

DEEP-SEA VALLEY-FILL SEDIMENTS:

CAP ENRAGE FORMATION, QUEBEC

By



FRANCES J. HEIN, B.S., M.Sc.

A Thesis

Submitted to the School of Graduate Studies

in Partial Fulfilment of the Requirements

for the Degree

Doctor of Philosophy

McMaster University

DEEP-SEA VALLEY-FILL SEDIMENTS:

CAP ENRAGE FORMATION, QUEBEC

DOCTOR OF PHILOSOPHY (1979)
(Geology)

McMaster University
Hamilton, Ontario

TITLE: Deep-Sea Valley-Fill Sediments:
Cap Enrage Formation, Québec

AUTHOR: Frances J. Hein, B.S. (University of Illinois
at Chicago Circle Campus)
M.Sc. (McMaster University)

SUPERVISOR: Professor Roger G. Walker

NUMBER OF PAGES: xiv, 514

ABSTRACT

The Cap Enragé Formation, Cambro-Ordovician in age, is approximately 250 m thick and consists of coarse clastic sediments in association with classical turbidites. Sediments are divided into seven major facies: (1) coarse-grained conglomerate; (2) graded-stratified/cross-stratified fine conglomerate and pebbly sandstone; (3) graded-dispersed fine conglomerate and pebbly sandstone; (4) graded-liquefied fine conglomerate, pebbly sandstone and sandstone; (5) ungraded-cross-stratified fine conglomerate, pebbly sandstone and sandstone; (6) structureless sandstone; and, (7) classical turbidites, mainly sandstone. Rare shale beds also occur.

Facies (7) beds follow the Bouma model and are interpreted as deposits from turbidity currents. Facies (5) beds are due to reworking of previous deposits by dilute flows associated with turbidity currents. Facies (1) to (4) and (6) record a two-stage process: i) grading patterns reflect segregation of clast sizes during main transport phases by turbidity currents; and, ii) sedimentary structures and fabrics record transport and deposition from basal dispersions, which developed at the base of turbidity currents.

Facies (1) beds have an a-axis flow-parallel bedding fabric, with a-axis upstream imbrication. Beds were deposited en masse from dispersions, in which there was strong grain interaction and high dispersive pressures. Grading patterns are interpreted in terms of decreasing applied shear stress and concentrations of sediment, as follows:

ungraded → inverse → inverse-to-normal → normal grading .

Coarse-grained Facies (2) beds have the same fabric as the Facies (1) beds and are interpreted as en masse deposits from dispersions, with dominant inertial effects. Stratification in both the coarse-grained Facies (2) and Facies (1) beds reflects pulsating deposition from the basal dispersions.

Finer-grained Facies (2) beds have flow-parallel or bimodal a-axis bedding fabrics, with a-axis upstream or bimodal imbrications. Beds were deposited from waning turbidity currents under high velocity tractional flow conditions. Bimodal bedding fabrics reflect clast re-orientation after initial deposition on the bed. Bimodal imbrications record deposition of clasts onto low-relief wave bedforms.

Facies (3), (4) and (6) beds all have a-axis flow-parallel, bimodal or random bedding fabrics. Differences arise in imbrication patterns: Facies (3) have bimodal imbrications; Facies (4) have bimodal or unimodal imbrications; and, Facies (6) have unimodal imbrications. All beds are interpreted as being deposited from basal dispersions, in which viscous effects dominated. Apparent viscous effects were due to high concentrations of sand, such that the coarser clasts responded to the flow as if it were very viscous. Facies (3) and (6) beds may have experienced some syn- or post-depositional deformation into low-relief wave-forms, yielding bimodal imbrications. Facies (4) beds experienced some syn- or early post-depositional liquefaction, producing fluid escape features. Some Facies (4) beds also underwent syn-depositional or early post-depositional deformation similar to Facies (3) and (6) beds.

The overall facies model suggests deposition within three main topographic levels: (i) main channels; (ii) bars within main channel networks; and, (iii) terraces above the main channel networks. Facies (1) beds are main channel deposits. Facies (2), (3) and (4) beds are bar-top deposits or marginal terrace deposits. Facies (6) are high terrace sediments. Facies (7) and shale were deposited on high 'distal' terraces, farthest removed from the main channel networks.

Small scale (\leq 1 m - 5 m) fining/thinning-up sequences record the abandonment of channels; coarsening/thickening-up sequences represent the occupation of channel sites. Large scale (10's - 100 m) sequences reflect interactions between main channel networks and high terrace sites. Transitions from channels to marginal terraces are fining/thinning sequences; sequences from marginal terrace to high terrace are fining/thickening; and, transitions from high terrace to 'distal' high terrace are fining/thinning.

Regional paleocurrent and facies trends within main channel networks suggest that sediments accumulated in a submarine braided valley system. Main channel networks were forced to swing parallel to the continental base-of-slope, perhaps by a small scale, uplifted continental block.

ACKNOWLEDGEMENTS

This work was performed under the supervision of Dr. Roger G. Walker, with funds provided by the National Research Council of Canada.

I thank Dr. Gerard V. Middleton, Dr. Jean Lajoie and Mr. Barry A. Johnson for their help and encouragement, particularly during the initial stages of this project. My advisory committee, Drs. R.G. Walker, G.V. Middleton and G.A. Round, all provided support and guidance throughout this study. Drs. R.G. Walker, G.V. Middleton and M.H.I. Baird provided helpful criticism of the thesis text. Special thanks are extended to Dr. Michael J. Keen and Dr. David J.W. Piper for providing the use of the facilities at Dalhousie University, during the laboratory phases of this project.

The field assistants were Ms. Deborah Hunter and Ms. Brenda McRae. Ms Hunter also prepared the acetate peels and enlarged photographs for the sandstone fabric analysis. Mr. H. Don Falkiner cut the oriented slab sections. Mr. Milton Graves helped with the petrologic analyses. Staff at the Denver Research Center, Marathon Oil Company, processed the field conglomerate fabric data with their computer and plotter facilities. Dr. William R. Normark, Dr. Donald R. Lowe and Mr. Timothy McHargue provided me with unpublished data.

Finally, I wish to thank my husband, Dr. Douglas J. Cant, for help with measurement of all those "blank-blank" grains in the sandstone imbrication plots; for help, encouragement and patience, especially during the grain orientation studies and the final months of thesis writing; and, last but not least, for nagging me to get this thing done.

TABLE OF CONTENTS

	<u>Page</u>
CHAPTER 1	
The Sedimentology of Deep-Sea Coarse Clastic Deposits and the Contribution of This Study	1
Introduction	1
Regional Setting of the Cap Enragé Formation	1
Deep-Sea Coarse Clastic Sediments -- The State of Knowledge	4
Purposes of the Present Study	15
Local Setting and Previous Studies of the Cap Enragé For- mation	17
Study Areas and Detailed Stratigraphy	27
Organization and Basic Results of the Thesis	31
CHAPTER 2	
Definition of the Facies	34
Sedimentary Facies	34
Basic Description of Facies	35
Facies (1) - Coarse Conglomerate	35
Facies (2) - Graded-Stratified/Cross-stratified Fine Conglomerate and Pebbly Sandstone	40
Facies (3) - Graded-Dispersed Fine Conglomerate and Pebble Sandstone	42
Facies (4) - Graded-Liquefied Fine Conglomerate, Pebbly Sandstone and Sandstone	47
Facies (5) - Ungraded-Cross-stratified Fine Conglomerate, Pebble Sandstone and Sandstone	51
Facies (6) - Structureless Pebbly Sandstone and Sand- Stone	54
Facies (7) - Classical Turbidites	57
Shale Facies	59
Gradation Between Facies	59

	<u>Page</u>
CHAPTER 2 (Cont'd)	
Facies Associations in Multiple Scour Fills	63
Small Scale Facies Associations	63
(1) Scour Fill Predominantly Facies (1)	63
(2) Scour Fill Predominantly Facies (2)	70
(3) Scour Fill Predominantly Facies (6)	73
CHAPTER 3	
Vertical and Lateral Facies Relationships	80
Vertical Facies Associations	82
Preliminary Analysis: Methods	82
Preliminary Analysis: Results	85
Detailed Analysis: Methods	88
(1) Pooling the Data	88
(2) Delineation of Detailed Sequences	91
Detailed Analysis: Results	93
(1) Markov Chain Analysis: Sequence of Beds	93
(2) Embedded Markov Chain Analysis: Sequence of Facies	94
(3) Substitutability, Cluster and Markov Analysis: Sequences of Groups of Facies	97
Lateral Facies Associations	97
Small Scale Facies Associations	99
CHAPTER 4	
Sedimentary Fabric and Size Analyses	102
Sedimentary Fabric	102
Conglomerate Fabric	103
Methods	103
Summary Statistics of Clast Orientation Patterns	104
Results	105
Discussion	109
Summary of Conglomerate Fabric Results	113
Pebbly Sandstone and Sandstone Fabric	113
Methods	113
Summary Statistics of Clast Orientation Patterns	116
Results	116
Summary of Fabric Results	123

	<u>Page</u>
CHAPTER 4 (Cont'd)	
Grain Size Analysis	124
Results	125
CHAPTER 5	
Depositional Mechanisms for Different Facies	128
Sedimentation of Deep-Sea Coarse Clastic Deposits	128
Hydrodynamic Implications of Major Sedimentary Features	132
Origins of Sedimentary Fabric Patterns	135
Fabric: A-axis parallel to flow, a-axis imbricate upstream	139
Fabric: A-axis parallel to flow, a-axis imbricate up- or downstream	143
Fabric: Random a-axis, unimodal or bimodal imbrication	147
Fabric: Bimodal a-axis, unimodal or bimodal imbrication	147
Summary -- Fabric Origins	149
Depositional Mechanisms for Different Facies	152
Facies (7)	152
Facies (1)	156
Facies (2)	169
Facies (5)	178
Facies (6)	180
Facies (3)	184
Facies (4)	186
CHAPTER 6	
Overall Facies Models for the Cap Enragé Formation	197
Introduction	197
General Paleotopographic Reconstruction	201
Reconstruction of Individual Outcrops	204
Main Channel Deposits	204
Marginal Terrace Deposits	218
High Terrace Deposits	229
General Sedimentation Model: Summary	231

CHAPTER 6 (Cont'd)	<u>Page</u>
Depositional Subenvironments for Different Facies	241
Main Channels	242
Braid Bars or Point Bars Within Main Channel Networks	244
High Terraces Above Main Channel Networks	246
Interpretation of Sequences in Terms of the Model	246
Large-Scale Relationships Between Conglomerates and Sandstones	249
Overall Setting of the Cap Enragé System	253
Comparison With Other Deep-Sea Coarse Clastic Sediments	255
Regional Paleotopography and General Setting	259
General Tectonic Setting	264
REFERENCES	269
APPENDIX 1 - List of Symbols and Abbreviations	283
APPENDIX 2 - Methods	286
APPENDIX 3 - Petrology	299
APPENDIX 4 - Descriptions of Sedimentary Features	301
APPENDIX 5 - Outcrop Maps and Stratigraphic Sections	364
APPENDIX 6 - Fabric Data From Conglomerates	424
APPENDIX 7 - Fabric Data From Pebbly Sandstones and Sandstones	431
APPENDIX 8 - Grain Size Analysis of Pebbly Sandstones and Sandstones	445
APPENDIX 9 - Statistical Analyses of Vertical Facies Sequences	450

LIST OF TABLES

<u>Table</u>		<u>Page</u>
1	Stratigraphic and Tectonic Setting: Cambro-Ordovician Conglomerates of Québec and Newfoundland	22
2	Grading and Types of Bases in Different Facies	39 ^b
3	Bed Thickness for Different Facies	43
4	Small-Scale Lateral Facies Associations	100
5	Bedding Plane Fabric and Imbrication Patterns	119
6	Classification of Sediment-Gravity Flows	129
7	Reports Dealing with Clast Fabric	133
8	Sedimentary Features and Their Possible Hydrodynamic Interpretations	136
9	Sedimentary Fabrics and Their Possible Hydrodynamic Interpretations	150
10	Minimum Estimates of Flows Depositing Facies (2) Beds	175
11	Observed Sedimentary Sequences	236
12	Dimensions of Some Submarine Canyons and Channels	256
13	Stratigraphic and Tectonic Elements, St. Lawrence Valley and Eastern Townships	266

LIST OF FIGURES

<u>Figure</u>		<u>Page</u>
1	Regional Geologic Map	3
2	Bouma Sequence	6
3	Interpretation of Bouma Sequence	6
4	Resedimented Conglomerate Models	6
5	Deep-Sea Sediment Transport and Deposition	8
6	Deep-Sea Fan	11
7	Deep-Sea Fan Sedimentary Facies	11
8	Sequences in Fan Sediments	11
9	Illustration of Paleoflow Controversy, Cap Enragé Formation	18
10	Outcrop Map	19
11	Generalized Stratigraphic Sections	19
12	Regional Paleoflow Directions	24
13	Petrologic Variations	24
14	Solitary Scour Fill - photo	36
15	Facies (1) Types	37
16	Facies (2) Types	41
17	Dispersed Pebbly Sandstone - photo	44
18	Conglomerate Filled Scour - photo	44
19	Facies (3) Types	45
20	Dish and Pillar Structures - photo	48
21	Pillar Structures - photo	48
22	Facies (4) Types	49
23	Trough Crossbedding - photo	52
24	Trough Crossbedding, in plan view - photo	52
25	Facies (5) Types	53
26	Structureless Sandstone - photo	53
27	Facies (6) Types	55
28	Classical Turbidite - photo	58
29	Facies (7) Types	58
30	Gradation Between Facies	61
31	Outcrop Sketch and Paleoflow Data - Rivière Trois Pistoles	64
32	Outcrop Sketch and Paleoflow Data - Grève de la Pointe	64
33	Multiple Scour Complex - St. Simon sur Mer (Shrine)	68
34	Multiple Scour Complex - Grève de la Pointe	68
35	Multiple Scour Complex - St. Simon sur Mer Est	72
36	Multiple Scour Complex - St. Simon sur Mer Est	72
37	Multiple Scour Complex - St. Simon sur Mer Est	75
38	Multiple Scour Fills - St. Simon sur Mer (Two Cottages) - photo	75
39	Multiple Scour Complex - St. Simon sur Mer (Two Cot- tages)	76

<u>Figure</u>		<u>Page</u>
40	Multiple Scour Complex - Anse à Pierre Jean 5	78
41	Multiple Scour Complex - Bic	78
42	Vertical Facies Relations	86
43	Facies Relationships	95
44	Facies Relationships	96
45	Facies Relationships: Groups of Facies	98
46	Graph of Semi-Angle of 3-D Vector Mean Versus the Mean Dip of Clasts	108
47	Illustration of R_z and R_{xy}	108
48	3-D Vector Mean Dip and Semi-Angle Cone of Confidence for Low Dips	112
49	Imbrication Patterns	114
50	Graphs of Modal Angle of Dip Versus Vector Strength and Imbrication	122
51	Conglomerate Fabrics	140
52	Production of Fabric in Flow	140
53	Forces on a Grain due to Collision	142
54	Conditions of Jumping and Rolling of Clasts	142
55	Bedform Stability Fields	153
56	Turbidity Current Sketch	155
57	Inclined Dish Structures - photo	189
58	Low-Angle Crossbedding - photo	189
59	Fluid Escape Structures in a Scour Fill	190
60	Fluid Escape Structures in Two Beds	192
61	Assemblage of Fluid Escape Structures	192
62	Fluid Escape Structures in a Single Bed	193
63	Fluid Escape Structures in a Single Bed	193
64	Liquefaction Structures	194
65	Conglomerate Pod Sketch	199
66	Paleotopographic Reconstruction of the Cap Enragé Depositional Setting	202
67	Generalized Sections and Paleotopographic Reconstruc- tion, Anse à Pierre Jean 3	205
68	Generalized Sections and Paleotopographic Reconstruc- tion, Anse à Pierre Jean 2	208
69A	Generalized Sections - Anse à Pierre Jean 1	212
69B	Paleotopographic Reconstruction - Anse à Pierre Jean 1	213
70	Paleotopographic Reconstruction - Niveau 3/4, St. Simon sur Mer - to - St. Simon sur Mer (Shrine)	216
71	Generalized Sections and Paleotopographic Reconstruc- tion - Cap à la Carre Ouest	219
72A	Generalized Sections - St. Simon sur Mer	222
72B	Paleotopographic Reconstruction - St. Simon sur Mer	223
73	Sedimentary Sequences - Channel and Terrace Interaction	235
74	Paleogeographic Interpretation of Facies	243
75A	Sedimentary Sequences due to Channel Network Abandonment	251

<u>Figure</u>		<u>Page</u>
75B	Sedimentary Sequences due to Channel Network Reoccupation	252
76d	Regional Setting of Cambro-Ordovician Conglom- erates in the Quebec-Gaspé-Newfoundland Flysch Belt	261
77-117	In Appendices	



CHAPTER 1

THE SEDIMENTOLOGY OF DEEP-SEA COARSE CLASTIC DEPOSITS

AND THE CONTRIBUTION OF THIS STUDY

INTRODUCTION

The Cap Enragé Formation consists of conglomerates, pebbly and massive sandstones in association with classical turbidites and occurs within the flysch belt of the Gaspé Peninsula of Québec (Fig. 1A). As such, the Cap Enragé sediments would be considered to be re-sedimented deep-sea coarse clastic deposits. In the following chapter, the regional setting of the Cap Enragé Formation is described. Next, a brief discussion is given of sedimentological studies of deep-sea coarse clastic deposits. This is followed by a section dealing with the specific geologic setting of the Cap Enragé Formation, detailed stratigraphy and previous studies of the formation. Finally, discussions of the study areas, organization and basic results of the thesis are presented.

REGIONAL SETTING OF THE CAP ENRAGE FORMATION

The Cap Enragé Formation belongs to the Québec Supergroup (Hubert et al., 1970) and occurs along the south shore of the St. Lawrence River. This formation is part of the flysch belt, consisting of a series of imbricated thrust slices and nappes of Cambrian to Middle Ordovician rocks, which delimit the western front of the Québec Appalachians

(Fig. 1A). In the Lower St. Lawrence valley (Fig. 1B), Cambrian and Ordovician rocks are grouped into three main types (St. Julien and Hubert, 1975): 1) shallow-water carbonates; 2) deep-sea clastic sediments; and 3) metamorphic and igneous rocks, in association with mélanges and ophiolites. The St. Lawrence lowlands are bounded to the north by Precambrian (Grenville) rocks of the Canadian Shield, and to the south by Silurian and Devonian continental sediments (Fig. 1B).

Northwest of the study area (Fig. 1B), a parautochthonous unit developed on the southeastern margin of the Precambrian platform. This parautochthonous unit consists of a basal late Middle Ordovician transgressive sandstone, succeeded by carbonate bank deposits and deeper water, mainly flysch sediments and resedimented conglomerates (Bussièrès et al in Béland and LaSalle, 1977). Along the south shore of the St. Lawrence River are outcrops of allochthonous structural units. The line separating the parautochthonous and allochthonous units is Logan's Line (Fig. 1B). The allochthonous units are further divided into an "external domain" and an "internal domain." The external domain consists of an outer belt of imbricate thrust slices and an inner belt of nappes, emplaced by gravity sliding (St. Julien and Hubert, 1975). The internal domain comprises metamorphic and igneous rocks, some of which rest upon continental (Grenville-like) crust, with other portions resting upon oceanic crust (St. Julien and Hubert, 1975) (Fig. 1B).

Cambro-Ordovician allochthonous nappes of the external domain consist mainly of shale - feldspathic sandstone-limestone & petromict conglomerate. In the lower St. Lawrence valley, this assemblage consists of the St. Roch and St. Damase Formations (Hubert, 1973) and the

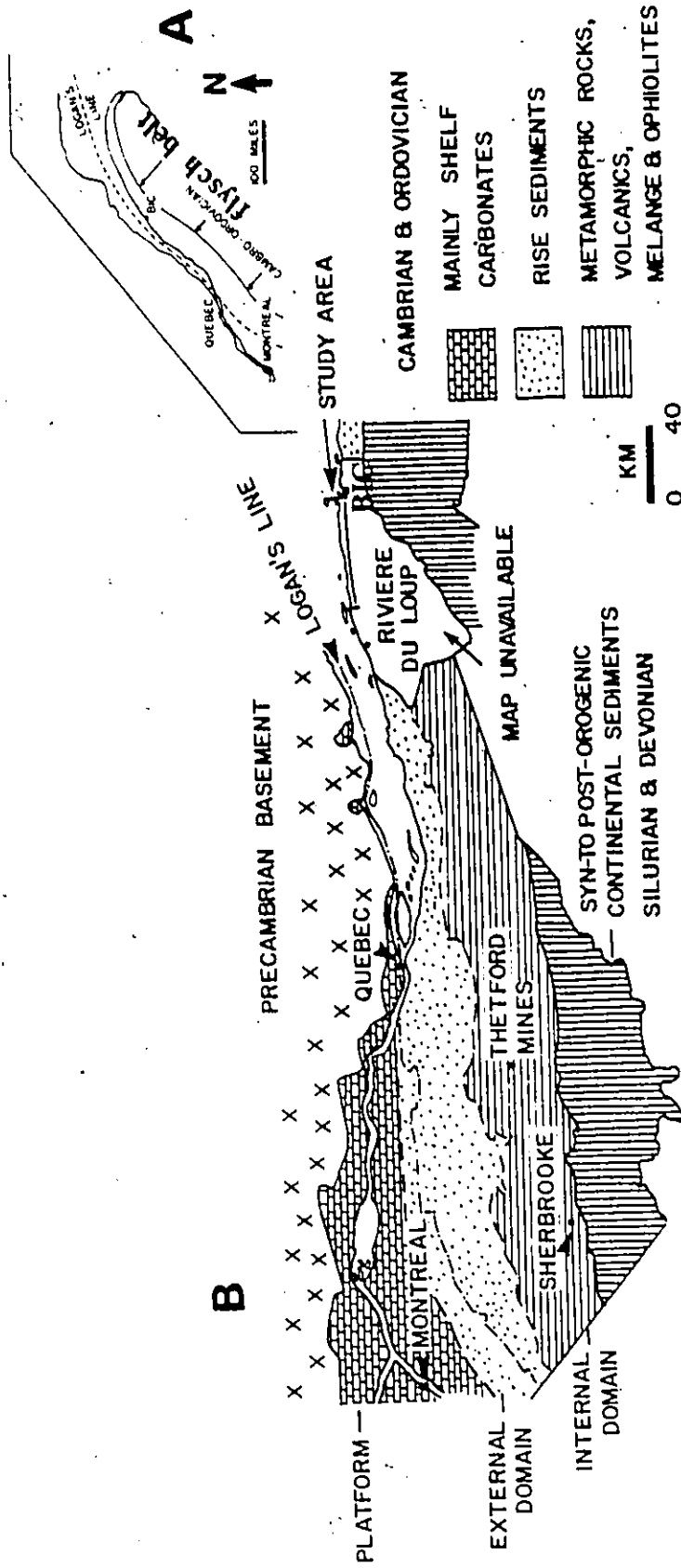


Fig.1 - Stratigraphic assemblages and tectonic domains in the St. Lawrence Lowlands and Eastern Townships, Québec Appalachians (redrawn from St. Julien and Hubert, 1975). Shallow water carbonates comprise the shelf carbonates. Rise sediments consist of an assemblage of deep-water shales, feldspathic sandstone, and limestone and petromict conglomerate. For detailed subdivisions within different tectonic domains see St. Julien and Hubert (1975, Fig.1).

4

Original, Cap Enragé and Ladrière Formations (Hubert et al, 1970) (Table 1). During the last five years, Vallières (1978: pers. comm.) has mapped the region on Figure 1B, for which, at present, a map is unavailable (blank area, Fig. 1B). Vallières will propose a unified nomenclature for the Cambro-Ordovician stratigraphy for this region and areas westward to Québec City. It is likely, although not definite, that the Cap Enragé name will be preserved (Vallières, 1978: pers. comm.).

The stratigraphic assemblages in the St. Lawrence lowlands and Eastern Townships have been interpreted by St. Julien and Hubert (1975) as representing four tectonic domains: Platform Sediments (shallow water carbonates); Rise Sediments (deep-sea clastic sediments); Metamorphic - Igneous Complex (metamorphic and igneous rocks, in association with mélanges and ophiolites); and, Syn- to Post-Orogenic Deposits (Silurian and Devonian continental sediments). The sedimentary, volcanic and structural history of the rocks grouped into these tectonic domains record the opening and closing of the proto-Atlantic basin. Generally, the tectonic model for the Lower St. Lawrence Valley - Gaspé Peninsula region follows the lithosphere plate tectonic models in the development of mountain belts (St. Julien and Hubert, 1975; see review by Dewey and Bird, 1970).

DEEP-SEA COARSE CLASTIC SEDIMENTS -- THE STATE OF KNOWLEDGE


Most sediment is thought to be transported into deep-sea basins by turbidity currents or, to a lesser extent, by debris flows (Kuenen, 1937, 1964; Hesse, 1975; Middleton, 1978). Many deep-sea sediments accumulate at the base of slope as depositional bulges, called submarine fans. There have been many recent review articles on the development of the

turbidite/submarine fan models. These include:

1. Evolution of the turbidity current concept (Walker, 1973);
2. Facies models applied to turbidites and associated coarse clastic deposits (Walker, 1975a, 1975b) (brief discussions);
3. Processes of transport and deposition from turbidity currents and associated sediment gravity flows (Middleton and Hampton, 1976);
4. Depositional, morphological and growth patterns on modern submarine fans (Normark, 1978);
5. General facies models for turbidite and associated coarse clastic sediments, integrated into a submarine fan model of sedimentation (based upon ancient examples, but modified by observations of modern submarine fans) (Walker, 1978).

In light of these full review articles, only the essentials of the turbidite/submarine fan models will be presented here. The basic concepts discussed will be used later, in the hydrodynamic implications and spatial arrangement of sedimentary facies within the Cap Enragé Formation.

Kuenen and Migliorini (1950) first proposed that most deep-sea clastic sediments were transported and deposited from turbidity currents. Dense suspensions of sediment, including pebbly sands and gravel, were envisioned as moving as turbulent flows, downslope under the influence of gravity. Bouma (1962) generalized the sequence of sedimentary structures within deposits from turbidity currents. This turbidite facies model, known as the "Bouma sequence," was later interpreted to be a consequence of decreasing flow power (both in time and space) in a waning turbidity current (Walker, 1978) (Fig. 2,3).



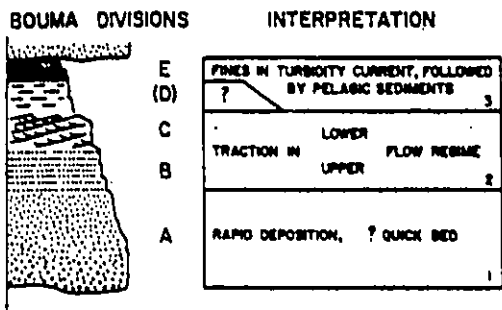


FIG. 2—Bouma model for classic turbidites. Division A is massive or graded, B is parallel laminated, C is rippled, D consists of faint laminations of silt and mud, and E is pelitic.

From Walker (1978)

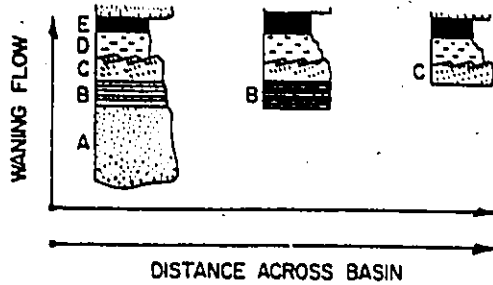


FIG. 3—Interpretation of ABCDE Bouma sequence in terms of waning flow suggests that groups of turbidites beginning with divisions B and C represent deposition from progressively slower flows. This can be related to increasing distance across basin, although it is emphasized in text that some CDE thin-bedded turbidites can be present on levees in proximal environments, and hence CDE turbidites are not necessarily distal.

From Walker (1978).

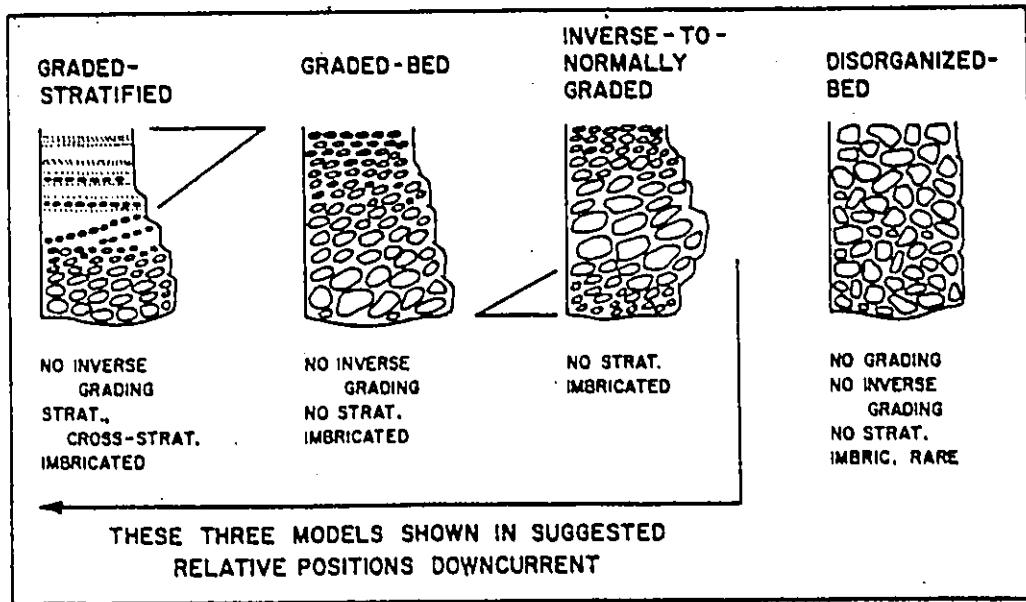


FIG. 4—Four models for resedimented conglomerates. Inversely to normally graded, graded-bed, and graded-stratified models are shown in relative downcurrent position, but this relation is suggested on theoretical grounds only.

From Walker (1978).

Although the recognition and interpretation of the Bouma sequence did provide a breakthrough in understanding the origin of turbidites, there were other deep-sea sediments that did not seem to conform to the model. This was particularly true for very proximal sediments, which Kuenen (1958) called "fluxoturbidites." Such sediments were interpreted as being deposited from "fluxoturbidity currents," transitional between slumps or slides and true turbidity currents. Since the time when workers were thinking in terms of "true turbidity currents" and "fluxoturbidity currents," it has become apparent that the fluxoturbidites actually comprise a wide number of mass flow deposits that operate in deep-sea settings.

The nature of mass flows, other than turbidity currents, has become understood to a much greater extent in recent years. Turbidity currents may originate as part of a continuum of subaqueous mass movements, from submarine landsliding to turbidity current flow. Middleton and Hampton (1973,1976) have proposed a conceptual model, which depicts the relationships in time and/or space of mass flow processes. Different processes are important for various flows, depending upon grain size in the flow and concentrations of sediment (Fig. 5).

Mass flows can be classified on the basis of the sediment support mechanism (Middleton and Hampton, 1973,1976) (Fig. 5): 1) turbidity currents (support by fluid turbulence); 2) liquefied sediment flows (support to a certain extent by fluid escaping from the sediment-water dispersion); 3) grain flows (support by dispersive pressure due to grain interaction); and, 4) debris flows (support by strength of a muddy matrix). Different gravity flow mechanisms may operate at the same time

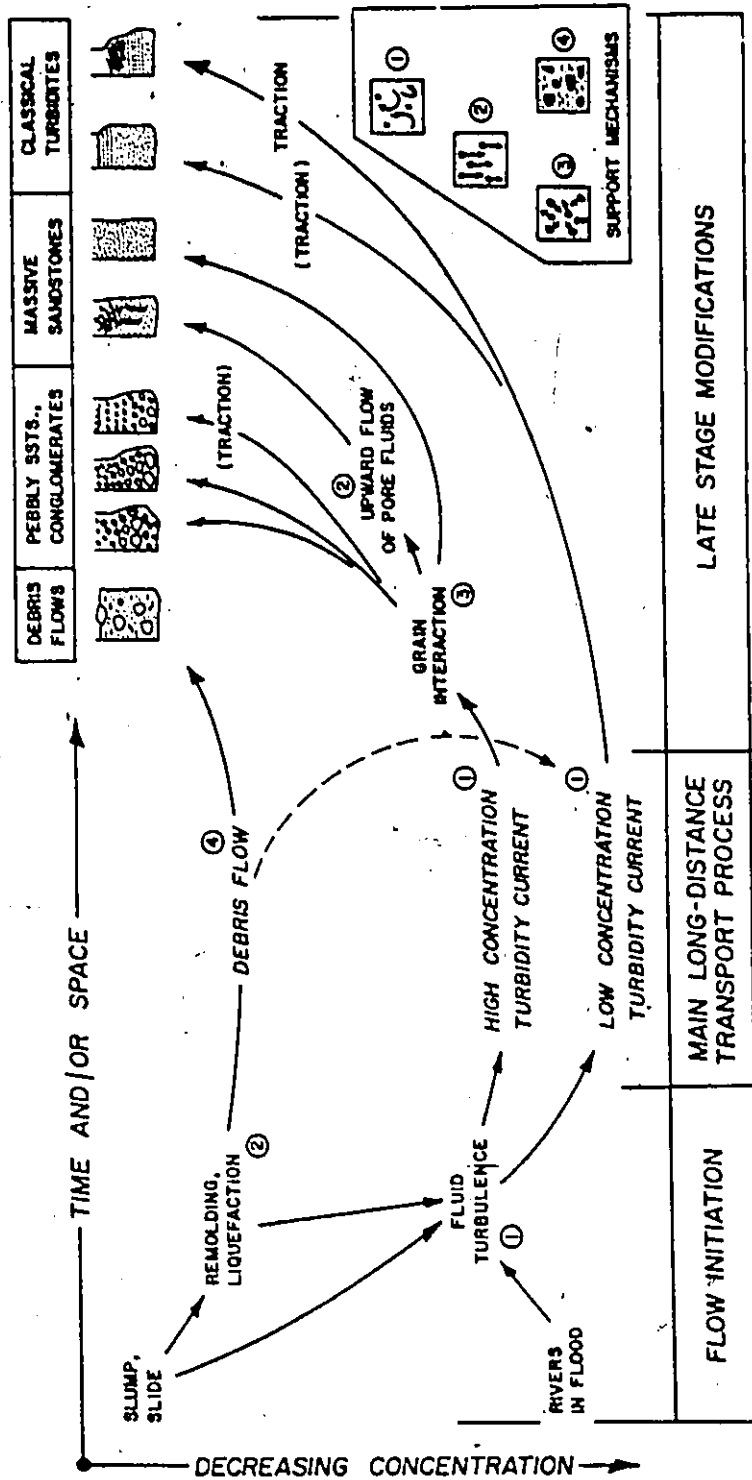


FIG. 5—Processes of initiation, long-distance transport, and deposition for currents transporting sediment into deep water. Framework is one of time and/or space, and concentration of flows. Grain-supporting mechanisms (insert, lower right) include: 1, fluid turbulence; 2, liquefaction; 3, collision between individual grains (dispersive pressure in grain flow); and 4, matrix strength (as in debris flow). Modified in discussion with Middleton (personal commun.) from Middleton and Hampton (1976), to show possibility of debris flows becoming turbid, and to eliminate grain flows as long-distance transport processes. From Walker (1978).

or, alternatively, in a temporal sequence during deposition from a single flow (Middleton, 1967; Skipper and Middleton, 1975).

Volumetrically, the classical turbidites (following the Bouma sequence and deposited from low-concentration turbidity currents) are the most important clastic deposit in deep-sea basins (Walker, 1976). Other deep-sea clastic sediments include: chaotic, pebbly and conglomeratic mudstones; clast-supported conglomerates, pebbly and massive sandstones.

Matrix-supported coarse deep-sea sediments include conglomeratic, pebbly and sandy mudstones. These deposits are thought to represent sediments deposited from mass flows near the source (slides or slumps) or sediments from subaqueous debris flows. Beds are chaotic or disorganized, with perhaps only a small basal zone of inverse grading. Clasts may protrude above the general bed level, representing the floating position of the coarser grains during transport.

Clast-supported deep-sea conglomerates have been studied by many workers (see Walker, 1975). However, a generalized facies model for deposition of these sediments has only been recently proposed by Walker (1975a) (Fig. 4). The trends in the resedimented conglomerate model show depositional patterns from currents which begin to deposit in proximal areas (Inverse-to-Normally Graded Conglomerates), to those currents which by-pass proximal areas and begin deposition further downcurrent (Graded-Stratified Conglomerates). The development of Graded-Stratified sequences in less proximal areas is mainly a consequence of decreased slope and greater distance of transport (Walker, 1978).

Massive and pebbly sandstones are not as well understood as the other deep-sea sediments. Some massive sandstones have well-developed fluid escape features, suggesting partial or complete sediment support by pore water expulsion. This pore water expulsion may have been during consolidation of the bed during deposition, or be due to post-depositional consolidation, as a consequence of loading (Lowe and LoPiccolo, 1974; Lowe, 1975). Other massive sandstones lack fluid escape features. Sequences of sedimentary structures within massive and pebbly sandstones have been studied by few workers (Aalto, 1976; Chipping, 1972; Keith and Friedman, 1977; Hiscott, 1977; Piper et al, 1978; Van/de Kamp et al, 1974). Pebbly sandstones show normal grading, have parallel stratification, crossbedding and fluid escape features (Walker, 1976, 1978). It is unknown whether these features show consistent patterns. Grain fabric studies are generally lacking from pebbly and massive sandstones (Hiscott, 1977; Sestini and Pranzini, 1965).

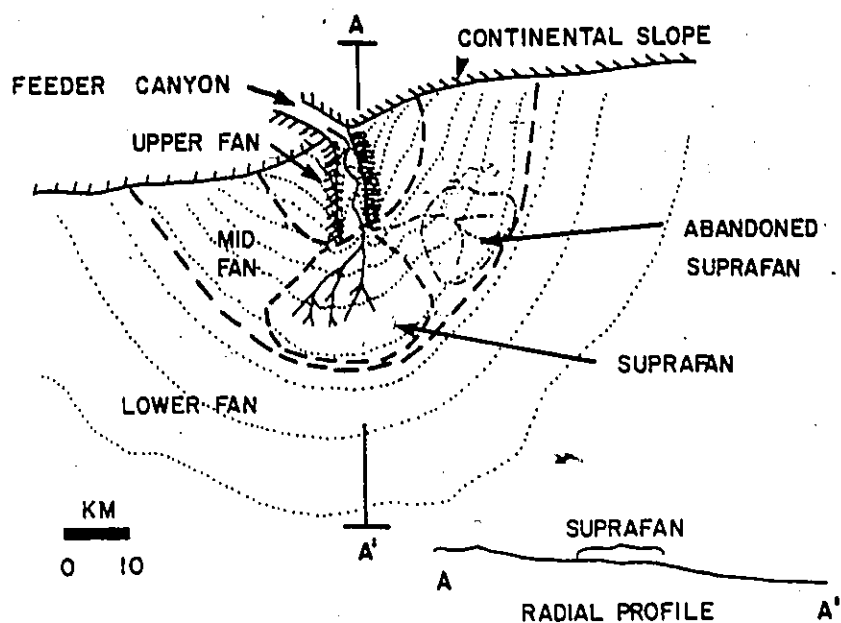
Hand-in-hand with studies dealing with sediment transport and depositional mechanisms, there have been many studies determining the geographic and topographic relationships amongst the various sorts of deep-sea sediments. The integration of these relations has led to the submarine fan model. This model is based upon trends in ancient deep-sea sediments, modified by what is known about sedimentation processes on modern submarine fans.

Many modern submarine fans have three broad morphologic features (Normark, 1974, 1978) (Fig. 6): 1) the upper fan, which is characterized by large leveed valley(s) (1-5 km wide). Sediments are the coarsest observed on fans and are deposited within shallow channels confined

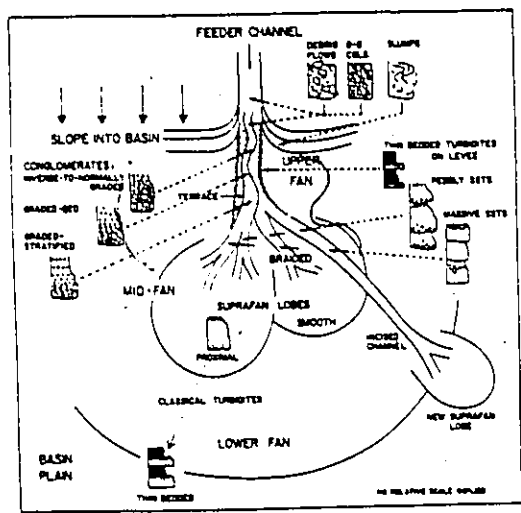
Fig.6 - Schematic representation of the model for submarine fan growth, emphasizing active and abandoned suprafan depositional lobes (redrawn from Normark, 1978).

Fig.7 - Schematic representation of the model for submarine fan growth, relating facies to fan morphology and depositional environment. D-B cgl indicates disorganized bed conglomerates (from Walker, 1978).

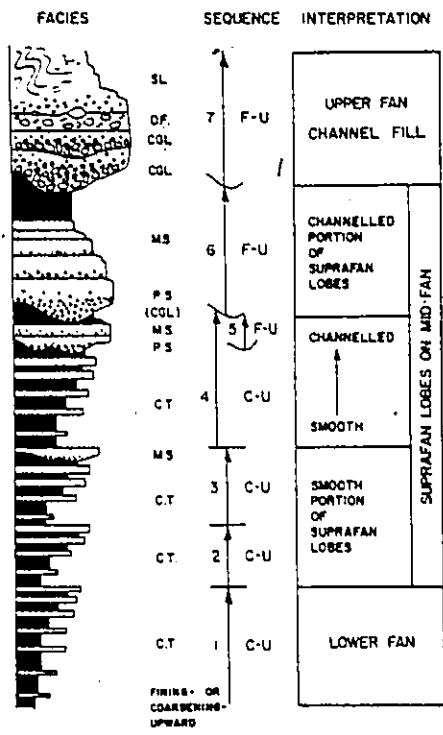
Fig.8 - Hypothetical stratigraphic sequence produced by fan progradation. C-U, thickening and coarsening upward sequence; F-U, thinning and fining upward sequence; C.T., classical turbidites; M.S., massive sandstone; P.S., pebbly sandstone; CGL, conglomerate; D.F., debris flow; SL, slumps (from Walker, 1978).



6



7



8

within the valley. Channel patterns may be meandering or braided.

2) The mid fan bulge (also called the suprafan), which occurs at the downslope end of the leveed upper fan valley. Sandy turbidites occur in the upper reaches of the suprafan, which is cut by many channels and isolated scours. Channels are generally less than 1 km wide. The finer grained, lower suprafan area is unchannelized. 3) The lower fan, which is unchannelized and receives only the fine-grained sediment from low-concentration turbidity currents. This lower fan lobe is almost flat and generally impossible to distinguish from flat, abyssal plain areas.

Basin shape, rate and size of sediment supply control the extent (if any) these morphologic divisions are developed on modern fans (Nor-mark, 1978). Fans with mainly coarse sediment input have a single leveed valley that ends downcurrent with a suprafan lobe. Fans which receive dominantly fine-grained silt and clay tend to have upper leveed fan valleys which may extend across most of the fan; or, at most, have only poorly developed suprafan lobes .

Aspects of the ancient submarine fan model are reviewed by Walker (1978) (Fig. 7). Classical turbidites are thought to be characteristic of the smooth, flat outer suprafan and lower fan lobes. Massive and pebbly sandstones tend to be more channelized, are coarser-grained and generally lack interbedded shales. Massive and pebbly sandstones are assigned to deposition within braided suprafan channels, where rapid channel migration accounts for the absence of shale deposits. Clast-supported conglomerates are thought to be from leveed channeled areas of the upper fan, or possibly the upper suprafan. Matrix-supported slump and debris flow sediments and disorganized conglomerates are thought to have

been deposited in very proximal, high slope areas, most likely at the base-of-slope contact between the feeder canyon and the upper fan leveed valley.

A model sequence produced by fan progradation (Fig. 8) (Walker, 1978) shows a variety of coarsening/thickening-up and fining/thinning-up sequences. Coarsening/thickening-up sequences of classical turbidites occur in outer fan and lower suprafan areas, due to lobe progradation. Fining/thinning-up sequences of pebbly and massive sandstones (minor amounts of conglomerate) occur in channeled portions of the suprafan. Fining/thinning-up sequences of conglomerates occur in the upper fan valley fills. The sequence is capped by disorganized conglomerates and/or matrix-supported slump and debris flow deposits. The overall sequence from the outer fan to the upper fan would be a coarsening/thickening-up sequence (Walker, 1978).

Not all deep-sea sediments follow the submarine fan model. Strong contour-flowing bottom currents can rework sand-size material (and finer) sediment, yielding new deposits, called "contourites" (Hubert, 1966; Bouma, 1972; Bouma and Hollister, 1973; Stow, 1977). In addition, some ancient and modern deep-sea troughs have turbiditic or turbidite-like sediments, which do not show any proximal-to-distal trends, as would be expected in a submarine fan system. Ancient turbidite-like deposits which do not conform to the fan model have been noted by the following workers: Enos, 1969 (Cloridorme Formation); Gonzalez-Bonorino and Middleton, 1976; Harms, 1974; McBride, 1962; Parkash, 1970 (Cloridorme Formation); Parkash and Middleton, 1970; Skipper and Middleton, 1975 (Cloridorme Formation). Modern deep-sea troughs which have

turbidite-like sediments which do not follow the submarine fan model, include: the Hispaniola-Caicos Basin (Bennets and Pilkey, 1976); the Maury Channel (Cherkis et al, 1973); the Northwest Atlantic Mid-Ocean Channel (Chough and Hesse, 1976).

PURPOSES OF THE PRESENT STUDY

The submarine fan model, which has served as a guiding light in the interpretation of coarse-grained (silt size and greater) deep-sea sediments for the past five years, has some obvious gaps that need specific documentation, in terms of flow processes and deposition:

(1) Although the generation of turbidity current flow is fairly well understood, the flow processes during depositional phases are not as well understood. Several workers have demonstrated that different gravity flow mechanisms may interact within a flow during deposition of a single bed. This has been shown experimentally (Middleton, 1967) and from field evidence (Skipper and Middleton, 1975; Hiscott, 1977) for generally sand size material, and from field evidence for coarse conglomerates (Davies and Walker, 1974; Walker, 1975a; Krause and Oldershaw, 1978). What type of flow mechanism(s) would account for the origins of deep-sea pebbly and massive sandstones?

(2) As yet a sedimentary model does not exist that adequately describes the facies of material intermediate in size between conglomerate beds (which may follow the models proposed by Walker, 1975a) and the sand and silt-size turbidites (which follow the Bouma model). Do pebbly and massive sandstones show consistent sedimentary features which allow the definition of facies? If so, how are these facies related to one another?

(3) What is the extent of gradation between pebbly and massive sandstones to more "proximal" conglomerates in upcurrent directions, and to more "distal" classical turbidites in downcurrent directions?

(4) Normark (1978) states that the degree of development of different morphological subdivisions of modern submarine fans depends greatly upon the size and rate of sediment supply. This is known from considerations of modern fans with mainly sand-size and finer sediment. Would submarine fans develop in systems that received very coarse sediment input (mainly coarse sand to coarse conglomerate) under conditions, of presumably, very rapid sediment supply?

These are some of the questions that were examined in this study.

The formation chosen for this project was the Cap Enragé Formation (Cambro-Ordovician) which is exposed along the north shore of the Gaspé Peninsula in Québec. This formation was chosen for several reasons:

(1) Sandstones, pebbly sandstones and conglomerates of the Cap Enragé Formation conformably overlie distal turbidites and, presumably, abyssal plain deposits (Orignal Formation) and grade conformably into distal turbidites (Ladrière Formation). Regionally the Cap Enragé Formation lies within the flysch belt of the Gaspé. By association, the Cap Enragé sediments are interpreted as being deposited within a deep-sea setting.

(2) The Cap Enragé Formation is well exposed along the coast between L'Isle Verte and Bic, Québec (approximately 50 km) and affords the opportunity for detailed section description on a bed-to-bed basis (Fig. 10, next section).

(3) Previous detailed sedimentological studies have been conducted on conglomeratic horizons within the Cap Enragé Formation (Davies, 1972; Davies and Walker, 1974; Johnson, 1974; Johnson and Walker, in prep.): Consequently, processes of deposition are understood for the coarser-grained units of this formation. Integration of these previous studies

with the present project (involving pebbly sandstones and sandstones) may yield an overall model, that would describe and interpret a coarse-grained deep-sea system.

(4) As will be covered in the next section, there is a disparity in the paleocurrent patterns for major sandstone horizons compared with paleoflow patterns for major conglomerate horizons, within the Cap Enragé Formation. Another reason for this study was to relate facies changes and paleocurrent changes within the sandstones and conglomerates of the Cap Enragé Formation (Fig. 9).

(5) Finally, before any detailed sedimentological study can be undertaken for an ancient deposit, good stratigraphic control must be present. The Cap Enragé Formation has been mapped in excellent detail in the Bic and St. Fabien sur Mer areas by Lajoie (in press and unpublished maps), and in the St. Simon and St. Simon sur Mer areas by Mathey (1970). (see location map, Fig. 10, next section): These maps provided the necessary stratigraphy, which enabled this detailed study to be conducted on a regional scale. For local outcrops, the map by Davies (1972) for Anse à Pierre Jean 1, and the conglomerate sections by Johnson (1974) for Anse à Pierre Jean 2 eastward to Cap Corbeau were a great help (see location map, Fig. 10, next section).

LOCAL SETTING AND PREVIOUS STUDIES OF THE CAP ENRAGE FORMATION

The Cap Enragé Formation consists of approximately 250 m of interbedded sandstones, pebbly sandstones and conglomerates associated with classical turbidites (Lajoie, in press; Hubert et al, 1970). It is exposed in the Lower St. Lawrence valley between L'Isle Verte and Bic (Fig. 10). Cap Enragé sediments conformably overlie claystones and siltstones of the

Fig. 9 - Cartoon illustrating one of the main purposes of this study -- to resolve and explain the disparity in paleoflows for the sandstones versus the paleoflows for the conglomerates within the Cap Enragé Formation.

Drawn by Ms. Lynn Johnston.



Non! C'est au SUD!!

Sorry, chap... the flow is to the west.

What the f--- am I getting into!!

Tsk, Tsk... Good luck, Fran... you'll need it!

SCRATCH SCRATCH

Dynam

Fig.10 - Location map of outcrops studied in the present project (shaded areas). Redrawn from topographic maps Trois Pistoles 22 C/3 (edition 2) and Rimouski 22 C/7 (edition 2)

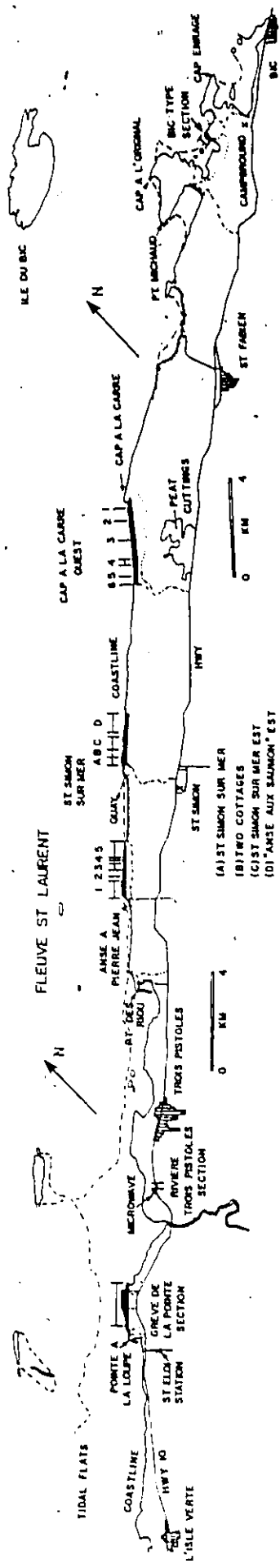
1 : 50,000 scale.

Fig.11 - Stratigraphic sections with nomenclature for the study areas. S11, Grève de la Pointe;

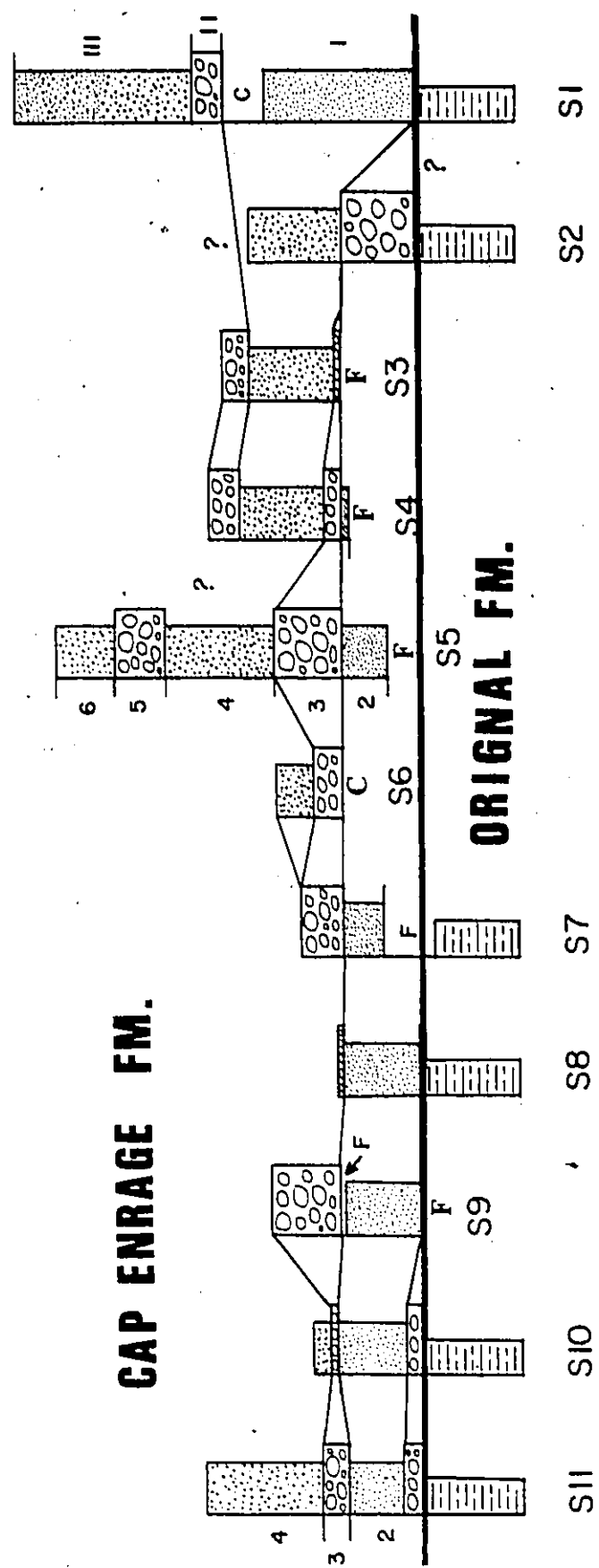
S10, Rivière Trois Pistoles; S9, Anse à Pierre-Jean 1; S8, Anse à Pierre-Jean 5; S7, St. Simon sur Mer (A); S6, St. Simon sur Mer, Two Cottages (B); S5, St. Simon sur Mer Est (C); S4, Anse aux Saumon Est (D); S2, Pt. Michaud; S1, Bic "Type" Section; S3, Cap à la Carre Ouest (6)

Arabic numbers refer to the "niveau" designations of Mathey (1970). Roman numerals refer to the "member" designations of Lajoie (in press). F - FAULT CONTACT; C - COVERED

- ○ ○ Conglomerate
- ● ● Pebbly Sandstone
- ○ ○ Sandstone



CAP ENRAGE FM.



ORIGINAL FM.

S11 S10 S9 S8 S7 S6 S5 S4 S3 S2 S1 E

Original Formation. Cap Enragé sediments are, in turn, conformably overlain by graded sandstones and pelites of the Ladrière Formation (Table 1). Sediments within the Cap Enragé Formation were derived from a carbonate bank and continental highland, located to the north of the depositional site (Lajoie et al, 1974). Tectonism associated with emplacement of the Lower St. Lawrence Valley Nappes has obliterated stratigraphic evidence for correlations between shelf platform and base-of-slope, deep-sea clastic sediments. The nappes now presently overlie and hide the original source material for the Cap Enragé sediments.

Petrologic and paleocurrent analyses (Lajoie et al, 1974) suggest that most of the Cap Enragé sediment was derived from a lower Paleozoic carbonate shelf, with less input from igneous and metamorphic rocks from the continental highlands of the Grenville craton. The carbonate bank supplied detrital sediment to the basin throughout the Cambrian. Although the bank is not preserved in outcrop, its presence is evident from Early Cambrian - Early Ordovician fossils within limestone clasts from deep-sea conglomerates, occurring as a narrow belt along the south shore of the St. Lawrence River (Hubert et al, 1970)

Conglomerates similar to those of the Cap Enragé Formation have been reported in the Lévis-Lauzon Formations (Osborne, 1956; Breakey, 1975) near Québec City; in the St. Roch Formation (Hubert et al, 1970; Rocheleau and Lajoie, 1974); in the Kamouraska and St. Damase Formations (Hubert, 1965); in the Tourelle Sandstone (regionally mapped with the Cap Chat mélange) (Hiscott, 1977); in the Cap des Rosiers conglomerates (Hendry, 1973; Aalto, 1972) -- all of the Lower St. Lawrence -- Gaspésie region. Similar conglomerates occur in Newfoundland in the Cape Comor-

ant Breccia (DeLong, 1977) and in the Cow Head Breccia (Hubert et al, 1977) (Table 1).

The age of the Cap Enragé Formation cannot be precisely dated. Trilobites collected from limestone clasts within the conglomerate are Early Cambrian (Lajoie, in press). Other fossils from limestone clasts are early Middle Cambrian (Rasetti, 1948 a, 1948b; Lajoie, in press). The overlying Ladrière Formation has Lower Ordovician fossils as the base (Lesperance, as quoted in Hubert et al, 1970). Hence, the Cap Enragé Formation cannot be older than early Middle Cambrian, and cannot be younger than Lower Ordovician, putting it in the age of 5×10^8 years.

There have been many studies of the Cap Enragé Formation (Léonard, 1969; Hubert et al, 1970; Mathey, 1970; Davies, 1972; Davies and Walker, 1974; Johnson, 1974; Lajoie et al, 1974; Chevalier, 1976; Lajoie, in press; Johnson and Walker, in prep.; Vallières, in prep.) Lajoie (in press) first mapped the formation, with the type section defined at Bic. Léonard (1969) did detailed mapping and description of the formation in the St. Fabien area. Mathey (1970) did detailed mapping in the St. Simon and St. Simon sur Mer area and conducted a general sedimentological study. Mathey (1970) interpreted the Cap Enragé sediments as deep-sea re-sedimented material, derived from the north, with paleocurrents toward the south-southeast (Fig. 12). Paleocurrent data was mainly from sandstones.

Hubert et al (1970) studied the 'type' section of the Cap Enragé Formation near Bic (Fig. 10). They interpreted the Cap Enragé sandstones and conglomerates as part of a submarine fan complex, with sediment supply from the north. Sediment was transported to the basin via

TABLE 1
 STRATIGRAPHIC UNITS AND TECTONIC ELEMENTS: CAMBRO-ORDOVICIAN
 CONGLOMERATES: QUEBEC AND NEWFOUNDLAND
 (DeLong, 1977; Hubert et al, 1977; St. Julien and Hubert, 1975)

		NORTH EAST				SOUTH WEST								
DOMAINS		AUTOCHTHONOUS DOMAIN		THRUST IMBRICATED STRUCTURES		EX T E R N A L D O M A I N								
SUB-DOMAINS		WESTERN NEWFOUNDLAND		NORTH COAST OF GASPE		LOWER ST. LAWRENCE VALLEY		QUEBEC CITY						
STRUCTURAL UNITS		W PLATFORM		KLIPPE		CAP ANNE RIVER NAPPE		LOWER ST. LAWRENCE VALLEY NAPPE						
ORDOVICIAN	UPPER	CAPE COMORANT BRECCIA	COW HEAD BRECCIA	St. Lawrence River Covered by Ice	CLORIDORME Fm.	CAP DES ROSIERS Fm and the "MAYANE BEDS"	CAP CHAT MELANGE	LADRIERE Fm	KAMOURASKA Fm	LEVIS Fm.				
	MIDDLE										ORIGINAL Fm	CAP ENRAGE Fm	ST. DAMASE Fm	ST ROCH Fm.
	LOWER													
CAMBRIAN	UPPER													
	MIDDLE													
	LOWER													



turbidity currents (and secondary bottom currents) in a direction toward the south.

Davies (1972) conducted a detailed study of the conglomeratic Niveau 3 at Anse à Pierre Jean, between Trois Pistoles and St. Simon (Figs 10,11). Initial studies by Davies indicated a paleoflow direction toward the west (determined from the conglomeratic fabric). This apparent anomaly with the south and southeast directions obtained by Mathey (1970) and Hubert et al (1970) prompted Davies (1972) to conduct detailed analyses of grain fabric and grain size within the conglomeratic beds to determine possible mechanisms of deposition and paleoflow directions. In Davies' model (Davies and Walker, 1974) conglomerates were interpreted as being deposited from dispersions, from suspensions and from tractional currents. Sediments were thought to be part of a submarine fan complex where paleoflow was mainly to the west-southwest (Fig. 12).

Johnson (1974) extended Davies' (1972) studies of conglomeratic horizons to other areas along the coastline (from Anse à Pierre Jean eastward to Cap Corbeau, northeast of Bic) to provide a basis for paleoenvironmental interpretation of the conglomerates. Detailed fabric and stratigraphic studies showed that the conglomerates were most likely deposited within a meandering submarine channel system, which at some localities and/or stratigraphic levels flowed toward the south (at Bic) or mainly toward the westerly directions (at other locations) (Fig. 12).

Lajoie et al (1974) studied the petrography of the sandstones in the Orignal, Cap Enragé and Ladrière Formations. This was done to determine the position, composition and relative relief of the source area.

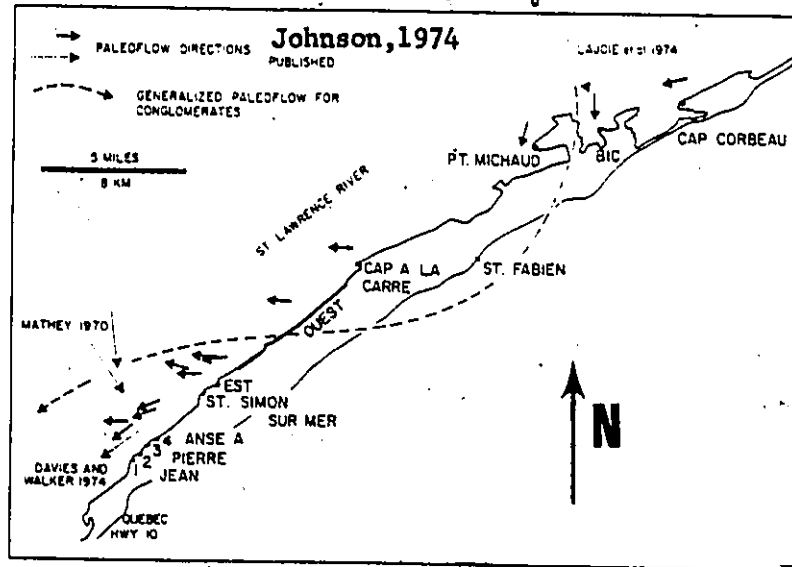


Fig. 12 - Location map with paleoflow directions in the Cap Eourage Formation (from Johnson, 1974).

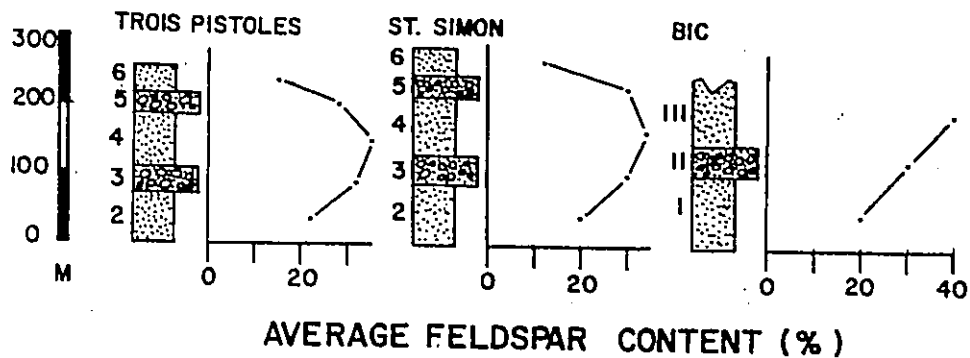


Fig.13- The Trois Pistoles, St. Simon, and Bic stratigraphic sections with stratigraphic nomenclature and variation in the mean feldspar content (redrawn from Mathey, 1970 and Lajoie et al., 1974)

Arabic numbers refer to the "niveau" stratigraphic subdivisions of Mathey (1970). Roman numerals refer to the "member" stratigraphic subdivisions of Lajoie (in press).

Detailed sections including the Cap Enragé Formation were studied at Trois Pistoles and Bic. To determine the location of the source area relative to the site of deposition, paleocurrent measurements were obtained which indicated an average paleoflow toward the southwest. Cap Enragé sediments were thought to be deposited in a submarine fan complex from sediment gravity flows which travelled mainly toward the south. (Fig. 12).

Chevalier (1976) studied the diagenesis of the sandstones of the Cap Enragé Formation near St. Fabien sur Mer, particularly in the Cap à la Carre Ouest outcrop. Diagenetic aspects are not considered in the present study. Chevalier found, in general, that a large part of the original matrix of the arkosic wackes and arenites were replaced by dolomite formed at the beginning of diagenesis. Later, iron-rich calcite replaced the dolomite as well as the rest of the matrix. Silica cement appeared after the formation of concretions and lenses, occurring after compaction of the sediment. Precipitation of the iron-rich calcite was followed by precipitation of calcite, less rich in iron.

Detailed discussions of the stratigraphy and structure are given by Hubert et al (1970) for the Bic -- St. Fabien area; by Mathey (1970) for the St. Simon and St. Simon sur Mer area; by Davies (1972) for the Anse à Pierre Jean outcrop; and, by Johnson (1974) for the Anse à Pierre Jean -- Cap Corbeau region. The regional structure and stratigraphy is being published by Lajoie (in press). As mentioned previously, Vallières (in prep., pers.comm) is preparing a map and revised stratigraphic nomenclature for the area.

Beds are generally folded into a series of northeast-trending

anticlines and synclines. In the St. Simon sur Mer -- Cap à la Carre outcrops, folds are broad and open with only low plunge angles. Folding is steeper in the Bic area (Hubert et al, 1970), although the plunge was not thought to be significant to affect the reorientation of paleo-current data (Johnson and Walker, in prep.).

The type section of the Cap Enragé Formation is exposed at Bic and has been described by Hubert et al (1970). It has since been divided into three members by Lajoie (in press) (Fig.11), where Member II of Lajoie (in press) includes Members II and III of Hubert et al (1970). In the St. Simon area, Mathey (1970) subdivided the Cap Enragé Formation into several different levels (called 'niveau') as shown in Fig. 11. Niveau 3 and Niveau 5 are conglomeratic; Niveau 2 is mainly sandstone; whilst, Niveau 4 and 6 are predominantly pebbly sandstone. Niveau 1 is the Original Formation. There is only one conglomerate level at the type Bic section, namely Member II (Lajoie, in press). Hubert et al (1970) thought that the conglomerate level at Pt. Michaud was equivalent to Member II at Bic. However, Johnson and Walker (in prep) suggest that (because the outcrops are discontinuous) perhaps the different conglomerate levels do not represent continuous bands; but, rather, that the conglomerates are discontinuous lenses on a regional scale. This idea is supported by Vallières (in prep, pers. comm.), who, as a result of regional mapping, believes that the niveau are lenticular and cannot be traced throughout the whole region.

STUDY AREAS FOR THE PRESENT PROJECT AND DETAILED STRATIGRAPHY

Outcrops were selected for study in this project if there was sufficient vertical exposure (generally greater than 5 m in height) of sandy or pebbly sandstone rocks. A few selected, mainly conglomeratic, sections were measured to discern sandstone associations, within conglomeratic units. Predominantly sandstone and pebbly sandstone sections were logged at Grève de la Pointe (S11), Rivière Trois Pistoles (S10), Anse à Pierre Jean 1 (S9), Anse à Pierre Jean 3, Anse à Pierre Jean 5 (S8), St. Simon sur Mer (S7), St. Simon sur Mer -- Two Cottages (S6), St. Simon sur Mer Est (S5), Anse aux Saumon Est (S4), Cap à la Carre Ouest, and Bic (S1) (Figs. 10, 11). Conglomeratic sections were logged at Anse à Pierre Jean 1 (S9), St. Simon sur Mer (S7), St. Simon sur Mer -- Two Cottages (S6), top part of Niveau 3 at St. Simon sur Mer Est (S5), Anse aux Saumon Est (S4), Cap à la Carre Ouest (S3), and Member II at Bic (Figs. 10, 11).

Outcrops in the Anse à Pierre Jean - St. Simon sur Mer area have been named and numbered following the designations of Davies (1972) and Johnson (1974). The exceptions to this are the St. Simon sur Mer -- Two Cottages and Anse aux Saumon Est sections. The St. Simon sur Mer -- Two Cottages section occurs between St. Simon sur Mer (to the west) and St. Simon sur Mer Est (to the east) (according to Johnson's terminology). The name 'Anse aux Saumon' is the local designation by the cottagers, in this area, for the bay east of the St. Simon sur Mer Est outcrop (Fig. 10). The outcrop called 'Anse aux Saumon Est' starts at the eastern side of the bay and extends eastward for about 4 km along the coast, towards Cap à la Carre Ouest.

The area between Rivière Trois Pistoles and L'Isle Verte (Fig. 10), has not yet been mapped and studied in detail. Detailed sections were measured at Rivière Trois Pistoles and Grève de la Pointe (Fig.10). The Rivière Trois Pistoles section is an inland exposure, along highway 10, across the road and east of a microwave telecommunications tower. The name 'Grève de la Pointe' is the local designation by cottagers for the outcrop between St. Eloi station (to the west) and Rivière Trois Pistoles (to the east). Vallières (1978: pers. comm.) refers to this outcrop as 'Pointe à la Loupe' -- the name which appears on the federal topographic map (Trois Pistoles 22 C/3 (edition 2) scale: 1:50,000). This name designates the southwestern part of the coastal exposure (Fig.10). In the present study, a section was not measured at the southwestern tip, consequently, the local name is thought to be a more adequate designation.

Detailed stratigraphy is established for rocks in the Cap Enragé Formation in the St. Simon sur Mer - Anse à Pierre Jean area (Mathey,1970; Davies,1972; Johnson,1974), in the St. Simon sur Mer Est region (Mathey,1970; Johnson,1974), and at the Bic - Pt. Michaud exposures (Lajoie,in press; Hubert et al,1970). Outcrops measured in the present study where stratigraphy has not been firmly established include: Cap à la Carre Ouest, Anse aux Saumon Est, Rivière Trois Pistoles and Grève de la Pointe.

Lajoie (in press) designated the conglomerate at Cap à la Carre as belonging to Member II, with the predominantly sandstones and pebbly sandstones of Cap à la Carre Ouest belonging to Member III. Johnson (1974) states that the conglomerate at Cap à la Carre Ouest is equiva-

lent to the conglomeratic Niveau 5 at St. Simon sur Mer Est (Johnson, 1974, p.96).

In the present study, contacts were traced in the field from St. Simon sur Mer Est east to Anse aux Saumon Est. These field correlations show that at Anse aux Saumon Est, Niveau 2 sediments are followed by thin Niveau 3 conglomerate. The Niveau 3 conglomerate is overlain by pebbly sandstone, which is capped by a thin, upper conglomerate horizon. Comparisons of detailed stratigraphic sections between Anse aux Saumon Est and Cap à la Carre Ouest, Section 6, show that the same sequence occurs at the western end of the Cap à la Carre Ouest outcrop. The only difference is that the Niveau 2 sediments are not exposed at Cap à la Carre Ouest, Section 6 (Fig. 11). General comparisons of the logged sections at Anse aux Saumon Est - Cap à la Carre Ouest, Section 6, suggest that the pebbly sandstones (overlying the Niveau 3 conglomerates) are equivalent to the top Niveau 3/ basal Niveau 4 at St. Simon sur Mer Est (to the west). Faulting of the Cap à la Carre Ouest outcrop prohibits determination of the stratigraphy for Sections 1-5, Cap a la Carre Ouest.

In the field, the rocks at Grève de la Pointe bear a close resemblance to the rest of the sediments within the Cap Enragé Formation. At the northeastern part of the outcrop, fine-grained siltstones, sandstones and shales outcrop. These sandstones, siltstones and shales are cut by feldspathic sandstones and fine conglomerates. The contact is a scoured margin, which forms an overhanging wall. The section at Grève de la Pointe consists of about 150 m of sediments, including sandstones, pebbly sandstones and conglomerates in association with classical turbidites. Petrologic analyses of sandstones (Appendix 3) in the present

study show that the mean feldspar content of the Grève de la Pointe sediments is about 33%. Comparisons with the results of Mathey's (1970) and Lajoie's et al (1974) studies of petrologic trends in the Cap Enragé Formation (Fig.13) suggest that the Grève de la Pointe sediments fall within the mean feldspar content of either Niveau 2 or Niveau 4 sediments. The maximum feldspar content within the Grève de la Pointe deposits, occurs in beds overlying a thick, chaotic conglomerate. The mean feldspar content of these beds reaches a maximum of 50%. This peak may reflect the one recorded in Niveau 4 sediments at Trois Pistoles by Lajoie et al (1974). If the beds above the thick conglomerate (see logged sections, Appendix 5) do, in fact, represent western equivalents of basal Niveau 4 sediments, then the thick conglomerate is, most likely, the western equivalent of Niveau 3. This would place the Grève de la Pointe section as including Niveau 2 through Niveau 4 deposits, with the fine-grained sandstones and shales at the base of the section representing Niveau 1 -- the Original Formation.

These correlations are confirmed, in a general way, by Vallières (in prep., 1978: pers. comm.). Vallières has not studied this outcrop in great detail and does not distinguish the fine stratigraphy within the Cap Enragé Formation. However, Vallières (in prep., 1978: pers. comm.) thinks that the outcrop of sandstone and conglomerate belongs to the Cap Enragé Formation, with the thin-layered grey pelitic and sandy sediment at the basal northeastern part of the outcrop, belonging to the Original Formation.

ORGANIZATION AND BASIC RESULTS OF THE THESIS

It is very difficult to describe and interpret the Cap Enrage sediments as belonging to a single sediment type. In order to simplify the description, beds are classified as belonging to specific sedimentary facies. The basis to the definition of the facies lie in the field descriptions of the individual beds -- lithology, sedimentary structures and sequences, and types of grading. As no new structures are defined, nor new interpretations given of features, all of the field descriptions are given as a catalogue (Appendix 4). Definitions of facies given in the thesis text are generally easily understood, with occasional reference needed to the catalogue of sedimentary features (Appendix 4).

The general organization of the thesis is as follows. Facies definitions are given in Chapter 2. Vertical and lateral facies relations are presented in Chapter 3. Grain fabric patterns and grain size distributions are presented in Chapter 4. Possible depositional mechanisms for the different facies are discussed in Chapter 5. An overall facies model and comparisons with other deep-sea systems are given in the final Chapter 6. The basic results of the thesis are given below as a preview.

The Cap Enrage Formation consists of sediments which can be grouped into the following facies: 1) coarse-grained conglomerate; 2) graded-stratified/cross-stratified fine conglomerate and pebbly sandstone; 3) graded-dispersed fine conglomerate and pebbly sandstone; 4) graded-liquefied fine conglomerate, pebbly sandstone and sandstone; 5) ungraded, crossbedded fine conglomerate, pebbly sandstone and sand-

stone; 6) structureless pebbly sandstone and sandstone; and, 7) classical turbidites (mainly sandstone).

Local sedimentary facies models for different outcrops fit what is called a 'scour-and-terrace' morphology. Coarser facies were deposited in topographically lower scours; and, finer facies were deposited on topographically higher, laterally-equivalent, depositional terraces. Small-scale (up to 5 m) fining-up or coarsening-up sequences are interpreted to reflect migration of scours away from a site (producing fining-up sequences) or migration of scours toward a site (producing coarsening-up sequences). Gradual fining-up or coarsening-up sequences represent migration of scours through meandering processes. Abrupt fining-up or coarsening-up sequences reflect migration by avulsion. Large-scale (10's-100m) fining-up and coarsening-up sequences are thought to represent migrations of large thalweg channels.

Regional grain size, bed thickness, facies and paleocurrent patterns are accountable in terms of large-scale scour-and-terrace morphological models. Sediments of the Cap Enragé Formation are interpreted as being deposited on at least three major topographic features:

1) major thalweg scours; 2) major depositional terraces within the thalweg channels; and, 3) major depositional terraces, which are much higher than the thalweg systems.

Facies (1) very coarse and coarse conglomerates are from major thalweg scours. Facies (2), (3) and (4) fine conglomerates and pebbly sandstones were deposited on major depositional terraces within the thalweg channels, or on high depositional terraces which are marginal to thalweg channel systems. Facies (6), (7) and shale beds are interpreted

as being deposited on high depositional terraces, generally far away from the thalweg systems. Facies (5) is not very common, although when it does occur it is widespread, associated with most of the other facies.

Overall depositional models and paleocurrent patterns suggest that the Cap Enragé sediments were deposited within a continental base-of-slope valley. Thalweg channels within the submarine valley may have formed a braided pattern. Outcrop restrictions prohibit one to determine whether the submarine valley fill represents: 1) deposits from an upper fan leveed valley, of the submarine fan model; or, 2) an isolated submarine valley, which has no association with a submarine fan.

Important Notes

The term "graded-liquefied" is used in the descriptive sense in this thesis. It implies that a bed shows normal grading and fluid escape features. As such no genetic implications are to be inferred.

Throughout this thesis the terms "member" and "niveau" will refer solely to the stratigraphic levels, as defined by Laiole (in press) and Mathey (1970). Any English translations of "niveau" -- i.e. "level, horizon" -- should be read in context of the thesis text, and not confused with the stratigraphic connotation (as used in this thesis) of "niveau."

A key to notation and abbreviations used in the thesis is given in Appendix 1.

CHAPTER 2

DEFINITION OF FACIES

SEDIMENTARY FACIES

As mentioned in the introduction, it is difficult to describe the Cap Enragé sediments as belonging to a single sediment type. Hence beds were classified as belonging to different sedimentary facies. The term 'facies' is defined as the "general appearance or nature of one part of a rock body as contrasted with other parts" (American Geological Institute, 1957). As applied to sedimentary rocks, the term 'facies' refers to a unit of rock that can be distinguished, in the field, from adjacent units of rock, in terms of lithologic characteristics, sedimentary and biogenic structures (de Raaf et al, 1965).

No biogenic structures were observed within beds of the Cap Enragé Formation. Thus, only lithologic characteristics and sedimentary structures contribute to the definition of facies. Each bed was catalogued according to 1) structures (or lack of structures); 2) grain size characteristics; and, 3) types of grading. Beds with similar structures, sequences of sedimentary structures and types of grading were classified as belonging to a given facies. Less importance was assigned to grain size criterion. Fabric patterns and imbrication types were not used in the definition of facies.

All of the field data, providing the basis for the definition of facies, are given in the appendices: 1) methods for section measuring and description (Appendix 2); 2) catalogue and description of sedimentary

features (Appendix 4); and, 3) logged field sections and location maps (Appendix 5).

In this chapter a basic description is given of each facies. Summary diagrams of the main sedimentary sequences are presented for each facies. Typical photographs of beds belonging to the various facies are cited. Many of these photographs are in the catalogue of sedimentary features (Appendix 4). To avoid repetition, where appropriate, references will be made to the photographs in Appendix 4.

Detailed work in the present study has led to the definition of 8 facies. Facies (1) through (6) comprise the coarser sediments of the Cap Enragé Formation, including very coarse conglomerate to medium sandstone. Facies (7) consists of finer-grained, mainly sandstone and siltstone classical turbidites. The final facies consists of rare shale beds.

BASIC DESCRIPTION OF FACIES

Facies (1) - Coarse Conglomerate (Figs.14,15,84,86,88,89,105)

The clast-supported coarse and very coarse conglomerates of the Cap Enragé Formation have been studied by Davies (1972) and Johnson (1974). Based upon their detailed work, these authors have recognized five types within the coarse conglomerates (Davies and Walker, 1974; Johnson and Walker, in prep.). These conglomerate types are mainly subdivided by clast size and include: cobble-boulder; cobble; coarse pebble and fine pebble conglomerate; and, granule sandstones. In the present study, the cobble-boulder, cobble and coarse pebble conglomerate types of these workers are grouped into a single facies, which is called the "coarse

SIP • II

FACIES 2

FACIES 1



Fig.14 - Large solitary scour fill of conglomerate- fine conglomerate
below Ms. McRae. Bed 1115, Cap a la Carre Ouest. Stratigraphic
top is up, p.411

FACIES I — COARSE CONGLOMERATE

N = 160

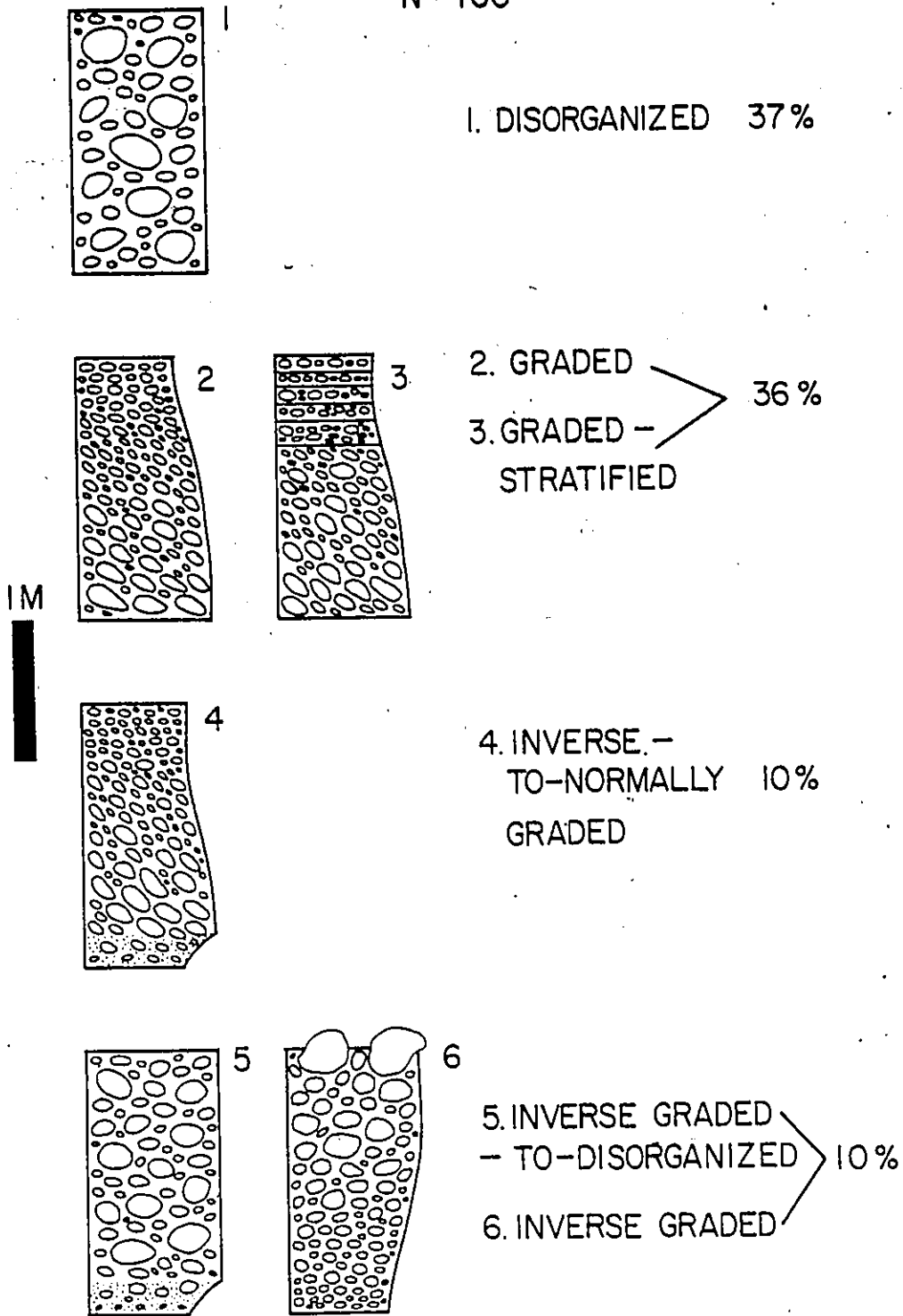


Fig.15 - Sketch of different Facies I types (and relative frequencies of occurrence).

conglomerate facies." A detailed description of the types of beds in this facies is given by Johnson and Walker (in prep.).

The coarse conglomerates have a variety of grading, stratification and fabric patterns which fit the models for resedimented conglomerates proposed by Walker (1975) (Fig.4). Walker's (1976) classification scheme was used to describe the coarse conglomerates (Fig.15). In addition to these four models proposed by Walker, two other types are recognized in the present study. These types are summarized in Fig.15 and include: 1. disorganized, 2. graded, 3. graded-stratified, 4. inverse-to-normally graded, 5. inverse graded-to-disorganized, and 6. inverse graded types (Fig.15).

In the present study, emphasis was placed upon finer sediments within the Cap Enragé Formation. Sections were measured in the finer-grained outcrops. Consequently, the coarser conglomerates, as logged in the finer sections, tend to be finer and thinner bedded than those described by Davies (1972) and Johnson (1974) from the predominantly conglomeratic sections. The cutoff between coarse conglomerate facies and the finer facies is a-axis of the 10 largest grains \geq 16 mm (Appendix 2).

Beds belonging to the coarse conglomerate facies account for 12% of the beds measured within the finer outcrops in the present study. Most of the coarse conglomerate beds had flat bases, less commonly scoured, and rarely loaded (Table 2). The maximum thickness reported by Johnson and Walker (in prep.) for beds of this facies was 7 m. In the present project, the average bed thickness was 1.9 m . Minimum thickness was 0.25

TABLE 2

GRADING TYPES IN DIFFERENT FACIES (IN %)

<u>Facies</u>	<u>N Beds</u>	<u>Ungraded</u>	<u>Normal</u>	<u>Abrupt</u> <u>Normal</u>	<u>Reverse</u>	<u>Reverse</u> <u>- Normal</u>	<u>Complex</u>
1	160	37	36	5	10	10	1
2	300	23	52	19	1	3	1
3	265	21	54	16	1	6	2
4	166	23	55	15	1	2	3
5	53	100	--	--	-	-	-
6	200	26	30	43	1	2	-
7	166	20	76	3	-	1	1

TYPES OF BASES IN DIFFERENT FACIES (IN %)

<u>Facies</u>	<u>N Beds</u>	<u>Flat</u>	<u>Scour</u>	<u>Load</u>	<u>Load &</u> <u>Scour</u>	<u>Irregular</u>	<u>Covered</u>
1	160	45	34	10	6	2	4
2	300	43	39	11	6	1	-
3	265	61	21	14	2	3	-
4	166	58	24	12	4	1	1
5	53	64	30	--	6	-	-
6	200	65	26	6	1	2	1
7	166	77	17	6	-	-	-

Irregular Base: Underlying bed has clast sticking out above the general bed level, making the base of the bed irregular

N Beds: number of beds

Reverse-Normal: Reverse-to-Normally graded beds

m. Beds in the present study were more commonly ungraded, disorganized or graded, graded-stratified (Fig. 15) (Table 2). Beds with reverse grading occurred less commonly. Complex and abrupt normally graded beds were rarely encountered (Table 2).

Disorganized beds are ungraded, unstratified and rarely show imbrication. Inverse-to-normally graded beds have a finer grained base which becomes coarser grained upsection. Overlying bed portions are normally graded, becoming finer-grained upsection. These beds are not stratified and show imbrication. Inverse graded beds become coarser grained from the base to the top and are unstratified with imbrication. Inverse-to-disorganized beds are gradational between the inverse graded and disorganized types (Fig. 15). Graded beds show normal grading -- they become finer grained from the base to the top of the bed, are not stratified and show imbrication. Graded-stratified beds are normally graded, become stratified (or cross-stratified) in finer upper bed portions and show imbrication (Fig. 15).

Facies (2) - Graded-Stratified/ Cross-stratified Fine Conglomerate and Pebbly Sandstone (Figs.14,16,108,112)

Beds of this facies are the most common beds within the finer portions of the Cap Enragé sediments. Twenty-three percent of the beds measured within the present study belong to this facies. Most of the beds had flat (43 %) or scoured (39%) bases; loaded bases were less common (11%) (Table 2). The average bed thickness was 1 m (range: 0.15 m to 5.5 m). Most of the beds belonging to this facies consisted mainly of fine conglomerate (a-axis: >4-16 mm), pebbly sandstone (grain diameter: >2-4 mm) and very coarse sandstone (grain diameter: >1-2mm). Over half of

FACIES 2-GRADED-STRATIFIED/CROSS-STRATIFIED
 FINE CONGLOMERATE & PEBBLY SANDSTONE N = 300

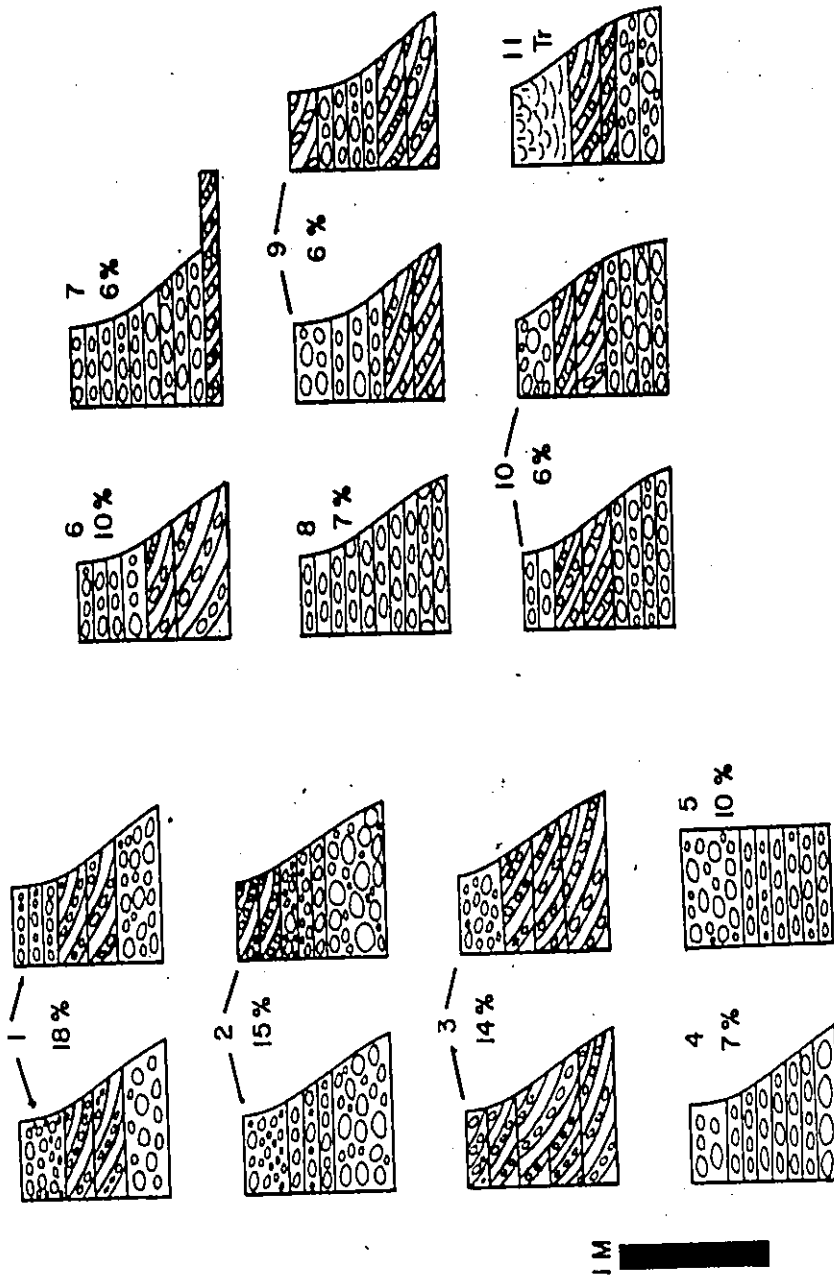


Fig. 16 - Sketch and relative frequency of different Facies 2 types.

the beds belonging to this facies were normally graded (52%) or abruptly normally graded (19%) (Table 2). Most of the beds were stratified or cross-stratified. Cross-stratification generally consists of medium scale trough cross-stratification (see Figs. 107-109). Parallel stratification is marked by alternating clast-supported and dispersed layers (Fig.104) or consists of alternating layers of different grain sizes, commonly marked by concentrated quartz pebble layers (Fig105). Beds less commonly have structureless basal portions. This latter case may represent beds that are transitional between the coarse conglomerate Facies (1) and the fine conglomerate - pebbly sandstone Facies (2).

Certain sequences occur within the Facies (2) beds. The most common sequences are: Graded/Stratified; Graded/Massive-to-Stratified or Graded/Dispersed-to-Stratified; Graded/Trough Crossbedded or Graded/Trough Crossbedded-to-Stratified; and, Graded beds with low angle cross-bedding. Average bed thicknesses for these different Facies (2) types are listed in Table 3. All of the mean thicknesses (of a random sample of 20 beds of each type) fall within two standard deviations of each other, suggesting that there is no significant difference in bed thickness amongst these Facies (2) types. These types are somewhat gradational to one another, with the more common ones illustrated in Fig.16 .

Facies (3) - Graded-Dispersed Fine Conglomerate and Pebbly Sandstone (Figs.17,18,19)

This facies is the second-most common facies within the finer grained beds of the Cap Enragé Formation. Twenty percent of the beds measured within this project belong to Facies 3. This facies is characterized by beds which display a "dispersed texture," in which

TABLE 3

BED THICKNESS FOR DIFFERENT FACIES

<u>Facies and Facies Type</u>	<u>Avg. Bed Thick. \bar{X}</u>	<u>S</u>	<u>($\bar{X} \pm 2S$)</u>	<u>N</u>
Facies 2:				
with oblique crossbedding	1.19	0.72	0-2.64	20
trough crossbedding or trough cross- bedding-to-stratified	1.38	1.14	0-3.65	20
dispersed or massive-to-stratified	1.11	0.65	0-2.40	20
stratified	1.10	0.74	0-2.58	20
Facies 3:				
dispersed or dispersed/stratified	0.68	0.55	0-1.78	35
massive-to-dispersed	0.92	0.41	0.1-1.74	20
dispersed-to-massive	1.32	0.89	0-3.1	20
dispersed-to-liquefied	1.30	0.55	0.2-2.4	20
dispersed-to-stratified	1.51	1.30	0-4.11	20
dispersed-to-crossbedded	1.18	0.57	0.04-2.32	17
Facies 4:				
mainly dish structures	1.59	1.27	0-4.12	20
mainly Type B pillars	1.32	1.00	0-3.32	20
dish-to-Type B pillars	2.55	2.40	0-7.35	20
Type B pillars-to-dish structures	2.13	1.53	0-5.18	16
Facies 6:				
massive and ungraded	0.92	0.68	0.24-1.6	20
massive and abrupt normally graded	0.73	0.64	0-2.0	20
massive and normally graded	1.20	0.81	0-2.82	20
dispersed-to-massive	1.25	1.01	0-3.28	20
massive-to-dish structure	2.14	2.46	0-7.06	20
massive-to-vague stratified	1.82	0.86	0.1-3.54	9
massive-to-stratified	3.23	3.19	0-9.61	16
massive-to-crossbedded	1.79	1.89	0-5.57	14
crossbedded-to-massive	1.36	0.83	0-3.02	13

S: standard deviation of bed thickness distribution

$\bar{X} \pm 2S$: confidence interval calculated two standard deviations either side of the mean bed thickness

N: number of measurements from a randomly drawn sample of each facies



Fig.17 - Dispersed pebbly sandstone. Book at left is 19 cm long. Bed 1402, Bic. Top of bed is up, p.422

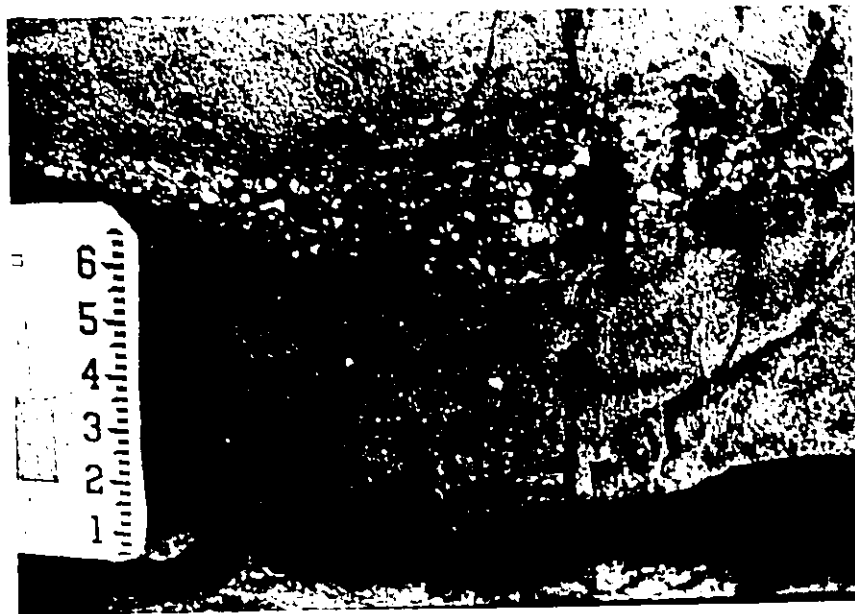
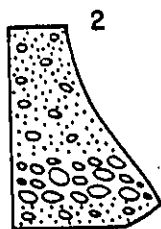
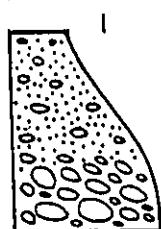


Fig.18 - Small scour at base of bed filled with clast supported fine conglomerate, above which fine pebbles are dispersed within finer sandstone. Bed 1421, Bic, p.422

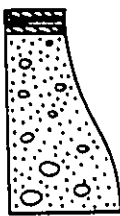
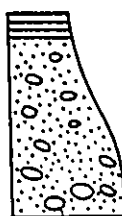
FACIES 3 - GRADED-DISPERSED FINE CONGLOMERATE
& PEBBLY SANDSTONE FACIES N=265

45



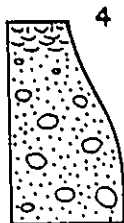
1. MASSIVE - TO - DISPERSED
2. INVERSE - TO - NORMALLY
GRADED, DISPERSED - TO -
MASSIVE - TO - DISPERSED

24 %



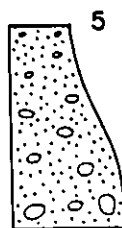
3. DISPERSED - TO -
STRATIFIED OR X. STRAT.

28 %

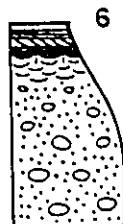


4. DISPERSED - TO - FLUID ESCAPE FEATURES

20 %



5. DISPERSED 17 %



6. DISPERSED - TO - FLUID ESCAPE FEATURES -
TO - STRATIFIED OR X. STRAT.

12 %

Fig.19 - Sketch and relative frequencies of different Facies 3 types.

coarser granules and pebbles do not touch one another, but rather are scattered throughout a finer grained sandy bed (Figs. 17 18).

Most of the beds had flat bases (61%), with less commonly scoured (21%) or loaded (14%) bases (Table 2). The average bed thickness was 1.3 m (range: 0.2 m to 11.6 m). Over half of the beds belonging to this facies were normally graded (54%) or abruptly normally graded (16%). Ungraded beds were less common (21%) (Table 2). Beds of this facies commonly had dispersed clasts in the fine conglomerate (a-axis: >4-16 mm) and pebbly sandstone (a-axis: > 2-4 mm) grain size classes. Dispersed coarse conglomerate (a-axis: > 16 mm) clasts were rare. The main portion of the beds are generally fine to medium sandstone (grain diameter: 0.13 mm to 0.5 mm); less commonly coarse to very coarse sandstone (grain diameter: > 0.5 mm to 1 mm) makes up the bulk of the bed.

Although the Facies 3 beds are characterized by dispersed texture throughout most of the bed, many of the beds have smaller portions characterized by other sedimentary features and textures (Fig. 19).

In coarser grained Facies 3 beds, structureless clast-supported portions occur near the base of beds (Cases 1 and 2, Fig. 19). Grading in these beds is either normally graded, or inverse-to-normally graded. In the latter grading pattern, the finer-grained base shows a dispersed texture, which is overlain by a coarser clast-supported unit. Beds with structureless, clast-supported basal divisions may represent beds that are transitional between Facies (1) and Facies (3). Finer grained Facies 3 beds may be wholly dispersed (17%), or have fine grained upper bed portions characterized by fluid escape features (dish structures and/or fluid escape tubes), stratification or cross-stratification (Fig. 19).

The main types of sequences within the Facies 3 beds are: dispersed; structureless-to-dispersed; dispersed-to-structureless-to-dispersed; dispersed-to-stratified and/or crossbedded; dispersed-to-fluid escape features; and dispersed-to-fluid escape features-to-stratified and/or cross-stratified (Fig. 19) As given in Table 3, there is no statistically significant difference in the bed thickness amongst beds with these different sequences.

Facies (4) - Graded-Liquefied Fine Conglomerate, Pebbly Sandstone and Sandstone (Figs. 20-22, 79, 90-103)

This facies is one of the less common facies within the Cap Enragé Formation, with only 13% of the beds measured in the present study being classed as Facies (4). Most of the beds had flat bases (58%). Scoured (24%) and loaded (12%) bases were less common. Average bed thickness was 1.6 m (range: 0.25 m to 16 m). Over half of the beds belonging to this facies had normal grading: 55% were normally graded; 15% were abruptly normally graded-to-normally graded. Ungraded beds were less common (23%) (Table 2). The term "liquefied" refers to flows in which the sediment support was partially due to the upward escape of pore fluid. "Liquefied" facies refer to those beds which show well-developed fluid escape features, suggesting that there was important influence of pore fluid expulsion on the sediment. Grain size ranges of Facies (4) beds are from 0.5 mm to 50 mm at the bases of beds, to 0.1 mm to 6 mm at the top of beds.

As with the other pebbly sandstone and sandstone facies, although the Facies (4) beds are characterized by fluid escape features in major bed portions, other, smaller units of beds may be structureless, disper-

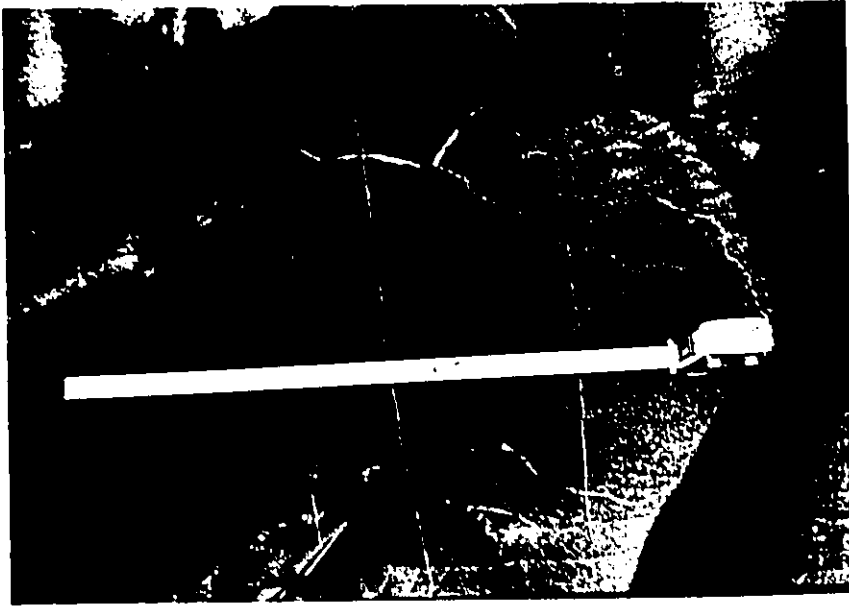


Fig.20 - Dish structures with Type A pillars (arrowed). Bed 911, St. Simon sur Mer Est. Tape is 50 cm long.- Stratigraphic top is up, p.404

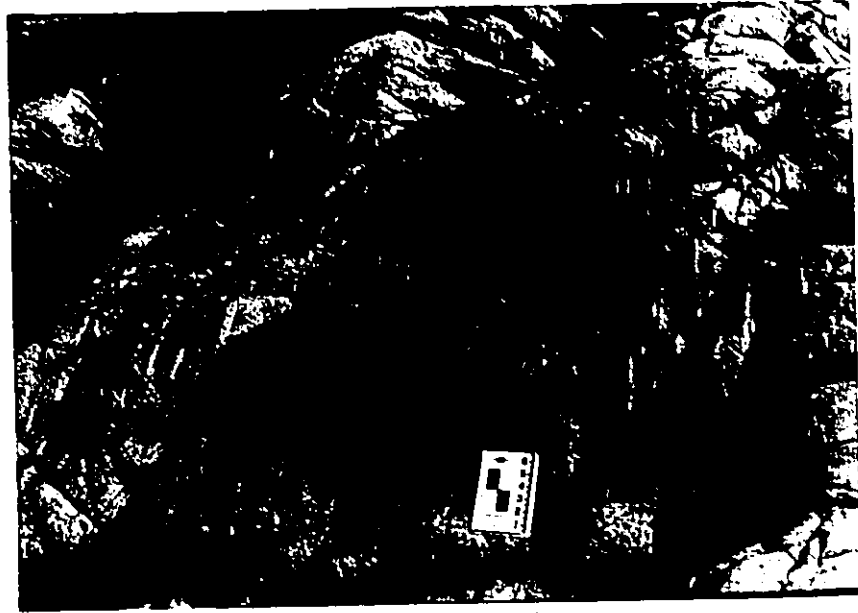
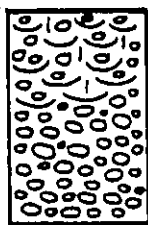
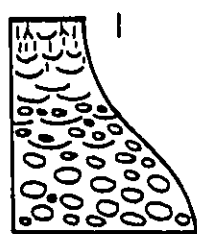


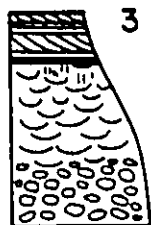
Fig.21 - Large, straight Type B pillars in cross-section. Bed 879, St. Simon sur Mer Est. Top of bed is up, p.403

FACIES 4 - GRADED-LIQUEFIED FINE CONGLOMERATE, PEBBLY SANDSTONE & SANDSTONE N=166



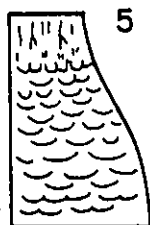
2 MASSIVE-TO-FLUID ESCAPE FEATURES

- 1. GRADED 35 %
- 2. UNGRADED 7 %



FLUID ESCAPE FEATURES - TO-STRATIFIED OR X.STRAT.

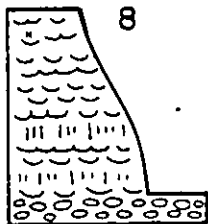
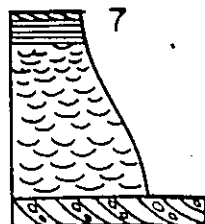
- 3. MASSIVE BASE 13 %
- 4. LIQUEFIED BASE 12 %



FLUID ESCAPE FEATURES

- 5. LIQUEFIED TOP 11 %
- 6. MASSIVE TOP 6 %

ABRUPTLY NORMALLY GRADED-TO-GRADED



7. X.STRAT.-TO-FLUID ESCAPE FEATURES -- TO-STRATIFIED OR X.STRAT. 9 %

8. MASSIVE-TO-FLUID ESCAPE FEATURES 7 %

Fig.22 - Sketch and relative frequencies of different Facies 4 types.

sed, stratified or crossbedded. In addition, in some beds, certain types of fluid escape features occur in different bed positions. The main kinds of Facies (4) sequences are: dish structures throughout the whole bed; Type B fluid escape tubes throughout the whole bed; Dish-to-fluid escape tubes; Fluid escape tubes-to-dish structures (Table 3). There is no statistically significant difference in bed thickness amongst beds with these different types of fluid escape feature sequences (Table 3). For the Facies (4) beds with mainly dish structures or dish structures-to-type B pillars, the sediment at the top of the beds is generally in the range of 0.15 mm to 0.5 mm, which fall within the optimum grain size range as stated by Lowe (1975) for dish structure formation. In the Facies (4) beds with mainly fluid escape tubes or tube-to-dish structure sequences, the sediment at the tops of beds range from about 0.15 mm to 5 mm. This is a coarser grained and wider range than those Facies (4) beds with mainly dish structures.

In beds with other structures, in addition to fluid escape features, the following sequences occur (Fig. 22): structureless-to-fluid escape features; fluid escape features - to- stratified and/or crossbedded; fluid escape features - to- structureless; crossbedded-to-fluid escape features-to stratified and/or crossbedded. Structureless-to-fluid escape feature sequences occur in beds which are fine conglomerate at the base. Beds are usually graded (35%); less commonly beds are ungraded (7%) or abruptly normally graded-to-graded (7%) (Fig. 22). Fluid escape features are found in finer grained upper bed portions in graded beds, or in upper bed portions of ungraded beds. Over 30% of the beds had stratified or crossbedded tops; all had normal grading, with the cross-stratification and

stratification occurring in the finer-grained tops of beds. Commonly, these stratification features truncated dish structures or fluid escape tubes. Some fluid escape tubes were bent or sheared in the direction of the paleoflow for overlying crossbedded units. Beds with crossbedded bases were abruptly normally graded-to-graded (Fig.22). Beds with fluid escape features-to-structureless sequences commonly had "free surface pillar structures (Figs. 97) or pillar structures which are deformed into convolute structures (Figs.98).

Facies (5) - Ungraded Cross-stratified Fine Conglomerate,
Pebbly Sandstone and Sandstone (Figs.23,24,25,107,109)

Facies (5) beds are ungraded and crossbedded throughout. Cross-stratification may be medium-scale trough cross-stratification (see description pages 344-346) (average set thickness = 0.45 m), small-scale cross-stratification (see description pages 346 to 348) (individual troughs on the order of a few cm or less in height in beds which average 0.33 m in thickness), and rare medium scale planar cross-stratification (average set thickness = 0.25 m in thickness). The range of set thickness for medium scale trough crossbedding is 0.3 m to 2 m , with a grain size range of 0.5 mm to 16 mm (average grain size = 6.6 mm). The range of bed thickness for small scale trough crossbedding is 0.1 m to 0.6 m, with a grain size range of 0.15 mm to 0.38 mm (average grain size = 0.27 mm). Beds belonging to this facies are ungraded and consist of cross-stratified sediment. The cross-stratification is medium scale in fine conglomerate and pebbly sandstone (a-axis: > 2-16 mm) and small trough cross stratification in the finer grained sandstones (grain diameter: > 0.125 mm to 2mm). Bases of beds may be scoured (30%), load-



Fig. 23 - Medium scale trough crossbedding in cross-section. Bed 1268, Cap à la Carre Ouest. Clipboard is 35 cm long. Paleoflow is to the right and into the page. Three sets of crossbedding occur, with reactivation structure (arrow) separating the top two sets. Stratigraphic top is up, p. 418

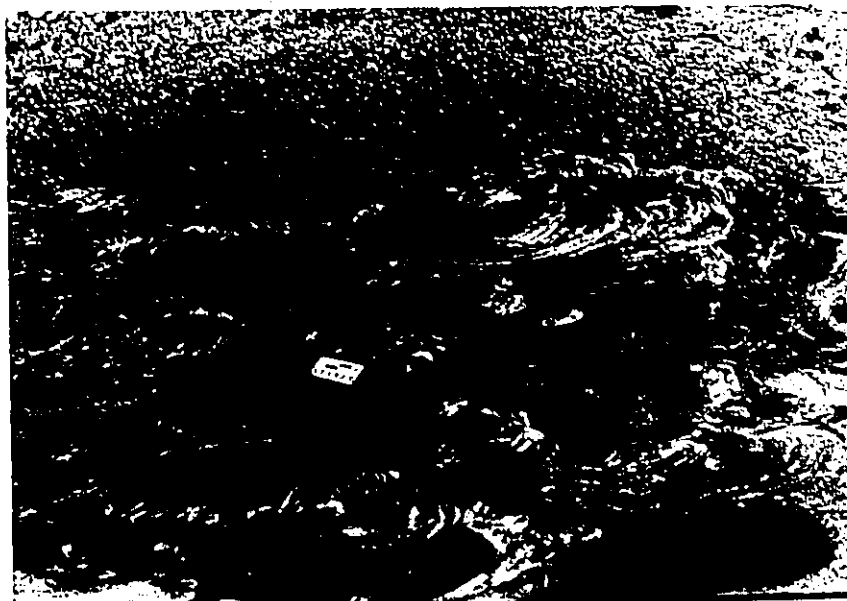


Fig. 24 - Medium scale crossbedding in plan view. Top Bed 1222, Cap à la Carre Ouest. Rectangles on the notebook are 5 cm long. Paleoflow is to the left, p. 417

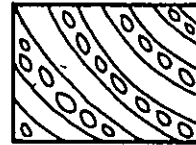
FACIES 5—UNGRADED CROSS-STRATIFIED FACIES

N = 53

1M



1



2



3



4



5

Fig.25 - Sketch of different Facies 5 types.



Fig.26 - Massive structureless sandstone. Top of bed is marked by arrow. Bed 1442, Bic. Stratigraphic top is up, p.422

ed and scoured (6%), or more commonly flat (64%) (Table 2). Cross-bedding is well defined. Cross-stratified sets are more commonly solitary, less commonly multiple. Multiple sets commonly have reactivation surfaces between the sets (Figs.23,25,107). Finer (grain diameter: 0.125 mm to 0.5 mm) sandstones are quite commonly overlain by shale beds.

Facies (6) - Structureless Pebbly Sandstone and Sandstone

(Figs. 26 27)

This facies is the third most common facies within the finer grained beds of the Cap Enragé sediments, with 15% of the beds measured in the present study belonging to this facies. Most of the beds had flat bases (65%), with less commonly scoured bases (26%) or loaded bases (6%) (Table 2). Most of the beds are abruptly normally graded (43%) or normally graded (30%), less commonly ungraded (26%). The average bed thickness was 1.5 m (range: 0.15 m to 13.2 m). The coarser basal zones of abruptly normally graded beds may consist of a relatively thin unit of clast-supported or dispersed fine conglomerate or pebbly sandstone. Overlying finer grained pebbly sandstone or sandstone is ungraded or normally graded (Fig. 27). Sedimentary structures are generally lacking within beds of this facies. Vague stratification or thin, discontinuous zones of fluid escape features may occur scattered within the finer grained, upper bed divisions. The coarser basal zones rarely show cross-stratification. The main impression of these beds is that they are structureless.

Although the Facies (6) beds are predominantly structureless, many of the beds have smaller bed portions characterized by dispersed clast zones, stratified or crossbedded, or fluid escape bed portions.

FACIES 6 - STRUCTURELESS PEBBLY SANDSTONE & SANDSTONE N = 200

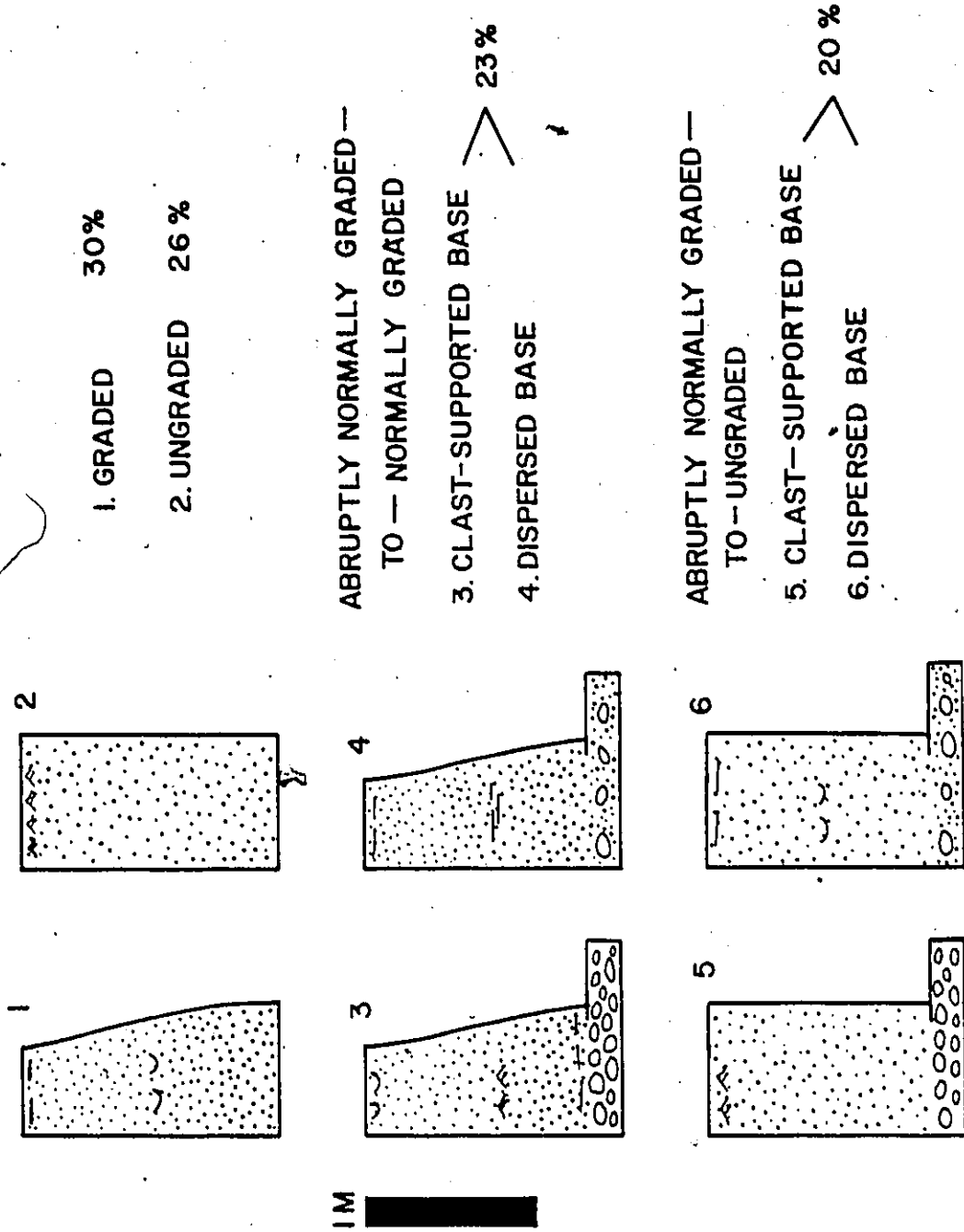


Fig. 27 - Sketch of different Facies 6 types, with relative frequencies. Internal structures, if they occur, are vague or occupy a very small bed portion. Internal structures do not occur in any order nor specific bed portion.

The main types of sequences within the Facies (6) beds are massive ; dispersed-to-massive; massive-to-dish structures; massive-to-stratified; massive-to-crossbedded; and, crossbedded-to-massive. In addition, the Facies (6) beds can be classed as ungraded, abruptly normally graded or normally graded. The average bed thicknesses of the different types are listed in Table 3. As shown in this table there is no statistically significant difference in the average bed thickness amongst the different Facies (6) types.

Stratification and crossbedding, where present, occupies a very small portion of individual beds and is generally ill-defined.

Stratification and crossbedding do not necessarily occur in consistent bed portions in all Facies 6 beds. The most striking feature within the Facies (6) beds is the occurrence of a coarser grained, clast supported or dispersed textured, base (Fig. 27). This feature is noted within 43% of the Facies (6) beds. Abruptly normally graded types (Cases 3 to 6, Fig. 27) had a much coarser grained lower 1/3 to 1/4 of the bed. The coarse clasts in the lower bed portions generally ranged in size from 0.5 mm to 150 mm. Upper portions of abruptly graded Facies (6) beds consisted primarily of material in the fine sandstone to very coarse sandstone classes (0.15 mm to 2 mm). Structureless beds with good overall normal grading (Case 1, Fig. 27.) tend to be somewhat finer grained, on the whole, than the other abruptly graded types. Basal grain size was in the range of 1 mm to 16 mm, whilst the upper bed portions are in the range of 0.25 mm to 4 mm.

Beds are generally abruptly normally graded-to-normally graded or ungraded. Abrupt grading usually occurs within the lower 1/3 of the beds. Basal grain size ranges from about 0.25 mm to 130 mm. In the structureless-to-fluid escape structure types, dish structures generally occur within the top 1/2 to top 1/3 of the beds. The grain size of the liquefied top portions ranges from about 0.15 mm to 3 mm. In some cases, the dish structures were truncated by parallel lamination. In the structureless-to-crossbedded types, cross-stratification is ill-defined and occurs in narrow bands. Where it does occur, it is usually in the top 1/4 of the Facies (6) beds. Sediment coarser than 0.5 mm shows either low angle oblique cross-stratification or trough crossbedding; sediment finer than about 0.5 mm is either ripple-crossbedded or exhibits convolute cross-lamination. Sediment at the top of Facies (6) beds with crossbedding is about the same size as that for the Facies (6) beds with liquefied tops -- in the range of about 0.2 mm to 3 mm grain size. Structureless-to-stratified types have upper bed portions somewhat finer grained than the Facies (6) beds with either crossbedded or liquefied tops. Stratification is ill-defined and occurs in narrow zones at the top of beds, where sediment is in the range of about 0.15 mm to 1.5 mm grain size.

Facies (7) - Classical Turbidites (Figs. 28, 29)

This facies is one of the less common facies within the beds of the present study, with only 13% of the measured beds falling into this category. Most of the beds had flat bases (77%). Scoured bases occur less commonly (17%) (Table 2). The average bed thickness was 0.6 m (range: 0.02 m to 3.7 m). Most of the beds were normally graded (76%).

117 • 11



Fig. 28 - Classical turbidite in pebbly-coarse sandstone showing Bouma A (massive), B (parallel laminated), C (rippled) divisions. Bed 189, Grève de la Pointe. Pen is 15 cm long, p. 376

FACIES 7
CLASSICAL TURBIDITE FACIES

N = 166

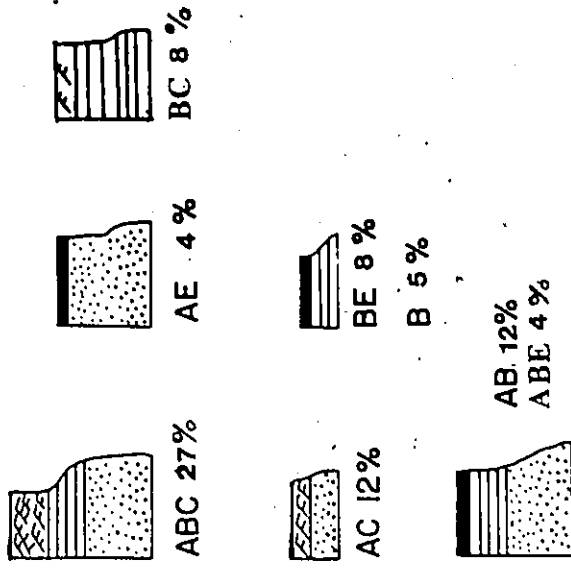


Fig. 29 - Sketch and relative frequencies of different Facies 7 types (greater than 4 percent).

Ungraded beds are less common (20%). Beds of this facies follow the Bouma model for turbidites, showing wholly or, in part, the following divisions (Fig. 29): A - the lower, graded, structureless division; B - the parallel stratified sandstone; C - the small scale trough cross-stratified sandstone; D - faint parallel stratified silt and mud; and, E - upper pelitic shale division. The most common type, of sequence observed within beds of this facies consists of an ABC sequence (32%) (Figs. 28, 29). AE and AC(E) sequences are less common. Other patterns rarely occur. Beds belonging to Facies (7) tend to be finer grained than the other facies and are generally composed of coarse to fine sandstone or silt (grain diameter generally less than 1 mm). Fine pebble conglomerate and pebbly sandstone classical turbidites (a-axis: > 2 mm to 16 mm) occur less commonly.

Shale Facies

Isolated shale beds rarely occur in the Cap Enragé sediments. Only 1% of the beds measured in the present study fall into this class. The average thickness of the shale beds was 0.16 m (range: from thin shale partings, about 1-2 mm thick to shale beds 0.2 m thick). The bases of shale beds are generally flat. Less commonly, shale beds occur as scour fill material.

GRADATION BETWEEN FACIES

Although the eight facies are defined in terms of unique combinations of lithologic criteria and sedimentary structures, the divisions are not as clear-cut in reality. Some beds display features which occur in more than one facies. In these cases, the beds were classed into the facies that characterized the greater proportion of the bed. Some of the

transitional types are: Facies (1)/ Facies (3); Facies (1)/ Facies (2); Facies (6)/ Facies (7) proximal turbidites; Facies (1)/ Facies (4); and, Facies (4)/ Facies (6) (Fig. 30).

Some of the graded-bed conglomerates belonging to Facies (1) have finer, dispersed pebbly sandstone tops. Some of the coarser-grained Facies (3) beds have structureless, graded conglomerate at the base. These occurrences suggest that the Facies (1) graded-bed conglomerates and the Facies (3) fine conglomerates and pebbly sandstones may be transitional to one another. The change from Facies (1) to Facies (3) consists of a decrease in grain size and bed thickness, along with an increase in the proportion of the bed showing dispersed texture.

Some of the graded-stratified conglomerates belonging to Facies (1) have finer-grained tops, in which stratification consists of alternating clast-supported and dispersed layers. Coarser, basal portions of Facies (2) beds also show this type of stratification. In addition, some Facies (2) beds have a relatively thin, coarser-grained structureless conglomerate at the base. These occurrences suggest that graded-stratified Facies (1) conglomerates may be gradational with Facies (2) beds (Fig. 30). The transition from graded-stratified Facies (1) to Facies (2) consists of a decrease in grain size and bed thickness. There is also a loss of the structureless basal division and an increase in the amount of stratification or crossbedding.

Facies (6) structureless sandstones are somewhat gradational with proximal classical turbidites of Facies (7). This transition from Facies (6) to proximal Facies (7) consists of a decrease in bed thickness and

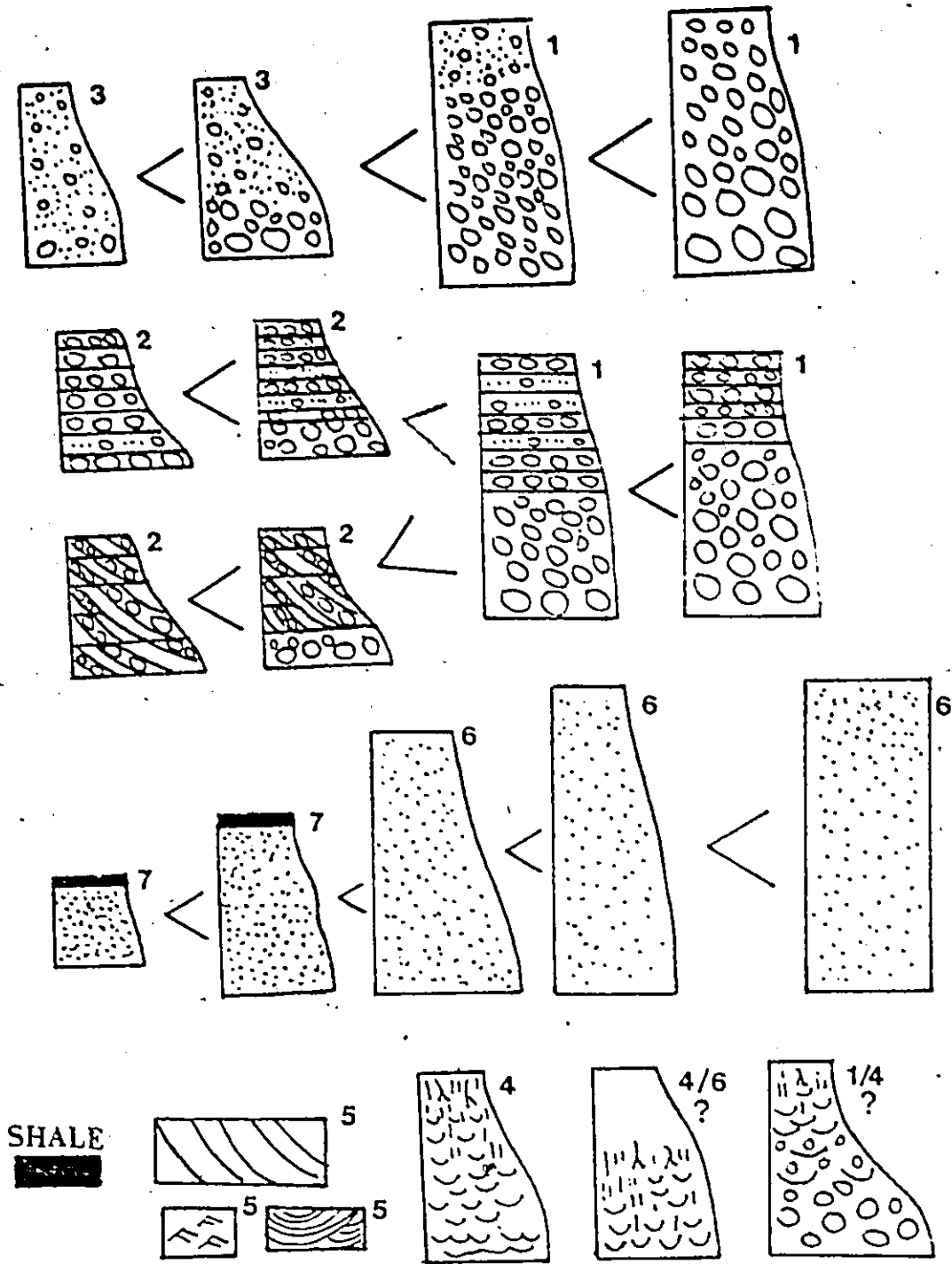


Fig.30 - Gradations Between Facies [<] as interpreted for beds
 Numbers indicate Facies.

slight decrease in grain size. Along with these changes is a better development of grading and an increase of interbedded shales (Fig.30).

Facies (4) graded-liquefied beds with structureless, conglomeratic bases may be gradational with Facies (1) conglomerates. However, Facies (1) conglomerates rarely have liquefied tops. Facies (4) beds with massive tops are not very common (6% of the Facies (4) beds). These beds with massive tops may be gradational between Facies (4) and Facies (6).

Shale beds and ungraded/crossbedded Facies (5) beds are not transitional with any of the other facies.

FACIES ASSOCIATIONS IN MULTIPLE SCOUR FILLS

Small-scale (Between Beds) Facies Associations in Multiple Scour Fills

Vertical and lateral facies relationships are revealed in the field in multiple scour and fill sequences. Two types of multiple scour fills occur: 1) Scour fills that have a single scour margin and have been filled by two or more separate events; or 2) Scour fills that have been multiply cut-and-filled by two or more different events.

Multiple scour fills are relatively rare within the Cap Enragé sections. Ten multiple scour fills were observed and measured in this study. These fills are present within different Members and Niveau and are not restricted to single major sedimentation units. A variety of facies comprise the fill material from the very coarse conglomerates (Facies (1)) to the fine-grained massive sandstones (Facies (6)). Complex facies relationships occur within the multiple scour fills; hence, each multiple scour fill sequence will be described separately.

(1) Scour Fill Predominantly Facies (1)

Three multiple scour fill sequences have the fill composed predominantly of Facies (1) conglomerates: St. Simon sur Mer (Shrine Section) (Niveau 4), Rivière Trois Pistoles (Niveau 2); and, Grève de la Pointe (Niveau 2).

(a) Rivière Trois Pistoles Section (Fig. 31)

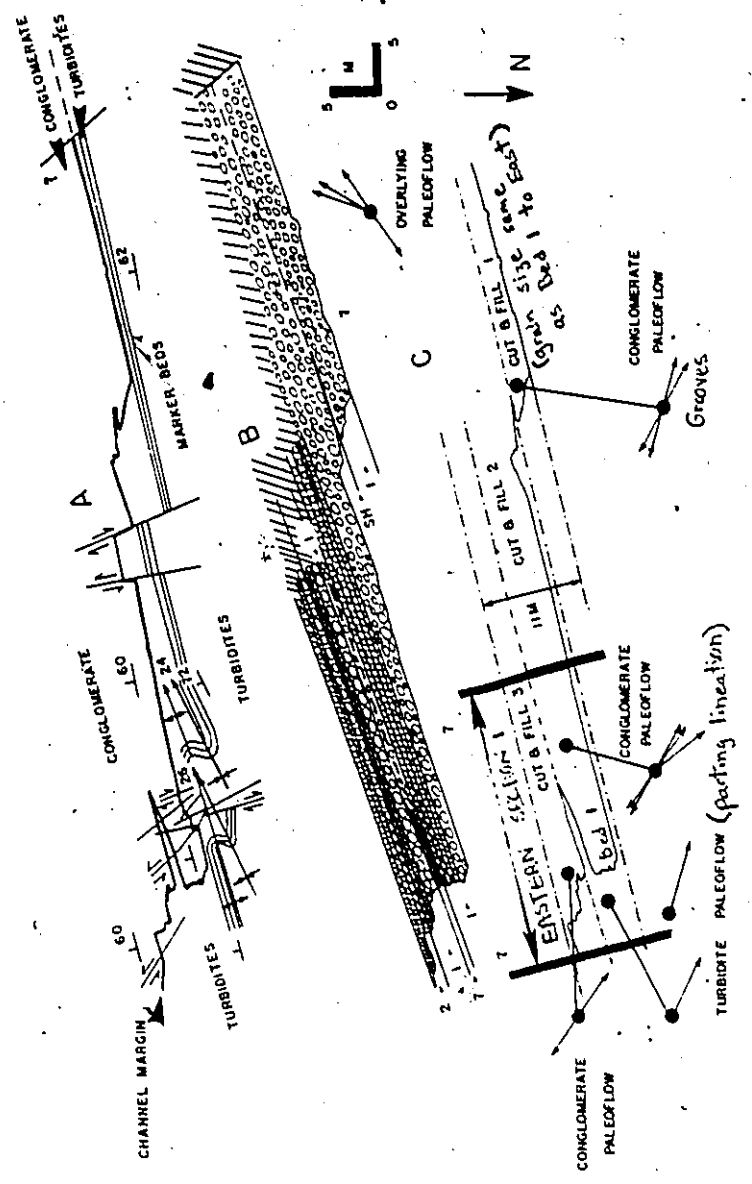
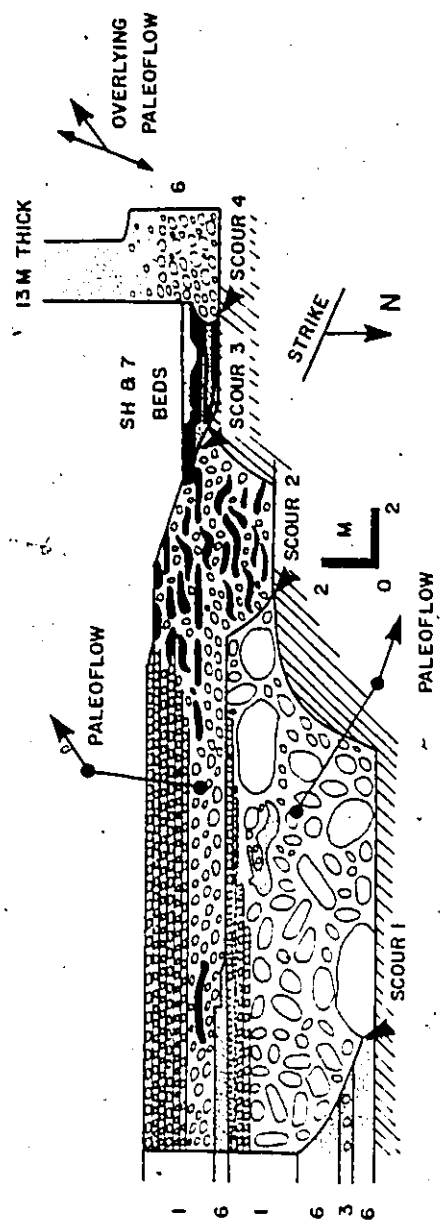
The initial scour surface is cut into predominantly massive sandstones (Facies (6)) with a thin interbed of dispersed pebbly sandstone (Facies (3)). This scour surface is about 4 m in apparent depth and traceable along strike for about 20 m (including extrapolation into

Fig. 31 - Outcrop sketch of multiple scour-fill sequence Beds 341-347, Rivière Trois Pistoles, p. 380

Fig. 32 - Pace and compass map (A) of multiply channelled contact between Original Formation (Niveau 1) and base of Cap Enragé Formation (Niveau 2), Grève de la Pointe.

Restored geometry and type of fill in channel complex (B). Out-and-fill sequences and paleoflow data (C).

Beds 1 - 5, Grève de la Pointe, p. 372



covered intervals). Scour fill is Facies (1) conglomerate which is disorganized with an abruptly graded-stratified top. This conglomerate is overlain by massive sandstone (Facies (6)), which is cut by the second scour surface. The fill of the second scour is also Facies (1) conglomerate. Eastward, this conglomerate is graded-stratified, whereas westward (at the lowest part of the scour) the conglomerate is very disorganized and had many bent and contorted shale intraclasts and appears to be a slumped portion. This slumped portion is cut by a third scour surface to the west. This third scour is much smaller than the first two scour surfaces (apparent scour depth is 1 m; traceable along strike for 4 m). Fill is very fine grained and consists of classical turbidites (Facies (7)) with shale interbeds. The western margin of the third scour fill is cut by the fourth scour, with an apparent depth of about 1 m. This fourth scour is filled with conglomerate, which is actually the base of a very thick, abruptly graded massive sandstone (Facies (6)).

An examination of the paleocurrent trends (Fig.31) shows an interesting pattern. The first scour fill material was deposited by a current that flowed toward the northwest. The finer-grained material in the second scour was deposited by a current that flowed toward the southwest. Beds overlying the multiple scour sequence also show paleocurrent trends toward the south or southwest.

(b) Grève de la Pointe Section (Fig. 32)

Scoured surfaces of the multiple scour fill are cut into classical turbidites and shales of the Original Formation. The scoured margin has an apparent depth of approximately 11 m and is traceable for about 200 m along strike (Fig. 32). Multiple cutting and filling seems to have occurred, where three events appear to have formed this complex. The basal 9 m of the fill (channel fill events 1 and 2, Fig. 32) may be enclosed within a scour that was cut as a result of a single flow. Two periods of fill are suggested by the presence of a shale parting between the two conglomerate fills. It is unlikely that this shale parting would be preserved, if the channel fill event 2 were scoured just before deposition. It is more plausible that the scour for events 1 and 2 was cut and then filled by two different events. The shale parting suggests a period of quiescence between the two events. The third scour was cut and filled by a later, separate event.

The first scour fill material consisted of ungraded Facies (1) conglomerate, which is overlain by shale. The second fill is graded-stratified Facies (1) conglomerate, which has the same grain size at the base as the first fill. After deposition of the second conglomerate, classical turbidites (Facies (7)) were deposited over the channel complex. After this relatively quiet period of sedimentation, more coarse material was supplied to the depositional site. Ungraded, disorganized conglomerates, with intraclasts and contorted large shale clasts, (Facies (1)) were transported to this site. The currents that transported this material scoured the margin, comprising the site of deposition for channel fill 3 (Fig. 32). This third scour is filled by separate events. The overall

trend is a fining-up sequence from coarse, ungraded and disorganized conglomerate (Facies (1)) --- graded-stratified conglomerate and fine conglomerate (Facies (1)) --- graded/stratified fine conglomerate and pebbly sandstone (Facies (2)) (Fig. 32).

An examination of the paleocurrent trends (Fig. 32), again shows a peculiar pattern. Paleocurrent data from the underlying Original sediments, suggest that the classical turbidites were deposited by currents that flowed toward the northwest. All paleocurrent data within the different scour fills also suggest that the currents that cut, and subsequently filled, the scour complex with coarse (Facies (1) and (2)) conglomerates flowed toward the northwest. Beds immediately overlying the scour fill complex were deposited from currents that flowed toward the south-southwest. Paleocurrents at the top of the section (Appendix 5) also indicate a paleoflow towards the southwest.

The beds overlying the scour fill complex are classed mainly as Facies (3) and (4), less commonly as Facies (7), (2) or (5) (Appendix 5). These overlying beds do not occur as scour fills, rather as continuous beds. Beds generally become finer-grained and slightly thinner-bedded upsection. The fining- and thinning-up trends are more gradual than those observed at Rivière Trois Pistoles section (Fig. 31, Appendix 5).

(c) St. Simon sur Mer (Shrine) Section (Fig. 33)

The first scour is about 1 m in depth and traceable along strike for about 4.5 m. Scour fill material consists of massive Facies (6) sandstone. This first scour fill is overlain by inversely graded-stratified conglomerate (Facies (1)). Westward this conglomerate has a scoured basal surface and exhibits large-scale crossbedding. The second scour surface has a depth of 4 m and is traceable about 12 m. Fill consists of conglomerate

Fig.33 - Multiple scour complex, Beds 792, 793, 797, St. Simon sur Mer (Shrine Section), p.389,400

Fig.34 - Multiple scour complex, Beds 296-300, Grève de la Pointe, p.378



ies (2) fills are both composed of mixed chaotic to disorganized zones of conglomerate, shale rafts and sandstone or conglomerate intraclasts. Top portions of the Facies (2) fills consist of crossbedded or stratified fine conglomerates. The top-most fill consists of a coarse grained Facies (1) conglomerate, which is ungraded and has well-developed imbrication (to the east) of large sandstone rafts. Paleoflows are toward the west.

(b) St. Simon sur Mer Est (Middle Horizon, Niveau 4)

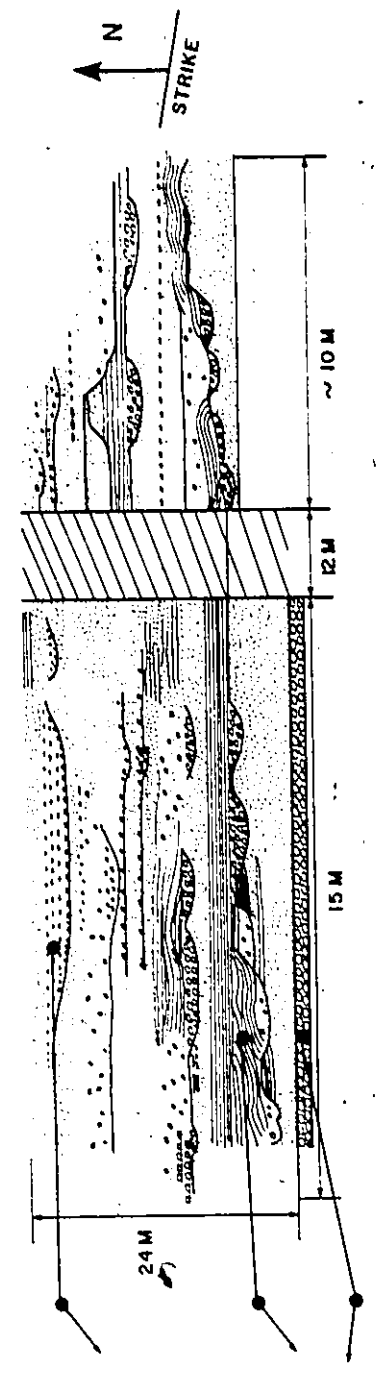
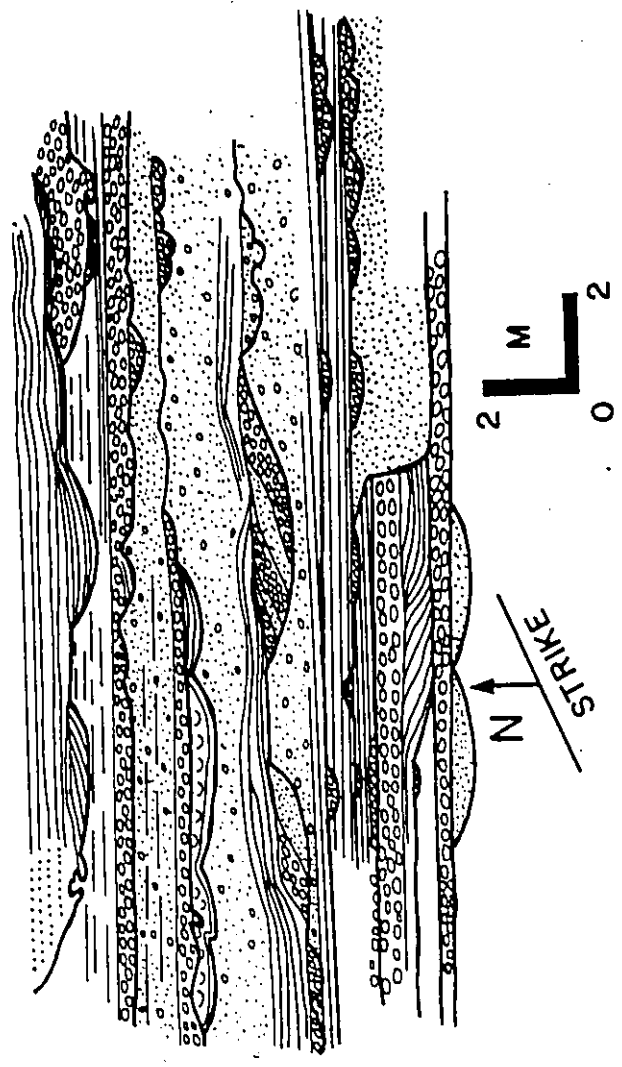
Sections 5 and 6 (Figs. 35,36)

The multiple scour fills of the St. Simon sur Mer Est section 5 and 6 are very similar to one another, in terms of the type of scouring and the facies that comprise the fill. In the lower scour (Section 5, Fig. 35) complex, the initial scour cuts into massive sandstone (Facies (6)). The initial scour of the upper complex (Section 6, Fig. 36) cuts into dispersed pebbly sandstone (Facies (3)). In both cases, dominant multiple scour fill consists of graded/stratified or crossbedded Facies (2) or massive Facies (6) sediments.

Scours in the upper Section 6 complex (Fig. 36) average 0.5-1 m in apparent depth and are traceable along strike for about 30 m. The pebbly sandstones and fine conglomerates, comprising the fill, are characteristically abruptly graded, with coarser clasts concentrated in the base of scours. Beds are marked by the occurrence of scalloped basal margins, which may or may not cross-cut one another.

Fig. 35 - Multiple scour complex, Beds 932-939, St. Simon sur Mer Est, p. 405

Fig. 36 - Multiple scour complex, Beds 949-954 and 967-974, St. Simon sur Mer Est, p. 406



Stratification in the lower part of the scours is scour-fill lamination or an irregular, "sweeping type" of lamination above the scours (Fig. 112). Upper parts of beds show horizontal stratification. In the lower part of the Section 6 complex (Fig. 36), beds are classed as Facies (2), whilst in the upper parts of this complex, beds belong to Facies (3) or (6). Associated with these trends is a slight fining-upsection of the maximum grain size of the beds. However, bed thickness tends to remain fairly constant, as do the scour dimensions.

The conglomerates and fine-pebble conglomerates of the Section 5 complex (Fig. 35) are, for the most part, normally graded/cross-bedded or normally graded/stratified. Coarser clasts are again concentrated in scours, but beds are less abruptly graded than those in Section 6 (Fig. 36). Beds are marked by scalloped basal margins. In lower parts of the complex, more beds belong to Facies (6) and are structureless; whereas, the upper parts of the complex tend to have beds that are wholly stratified or crossbedded. Dimensions of scours become larger upsection, along with an increase in the proportion of Facies (2) beds. As in Section 6, stratification within beds seems to grade from scour-fill cross-lamination within basal portions, to a sweeping type of lamination, which becomes low-angle to horizontal towards the tops of beds.

(3) Scour Fill Predominantly Facies (6) (Fig. 37)

Scours filled with predominantly massive Facies (6) sandstones only occur in Niveau 2 at St. Simon sur Mer Est (Fig. 37). These sediments are abruptly graded pebbly sandstone and fine pebble conglomerate, which are overlain by medium to fine sandstone. Dispersed coarser clasts occur in basal scours. The main impression of these beds is that they are struc-

tureless; less commonly, beds display scour-fill lamination (Appendix 4), stratification or dish structures. Beds are marked by the occurrence of prominent, scalloped basal surfaces. Apparent scour depth of individual scours is about 0.5 - 1 m. Several beds have laterally linked basal scours, which progressively cut downsection to a depth of about 2 m. Scours are traceable along strike for most of the outcrop width, about 50 m.

(4) Scour Fill Mixed Facies

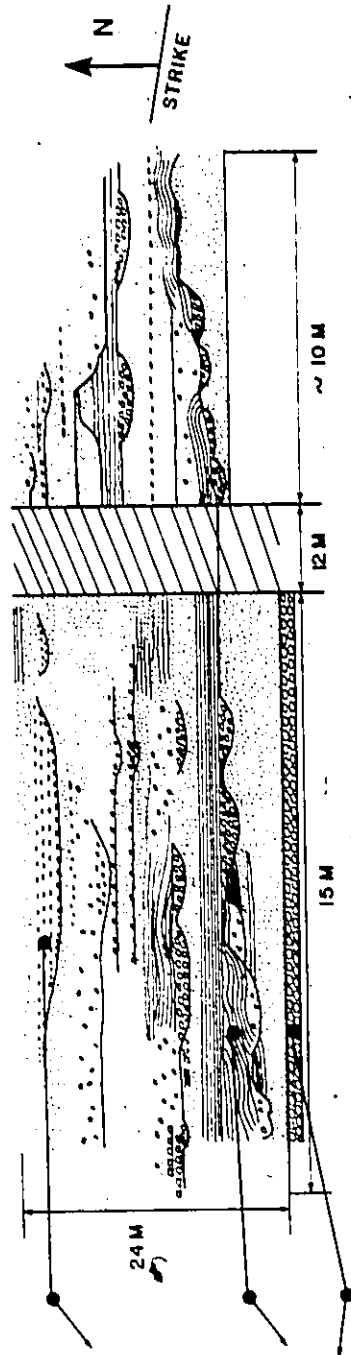
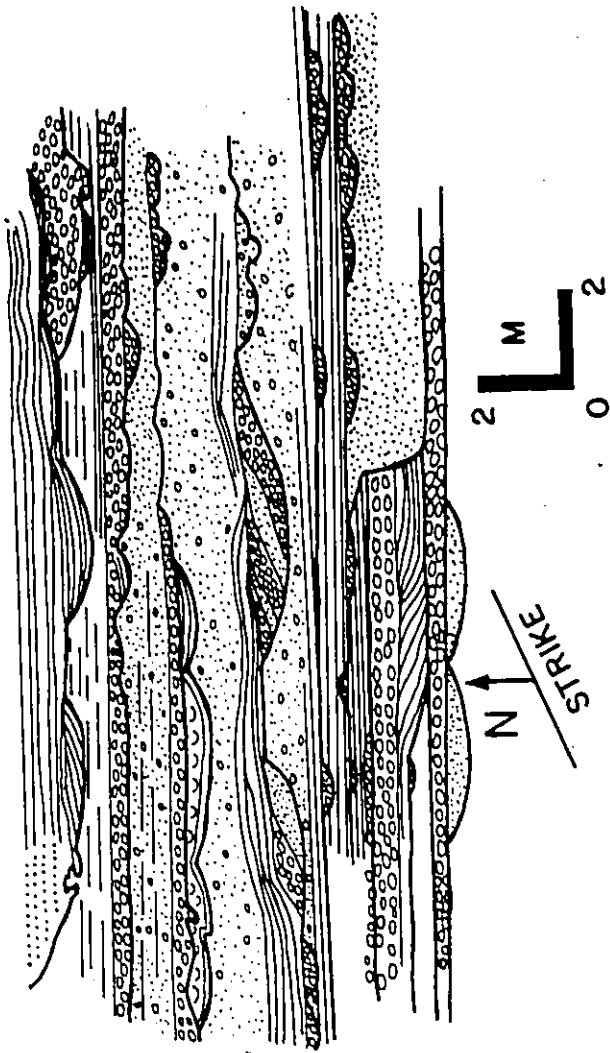
Four small multiple scour complexes have scour fills which belong to a variety of facies. These complexes occurred within sections at Grève de la Pointe, St. Simon sur Mer (Two Cottages), Anse à Pierre Jean 5 and Bic.

(a) St. Simon sur Mer (Two Cottages) (Figs. 38,39)

The first scour cuts into ungraded Facies (1) conglomerate. Lower scours of this complex are filled with structureless Facies (6) pebbly sandstone. Upper portions have fills classed as belonging to predominantly Facies (2). Fabric measurements and other paleocurrent data suggest that the currents that cut-and-filled the scours were flowing to the west-southwest. This paleoflow pattern is coincident with that found in immediately overlying and underlying beds. Scours are quite small: average apparent depth is about 0.5 m; and, scours are traceable along strike for about 7 m.

(b) Grève de la Pointe (Beds 81-91, Appendix 5)

One small multiple scour fill is associated with these beds. The first scour cuts into dispersed Facies (3) pebbly sandstone. Scours average 1 - 1.5 m in apparent depth and are traceable along strike for 3 - 6 m. The fill of the first scour is graded/crossbedded Facies (2) conglom-



Stratification in the lower part of the scours is scour-fill lamination or an irregular, "sweeping type" of lamination above the scours (Fig. 112). Upper parts of beds show horizontal stratification. In the lower part of the Section 6 complex (Fig. 36), beds are classed as Facies (2), whilst in the upper parts of this complex, beds belong to Facies (3) or (6). Associated with these trends is a slight fining-upsection of the maximum grain size of the beds. However, bed thickness tends to remain fairly constant, as do the scour dimensions.

The conglomerates and fine-pebble conglomerates of the Section 5 complex (Fig. 35) are, for the most part, normally graded/cross-bedded or normally graded/stratified. Coarser clasts are again concentrated in scours, but beds are less abruptly graded than those in Section 6 (Fig. 36). Beds are marked by scalloped basal margins. In lower parts of the complex, more beds belong to Facies (6) and are structureless; whereas, the upper parts of the complex tend to have beds that are wholly stratified or crossbedded. Dimensions of scours become larger upsection, along with an increase in the proportion of Facies (2) beds. As in Section 6, stratification within beds seems to grade from scour-fill cross-lamination within basal portions, to a sweeping type of lamination, which becomes low-angle to horizontal towards the tops of beds.

(3) Scour Fill Predominantly Facies (6) (Fig. 37)

Scours filled with predominantly massive Facies (6) sandstones only occur in Niveau 2 at St. Simon sur Mer Est (Fig. 37). These sediments are abruptly graded pebbly sandstone and fine pebble conglomerate, which are overlain by medium to fine sandstone. Dispersed coarser clasts occur in basal scours. The main impression of these beds is that they are struc-

tureless; less commonly, beds display scour-fill lamination (Appendix 4), stratification or dish structures. Beds are marked by the occurrence of prominent, scalloped basal surfaces. Apparent scour depth of individual scours is about 0.5 - 1 m. Several beds have laterally linked basal scours, which progressively cut downsection to a depth of about 2 m. Scours are traceable along strike for most of the outcrop width, about 50 m.

(4) Scour Fill Mixed Facies

Four small multiple scour complexes have scour fills which belong to a variety of facies. These complexes occurred within sections at Grève de la Pointe, St. Simon sur Mer (Two Cottages), Anse à Pierre Jean 5 and Bic.

(a) St. Simon sur Mer (Two Cottages) (Figs. 38,39)

The first scour cuts into ungraded Facies (1) conglomerate. Lower scours of this complex are filled with structureless Facies (6) pebbly sandstone. Upper portions have fills classed as belonging to predominantly Facies (2). Fabric measurements and other paleocurrent data suggest that the currents that cut-and-filled the scours were flowing to the west-southwest. This paleoflow pattern is coincident with that found in immediately overlying and underlying beds. Scours are quite small: average apparent depth is about 0.5 m; and, scours are traceable along strike for about 7 m.

(b) Grève de la Pointe (Beds 81-91, Appendix 5)

One small multiple scour fill is associated with these beds. The first scour cuts into dispersed Facies (3) pebbly sandstone. Scours average 1 - 1.5 m in apparent depth and are traceable along strike for 3 - 6 m. The fill of the first scour is graded/crossbedded Facies (2) conglomerate.

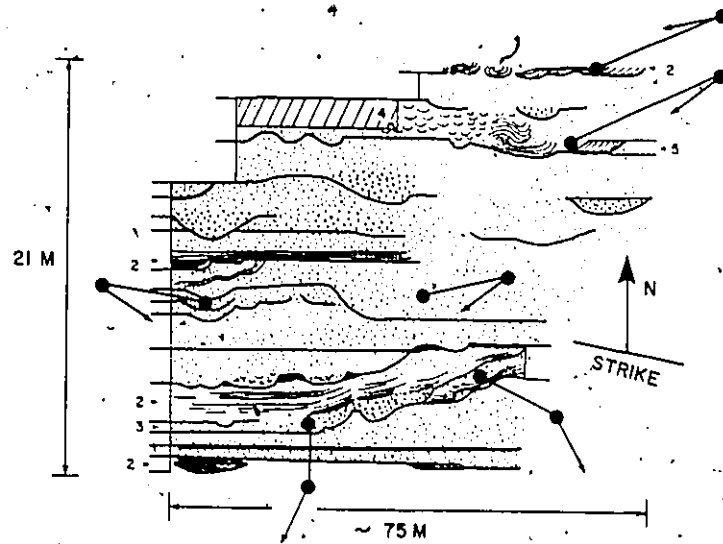


Fig.37 - Multiple scour complex, Beds 849-869, St. Simon sur Mer Est, p.402



Fig.38 - Small multiple scour fills. Beds 771-787, St. Simon sur Mer (Two Cottages) Section. Rectangles on notebook are 5 cm long. Stratigraphic tops are upward, p.398

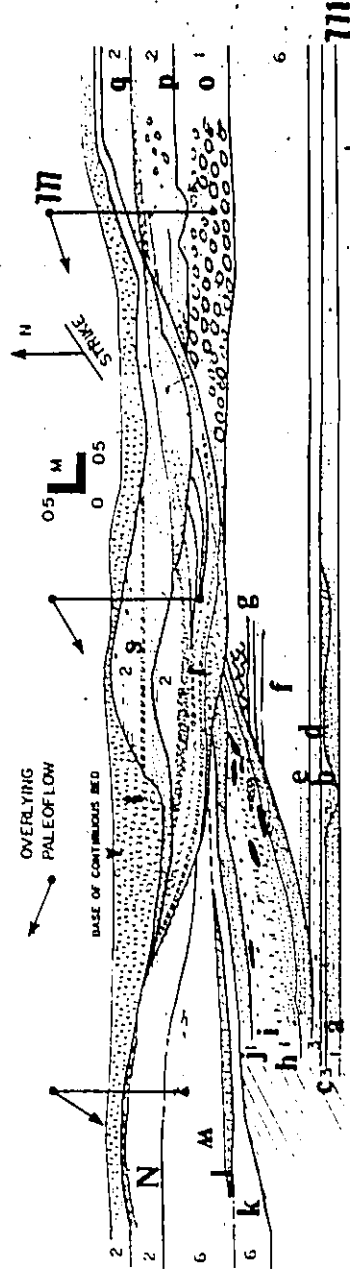


Fig.39 - Multiple scour complexes, Beds 771-787, St. Simon sur Mer, Two Cottages, p.398

grain size data: a (20mm); b (29mm); c (13mm); d (12mm); e (10mm); f (7mm); g (5mm); h (88 mm); i (3mm); j (17mm); k (4mm); l (11mm); m (2mm); n (10mm); o (30 mm, base; 2mm, top); p (28 mm, base; 0.75 mm, top); q (15 mm, base; 2mm, top); r (23mm, base; 5 mm, top); s (46mm, base; 8mm, top); t (20mm).

erate. To the northwest, this fill is truncated by four cross-cutting scour fills. The lower two fills are graded, liquefied Facies (4) pebbly sandstone and sandstone. The top-most fills are dispersed Facies (3) conglomerate and pebbly sandstone. No paleocurrent data is available for these scour fills. This small-scale multiple scour complex overlies a thick disorganized Facies (1) conglomerate. The transition with this underlying conglomerate is very abrupt.

(c) Anse à Pierre Jean 5 (Fig. 40)

The initial scour of this complex cuts into fine grained, stratified sandstone (Facies (2)). The first scour is about 1 m deep and is traceable for about 5 m along strike. Fill consists of predominantly structureless Facies (6) sandstone with only a thin line of inclined dish structures, post-depositional in origin. This first fill is succeeded by a liquefied Facies (4) bed, which is cut by the second scour. The second scour has an apparent depth of about 2.5 m and is traceable along strike for 8 m. This scour has been filled by two depositional events. The basal fill consists of a liquefied Facies (4) bed, which is overlain by a graded-stratified (and partly liquefied) Facies (2) bed. The basal fill of this second scour probably became liquefied due to emplacement of the overlying Facies (2) bed. All of these scours open up toward the east. Inclined stratification suggests an eastern paleoflow. No other paleocurrent information is available. This complex most closely resembles the scour complex at St. Simon sur Mer Est (Lower Horizon) (Niveau 2) (Fig. 37).

(d) Bic (Fig. 41)

The initial scour of this complex cuts into a liquefied Facies (4) bed. Fill of the first scour consists of Facies (1) conglomerate to

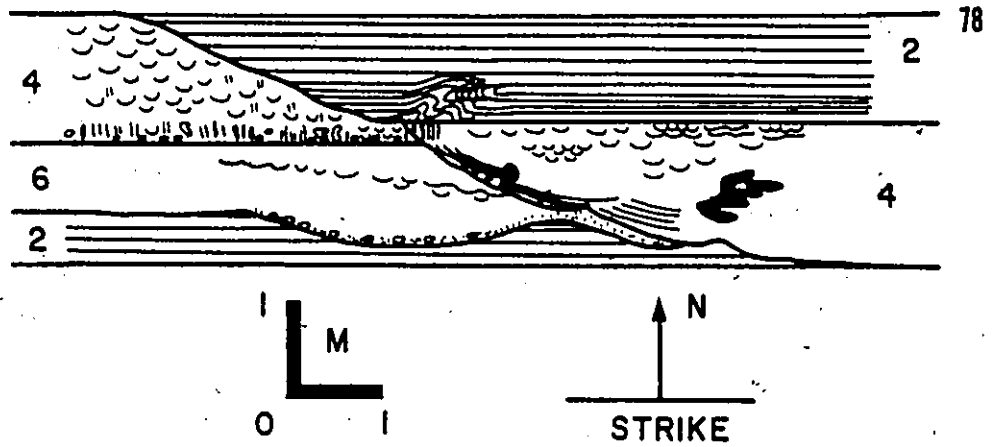


Fig.40 - Multiple scour complex, Beds 573-576, Anse à Pierre

Jean 5. Regional paleoflow to the south-southwest, p.390

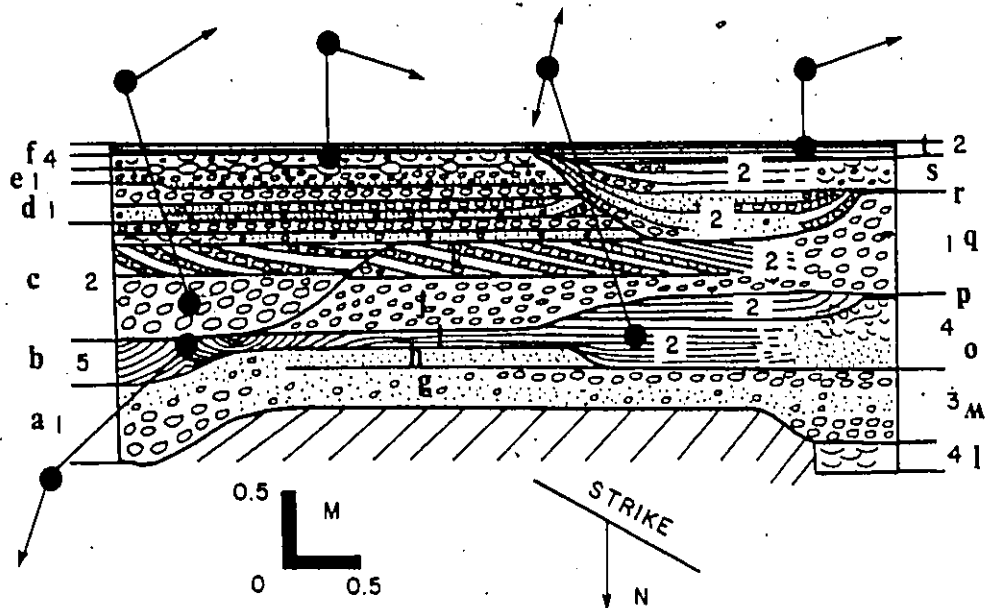


Fig.41 - Multiple scour complex, Beds 1331-1346, Bic, p.419

Grain size data: a-93mm; b-0.5mm; c-29-14 mm; d-26mm; e-40mm; f-35mm; g-70mm; h-0.5mm; i-0.4mm; j-30mm; k-66 mm; l-0.3mm; m-95mm; o-0.4mm; p-0.4mm; q-32mm; r-184-35mm; s-35mm; t-4mm.

the east and Facies (3) dispersed pebbly sandstone to the west. The area between the scour consists of Facies (3) dispersed pebbly sandstone and Facies (6) massive sandstone. The next series of four scours are filled mainly with Facies (2) deposits. The first of these scour fills consists of a Facies (2) bed which changes westward into a liquefied Facies (4) deposit. To the east the Facies (2) bed becomes an ungraded, crossbedded Facies (5) unit.

The four scours are topped by very thin, inverseby graded Facies (1) and ungraded Facies (1) conglomerates. A thin liquefied Facies (4) pebbly sandstone occurs at the top of the Facies (1) beds. To the west the thin Facies (1) beds and the Facies (4) bed are cut by nested scour fills, consisting of Facies (2) deposits.

Paleoflows for the Facies (5) fill of the second scour are toward the north. All other paleoflows within this complex are generally toward the west-southwest.



CHAPTER 3

VERTICAL AND LATERAL FACIES RELATIONSHIPS

Sedimentary environments are complex dynamic systems. Their deposits, in turn, can also be quite complex. In order to work backward from "results" to "processes," models are commonly erected of sedimentary systems. Models may be in terms of a reduction in physical scale (as the dedicated model railroader scaling-down trainloads of boxcars for ease in handling and observation) or, alternatively, the models may consist of actual simplification of the observed system. In the present study, physical scale-modelling of the system was not attempted. Rather, simplification of the observed field relationships was done. This chapter presents the summaries (simplifications) of the observed facies associations. These simplifications will be integrated into an overall model for the Cap Enragé sediments, in the final Chapter 6.

The first step in the simplification of a stratigraphic succession is done by recognizing different sedimentary facies. This was done in Chapter 2. The next step is to try and delineate environments from the sedimentary facies associations. To do this, geologists have used Johannes Walther's Law of Succession of Facies as a guide. This law is stated as follows: "The various deposits of the same facies area and, similarly the sum of the rocks of different facies areas were formed beside each other in space, but in crustal profile we see them lying on

top of each other ... only those facies and facies areas can be superimposed, without a break, that can be observed beside each other at the present time" (Walther, 1894, free translation as given in Blatt et al, 1972, pp. 187-188; emphasis added). As listed in Blatt et al (1972) there are several corollaries to this law:

1. No major breaks can occur in the stratigraphic sequence.
2. One location is unlikely to display all of the facies which occur in lateral association.
3. An oversimplified model vertical succession, necessarily, leads to an oversimplified interpretation of the lateral facies associations.

A good facies model must, implicitly, account for the observed lateral and vertical facies associations. Hence, a good description of the observed associations must be given. The associations must be simplified to the extent that "one can see the forest for the trees"; however, they must not be oversimplified to the extent that one ends up with a simple-minded interpretation. A delicate balance must be maintained. One must also be assured that personal bias does not enter into the delineation of associations. An objective method must be used to determine significant facies relationships.

In the following chapter, the observed vertical and lateral facies associations are presented for the Cap Enragé sections measured in the present study. As with most ancient successions, the vertical associations are much easier to observe than the lateral facies relationships. Consequently, more data is available to discuss the vertical patterns, with some refinements gleaned from the lateral trends.

VERTICAL FACIES ASSOCIATIONS

Preliminary Analysis: Methods

In the study of stratigraphic successions, one is interested in determining if there is any evidence of recurrent or cyclic repetitions of different facies, which would yield valuable information about possible repetitive sedimentation processes. There are many ways to objectively analyze sequences of data. The nature of the data and its spacing in the section dictates what sort of technique should be used. In the present study, one is concerned with the possibility of recurrent patterns in the chronological succession of facies. The variable is the "facies." Facies are nominal data in that the magnitudes of the facies (1,2,3,...,7) are irrelevant. In this preliminary analysis, the spacing of facies in vertical sections is not important -- only the sequence of facies is considered.

Three types of statistical techniques are appropriate to use for nominal data in successions in which the spacing is not considered. These techniques are: auto-association and cross-association, markov analysis of transition matrices, and runs tests (Davis, 1973). Markov and semi-markovian models have been successfully applied to stratigraphic problems, both in the simulation of observed sections and to determine whether observed successions are accounted solely in terms of independent random processes. Many workers have used these techniques in the analysis of deep-sea sediments (Davies and Walker, 1974; Doveton and Skipper, 1974; Hattori, 1976; Hiscott, 1977; Miyamura, 1965; Simpson, 1970; van Andel and Komar, 1969; Vistelius and Faas, 1965; Vistelius and Feygel'son, 1965).

In the preliminary analysis, it was chosen to use markovian analysis of observed facies transitions to determine if there is any pattern that is not explained in terms of independent random sedimentation processes. There are many sources of error in the geologic application of Markov analysis.

The first problem involves the test against randomness. There is no exact test of cyclicity for nominal data. Consequently, to determine whether a given sequence of categorical data is random or not, a χ^2 test is conducted. The null hypothesis is that the sequence of lithologic events is random. One must be careful as to the number of states defined: as the number of states increases, so does the number of transitions needed for statistical certainty. The manner in which the states are defined is also important: different χ^2 values may result if the definition of states is by lithologic or bedding thickness, rather than facies criteria. One should strive for a low number of states, both for statistical analysis and in the portrayal of data. Patterns within transition probability matrices are commonly shown by plotting them as flow graphs. Incipient patterns are more apparent if the transition matrices have a low rank.

Other problems arise in the use of Markov analysis. Covered intervals or incomplete sections (due to erosion or faulting) may affect the decision of "randomness" or "non-randomness." In addition, as with all χ^2 tests, one has to arbitrarily decide on a certain significance level within the difference matrix, between random and observed transition probabilities. One has to keep in mind the geologic significance of why certain associations occur; and, conversely, why others rarely

occur. Much geologic insight must be used to define the states and to recognize the significance of their transitions.

In the present study, nine states were defined for the Markov analysis. The nine states comprise the eight facies defined in Chapter 4 (Facies 1,2,...,7 and shale) as well as the "scoured surface" state (abbreviated SS). The scoured surface state consists of large scale scours, with an apparent depth greater than or equal to 1 m (range: 1-11 metres). This scoured surface state differs from the other states, in that it does not describe a "unit of rock." Rather, it represents a major break in the deposition of sediments and signifies a period of erosion. None-the-less, the scoured surface state is recognizable in the field, and is extremely important in trying to describe sequences of sedimentation.

After the definition of the nine states, the transition sequences were tabulated. Transitions of one state back to itself is not allowed in the analysis of facies sequences -- this is an embedded Markov-chain analysis. Consequently, states may consist of one bed (in the case of an isolated facies) or a series of beds of the same facies in multistorey sequences. If a section break occurred, as a covered interval or fault contact, a new transition sequence was started. This complication results in truncated sequences.

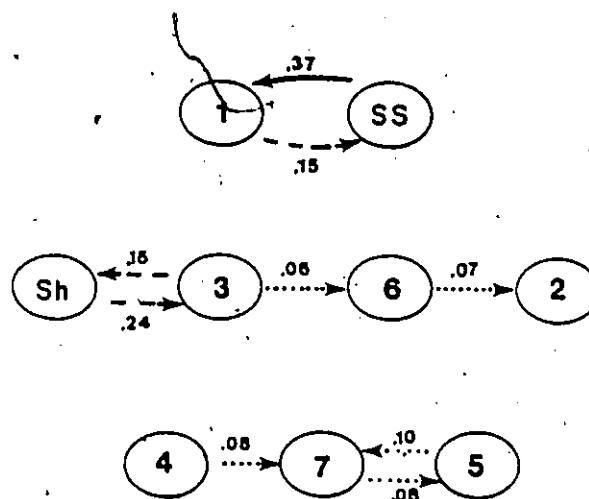
After the definition of the nine states and compilation of the transition sequences, the next step was to analyze possible patterns of transitions between states or facies. Facies relationships can be shown by facies relationship flow or "spider" diagrams drawn from the original field transition counts. In this study, these diagrams based on transi-

tion counts are quite complex and very difficult to understand. Simplification of the facies relationship diagram is necessary.

The facies relationship diagram was simplified by eliminating those transitions which have a probability of occurrence less than or equal to the probability if the transitions were random. In order to determine which transitions are significantly different from random, transition count, transition probability and difference matrices were tabulated using the methods outlined in Davis (1973, pp. 278-288), Harbaugh and Bonham-Carter (1970, Chapter 4) and Miall (1973) (Appendix 9). Davies and Walker (1974) selected a cutoff value of 0.35 for the difference matrix scores to distinguish random and non-random transitions. If this is done for the present study (Appendix 9), only one transition is significant for all the transitions within the Cap Enragé Formation that were measured. Hence, it was thought that this value was not very useful. A difference of +0.05 between the observed and random transition probabilities was arbitrarily selected as being the boundary between random and non-random transitions (as was done by Cant and Walker (1976) for fluvial sediments).

Preliminary Analysis: Results

Transition Count, Transition Probability, Random Probability and Difference Matrices are tabulated in Appendix 9 for all the transitions observed within the measured sections. A summary facies relationship diagram is shown in Fig. 42). As shown in this diagram, there is lack of a well-defined sequence or even associations of facies. The only well-defined association is the trend of scour surfaces to be overlain by coarse conglomerates (Facies 1). One does not need sophisticated



Key

1, ..., 7: Facies 1 through 7

sh: Shale Facies

SS: Scoured Surfaces

Numbers in decimal form indicate the difference matrix scores

..... Difference matrix scores: .05-.1

----- Difference matrix scores: >.10-.3

————— Difference matrix scores: >.3

Fig.42 - Facies relations in the Cap Enragé Formation, using
all the transitions observed in the measured section.

markovian analyses to show that scoured surfaces tend to be overlain by coarse conglomerates -- it is obvious in the field and is not at all surprising. The value of this analysis is that it demonstrates, that, on the whole, the other facies do not show consistent patterns in their distribution within all the sections that were measured in this study.

The lack of consistency can be partly attributed to the fact that all of the sections, regardless of their stratigraphic position or geographic location, were lumped into one grand section. The obvious trends, based upon Johnson's (1974) work, of Facies (1) to Facies (2) in vertical sections through pod conglomerates do not show up as significant transitions. Similarly, the trend from predominantly A-division turbidites (equivalent to Facies (3) and Facies (6) beds) to complete classical turbidites (equivalent to Facies (7)) at the Bic Member III section (Hubert et al, 1970) are not significant in the present analysis. The problem is that by considering the overall transitions within the whole Cap Enragé, one is lumping "peaches with oranges" by considering Niveau 2. through Niveau 6 and Member I through Member III sediments as representing a homogeneous set. One of the basic premises of the Markov chain is that a stationary (or fixed) transition matrix applies to all transitions. This is clearly not the case: beds in Member II and Niveau 3 and 5 are composed mainly of Facies (1) conglomerates, whereas Members I and III and Niveau 2, 4 and 6 (Fig. 11) comprise the finer facies (Facies (2) through Facies (7) and Shale). A more detailed analysis is needed.

Detailed Analysis: Methods

(1) Pooling the Data: Definition of Major Sedimentation

Units

One of the major difficulties in doing the Markov analysis is in trying to decide which sections can be lumped together and considered as essentially a homogeneous set of data for statistical purposes. As mentioned before, there are various Members and Niveau which can be mapped on a regional scale for the Cap Enrage sediments, although they are lenticular across the entire outcrop belt. Member I at Bic is predominantly sandstone. Similarly, Niveau 2 in the Anse à Pierre Jean - St. Simon region is mainly sandstone. When taken out of stratigraphic context, these sediments of Member I and Niveau 2 are virtually indistinguishable from one another in the field. Consequently, these will be considered one major sedimentation unit. Member II at Bic and Niveau 3 and 5 in Anse à Pierre Jean - Cap à la Carre Ouest are mainly composed of Facies (1) and Facies (2) beds, and are difficult to distinguish from one another without complete chronology, as in fault blocks. These will be the second major sedimentation unit. The third major unit comprises Niveau 4 and Niveau 6 pebbly sandstones in the St. Simon - Cap à la Carre Ouest region, which are equally difficult to distinguish without complete sections. Member III at Bic consists of pebbly sandstones and sandstone and resembles the pebbly sandstones in Niveau 4 and 6. Member III differs significantly in that a well-defined overall fining-up sequence occurs at Bic, which is not seen in Niveau 4 and 6 in the St. Simon - Cap à la Carre Ouest outcrops. Hence, Member III will be a separate set. Niveau 2 at Rivière Trois Pistoles and Grève

de la Pointe have thick Facies (1) conglomerate beds at the base of the sections. This is only seen at one other outcrop -- Pt. Michaud, between Bic and Cap à la Carre. For this reason, the Niveau 2 sections are not considered in the same set at Niveau 2 in the Anse à Pierre Jean - St. Simon region. The geographic position of Grève de la Pointe at the farthest western part of the outcrop for the Cap Enragé suggests that it would be unwise to group it with the eastern equivalents -- Member I. Hence, Grève de la Pointe sections will be their own set. Niveau 2 at Rivière Trois Pistoles has aspects similar to both the Niveau 2 sediments at Anse à Pierre Jean, to the east, and Grève de la Pointe, to the west. Consequently, the Rivière Trois Pistoles section will be considered on its own. This results in six major sedimentation units, for statistical analysis, which are designated:

1. Sandstone Horizons (Member I and Niveau 2: Anse à Pierre Jean - St. Simon area and Bic)
2. Conglomerate Horizons (Member II, Niveau 3 and Niveau 5: Anse à Pierre Jean - Cap à la Carre region and Bic)
3. Bic III (Member III: Bic)
4. Pebbly Sandstone Horizons (Niveau 4 and Niveau 6: St. Simon - Cap à la Carre Ouest area)
5. Rivière Trois Pistoles Section
6. Grève de la Pointe Section

In order to test that the sections have not been over subdivided into the six major sedimentation units, a Chi-squared test and a one-way ANOVA were performed. In order to test if there are differences in facies occurrences with respect to the sedimentation units, the chi-

squared test was done (Appendix 9). The prob-value of the calculated χ^2 value suggests that the null hypothesis (that the facies in the different sedimentation units occur equally often) is false. A serious drawback of the Chi-squared test is that it does not state how much the facies differ between the sedimentation horizons. To overcome this aspect, the data were reworked and the one-way ANOVA was conducted (Appendix 9). The results of the ANOVA are listed in Appendix 9 and are summarized as follows:

1. The null hypothesis of equal facies percentages was rejected for the coarse conglomerates (Facies 1).
2. The null hypothesis was marginally acceptable for the ungraded cross-bedded Facies (5) sediments and may be due to the small number of beds.
3. The null hypothesis was marginally rejected for the classical turbidites (Facies 7).
4. All of the other facies show that there is no evidence, from this sample, to state that the null hypothesis of equal facies percentages in the different sedimentation units was false.

There is not enough data to test the validity of the assumptions of normality and equal variances basic to the ANOVA test. Lists of the confidence bands about the mean % facies occurrence ($\bar{X} \pm 2s$) (Appendix 9) suggest that the assumption of homoscedasticity may not be valid: Facies (4) and Facies (6) percentages in the Sandstone Horizons have much greater variances than those facies observed in other horizons. However, the mean percentages of Facies (4) and Facies (6) in the Sandstone Horizons fall within the confidence bands of the other horizons. It is, therefore, not thought that the conclusions from the ANOVA are wrong.

(2) Delineation of Detailed Sequences

There are several scales of sequences that can be examined: 1) sequences of beds; 2) sequences of facies; and 3) sequences of groups of facies which occur together. Each of these has different implications as to sedimentary processes and environmental reconstructions.

In the first case, the beds are all classed into facies and a Markov-chain analysis is done in which one state is allowed to go back to itself. Beds are independent events and, as such, the facies class of a given bed does not, necessarily, depend upon the facies class of the immediately preceding bed. A Markov-analysis of the facies patterns, using beds as divisions, would show if beds of a given facies tend to be overlain by beds of the same facies or different facies. A parameter, called the "facies stability", can be derived to express the trend of beds of the given facies to be overlain by beds of the same facies. The expression for the facies stability is:

$$(1) \quad \text{Facies stability} = (\text{number of transitions of a state back to the same state}) / (\text{total number of transitions from the state}).$$

This facies stability coefficient ranges from 0 (for those states in which beds of a given facies are never overlain by another bed of the same facies) to 1 (for those states in which beds of a given facies are always overlain by beds of the same facies). A two-factor ANOVA is conducted to test if there is a significant difference in the facies stability between facies as observed in the major sedimentation horizons.

Methods used in this analysis are given in Appendix 9.

In the second case, where stratigraphic units are divided by

facies and not beds, the embedded Markov-chain analysis is done. The methods are identical to those used in the preliminary analysis of facies associations.

In the third case, one is concerned with sequences within the distribution of groups of facies. In order to define facies groups one has to objectively decide which facies occur in similar stratigraphic context. In complex sequences it is often difficult, with large amounts of data, to readily discern what facies occur in similar positions. The capacity of one facies to substitute for another in a preferred section is called "substitutability." Cluster and substitutability analysis enable one to discern facies that may proxy for one another. One can construct a "tree diagram" (also called dendrogram) of facies based upon mutual substitutability. Facies with high mutual substitutability would cluster "high up in the tree"; whereas facies with low mutual substitutabilities would link at lower levels. Clusters of facies at high mutual substitutability values would be considered to be "groups of facies," in that they occur within similar stratigraphic contexts.

Cluster analysis is quite useful in the discernment of relationships amongst facies. This analysis demands no prior knowledge about facies relationships. The dendrogram clustering method allows the data to classify itself (individual facies are free to enter any group that emerges) and is an efficient display of complex relationships. There are, however, several disadvantages of this method: 1) distortions can result from trying to represent multi-dimensional data in two-dimensions, as a consequence of averaging substitutability values; 2) no statistical tests of significance exist; 3) statistical groups may or may

not be geologically significant. Computational techniques for cluster and substitutability analysis are given by Davis and Cocke (1972) and Davis (1973) and are summarized in Appendix 9. In order to look for vertical associations between groups of facies, a Markov-chain analysis and an embedded Markov-chain analysis were done in which the states were defined by groups of facies (Appendix 9).

Detailed Analysis: Results

All of the matrices used in the embedded Markov-chain and Markov-chain analyses are given in Appendix 9. Likewise, matrices and dendrograms for the cluster and substitutability are tabulated in Appendix 9. Flow charts for preferred facies associations are also given. Results of the test for Markov property using the χ^2 statistic (Gingerich, 1969), ANOVA tests, and facies stability coefficient values are also all tabulated in Appendix 9.

(1) Markov-Chain Analysis: Sequences of Beds

Results of the two-factor ANOVA on facies stability shows that there was no evidence that facies stability is different in the six major sedimentation horizons. Similarly, the tests for differences between facies show that facies stability values are similar in the different facies.

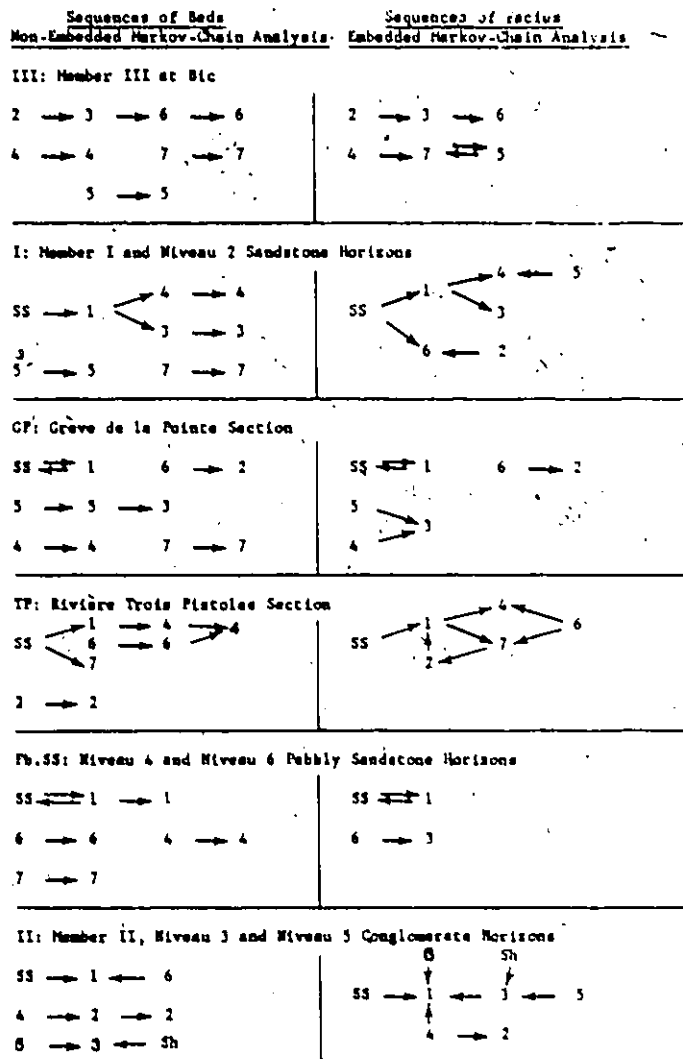
No χ^2 test exists that can test the Markov-property in Markov-transition count matrices (where transitions are allowed back to the same state) in which there are off-diagonal zero entries (as in the present study) (see discussion in Appendix 9). Hence, one cannot test if the whole observed probability matrix is significantly different from random. This is not the objective of this exercise. Rather, one is inter-

ested in finding those individual transitions between facies which are significantly different from random.

An examination of the flow diagrams for the major sedimentation units suggest that there are some significant facies associations on a bed-to-bed basis (Fig.43). There are however, few consistent associations that are seen in all sedimentation horizons. There are some trends which seem to prevail. Scoured surfaces tend to be followed by Facies (1) coarse conglomerates. Liquefied Facies (4) beds are generally followed by beds of the same facies. In major sedimentation units which have dominant transitions involving beds belonging to Facies (5), (6) and (7), the transitions are usually back to beds of the respective facies (i.e. beds belonging to Facies (5) are usually followed by more Facies (5) beds, etc.). If one looks at the dominant overlying transitions (difference matrix scores greater than 0.1) (Fig. 44) Facies (1) beds tend to be overlain by beds belonging to a number of different facies. Beds belonging to other facies are overlain by beds belonging to two or three different facies. The type of facies that overlies a given facies bed, generally varies with the major sedimentation unit (Fig. 44).

(2) Embedded Markov-Chain Analysis: Sequences of Facies

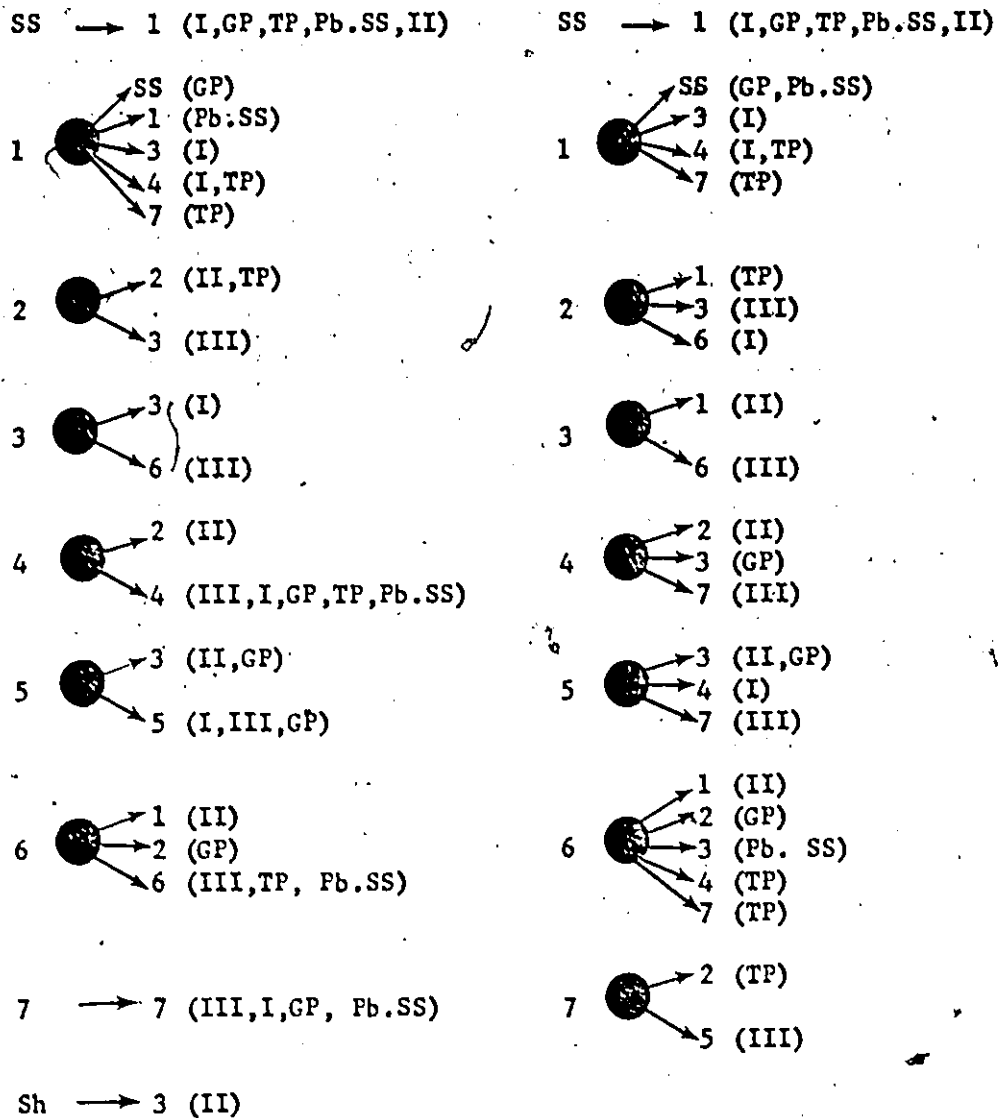
Results of the χ^2 test suggest that the total transition probability matrices differ from random in only two of the six major sedimentation units: Greve de la Pointe Section and the Pebbly Sandstone Horizons. This is likely due to the large sample size of these two sets of data (number of transitions are 245 and 295 respectively). With nine states, a very large number of transitions is required for sta-



Abbreviations same as in the previous figure.

Fig.43 - Summary of facies relations in different sedimentation horizons. Difference matrix scores $> +.30$.

Sequences of Beds Sequences of Facies
Non-embedded Markov Chain Analysis Embedded Markov Chain Analysis



Abbreviations: 1,...,7: Facies 1 through 7

Sh: Shale Facies; SS: Scoured Surfaces

I: Member I and Niveau 2 Sandstone Horizons

II: Member II, Niveau 3 and Niveau 5 Conglomerate Horizons

III: Member III at Bic

Pb. SS: Niveau 4 and Niveau 6 Pebbly Sandstone Horizons

TP: Rivière Trois Pistoles Section

GP: Grève de la Pointe Section

Fig.44 - Facies relations in different sedimentation horizons. Difference matrix scores > +.30.

tistical significance of the entire transition probability matrix. As mentioned before, one is mainly interested in those individual transitions that differ from random.

As with the bed sequences, the flow diagrams show very few consistent patterns within the whole formation (Fig. 43). Scoured surfaces are generally overlain by Facies (1) conglomerates. At Grève de la Pointe and in the Pebbly Sandstone Horizons, Facies (1) conglomerates tend to be succeeded by scoured surfaces. If one examines the dominant overlying transitions (Fig. 44), Facies (1) and (6) units are succeeded by a number of facies. The other facies are generally overlain by two or three types of facies, where the succeeding facies varies with the major sedimentation unit.

(3) Substitutability, Cluster and Markov-Chain Analysis:

Sequences of Groups of Facies

None of the groups of facies delineated from the substitutability and cluster analyses are consistent throughout the major sedimentation units. Results of the Markov-chain and embedded Markov-chain analyses for the groups of facies within the major sedimentation units are given in Fig. 45. Examination of these flow diagrams suggest that there are few consistent "facies group" associations seen in all sedimentation units. This is to be expected when each major sedimentation unit tends to show a different grouping of facies.

LATERAL FACIES ASSOCIATIONS

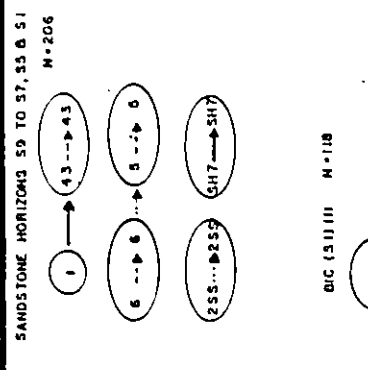
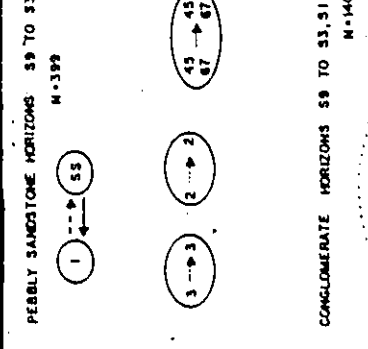
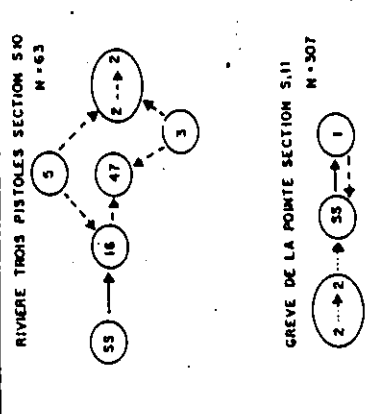
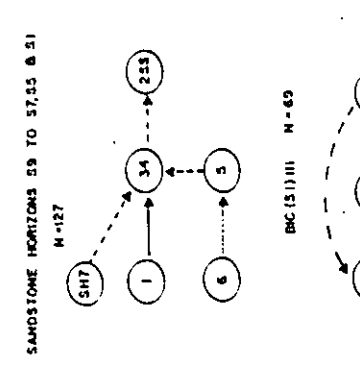
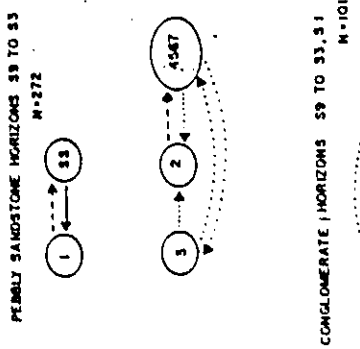
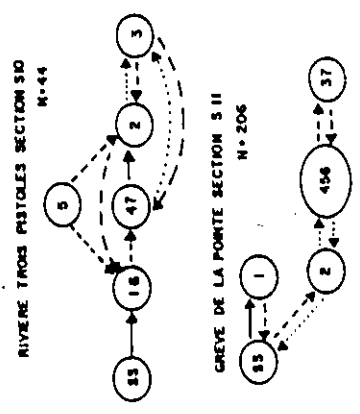
As mentioned in the beginning of this chapter, it is usually difficult to get good, continuous lateral exposures to adequately portray lateral facies associations. Small, outcrop-scale lateral facies

Fig.45 - Facies relations of groups of facies in different sedimentation horizons.

Key same as in Fig . S1...S11 indicate sections on location map (Fig.).

Upper part of diagram refers to embedded markovian analyses of groups of facies.

Lower part of diagram refers to non-embedded markovian analyses of groups of facies.



relationships can be observed in some beds in spatial along-strike sections as well as in single and multiple scour fills. Regional facies associations are evident only by comparing major sections within Niveau and Members, at outcrops that are fairly continuous along the coast (parallel to strike). In the first part of this section, lateral facies changes within individual beds are presented. Secondly, the relationships within scour fills will be examined. Facies associations are described from field observations. Not enough data is available for statistical analysis of preferred associations. Regional associations will be examined in the next chapter in conjunction with the paleocurrent patterns.

Small-scale (Within Beds) Facies Associations

Along-strike facies associations within individual beds can be observed in 66 beds within the sections measured in this study. Of these, 27 beds were in sections parallel to local paleocurrent directions; 17 beds were in sections transverse to the local paleoflow; and, 22 beds were in sections oblique to the local paleocurrents. All of these beds show complex lateral facies relationships and all of these changes are shown in the section diagrams (Appendix 5).

Beds thin or thicken in both along-strike directions. Grain size within individual beds may coarsen, become finer and even coarsen again in one direction along strike. Due to this variation, in both grain size and thickness within individual beds, it is difficult to know how to define a "starting" position for a given bed. The coarsest-grained portion of a bed was selected as the starting point to describe the along-strike facies associations within the beds. A summary is in Table 4.

TABLE 4SMALL-SCALE (WITHIN BED) LATERAL FACIES ASSOCIATIONSCoarsest Portion of Bed: Facies (1)

The following trends are on the scale of "pod" fills of Johnson and Walker (in prep.).

1. Facies (1) portions of beds within current-parallel and current-transverse sections become finer-grained and thinner-bedded in all directions. In beds involving transitions of Facies (1) conglomerates, thick, inverse or normally-graded conglomerates tend to occur upcurrent and grade downcurrent into thinner, normal-graded-to-stratified conglomerates. The thinning- and fining trends occur with Facies (1) in relation to other facies (1,3,4 and 6) portions of beds, although no overall consistent patterns occur.
2. In current-oblique sections beds become finer-grained and may thicken or become thinner in both easterly and westerly directions. Associated with these changes is the change from coarse Facies (1) bed portions to Facies (2), (3) and (6), although no consistent overall patterns occur.

Coarsest Portion of Bed: Facies (2)

1. In current-parallel sections there are no consistent bed thickness trends nor facies associations. Beds become finer-grained in both up- and down-current directions. Most facies as associated with the coarser Facies (2) portions of beds, with the exception of the coarser Facies (1) conglomerates.
2. In current-transverse sections, the coarsest Facies (2) portions of beds occurred in a most-westerly position. Beds tend to become thicker and finer-grained in an easterly direction. Associated with this change is a transition of Facies (2) to Facies (3) and/or Facies (6).
3. In current-oblique sections beds become finer-grained in both easterly and westerly directions. Beds may thicken or become thinner-bedded. Facies (3), (6) and (5) are associated with the coarser, Facies (2) bed portions. No consistent overall patterns occur.

Coarsest Portion of Bed: Facies (3)

1. In current-parallel sections most of the beds tend to become finer grained and thinner-bedded in up- and downcurrent directions. Facies (2), (3), (4) and (6) are associated with the coarser Facies (3) bed portions, although no consistent overall patterns emerge.

TABLE 4 (continued)

2. In current-transverse sections most of the beds become finer-grained and thicker-bedded in an easterly direction. Coarse Facies (3) bed portions grade into thicker, finer-grained Facies (3) and/or Facies (6) bed portions.
3. In current-oblique sections beds become finer-grained and may become thinner or thicker bedded in both easterly or westerly directions. Facies (2), (4) and (6) bed portions occur in association with the coarser Facies (3) portions, although no overall patterns are evident.

Coarsest Portion of Bed: Facies (4)

1. In current-parallel sections, the coarsest Facies (4) bed portions are in a downcurrent position. Beds tend to become finer-grained and thinner-bedded upcurrent. Associated with this change is a tendency for Facies (4) bed portions to be replaced by finer Facies (2), (3), (4) or (6) bed portions.
2. In current-transverse sections the coarsest Facies (4) bed portions occur in a most westerly direction. Beds become finer-grained in easterly directions. Beds may become thicker or thinner towards the east. Associated with these changes, the coarse Facies (4) portions change into Facies (2), (4), (6) or (7) finer bed portions.
3. In current-oblique sections beds become finer-grained with no bed thickness change in both easterly and westerly directions. Finer Facies (1), (3), (2) and (5) bed portions are associated with the coarser Facies (4) portions, although no overall consistent patterns occur.

Coarsest Portion of Bed: Facies (6)

1. In current-parallel sections Facies (6) portions became thinner and finer-grained in both up- and downcurrent directions. Facies (2), (3) and (4) portions were associated with the coarser and thicker Facies (6) bed portions, although no overall patterns were consistent.
2. In current-transverse and current-oblique sections, the coarsest Facies (6) portions of bed occurred in a most westerly direction. The coarsest Facies (6) portions became thinner and finer-grained to the east. Associated with this change is usually a transition from thick Facies (6) to thin Facies (6) (less commonly, thin Facies (2), (3), (5), (7)) in an easterly direction.

CHAPTER 4

SEDIMENTARY FABRIC AND SIZE ANALYSES

SEDIMENTARY FABRIC

The term 'fabric' refers to the spatial orientation of the elements of which a rock is composed (American Geological Institute, 1957). As applied to sedimentary rocks, fabric includes the a-axis (long axis) orientation of grains, and the angle of imbrication, with a-axis or b-axis (intermediate axis) dipping upstream. Grain fabric depends upon many factors, including: 1) mode of deposition of the grains; 2) grain size, shape and roundness; 3) sorting of the sediment being deposited; 4) boundary conditions on the bed at the time of deposition, especially bed roughness factors and bed slope.

In many clast-supported conglomerates and pebbly sandstones, of both terrestrial and marine origin, there is a lack of useful sedimentary structures. Commonly, the only clue to the nature and the direction of the depositing currents lies in the orientation of the individual grains -- the sedimentary fabric. For this reason, detailed fabric studies were done in the coarser Cap Enragé sediments (which lacked other paleoflow features) to discern possible mechanisms and environments of deposition, as well as broad-scale paleocurrent patterns.

In this chapter, the results of the fabric and size analyses are presented. These studies were done on material from coarse conglomerate, pebbly sandstone and sandstone beds. Detailed methods used in field

sampling, field measurement and laboratory methods are given in Appendix 2 . Methods will only be discussed briefly in this chapter.

Stereonet plots and summary statistics of the conglomerate fabric data are given in Appendix 6 . Rose diagrams and summary statistics of the pebbly sandstone and sandstone fabrics are presented in Appendix 7 . Grain size cumulative frequency curves and summary statistics for the pebbly sandstone and sandstones that were studied are in Appendix 8 .

CONGLOMERATE FABRIC

Methods

Strike and dip measurements of the apparent "ab-planes" of individual clasts were measured within conglomerate and fine conglomerates in the field. Within each bed, the orientation of 100 clasts was measured. The field orientation of the clasts was then rotated back to the horizontal (correcting for regional dip of beds) and summary statistics were calculated, using computer facilities. Original, corrected to horizontal, stereonet plots of conglomerate fabrics were drawn by computer plotter routines.

To date, few studies have dealt with the analysis of three-dimensional fabric in deep-sea conglomerates (Davies and Walker, 1974; Johnson, 1974; Rocheleau and Lajoie, 1974; Walker, 1975a; 1975b; in Harms et al, 1975; 1977). In his discussion of conglomerate fabrics, Walker (1977) discusses the fabric in terms of the following statistics: three-dimensional vector mean dip; the semi-angle cone of the three-dimensional vector mean; the semi-angle of confidence of the vector mean azimuth. In addition, (although not used by Walker, 1977) the estimate of the precision constant 'k' gives a measure of the dispersion of the

distribution.

Summary Statistics of Clast Orientation Patterns

The statistics that were used in Walker's (1977) study and in this project, are summarized by Irving (1964) and Nederlof and Weber (1971). These statistics will only be briefly described here. A list of notation and abbreviations for the text is given in Appendix 1 .

The three-dimensional vector mean is the average attitude of a given set of poles to planes (in this case, the 'ab planes' of individual clasts in a bed). The uncertainty of this vector mean is a function of the sample size and the variance of the parent population. In the analysis of three-dimensional data, this uncertainty can be described by an estimate of the "semi-angle of the confidence cone" of the vector mean, at a given probability level. In this study, a 95% confidence level was used. The estimate of the "semi-angle of confidence" of the azimuth gives the spread of the confidence cone of the three-dimensional vector mean, as projected upon a two-dimensional surface (the "xy-plane", in this case the "EW-NS plane of the earth, excluding the up direction) (see Nederlof and Weber, 1971). The precision constant "k" is also a measure of the uncertainty of the vector mean. Unlike the semi-angle of the confidence cone, k is not a function of sample size. Fisher (1953) presents a method for handling data that have positions on a sphere. The parameter "k" determines the precision of the point distributions on a sphere. If points are randomly distributed, $k = 0$; if points are clustered into a small region of the sphere, k is very large.

Two parameters describe the dip of the imbrication planes ("ab-planes") of the clasts: the absolute dip average and the three-dimensional vector mean dip. The absolute dip average is the mean of the angles of dip of the imbrication planes, as measured from the horizontal, regardless of the direction of dip. The three-dimensional vector mean dip is defined as follows:

$$(2) \quad \delta_{xyz} = \arctan (R_{xy} / R_z), \text{ where}$$

R_{xy} is the vector sum in the xy (NS-EW plane) plane and R_z is the vector sum in the vertical (up) or z plane.

Results

Strike and dip measurements were made of "ab planes" of 100 clasts in each of 45 beds in the field. Locations of the beds in which the fabric was measured are indicated in Appendix 6, Summary Statistics Table, and on the logged section diagrams, Appendix 5. Stereonet plots of the conglomerate fabric, rotated about strike back to the horizontal, are illustrated in Appendix 6. Summary statistics pertaining to these stereonet plots are listed in Appendix 6. Field methods are discussed in Appendix 1. Field observations indicated an a-axis upstream imbrication. Fabric measurements were done in clast-supported conglomerate and fine conglomerate units. These units may have comprised a whole conglomerate bed, or consisted of basal conglomerate units of beds, that were graded from conglomerate, at the base, to pebbly sandstone and sandstone, at the top. Beds in which the fabric was measured can be classed, generally, as belonging to Facies (1), although some beds belong to Facies (2), (3) and (4) (see logged sections, Appendix 5).

Individual conglomerate units fall into three categories:

1) poorly organized or disorganized conglomerates, which are ungraded or inversely graded; 2) structureless graded conglomerates; and, 3) normally graded conglomerates which show stratification in finer-grained, upper bed portions. Most of the conglomerates, in which the fabric was measured, are graded-bed conglomerates (31), with less common occurrences of disorganized (10) or graded-stratified (8) conglomerates.

In the following section, the fabric results will be discussed in terms of: absolute dip average, three-dimensional vector mean dip, and uncertainties of the vector mean, in relation to type of conglomerate, grain size and thickness of conglomerate units.

(1) Absolute Dip Average of Imbrication Planes

Due to the small sample size of different conglomerate types, it was impossible to test if there was a significant difference in the absolute dip average amongst the different conglomerate types. No significant correlation ($r = +0.24$) exists between the absolute dip average and the grain size of the conglomerate units. Similarly, no significant correlation was found between absolute dip average and conglomerate unit thickness ($r = +0.42$).

(2) Three-dimensional Vector Mean Dip (δ)

The three-dimensional vector mean dip values range from 2.7° to 30.2° . Over 25% of the plots (13 plots) have three-dimensional vector mean dip values less than 10° . This is particularly disturbing because none of the stereonet plots (Appendix 6) have girdles, dipping less than 10° . There is insufficient data to test if the three-dimensional vector mean dip varies with conglomerate type. Plots of the three-

dimensional vector mean dip versus grain size or conglomerate thickness are extremely scattered and no correlation coefficients (r values) were calculated.

(3) Semi-angle Cone of Confidence of the Vector Mean

Insufficient data exists to test if there is a significant difference in the values of this parameter ($\hat{\theta}$) amongst the disorganized, graded and graded/stratified conglomerates. No significant correlation ($r = +0.002$) exists between $\hat{\theta}$ and the grain size of the conglomerate unit. Similarly, no significant correlation was found between $\hat{\theta}$ and conglomerate unit thickness ($r = +0.4$).

(4) The Precision Constant (\hat{k})

There was insufficient data to test if there was a significant difference in the \hat{k} values amongst the different conglomerate types. Plots of \hat{k} values versus grain size or conglomerate thickness are extremely scattered and no correlation coefficients (r values) were calculated.

(5) Semi-angle Cone of Confidence of the Vector Mean ($\hat{\theta}$)

Versus the Absolute Dip Average of Imbrication Planes

A strong positive correlation ($r = +0.93$) (Fig.46) exists between the semi-angle of the cone of confidence of the vector mean ($\hat{\theta}$) and the absolute dip average of the clasts. A similar relation was noted by Walker (1977) for $\hat{\theta}$ values versus the three-dimensional vector mean dip, for deep-sea conglomerates in Oregon. This high degree of correlation between these two parameters is somewhat suspect in the present study. It is disturbing that this plot has such a high correlation coefficient, whilst all of the other plots are not signifi-

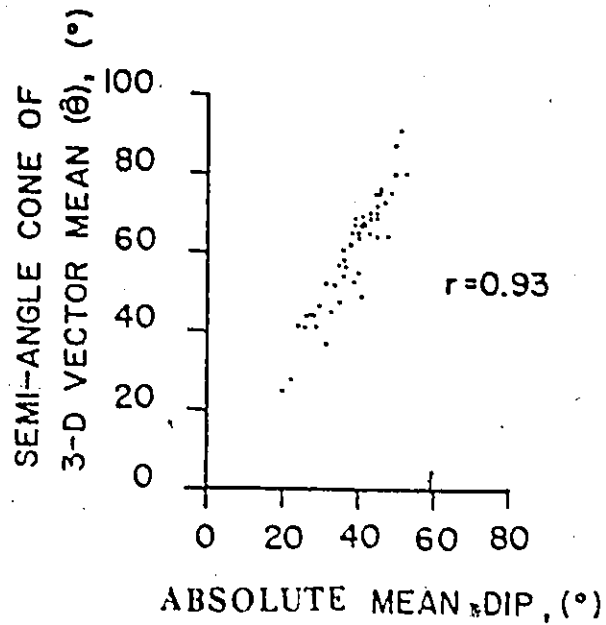


Fig. 46 - Graph illustrating the strong correlation between the semi-angle cone of the three-dimensional vector mean (95% confidence level) and the absolute mean dip. r = correlation coefficient. The definition of the semi-angle cone of the three-dimensional vector mean (see Nederlof and Weber, 1971) indicates that there may be some autocorrelative interaction between these variables.

cant, with very low correlation coefficients or extremely scattered plots.

Discussion

Most of the parameters describing the conglomerate fabric bear no relation to the grain size nor thickness of the conglomerates. Two puzzling results are evident from these conglomerate fabric studies:

1. Low three-dimensional vector mean dips (10° or less) can result from distributions, whose stereonet plots do not show girdles dipping at 10° or less; and,
2. A high correlation coefficient suggests that a strong relation exists between the semi-angle cone of the 3-D vector mean and the absolute mean dip. Ordinarily, one would be delighted with such a good correlation, but the fact that all other plots are not significant and this one is very significant, sheds some doubt upon this correlation.

(1) Three-dimensional Vector Mean Dip (δ)

At first glance, one would think that the δ measure of imbrication would more adequately portray the average orientation of a given set of planes, as compared with the absolute dip average. The problem with δ is that it takes into account direction as well as absolute deviation from the horizontal, in describing the average imbrication. Consequently, very low δ values can result from two entirely different orientation patterns: 1) those populations which have clasts dipping at near-horizontal angles; and, 2) those populations which have clasts dipping at high angles, but in opposite directions.

In the first case, all clasts have very low dips (near horizontal). The vector sum R_{xy} will have a certain value, depending upon the spread of the a-axis orientations in bedding. The vector sum R_z will always tend to be very large. Unless there is a constant orientation of the a-axes in bedding, the resulting quotient (R_{xy} / R_z) will be a small number. The three-dimensional vector mean dip (δ_{xyz}) will also be a low value.

In the second case, clasts have imbrication planes which dip in opposite directions (Fig. 47). The dip angles need not be low. If clasts have imbrication planes which strike in the same direction, but dip in opposite directions, a very low δ_{xyz} value will result (Fig. 47). The resulting vector sum R_z is large, whilst the vector sum R_{xy} has a very small magnitude. As in case (1), the resulting quotient (R_{xy} / R_z) will be a small number. The three dimensional vector mean dip (δ_{xyz}) will also be a low value.

This problem of low, three-dimensional vector mean dips, resulting from different orientation patterns suggests that this parameter (δ_{xyz}) is an inadequate representation of "average dip" for populations, which have clasts dipping at various angles (as in the present study). It is not a sufficient measure of average dip of pebbles in beds that show poor, or scattered, distributions on stereonet. It may be an adequate measure of the average dip of a population if the clasts show a well-ordered, clustered distribution.

The value of using three-dimensional orientations of clasts within conglomerate beds lies in the fact that individual pebbles can be measured in the field. It is quite often very difficult to obtain an adequate sample of a conglomerate bed for future analysis in the

laboratory. Also δ_{xyz} values do not affect the three-dimensional measures of dispersion, nor the orientation of the vector mean azimuth. So, although the statistical analysis of the conglomerate imbrication has been reduced to two dimensions (by using the absolute dip average) the original measurement of the three-dimensional clast orientations is justified.

The δ_{xyz} values do, however, affect the semi-angle of confidence of the vector mean azimuth. On a two-dimensional representation it is impossible to adequately portray the three-dimensional range of the uncertainty of the vector mean. For this reason, $\hat{\theta}_L$ is commonly used to show this uncertainty on two-dimensional maps or section diagrams. However, $\hat{\theta}_L$ is a function of both $\hat{\theta}$ and δ_{xyz} (see Nederlof and Weber, 1971). The previous discussion pertaining to the problems of using δ_{xyz} with scattered pebble plots suggests that some $\hat{\theta}_L$ values may also be spurious. Hence, in beds that show poor or scattered distributions on stereonet plots, only the semi-angle cone of confidence of the three-dimensional vector mean ($\hat{\theta}$) and estimates of the precision constant (\hat{k}) can be used as measures of the scatter of the distribution.

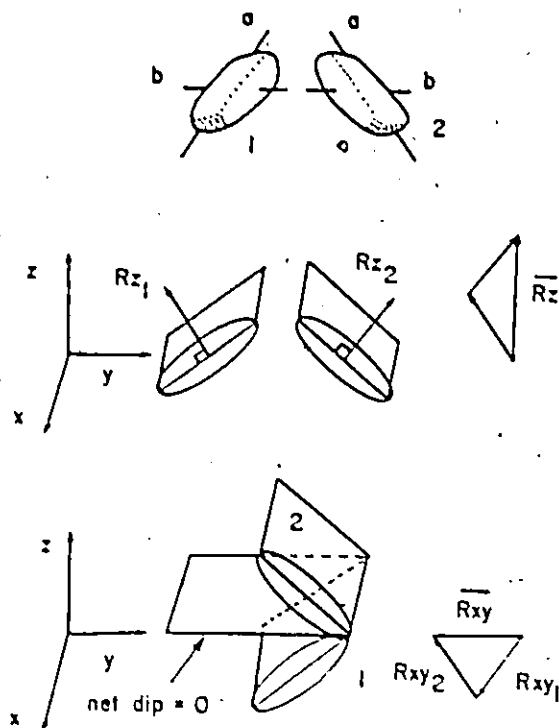


Fig.47 - Schematic representation of vectorial sums R_z and R_{xy} of clasts with the same strike but opposite dips.

Summary of Conglomerate Fabric Results

1. Field observations indicated that the conglomerate fabric within the beds measured in this study was a-axis imbricate upstream, a-axis parallel to flow (by comparison with other conglomerate paleoflow data).
2. Parameters indicating the scatter of three-dimensional orientations ($\hat{\theta}$ and \hat{k}) and the absolute mean dip show no relations to grain size nor thickness of the conglomerates.
3. Plots of $\hat{\theta}$ versus δ_{xyz} and plots of $\hat{\theta}$ versus absolute dip average may have a certain autocorrelative influence.
4. In distributions which have scattered stereonet plots, with clasts dipping in opposite directions, estimates of δ_{xyz} and $\hat{\theta}_\alpha$ may be spurious.

PEBBLY SANDSTONE AND SANDSTONE FABRIC

Methods

In the study of sandstone fabric, two preferred grain orientations are important: the a-axis fabric in bedding and the imbrication pattern, measured in a plane cut perpendicular to bedding. In beds that have a-axis parallel to flow, a-axis imbricate upstream orientations (Fig. 49, Case 1), grain measurements in a plane cut perpendicular to bedding, in a direction parallel to the preferred a-axis direction (in bedding), will yield imbrication information. In beds that have a-axis perpendicular to flow, b-axis imbricate upstream (Fig. 49, Case 2), grain measurements in a plane cut perpendicular to bedding, in a direction perpendicular to the preferred a-axis direction (in bedding), will yield the imbrication information.

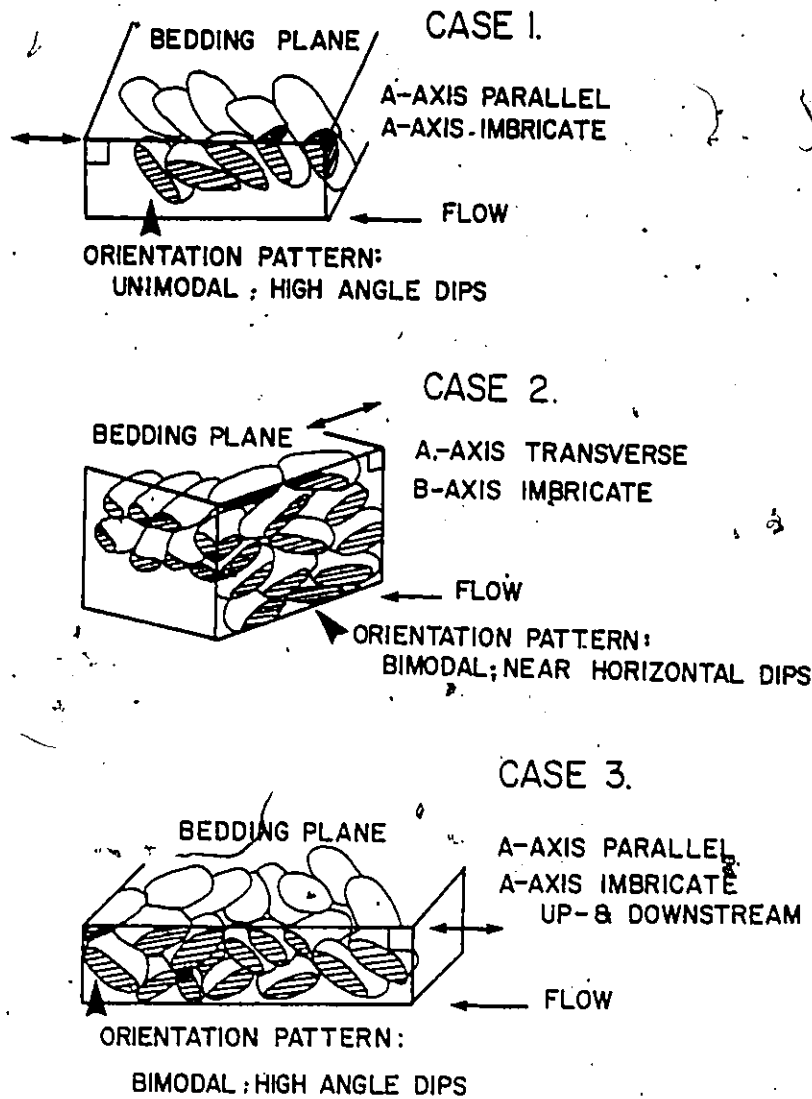


Fig.49 - Imbrication patterns in sections cut parallel to preferred a-axis in bedding for different original sedimentary fabrics.

One has no a priori way of knowing whether a sandstone will possess an a-axis parallel to flow or a-axis perpendicular to flow fabric. Thus, the imbrication cuts were initially done in a direction parallel to the preferred a-axis direction in bedding. Imbrication patterns vary according to the type of original fabric pattern (Fig.49). Thus, by examining the grain orientations in both bedding and imbrication planes, one can ascertain the original sedimentary fabric.

Most workers who study sandstone fabric, conduct this analysis in thin section. In the present study, a method similar to that used by Hiscott (1977) was employed. Details of the measurement and preparation techniques are given in Appendix 2. Briefly, acetate peels were made of stained, cut and polished surfaces of oriented sandstone and pebbly sandstone samples. Orientations of apparent a-axes of 100 grains were measured on enlarged photographs, made from the acetate peels. Thus, for each sample, 200 grains were measured: 100 grains in the bedding plane, and 100 grains in the imbrication plane.

Rose diagrams were made of each of the bedding plane plots. These plots were separated into those which showed bimodal patterns and those which did not show bimodality. The criterion used for bimodality is discussed in Appendix 2. For those beds which had bimodal plots, the imbrication cut was made in a direction parallel to the dominant mode of the bimodal pattern, as observed in bedding. For those beds which did not show bimodality, two-dimensional vector mean azimuths were computed (Curry, 1956). For samples with good a-axis bedding patterns, poor a-axis bedding fabrics, and random a-axis bedding fabrics, the imbrication cut was made in a direction parallel to the computed

vector mean. Vector mean azimuths computed from random or poor unimodal patterns may not have real meaning. The computed vector means, however, provided a standard and arbitrary direction in which to cut the imbrication slabs in beds that had random or poor unimodal bedding fabrics.

Summary Statistics of Clast Orientation Patterns

Standard statistical methods were used to analyze the bedding and imbrication patterns. The following statistics are important: the vector mean direction, significance level of the distribution (based upon the Tukey χ^2 test), the vector strength (L%) (which indicates the amount of scatter of the pattern), and the standard deviation (σ).

Bedding plane fabric data is "line of motion" (or 180° data), in that only a sense of the flow is indicated. Imbrication data is oriented, with respect to the horizontal a-axis preferred direction in bedding. Imbrication data is, therefore, considered to be vectorial (or 360°) data. Methods for computation of the statistics of both 180° and 360° data are given by Curray (1956). These computations were only done on the samples that did not have bimodal orientation patterns.

Results

Oriented hand-specimen samples of pebbly sandstones and sandstones were taken from 95 beds for fabric analysis in the laboratory. Locations of the beds from which samples were taken are indicated in Appendix 7, Summary Statistics Table, and on the logged section diagrams, Appendix 5. In 13 beds, samples were taken at various intervals within the same bed. Bedding fabric patterns were done on 116 samples. Of the 95 beds, imbrication plots were done on 71. Rose diagrams

of individual measurements for bedding fabric and imbrication studies are given in Appendix 7. Summary statistics for bedding plane fabric patterns and imbrication patterns are also all listed in Appendix 7, just prior to the respective fabric and imbrication rose diagrams.

Fabric measurements were done in samples from units that may have comprised whole sandstone beds, or consisted of certain levels within beds that were graded from conglomerate to sandstone. Beds in which the fabric was measured are classed as belonging to primarily Facies (3) and (4); less commonly beds belong to Facies (1), (2) and (6). Rarely were Facies (7) beds measured. Fabric was not measured within the cross-stratified beds of Facies (5). Individual sandstone units from which the samples were taken fall into four categories: 1. dispersed pebbly sandstones; 2. liquefied sandstones; 3. stratified sandstones; and, 4. massive (or structureless) sandstones.

In the following section, the fabric results will be discussed in terms of the type of orientation pattern, clast dip and uncertainties of the vector mean. These aspects of the orientation patterns will be related to the type of sandstone unit, grain size and thickness of the units. Paleoflow patterns, as determined from the fabric and imbrication patterns, will be discussed in conjunction with the paleocurrent patterns of the conglomerate beds in the final Chapter 6.

(1) Orientation Patterns of Bedding Plane Fabric

Four types of orientation patterns are recognized: 1. Bimodal (as determined from rose diagrams, see Appendix 2); 2. Random: significance level = 1.0 - 0.2 (χ^2 test); 3. Unimodal: significance level:

0.2 - 0.05 (χ^2 test); and, 4. Well-developed Unimodal: significance level = less than 0.05 (χ^2 test).

A summary of the type of orientation pattern for the different sandstone types is given in Table 5. Dispersed, liquefied and massive units have about equal proportions of random, bimodal and unimodal patterns. Unimodal patterns within dispersed and liquefied units are well developed (significance level = less than 0.05); less commonly they are not as well developed (significance level = 0.2 - 0.05) (Table 5). In massive units, the unimodal patterns are not as well developed (significance level = 0.2 - 0.05); less commonly, they are well developed. Stratified units have predominantly unimodal patterns, less commonly bimodal and rarely random patterns (Table 5). The unimodal patterns are usually well-developed, less commonly not so well developed.

All of the samples with bimodal a-axis orientation patterns were re-examined to determine whether the grain size of the clasts was influencing the orientation pattern. The orientation of the 25 largest clasts within each enlarged photograph was noted. In 47 % of the bimodal plots, the largest grains aligned parallel with the dominant mode of the bimodal distribution. In 31 % of the bimodal plots, the largest grains fell within the secondary mode. In 22 % of the bimodal plots, the largest grains were oriented between the two modes. All of the bimodal plots from stratified sandstones (7 samples) had the largest grains parallel to the secondary mode. Those bimodal plots from dispersed, massive and liquefied sandstones had the largest grains usually parallel to the main mode; less commonly, in the secondary mode or between them.

TABLE 5

BEDDING PLANE FABRIC AND IMBRICATION PATTERNS FOR DIFFERENT FACIES

Facies	N	Bedding Plane Fabric Patterns		Unimodal Facies		Imbrication Patterns				
		% Random	% Bimodal	% V. Good	% Good	Avg. L%	Avg. L%	N Unimodal	N Bimodal	
Dispersed	47	38	34	19	9	20.05	12.44	30	37	63
Liquefied	27	33	37	26	4	21.71	14.35	13	54	46
Massive	19	37	32	5	26	15.24	11.37	9	78	22
Stratified	23	9	30	48	13	22.37	20.21	19	47	53

Dispersed: Facies (3); Liquefied: Facies (4); Massive: Facies (6); Stratified: Facies (2)
 V. Good Unimodal: Significance Level less than 0.05; Good Unimodal: Significance Level: 0.2 - 0.05;
 Random: Significance Level: 1.0 - 0.2. L%: vector strength, vector magnitude expressed in percent.

(2) Imbrication Patterns

Two types of imbrication patterns are recognized: 1. Unimodal Patterns, with high dips (average dip = 36° ; range: 15° - 60°); and, 2) Bimodal Patterns, with a dominant mode and high dips (average dip = 31° ; range: 5° - 65°). A summary of the imbrication patterns for the different sandstone types is given in Table 5. Dispersed sandstones show mainly bimodal imbrication patterns. Liquefied and stratified sandstones tend to have about equal proportions of bimodal and unimodal imbrication patterns. Most of the massive sandstones display unimodal imbrication patterns. No grain size influence was seen in bimodal plots.

(3) Modal Angle of Imbrication

In the analysis of the imbrication patterns, which showed a unimodal distribution, a vector mean was computed (Curry, 1956) for vectorial (360°) data. This vector mean tends to have a very high value for all of the samples, with an average imbrication dip of 76° . Examination of the rose diagrams for the imbrication plots (Appendix 7) shows, however, that most of the clasts do not dip at such high angles. The problem arises from the fact that the clasts (even those belonging to unimodal distributions) may have some components of the distribution which dip in a downstream direction, resulting in a net vectorial dip which is greater than the dip of most of the individual clasts. Consequently, it is thought that the "modal angle of dip" would more accurately depict the average dip of the individual clasts. This modal angle of dip is taken as the midpoint of the largest mode in the rose diagram of each imbrication plot.

Modal dips for the bimodal plots and unimodal distributions are tabulated in Appendix 7 . The average modal dip for the unimodal imbrication plots is 36° . In the bimodal imbrication plots, the modal dip of the strong mode averages 33° , whereas the weak mode has an average modal dip of 29° .

There is no relationship between the modal angle of dip and sandstone thickness nor grain size for any of the different sandstone types. There is insufficient data to test if there is any significant difference between the modal angle of dip as noted amongst the different sandstone types.

(4) Vector Strength of the Vector Mean

The vector strength of the vector mean is a measure of the scatter of the distribution, and is the magnitude of the resulted vector mean, expressed in per cent (Curry, 1956). These can only be calculated for unimodal patterns.

No relationships were found between the bedding or imbrication vector strengths versus sandstone thickness or grain size. No relationship exists between the vector strength in bedding and the vector strength in the imbrication plot. These plots are extremely scattered and no correlation coefficients were calculated.

A negative correlation ($r = -0.67$) exists between the vector strength of the bedding vector mean and the modal angle of dip (Fig. 50). A positive correlation ($r = +0.61$) exists between the vector strength of the imbrication vector mean and the modal angle of dip (Fig. 50). These relations suggest that at high modal angles of imbrication, bedding plane orientations have low vector strength values, suggesting a high amount

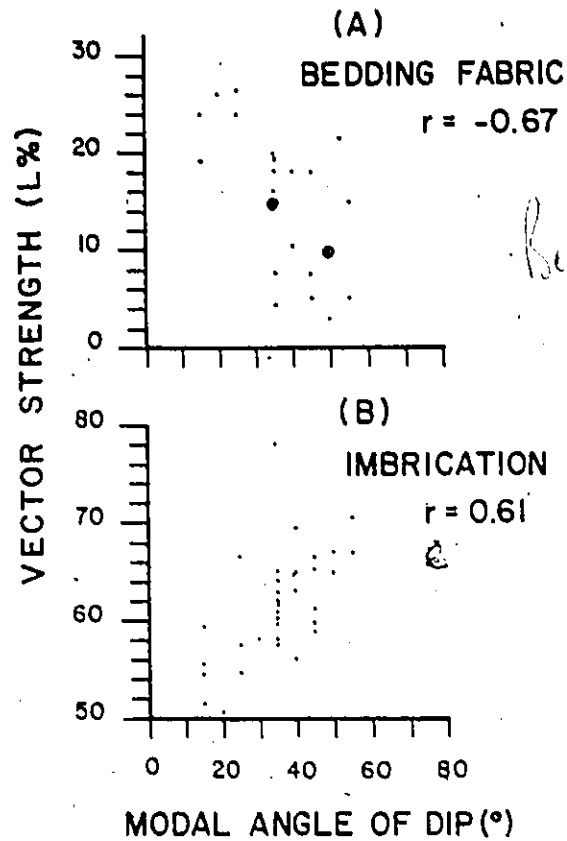


Fig.50 - Graphs of modal angle of dip vs. vector strength of bedding fabric pattern (upper plot) and imbrication fabric pattern (lower plot). r = correlation coefficient.

of scatter. As modal angles of imbrication decrease, the vector strength values become larger, suggesting a better-ordered distribution. The reverse trend occurs in imbrication plots: the amount of scatter of the imbrication plots decreases, as the modal angle of imbrication increases.

Summary of Sandstone and Pebbly Sandstone Fabric Results

1. Dispersed, liquefied and massive sandstones have about equal proportions of random, bimodal and unimodal patterns in bedding. Unimodal patterns are well developed within dispersed and liquefied sandstones, whilst in massive sandstones they are not so well developed. Stratified sandstones have well developed unimodal patterns in bedding, less commonly bimodal patterns in bedding.
2. Bimodal bedding plots from stratified sandstones had the largest grains parallel to the secondary mode. Those bimodal bedding plots from dispersed, massive and liquefied sandstones had the largest grains usually parallel to the main mode; less commonly, in the secondary mode or between them.
3. Dispersed sandstones have mainly bimodal imbrication patterns. Liquefied and stratified sandstones tend to have about equal proportions of bimodal and unimodal imbrication patterns. Massive sandstones have unimodal imbrication patterns. No grain size influence was seen, where largest clasts dip both up- and downcurrent, in bimodal imbrication plots.
4. No relationship exists between modal angle of dip and sandstone thickness nor grain size for any of the different sandstone types. Such plots have widely scattered patterns.
5. Vector strengths of bedding and imbrication plots bear no relation

to each other, nor to sandstone thickness nor grain size.

6. Bedding plane orientation patterns are more scattered in beds which have high modal angles of imbrication; conversely, bedding plane orientation patterns become better developed in beds which have low modal angles of imbrication.
7. Imbrication plane orientation patterns are more scattered in beds which have low modal angles of imbrication; conversely, imbrication plane orientation patterns become better developed in beds which have high modal angles of imbrication.

GRAIN SIZE ANALYSIS

Just as the processes of deposition influence the fabric of a sediment, these processes are also thought to leave an imprint upon the distribution of grain sizes within the sediment. For this reason, there has been much work in sedimentology trying to relate characteristics of grain size distributions to depositional mechanisms and environments.

In the present study, grain size analyses were conducted on samples from different sandstone types, including liquefied, dispersed, stratified, stratified: B-division of classical turbidites, and massive types. With the exception of the B-division turbiditic samples, the rest of the samples were obtained near the base of beds.

Detailed methods of field sampling and laboratory measurement are given in Appendix 2 .

Results

Grain size analyses were done for 26 samples. Replicate measurements by an independent operator were done for 4 samples. Summary statistics and cumulative frequency curves are given in Appendix B. Comparisons of the replicate measurements, by independent operators, of identical thin sections, show that the curves are not repeatable.

Problems in consistency of measurements arise in estimates of the coarsest one-percentile and in estimates of the inclusive graphic skewness (Sk_T). This is thought to be due to two factors: 1. Most of the samples show moderate or poor sorting. Inhomogeneity with samples with the uneven distribution of scattered coarse grains may partially account for these inconsistencies. 2. Many of the smaller grains, especially the unstable rock fragments, are partially or wholly recrystallized (Chevalier, 1977), making estimates of the finer portions difficult. Another characteristic of the grain size curves seems to be an artifact of the measurement technique. Examination of the cumulative frequency curves (Appendix B) suggests that most of the samples show a paucity of grains in two grain size classes: 2.5 ϕ to 2.75 ϕ and 3.75 ϕ to 4 ϕ . It was discovered, subsequently, that it is difficult to distinguish grains within the 2.5 ϕ and 2.75 ϕ classes from one another, and the 3.75 ϕ and 4 ϕ from one another. Consequently, these low values on the grain size curves are thought to be due to measurement error and not due to depositional processes nor to be a function of sediment supply.

Results from the grain size analyses are not very encouraging. Liquefied, massive and stratified sandstones all tend to be positively (fine) skewed or have near-symmetrical or symmetrical distributions.

Dispersed sandstones tend to be near-symmetrical or negatively (coarse) skewed. Most of the liquefied, massive and stratified samples show moderate sorting. Dispersed sandstones tend to be poorly sorted. No relationship was found between the inclusive graphic standard deviation (σ_I) and the vector strength (L%) of the fabric for any of the sandstone types.

Passaga (1957,1964) found that depositional environments (and the different dominant depositional mechanisms) could be distinguished by plotting the coarsest one-percentile (C) versus the median grain size (M). One advantage of this plot is that it used the coarsest and median percentiles, which were most-likely unaffected by diagenesis. It was hoped that C-M plots in the present study would be useful in distinguishing different mechanisms of deposition for the different sandstones. However, no trends were evident from these C-M plots in the present study.

In fluvial sediments grain size distributions show straight line segments when plotted on probability paper (Middleton,1976), which are thought to represent different subpopulations of grains moved by different transport processes. Visher (1978,pers. comm., SEPM Research Colloquia: Turbidites, AAPG-SEPM Annual Convention) has recently tried to apply these ideas to mass flow deposits. However, these ideas cannot be applied to mass flow deposits. Shape of the grain size curves in mass flows is not a function of processes of transportation, but rather a function of the source material supply. In the fluvial sediments the subpopulations develop as a result of the relative magnitudes of the settling velocities of the grains and the shear

velocities of the stream (Middleton, 1976). This determines whether a grain will be transported by traction or intermittent suspension. Nothing is known about liquefied flow velocities, if they even exist. Velocities of debris flows vary with the water content of the flow. Deposition from mass flows is a consequence of freezing of the mass flow, due to loss of inertia and due to the effect of gravity (Middleton, 1970). Consequently, the shape of grain size distribution curves from mass flow deposits are no help in trying to ascertain depositional mechanisms, as in the fluvial case (Middleton, 1976).

CHAPTER 5

DEPOSITIONAL MECHANISMS FOR DIFFERENT FACIES

SEDIMENTATION OF DEEP-SEA COARSE CLASTIC DEPOSITS

Coarse grained sediment is thought to be deposited into deep-sea basins by a variety of gravity-induced mechanisms, including submarine slumps, slides and sediment-gravity flows. Material within the Cap Enragé sediments seems to have been transported as individual grains within flows, as opposed to en masse transportation of large blocks of sediment masses (as in slumps and slides). For this reason, in the following section only sediment-gravity flow mechanisms will be discussed.

Middleton and Hampton (1973) proposed that there are four "end members" of subaqueous gravity flows, classed on the basis of the dominant sediment support mechanism: 1) turbidity currents (support by fluid turbulence), 2) fluidized sediment flows (support by the upward flow of a fluid escaping from the sediment-water dispersion), 3) grain flows (support by dispersive pressure); and, 4) debris flows (support by strength of a muddy matrix). More recently, Lowe (in prep.) has revised gravity flow classification and nomenclature (Table 6). In this classification, Lowe (in prep.) suggests that gravity flows are separated on the basis of flow behaviour. Debris flows are separated as a rheological group, in which debris flows are sediment-gravity flows of Coulomb viscous or Bingham substances. The

TABLE 6

CLASSIFICATION OF SEDIMENT-GRAVITY FLOWS

(from Lowe, in prep.)

Flow Behaviour	Flow Type		Sediment Support Mechanism
Fluid	Fluidal Flow	Turbidity Current	Fluid Turbulence
		Fluidized Flow	Escaping Pore Fluid (Full Support)
Plastic (Bingham)	Debris Flow	Liquefied Flow	Escaping Pore Fluid (Partial Support)
		Grain Flow	Dispersive Pressure
		Cohesive Flow	Matrix Strength Matrix Density

strength of the flow originates from cohesive forces (cohesive flows containing clays) or from frictional grain interactions (grain flows). Liquefied and fluidized flows have low strength and are somewhat transitional between debris flows and fluidal flows (Lowe, pers. comm. and in prep.).

Coarse sediment is usually transported into deep-sea basins by turbidity currents or debris flows (see reviews by Kuenen(1964) and Hesse (1975); Middleton,1978). At the time of deposition, however, other gravity flow mechanisms may predominate, yielding characteristic sediments which differ significantly from classical turbidites or debris flow deposits (Davies and Walker, 1972; Hiscott,1977; Howell and McLean,1976; Hubert et al,1970; Kruit et al,1972; Middleton and Hampton 1973, 1976 ; Walker,1975,1978; Lowe,1975; Lowe and LoPiccolo,1974).

Turbidity currents may originate as part of a continuum of subaqueous mass movements from submarine landsliding to turbidity current flow (Cook et al,1972; Dott,1963; Kuenen,1952; Morgenstern,1967; Heezen and Ewing,1952). This process is understood to a certain degree. The transition from submarine landsliding to debris flow (or other mass flows) involves a change in the physical state of the sediment. At the time of mobilization of the sediment, there is a breakdown of the metastable grain packing, as well as liquefaction or fluidization in some flows (Andresen and Bjerrum,1967; Moore,1961; Shepard and Dill,1966). During mass flow movement the transition from subaqueous debris flow to turbidity current flow involves extensive dilution of the flow as a natural consequence of the debris flow moving downslope in a fluid medium (Hampton,1972). Turbidity currents can also result from the input

of sediment-laden flood waters from fluvial systems feeding and funneling down submarine canyons (Fleischer, 1970; Heezen et al, 1964; Malouta, 1978; Shepard, 1978; Shepard and Emery, 1973; Stow, 1977).

The flow mechanics involved in transport and deposition of sediment from turbidity currents are not so well understood as those involved in the generation of the currents. As demonstrated experimentally (Middleton, 1967) and from field evidence (Skipper and Middleton, 1975), several different gravity flows (other than turbidity currents) may operate together, or at different times, during deposition of sediment from single flows (Hiscott, 1977; Krause and Oldershaw, 1978; Middleton, 1978; Skipper and Middleton, 1975; Walker, 1976; Davies and Walker, 1972; Sadler, in prep).

As mentioned in the introductory chapter, Middleton and Hampton (1973, 1976) have proposed a conceptual model (Fig. 5) that shows the dynamic relations of flow processes that are operative for submarine mass flows. This conceptual model seems to work for the spatial distribution of very coarse grained mid-Miocene deep-sea sediments on Santa Cruz and Santa Rosa Islands, California Borderland (Howell and McLean, 1976). This model has not yet been generally applied to finer-grained conglomerates, pebbly sandstones and sandstones.

In the following chapter, each of the eight lithofacies described in the previous Chapter 2 are discussed in terms of possible depositional mechanisms. Emphasis will be placed on the origins for individual beds. The discussion will rely on field evidence, as well as fabric and imbrication patterns. Flow mechanisms will be discussed in light of the classification of Lowe (in prep.) (Table 6) and the conceptual

model of Middleton and Hampton (1973,1976) (Fig. 5). Clues to the depositional mechanics lie in the grain fabric and imbrication, in the type(s) of grading, and in the sequences of sedimentary structures. To avoid repetition, implications of these different features will be presented first. This is followed by an interpretation of the depositional processes for each of the facies.

HYDRODYNAMIC IMPLICATIONS OF MAJOR SEDIMENTARY FEATURES

Implications of clast fabric and imbrication patterns are based upon theoretical and experimental work, as well as empirical data. Theoretical and experimental work has dealt mainly with sand-size material, with the exceptions of Lindsay's (1968) study (which dealt with the theoretical development of fabric in pebbly mudstones) and Johansson's (1963,1965,1976) experimental work (clast orientations of pebbles and pebbly sands) (Table 7). Empirical data on grain orientations in deep-sea sediments have been obtained by many workers (Table 7). Most of these studies have dealt with fabric in deep-sea conglomerates or in classical turbidites. Few studies have examined grain orientations in massive sandstones, which are not obviously turbiditic in origin (Table 7).

Two main types of grading are generated in fine-grained density currents: 1) distribution grading, in which the whole grain size distribution of a sediment becomes shifted toward the coarser or finer sizes; and, 2) coarse-tail grading, in which only the size of the coarsest few percentiles of the distribution change (Middleton,1966). Implications of these grading types, as determined from experimental results, are discussed by Middleton (1967,1970). In general, studies of deep-

TABLE 7

REPORTS DEALING WITH CLAST FABRIC

<u>Theoretical and Experimental</u>	<u>Empirical-Deep-sea Conglomerates</u>	<u>Empirical-Deep-Sea Pebbly Sandstones and Sandstones</u>
Dapples and Rominger, 1945	Aalto and Dott, 1970	<u>Classical Turbidites (< 1 m thick)</u>
Jeffrey, 1922	Aalto, 1972	Colburn, 1968
Johansson, 1963, 1965, 1976	Breaky, 1975	McBride and Kimberly, 1963
Kelling and Williams, 1967	Cook et al, 1972	Ksiazkiewicz, 1952
Koster, 1977	Davies and Walker, 1974	Kuonen and Carozzi, 1953
Lindsay, 1968	DeLong, 1977	Parkash and Middleton, 1968
Rees, 1968	Eder, 1970	Scott, 1966
Rusnak, 1957	Engel, 1970	Smoor, 1960
Rukavina, 1965	Fisher and Mattinson, 1968	Stanley, 1963
Schwarzacher, 1951	Harms, 1974	Taira, 1976
Taylor, 1923	Helwig and Sarpi, 1969	<u>Massive Sandstones (1-2 m thick)</u>
Taira, 1976	Hendry, 1972, 1973, 1976	Bouma, 1962
	Hubert et al, 1977	Hand, 1961
	Johnson, 1974	Onions and Middleton, 1968
	Johnson and Walker, in prep.	<u>Thick Massive Sandstones (> 2 m thick)</u>
	Marschalko, 1964	Hiscott, 1977
	Mutti, 1969	Sestini and Pranzini, 1965
	Mutti and Ricci Lucchi, 1972	
	Nilson and Simoni, 1973	
	Piper, 1970	
	Ricci Lucchi, 1969	
	Rocheleau and Lajoie, 1974	
	Rust, 1966	
	Scott, 1966	
	Srivastava et al, 1972	
	Thompson and Thomsson, 1969	
	Unrug, 1963	
	Walker, 1975a, 1975b, 1977	

sea sandstones and pebbly sandstones have not been done in sufficient detail to ascertain the relative importance of these two grading types.

Different grading patterns in deep-sea conglomerates have been reviewed and integrated into a model by Walker (1975a; in Harms et al, 1975; 1977; 1978). In Walker's model, there are three main patterns: lack of grading (ungraded), inverse grading, and well-developed normal grading. Explanations for the origins of inverse grading are given by Middleton (1970) and Walker (1975a, 1977, 1978); explanations for the occurrence of well-developed normal grading are presented by Walker (1965, 1975a), Middleton (1966, 1967) and Middleton and Hampton (1976). Few studies have examined the development of grading in predominantly structureless, pebbly sandstones and sandstones. (Gonzalez-Bonorino, 1976; Hiscott, 1977).

There are two kinds of sedimentary structures that give information as to the relative rates of deposition of deep-sea sediments. These are: tractional current features (stratification and crossbedding) and syndepositional fluid escape features (dish structures and fluid escape tubes). Many, although not all, liquefaction features in deep-sea, massive sandstones, are thought to form during early syndepositional stages. Tractional current structures need time for clasts to roll along the bed just prior to deposition and, consequently, imply slower rates of deposition (Walker, 1978). Tractional current structures can indicate flow strength at the time of deposition (Guy et al, 1966; Harms and Fahnestock, 1965; Middleton and Southard, 1977; Simons et al, 1965; Southard, 1971; Southard in Harms et al, 1975; Williams, 1967). Syndepositional liquefaction features form as a consequence of very rapid

depositional rates (Walker, 1978). Different liquefaction features can denote relative rates of pore water expulsion (Lowe, 1975).

In order to avoid an extensive review in the text (it would take at least 50 pages to do an adequate job), the more important hydrodynamic implications, gleaned from a literature review (see citations in Table 7 and discussion on the previous pages), are presented as a summary table -- Table 8. Relevant data from other studies will be discussed explicitly in the discussions on the origins of individual facies. The exception to this will be the theoretical discussion of the origins of sedimentary fabric, which is presented first. Many of the ideas on the development of sedimentary fabric are based upon results of experimental work. Theoretical understanding of the origins of sedimentary fabric patterns is, at its best, still in a rudimentary state. This is especially true for the new types of fabrics that have been discovered in the present study, as well as for the other fabric types which have been recognized for many years.

ORIGINS OF SEDIMENTARY FABRIC PATTERNS

The main factor which influences a certain fabric pattern is the mechanism of transport. Clasts which are rolled along the bed as tractional load display a-axes perpendicular to flow, b-axes imbricate upstream patterns (Fig. 51). This is because rotations about the b-axis or c-axis (short axis) would necessitate that the centre of gravity of each clast be lifted higher above the bed for each rotation (in comparison to rotations about the a-axis) (Walker, 1975a). The a-axis parallel to flow, a-axis imbricate upstream pattern implies no clast rolling, but is more difficult to account for.

TABLE 8: SEDIMENTARY FEATURES AND THEIR POSSIBLE HYDRODYNAMIC IMPLICATIONS

Sedimentary Feature	Possible Hydrodynamic Implications
Absence of Grading	<ol style="list-style-type: none"> 1. Complete recycling of material within the current -- no lateral segregation of sizes in the flow ; velocity of the body greater than the head velocity (?) in high slope areas 2. syndepositional deformation (churning and/or fluidization) completely mixed the sediment, destroying any grading 3. Very rapid depositional phase in relation to rate of loss of flow competence -- no opportunity for separation of sizes before deposition 4. Grains were not free to move within the flow to develop grading
Abrupt Normal Grading	<ol style="list-style-type: none"> 1. Some loss of flow competence before rapid deposition of most of the bed 2. Only the largest sediment settled out, with all of the finer sizes kept in suspension or dispersion until all was deposited at once
Normal Grading	<ol style="list-style-type: none"> 1. Good lateral separation of sizes in current with less recycling of material between body and head, implying velocity of head and body were about the same (? in low slope areas) 2. Grains were free to move in the flow 3. Intermediate depositional rate in relation to rate of loss of flow competence -- opportunity for good separation of grain size prior to deposition
Inverse Grading	<ol style="list-style-type: none"> 1. At least the fine grains were free to move within the flow 2. High applied shear stress in cross section and strong grain interaction with high dispersive pressures

TABLE 8 (continued)

Sedimentary Feature	Possible Hydrodynamic Implications
Complex Grading	1. Moving pulses of coarse and fine material in the flow 2. Amalgamation of beds
Fluid Escape Features	1. V. rapid depositional rates with entrapment of significant pore water, leading to syndepositional or early post-depositional liquefaction 2. Rapid post-depositional loading inducing post-depositional liquefaction
Stratification and Crossbedding	1. Slower depositional rates -- time for grains to roll along the bed and to be molded into bedforms 2. Less confined flow conditions, with slower rates of sedimentation and greater low velocity zones for deposition under concentrated gravity flows

Although one of the most important factors affecting the sedimentary fabric is the mechanism of clast transport, other factors may also significantly influence the fabric. These include: 1) size and shape of the clasts; 2) sorting of the sediment; 3) flow factors, including bottom shear-stress and velocity; 4) mobility of the clast within the flow (flow viscosity); and, 5) bed surface features: slope of the bed, bed roughness factors, and form of the bed surface, whether flat, undulating or wave-form, or very irregular. In addition to all of these factors, the orientation of individual clasts may record different aspects of the interactions between individual clasts and the flow:

1. The orientation may reflect the attitude of the clast as it was most easily transported in the flow;
2. Clast fabric may indicate the orientation which is the result of the flow's rotating the clast about a pivot point on the boundary after initial clast deposition on the bed; or,
3. In the case of flows with very high concentrations of clasts, the fabric may be a result of strong clast interaction at the moment or just prior to depositional phases, and may not actually record the true nature of the transporting flow.

Hence it is no wonder that theoretical aspects on the origins of sedimentary fabrics are poorly understood.

All in all, there are six different fabric patterns that are recognized within the Cap Enrage sediments (Table 5). These include:

- 1) a-axis flow-parallel, a-axis imbricate upstream (unimodal bedding fabric, unimodal imbrication);
- 2) a-axis random, a-axis imbricate

upstream (random bedding fabric, unimodal imbrication); 3) a-axis bimodal, a-axis imbricate upstream (bimodal bedding fabric, unimodal imbrication); 4) a-axis flow-parallel, a-axis imbricate up- and downstream (unimodal bedding fabric, bimodal imbrication); 5) a-axis random, a-axis imbricate up- and downstream (random bedding fabric, bimodal imbrication); and, 6) a-axis bimodal, a-axis imbricate up- and downstream (bimodal bedding fabric, bimodal imbrication).

Several of these fabric patterns are new and have not been reported elsewhere; and, no theoretical nor experimental work can shed light onto their origins. Other fabric patterns are similar to those reported elsewhere; and, some tentative explanations can be given as to their derivations. In the following section, possible explanations will be presented for the different fabric types. In summary, a speculative outline for the origins of the main fabric types will be proposed. This will be used later, in conjunction with other sedimentary features, as a tentative basis for the interpretations of the different flows which gave rise to the various facies.

Fabric: A-axis parallel to flow, a-axis imbricate upstream

Theoretical studies on sand-size material (particularly Rees, 1968) have helped to explain the origins of this fabric pattern (Walker, 1977) (Fig. 52). Random oriented clasts will, when under applied shear, orient themselves such that the average angular momentum transfer per clast collision is minimized. The angular momentum is zero when collisions take place on principal axes. Clasts of overlying layers (as seen in cross-section) can only collide along their principal axes, if these axes are tilted upstream to meet the collision -- hence

Fig.52a Collisions between particles in layers with overlap. Arrow indicates direction of motion. Collisions are symmetrically distributed with respect to principal axes if the clasts are tilted away from the direction of motion as in part B (after Rees, 1968).

Fig.52c Vertical cross-section through the flow in which ellipsoidal clasts are free to collide with one another. Arrows indicate increasing velocity and shear stress upward. The only statistically stable orientation is illustrated (after Walker, 1977).

Fig.52d An assemblage of randomly oriented clasts under shear will be oriented so that average angular momentum transfer on collision is minimized. There is a tendency for a particle to adopt one of the two illustrated preferred orientations. Collisions are more glancing where particles have long axes flow-parallel (after Rees, 1968).

Fig.52e Plan view of a conglomerate flow in a channel. As indicated by arrows, flow velocities and shear stresses increase toward the centre of the flow, but gradients of these parameters decline. At margins, clasts are in a stable orientation as drawn. In the flow centre, clasts in transverse orientations (iii) will be rotated to oblique (ii) or flow parallel orientations (i) which are stable (after Walker, 1977).

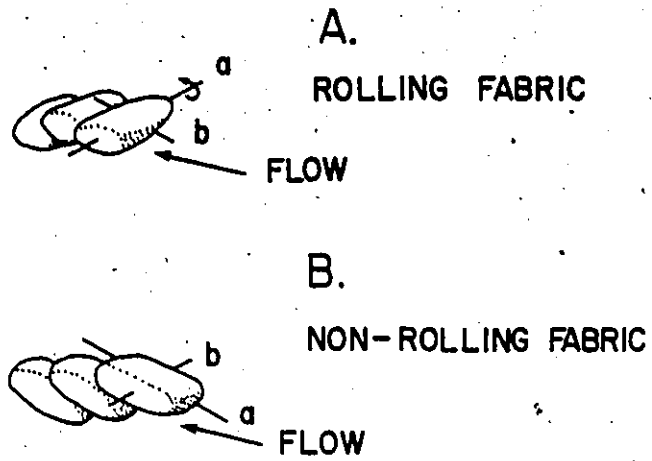


Fig. 51 - Contrast between conglomerate fabrics produced by rolling clasts (long axis transverse to flow) with "typical" resedimented fabric (long axis parallel to flow). After Walker (1976).

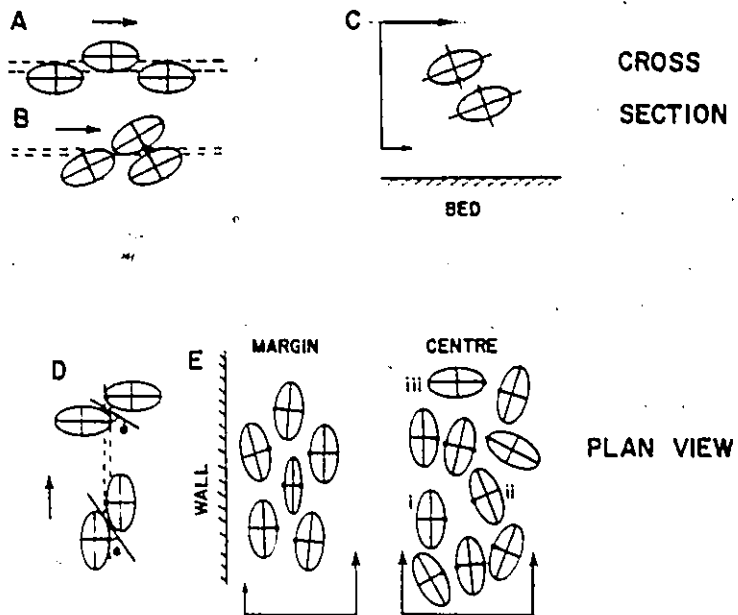


Fig 52 .

the a-axis upstream imbrication (Figs. 52A,B,C). Collisions are more glancing and involve less momentum transfer, if the a-axes are aligned parallel to flow (Fig. 52 D) (Rees, 1968). The main question remains: what is a stable orientation in flows with high sediment concentrations? In collisions between clasts there is generally an angular momentum transfer, which causes the clasts to be rotated. Assuming that there is friction, in collisions between clasts, there is a couple generated about the centre of mass, which leads to rotation of the clasts. The only cases in which there is no angular momentum transfer are the cases where collisions are head-on, along principal axes (Fig. 52D). Therefore, only those clasts which collide along principal axes and are oriented either flow-parallel or flow-transverse will not be rotated. These orientations can be thought of being 'stable,' in that only those clasts in either one of these orientations are not rotated in the flow. Consideration of Rees' (1968) analysis, a-axis flow-parallel orientations would be 'more stable' than flow-transverse orientations.

The pressure resulting from grain collisions is the 'dispersive pressure' (Bagnold, 1954). Bagnold (1954, 1973) stated that the ratio of tangential shear stress to the dispersive pressure (T/P) (Fig. 53) is constant and equals 0.63 for flows in which the grain inertia effect is dominant. In flows for which the viscosity of the fluid is dominant, the T/P ratio is 0.75. Hence for flows in which the grain inertia is more important, the angle of imbrication is about 30° ($\tan 30^\circ = 0.58$). Imbrication angles are higher (36°) for flows in which the viscosity of the fluid predominates. Steep imbrication angles are also associated with rapid deposition from suspension (Schwarzacher, 1951) or deposition from

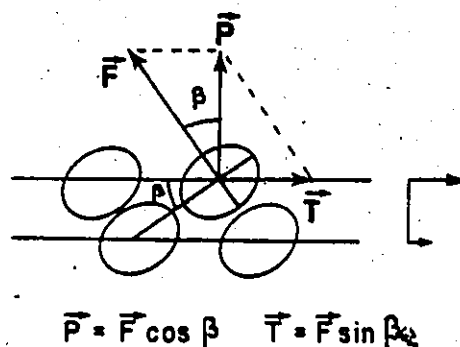
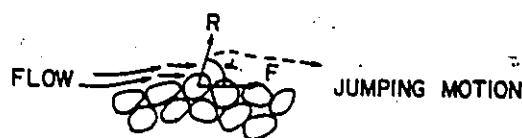


Fig. 53 - Forces on a grain and their orientation due to grain-to-grain collision. Arrows at right indicate increase in applied shear stress. T = tangential shear stress; P = dispersive pressure; F = resultant force; β = imbrication angle of grains (after Bagnold, 1954 and Rees, 1968).

A. WELL SORTED



B. POORLY SORTED

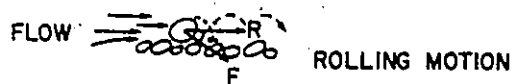


Fig. 54 - Conditions of jumping and rolling motion. α = angle between resultant force (R) and flow direction (F). For $\alpha > 0^\circ$ the particle will jump, whereas for $\alpha \leq 0$ the particle will stay in contact with the bed, and roll (after Johansson, 1976).

high velocity flows (Johansson, 1976).

Fabric: A-axis parallel to flow, a-axis imbricate up- and down-stream

The occurrence of bimodal imbrications was an unexpected result and is not easy to explain. Bimodal imbrications in the present study have clasts dipping in both upcurrent and downcurrent directions, with a more dominant mode dipping upstream. Bimodal imbrications have only been reported in a few deep-sea sediment studies (Bouma, 1962; Hiscott, 1977; Lindsay, 1966). In the previous discussion dealing with the development of a-axis flow-parallel, a-axis imbricate upstream fabric it was assumed that clasts were deposited from dispersions, in which clasts were relatively free to collide and rotate with respect to other clasts in the flow. If clast mobility is hindered (by high concentrations of sediment and/or fluid viscosity) the 'stable' fabrics may not develop. Similarly, under conditions of very rapid deposition, there may not be enough time for the clasts to obtain a stable orientation before they are buried. The combined effects of high clast concentrations and rapid sedimentation are thought to explain the origin of bimodal imbrications, in beds with a-axis flow-parallel orientations.

Jeffrey (1922) examined theoretically the orientation of clasts in viscous fluids. Ellipsoids were found to rotate in elliptical orbital paths about the centre of each clast, returning to original clast orientations after completion of an orbit. Lindsay (1968) subsequently did computer simulation of such particle motion in viscous laminar flows, where clasts do not actually touch one another. Lindsay (1968) found that strong a-axis patterns can develop in a very short period of time.

Lindsay (1968) found that long-axis fabric in mudflows most likely develops under laminar flow conditions, just prior to the arrest of the mudflow. A-axis modes develop parallel to the flow direction, although the a-axis can imbricate in either up- or downflow directions. The development of preferred a-axis fabric is cyclic: the initial fabric pattern is characterized by weak modes that dip in an upstream direction. In time, the modes coalesce to form a strong unimodal fabric with a-axis parallel to flow and negligible (near-horizontal) imbrication. The maximum preferred orientation is developed in this near-horizontal imbrication. Next, the fabric degenerates: firstly, to a single a-axis mode parallel to flow, but imbricate downstream; then, to a weak girdle; and, finally a random fabric. The fabric development is cyclic and reflects individual particle motion. The strength of the a-axis orientation and the amount and direction of imbrication depend upon the instant that the mudflow motion is arrested, "freezing" the flow simultaneously at all depths. Preferred fabric patterns developed very rapidly, in about 3% of the time for a clast to complete one period of motion.

The effect of grain reorientation during settling is thought to be negligible in highly viscous, clayey mudflows and may be somewhat more important in less viscous, sandy mudflows (Lindsay, 1968). If reorientation of grains takes place during settling after the mudflow has ceased moving the larger, more elongate as asymmetric grains will reposition with the maximum cross-sectional area being near-horizontal. This does not affect the a-axis orientation, but does reduce the imbrication angle (Lindsay, 1968).

Comparisons by Lindsay (1966,1968) to fabric patterns in subaqueous mudflow and tilloid deposits show similar patterns to the results from the computer simulations. These field examples had a-axis fabrics with distinctive girdles that dipped in either up- or downstream directions. Based upon grading patterns, presence of outsized clay clasts and continuity of beds, Lindsay (1966) concluded that some of the tilloid sediments were transported under turbulent flow conditions and developed the fabrics in a laminar stage just before movement was arrested. A smaller number of flows had higher viscosities were confined to laminar flow conditions throughout phases of transport.

The a-axis parallel to flow orientations in flows which are dominated by viscosity effects are accounted by consideration of Bagnold's (1954) results. Bagnold (1954) demonstrated that even when the fluid viscosity prevented direct grain collisions from taking place, a dispersive pressure still existed on the clasts floating in a fluid which is being sheared. As in the case of concentrated clast dispersions under shear, an orientation in the grains will develop to minimize the effect of the dispersive pressure force -- resulting in an a-axis parallel to flow orientation for flows with 'close encounters of the dispersive kind.'

There is an alternative explanation for the origins of a-axis flow-parallel, bimodal imbrications, although very speculative. Wave fabrics have been reported by Hubert et al (1977) and Aalto (1972) in clast-supported conglomerates. Many of the breccias studied by Hubert et al (1977) have wave-form fabrics, with average wave lengths of 2.4 m and mean amplitude of 0.6 m. Many of the wave-forms are overturned in a downslope direction, with the result that most of the clasts dip in a downslope direction, due to the overturning of the anticlinal limbs.

In their interpretation of the flow mechanisms, Hubert et al (1977) suggested that the flows moved downslope as highly viscous, surging masses of mud and limestone clasts. The platy limestone clasts slid past one another in the muddy flow to yield either horizontal or wave-form fabrics. Inclined clast fabrics were generated in the direction of downslope movement and were interpreted as representing response to increase shear within the flow, produced by friction that increased toward the base. Upslope orientation of clasts occur where clasts are aligned on the upslope synclinal limb of low amplitude waves. Conversely, downslope orientation of clasts occur where clasts are aligned on the downslope, upright anticlinal limb of low amplitude waves. Although, as evident from the fabric sketches (Figs.9,11,12 in Hubert et al,1977), the a-axis orientations in bedding of the wave-form features is transverse to the paleoslope, a similar mechanism may account for the generation of bimodal imbrications in beds with a-axis flow-parallel orientations.

The necessary requisite is to generate low-relief waves -- either within the flow, as the syndepositional wave-forms of Hubert et al (1977); or, alternatively, to generate low-relief waves on the bed, perhaps as low-relief bedforms similar to antidunes. In the first case, the flows would be very viscous and the wave-forms would record moving pulses within the flow, which are preserved by en masse deposition from the flow. In the second case, clasts would be deposited on the bed individually. Those that fall on the upcurrent limbs of the low-relief waves on the bed would have an upcurrent dip, whilst those that fall on the downcurrent limbs of the low-relief bedform waves would have a downcurrent dip. Clasts would not roll prior to deposition, and local bed microtopography would --

determine the direction of clast imbrication.

Fabric: Random a-axis, unimodal or bimodal imbrication

Matrix-supported sediments, including pebbly mudstones, sandy mudstones and olistostromes, commonly have little preferred fabric. This is thought to reflect hindered clast mobility due to the high viscosity of the mudflow (Crowell, 1957). Matrix-supported conglomerates (also called olistostromes) may have chaotic or random fabrics (Breakey, 1975; Gorler and Reutter, 1968; Harms, 1974). Gorler and Reutter (1968) and Lindsay (1966) found that clasts had a-axes aligned in broad, near random, girdles but with a-axes imbricate upstream. This type of fabric pattern might be analogous to the initial long-axis fabric that is developed in mudflows. Lindsay (1968) in his simulations (see discussion on previous pages) stated that the initial fabric in bedding is weakly developed, but has an upstream imbrication. Random a-axis patterns in bedding with bimodal imbrications may reflect the degeneration of the mudflow fabric, just prior to the completely random pattern. The other way to explain random fabrics is to say that they represent the en masse deposits from turbulent suspensions or dispersions.

Fabric: Bimodal a-axis, unimodal or bimodal imbrication

Answers to the generation of bimodal a-axis fabric in bedding may lie, perhaps, in the results of Johansson's (1976) flume studies on deposition of non-uniform sediment, under changing flow conditions. Experiments were conducted under rough, fully turbulent flow with pebble, granule and sand-size material. Pebble fabric patterns were found to vary with the velocity of the flow, slope of the bed, and sorting of the sediment.

An a-axis transverse to flow, b-axis imbricate upstream pattern is typical for 1 cm+ clasts in gravelly sands with shear velocities up to 7 cm/sec (Johansson, 1976). With slightly higher shear velocities (8 cm/sec), the a-axis transverse orientation becomes less pronounced, with an increasing number of clasts assuming an a-axis flow-parallel, a-axis imbricate upstream fabric. A stronger a-axis flow-parallel, a-axis imbricate upstream pattern is produced under increasing flow velocities and tractive forces. Under high flow conditions, all clasts with a-axes transverse to flow are transported as rolling bed load -- only those clasts with an a-axis parallel to flow orientation have a stable alignment with the flow and will be deposited (Johansson, 1976). Bimodal patterns, with approximately 90° separation between modes, may result in flows which have shear velocities (for a given sediment size and sorting) intermediate between those velocities in which a-axis parallel or a-axis transverse orientations are stable (Johansson, 1976).

The second factor affecting clast orientation is the sediment sorting -- the relative size of a clast with its surrounding neighbors (Fig. 54) on a bed (Johansson, 1976). Clasts which rest on a bed of similar size material would require a greater velocity to initiate movement and reorientation, after initial deposition on the bed. Larger clasts that stick up above the general bed level (Fig. 54) are more easily transported and may be rolled along the bed. This may result in possible reorientation from an a-axis flow-parallel orientation to an a-axis flow-transverse orientation during redeposition on the bed (Johansson, 1976).

Most of the bimodal bedding fabric plots are asymmetric, with the dominant mode flow-parallel and the secondary mode flow-transverse (as determined from the imbrication data and other independent paleocurrent indicators). Asymmetric bimodal bedding fabrics, with unimodal a-axis imbrication patterns in an upstream direction, may reflect re-orientation of clasts after initial deposition on a bed. After deposition, some of the clasts, including the larger ones (which protrude above the general bed level, as in Fig.54) were remobilized and rolled along the bed. Upon redeposition these remobilized clasts had an a-axis transverse to flow orientation, with b-axis imbricate upstream. Although some of the clasts were reoriented, most of the clasts did not move and retained the initial a-axis flow-parallel, a-axis imbricate upstream fabric. On the average, this would yield an asymmetric a-axis bimodal pattern, with an a-axis imbricate upstream pattern.

Bimodal bedding fabrics with bimodal imbrication patterns cannot be interpreted at the present time. This is the first time that such a fabric has been reported. No experimental data can help explain its origins. Interpretations will only be possible after more work is done by other researchers on the fabric development under high velocity and high sedimentation rates.

Summary: Tentative Schema of Sedimentary Fabric Origins

As evident from the previous discussions, the origins of sedimentary fabrics are not well understood. Many of the fabric types can be explained in terms of two or more processes. In summary, a tentative outline (Table 9) is proposed to account for the development of the various fabric types. Only considerations of other sedimentary features

TABLE 9

SEDIMENTARY FABRICS AND THEIR POSSIBLE HYDRODYNAMIC IMPLICATIONS

Sedimentary Fabric	Possible Hydrodynamic Implications
Random A-axis Bedding Fabric	<ol style="list-style-type: none"> 1. Clasts were not free to move in the flow 2. Very rapid depositional rates -- clasts did not have enough time to obtain a stable orientation prior to deposition 3. Any fabric that was developed, was destroyed by syn-depositional or early post-depositional deformation (churning or fluidization) of the sediment
Unimodal A-axis Bedding Fabric Aligned Parallel to Flow	<ol style="list-style-type: none"> 1. Clasts were mobile in the flow 2. High applied shear stress 3. Strong grain interaction, with high dispersive pressures 4. Clasts did not roll along the bed 5. Intermediate depositional rates -- clasts had enough time to obtain a stable orientation in the flow, but were buried quickly to preserve the grain transport orientation, with no clasts becoming reoriented after initial deposition on the bed
Bimodal A-axis Bedding Fabric Aligned Transverse and Parallel to Flow (Case 1)	<ol style="list-style-type: none"> 1. Clasts were not completely mobile in the flow 2. Rapid depositional rates -- not all of the clasts had enough time to obtain a stable orientation prior to burial. Those clasts that assumed a stable orientation aligned flow-parallel; those that did not, assumed an a-axis flow-transverse orientation. 3. Clasts did not roll along the bed, with no clast reorientation after initial deposition on the bed

TABLE 9 (continued)

Sedimentary Fabric	Possible Hydrodynamic Implications
Bimodal A-axis Bedding Fabric Aligned Transverse and Parallel to Flow	<ol style="list-style-type: none"> 1. High applied shear stress 2. Clasts were mobile in the flow 3. Slightly lower depositional rates -- clasts had enough time to obtain a stable transport orientation, but some clasts were rolled along the bed after initial deposition. 4. Strong grain interaction and some clast rolling prior to burial
Unimodal A-axis Imbrication High angle in an Upstream Direction	<ol style="list-style-type: none"> 1. High applied shear stress 2. Clasts were mobile within the flow 3. Strong grain interaction 4. Clasts did not roll along the bed 5. Intermediate depositional rates -- clasts had enough time to obtain a stable grain transport orientation, but were not reoriented after initial deposition on the bed.
Bimodal A-axis Imbrication High Angle in both Upstream and Downstream Directions	<ol style="list-style-type: none"> 1. Hindered clasts mobility 2. Less strong clast interaction 3. Clasts did not roll along the bed prior to burial <p style="text-align: center;">or</p> <ol style="list-style-type: none"> 4. Bimodal imbrication induced by either 1) deposition onto a wavy bed; or, 2) syn-depositional or early post-depositional deformation of internal structure of bed into low-amplitude wave-forms.

in conjunction with the fabric patterns, will help one to decide the most-likely mechanisms for the origins of the various facies.

DEPOSITIONAL MECHANISMS FOR DIFFERENT FACIES

Discussions will be made first for those facies which follow previously-defined sedimentary models --- namely, the classical turbidites (Facies 7), following the Bouma (1962) model; and, the coarse conglomerates (Facies 1), following Walker's (1975a) model for resedimented conglomerates. Concepts presented in the interpretation of the depositional mechanics for the origins of Facies (1) and (7) beds will be used, in part, to explain the origins of beds belonging to the other facies.

Facies (7) -- Classical Turbidites

The internal structure of the "model" classical turbidite (Bouma, 1962) (Fig. 2) consists of five divisions, which occur in a regular sequence: (A) graded or massive sandstone; (B) parallel laminated division; (C) rippled crossbedded sandstone; (D) faint, parallel laminated silt and muddy sediment; and, (E) pelitic division. This sequence of stratification types has been interpreted by workers (Harms and Fahnestock, 1965; Walker, 1965) as being due to a sequence of bedforms that would result under conditions of deposition from waning turbidity currents. This is based upon flume data (Guy et al, 1966; Simons et al, 1965; Williams, 1967) (Figs. 2, 55). B-division parallel lamination is thought to be the result of upper flow regime tractional flow. C-division ripple crossbedding is due to tractional flow in lower flow regimes (Fig. 2). D- and E-divisions are due to sediment settling out of suspension from the tail of the turbidity current, followed by pelagic

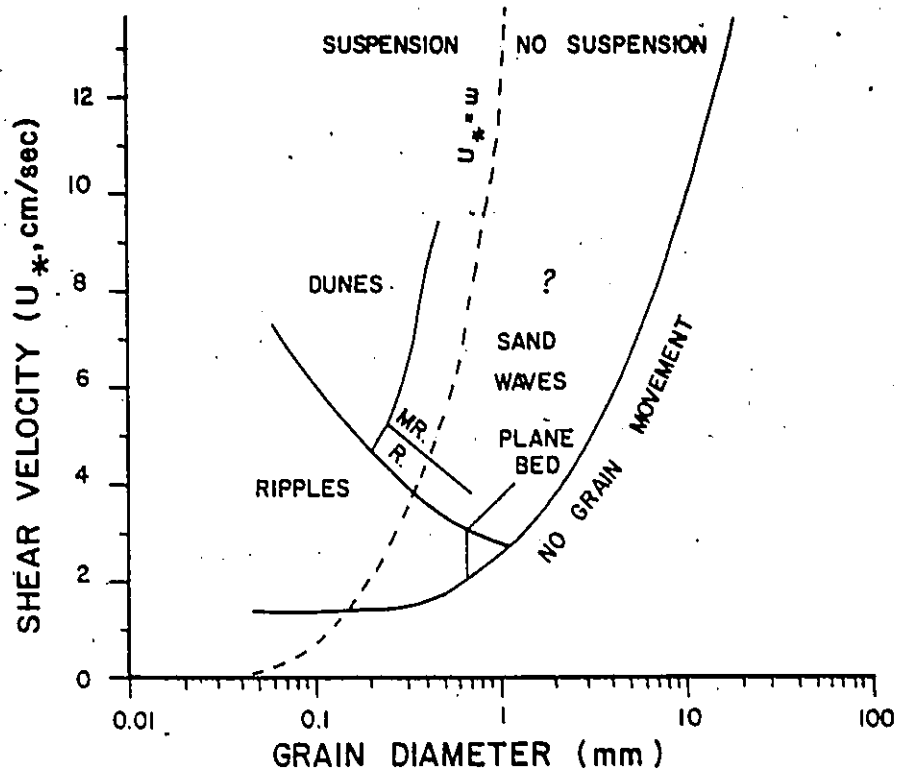


Fig.55 - Bedform stability fields plotted on a graph of grain diameter vs. shear velocity (after Hiscott, 1977).

sedimentation.

Within the Cap Enrage sediments, most of the classical turbidites are ABC (27%), AB(E) (16%), B(E) (14%) or AC (12%) types. Under the Bouma model, the ABC types would reflect deposition under waning flow conditions of rapid deposition, to traction in upper and lower flow regimes. AB(E) types would have been deposited under very rapid fallout from the turbidity current, followed by tractional deposition in upper flow regimes, and, in some cases, pelagic sedimentation. B(E) beds would have formed under mainly upper flow regimes, followed by pelagic sedimentation, in some cases. AC types were deposited firstly under conditions of rapid sedimentation, followed by traction in the lower flow regime.

It is thought that some sediment gravity flows may be layered (Fig. 56). A lower, 'modified grain flow' may occur near the bed (Lowe, 1976b; Middleton, 1970; Middleton and Southard, 1977), where dispersive pressure is maintained by shear stress exerted by an upper, turbulent turbidity current (Middleton, 1970; Lowe, 1976b). The term 'modified grain flow' means a flow in which the shear stress is increased without a corresponding increase in pressure. This can be accomplished by flows moving over the top. Entrained fluid flow is always present above a turbidity current, due to drag at the upper interface between the turbidity current and sea water. Entrained fluid flows are very dilute and probably have little effect by reworking on the sediments that are deposited from the underlying turbidity currents.

Absence of stratification within lower A-divisions of turbidites can be explained as a combination of 1) deposition in a liquefied state;

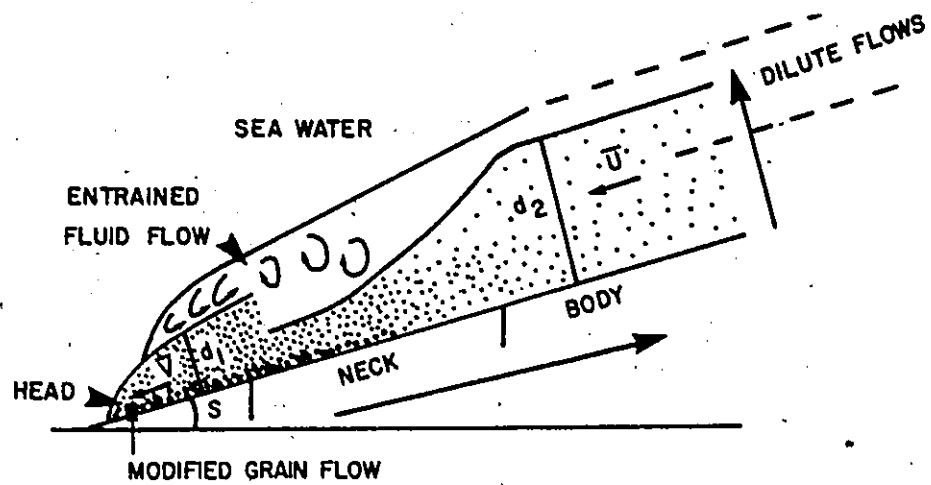


Fig.56 - Head, neck, and body of a turbidity current travelling down a slope of angle S . Large arrows indicate directions of decreasing sediment concentration. Modified grain flow and entrained fluid are shown. \bar{V} = average head velocity; \bar{U} = average body velocity (modified from Komar, 1977).

and, 2) churning of the sediment by internal (? Helmholtz) waves, which move along the upper interface (Middleton and Hampton, 1976; Walker, 1978). Liquefaction coupled with churning of the sediment result in structureless division. Deposition under waning flow conditions accounts for the normal grading. The lack of identifiable antidune crossbedding (presumably formed at higher stream power conditions than B-division lamination) may be due to 1) a consequence of a very long wavelength, which, in practice appears to look like plane lamination in outcrop (Middleton, 1978: pers. comm.); 2) rapid sedimentation rates, with insufficient time for bedforms to develop; or, 3) damping out of bedforms, due to high suspended sediment concentrations, during deposition of division A.

Facies (1) -- Coarse Conglomerates

Most of the coarse conglomerates measured in the present study are disorganized (37%) or graded-bed and graded-stratified (36%) (see logged sections, Appendix 5 and Fig. 15). Conglomerate fabric within each measured bed (those in which fabric was measured) is described as being a-axis flow-parallel, a-axis imbricate upstream. This is the general, overall, fabric in each bed. Individual clasts do show a fairly wide scatter in the directions of dip within each bed, with some clasts dipping in oblique or downcurrent directions (see stereonet plots, Appendix 6). Fabric is developed to about the same degree in all of the conglomerates that were measured, with parameters describing the scatter and dip of the clasts having no relation to grain size nor thickness of the conglomerates.

Fabric patterns within conglomerates were measured upsection in different levels of the same bed. This was done for only three beds.

Of these, two beds had consistent paleoflow directions upsection within individual beds; whereas, the third had about a 70° change upsection within the same bed (see Appendix 6 and logged sections, Appendix 5). The change in paleoflow within the third bed may be due to an amalgamation of beds, or reflecting actual meandering within a single flow.

The first question to be answered is whether the coarse conglomerates were transported and deposited essentially en masse; or, alternatively if the coarse conglomerates were transported and deposited as individual clasts within a flow. The en masse deposition is favoured by the occurrence of 1) a-axis flow-parallel, a-axis imbricate fabric, 2) homogeneity of fabric vertically, in two out of three beds; 3) lack of correlation between grain size and bed thickness; and, 4) lack of correlation between scatter of the fabric plots and dip of the clasts versus either grain size or bed thickness. Features which are incompatible with en masse transport are 1) the occurrence of grading in over 60% of the Facies (1) beds; 2) the fact that some of the Facies (1) conglomerates have graded-stratified sequences; and, 3) the difficulty of transporting large clasts en masse as coherent units. Of course, the same mechanism need not be invoked to account for the origins of all of the different types of Facies (1) conglomerates (Fig. 15).

One way to explain the transport and deposition of Facies (1) conglomerates is to invoke different processes for main transport phases and for main depositional phases. Sediment is transported into deep-sea basins via turbidity currents or debris flows. The lack of muddy matrix within the coarse conglomerates as well as the development of grading and stratification within many of the beds (Fig. 15) suggest that the beds

were not deposited from debris flows. This leaves turbidity currents as the main transport mechanism of sediment into the depositional basin. Most of the Facies (1) conglomerates were, therefore, thought to be transported by fluidal turbidity currents down the continental slope to the base-of-slope setting for the Cap Enragé deposits. Upon emergence at the base-of-slope, the turbidity currents lost momentum, due to the decrease of slope. As currents slowed down, sediment was deposited from the base of the flows. It is unlikely that the currents dumped all of their load at the contact between the continental slope and the basin, as most of the Facies (1) conglomerates are not disorganized. Currents probably deposited their load gradually as velocities waned, while continuing to travel in the base-of-slope setting. Sediment may have been transported long distances (up to 40 km⁺) before being deposited.

It is probable that during the transport stages within the base-of-slope setting, concentrated clast-dispersions developed at the base of the turbidity currents, once they emerged from the submarine feeder canyons. Deposition from the concentrated clast dispersions may have been en masse, when the strength of the basal dispersion exceeded the applied shear stress from the over-riding turbidity current. For the Facies (1) conglomerates the dominant support mechanism within the basal dispersions may have been dispersive pressure, generated by a high number of clast collisions. This is suggested by the fabric, which is a-axis flow-parallel, a-axis imbricate upstream. The sedimentary features within the Facies (1) conglomerates would reflect transport phases under fluidal turbidity currents; and, secondly deposition from concentrated clast dispersions, possibly 'modified grain flows.' The turbidity current

mechanism was operative for long distances, whereas influences due to transport and deposition from basal modified grain flows were felt over somewhat shorter distances. The different grading patterns are interpreted as reflecting the segregation of sizes within the turbidity current, prior to deposition. The grain fabric would reflect strong clast interaction within the basal modified grain flow layers. The extent to which a basal modified grain flow would develop would depend mainly upon two factors: the amount of applied shear stress by the over-riding turbidity current and, secondly, on the concentration of clasts at the bottom of the turbidity current.

The reason that the coarse conglomerates cannot be transported and deposited from true grain flows is 1) the sediments were likely not deposited on avalanche slopes (most of the beds are well-graded and some show stratification, suggestive of slower rates of deposition than in avalanche slope settings); and, 2) some of the coarse conglomerates were transported long distances. As shown by Middleton (1978) and Middleton and Southard (1977), only high slopes with a minimum dip of about 30° can maintain steady, uniform grain flows with dispersive pressure as the dominant support mechanism. True grain flows are not thought to be very important in nature and would only be active on avalanche slopes. Hence, sediments which have features of grain flows, but have obviously been transported long distances, are thought to be the product of 'modified grain flows' (Middleton, 1970; Middleton and Southard, 1977; Lowe, 1976b), see Figure 56 .

The type of basal dispersion that is envisaged is similar to that described by Bagnold (1973) for saltation of grains. Bagnold (1973) thinks that saltation under bed load transport is possible because of fluid drag on the grains. The grains, however, are maintained above the bed by dispersive pressure. Hence, the saltating layer is a 'modified grain flow,' in which over-riding fluid applied the shear stress requisite for the generation of high dispersive pressures. Rough calculations can be made, for simplified models, of the possible thicknesses for such modified grain flow layers. It is impossible to estimate the actual density of turbidity currents that were capable of transporting the coarse conglomerate debris. There is no evidence of fine-grained muddy matrix, therefore, the flow densities were probably less than that for debris flows ($S_f = 1.5 \text{ g/cm}^3$, Hampton, 1972, p.791) and may be in the order of 1.2 g/cm^3 , the maximum turbidity current densities calculated by Komar (1970) for currents that could transport gravel-size material in Doheny Channel deposits. Nelson *et al* (1970) give average slopes of 0.008 in the inner fan valley of Astoria Fan. Using these slope and fluid density estimates, the shear stress at the base of the turbidity current is given by

$$(2) \quad \tau_o = S_f \left\{ \frac{\Delta S}{S_f} \right\} g d S,$$

$$\text{where } g = 981 \text{ cm/sec}^2$$

$$S = 0.008$$

$$\Delta S = 0.2 \text{ g/cm}^3$$

Assuming a turbidity current thickness of 100 m (d), this results in a basal shear stress of about $15,700 \text{ dynes/cm}^2$.

Assuming that the shear stress at the base is transferred to the grains (i.e. τ_0 becomes T), then the dispersive pressure (P) is given by:

$$(3) \quad P \sim T / 0.6 = 15,700 / 0.6 \approx 26,000 \text{ dynes/cm}^2$$

This dispersive pressure (P) balances the vertical component of the gravitational force acting on a column of dispersed grains. Assuming that the dispersed layer has a bulk density of 2 g/cm^3 , the height of the column of dispersed grains can be calculated:

$$(4) \quad P = \rho_f \left\{ \frac{\Delta \rho}{\rho_f} \right\} g \cdot h,$$

$$\text{where } g = 981 \text{ cm/sec}^2$$

$$\rho_f = 2 \text{ g/cm}^3$$

$$\Delta \rho = 1 \text{ g/cm}^3$$

$$P = 26,000 \text{ dynes/cm}^2$$

Hence a grain flow of only 27 cm thick can be maintained at the base of a turbidity current which is 100 m thick (assuming a bulk density of 2 g/cm^3 for the basal grain flow).

These calculations show that if the modified grain flow layer does exist at the base of large turbidity currents, it influences only a very thin zone of the flow. This has several implications. Firstly, in order to accumulate beds on the average of about 2 m thick (assuming that deposition is from basal grain flow layers) would mean that the clasts were deposited piecemeal within a narrow zone at the base -- i.e. on the order of 30 cm thick layers. In basal parts of beds, where there may not have been good size segregation of clasts during initial depositional stages, the layers may not be distinguishable from one another. In upper parts of beds, presumably under slower rates of deposition and longer distance of transport, this piecemeal, layer

by layer en masse deposition of sediment may be reflected in crude stratification or layering. Alternatively, deposition from the basal parts of modified grain flows may lead to an expansion of the grain flow, with the result that thin layers are deposited continuously, with no break in deposition. This may be operative in lower parts of flows, where under initial conditions of deposition, sediment concentrations are very high and reconstruction or expansion of the modified grain flow layer may be almost instantaneous. The second major implication of the thin nature of the basal modified grain flow layers is that bottom-hugging, clast-supported dispersions may be very sensitive to pre-existing topography on the ocean floor. The overlying, less dense thicker turbidity currents would be insensitive to topography and may travel more as blanket flows.

The problem with the above calculations is that they apply to minimum conditions of transport and may not strictly apply to conditions dominated by deposition, which is the record that is preserved in the sedimentary deposits. Thicknesses of modified grain flow layers under conditions of deposition may be actually thicker than those calculated above for minimum transport conditions.

The next point concerns the generation of different grading types within the Facies (1) conglomerates. Within the sections measured in this study, there are about equal proportions of disorganized, graded-bed and graded-stratified types. A slightly lower percentage of coarse conglomerates have inverse grading at the base (Fig.15). According to Walker's (1975a) model the following trends are observed from areas of high applied shear stress to sites with low applied shear stress:

Inverse grading forms in concentrated clast dispersions in response to the collisions of the clasts, which generate dispersive pressure. In experimental grain flows (sand avalanches) and in beach laminations, inverse grading is formed by dispersive pressure (Sallenger, in prep., as quoted by Middleton, 1978: pers. comm.). The other way inverse grading may form is by a 'kinetic sieve' mechanism (Middleton, 1970). In this method, as clasts collide in dispersions, smaller clasts filter their way between the larger clasts to the base of the flow (Middleton, 1970). Whatever the cause of inverse grading, very high applied shear stresses are needed to produce a high rate of strain on a dispersion, which, in turn, results in a high rate of collision. As applied shear stress decreases, the ability for a dispersion to maintain high rates of clast collisions is lessened, with a loss of inverse grading at the base of the flow. Under lower applied shear stresses graded bedding develops (Walker, 1975a). With waning flow conditions, currents are slower and carry finer debris, such that there is a greater potential for the development of stratification. Thus, graded-stratified beds imply deposition from slower flows than graded-bed conglomerates (Walker, 1975a). According to Walker's model (1975a) ungraded, disorganized conglomerates have a chaotic appearance and are very coarse-grained. They are tentatively interpreted by Walker (1975a) as being deposited under conditions of even greater applied shear stress, than either the inverse-to-normally graded conglomerates or the graded-bed conglomerates (Fig. 4).

One way to explain the different grading types in the Facies (1) conglomerates is to say that they reflect deposition under conditions with varying applied shear stresses. Applied shear stress is a function of the bottom slope and the force exerted by the over-riding flow on the sediment being deposited at the base of the flow. As will be demonstrated in Chapter 6, and as pointed out by Johnson (1974), grading patterns within the coarse conglomerates change along-strike. No high-slope channel walls coincide with these changes in grading patterns. Thus, it is not thought that the bottom slope changed significantly during deposition of the laterally-changing conglomerates. The main influence upon the applied shear stress would, therefore, be the force of the over-riding flow.

One must also consider the influence of sediment concentration on the development of grading. Highly concentrated clast dispersions deposit sediment when the strength of the dispersion exceeds the applied shear stress. This may be accomplished by decreasing the applied shear stress (by decreasing the slope of flow depth, equation (2)), or by increasing the sediment concentration, which increases the strength. Therefore, implicit with high-to-low concentrations is the trend from very rapid-to-slower depositional rates. Grain mobility (and the capacity to form graded beds) is also increased with decreasing sediment concentrations.

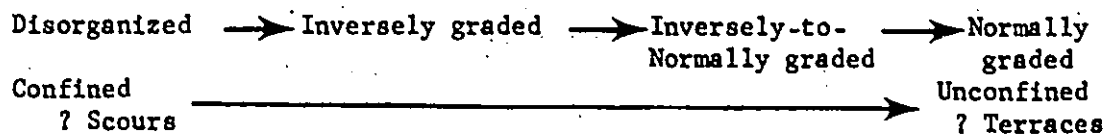
Experimental work (Middleton, 1967) demonstrates that high concentration flows deposit beds with coarse-tail grading, in which the vertical grading is only evident in the coarsest few percent of the grain size distribution. Deposits from low concentration flows show

distribution grading, in which all of the percentiles of the grain size distributions show vertical grading. Qualitatively speaking, grading becomes better developed in deposits from low concentration flows. One can rank the different grading patterns in terms of probable concentrations of flows, assuming constant clay contents. Sediment flows with very high sediment concentrations (and very rapid depositional rates) would be disorganized. As sediment concentrations decrease (with an increase in grain mobility and a decrease in depositional rates), the following trends would occur:

Inverse graded - to - Inverse Inverse-to- Normally
 Disorganized → graded → Normally graded → graded
 Very High Concentration → High Concentration → Lower Concentration

As mentioned before, conglomerates can change grading patterns along-strike. Hence the next problem is to explain the spatial variations of sediment concentrations during deposition from single flows. A pre-existing topography, consisting of topographic 'highs' and 'lows', existing on the ocean bed, may have influenced deposition. Many small-scale turbidity currents are deflected and controlled by topographic features on the ocean bottom (Gonzalez-Bonorino and Middleton, 1976; Bennets and Pilkey, 1976). This is also true of large-scale, air-borne catastrophic rockflows (Heim, 1932, translated in Hsü, 1975) and base-surge tephra deposits (Crowe and Fisher, 1973; Sheridan and Updike, 1975). It is not unreasonable to expect that bottom-hugging, large-scale sediment gravity flows may have, similarly, been affected by topographic constraints on the ocean floor.

If a scour-and-terrace topography existed on the ocean floor, flows that were bottom-hugging would likely be confined to travel and deposit material within lower scour sites. The main influence of this confinement would be an increase in flow depth and an increase or continuance of high flow velocities. In unconfined areas, perhaps on higher terraces separating scour sites, the shear stress on the bed would decrease, concomitant with a reduction in both flow depth and flow velocity. These reductions in shear stress, depth and velocity would all favour deposition of sediment, which results in lower-concentration flows travelling across unconfined areas. For a given original sediment concentration, as a dispersion travels from confined to unconfined areas, the deposits would show the following grading trends:



The next major point is to consider the generation of stratification in the graded-stratified Facies (1) conglomerates. Stratified, upper, finer-grained portions show clast-supported pebbly layers alternating with more sandy layers. The sandy layers have a dispersed texture, in which the coarse clasts do not touch one another, but rather 'float' in the finer sandstone. The fabric of the clast-supported layers was measured within the finer, stratified parts of 16 beds. All of these beds showed an a-axis flow-parallel, a-axis imbricate upstream fabric (Appendix 6, also logged sections, Appendix 5). This suggests that the clasts within the concentrated, clast-supported stratification bands did not roll along the bed as tractional load; but, rather the clasts were

deposited from dispersions. This makes it more difficult to explain the origin of the stratification.

In their study of the Cap Enrage Facies (1) conglomerates, Davies and Walker (1974) describe a similar type of stratification to that pondered here. Stratified, upper finer-grained portions of coarse conglomerates were described, quite often, showing pebble or cobble layers alternating with more sandy layers. Some of the contacts were gradational, suggesting pulsating or fluctuating flow conditions (Davies and Walker, 1974). Graded-stratified beds were thought to have been deposited from dispersions, in which fluid turbulence was the dominant support mechanism for the lower bed portions, with bed load movement becoming increasingly important in the deposition of finer-grained portions. Fluctuations in shear velocity were thought to account for the stratification bands, where alternations yielded sand deposition from suspension and granule transportation by traction. In their work (Davies and Walker, 1974) no study of the fabric of the stratification bands: fabric determinations were only made in the coarser, lower parts of graded-stratified beds. Clearly, their mechanism cannot be used to explain alternating clast-supported and clast-dispersed stratification bands of Facies (1) beds examined in the present study. The a-axis flow-parallel, a-axis imbricate upstream fabric implies that the clasts within clast-supported layers were not rolled in traction.

The alternating concentrated/dispersed bands may reflect pulsating deposition from basal modified grain flow layers. As discussed previously sedimentation at the base of turbidity currents may be gradual and from successive grain flow layers. Immediately after deposition of a clast-supported, basal grain flow layer, the overlying turbidity current will

be somewhat depleted in a specific size, until more clasts of a similar size sink down to the base of the flow. During this interval, only fine-grained sediment and coarser clasts are within the basal layer of the turbidity current. Depending upon the strength of the basal layer, relative to the applied shear stress from the over-riding layer, the basal mixture of fine and isolate coarse clasts may be deposited. This may explain the crude stratification, in which fabric of the clast-supported layers indicated deposition under conditions of high rates of clast collision.

The final point to consider is the magnitude of the fluidal turbidity currents necessary to transport the coarse conglomerates into the basin. Davies and Walker (1974) calculated velocities in the range of 50 m/sec - 125 m/sec to suspend cobble/boulder to fine pebble debris by fluid turbulence (assuming spherical clasts with density of 2.65 g/cm³ and grain size of the ten-percentile, 39-88 cm). Where there is a large range of clast sizes within a flow, the large grains may respond to the smaller ones in the fluid, as if the fluid had a higher viscosity. This would produce a buoyancy effect for the larger clasts as well as increasing the bulk viscosity of the flow, both factors which decrease the settling velocity of the larger clasts and the strength of the turbulence requisite for suspension of the large clasts. Thus, with appreciable concentrations of fine sand in the flow, velocities needed for suspension of cobble/pebble size clasts might be reduced by a factor of two (Simons et al., 1965, p.49), yielding a velocity range of 25-50 cm/sec to suspend all but the coarsest 10-percentile clast sizes.

The most puzzling point concerns the transport of very large boulders into the basin. It is difficult, by any stretch of the imagination, to envisage large blocks (range: 2-4 m long x 1 m wide) being transported into the basin by turbidity currents, supporting the clasts mainly by fluid turbulence. These large clasts are not very common and comprise less than 10% of the Facies (1) conglomerates. It may be that the large clasts tumbled downslope at the base of large-scale turbidity currents, which carried the finer conglomerate debris. Although it cannot be demonstrated in the field, it is possible that the large blocks were dislodged as part of the rockfalls or slides that initiated the turbidity current flows. Due to their large size (and mass) the large blocks gathered much momentum as they came down the continental slope and would travel long distances, before coming to a halt in the base-of-slope setting.

Facies (2) -- Graded-Stratified/Cross-stratified

Fine Conglomerate and Pebbly Sandstone

Most of the beds belonging to this facies are normally graded and stratified and/or crossbedded throughout (Fig. 16 and logged sections, Appendix 5). Fabric in coarser, stratified portions, toward the base of Facies (2) beds is identical with that for Facies (1) conglomerates -- a-axis flow-parallel, a-axis imbricate upstream (Appendix 6 and logged sections, Appendix 5). Finer-grained, upper bed portions show unimodal bedding fabrics, less commonly bimodal fabric patterns in bedding. Bimodal bedding plots have the largest grains oriented parallel to the secondary mode. Imbrication patterns show about equal proportions of unimodal and bimodal distributions. No grain size influence was seen

in the imbrications, where large clasts dip both up- and downcurrent in the bimodal imbrication plots. Modal angle of dip does not vary with bed thickness nor grain size. Similarly, vector strengths in bedding and imbrication plots are not related to thickness nor grain size of the bed nor to each other.

Paleoflow directions were measured upsection at different levels within 15 beds (Appendices 6 and 7, and logged sections Appendix 5). Of these beds, 10 showed consistent patterns from the base to the top of the bed. The other 5 beds showed variable patterns, with paleoflows commonly differing 90° or more. All of the beds showed progressive normal grading and sequences of structures coincident with waning flow conditions (by comparisons to massive and b-laminated classical turbidites) Hence beds are thought to have been deposited from single flows. Beds with varying paleoflow patterns were deposited from flows that switched directions, or meandered, during deposition.

Parallel stratification in lower parts of Facies (2) beds is commonly defined by alternating clast-supported and clast-dispersed bands. This fact, coupled with the a-axis flow-parallel, a-axis imbricate upstream fabric of the coarser Facies (2) bed portions, suggests that this stratification may have originated similar to that in the upper parts of Facies (1) beds -- i.e. as pulsating deposition from basal concentrated clast dispersions.

Finer-grained, upper bed portions of Facies (2) sediments have stratification that is defined by clear-cut alternations of grain sizes between the layers. This stratification implies that there was good segregation of grain sizes prior to deposition. The occurrence of medium-

scale trough crossbedding in many of the beds (Fig. 16) also suggests tractional influence during deposition of the finer-grained bed portions. The fabric data, however, are not indicative of pure tractional bed-load transport.

Fabric within well-defined, stratified pebbly sandstones and fine conglomerates of this facies are described as: well-defined unimodal, good unimodal or bimodal bedding fabrics. Imbrication patterns are either unimodal or bimodal, with high angles of dip. In light of Johanson's (1976) work, the fabric patterns are interpreted as follows:

Well-developed unimodal bedding fabrics, with a-axes imbricate upstream reflect deposition under high velocity conditions. Only those clasts with a-axes both parallel to flow and imbricate upstream were stable and were not rolled in transport by the flow. All clasts with other orientations were maintained in transport. Good unimodal bedding fabrics, with a-axes imbricate upstream reflect deposition under slightly lower velocity conditions. Unimodal bedding fabrics, with bimodal imbrications may reflect deposition under very high velocity conditions in which there was perhaps a 'wave-form' topography on the bed. Only those clasts with a-axes parallel to flow were deposited on the bed. Clasts deposited on upflow limbs of wave bedforms showed an upstream imbrication; whilst, those clasts deposited on downflow limbs of wave bedforms attained downstream imbrications.

Bimodal bedding fabrics with bimodal imbrications cannot, at present be interpreted. It is difficult to understand the origin of this pattern, and no experimental work can help explain its development.

Bimodal bedding fabrics with a-axes imbricate upstream reflect deposition under lower velocity conditions, compared to Facies (2) beds with unimodal flow-parallel bedding fabrics. The bimodal bedding fabric is thought to be due to some clast reorientation after initial deposition on the bed. Although some of the clasts are reoriented by tractional rolling on the bed, most of the clasts retained the a-axis flow-parallel, a-axis imbricate upstream pattern. On the average, this yields a bimodal a-axis bedding fabric, with a-axes imbricate upstream. The flow-transverse mode in the bedding plot would not be as strong as the flow-parallel mode, as most of the clasts are not reoriented.

The next major point concerns estimates of flow conditions to generate the observed sequences of structures and grading patterns within the Facies (2) beds.

Oblique crossbedding is described in Appendix 4, and is low-angle crossbedding. Usually the lower contact is parallel laminated. Consequently, it is impossible to explain this crossbedding as being a result of infilling of low-relief scours on the bed. It is possible, as postulated by Hendry (1972) and Rocheleau and Lajoie (1974) that this type of crossbedding is formed by migration of large dunes.

Crossbedding in lower and upper parts of Facies (2) beds suggests that the flows were fully turbulent. Assuming Shield's relations are valid for fine pebble transport at the base of low-concentration turbidity currents, Shield's criterion can be used to calculate minimum (at the threshold of clast movement) shear velocities needed for movement as bedload of given grain sizes.

Minimum shear velocity values can then be used to obtain estimates of minimum flow velocity and critical shear stress. The following relations are used.

$$(5) \quad \tau_c = \beta (\gamma_s - \gamma_f) d_s$$

$$(6) \quad \tau_c = S_f U_{*c}^2$$

For fully turbulent flow ($Re > 1000$), Shield's $\beta = 0.06$. By substitution and rearranging:

$$(7) \quad U_{*c} = \left\{ \frac{0.06 (g) [\rho_s - \rho_f] d_s}{S_f} \right\}^{\frac{1}{2}}$$

Because most of the fine conglomerate with stratification consists of quartz-pebble stratification, the density of quartz (2.65 g/cm^3) was used to be the average density of the sediment (ρ_s). A turbidity current density of 1.18 g/cm^3 was used (ρ_f). Estimates for shear velocities needed at the base and top of beds for the different Facies (2) types are listed in Table 10. The minimum shear velocities for the Massive-to-Stratified and Graded/Stratified Types were in the range: 11-14 cm/sec at the base of beds and 5-9 cm/sec at the top of beds. The minimum shear velocities for the Graded/Trough Crossbedded and Graded/Oblique Cross-laminated types were in the range: 10 cm/sec at the base of beds and 8-10 cm/sec at the tops of beds.

Assuming that the flow is predominantly two-dimensional and that the low concentration turbidity currents were flowing in essentially 'open channel' conditions, one can use the following equation to obtain an estimate of the average flow velocity:

$$(8) \quad \frac{\bar{U}}{U_*} = \left\{ \frac{8}{f} \right\}^{\frac{1}{2}}$$

where f is actually $(f_0 + f_1)$. Friction factor values (f) are listed in Table 10. Calculations show that the velocity for the Massive-to-Stratified and Graded/Stratified types range: 160 - 215 cm/sec at the base of beds to 70 - 141 cm/sec at the tops of beds. Velocities for the Graded/Trough Crossbedded and Graded/Oblique Cross-laminated types range: 140 - 156 cm/sec or 71-78 cm/sec (depending upon the f values) at the base of beds to 114-142 cm/sec or 57-71 cm/sec (depending upon f values) at the top of beds. Because Shield's criterion was used to estimate critical shear velocities, these flow velocity averages are minimum estimates.

With estimates of minimum flow velocities, approximations can be made of minimum flow heights. Middleton (1966) showed that the velocity of the head of a density current is given by:

$$(9) \quad \bar{V} = C \left\{ \left[\frac{\Delta S}{S_f} \right] g d_1 \right\}^{\frac{1}{2}}$$

where, $C = \text{constant} = 0.7$. Estimates of the flow depth (d_1) were made using a turbidity current density of 1.2 g/cm^3 ; estimates of the minimum velocities calculated for maximum grain sizes at the base of beds (\bar{U}); and, lower friction factor approximations (f -values). Results of these calculations (Table 10) yield minimum flow heights of 5-50 m for the Massive-to-Stratified types, 3-19 m for the Graded/Stratified types, and about 6 - 25 m for the Graded/Trough Crossbedded and Graded/Oblique Cross-laminated types.

TABLE 10

MINIMUM ESTIMATES OF FLOWS DEPOSITING FACIES (2) BEDS

Facies (2) Type	f	U* (cm/sec)	\bar{U} (cm/sec)	Maximum Grain Size (mm)	Mean Grain Size (mm)	Part of Bed
Massive-to-Stratified	.035	14.3 - 43.3	215 - 650	256	28	Base
Stratified Throughout	.035	10.8 - 27.1	163 - 406	100	16	
Trough Crossbedded	.042	10.1 - 33.2	232 - 464	150	14	
Oblique Crossbedded	.042	11.2 - 33.2	253 - 464	150	17	
Massive-to-Stratified	.035	9.4 - 15.3	141 - 230	32	12	Top
Stratified Throughout	.035	4.7 - 10.8	70 - 163	16	3	
Trough Crossbedded	.042	8.1 - 33.2	232 - 464	150	9	
Oblique Crossbedded	.042	7.7 - 10.1	54 - 107	80	14	

CURRENT HEAD HEIGHT ESTIMATES, BASED ON BASAL AVERAGE VELOCITY VALUES *

Facies (2) Type	Head Height (m)	* Note:
Massive-to-Stratified	5 m - 49 m	$S_s = 2.65 \text{ g/cm}^3$
Stratified Throughout	3 m - 19 m	$S_f = 1.18 \text{ g/cm}^3$ for lower heights
Trough Crossbedded	6 m - 25 m	$S_f = 1.65 \text{ g/cm}^3$ for greater heights
Oblique Crossbedded	7 m - 25 m	Average velocities used were the U values calculated for the base of the beds.

f value estimates are based on data given by Simons et al (1965) and Koster (1977).

The final point concerns the generation of trough and oblique crossbedding. Medium-scale and large-scale trough crossbedding attributed to the migration of dunes is generally lacking in deep-sea sediments, with the exception of those structures reported by Rocheleau and Lajoie (1974), Hendry (1972) and Winn and Dott (1977). It is generally accepted that increased concentrations of sediment and increasing rates of deposition from suspension suppress turbulence and the generation of bedforms. Thus, most workers have invoked this concentration effect to account for the absence of crossbedding of dune migration in deep-sea sediments. This is especially true in denser fluids ($S_f = 1.1+$) where, for example, sand grains (due to their reduced settling velocity) will behave hydrodynamically like coarse silt. For a given shear velocity, this will take the sand grains out of the dune stability field and into the ripple field (Fig.55).

The generation of oblique cross-lamination is not understood very well. Rocheleau and Lajoie (1974) interpreted oblique low-angle crossbedding due to the migration of dunes under relatively high rates of suspended sediment fall-out, with a diminishing of the stoss side slope. This effect has been observed by Jopling (1965) in his study of avalanche fronts of laboratory deltas. Oblique cross-lamination in the present study, is similarly thought to be due to bed form migration under conditions of high suspension fallout. The irregularly inclined stratification in some Facies (2) beds may have a similar origin (Fig.112). Alternatively, this feature may represent suppression of upper flow regime antidunes under high suspension fall-out.

The absence of dune crossbedding has been explained (see previous page), now the presence of dune crossbedding within many of the Facies (2) beds must be accounted for. Dune structures need certain flow depths and a given amount of time to develop (Middleton, 1974; 1977: pers. comm.). As discussed by Middleton (1974) dunes require a well-developed separation zone, for the generation of large-scale and medium-scale crossbedding. Hence, the transition from plane bed to dunes implies an increase in the friction factor values by a factor of 2½. Under conditions of slowly decreasing stream power, this would imply that such a large increase in friction factor can only be accounted for by an increase in flow depth. Considerations of the stream power equation, in relation to the formation of dune structures, suggests that for turbidity currents (in which the density difference is low, i.e. $\Delta \rho = 0.1$), dunes can only form if the flow depths are greater than 150 cm. For flow depths less than 150 cm, with bed slopes sufficiently high to give requisite stream power values for dune formation ($\text{Re} = 1000 \text{ ergs/cm}^2/\text{sec}$), the flows will be supercritical and dunes will not be able to form.

Flow depth estimates for the Graded/Trough Crossbedded and Graded/Oblique Crossbedded types are in the general range of 6 - 25 m, well within the range of values needed for dune formation. One must also consider the time factor needed to develop dune forms. Higher shear stress values are needed for the generation of dune structures, as opposed to ripple bedforms. Slightly longer duration currents are requisite, such that dunes will be stable bedforms. These flow conditions (longer duration currents with flow depths at least 150 cm)

may only be possible in the thicker, coarser-grained, large-scale turbidity currents.

In summary, the different Facies (2) types can be arranged in a possible hierarchy of flow conditions and/or sedimentation rates. The Massive-to-Stratified types, with ungraded bases and alternating concentrated-clast and dispersed-clast stratification bands, are thought to have been deposited under high flow conditions and/or sedimentation rates. Deposition was from concentrated clast dispersions, perhaps modified grain flows, at the base of large-scale turbidity currents. During final flow stages tractional currents became predominant. These tractional currents may record tractional upper flow regime conditions.

Graded/Trough Crossbedded types are dominated by tractional current features and formed under lower flow conditions than the Massive-to-Stratified types. Graded/Stratified and Graded/Oblique Cross-laminated types are both dominated by tractional current deposition, which were not as strong as the flows generating the Graded/Trough Crossbedded types. In addition, Graded/Oblique Cross-laminated types may have formed under conditions of high sediment fall-out from suspension.

Facies (5) -- Ungraded Cross-stratified Fine Conglomerate

Pebbly Sandstone and Sandstone

Facies (5) beds are ungraded and crossbedded throughout (Fig. 25). Because the beds are ungraded, one must assume that the flows were predominantly tractional with very little suspended sediment fall-out. Facies (5) beds are rare within the Cap Enrage sediments, suggesting that the tractional flows that molded the bedforms (to yield the small and medium-scale trough crossbedding) were not likely due

to strong bottom currents that continually swept across the depositional setting. Rather, it is more likely that the tractional flows were associated with turbidity current flow. These tractional flows may have been dilute spillover flows from turbidity currents, that were travelling in other parts of the depositional system. Grain size for beds with medium-scale, ungraded trough crossbedding averages about 7 mm (minimum: 0.5 mm, maximum: 16 mm). The grain size for beds with small-scale, ungraded trough crossbedding averages 0.3 mm (minimum: 0.15 mm, maximum: 0.38 mm).

No experimental work has been done on bed form genesis for sediment in the range of that observed for the medium-scale trough crossbedding (Middleton and Southard, 1977, Fig. 7.19; Fig. 57 in this thesis). Similarly, recent work by Dalrymple *et al* (1978) on bed configurations in the Bay of Fundy tidal environment do not have data within the grain size range for medium-scale trough crossbedded sediments in the Cap Enrage deposits. A rough estimate can be made of flow velocities by using the minimum grain size, 0.5 mm, and the bedform stability plot given in Fig. 57. For a grain size of 0.5 mm, the shear velocity (U_*) needed to generate dunes is about 9 cm/sec. Using a friction factor value of 0.042 (f) along with the above grain size and shear velocity values, the average velocity (\bar{U}) calculated from equation (8) is 124 cm/sec. Similar calculations for the small-scale trough crossbedded Facies (5) sediments (using $U_* = 5.8$ cm/sec; grain size = 0.27 mm; and, $f = 0.052$) yield an average velocity of 72 cm/sec. This average velocity for generation of small-scale trough crossbedding corresponds with those calculated in other environments for similar size material. For medium sand in rivers dunes are formed in flows with velocities of 50-70 cm/sec,

depending upon flow depth (Cant, in press). For this size sediment (0.27 mm) in the tidal Bay of Fundy, dunes are formed in flows with velocities of 78 cm/sec (Dalrymple et al, 1978).

Dilute spillover flows from turbidity currents with velocities in the range of about 70 - 125 cm/sec, are thought to have reworked previously deposited sediments and molded them into bedforms, which migrated, yielding ungraded crossbedded Facies (5) beds.

Facies (6) -- Structureless Pebbly Sandstone and Sandstone

Fabric within the massive Facies (6) sandstones may be unimodal, random or bimodal in bedding, with a-axis imbricate upstream. Paleoflow directions in different levels of individual beds were measured in 4 beds, all of which showed consistent vertical patterns (Appendix 7, and logged sections, Appendix 5). Most of the beds are abruptly normally graded (43%) or slightly normally graded (30%). Less commonly beds are completely ungraded (26%) (Fig. 27). The lack of good, overall progressive grading suggests either 1) sediments were deposited very rapidly, from turbulent suspensions, with very little time for good lateral segregation of grains within the current before deposition; or, 2) grain mobility was hindered, perhaps by high viscosity of the flow, or apparent viscosity due to appreciable concentrations of fine sand, which make the coarser grains respond to the flow as a more viscous fluid.

The variable a-axis bedding fabrics with unimodal, a-axis imbricate upstream patterns are akin to those patterns generated by Lindsay (1966) for flows in which viscosity effects are dominant. The type of grain fabric that is generated and preserved in the deposit depends upon the time within the cycle of particle motion that the viscous flow is

arrested. The only fabric pattern that is difficult to explain in terms of deposition from viscous flows is the bimodal bedding fabric, with a-axis imbricate upstream. Other workers have reported a-axis transverse to flow bedding fabrics in deposits from laminar debris flows (Johnson, 1970) (in rigid plug areas) or from laminar lava flows (Khan, 1962). The reason for flow-transverse bedding fabric orientations under laminar flow conditions is not understood.

As with the Facies (1) conglomerates, some features of the Facies (6) beds suggest deposition of sediment en masse, whilst other features suggest transportation was not as coherent masses of debris flows, slides or slumps. Fabric patterns resemble most closely those developed within viscous laminar flows. The occurrence of abrupt or slight normal grading suggests that there was some grain mobility and segregation of clasts prior to deposition. As with the Facies (1) conglomerates, the massive Facies (6) sandstones were thought to have been transported to the basin by turbidity currents. During transport stages within the base-of-slope setting, concentrated clast-dispersions developed at the base of the turbidity currents. Deposition from the concentrated clast dispersions may have been en masse, when the strength of the basal dispersion exceeded the applied shear stress from the over-riding turbidity current. Grading patterns reflect sorting of sediment within the turbidity currents prior to deposition. Fabric patterns reflect transport and deposition from basal concentrated-clast dispersions.

In contrast to the Facies (1) conglomerates, the basal dispersions for flows which deposited the Facies (6) sandstones may have been dominated

2, by viscous, rather than inertial, effects. The viscous effects are thought to be due to very high concentrations of sediment coupled with a range in the sizes of the dispersed grains, with the result that the larger grains respond to the smaller grains in the dispersion, as though the dispersion were a fluid of larger density viscosity. This apparent increase in the bulk viscosity of the concentrated clast-dispersion 1) damps turbulence, tending to make the dispersion behave more in terms of laminar flow conditions; and, 2) reduces the amount of grain interaction between the coarser grains. This results in a fabric which records the orientation of clasts in viscous fluids, where interaction with other clasts is eliminated.

As for the Facies (1) conglomerates, for simplified models one can calculate the thickness of a concentrated-clast dispersion, at the base of a turbidity current, in which viscous effects dominate. Assuming the same type of turbidity current as in the Facies (1) calculations with a thickness of 100 m, results in a basal shear stress of about 15,700 dynes/cm² (using equation 2). Assuming that the shear stress at the base of the turbidity current is transferred to the grains, then the dispersive pressure (P) for grains in the viscous regime is given by:

$$(10) \quad P \sim T/0.75 = 15,700/(0.75) \approx 20,933 \text{ dynes/cm}^2$$

The height of the column of dispersed grains can be calculated by equation (4), using a bulk density of 2.4 g/cm³ (debris flow specific gravity calculations, Johnson, 1970). Results of these calculations show that a dispersion (in which viscous effects dominate) of only 15 cm thick can be maintained at the base of a turbidity current that is 100 m thick. These results show that if a viscous dispersion does exist at the base

of large turbidity currents, it influences only a very thin zone of the flow. If sediment is deposited layer-by-layer, the layers may be indistinguishable from one another in flows in which there is little or poor grain segregation prior to deposition (as in the case of Facies (6) beds). Alternatively, as deposition from basal dispersions occurs, expansion of the dispersion may work vertically up in the turbidity current with no loss of a basal dispersed layer upon deposition. As with the calculations of modified grain flow thicknesses, thicknesses of viscous dispersions, at the base of turbidity currents, under conditions of deposition may be greater than those calculated for minimum transport conditions.

In summary, Facies (6) beds are thought to have been transported by high-velocity, mainly sandy turbidity currents. Rates of deposition were high, compared to loss of flow power of the currents, with little segregation of grains occurring before burial. Deposition is thought to be mainly from basal concentrated-clast dispersions, in which viscous effects were dominant. Features of Facies (6) beds reflect influences of transport by turbidity currents, and deposition from basal viscous dispersions. Grading is due to lateral segregation of sizes within the transport turbidity current phase, and the variable fabrics reflect the time that the viscous dispersions were arrested.

Facies (3) -- Graded-Dispersed Fine Conglomerate and
Pebbly Sandstone

An equal number of Facies (3) beds have unimodal, bimodal or random a-axis fabric patterns in bedding. Imbrication is usually bimodal, with no grain size influence on the bimodality (i.e. largest clasts dip both up- and downcurrent) (Table 5). Paleoflow directions in different levels of the same bed were determined for 16 beds (Appendix 7, and logged sections, Appendix 5). Of these beds, only 4 showed consistent paleoflow directions from the base to the top of the beds. In the other beds, directions varied on the average 57° from base to top (range: 24° - 99°). All of the beds showed normal grading, although it was the coarse-tail variety. Hence, beds are not thought to be amalgamated. The variable paleoflow patterns within individual beds may reflect meandering within flows during deposition, or be a consequence of rapid deposition in which no fabric orientation is consistently preferred throughout deposition of the beds.

Most Facies (3) beds have normal coarse-tail grading (Fig.19). Over 30% of the beds have stratified and/or crossbedded thin bed portions at the top of the beds. About a third of the beds have well-developed fluid escape features, in the finer-grained upper bed portions (Fig.19). Stratified, crossbedded and liquefied upper bed portions are usually quite thin. Hence tractional and liquefied flows are not thought to be the main transport mechanism of the bulk of Facies (3) beds.

Fabric within Facies (3) beds is very similar to that found in the massive Facies (6) beds, with the exception that only (for the most part) bimodal imbrications are dominant. The occurrence of coarse-tail

grading and characteristic dispersed textures suggest that the Facies (3) beds may represent conditions of very rapid sedimentation. As with the other facies discussed previously, the features of the Facies (3) beds are thought to record a two-fold (at least) sedimentation process. Grading is interpreted as the result of lateral size segregation during transport phases by turbidity currents. Fabric development is thought to occur during transport and depositional phases as basal, concentrated-clast dispersions. It is the nature of these proposed basal dispersions that is of interest.

The variable a-axis bedding fabrics are again similar to those generated by Lindsay (1966) for viscous laminar flows. In Lindsay's models (1966) the imbrication is usually a-axis imbricate upstream; less commonly bimodal imbrications occur. The predominant bimodal imbrication pattern within the Facies (3) beds suggests that, perhaps, a viscous flow model for the basal dispersion does not wholly account for the fabric pattern. The bimodal imbrications may be explained in terms of wave-forms that are generated within the dispersion, which are preserved by en masse deposition from the dispersion. Syndepositional wave-forms may be generated by pulses moving within the dispersion. Alternatively, the wave-forms may have been generated by interface waves travelling along the contact between the basal, depositing dispersion and the over-riding turbidity current.

In summary, Facies (3) beds were deposited rapidly from high concentration turbidity currents. Good lateral segregation of grain sizes did not occur within the current before deposition, where mixing processes and turbulence within the head probably kept the sediment

homogenized. Beds were deposited rapidly, in relation to loss of competence of the turbidity currents, with little time for grain segregation. High concentrations of sediment may have also hindered the settling of clasts. Deposition was from basal concentrated-clast dispersions, which were likely viscous flows that experienced syn-depositional deformation. This syndepositional deformation formed internal wave-forms within the dispersions, which account for the bimodal imbrication patterns. Thin, fine-grained upper bed portions show liquefaction features, stratification and/or crossbedding. This suggests that liquefied flows and/or tractional flows may have been important during deposition of the upper bed portions. This may reflect more deposition from turbidity current phases, under lower-concentrations and less-rapid sedimentation rates. Development of fluid escape features within lower bed portions may have also been a consequence of the poorly sorted nature of the bulk of Facies (3) beds.

Facies (4) -- Graded-Liquefied Fine Conglomerate, Pebbly

Sandstone and Sandstone

Liquefied sandstones and pebbly sandstones have about equal percentages of random, bimodal and unimodal bedding fabrics. Bimodal bedding plots had the largest grains usually aligned parallel to the dominant mode. Less commonly, large grains were in the secondary (transverse to flow) mode or between the dominant and secondary modes. Equal percentages of bimodal and unimodal imbrication patterns occurred. No grain size influence occurred in the bimodal imbrication plots, where large clasts dipped both up- and downcurrent. No relationships existed between modal angle of dip and vector strengths of bedding and imbrica-

tion plots. Similarly, no relationships were found between these parameters and bed thickness nor grain size.

Paleoflow directions were obtained in different levels within individual beds, for 11 beds (Appendix 7, logged sections, Appendix 5). Of these beds, the 7 coarser beds showed good agreement in paleoflows vertically within beds. The finer-grained beds had variable patterns from the base to the top of beds. Three of the four finer grained beds had upsection changes of 90° or greater. In one bed, the flow patterns were coincident at the base and the top of the bed, but differed by about 40° in the middle of the bed. Most of the Facies (4) beds are normally graded with no internal nor load or scour features. The divergent paleoflows are not thought to be due to amalgamation of beds; rather, the upsection changes within individual beds are thought to reflect meandering within flows during deposition.

Most of the liquefied beds have overall, progressive normal grading (Fig. 22 and logged sections, Appendix 5), with only a small proportion being ungraded or inversely graded. The abundance of beds with good, overall normal grading suggests that there was good lateral segregation of grains within the flow prior to deposition. As for the other facies previously discussed, grading is thought to reflect the transport phases by turbidity currents. Fabric patterns are interpreted as recording transport and deposition from concentrated-clast dispersions at the base of the turbidity currents. Facies (4) beds have fabric patterns similar to those belonging to Facies (3) and Facies (6). Facies (4) beds are similarly interpreted as being deposited from dispersions in which viscous effects were dominant. Some of the dispersions

may have also undergone syndepositional deformation, to yield the bimodal imbrications as in the Facies (3) beds.

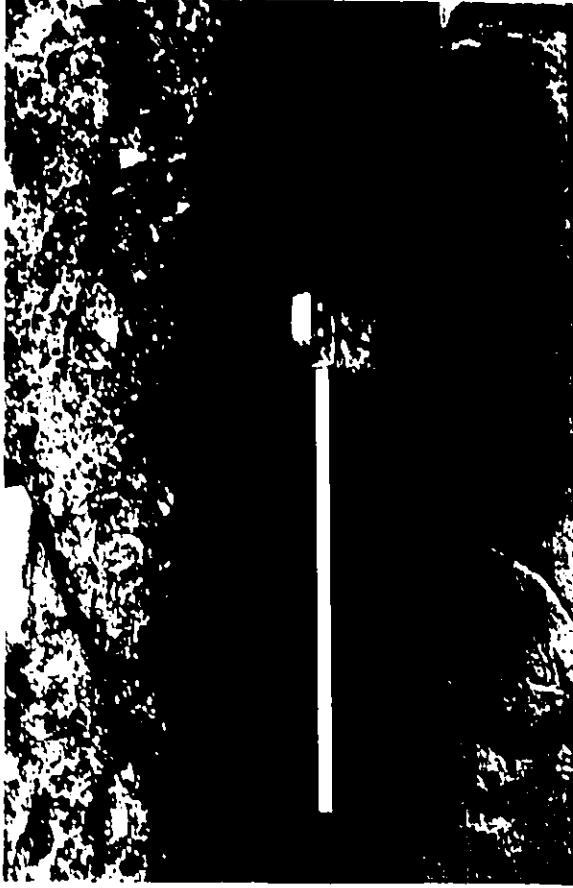
The next major point concerns the estimation of the time of liquefaction of the sediment. Liquefaction due to the release of entrapped pore fluid can occur at various times: 1) during syn-depositional or early post-depositional stages; 2) later post-depositional stages, as a consequence of loading during deposition of the next bed; or, 3) much later, due to sudden loading of a packet of sediments or due to overburden weight and compaction (Lowe, 1975). These different times of liquefaction for individual beds are not always easily distinguished. Beds which have stratified or crossbedded upper bed portions (Types 3, 4, 7 on Fig. 22 and Fig. 60) are syn-depositional, where parallel lamination and crossbedding would represent slower rates of deposition from the over-riding turbidity current flow. By contrast, large sandstone sills and dykes and conglomeratic injections (Fig. 102, 103, 63) would be late post-depositional.

Over 30% (Fig. 22) of the liquefied beds are topped by stratified and/or crossbedded sandstones. An additional 6% of the beds have free-surface pillars, followed by massive upper bed levels. These occurrences suggest that for about 40% of the liquefied beds, liquefaction was syn- or early post-depositional (before deposition of the next bed). Liquefaction may have been a result of pore fluid expulsion during consolidation of deposits from the concentrated-clast dispersions.

Other beds are interpreted as being due to early post-depositional liquefaction. Inclined dish structures have been traced along strike to undisturbed crossbedding (Fig. 58). Liquefied beds which are deformed



57



58

Fig. - Inclined dish structures (left) which are traceable to undisturbed low-angle crossbedding

(right) about 4 m to the east. Bed 911, St. Simon sur Mer Est. Tape is 50 cm long.

Paleoflow is to the left. Stratigraphic top is up, P.404

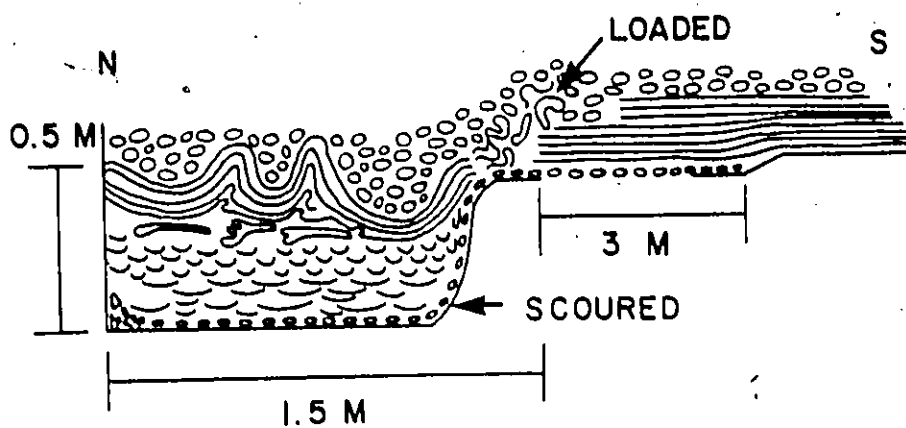


Fig.59 - Differences in fluid escape structures in a scour fill bed. The trend is from broad, flat dishes to more concave dishes to convolute laminations and flame structures. Liquefaction is interpreted as a result of loading during deposition of the overlying bed. Bed 1325, B1c, p.419

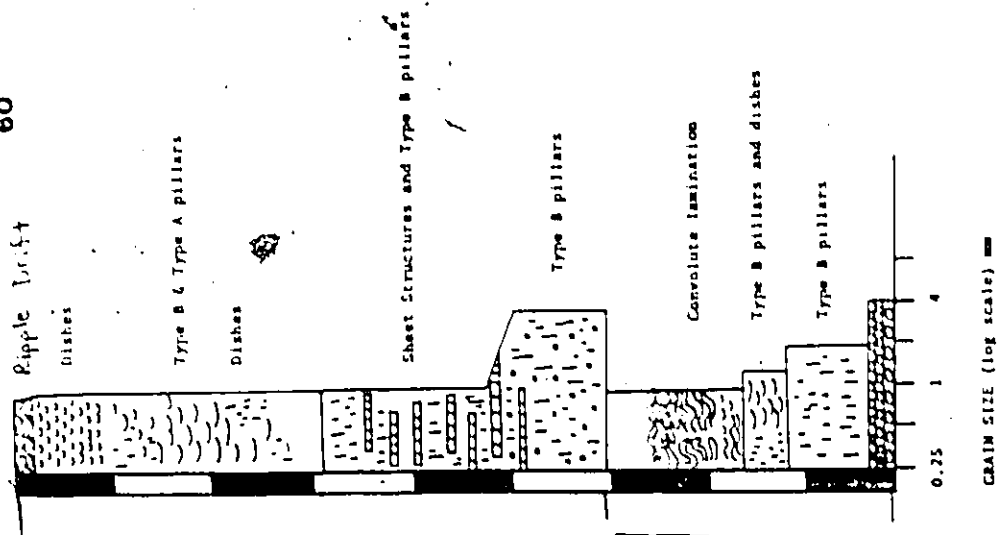
in response to load structures in the overlying beds (Figs. 59, 79) are interpreted as representing beds in which liquefaction was probably induced by deposition and sudden loading by the overlying bed. By contrast, beds with rapidly changing types of fluid escape features alternating with massive layers (Fig. 61), those with free surface pillars at the top bed portions (Figs. 61, 62), and those liquefied beds which do not disrupt immediately overlying sandy sediment are all interpreted as being syn-depositional or early post-depositional (before deposition of the next bed) liquefaction.

Within the Facies (4) beds there are some internal sequences of fluid escape features. These include: 1) flat dish structures → more concave dish structures → very concave dish structures with Type A pillars (Figs. 59, 62), some of which may be capped by free surface pillars (Fig. 62) or convolute lamination (Fig. 61); and 2) the reverse sequence from Type B pillars → Dish structures with Type A pillars → Dish structures. The first sequence occurs more commonly and is the type of sequences expected from the base to the top of a graded bed, with decreasing grain sizes and greater pore fluid discharges at the tops of the beds (Fig. 64). The second sequence would represent decreasing pore fluid discharges upsection and may represent cases where the bed was deposited in pulses -- with basal zones having more rapid rates of expulsion than upper bed layers. Beds with massive bases (Types 1, 2, 3, 8, Fig. 22) tend to be coarser grained than those beds that have fluid escape features at the base. This may be due to the fact that coarser sediment is more difficult to liquefy than finer sediment. Massive fine grained tops of beds are more common in beds in which the top

Fig. 60 - Differences in fluid escape structures in two beds, interpreted as being syn- or early post-depositional in origin. In both cases, the liquefaction became less forceful upsection. These are laterally equivalent to Beds 1176, 1177, and 1178, Cap à la Carre Ouest Section 6, p.413

Fig. 61 - A complex assemblage of various fluid escape features and structureless subunits within a single bed, interpreted as representing pulsing depositional / liquefaction stages during the deposition of a single bed. Bed 549, Anse à Pierre Jean 5, p.390

60



61

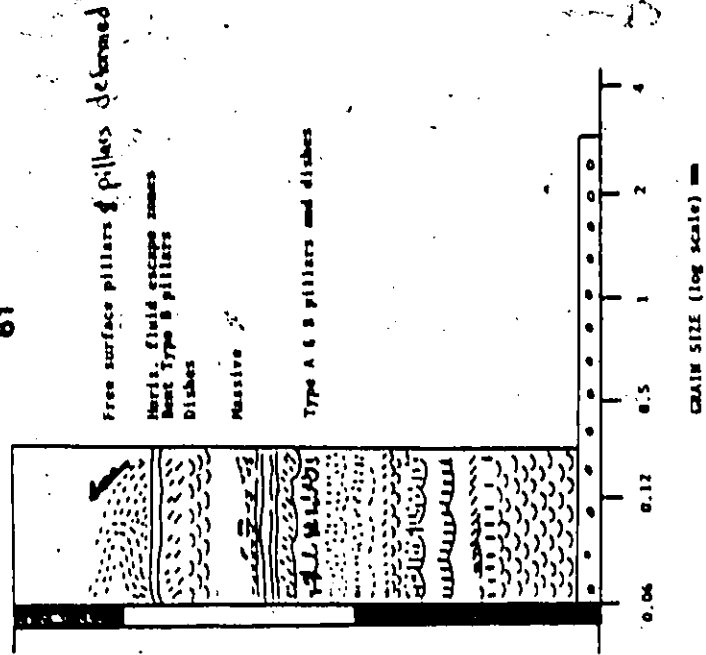
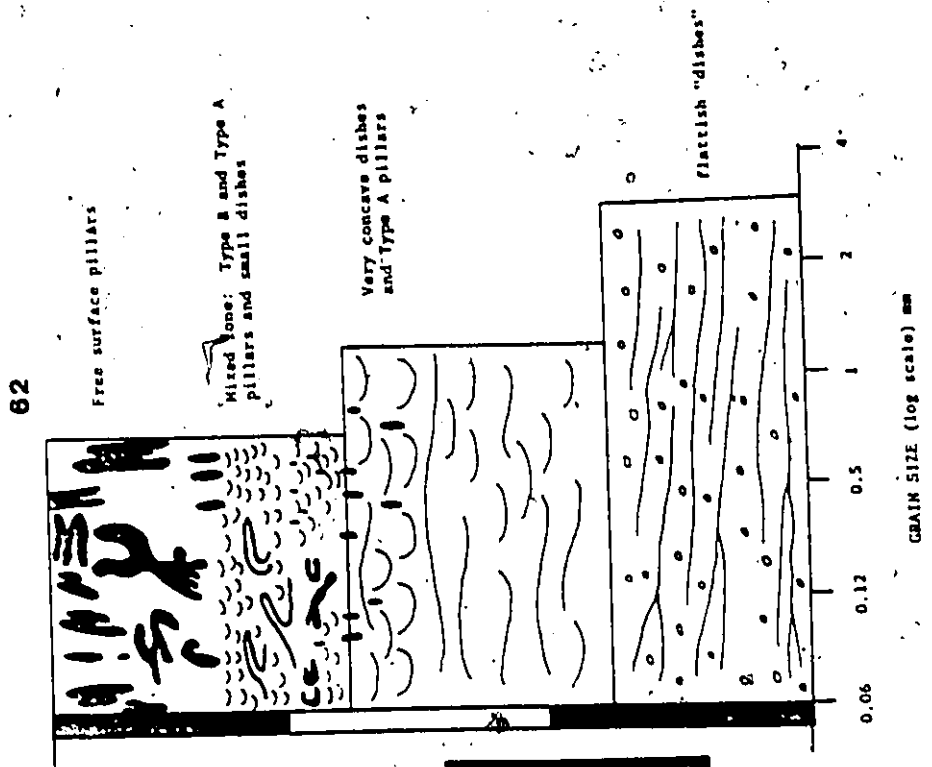
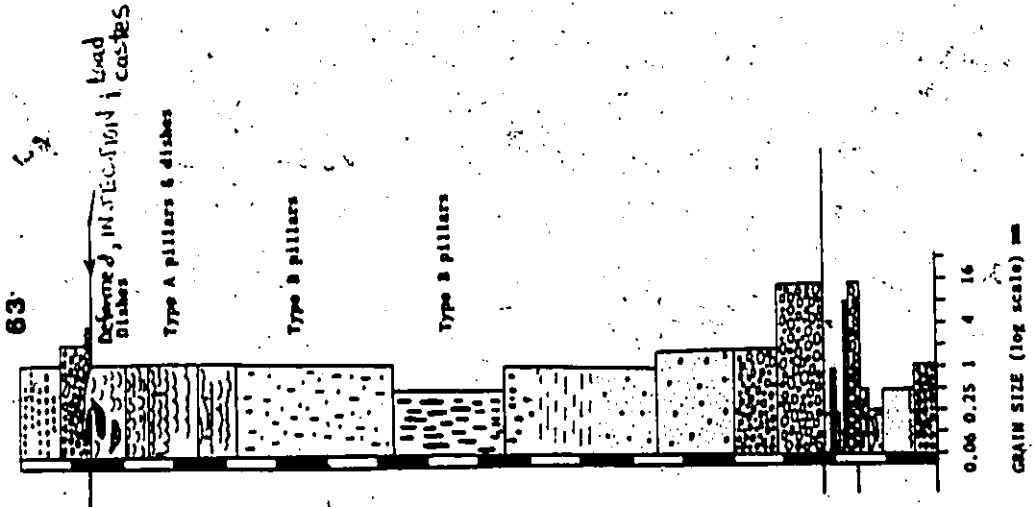


Fig. 62 - Differences in fluid escape features in a single bed, interpreted as being syn- or early post-depositional in origin. Liquefaction became more forceful upsection. Bed 1352, Bic, p.419

Fig. 63 - Differences in fluid escape features in a single bed. Liquefaction became less forceful upsection. Although the overlying bed has a loaded base, it is believed that loading due to deposition of the thin (1.3 m) bed did not cause liquefaction of the underlying thicker (14.5 m) bed. Rather, the sequence is interpreted as representing syn- or early post-depositional liquefaction. Detached load casts and injections are a consequence of depositional/consolidation processes associated with the later event. Bed 878, St. Simon sur Mer Est, p.403



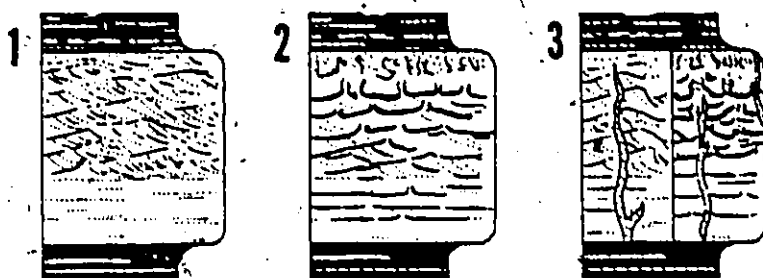


Fig.64- Liquefaction structures that develop in turbidite BCDE beds with non-cohesive C and D divisions. Grain size decreases up through the bed. (1) unmodified BCDE turbidite bed; (2) at fluid discharges just above pure seepage: elutriation and redistribution of mobile grains in B division results in very flat dish structures (or consolidation laminations, Lowe's (1975) terminology) and small Type A fluid escape tubes. Collapse of C division results in partial liquefaction with development of strongly curved dish structures and Type A pillars; (3) at highest water escape rates, structures depend upon the rate of discharge increase. If discharge rises rapidly large Type B pillars can cut across unmodified primary structures (left); if discharge rises gradually, large Type B pillars can form cross-cutting lower discharge fluid escape features.

(from Lowe, 1975)

fluid escape feature consists of free surface pillars (Type 6, Fig.22, Fig.61). These massive fine grained tops (medium to fine sandstone) may represent bed portions that were completely fluidized, leaving no trace of fluid escape features due to the complete washing out of fine material from the bed.

Liquefied flows are not thought to be significant transport agents of sediment into deep-sea depositional sites. Following the discussion of Lowe (1976), in the simplest case, liquefied flow is laminar with no grain interaction. From Lowe's (1976) estimates, laminar liquefied flows are only effective transport agents for thin flows (a few cm thick) of sediment finer than 1 mm. It is, therefore, most probable that graded-liquefied fine conglomerates, pebbly sandstones and sandstones experienced liquefaction during the final transport stages and beginning depositional stages, due to pore water expulsion during initial compaction.

In summary, the Facies (4) graded-liquefied beds are interpreted as being transported into the basin by turbidity currents. During this main transport phase lateral grain size segregation developed, which during deposition led to the formation of graded bedding. Prior to deposition, concentrated-clast dispersions developed at the base of the turbidity currents. Sediment was deposited from the basal dispersions, which, due to high concentrations of sediment may have behaved more as viscous flows. Syndepositional or early post-depositional churning of the sediment produced wave-forms within the dispersions, which explains the bimodal imbrication. Variable bedding fabrics are explained by deposition from dispersions in which viscous effects were dominant. Deposi-

tional rates were very high entrapping significant portions of pore water between the grains. The significant entrapment of pore water and perhaps subsequent churning of the sediment favoured syn- or early post-depositional liquefaction in many beds. Less commonly, beds became liquefied as a consequence of post-depositional loading. Thus, deposition of Facies (4) beds is a multiphase process. Lateral sorting within turbidity currents during transport accounts for the progressive, normal grading. Fabric development is a consequence of rapid deposition from concentrated dispersions at the base of turbidity currents. During these depositional stages, liquefied flows became important, forming prominent fluid escape features. In some beds, reworking by turbidity current flow formed stratification and crossbedding in the finer, upper bed portions.

CHAPTER 6

OVERALL FACIES MODEL FOR THE CAP ENRAGE SEDIMENTS

"Models are to be used, but not to be believed." (Henri Theil)

INTRODUCTION

As mentioned in the introductory chapter, detailed studies by many workers (Davies and Walker, 1974; Hubert *et al.*, 1970; Johnson, 1974; Johnson and Walker, in prep.; Lajoie *et al.*, 1974; and, Mathey, 1970) show a complex paleocurrent pattern for the Cap Enrage sediments (Fig. 12). The most comprehensive study on a regional scale has been Johnson's (1974) work on the conglomeratic members and niveau between Anse a Pierre Jean and Cap Corbeau (Fig. 10). Paleoflows within the conglomerates were mainly west-southwestward, with southerly flows at two locations (Johnson and Walker, in prep.). Compared with local paleoflow directions, conglomerates show horizontally fining and thinning trends in various directions, including upstream, downstream and cross-stream directions (Johnson and Walker, in prep.).

The overall conglomerate paleoflow is toward the southwest (Johnson and Walker, in prep.). Based upon source areas for the sediment (Lajoie *et al.*, 1974) and orientation of present tectonic strike, the conglomerate paleoflows were determined to be parallel to the base-of-slope during Cap Enrage time (Johnson and Walker, in prep.; Davies and Walker, 1974). The large-scale swing of paleoflows from a slope-normal to a slope-parallel direction (at the base-of-slope), prompted Johnson and

Walker (in prep.) to interpret the whole Cap Enragé Formation as being deposited within the confines of a submarine trough or valley. Individual conglomerate members and niveau within the formation are interpreted as meandering, main channel deposits from the valley floor (Johnson and Walker, in prep.).

Within the submarine valley context, the horizontally fining and thinning trends within the conglomerates were conceptualized by Johnson (1974) as sequences which radiate from single, cobble-boulder conglomerates. This radiating, fining and thinning-outward pattern defined what Johnson (1974) called a "pod." Pods have vertically fining-up sequences on the order of 5 m thick. Largest pods were 100-200 m wide and 400 m long (Fig.65). Pod fills were interpreted by Johnson (1974) as representing the fill of incised, deeper scours within the main channel floor.

The field outcrop usually permits only one horizontally thinning and fining sequence to be seen -- either in upstream, downstream or, rarely, in cross-stream directions (Johnson and Walker, in prep.). As pointed out by Johnson and Walker (in prep.) the main problem with the pod model is that it does not adequately explain the horizontally fining and thinning trends in upstream directions. Downstream horizontally fining and thinning trends can be accounted by decreasing flow velocities and rates of deposition, as currents emerge from deeper scours. An alternative interpretation, which is presented in this chapter, is that the horizontally fining and thinning sequences represent facies changes from coarser, main channel deposits to finer, topographically higher, terrace or braid bar top deposits.

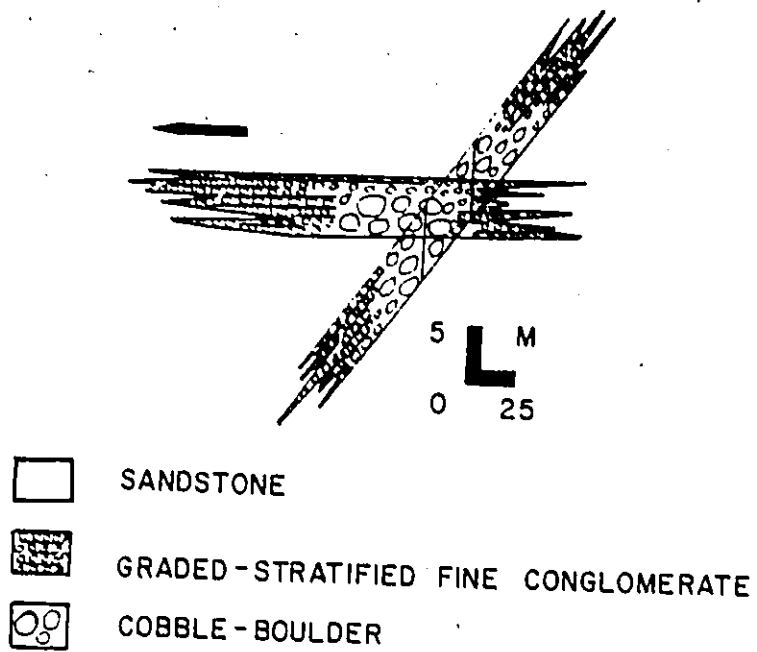


Fig.65 - Generalized sketch of a conglomerate "pod". Arrow indicates conglomerate paleoflow.

In the present project, the overall Cap Enragé model was developed only after detailed comparisons of individual sections, and by glean- ing the common denominators from all of the sections. Understanding the whole Cap Enragé Formation, as an integrated network, means that one would have to put all of the sections together in one complete, yet very detailed, diagram. The detail of the sections and the limitations of pre- senting the data in thesis format, prohibit the use of large detailed diagrams. Therefore, one has to examine the individual parts of the sys- tem piecemeal; and, show how the different parts give information about the whole system. Once the different parts are interpreted, these inter- pretations can be integrated into the facies model for the whole forma- tion.

In this chapter the basic model is presented first. This is done to keep a certain frame of reference for the different interpretations and to provide a description of the basic terminology. By reading the interpre- tations of individual outcrop sections, the reader can see how the various parts fit into the whole system. In addition, one can see how the author devised the model for the whole formation. An analogy to this presentation would be someone coming in on the tail end of the first showing of "Murder on the Orient Express," when Hercule Poirot is explaining how everyone killed the victim. Then, one would sit through the second showing of the film to see how Agatha Christie's clues, throughout the film, led up to Poirot's final solution of the case.

In this chapter the order is as follows. The basic model is present- ed first, with the terminology that will be used. Next, interpretations of individual outcrops that fit into the different subenvironments are

presented. This is followed by an integration of the different interpretations into an overall facies model for the Cap Enragé sediments. Comparisons are made with other deep-sea sediments. Finally, a general tectonic setting is discussed.

GENERAL PALEOTOPOGRAPHIC RECONSTRUCTION OF THE CAP ENRAGÉ SYSTEM

The general interpretation of the paleotopography of the setting for the deposition of the Cap Enragé sediments is sketched in Figure 66. An aggraded channel system, with a braided pattern, flowed within a submarine valley (denoted by 'valley walls', Fig.66). Within the submarine valley, there were different topographic levels of deposition, including:

1. Main Channels (MC, Fig.66): depths in the range of 1-5 m; individual channel widths up to about 250 m. Channels, for the most part, have gently sloping walls: only three scour contacts, of what were interpreted as main channel fills, had steep, near vertical, sides. The main channels, most likely, formed a braided or anastomosing pattern. The braided channel network had a possible width of about 10 km across the submarine valley (to accommodate the outcrop belt of conglomeratic members and niveau).
2. Pods (P, Fig.66): depths in the order of 1-5 m; maximum widths of 100-200 m; and, maximum length of 400 m. These pods are defined by Johnson (1974) and are interpreted as representing incised scour deposits from main channels. Maximum depths of incision would be about 5 m.
3. Cut-off Channel (CC, Fig.66): depths in the order of 0.5 - 2 m; maximum lengths traceable along strike for about 50 m. Many of the individual scour traces have steep, near vertical, sides. Quite often individual scours may be laterally linked along the base of a bed, giving the

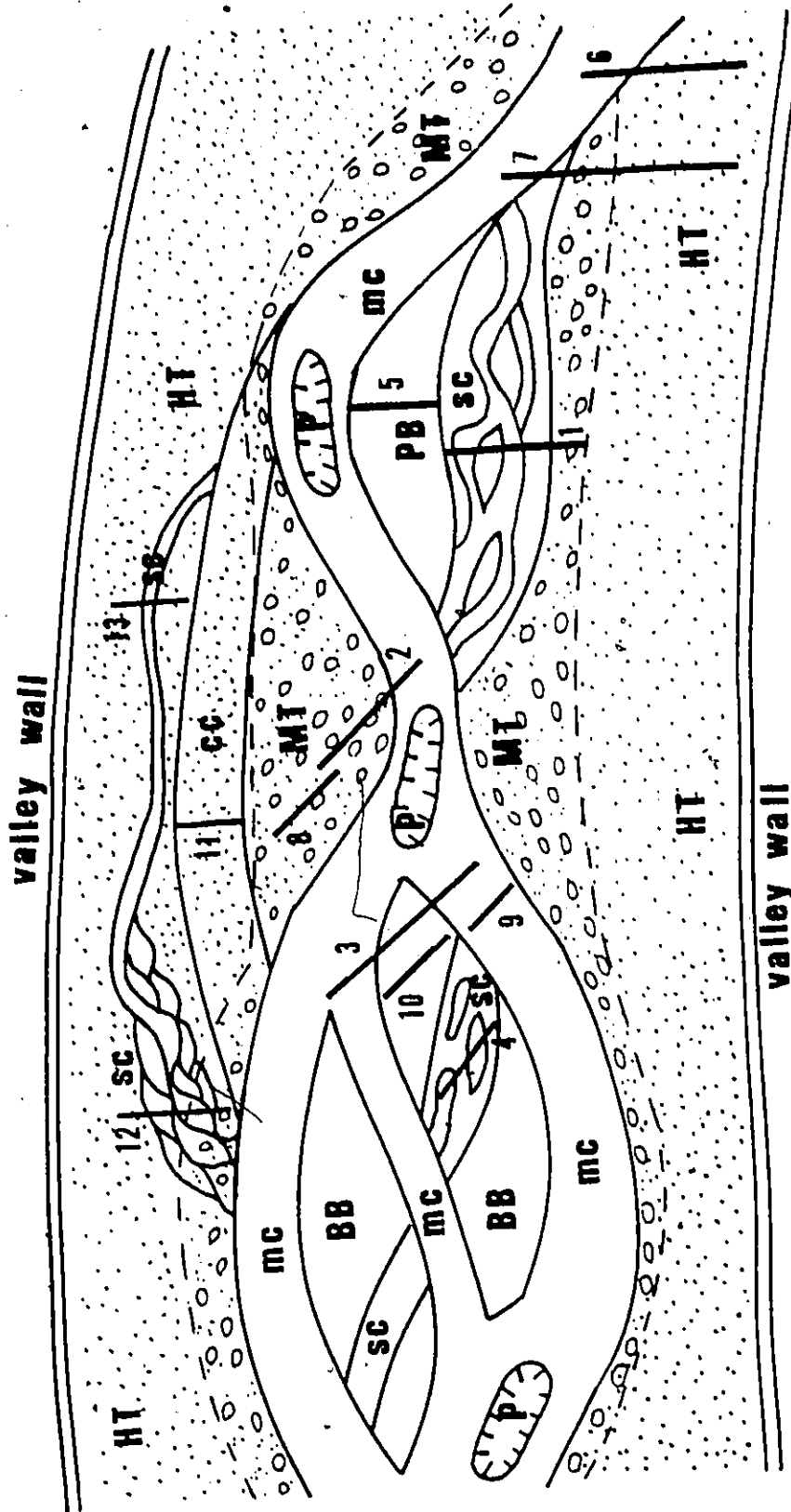


Fig. 66. General paleotopographic reconstruction of the Cap Enrage system. Numbers and heavy lines refer to lines of section. Key: Main channels (mc); pods (P); cut-off channel (cc); point bars (PB); braid bars (BB); marginal terrace (MT); high terrace (HT); secondary channels (sc). : : : : sandstone; ○ ○ ○ ○ pebbly sandstone; □ conglomerate

base a scalloped appearance. Most of the scour fill material consists solely of the finer-grained facies. These scour-fill, fine grained deposits are interpreted as being deposited from main channel sites, which are cut-off from coarse sediment supply.

4. Point Bars (PB, Fig. 66): relief of 1-5 m above the main channel and lengths up to 600 m. These are topographic high areas which occur in meander bends of the main channels.
5. Braid Bars (BB, Fig. 66): heights on the order of 1-5 m above the main channels and widths between channels of 50-100 m. These are interchannel, topographically high, areas within the aggrading main channel network. These braid bars separate the main channels.
6. Terraces (MT and HT, Fig. 66): marginal terraces on the order of 5-10+ m above the main channel network (MT), and high terraces (HT) on the order of 25-50+ m above the aggrading main channel system. The terraces are depositional high areas, above the general level of the main channels and bars of the channel network. Although it cannot be proved, the terraces (for simplicity sake) are interpreted as being continuous borders to the aggrading channel network. These terraces would be within the confines of the submarine valley. Marginal terraces (MT, Fig. 66) are those terrace sites which are near the main channels and receive some coarse sediment input. High terraces (HT, Fig. 66) are those terrace areas which are far away from the main channels and receive mainly fine sediment.
7. Secondary Channels (SC, Fig. 66) are small channels which are superimposed upon braid bars, point bars or terraces. Small channels are generally less than or equal to 1-2 m in depth. Widths of individual channels

range from a few m to about 25-50 m. Small channels occur singly, or form braided or anastomosing patterns on bar or terrace tops.

8. Secondary Braid Bars (Fig.66) are small, interchannel areas which separate the secondary channels. Small braid bars range from less than 1 m in height to about 2 m in relief. Widths range from a few m to about 25-50 m.

PALEOTOPOGRAPHIC RECONSTRUCTIONS FOR INDIVIDUAL OUTCROPS

Main Channel Deposits

(1) Anse à Pierre Jean 3 (Niveau 3) (Fig.67)

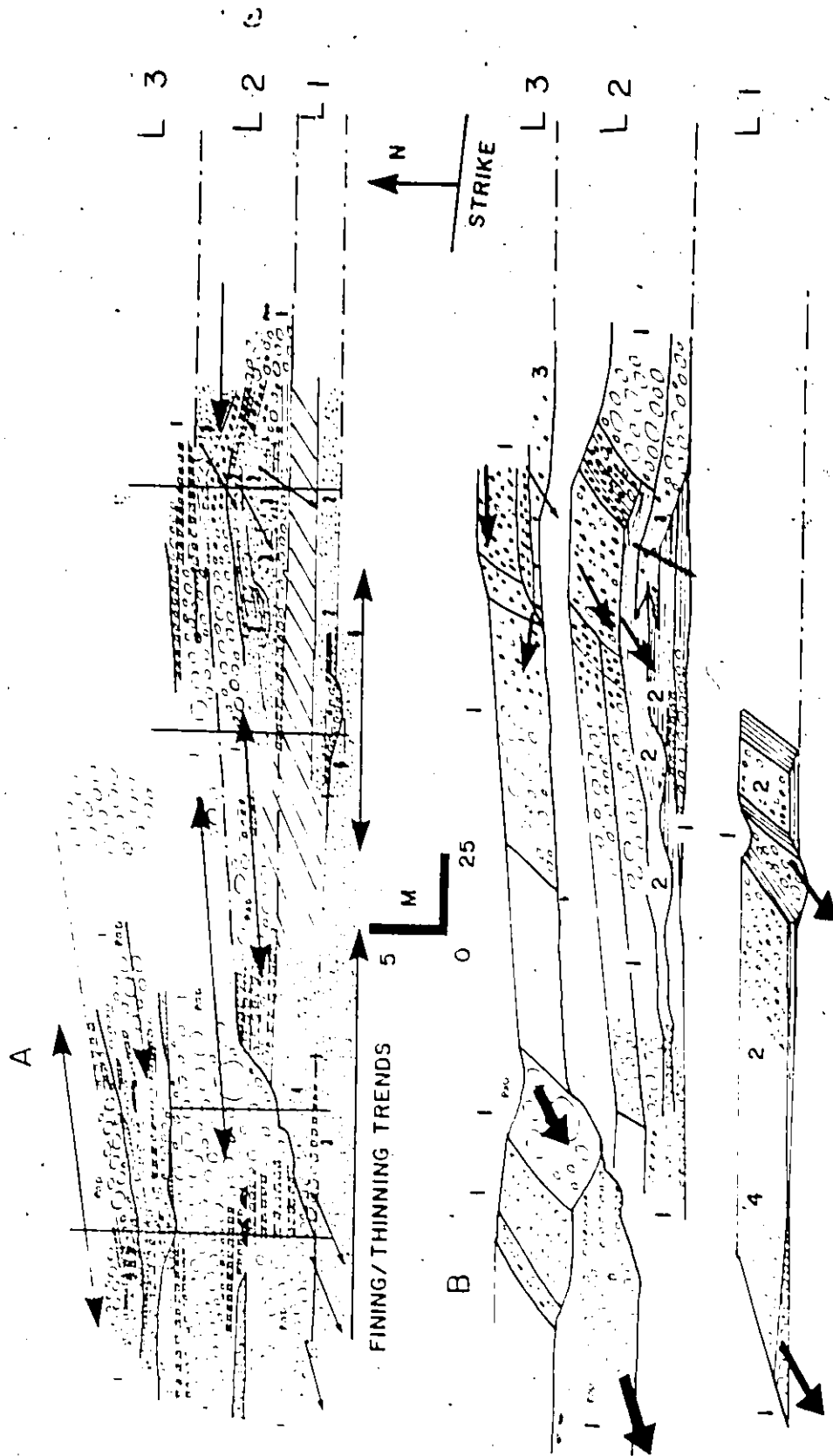
This reconstruction is based upon detailed sections from this study (Beds 484-506, Appendix 5, p.387) as well as detailed conglomerate sections of this outcrop given by Johnson (1974). Beds which fit Johnson's pod model, in the descriptive sense, are labelled as 'pod' on the generalized section (Fig.67A) and will be referred as 'pod sediments' in this discussion.

In general, the sections at Anse à Pierre Jean 3 (Niveau 3) appear to represent a series of superimposed pod sediments. Sediments become coarser-grained, and pod dimensions become larger upsection (Fig.67A). Niveau 3, for ease in discussion, is divided into three levels (L1-L3, Fig.67A).

A small pod occurs in the eastern basal part of Level 1 (L1, Fig. 67). Basal pod fill consists of Facies (1) conglomerate, which grades into Facies (2) fine conglomerates, along the eastern and western margins of the scour surface. The basal Facies (1) conglomerate thins westward, where it has large boulders sticking out above the general bed level. A thick, liquefied Facies (4) bed overlies this irregularly-topped

Fig. 67. Generalized sections (A) and paleotopographic reconstruction (B). In (A), dotted portions are the finer-grained facies, excluding Facies (1); open ellipses are Facies (1) units. Beds conforming to the pod model (Johnson and Walker, in prep.), in the descriptive sense, are labelled as 'POD.' Heavy arrows show fining/thinning trends. Light arrows are paleocurrent directions. Numbers 1, ..., 6 are facies designations. L1, ..., L4 are level designations for specific outcrops. Cross-hatched portions are covered intervals. Dashed lines are boundaries between levels. Strike line is regional strike of the outcrop. In (B), arrows indicate paleoflow directions, with relative flow strengths suggested by arrow size. Numbers 1, ..., 6 are facies designations. Scale as indicated is the same in both (A) and (B).

Anse à Pierre Jean 3, Beds 484-506, p.387



conglomerate. No paleocurrent data is available for the liquefied bed. It is continuous along strike and shows no evidence of scouring nor channelization. Paleoflows within the irregularly-topped conglomerate are identical with those for the scoured Facies (1) conglomerate located to the west. Both paleoflows are toward the southwest. The thick Facies (1) conglomerates at the west end of the outcrop conform to Johnson's (1974) pod model, in a descriptive sense, and are interpreted as being main-channel deposits.

The association of the thick liquefied Facies (4) bed with the Facies (1) conglomerate, immediately overlying and along-strike to the liquefied bed, suggest that the thick liquefied bed may have been deposited near a main channel. The continuous nature of the bed suggests that it was not deposited within a scour or channel. The most likely site would be a marginal terrace setting (Site 2, Fig.66) near a main channel. The thin, underlying and irregularly-topped Facies (1) conglomerate may have been deposited from flows which overtopped the main channel and deposited thin conglomerate on top of the marginal terrace. This thin conglomerate is inversely-graded, clast-supported, with no evidence of fine matrix and has large clasts protruding above the general bed level. The interpretation of the origin of this conglomerate is that it is a lag deposit from a coarse-grained flow, which travelled mainly down the main channel (to the west). There was a brief interlude of overtopping the channel, leaving a coarse-grained, inversely-graded, lag on top of the marginal terrace. Subsequent deposition from later flows covered the boulders and clasts sticking up above the general bed level -- producing an irregularly-topped conglomerate.

The facies associations in Levels 2 and 3 (L2, L3, Fig.67) can be explained by a series of channel/braid bar deposits, which were superimposed upon one another. Facies (1) coarse conglomerates are laterally associated with thin Facies (1) beds and Facies (2) and (3) beds. These associations are interpreted as representing changes from main channel sites (thick Facies (1) beds) to slightly higher braid bar tops (thin Facies (1), (2) and (3) beds), where flows which overtop the channels are of a lower concentration and somewhat slower, depositing thinner and finer-grained deposits.

The coarse-grained nature of the fills and the large dimensions of the scoured surfaces (up to 5 m depth at the west end of the outcrop) suggest that the channel/braid bar complexes are part of the aggrading main channel network (Site 3, Fig.66). Arbitrary vertical sections through the superimposed pod sediments do not show overall trends, aside from the tendency of Facies (2) and (3) sediments to be followed by Facies (1) conglomerates. However, when one looks at the superimposed pods, the sediments of each successive pod seems to become coarser-grained and pod dimensions become larger upsection (from the base of Level 2 to Level 3). This overall coarsening/thickening-up sequence of pod sediments may reflect gradual occupation of a main channel site by successively larger, and more competent, sediment gravity flows.

(2) Anse à Pierre Jean 2 (Niveau 3) (Fig.68)

This reconstruction is based upon detailed sections from this study (Beds 456-483, Appendix 5, p.386), as well as detailed conglomerate sections of this outcrop given by Johnson (1974). Beds which fit Johnson's pod model, in the descriptive sense, are so labelled on the

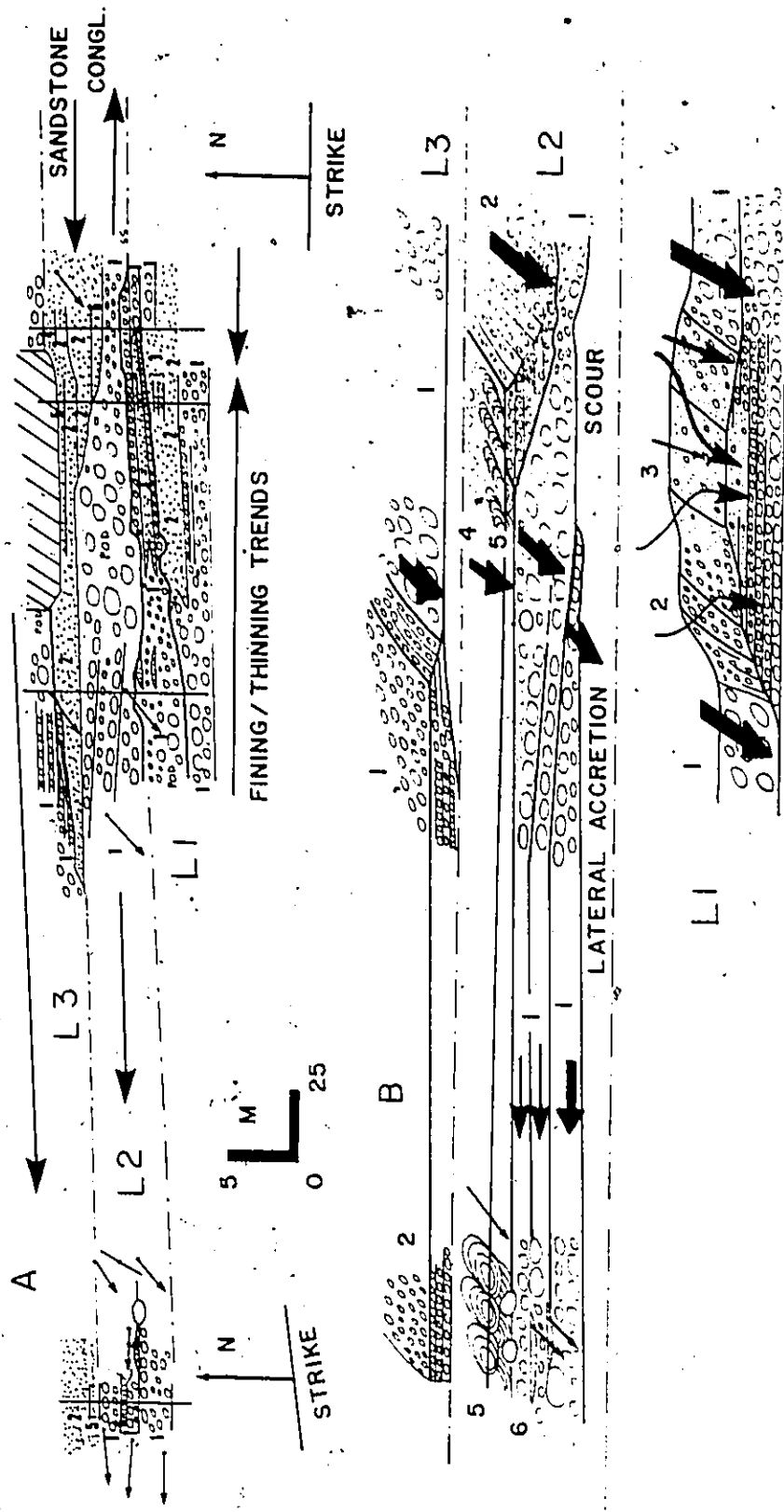


Fig. 68. Generalized sections (A) and paleotopographic reconstruction (B). Key same as in Figure 67. Anse à Pierre Jean 2, Beds 456-483, p.386

generalized section (Fig.68A). For simplification of the following discussion, the section is divided into three levels of facies associations, within the predominantly conglomeratic sections (Fig.68A).

In the lowest Level 1 (L1, Fig.68A) Facies (1), (2) and (3) occur in lateral association with one another. Paleoflows are mainly toward the southwest. These deposits are interpreted as representing deposition within shallow, secondary channels (Facies (1)), which are separated by low-relief, secondary braid bars (thin Facies (2) and (3)) (Fig. 68B). Within Level 1 there are two superimposed secondary channel/secondary braid bar deposits.

Level 2 (L2, Fig.68A) sediments are mainly Facies (1) conglomerates in the lower part, and Facies (2) fine conglomerates in the upper part. At the eastern end of the outcrop, conglomerates and sandstones have paleoflows toward the southwest. In the western part of the outcrop, the Facies (1) conglomerates were deposited by currents that flowed westward, whereas the massive Facies (6) and crossbedded Facies (5) sandstones were deposited from southwesterly flowing currents (Fig.68A). These patterns suggest that the western block was not tectonically rotated, as suggested by Johnson (1974); rather, the divergence of paleoflows within the conglomerates across the outcrop is real. Within Level 2, the conglomerates fine and thin westward, with the accompanying paleoflow switch from southwesterly to westerly flow directions. It is noteworthy that the low-angle, inclined crossbedding in the conglomerate occurs in about the middle of the exposure (Fig.68A).

The observed paleoflow, facies, bed thickness and grain size patterns suggest that this complex may represent a coarse, mainly conglomeratic

erate channel/braid bar or channel/point bar couplet (Fig.68B). Coarse conglomerates at the east end of the outcrop are interpreted as being deposited within a channel, which was prograding eastward. Low-angle inclined stratification within the conglomerate is interpreted as being lateral accretion deposits on the bar margin. The thin, inversely-graded, irregularly-topped conglomerates at the west end of the outcrop, are thought to be conglomerate lag deposits from flows that overtopped the channel and deposited material on the bar top. The coarse-grained nature of the deposits in this outcrop and apparent scour depths in the range of 2-5 m suggest that the channel/bar couplet is within a main channel network (Site 5 or 3, Fig.66). It is impossible to say whether the bar is a braid bar separating two channels or a point bar, occurring within a meander bend of one channel. Outcrop limitations prohibit such fine subdivision of the interpretation.

The top part of Level 2 and all of Level 3 (L2,L3, Fig.68A) consist of mixed, thin bedded facies (Facies (1),(2),(4) and (5)), which occur in very thin 'pods'. These are interpreted as being deposited within very shallow, secondary channel/secondary braid bars which are superimposed upon one another. The association with coarse-grained deposits of the lower part of Level 2, suggests that the depositional site is also within the main channel network, perhaps on top of a large braid bar or point bar (Sites 1 or 4, Fig.66).

The overall sequence from Level 1 to Level 2 is a coarsening and thickening-up sequence. The sequence from Level 2 to Level 3 is fining and thinning upsection. This is thought to represent migration of a main channel to-and-from the depositional site preserved in this outcrop.

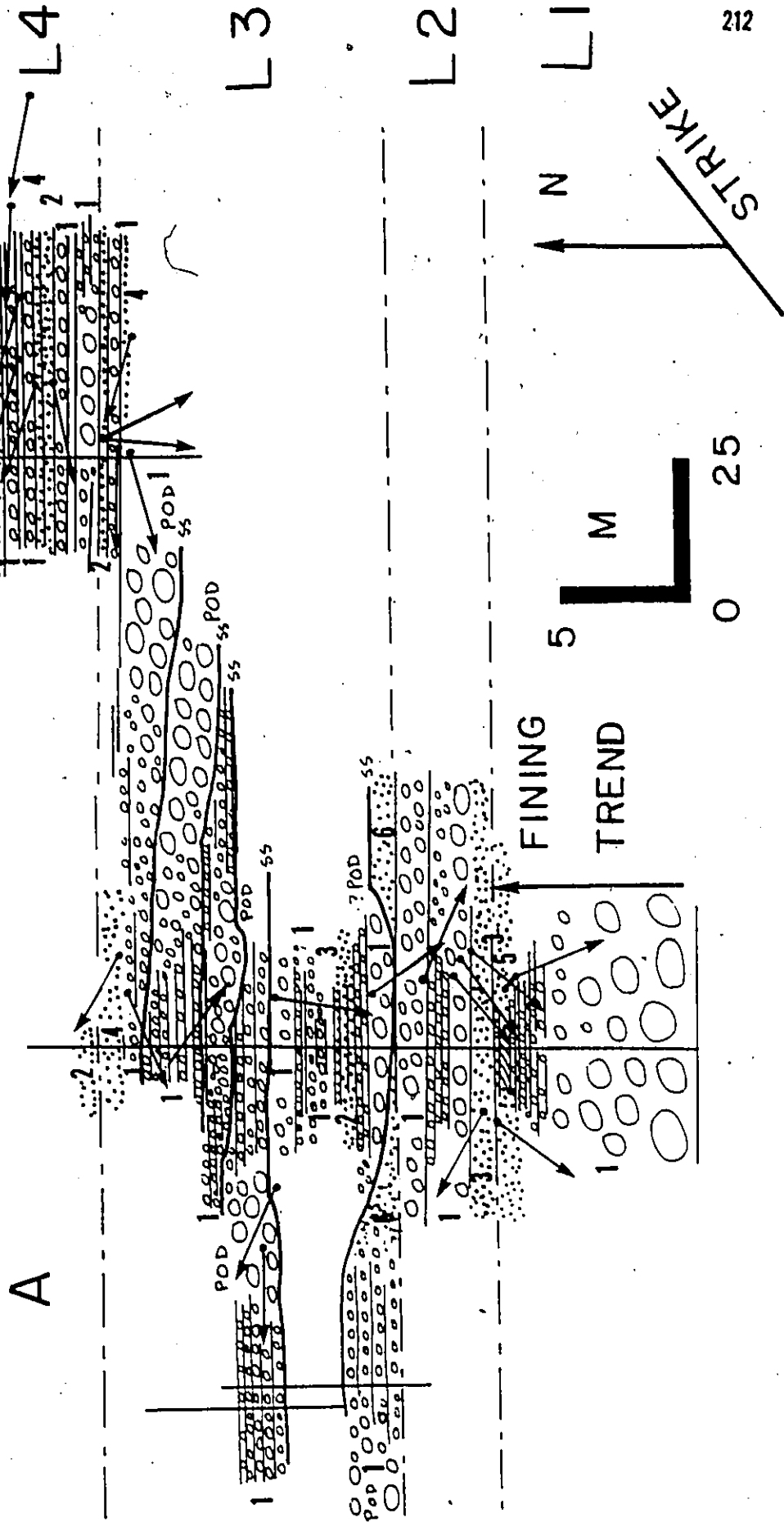
(3) Anse à Pierre Jean 1 (Niveau 3) (Fig. 69)

This reconstruction is based upon detailed sections from this study (Beds 429-455, Appendix 5, p384). Beds which fit Johnson's (1974) pod model, in the descriptive sense, are labelled on the generalized section (Fig.69A). Coarser-grained conglomerates, which also fit the pod model, occur to the west of the section that is described here. These conglomerates were interpreted by Johnson (1974) as being main channel deposits. Flows which deposited these main channel conglomerates travelled toward the southwest (Johnson,1974).

For ease in description and in presentation of the interpretation, this outcrop is divided into four levels (L1-L4, Fig.69A). Level 1 consists of a thick, graded-stratified Facies (1) conglomerate, which appears to be continuous and unchanged across the outcrop. This thick, graded conglomerate was deposited from westerly flowing currents. Because of the very coarse-grained nature of this bed it is thought to have been deposited within a main channel. However, it does not show any evidence of channelization. The thickness of the bed (Fig.69A) also suggests that it was deposited from a very large flow. Hence it is thought that the very large flow travelled unconfined within a main channel. This large flow was oblivious to pre-existing topography and did not follow patterns of deposition corresponding to channel/braid bar topographies (Site 9 ?, Fig.66).

Level 2 consists of a series of mainly flat, continuous beds belonging to Facies (1), (2) and (3), which do not conform to a channel/bar model. Rather, these beds are all continuous and unchanged across the outcrop. No obvious grain size, bed thickness, paleocurrent nor facies patterns emerge, suggesting deposition in an unconfined, unrestrictive

Fig. 69A. Generalized section. Anse à Pierre Jean L, Beds 429-455. Key as in Figure 67. Note that the scale in Fig. 69A differs from that used in Fig. 69B (next page), p. 384



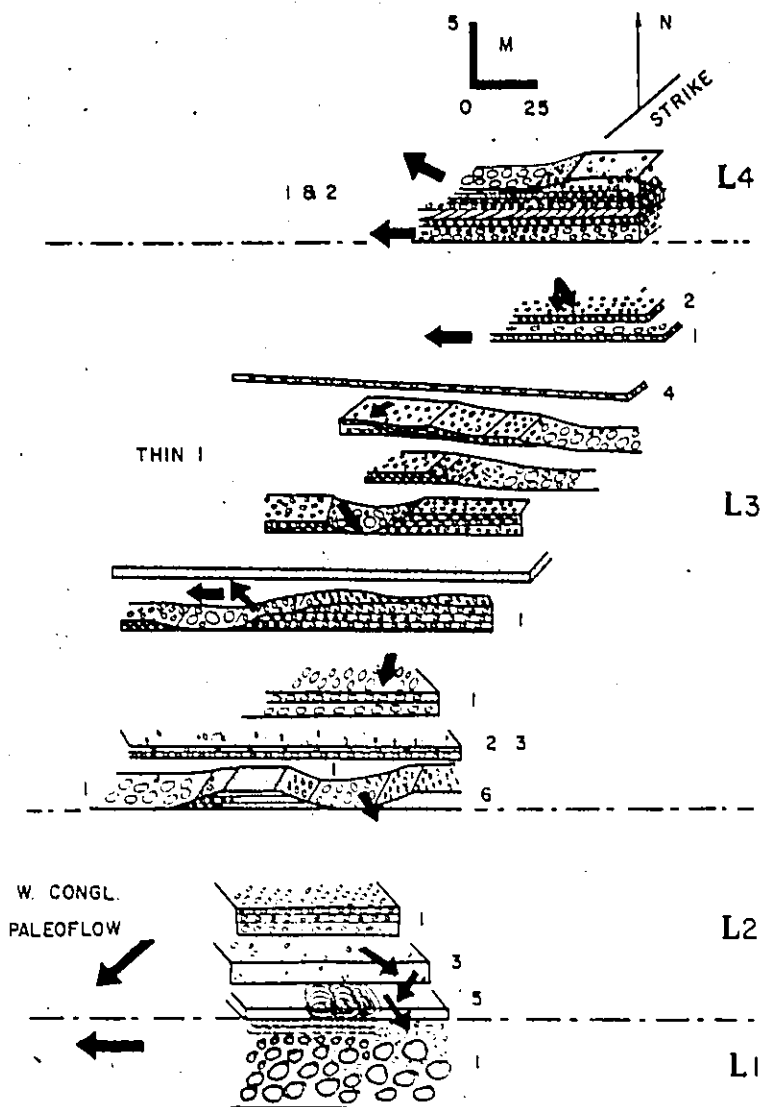


Fig. 69B. Paleotopographic reconstruction. Anse à Pierre Jean 1, Beds. 429-455. Key as in Fig. 67. Note that the scale in Fig. 69B differs from that used in Fig. 69A (previous page), p. 384

area. These deposits most likely represent sediments from coarse-grained overchannel flows that travelled from main channels to flat, unconfined, marginal terrace sites (Site 5, Fig.66). One small pod deposit occurs near the top of Level 2 (Fig.69A). This small pod may represent deposits from a secondary channel that was carved into the top of the marginal terrace (Site 1, Fig.66).

Level 3 sediments belong to Facies (1), (2) and (4) and conform to the pod model, in the descriptive sense. Average paleoflow is toward the west-northwest. Grain size and dimensions of the pods become greater upsection and toward the east. These deposits are interpreted as representing sediments from secondary channel/secondary braid bar complexes. Because of the coarse sediment size at this outcrop and the relatively thin nature of the finer-grained facies, these secondary channel/braid bar deposits are interpreted as being from the main channel network, perhaps on top of large braid bars or point bars, cutoff from the very coarse sediment supply (Sites 1 or 4, Fig.66). The overall coarsening/thickening-up sequence from the base of Level 2 to the top part of Level 3 may reflect meandering processes of the main channel closer to the bar top -- supplying coarser sediment, through time, to the secondary channels on the bar top.

Level 4 consists of thin bedded Facies (1) conglomerates, interbedded with sandstones of a variety of facies. Beds do not fit the channel/bar model nor the pod model, in the descriptive sense. Beds are continuous and unchanging across the outcrop. Paleoflows are generally toward the west. The change from the top of Level 3 to Level 4 is a fining and thinning-up sequence. This may reflect migration of the main channel

farther away from the depositional site, leaving a stranded bar, which received mainly finer-grained, thin, continuous overchannel flow deposits. The depositional setting is thought to be a bar top which was unchanneled and somewhat marginal to main channel settings, such that it sporadically received coarse conglomerate debris (Site 1, MT, Fig. 66).

(4) St. Simon sur Mer to St. Simon sur Mer (Shrine Section)

(Niveau 3 - Niveau 4) (Fig. 70)

This reconstruction is based upon detailed sections from this study (Beds 674-824, Appendix 5, p. 396), as well as detailed conglomerate sections of the outcrop at St. Simon sur Mer by Johnson (1974). This discussion concerns the broad-scale interpretation of sediments between the point at St. Simon sur Mer, eastward to the bay near the Shrine Sections (see outcrop maps, Appendix 5, p. 392), a shoreline distance of about 1.1 km. Detailed interpretations of the St. Simon sur Mer (point) outcrop, at the western tip of the exposure, are given under the next discussion on marginal terraces. Because of the great detail of the sections in this outcrop, it is impossible to reconstruct them into a generalized section that would conform to thesis format. The reader is referred to the logged sections (Appendix 5, p. 393 - 400) for the different grain size, bed thickness, paleocurrent and facies patterns. A generalized paleotopographic reconstruction is given in Figure 70.

The main conglomerate between the point at St. Simon sur Mer and the Two Cottages section has been studied in detail by Johnson (1974) and is interpreted by Johnson and Walker (in prep.) as being a main channel deposit. From Two Cottages east to the Shrine Section (Fig. 70) a series of small scour-fill conglomerates occur along strike, at the base of the

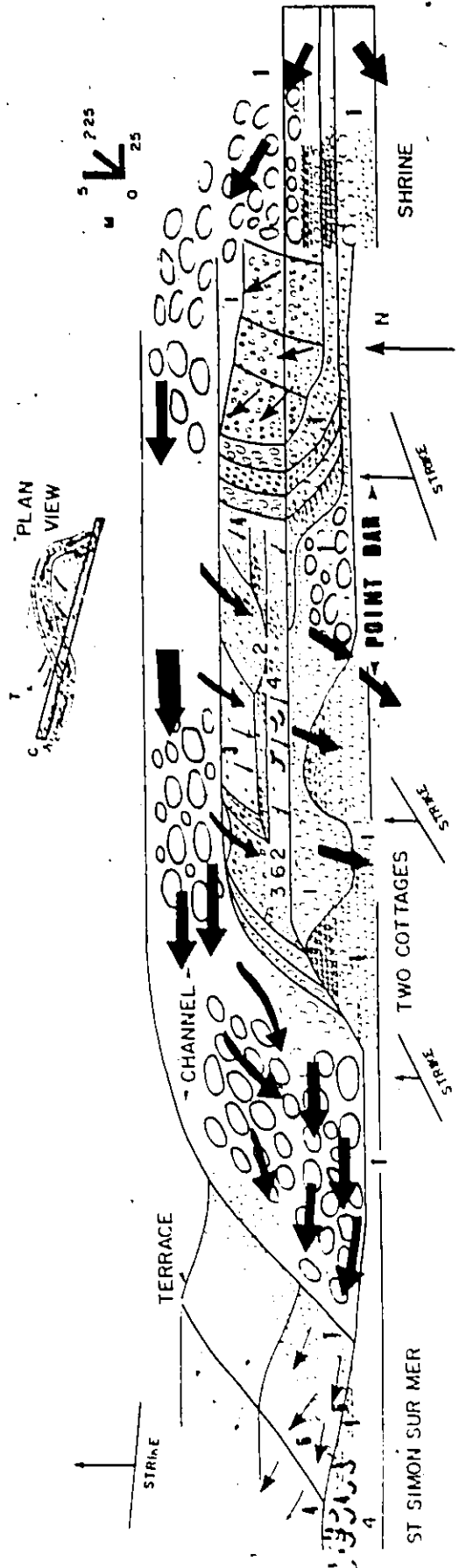


Fig. 70. Paleotopographic reconstruction of Niveau 3/4 sediments: St. Simon sur Mer eastward to St. Simon sur Mer (Two Cottages) and (Shrine) Sections. Key is the same as in Fig. 67B. For details of individual beds, see outcrop maps and logged sections, Appendix 5, p384-400

section. These conglomerates are generally thinner-bedded and somewhat finer-grained than the very coarse conglomerates studied by Johnson (1974) (designated 'channel' Fig.70). The coarse conglomerates at St. Simon sur Mer were deposited from westward flowing currents, whilst the paleoflows for these smaller scour-fill conglomerates are generally toward the south-southwest. Exceptions to this are the lateral accretion scour-fill and equivalent beds at the Shrine section (Fig.33), where paleoflows are toward the northwest. Not all of the conglomerates are scour-fill deposits. Many of the conglomerates are thin and do not change character along strike.

The mixture of small scour-fill conglomerates with continuous conglomerates and sandstones, which have a paleoflow divergence to the main channel conglomerates (to the west), suggest that these sediments may represent deposits from a broad marginal terrace or point bar, near a main conglomerate channel (Site 5, Fig.66).

The overlying Niveau 4 sediments belong to a variety of facies and do not show prominent scour surfaces. Beds thin/fine or coarsen/thicken in both easterly and westerly along-strike directions. Facies character of the beds also vary along strike. Paleoflows are toward the south, southwest and west-northwest. The variability of the paleoflows and characteristics of the beds, suggests deposition in an unconfined, nonrestrictive area. Beds are interpreted as being deposited in shallow, low-relief secondary channels or secondary channel/secondary braid bar complexes. Coarse sediment input suggests that the proposed area was near a main channel.

The reconstruction of the outcrop paleotopography (Fig.70) consists of a meandering main channel (Niveau 3 at St. Simon sur Mer, 'chan-

nel' Fig.70) with alternating point bars: 1) a low relief, coarse-grained point bar within the main channel network (Niveau 3 and 4, Two Cottages and Shrine Section) (Site 1, Fig.66: Niveau 3 and multiple channel complexes (Fig.38,39) Niveau 4; Site 5, Fig.66: most of Niveau 4); and, 2) a topographically higher, finer-grained marginal terrace (sandstone packet at St. Simon sur Mer, which is discussed in the next section) (Site 2, Fig.66).

Marginal Terrace Deposits

(1) Cap à la Carre Ouest (? Niveau 3 to Niveau 4) (Fig. 71)

This reconstruction is based upon detailed sections from this study (Beds 1098-1140, Appendix 5, p.411). Beds which conform to Johnson's (1974) pod model, in the descriptive sense, are labelled on the generalized section (Fig. 71A).

A small conglomerate complex, following the fining and thinning trends in cross-stream directions of Johnson's (1974) pod model, occurs in the northeastern part of the outcrop (Fig.71A). The pod conglomerates are traceable along strike for about 100 m. Paleoflow patterns within the conglomerates are towards the southwest. The Facies (1) pod conglomerates become finer-grained and take on an aspect of Facies (2) or (4) beds towards the west. Beds become finer-grained and thinner-bedded westward, where they merge with beds belonging to a variety of facies, including Facies (2), (3), (4), (5) and (6). Associated with this lateral fining and thinning trend, the paleocurrents become quite variable within the pebbly sandstone and sandstone facies and tend to have a near-random, overall pattern (Fig.71A). Sandstones and pebbly sandstones show lateral, as well as vertical fining/thinning trends (Fig.71A).

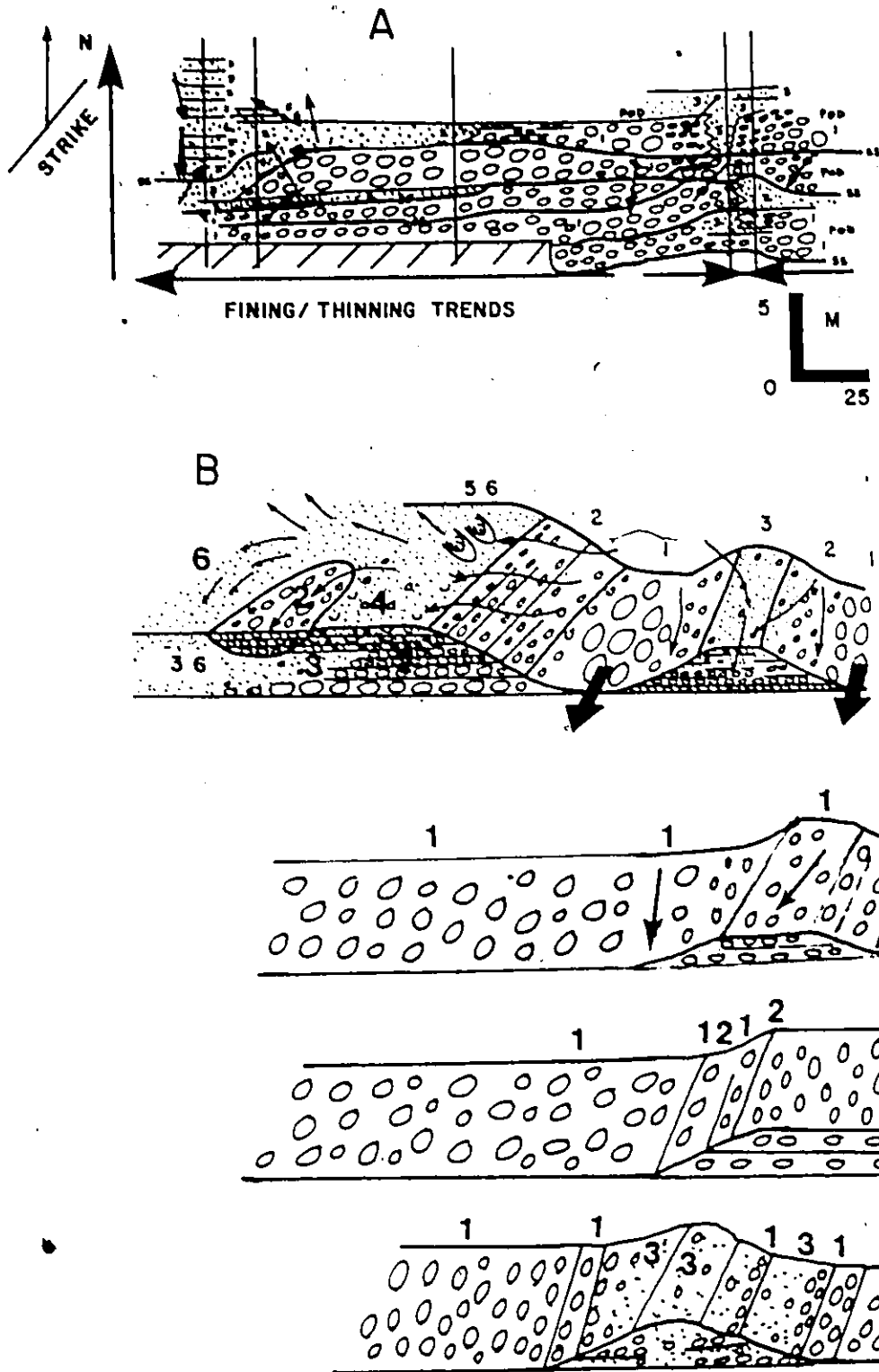


Fig. 71. Generalized sections (A) and paleotopographic reconstruction (B). Key is the same as in Fig. 67. Cap à la Carre Ouest, Beds 1098-1140, p.411

A simple channel/braid bar model can account for the observed grain size, bed thickness, and paleocurrent patterns within the different pod sediments at the northeast end of the outcrop. Coarse Facies (1) conglomerates occur in, generally, concave-up, scour-based units (Fig. 67A). These are interpreted as representing channel sediments. Depths of the channels range from about 2 m to a maximum of 5 m. Thinner and finer-grained facies are interpreted as representing braid bar deposits, which were topographically higher than the channels and received somewhat finer-grained and lower-concentration flow deposits. The northeast part of the outcrop is thought to represent the deposits from at least 4 superimposed small-scale (? secondary) channel/braid bar complexes.

Towards the west, the facies (1) coarse conglomerates grade into a mixture of facies, along with a fining and thinning trend. The paleocurrent patterns are quite complex in the sandstones. One model that may account for these relations is spillover from coarse conglomerate scours or channels onto a broad, topographically higher terrace. Spillover flows from the conglomerate scours onto the broad terrace assumed a variety of natures. Low concentration, predominantly tractional currents, deposited ungraded, trough cross-stratified Facies (5) beds, and likely reworked previously deposited sediment on the terrace. High concentration, high velocity, fine-grained flows accounted for the deposition of Facies (3) and (6) beds. Facies (2) flows had deposition from concentrated clast dispersions, as well as tractional deposition during later flow stages. Some facies (2) flows were capable of scouring the bed, producing small scours on the broad terrace.

The small dimensions of the scour surfaces and the relatively finer-grained nature of the fill, suggest that the deposits at the east end of the outcrop represent deposits from secondary channel/ secondary braid bar settings. Sediments overlying the deposits to the west are not channelized and are mainly fine-grained, continuous sandstones and pebbly sandstones. These associations suggest that the secondary channel/ braid bar sediments at this outcrop may represent secondary braided channel networks that are not within the main channel system. Rather, the secondary channel/braid bar complexes are interpreted as being topographically above the main channel system -- perhaps in the marginal terrace setting, which only occasionally received coarse sediment input (Site 1, Fig. 66).

(2) St. Simon sur Mer (Niveau 3) (Fig. 72)

This reconstruction is based upon detailed sections obtained in the present study (Beds 610-641, Appendix 5, p. 394), as well as detailed conglomerate sections by Johnson (1974). Units which conform to Johnson's (1974) pod model, in a descriptive sense, are labelled on the generalized sections (Fig. 72A).

One of the best outcrops to observed the peculiar conglomerate and sandstone relations is at St. Simon sur Mer (Niveau 3) (Fig. 72). At this locality several pod sequences are superimposed upon one another (Levels 1, 2 and 3, Fig. 72). A large-scale coarsening-thickening-up sequence of pod conglomerates (from Level 1 to Level 3, Fig. 72) occurs here.

Level 1 consists of a series of small pods. Basal scours are composed of Facies (1) conglomerates, which thin and fine between scour

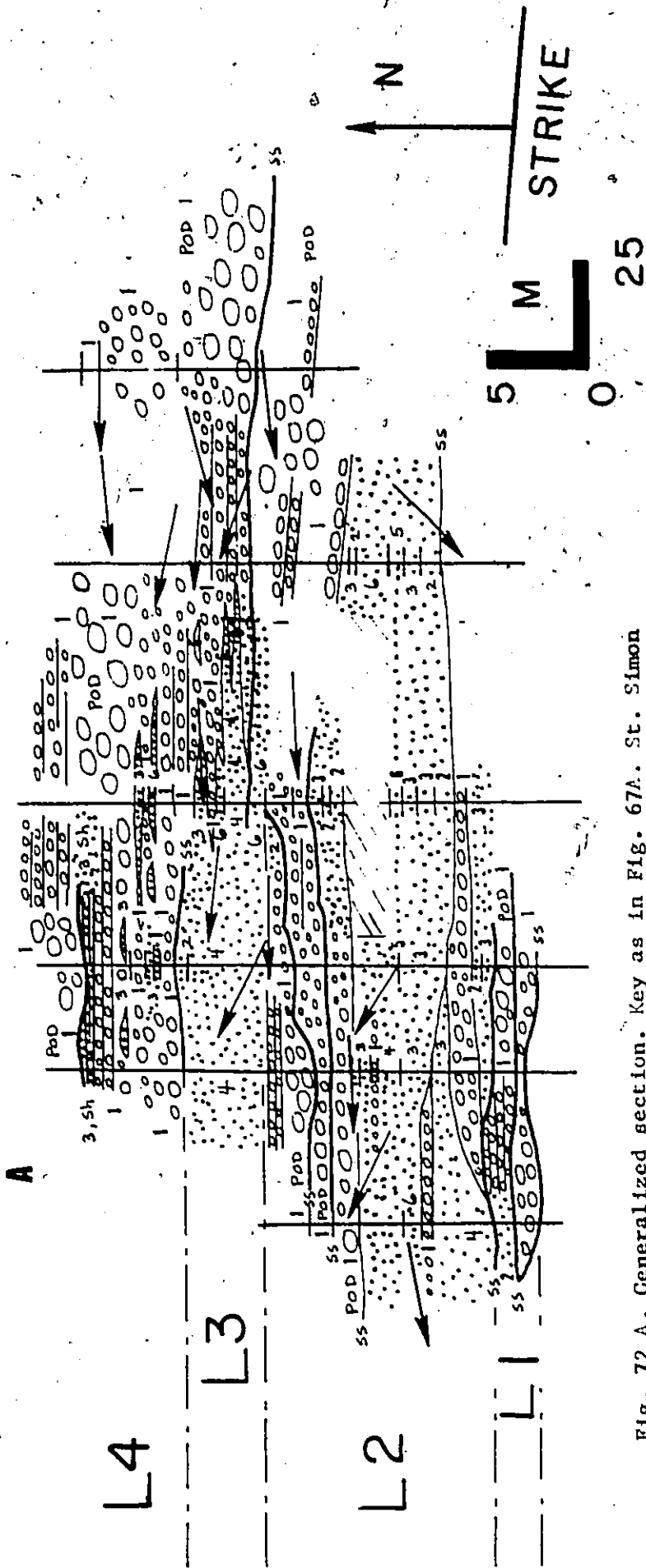


Fig. 72 A. Generalized section. Key as in Fig. 67A. St. Simon
 bur Mer, Beds 610-641. Note that the scale in Fig.
 72 A differs from that used in Fig. 72B (next page), p.394, 395

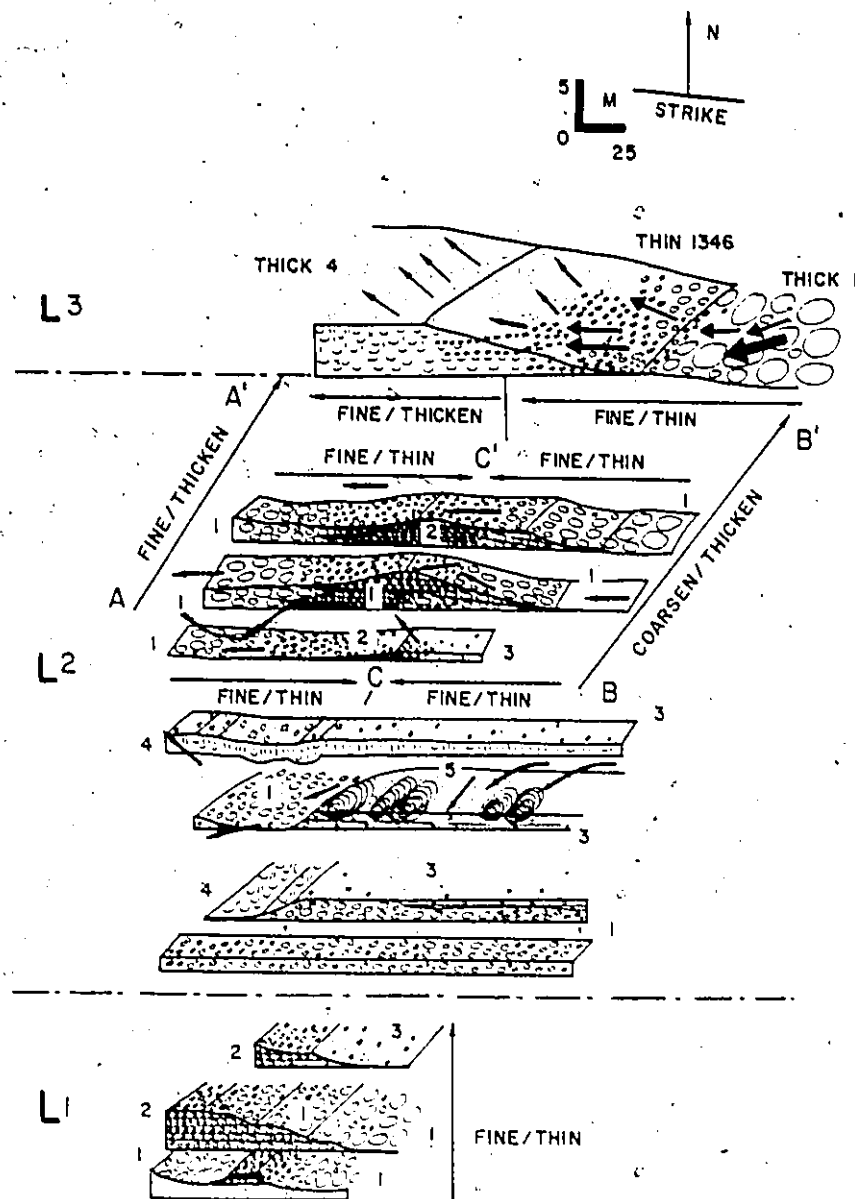


Fig. 72 B. Paleotopographic reconstruction. Key as in Fig. 67B. St. Simon sur Mer, Beds 610-641. Note that the scale in Fig. 72B differs from that used in Fig. 72A (previous page), p. 394, 395

fills. At the top of Level 1, scours are shallower and filled with Facies (2) and (3) beds. This overall fining/thinning sequence within Level 1 is thought to represent gradual abandonment of a small channel site, cut into a previously unchannelized site (Niveau 2). The small channel site was depleted from coarse sediment supply and received only finer and finer sediment through time. As a result of this depletion of coarse sediment input (reflecting deposition from less competent flows) shallower scours were carved, resulting in thinner pod dimensions upsection.

Level 2 sediments consist of flat, continuous sediments as well as discontinuous, channelized 'pod' deposits. A mixture of facies occurs, consisting of Facies (1), (2), (4), (5) and (6). Paleoflow patterns are variable, with slight divergence between that for the conglomerate Facies (1) beds and the finer pebbly sandstone facies (Facies (3) through (6)). Deposits in this level are thought to represent secondary channel/braid bar fills and deposits, as well as continuous broad terrace deposits. The environment is envisioned to be similar to that interpreted for the Cap à la Carre (Section 5) deposits (Fig. 71). Coarser sediment started to cut-and-fill on a predominantly flat terrace. Depletion of coarse sediment supply to the secondary channel/braid bar complex on the terrace top may reflect meandering of a main channel further away from the terrace setting.

Level 3 sediments consist of a series of superimposed pods, comprising mainly Facies (1), (2) and (3). There is a slight paleocurrent divergence between the coarse Facies (1) conglomerates and the other, finer-grained, facies (Fig. 72). The top of the sequence consists of a larger, very coarse-grained scour that was filled by sediment deposited from west-southwesterly flowing currents. In the western part of the sec-

tion, thin Facies (1) conglomerates are interbedded with thin, massive Facies (6) sandstones and thin, liquefied Facies (4) sandstones. Further westward these thin beds merge into a thick, liquefied Facies (4) sandstone. These facies and paleocurrent associations are interpreted as reflecting the transition from a coarse-grained, main channel site to a finer-grained, topographically higher, terrace setting (Site 2, Fig.66). The downstream fining and thinning of coarse Facies (1) conglomerate into liquefied Facies (4) sandstone and thin Facies (1) conglomerate can be explained by considering a section cut through a meander bend, from the main conglomerate channel downstream to the high terrace site (see plan sketch, Fig. 70 and Site 2, Fig.66).

Vertical sections are fining/thickening-upward along AA' (Fig. 72), which are interpreted as representing gradual abandonment of a small channel system, with the concomitant replacement by deposition on a terrace site, where amalgamation of fine-grained deposits yields thicker-bedded sediments. Vertical sections are coarsening/thickening-upsection along BB' (Fig.72). This is thought to reflect the gradual migration of a main channel into what was originally an unchannelized, possibly terrace site. Vertical sections along CC' (Fig. 72) comprise a variety of facies and do not have obvious trends in facies, grain size, nor bed thickness distributions. This mixture is interpreted to represent a marginal terrace or marginal channel site: the transition between main channel deposition and terrace sedimentation (Site 2, Fig.66).

(3) Grève de la Pointe (? Niveau 4) (Fig.34)

The following interpretation is based upon detailed sections from the present study (Beds 296-300, Appendix 5, p.378).

The overall sequence in the multiple scour fill complex is a coarsening-up, thickening-up sequence, which is accompanied by an increase in apparent scour depth from 0.5 m at the base to 1 m at the top. Most of the scour fill consists of Facies (2) conglomerate, which becomes coarser-grained upsection. In contrast to the predominantly Facies (1) conglomerate fills at other locations, this scour fill sequence does not show a divergence in paleoflow directions, with respect to underlying and/or overlying sediments. All paleocurrent indicators within the scour fill complex and associated beds are toward the westerly direction (west, northwest or southwest).

This complex is interpreted as being deposited wholly within a channel site. The relatively finer-grained nature of the fill (in comparison to the very coarse conglomerates of main channel deposits within Niveau 3 in the Anse à Pierre Jean - St. Simon sur Mer area) and the shallow apparent depth of the scour surfaces is suggestive of deposition within secondary channel settings. The channels did receive some coarse sediment input. Perhaps the secondary channel complex occurred in a marginal terrace location. Flows became more competent within the channel complex through time. After cut-and-fill of the top-most scour, the secondary channel system was cutoff from coarse sediment supply and received only fine-grained material, which was deposited as continuous beds by westerly-flowing currents (Appendix 5, p. 379). The depositional setting preserved in this outcrop may be a secondary channel system, perhaps on a marginal terrace, which became abandoned through time, due to the migration of main channels, which fed the marginal terrace site. Overlying beds are interpreted as unchannelized, marginal terrace sediments (Beds 301-310,

Appendix 5, p.378). The depositional setting would be similar to that in Site 1, Figure 66.

(4) St. Simon sur Mer Est Multiple Channel Complexes (Niveau 4)

(Figs. 35,36)

The interpretations of the depositional settings of these two multiple channel complexes are based upon detailed sections from the present study (Appendix 5, p.405,406). Both multiple channel fills overlie predominantly unchanneled beds, comprising mainly Facies (3), (6) and thin Facies (2) deposits. Dominant scour fill material consists of graded/stratified or graded/crossbedded Facies (2) conglomerates and pebbly sandstones, or massive Facies (6) sandstones. Scours generally reach a maximum of 1 m in apparent depth.

As with the Grève de la Pointe Facies (2) complex (Fig. 34), the paleoflow patterns within the Section 6 complex (Fig. 36) agree with those of overlying and underlying beds. Paleoflows are towards the west-southwest. No paleocurrent data is available from the lower Section 5 (Fig.35) complex. Beds overlying and underlying the Section 5 (Fig.35) scour complex are also toward the west-southwest, coincident with paleoflows of the upper Section 6 (Fig.36) scour fills. The multiple scour fill complexes of Section 5 and Section 6 (Figs.35,36) are interpreted as being deposits from a channel complex that was cutoff from coarse sediment supply. Flows that transported material to the cutoff channels were high velocity flows (capable of significant scouring), but lacked coarse debris, which may have been previously deposited as coarse-grained lags.

The channel complex at Section 5 (Fig.35) shows a slight coarsening/thickening-up sequence, whereas the complex at Section 6 (Fig.36) has

a fining/thinning-up trend. This suggests that flows within the Section 5 complex became more competent upsection, whereas flows within the Section 6 complex became less competent through time. The general depositional site is thought to be a channelized site which is cutoff from much coarse sediment input. It may be akin to a cutoff channel in a marginal terrace setting (Site 11, Fig.66). Size of material being fed into the cutoff channel would depend upon the proximity of main channels to the cutoff channel, and the relative strengths of flows travelling down the main channels. Overall coarsening/thickening-up sequences within cutoff channel deposits would reflect migration of main channels closer to the cutoff channel. Overall fining/thinning-up sequences within the cutoff channel deposits would reflect migration of major channels away from the cutoff channel site.

(5) Bic (Member I) (Fig.41)

The following interpretation is based upon detailed sections from the present study (Beds 1331-1346, Appendix 5, p. 419). As shown in Figure 41, a mixture of facies occurs in this complex. All of the scours are quite small: apparent scour depths range from about 0.2 m to a maximum of 0.5 m; scours are traceable for a few metres along strike. No consistent grain size trends occur from the base to the top of the complex; rather, a mixture of coarse and fine beds occurs. Immediately preceding and succeeding beds are, on the whole, much finer-grained and thicker-bedded than the beds within the scour complex.

An examination of the paleocurrent indicators suggests that in the lower part of the multiple scour complex, flow was towards the northeast. About half-way upsection, the flow shifted towards the southwest-west.

It is not thought that this multiple scour complex represents deposits from a main channel, due to the relatively fine-grained nature of the fill and the small dimensions of the scours. The cross-cutting nature of the scour fills suggests a braided pattern. The depositional setting might have been an unconfined, broad terrace site near a main channel, which sporadically received thin, coarse and fine conglomerate debris as spillovers from the main channel. The small channel fills would represent deposits from secondary channels, perhaps within the marginal or high terrace setting (Site 12, Fig.66).

High Terrace Deposits

(1) Rivière Trois Pistoles (Niveau 2) (Fig.31)

The following interpretation is based upon detailed sections from the present study (Beds 341-347, Appendix 5, p.380). The overall sequence from the base to the top of the multiple scour fill is from coarse grained Facies (1) conglomerates, to shale and classical turbidites (Facies (7)). Scour dimensions become smaller upsection, from apparent scour depths of 4 m at the base, to less than 1 m at the top of the multiple scour complex. The transition from the coarse-grained to the fine-grained fills is very abrupt. Associated with the fining- and thinning-up trend is a shift in the paleoflow patterns. Initial cut-and-filling was done by northwesterly flowing currents that deposited very coarse conglomerates. A shift in the flows occurred to the south-southwest, with finer-grained material being deposited from less competent southerly flows. This shift in paleoflows is accompanied by a shallowing and decrease in the apparent width of the scours, a decrease in the size of the scour-fill sediment, and an abrupt overall fining- and thinning-up trend (Beds 341-345, Appendix 5, p.380).

The multiple scour-fill sequence is overlain by continuous beds. The transition from the scour-fill sediments to the continuous deposits may reflect a transition from main channel (initial Facies (1) scour fills) to unchannelized areas, perhaps marginal or high terrace sites. The fine-grained nature of the top scour-fill and the fairly fine-grained aspect of the beds overlying the multiple scour complex (Beds 347-354, Appendix 5, p.380) suggests deposition in an unchannelized site cutoff from significant coarse sediment input. The depositional site may be a high terrace setting, near a main channel, which occasionally received minor amounts of coarse sediment. The overall sequence from Bed 341 to Bed 347 would, most likely, represent the type of pattern generated at Site 6, Fig. 66.

(2) Grève de la Pointe Multiple Scour Fill (Fig.32)

The following reconstruction is based upon detailed sections from the present study (Beds 1-5, Appendix 5, p.372). The multiple scour fill sequence at the base of the Grève de la Pointe section consists of thick, coarse-grained Facies (1) conglomerates. The beds overlying the multiple scour fill complex are finer grained and continuous. Along with the trend to unchannelized, finer sediments there is a switch in the paleoflows from a northwesterly direction in the coarse Facies (1) conglomerates (Beds 1-5, Fig.32) to a southwesterly direction in the overlying beds (Beds 6-33 and Beds 42-73, Appendix 5, p.372, 373).

These transitions may reflect a gradation from channelized sedimentation to non-channelized deposition. The transitions are more gradual than those observed at the Rivière Trois Pistoles section (Fig. 31) and are interpreted as reflecting transitions from main channel settings-to-marginal terrace-to-high terrace settings (Site 7, Fig.66).

(3) St. Simon sur Mer Est (Niveau 2) (Fig. 37)

The following interpretation is based upon detailed sections from the present study (Beds 849-869, Appendix 5, p.402). As shown in Figure 37, most of the beds are massive Facies (6) sandstones. Scour depths of scour surfaces range from 0.5 - 2 m and scours are traceable along strike. Paleoflows are consistently toward the south-southwest. No obvious grain size, bed thickness, nor changes in scour dimensions trends occur. Most of the beds are bounded by prominent scoured basal surfaces. This suggests deposition in a channelized site. However, the fill is predominantly sandstone, with rare input of pebbly sandstone or conglomerate material. The relatively shallow scour depths suggest deposition within secondary channels. The uniformly fine-grained nature of the scour-fills suggests deposition in a site that was mostly cutoff from any coarse sediment input. The depositional setting may be secondary channels in a high terrace area, which receive only the finer sandy spillover flows from the main channel (Site 13, Fig.66).

GENERAL SEDIMENTATION MODEL: SUMMARY

Geomorphic elements within the Cap Enrage depositional system have been deduced from field relations, including: grading patterns, facies relationships, bed thickness changes and paleocurrent trends. Different facies are interpreted as being deposited in main channels, on braid or point bars, or on terraces, above the general level of the main channel network (main channels and bars). Different rates of sedimentation in conjunction with varying concentrations and size of sediment account for the distribution of the different facies. The general model of sedimentation consists of rapid deposition within channels, with less rapid

deposition on topographically higher braid bars, point bars and terraces. This model is operative on all scales, from deposition of individual beds to the large-scale organization of major conglomerate and sandstone horizons.

Channel-and-braid bars can be very low relief features, almost sheet-like, accounting for the observed changes within individual beds: the result of deposition from single flows. The next higher scale consists of secondary channel/secondary braid bar complexes which explain the relationships of superimposed and laterally adjacent beds: the result of deposition from several or many flows. Small-scale (< 1m-5m) vertical sequences can be interpreted as the interaction of secondary channel/secondary braid bar or secondary channel/secondary point bar couplets. The largest scale features consist of main channel networks, consisting of main channel/braid bar or main channel/point bar couplets, and terraces, which border the aggrading channel system. Large-scale (10's - 100 m) thick sequences are interpreted in terms of the interactions between the main channel networks and the terraces.

Three main depositional settings are thought to exist within the Cap Enragé system: 1) main channels; 2) braid bars or point bars within the main channel network; and, 3) terraces above the main channel network. The coarsest and thickest beds are interpreted as being deposited within the main channels. Towards the margins of channels, beds become finer-grained and thinner bedded -- reflecting decreasing flow conditions and sedimentation rates, as flows spilled out from main channels to topographically-higher, interchannel areas. Terraces have predominantly finer-grained sediments, with coarse sediment only being supplied to marginal terrace

sites, which occur near the main channels. The terraces are envisioned as being high above the general level of the main channel network (25-50m), with only fine sediment being carried to this site by overchannel flows. The transition between terraces and main channels is probably very gradual -- perhaps a depositional slope of $\leq 10^\circ$, as near-vertical channel walls are rarely seen at the contacts between major conglomerate and sandstone horizons. Beds which are interpreted as being high terrace deposits are generally finer-grained and thicker-bedded than marginal terrace sediments. The thicker-bedded nature of the high terrace sediments may be a consequence of two factors: 1) a sudden loss of flow competence as flows overtop main channel networks, with rapid deposition of great thickness of fine sediment; and, 2) amalgamation of finer-grained deposits from separate flow events. In summary, the deposits from the different major depositional sites are:

1. Main Channel Networks, including main channels/bars: coarse-grained and thick bedded sediments;
2. Marginal Terrace Settings: finer-grained and thinner bedded deposits; and,
3. High Terrace Areas: finest-grained and thicker bedded (than marginal terrace deposits), except in sites far away from the influence of main channels, receiving only the finest-grained classical turbidites and shales.

A variety of different vertical facies sequences and trends have been observed in outcrop, which can be interpreted as being the result of:

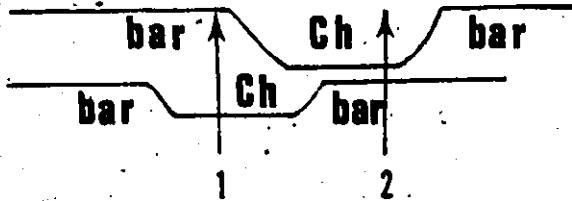
- 1) interactions between main channels and interchannel areas (braid bars or point bars) wholly within the main channel network; or
- 2) interactions between main channel networks (including channels and bars) and terraces.

Vertical bed thickness and grain size changes may be gradual and these are here termed 'sequences;' alternatively, the changes may be very abrupt and are referred to as 'abrupt vertical trends.' The different types of observed vertical sequences and trends, observed within the Cap Enrage sediments, are listed in Fig. 73, Table 11. General interpretations as to their origins and all the beds which show a particular sequence are indicated in Table 11. The reader is referred to the logged sections (Appendix 5) for the details of the bed thickness, grain size and facies characteristics. In general there are six main types of sequences or trends (Fig. 73); 1) fining/thinning-upsection; 2) coarsening/thickening-upsection; 3) coarsening/thinning-upsection; 4) fining/thickening-upsection; 5) abrupt fining-upsection, with little apparent change in bed thickness; and, 6) abrupt coarsening-upsection, with little apparent change in bed thickness. These sequences are observed on two scales of magnitude: those that are generally less than 1 m to about 5 m in height; and, those vertical sequences or trends that are 10's - 100 m in height.

Fining/thinning-up sequences are interpreted as reflecting the gradual migration of channels away from the depositional site preserved in a given outcrop. This interpretation is based upon comparisons with fluvial fining/thinning-up sequences (Allen, 1964, 1965, 1970) as well as interpretations of fining/thinning-up sequences of, what are interpreted as being, deep-sea channel deposits (Hendry, 1978; Mutti and Ghibaudo, 1972; Mutti and Ricci Lucchi, 1972; Ricci Lucchi, 1975; Walker, 1975b, 1975c, 1977, 1978). This is the most-likely interpretation for fining/thinning-up sequences, unless one invokes long-term tectonic controls on sedimentation

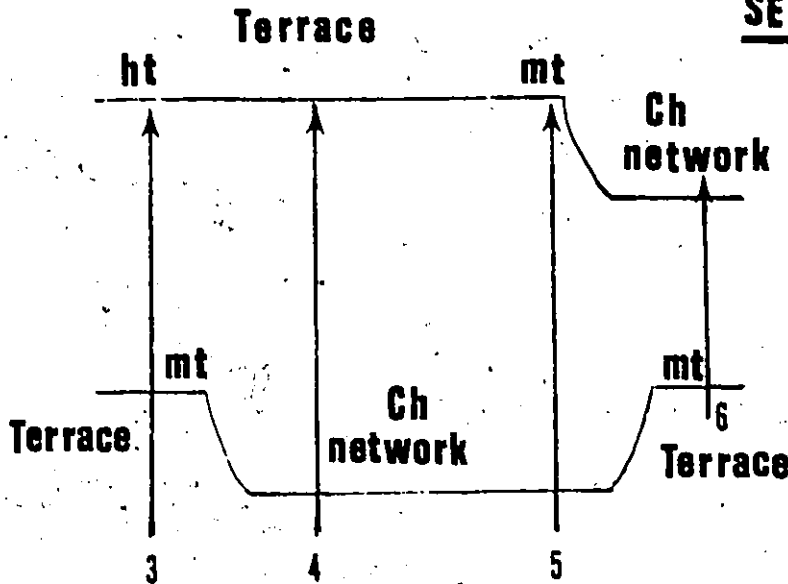
Fig. 73. Sedimentary sequences due to interactions between channels-and-bars, or due to interactions between main channel networks-and-terraces.

SEQUENCES : < 1-5 metres

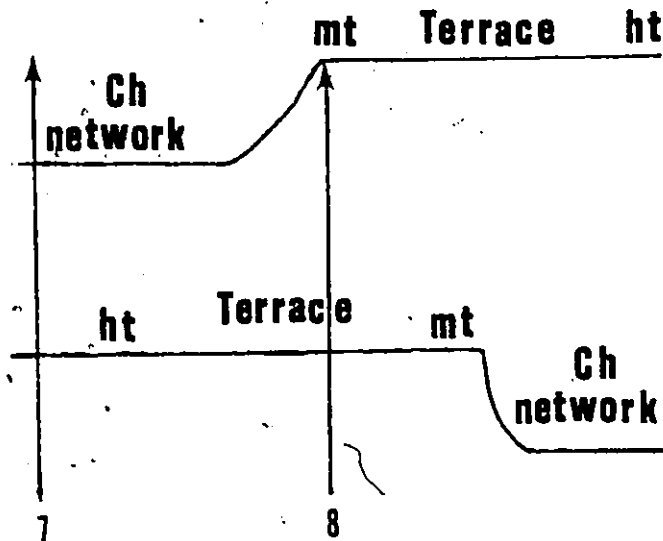


- 1 FINE / THIN
- 2 COARSEN / THICKEN

SEQUENCES : 10-100 metres



- 3 FINE / THICKEN
- 4 ABRUPT FINE
- 5 FINE / THIN
- 6 COARSEN / THICKEN



- 7 ABRUPT COARSEN
- 8 COARSEN / THIN

TABLE 11

OBSERVED SEDIMENTARY SEQUENCES

SEQUENCE	Fine/Thin		TYPE SEQUENCE
	<u>Main Channels</u>	<u>Bars in Main Channel Network</u>	
BEDS	429	430 - 443	Vertical
	475	456 - 460	Lateral
	475	476-478, 479-481	Vertical
	492	500 - 503	Lateral
	1084	1078 - 1080	Lateral
	1081	1092, 1093, 1097	Lateral
	1101	1102 - 1103	Vertical
	1107	1109	Lateral
	1115, 1111	1102 - 1103	Lateral
	1363	1364 - 1365	Vertical
Mean Bed Thickness	5.2 m	1.0 m	
Mean Grain Size	586 mm	122 mm	

SEQUENCE	Fine/Thin		Fine/Thicken	TYPE SEQUENCE
	<u>Main Channels</u>	<u>Marginal Terrace</u>	<u>High Terrace</u>	
BEDS	1 - 5	6 - 24		Vertical
	36 - 39	40 - 68		Vertical
		176-184	194-202	Lateral
		242-245	194-202	Lateral
		262-264	194-202	Lateral
		297-302	284-289	Lateral
		494-498	491	Lateral
		507-515	509, 516	Lateral
		522-531	541-544	Lateral
		522-531	552-556	Lateral
	675	667-670	627	Lateral
		619-626	627	Vertical
	675	676-692	693-696	Vertical
		676-692	706-715	Lateral
	887	874-875	878	Lateral & Vertical
	889	890-892	893	Vertical
		894-901	908, 909, 917	Lateral
		921-923	924-930	Vertical
		931-939	940-942	Vertical
	985-986	984-988	990-994	Vertical
	985-986	989	995-997	Vertical

TABLE 11 (cont.)

SEQUENCE	Fine/Thin		Fine/Thicken	TYPE SEQUENCE
	Main Channels	Marginal Terrace	High Terrace	
SUBENVIRONMENT				
BEDS	1098-1121	1122-1126 1165-1173	1174- 1180 1301- 1311	Lateral Vertical Vertical
Mean Bed Thickness	4.9 m	1.2 m	4.2 m	
Mean Grain Size	560 mm	88 mm	1 mm	

SEQUENCE	Fine/Thin		TYPE SEQUENCE
	High Terrace	'Distal' High Terrace*	
SUBENVIRONMENT			
BEDS	404 - 406 1302-1311 1473-1488	407 - 415 1312-1316 1489-1489+	Vertical Vertical Vertical
Mean Bed Thickness	2 m	0.4 m	
Mean Grain Size (excluding shale)	15 mm	0.6 mm	

SEQUENCE	Coarsen/Thin		TYPE SEQUENCE
	High Terrace	Marginal Terrace	
SUBENVIRONMENT			
BEDS	347 400 493	348 - 370 401 - 403 494 - 498	Vertical Vertical Vertical
Mean Bed Thickness	11 m	1 m	
Mean Grain Size	4 mm	26 mm	

SEQUENCE	Abrupt Fine/Thicken Trend		TYPE SEQUENCE
	Main Channel Network	High Terrace	
SUBENVIRONMENT			
BEDS	341 - 344 1382-1397	347 1398-1408	Vertical Vertical
Mean Bed Thickness	2 m	8 m	
Mean Grain Size	307 mm	9 mm	

TABLE 11 (cont.)

SEQUENCE SUBENVIRONMENT	Coarsen/Thicken		Main Channel	TYPE SEQUENCE
	'Distal' High Terrace *	High Terrace		
BEDS	577 - 586	587 - 592	593	Vertical
	893	894 - 900	901	Vertical
	1025-1063	1064-1070		Vertical
	1312-1319	1320-1346		Vertical
Mean Bed Thickness	1 - 0.5 m	1.3 m		
Mean Grain Size	7 mm	17 mm		

* Note: 'Distal' High Terraces are those high terrace settings farthest away from the main channel networks and received predominantly only fine-grained debris from lower velocity flows.

The interpretation of the fining/thinning-up sequences as a result of gradual abandonment of channels, implies, necessarily that the channels were utilized by successive gravity flows. Abandonment of the channel may be due to gradual migration processes of the channel, coupled with aggradation of the channel network -- with the result that eventually, due to shallowing of the channel, subsequent flows would overtop the channel, creating a new channel site. Diversion of most of the successive flows down the new channel results in only the finer, overchannel flows reaching the old channel site. This results in a fining/thinning-up sequence at the abandoned channel location. Channel abandonment may also be caused by the complete filling of a channel by deposits of a large flow, which effectively plug the channel and prohibit its use by successive flows.

The small scale (≤ 1 m - 5 m) sequences are interpreted as representing channel fills -- either main channels or secondary channels. Those sequences with mainly conglomeratic fill and with greater thicknesses (2-5m) are thought to record the progressive abandonment of main channels within the main channel network (Fig.73). Those sequences with finer-grained fill and smaller thicknesses ($\leq 1-2$ m) are interpreted as recording the gradual abandonment of secondary channels, which occur on bar tops within the main channel or terrace tops, above the main channel network. Large-scale (10's-100m) sequences are interpreted as representing the progressive abandonment of main channel networks, with the concomitant replacement by terrace deposition at a particular site. Fining/thinning-up sequences are not that common within the Cap Enragé Formation. Most beds do not show vertical sequences; although of

those sequences that occur, the fining/thinning-up type is most common.

Coarsening/thickening-up sequences are interpreted as reflecting the gradual migration of channels toward a depositional site preserved in a given outcrop. This interpretation is based upon the occurrence of coarsening/thickening-up sequences preceding what have been interpreted as main channel or secondary channel fills (Fig.73). Coarsening/thickening-up sequences have similarly been interpreted in fluvial sediments as representing the reoccupation of old channels and incorporation of old channels into active parts of the fluvial system (Costello and Walker, 1972).

Coarsening/thickening-up sequences with mainly conglomeratic fill and dimensions of 2-5 m are interpreted as recording the progressive reoccupation of main channels within the main channel network (Fig.73). Those sequences with finer-grained fill and smaller dimensions ($\leq 1-2m$) are thought to record the reoccupation of secondary channels, which were located on bar tops or terrace top settings. Large-scale (10's - 100 m) sequences are interpreted as representing the gradual reoccupation of main channel networks, replacing what was previously a terrace setting. Coarsening/thickening-up sequences are not very common within the Cap Enragé Formation. When they do occur they are rarely large-scale, and more commonly, small-scale sequences.

The other four types of sequences observed within the Cap Enragé sediments are explained in terms of interactions between main channel networks and terrace settings. These interpretations are based solely upon the features and relationships observed in the present study. Different sequences are generated depending upon whether a site is being

reoccupied or abandoned by a main channel network and the rate of migration of the main channel system. Fining/thickening-up sequences occur when high terrace sediments are superimposed upon what was previously a marginal terrace setting. Abrupt fining-up trends are interpreted as representing the rapid abandonment of a main channel network, with the replacement being a high terrace depositional setting. Coarsening/thinning-up sequences are thought to reflect the superpositioning of marginal terrace deposits on what was previously a high terrace setting. Abrupt coarsening-up trends are interpreted as reflecting the rapid migration of a main channel network onto what was previously a high terrace setting. The generation of these different types of sequences are schematically drawn in Figure 73.

The implications of these various vertical sequences are far-reaching. Many workers (Normark, 1978) suggest that the fill of submarine channels would be predominantly fining/thinning-up sequences, due to progressive abandonment of a channel site. The results and synthesis from this study show that many different vertical sequences may result from the interactions between: 1) main channels and braid bars within the main channel network; and, 2) main channel networks (including main channels and braid bars) and terraces.

DEPOSITIONAL SUBENVIRONMENTS FOR DIFFERENT FACIES

Based upon the various field relations a suite of facies can be assigned to each of the major geomorphic elements of the system, including: main channels; bars within the main channel network; and, terraces.

Main Channels

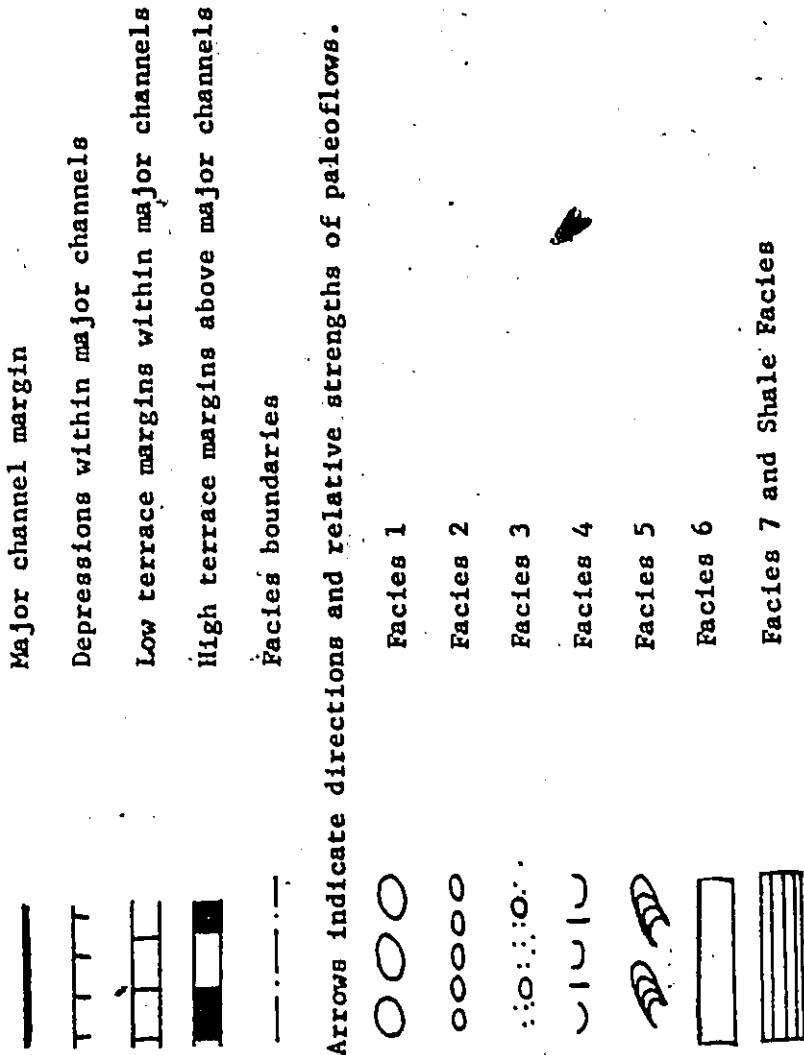
The main channels are relatively shallow (up to 5+ m deep) features on the floor of the submarine valley. Sides of shallow channels are interpreted as being low-relief (? 10° slopes) and are, most likely, mainly depositional rather than erosional in origin. Main channel conglomerates commonly fine and thin in downstream, cross-stream and upstream directions. The downstream and cross-stream fining/thinning trends would be related to decreasing rates of deposition and flow velocities, as flow spilled out from main channels to topographically higher braid bars, point bars or terraces. The facies changes occurring from the centre of a main channel to a main channel margin would be:

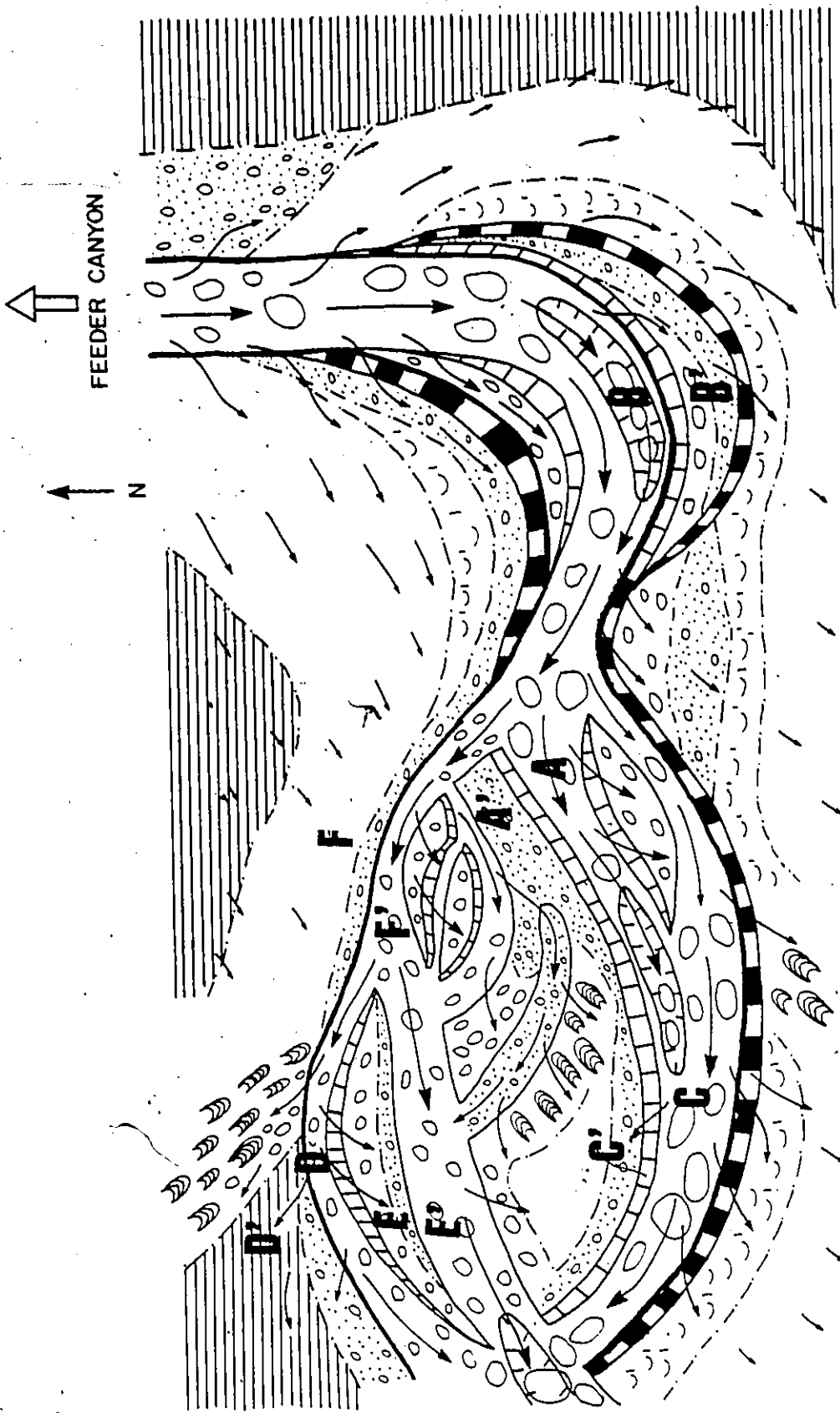
Inversely Graded Facies (1) → Graded Facies (1) → Graded-Stratified Facies (1)

Sequences that fine in directions which are transverse to local paleoflow directions would represent channel-to-bar or channel-to-terrace sequences (AA' and BB', Fig. 74). Sequences that fine and become thinner in directions which are parallel to local paleoflows and in a downstream direction are interpreted as representing spill from channels to bars or terraces at meander bends (CC' and DD'). Sequences that fine and become thinner in directions which are parallel to local paleoflows and in an upstream direction are interpreted as representing the progradation of bar or terraces downstream into coarser-grained channel sediments (EE' and FF', Fig. 74).

The only way that conglomerate flow deposition can be controlled by shallow main channel topography is if: 1) dispersions which carry the conglomerate debris are bottom-hugging flows, and 2) the conglomerate is

Fig. 74 - Regional paleogeographic interpretation of depositional environments of different facies.





OBSTRUCTION

carried within a relatively thin basal zone of the dispersion -- most likely within a zone less than 5 m thick. These two restraints have some serious implications about the conglomerate channels. Firstly, many of the conglomerates may actually have multiple-flow origins. Multiple origins for the conglomerates are also suggested by the following:

- 1) grain size and bed thickness are not related to one another for the Facies (1) and (2) conglomerates;
- 2) fabric data, including scatter of data and absolute mean dip, show no relations to grain size nor thickness of the conglomerates; and,
- 3) many of the conglomerates have feather-edge contacts with laterally-adjacent, or flow-parallel, finer-grained facies ('pod' deposits).

Secondly, some of the apparent grading patterns within some of the conglomerates, which occur in the centre of main channels, may actually be due to amalgamation of the deposits of several flows -- and not the consequence of deposition from a single flow. Thirdly, the main channels most likely form a continuous network which serve as conduits for many successive thin conglomerate flows. The occurrence of thick, continuous coarse-grained conglomerates can be explained as being the deposits of relatively uncommon, very-large flows, which blanketed the whole floor of the submarine valley and were not constrained by pre-existing topography.

Braid Bars or Point Bars within Main Channel Networks

Braid bars and point bars within the main channel network would be topographically above the main channels. Consequently, most of the flows reaching these sites would be somewhat finer-grained and lower-velocity and would, most likely, be spillover flows from the main

channels. The trend from bar margins (at contacts with main channels) to bar centres would be:

Facies (2) → Facies (3) → Facies (4)/(6)

Although the bar sites are topographically above the main channels, rates of sedimentation would still be quite high, due to the proximity of major channels. Initial stages of deposition are from concentrated clast dispersions and deposition is quite rapid. Only during later flow stages, in some beds, is deposition slower to the point that tractional influences become important.

Thin Facies (1) conglomerates also occur in association with the other finer-grained facies. Some of these Facies (1) beds are very thin (10-30 cm), continuous and unchanging across the outcrops. These are interpreted as being overchannel, continuous bar-top deposits. Other Facies (1) and some of the coarser-grained Facies (2), (3) and (4) beds occur as multiple scour fills, as solitary scour fills or as pod sediments, in the descriptive sense. These are interpreted as representing secondary channel and/or braid bar complexes which occur in bar-top settings. Many of the finer-grained Facies (3), (4) and (6) beds change facies, become thinner-bedded and finer-grained in various directions, including flow-transverse, flow-parallel and flow-oblique directions. Usually these changes only show consistent patterns within individual beds and not successive beds. Such features are interpreted as representing the fill of very low relief, almost sheet-like, secondary channels/secondary braid bars which were in bar-top settings. Some Facies (5) beds occur in association with the other bar-top deposits and are thought to be due to tractional reworking of previously deposited bar-top sediments.

High Terraces Above Main Channel Network

These terraces are unconfined, broad areas that receive mainly fine debris. They are envisaged as being perhaps 25-50+m above the main channel network. Coarser debris would occur in marginal terrace settings, near main channel contacts, whereas the finest debris would be deposited in terrace sites, farther away from main channels. The trend from terrace sites marginal to channels to terrace sites, isolated from major channels, would be:

Thin Facies (2) → Facies (3)/(4) → Facies (6) → Facies (7)/Shale

Some secondary channels may be carved on terrace tops, due to overchannel spilling of very competent flows. Some of these secondary channels formed braided networks, whereas other secondary channels were associated only with the deposition of individual beds (i.e. channels were cut and then rapidly filled by the same flow). Tractional reworking of previously deposited terrace top sediments yielded ungraded, crossbedded Facies (5) beds.

INTERPRETATION OF PREFERRED SEQUENCES IN TERMS OF THE PROPOSED MODEL

Markov and embedded Markov-chain analyses of bed-to-bed trends show that scoured surfaces are followed by Facies (1) conglomerates (Figs. 43, 44), which probably reflects the occurrence of Facies (1) beds mainly within major channels, some of which may be incised a depth of 5 m into the valley floor. Major sedimentation units which have Facies (4, 5, 6, 7) beds have a tendency for beds of respective facies to be overlain by beds of the same facies. This suggests that the spatial segregation of the different facies is fairly stable within the submarine valley system.

The variable patterns of the embedded Markov-chain analysis on a bed-to-bed basis would be expected if one is dealing with channel abandonment or channel reoccupation at given sites preserved in different outcrops.

Cluster and Markov-chain analysis (Fig. 45) show that within conglomerate horizons, interpreted as main channel deposits, Facies (1) beds are underlain and overlain by Facies (2,6,SS). These transitions might be interpreted as reflecting trends from main channel centres \longleftrightarrow main channel margins \longleftrightarrow braid bar sites. Facies (3,4) are associated with shales, which are then succeeded by Facies (1). These trends are thought to reflect reoccupation of a cutoff channel site or, alternatively, creation of a new channel on what was previously a terrace setting.

The pebbly sandstone horizons are interpreted as being deposited mainly within the main channel network, as bar top deposits, or as marginal terrace sediments. Within the pebbly sandstone horizons scour surfaces are again associated with Facies (1) conglomerates, reflecting the channelization of the coarse conglomerates. Shale tends to be overlain by Facies (4,5,6,7) which is thought to represent a progradation of 'nearer-to-channel' terrace sediments over those terrace sediments isolated from any coarse sediment input. Facies (3) is assigned to marginal terrace sites because of its relations with both Facies (4,5,6,7) and Facies (2).

The sandstone horizons, interpreted generally as high terrace deposits, show a trend of Facies (1) to be overlain by Facies (3,4), which, in turn, are followed by Facies (2,SS). These passages are interpreted to represent transitions between the high and marginal terrace settings. Facies (3,4) would be the high terrace sediments, with Facies (1,2,SS) all being due to spillover flows from the main channels to marginal ter-

faces. Facies (Sh,7) are followed by Facies (3,4) which reflect the progradation of marginal terrace deposits onto high terrace sediments, far away from the main channels. Facies (6) is followed by Facies (5); otherwise, Facies (6) is generally isolated from the other facies. Those Facies (5) beds that overlie Facies (6) beds may be due to tractional reworking of previously deposited massive Facies (6) sandstones.

The Bic section shows a tendency of either Facies (4,6) or Facies (5) to be succeeded by Facies (7,2). This pattern would reflect a change in deposition from clast dispersions (Facies 4,6) to deposition under greater tractional influence. This may record the passage from marginal terrace sites (Facies 4,6) to high terrace sites (Facies 7,2) and Facies (5), where deposition is slower. Facies (7,2) show a trend of being overlain by Facies (3), which would suggest a change from high terrace sites back to marginal terrace settings.

The Grève de la Pointe section shows a preferred relationship between Facies (1) and Facies (2) both with scoured surfaces, interpreted as representative of deposition within large and small channel complexes. Facies (2) occurs with Facies (4,5,6) which, in turn, tend to be found with Facies (3,7). These patterns are all thought to characterize passage from small channels on marginal terrace sites to terrace sites, farther away from the main channels. Shale is overlain by Facies (3,7), which is interpreted as recording the progradation of main terrace deposits onto those which are very isolated from coarse sediment input.

The Rivière Trois Pistoles section has a very complex flow pattern of facies relationships and is interpreted as recording deposition from several different settings, including main channel/braid bar, bar-

tops within the main channel network, and terrace settings.

When non-embedded Markov-chain analyses are done of the facies clusters, many of the clusters tend to be overlain by facies of the same groups. This suggests an overall stability of the spatial distribution of suites of facies, with respect to the inferred main channel systems.

LARGE-SCALE RELATIONSHIPS BETWEEN CONGLOMERATES AND SANDSTONES

Large-scale relationships occur on the scale of 10's-100 m thick. These relationships concentrate on the interactions of the conglomeratic members/niveau with the sandstone and pebbly sandstone members/niveau. In general, the transition from main channel conglomerates to terrace pebbly sandstones and sandstones is an overall fining-up sequence. The transition from terrace pebbly sandstones and sandstones to main channel conglomerates is an overall coarsening-up sequence.

As described by Johnson and Walker (in prep.) conglomerate members or, niveau vary between 35-50 m thick and consist of horizontally fining- and thinning-sequences. These sequences are explained, in the present study, by considering transitions from main channels to braid or point bars between main channels, but still within the main channel network. No consistent overall thinning- and fining-up sequences occur. Similarly, no overall trends are seen in facies types, clast size nor in sedimentary structures (Johnson and Walker, in prep.). This is not surprising, as demonstrated in the previous section, a whole variety of different sedimentary sequences can be generated by the interaction of main channels and braid or point bars.

Johnson and Walker (in prep., their Fig.9) show a transition zone 4-15 m thick as recording the passage from main conglomerate members/

niveau to main sandstone horizons. The transition zone consists, in their interpretation (Johnson and Walker, in prep.), of interbedded conglomerates and sandstones, many of which occur as small multiple-scour fills. Conglomerates become finer-grained, thinner-bedded and less common, up-section within the transition zone. This transition zone was interpreted as representing final stage of conglomerate deposition within a main channel (Johnson and Walker, in prep.). The sequence is topped by nonchannelized mainly sandstone deposits.

Examination of individual sequences within the various outcrops measured within the present study suggest that the transition zone of Johnson and Walker (in prep.) is not usually developed. In light of the main channel network/terrace model, which is presented in this chapter, -- the transition zone marks deposits that accumulate in marginal terrace settings. The marginal terrace subenvironment may be bypassed if main channel migration is very rapid and not through gradual processes. A variety of sequences or trends are developed between the main conglomerate and sandstone horizons, depending upon whether main channels are abandoning or reoccupying a site ; and, depending upon whether the migration is gradual or very rapid (Fig. 73,75 and Table 11).

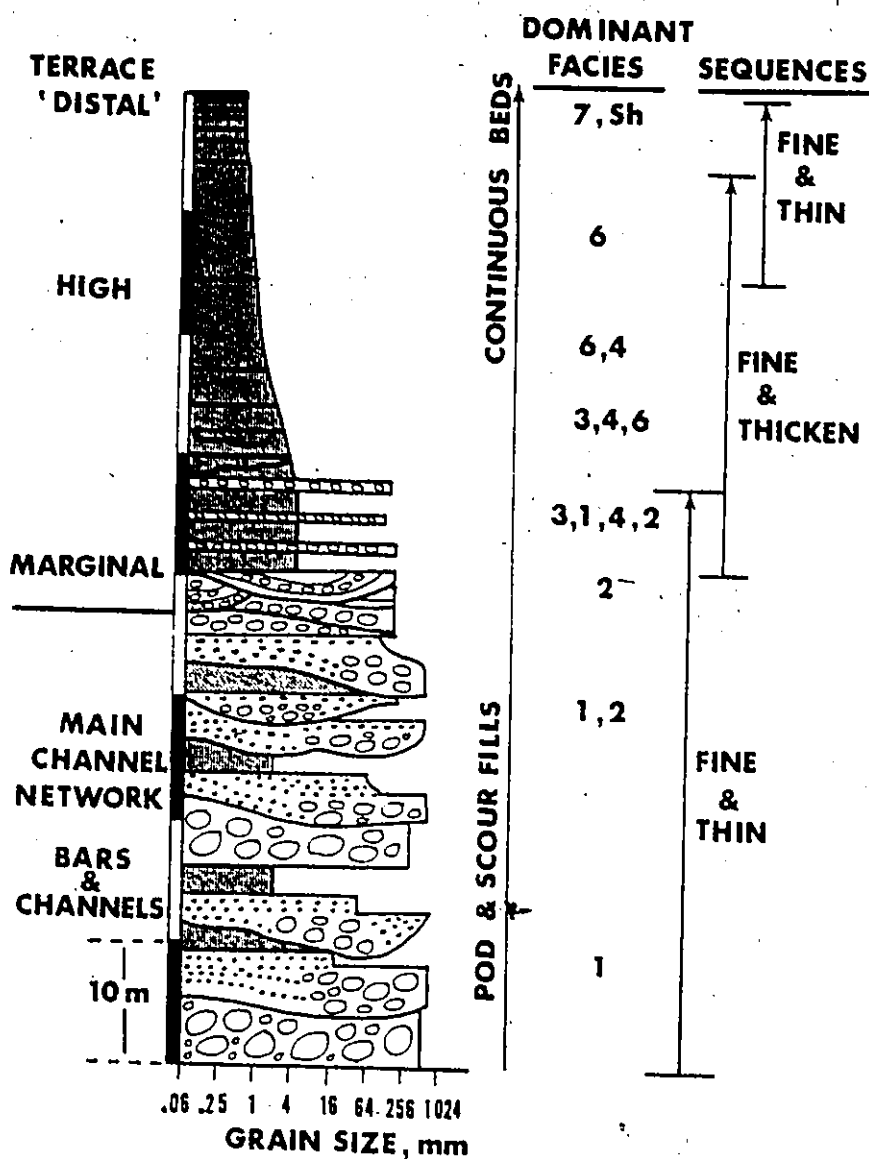


Fig. 75A Types of sedimentary sequences generated by the gradual abandonment of a main channel network, with the replacement by marginal terrace and high terrace settings. 'Distal' high terrace refers to those terrace settings farthest removed from the main channel network. Scale bar = 10 m.

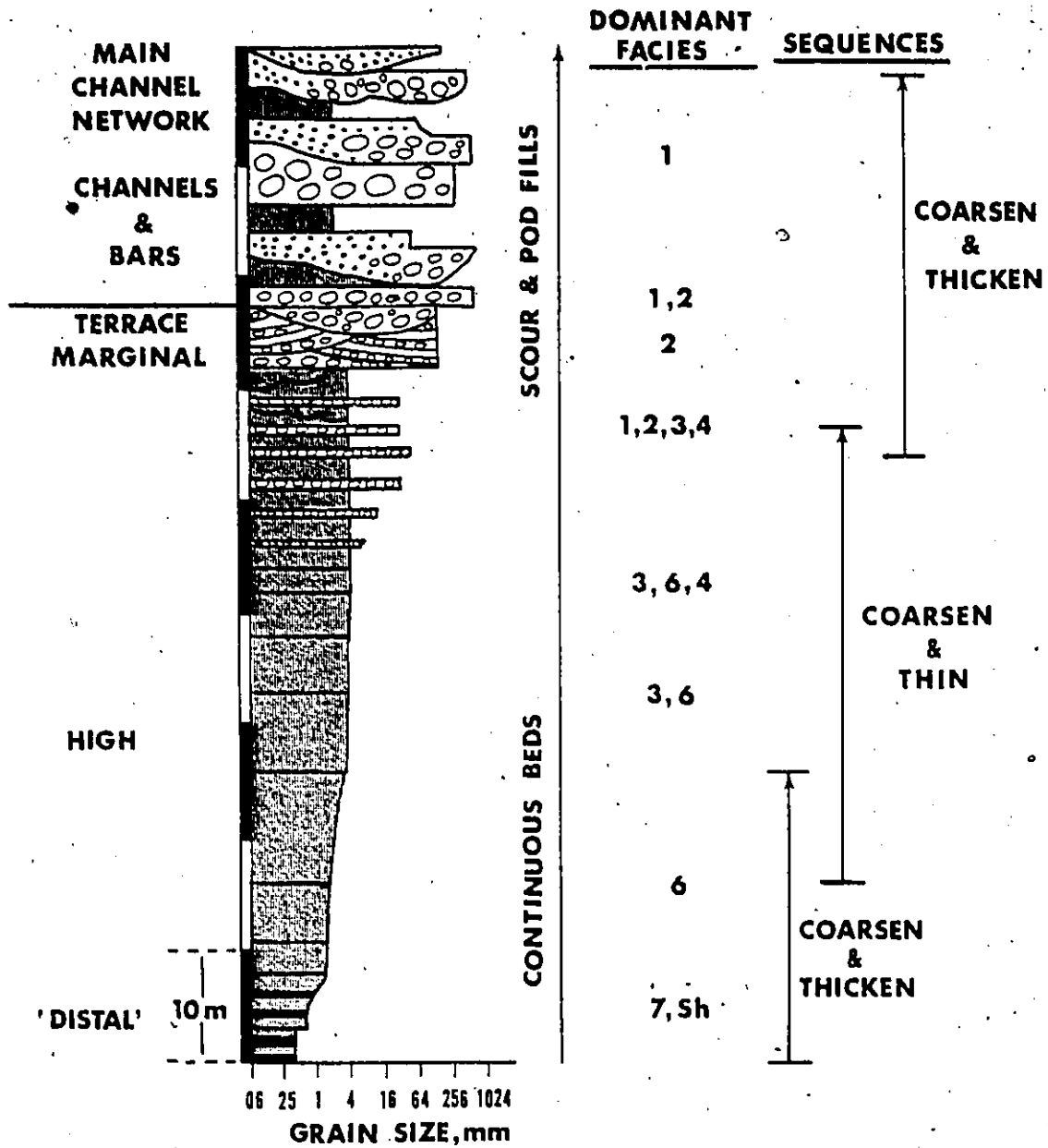


Fig. 75B. Types of sedimentary sequences generated by the gradual reoccupation of a site by a main channel network, with the abandonment of high terrace and marginal terrace settings. 'Distal' high terrace refers to those terrace settings farthest removed from the main channel network. Scale bar = 10 m.

The main channel network/terrace model explains the differences in paleoflow directions between the main conglomerate and sandstone horizons. As shown by Johnson and Walker (in prep.) conglomerate paleoflows are generally toward the west-southwest. Results from this study, as well as Mathey (1970) and Lajoie et al (1974), show mainly southerly directions for the sandstone horizons. Conglomerates are confined and follow the 'main thalweg' directions (Johnson and Walker, in prep.) Finer sediment is swept up onto marginal and high terraces, at angles to the local main channel orientations (mainly conglomerate).

Finally, implicit in the main channel network/terrace model is the fact that the main channel conglomerates may be time equivalent to topographically-higher sandstones deposited on terraces. Due to this complication, plus difficulties in correlations between fault-bounded outcrops, it is impossible to confidently reconstruct the regional paleogeography of the Cap Enrage Formation, as seen through different time-equivalent stratigraphic zones.

OVERALL SETTING OF THE CAP ENRAGE SYSTEM

The different members and niveau within the Cap Enrage Formation consist of different suites of facies. Member I and Niveau 2 are composed mainly of thick Facies (3), (6) and (4) beds, in association with classical turbidites (Facies (7)) and shale beds. These sediments are generally assigned to the high terrace setting, with some of the coarser sediments belonging to marginal terraces. Member II, Niveau 3 and Niveau 5 beds are mainly conglomeratic Facies (1) and (2) deposits and are interpreted to be the results of deposition within main channels and braid bars of the main channel network, comprising the submarine channel floor. Niveau 4

and Member III (near the contact with Member II) and Niveau 6 are predominantly coarse-grained Facies (2), (3) and (4) beds and are interpreted to be marginal terrace deposits. The top part of Member III consists of mainly classical turbidites (Facies (7)), shale beds and thin Facies (3) and (6) beds. This is interpreted to represent high terrace deposits. Lack of sufficient stratigraphic control, on a regional scale, prohibits the reconstruction of the whole formation through time-equivalent horizons.

Flow patterns within the conglomerates, interpreted as main channel sediments, are toward the south at Pt. Michaud and Bic (Fig. 12) but swing to the west-northwest at other localities to the west. This large-scale meandering of the main channel(s) is thought to be due to some sort of obstruction that prohibited further southern flow of coarse, bottom-hugging dispersions that travelled in channels. The general south-southwest trend of the finer sediment flows may have been enhanced by a regional tilt to the southerly direction.

The whole Cap Enragé Formation is interpreted as being deposited within the confines of a submarine channel. Although levee deposits are never seen in outcrop, the switch in regional paleoflows for the conglomerates (Johnson and Walker, in prep.), coupled with the rarity of fine-grained sandstones and shales, suggest channelization. There is insufficient data to state whether the Cap Enragé channel would be an "Upper Fan, Leveed Channel" (Fig. 6,7) or if it is an independent submarine channel, not associated with a submarine fan.

COMPARISONS WITH OTHER DEEP-SEA COARSE CLASTIC SEDIMENTS


Johnson and Walker (in prep.) suggest that the minimum width of the Cap Enragé channel would be 10 km (to include outcrop width) and minimum depth would be 300 m (assuming the whole formation fits inside the submarine channel). These estimates are not outlandish in comparisons to the dimensions of large, modern and ancient, submarine channels (see reviews by Normark (1978) and Walker (1978); McHargue et al, 1978; Scholl et al, 1970; Stow, 1977) (Table 12).

The next point is the type of channel pattern within the Cap Enragé system. Johnson and Walker (in prep.) suggest that the system was an incised meandering thalweg that occurred within the major channel system. The thalweg had a depth of 5-10 m and a possible (?) width of 50-100m. Johnson (1974) found that groups of conglomerate pods, alternating with sandstones, are on the order of 5-10 m thick -- hence, the estimate of depth of incision within the channel floor. This thalweg is the same order of magnitude of known channels within larger deep-sea valleys: the La Jolla channel thalweg is 200-300 m wide and 20 m deep; the Ascension thalweg is 100 m deep; and, the Northwest Mid-Ocean channel thalweg is 4-10 m deep and 400-1200 m wide (Johnson and Walker, in prep.).

Models from the present study show that Johnson and Walker's estimate of thalweg dimensions apply to the relationships between scours and low-relief, coarse-grained, terraces within major channels. In addition there were higher, fine-grained, terraces which stood perhaps 25-50 m above the base of the channel thalweg. This estimate is based upon the thickness of sandy niveau in relation to along-strike conglomerate niveau and members.

TABLE 12

DIMENSIONS OF SOME OF THE LARGER SUBMARINE CANYONS AND CHANNELS

<u>Channel or Canyon System</u>	<u>Floor Width</u>	<u>Height to Levee</u>	<u>Length</u>	<u>Reference</u>
Bering Canyon	3-4 km	0.8 km	400 km	Scholl et al., 1970
Bering Canyon (near mouth)	11.5 km	0.35 km		
Pribilof Canyon (outer shelf trough)	30 km	1.5 km	90 km	
Zhemchug Canyon (central axis)	25-30 km	2.6 km	160 km	
Laurentian Fan channels (upfan area)	26 km	0.85 km	330 km	Stow, 1977
Laurentian Fan channels (further downfan)	2-10 km	0.1 km		
Late Paleocene Meganos	3.2-9.7 km	0.6 km	80+km	Walker, 1978
Mid-Eocene Yoakum	16 km	0.9 km	80 km	
Pleistocene Mississippi	3.3 km	0.6 km	80 km	
Early Cretaceous Gevarum	max. 15 km	0.9 km	16+km	
Miocene Indus Cone (average dimensions of the larger channels, not the largest)	10-15 km	0.5-0.8 km		McHargue and Kessler, 1978
Upper slope channels	25-30 km	1.2 km (?)		McHargue, Kes- sler and Webb, 1978: pers. comm.
Lower slope-Upper Rise channels	8 km 	10-12 km		

Models developed in the present study suggest that the channel pattern within the confines of the Cap Enragé valley was a braided and not meandering pattern. The A.G.I. dictionary of geologic terms (1957) defined a 'braided stream' as "one flowing in several dividing and reuniting channels resembling the strands of a braid, the cause of the division being the obstruction by sediment deposition by the stream." The extension of a braided channel interpretation to a deep-sea submarine valley is not unreasonable. Bathymetric and seismic profiles of many modern and sub-Recent fans show braided channel patterns, including Redondo (Haner, 1971), Hatteras (Cleary and Conolly, 1974), Laurentian (Stow, 1977), Navy and Ascension (Normark, 1978) Fans. On Hatteras Fan (Cleary and Conolly, 1974) interchannel terraces, up to 5 km across, have irregular surfaces, presumably formed by small channel networks developed on the terrace-top surfaces. Major channels of the Laurentian Mid Fan area are up to 26 km wide and have several distinct thalwegs. Deep-tow bathymetric profiles of Navy and Ascension Fan valleys show that the valleys are floored with irregular shallow channels, up to 8 m deep and 50-200 m wide on Navy Fan, and a depth of 20 m on Ascension Fan (Normark, 1978).

Few ancient deep-sea sediments have been interpreted as being deposited within braided, submarine channel networks. The one, well-documented case is the Repetto Formation of the Los Angeles Basin (Hsü, 1977). Isopach maps over an area 2.5 km wide x 5 km long, show a pattern of branching and anastomosing elongate sand stringers (Hsü, 1977, Fig. 18), that essentially form a braided pattern (Walker, 1978). Individual sand stringers, possibly channel deposits (Walker, 1978), are about 250-450 m wide and up to 13 m thick (Hsü, 1977).

The scale of all of the features reconstructed for the Cap Enragé valley fall within those dimensions of similar features found in modern submarine settings (see discussions previous two pages). The only features for which there are not obvious analogies are the very low-relief scour-and-terraces which account for the deposition of individual beds on low-relief and high-relief terraces within the Cap Enragé system. Stow (1977) notes the occurrence of small transverse (with respect to main channel directions), tributary (and distributary?) channels across the backs of major channel levees. Many of the levees have a "hingeline" across which the seismic reflectors are either discontinuous or bent, which was interpreted by Stow (1977) as representing filling-in of depressions or channels within the back levee area by sheetflow.

Deep-tow side-scanning sonar data from Navy Fan (Normark et al, in prep.) show the existence of flute-shaped scours, many 5-30 m across and 1-2 m deep. The origin of these scours is not known and may be due to either scouring or rotational slumping. Although the depth of the flute-shaped depressions is given as 1-2 m, this is the limit of the vertical resolution of the sounding system. D.J.W. Piper (1977:pers. comm.) states that these scour or depression features are observed down to the smallest scale, a few 10's of centimetres discernable on bottom photographs.

The smallest scour-and-terraces, accounting for deposition of individual beds within the Cap Enragé Formation, appear similar to those reported by Normark et al (in prep.) and Piper (pers. comm.) for Navy Fan. The origin of these features on Navy Fan is not known. Within the Cap Enragé there is no evidence of separate periods of scouring and deposi-

tion; likewise, there is no evidence of slumping within these small scour-and-terraces. Consequently, they are interpreted as representing scour-and-fill events associated with deposition of individual beds within the Cap Enragé system. The next larger scale scour-and-terraces, accounting for the deposition of several or many beds, are similar to the small scour and channel complexes reported by some workers as being on the tops of interchannel terraces (Cleary and Conolly, 1974; Stow, 1977) and within major channels (Normark et al, in prep.). As with the origin of the smallest scours, these are interpreted for the Cap Enragé deposits as representing scour-and-fill events associated with the deposition of several flows, and not due to slumping nor filling of pre-existing topography. The largest scour-and-terraces, accounting for the deposition of the different members and niveau within the Cap Enragé Formation, are the same size as many of the thalweg channel and interchannel terraces described from many submarine fan and submarine channel settings (Chough and Hesse, 1976; Cleary and Conolly, 1974; Hand and Emery, 1964; Hsü, 1977; Haner, 1971; McHargue et al, 1978 and pers. comm.: 1978; Normark, 1978; Normark et al, in prep.; Stow, 1977).

REGIONAL PALEOTOPOGRAPHY AND GENERAL SETTING

As mentioned in the introductory chapter, conglomerates of deep-sea origin have been reported in a narrow belt of Early Cambrian to Early Ordovician rocks along the lower St. Lawrence, Gaspésie and Newfoundland areas. Although the rocks are not all representative of the same time period, general comparisons with respect to basinal setting can be made with the Cap Enragé sediments.

The Lévis-Lauzon conglomerates at Québec City (Osborne, 1928; Breakey, 1975) have a general paleoflow within the conglomerates due south (Fig. 76). Conglomerates show normal grading, but without good fabric nor stratification. Conglomerates were thought to be deposited from debris flows, mass flows and slumps (Breakey, 1975). These breccia beds are associated with ribbon limestones, regular classical turbidites, pebbly mudstones and shale beds. The general environment is interpreted as being a very proximal, immature deep-sea environment, perhaps at a base of slope setting at the mouth of submarine canyons (Breakey, 1975).

The St. Roch conglomerate channel fill at L'Islet sur Mer (Rocheleau and Lajoie, 1974) shows conglomerates with normal grading, well developed fabric and imbrication, and parallel and oblique cross-bedding. Topping the conglomerate fill are massive sandstones. Both conglomerate and sandstone beds are interpreted as being transported by high density turbidity currents into the basin. The channel cuts into classical turbidites, which are neither truly proximal nor distal, but on smooth fan lobes (Walker, 1978). This would place the turbidites on smooth lobes of the lower mid-fan or middle, lower-fan. Turbidite flow was toward 170° , whereas erosional markings on the base of the conglomerate channel suggest flow towards 210° (Walker, 1978). Conglomerates within the fill have an average paleoflow towards the south-south-west; similarly, oblique crossbeds in the sandstone fill have long axes of the troughs oriented NNW-SSE, with the foresets dipping toward the south (Rocheleau and Lajoie, 1974). Turbidites and channel fill are thus interpreted as being parts of the same fan complex, with the coarse chan-

Fig. 76 - Regional setting for different Cambro-Ordovician conglomerates in the Quebec-Gaspe-Newfoundland flysch belt. The sketch is not meant to represent deposition at a single time or basin setting, rather relative basin settings within carbonate platform-slope-rise systems are shown. 1. Cow Head Breccia 2. Cape Cormorant Breccia 3. Cap-des-Rosiers Conglomerate 4. Cap Enragé Formation 5. St. Roch Formation at L'Islet sur Mer 6. Lévis-Lauzon Conglomerate.

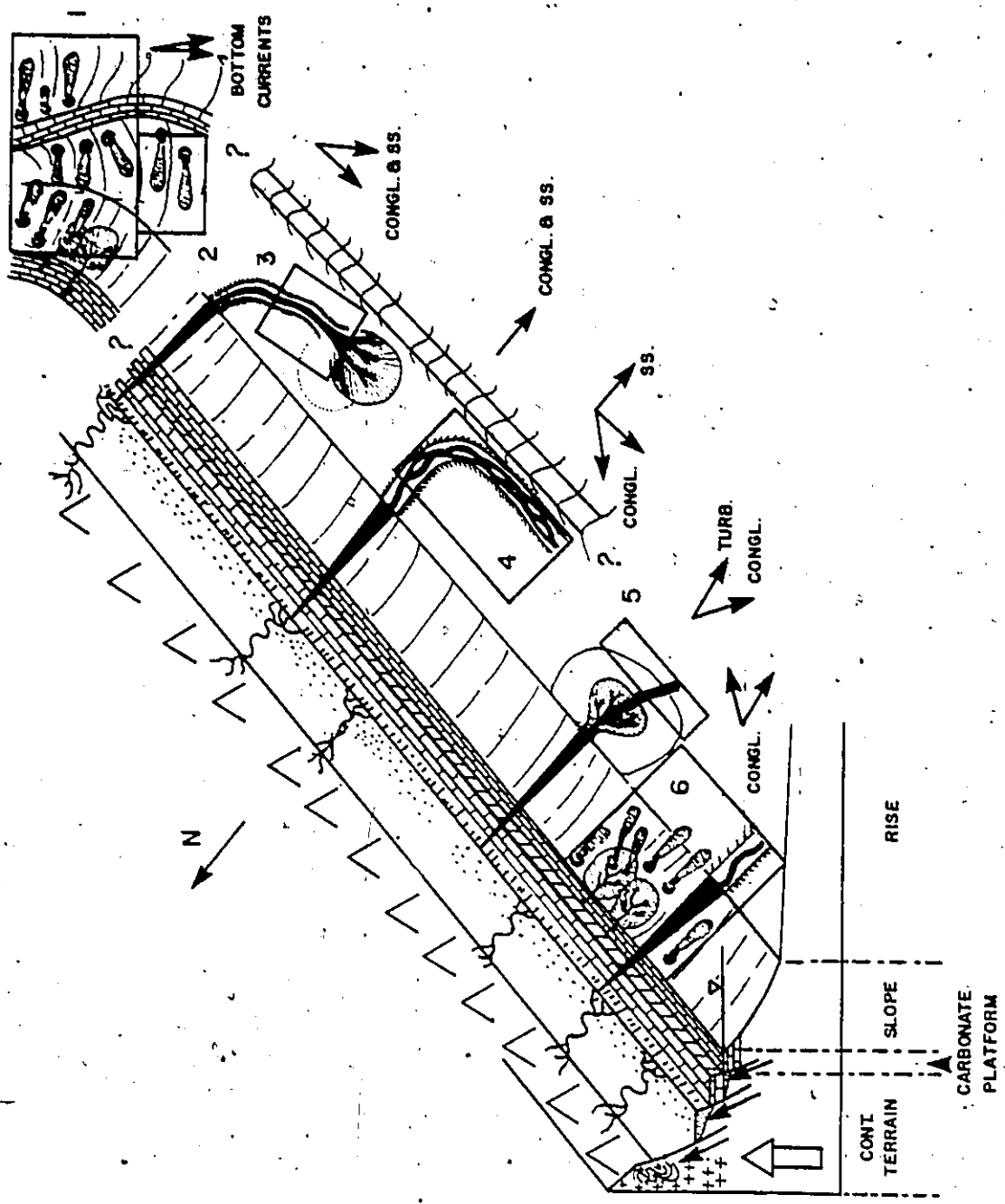


Fig. 76A- Generalized tectonic map of the St. Lawrence Lowlands and Gaspésie Peninsula of Québec and the Western Platform of Newfoundland. Locations of the different Cambro-Ordovician conglomerates in the Quebec-Gaspé-Newfoundland flysch belt are numbered as follows:

1. Cow Head Breccia
2. Cape Cormorant Breccia
3. Cap-des-Rosiers Conglomerate
4. Cap Enragé Formation
5. St. Roch Formation at L'Islet sur Mer
6. Lévis-Lauzon Conglomerate.

Redrawn from the Geological Survey of Canada Tectonic Map of Canada, Map 1251 A, 1968,

Scale 1:5,000,000.

261A

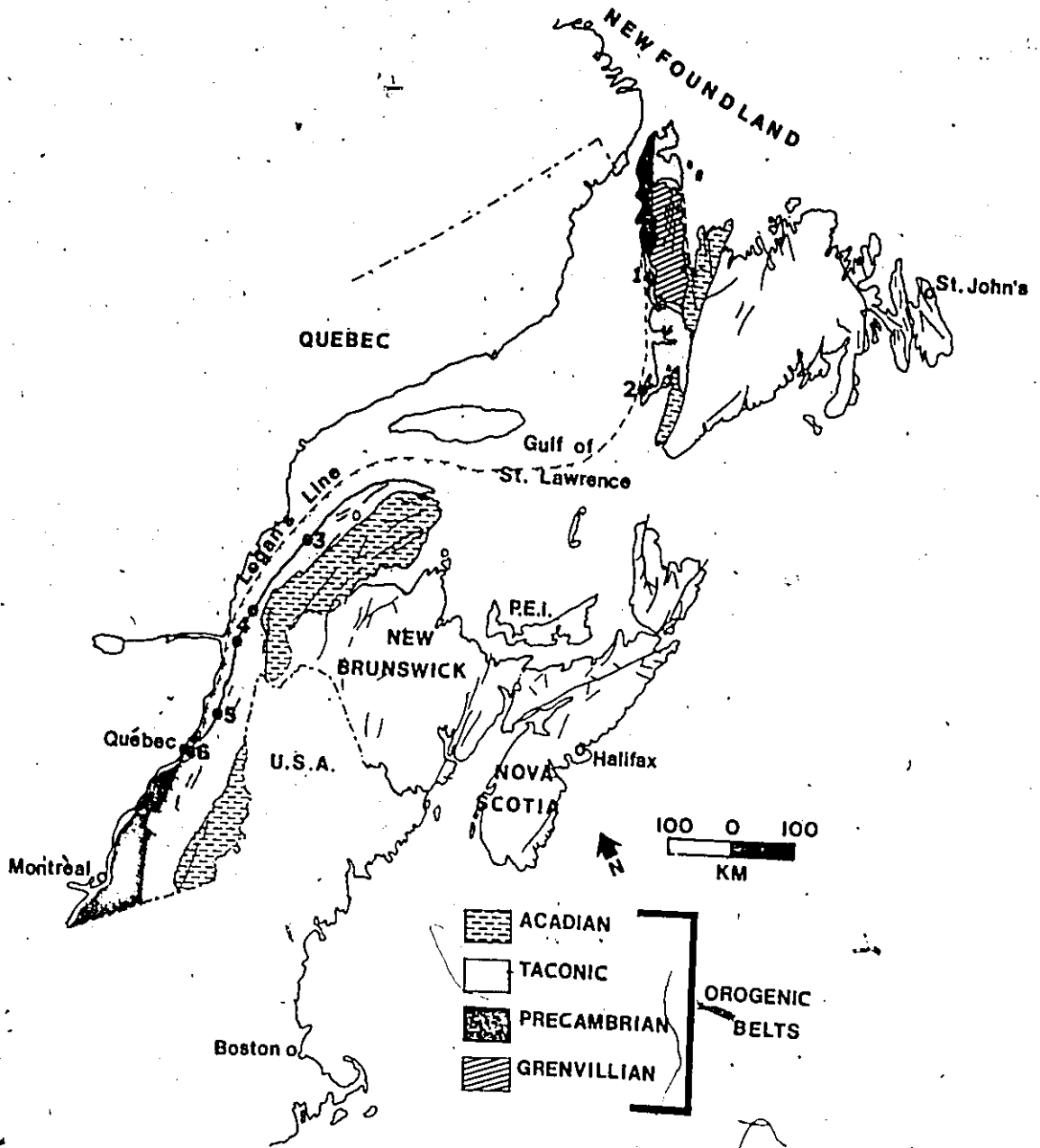
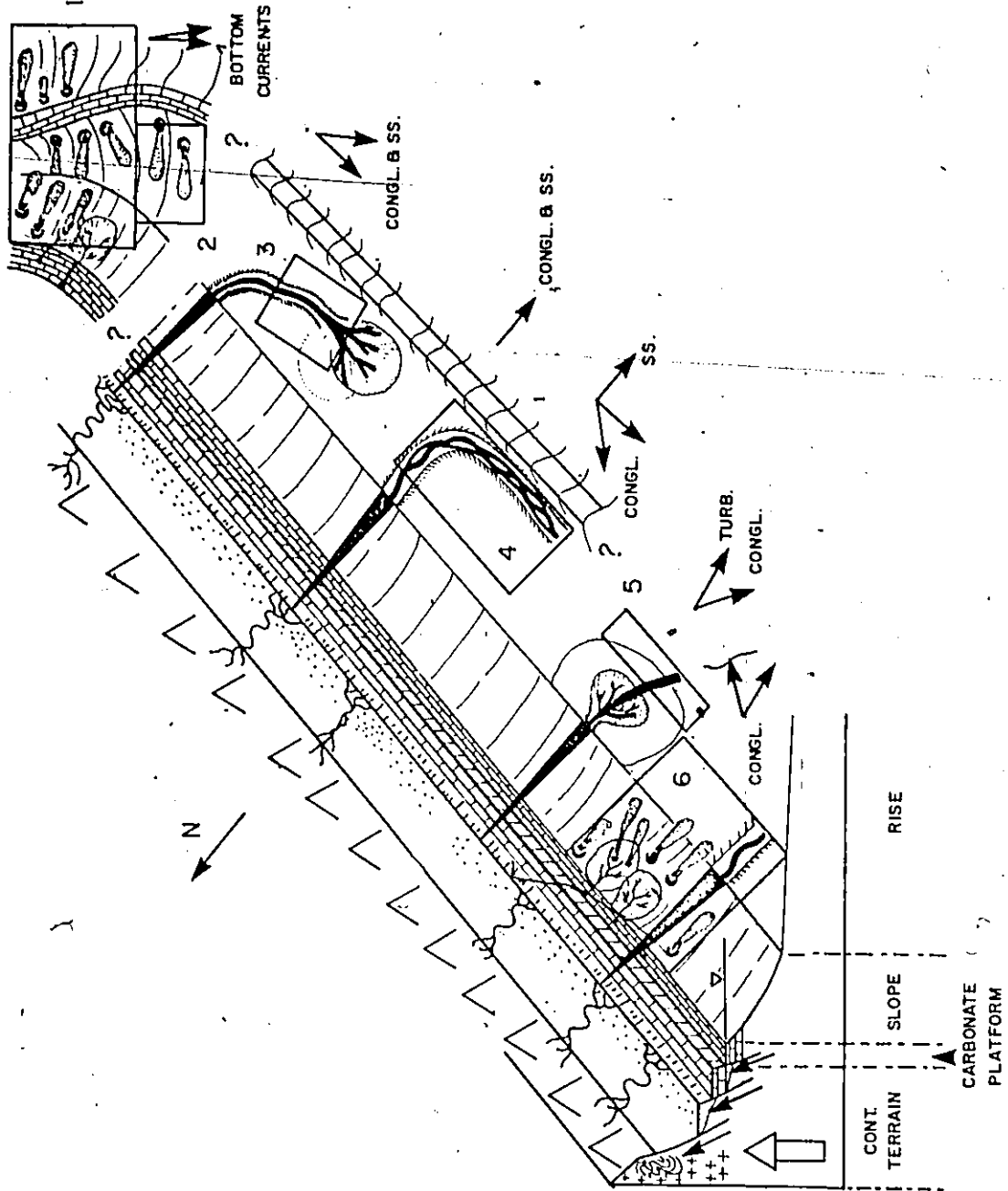


Fig. 76B - Regional setting for different Cambro-Ordovician conglomerates in the Quebec-Gaspé-Newfoundland flysch belt. The sketch is not meant to represent deposition at a single time or basin setting, rather relative basin settings within carbonate platform-slope-rise systems are shown. 1. Cow Head Breccia 2. Cape Cormorant Breccia 3. Cap-des-Rosiers Conglomerate 4. Cap Enragé Formation 5. St. Roch Formation at L'Islet sur Mer 6. Lévis-Lauzon Conglomerate.



nel fill being representative of an incised-fan channel (Walker,1978) (Fig. 76).

The Cap-des-Rosiers conglomerate at Grosses Roches (Hendry,1973) occurs mainly as channel fills that cut claystones and turbidites. Conglomerates show normal grading, rip-up structures, poor sorting, very large clasts and, in some beds, chaotic fabric. Traction structures are rare within the conglomerates, suggesting very rapid depositional rates (Hendry,1973). Most of the conglomerate beds are composite, in which the successive conglomerate flows were thought to result from progressive liquefaction of sediment. Sediment was transported and deposited by high density, sediment gravity flows, which were probably associated with gravity slides. The Grosses Roches conglomerate has been assigned to the upper fan (or upstream part of the braided supra-fan) (Walker,1978), as evidenced from silty mudstone outside the channel and the disorganized nature of the conglomerate channel fill. The sediments of the fill were deposited by flows that travelled towards the south, southwest and west (Hendry,1973,1976), although all of the sediment was derived from the north. This is strikingly similar to the switch in paleoflows as observed for the Cap Enragé deposits. The Grosses Roches coarse flows may have also been deflected by a similar, although not necessarily the same, obstruction.

The Cow Head Breccia (Hubert et al,1977) consists of limestone breccia interbedded with thin lime mudstone, calcarenite, shales, marls and radiolarian cherts. Every breccia bed has mud matrix (5-25% of individual beds) and some bed portions may be matrix-supported breccias. About 90% of the clasts within the beds show subparallel alignment or

wave-form fabrics. Clast imbrication is downslope and many breccia beds show transitions amongst the horizontal, waveform and downslope-inclined fabrics. Breccias are thought to have been deposited from gravity-induced viscous mass flows, with surging motions within the flows causing the peculiar clast fabric and imbrication patterns. Mass flows were shed off small carbonate platforms (at least two) that trended NW-SE. Breccias are slope deposits. Finer-grained calcarenites were deposited by contour currents that swept the slope setting.

The Cape Cormorant Breccia (DeLong, 1977) overlies slope facies and is topped by turbiditic sandstones. Associated with the conglomerate breccias are calcarenites, which may be massive, normally graded or show Bouma sequences. Breccias are disorganized, reversely or normally graded. Large clasts may protrude out above the general bed level. Matrix content varies from 15% to matrix-supported breccias. Some breccia beds have calcarenite caps that are massive or graded and may represent the same depositional event as the underlying breccia unit. Slump horizons associated with the breccias suggest that paleocontours ran NE-SW. Clast imbrication within the breccia beds was downslope. Breccias may have been deposited from debris or mass flows, some of which generated turbidity currents forming calcarenite caps with Bouma sequences. The general setting would be a slope environment (Middleton, 1978: pers. comm.; DeLong and Middleton, 1978), although the slope direction for the Cape Cormorant Breccia is still in doubt (Middleton, pers. comm.)

GENERAL TECTONIC SETTING

The most striking information about the paleotectonic setting was that both the Cap Enragé and the Cap des Rosiers conglomerates were deflected by some obstruction, to travel in a direction parallel to the ancient base-of-slope. Main conglomerate members within the Cap Enragé Formation showed paleoflows consistently toward the west-southwest, throughout deposition of the whole formation (Johnson and Walker, in prep.). This suggests that the obstruction was probably at least 300 m high (the Cap Enragé Formation is about 250 m thick) or the obstruction grew progressively through time, to continually obstruct Cap Enragé deposition to the south. It is the nature of this obstruction that is most intriguing.

All of the evidence shows that during Cap Enragé time the basin was expanding and not contracting. The northern Appalachian system (Eastern Townships - Gaspé - New Brunswick) developed in subsiding basins that formed between, what is presently, the Canadian Shield and the Avalon Landmass (Bird and Dewey, 1970; Church and Stevens, 1971; Poole, 1976; Ruitenberg et al, 1977; St. Julien and Hubert, 1975). During the late Precambrian or Cambrian initial distension began. This resulted in the formation of a southern basin and a disrupted microcontinental block (Avalon Landmass), south of the Canadian Shield (Ruitenberg et al, 1977). Further extension between the microcontinent and the Canadian Shield resulted in the opening of a northern basin during Cambrian time. This northern basin developed on subsiding continental crust, with extension being by mainly thinning and normal faulting of continental crust (Poole, 1976). This northern basin served as the depocentre for the Cap Enragé and Cap des Rosiers sediments.

During Cambro-Ordovician time a variety of sediments were deposited

in the northern marginal basin, in what is presently the Lower St. Lawrence Valley. The basinal sediments included shales, feldspathic sandstones, and conglomerates, composed of limestone and petromict clasts. These sediments compose what are called the St. Roch, St. Damase, Kamouraska, Orignal, Cap Enragé and Ladrière Formations (Table 13).

In the Sherbrooke-Thetford Mines area (Fig. 1), a shale mélange developed during middle Lower Cambrian to Middle Ordovician time. This mélange, the St. Daniel Formation, accumulated on newly formed oceanic crust, as suggested by ophiolite assemblages (St. Julien and Hubert, 1975) (Table 13). Ophiolites also occurred in western Newfoundland (Dewey and Bird, 1971; Kennedy, 1973) and in northern New Brunswick (Ruitenberg *et al.*, 1977). During Middle Ordovician time, the oceanic crust in the Sherbrooke-Thetford Mines area was covered by a variety of deposits, including shales, sandstones and tuffs of the Magog Group and calc-alkaline volcanic assemblages (St. Julien and Hubert, 1977). These rock assemblages were interpreted by St. Julien and Hubert (1977) as representing deposition within an expanding marginal basin along the eastern edge of the Canadian Shield.

In the early Ordovician time, obduction of part of the oceanic crust occurred (St. Julien and Hubert, 1977). The ophiolite assemblage was thrust upon and over shale and feldspathic sandstones of the Caldwell Group and dark grey phyllites and feldspathic sandstones of the Rosaire Group (Table 13). Concomittant with this obduction, St. Julien and Hubert (1977) propose that there was subduction of oceanic crust to the east. A Benioff zone was thought to have formed, above which a broad volcanic island arc system evolved. In the Sherbrooke - Eastern Townships area calc-alkaline lavas and pyroclastic material of the Ascot-Weden Formations

TABLE 13

STRATIGRAPHIC AND TECTONIC ELEMENTS: CAMBRO-ORDOVICIAN, LOWER ST. LAWRENCE VALLEY AND EASTERN TOWNSHIPS, QUEBEC (St. Julien and Hubert, 1975)

DOMAINS		E X T E R N A L		I N T E R N A L		D O M A I N	
SUB-DOMAINS		N A P E S		S I A L I C C R U S T		O C E A N I C C R U S T	
LOCATION		LOWER ST LAWRENCE VALLEY		E A S T E R N T O W N S H I P S		S H E R B R O O K E	
STRUCTURAL UNITS		LA POCATIERE BIC		M O T R E - D A M E A N T I C L I N O R I U M		S T . V I C T O R S Y N C L I N O R I U M	
UPPER		LOWER ST LAWRENCE VALLEY NAPPES				M A S O O G G R	
MIDDLE						F L Y N C H S T V I C T O R M A S O O G R	
LOWER		K A M O R A S K A F m				F L Y N C H S T V I C T O R M A S O O G R	
UPPER		L A D R I E R E F m				A S C O T F m	
MIDDLE		C A P E M A S E F m				F L Y N C H S T V I C T O R M A S O O G R	
LOWER		S T R O C H F m		C A L D W E L L G r		S T . D A N I E L F m	
		O R I G I N A L F m		O A K H I L L G r		S T . D A N I E L F m	
				R O S A I R E G r		O P H I O L I T E A S S E M B L A G E	
				P S		O P H I O L I T E A S S E M B L A G E	

— Base of the nappe
 ~~~~~ Unconformity

(Table 13) were deposited on oceanic crust (St. Julien and Hubert, 1975). In New Brunswick, the volcanic arc system developed upon sialic crust (Ruitenberg et al, 1977). The development of this volcanic arc system is interpreted by Ruitenberg et al (1977) and St. Julien and Hubert (1975) as recording the closing of the northern marginal basin, which was closed completely by late Ordovician time. Hence, it is clear that during Cap Enragé and Cap des Rosiers time the northern basin was in an extensional phase. No plate tectonic obstructions, as a consequence of creation of volcanic arcs or associated with deformation in creation of a subduction zone, can account for obstruction that served as a barrier to sediment dispersal to the south, in the northern basin.

During accumulation of the Cap Enragé sediments, the northern marginal basin was undergoing expansion and was developed upon, from all evidence available, continental crust. Development of an arc-trench gap did not occur until later. Therefore, the depression could not have been a trench; also the obstruction could not have been a volcanic arc highland. The barrier to southerly-flowing main channels of the Cap Enragé Formation may have been uplifted continental blocks (perhaps at least 300 m high, or with continued uplift during Cap Enragé time), which were associated with marginal normal faulting during expanding phases of the northern marginal basin.

The next point concerns whether the proposed uplifted block was a large-scale microcontinental block or a smaller scale feature. Hubert (1973) interpreted, based upon paleocurrent evidence, that the arkoses of the St. Roch and St. Damase Formations were derived from islands and/or landmasses located to the southeast of the depocentre -- the northern

marginal basin. In Hubert's interpretation (1973) the source area was above sea level and the rocks were similar to those of the Canadian Precambrian Shield. Most of the basis for this interpretation involves the paleocurrent data derived by Hubert (1973) in his study. More recent studies by Strong (1977) show that a landmass and/or islands did not, in fact, supply sediment to the depocentre for the St. Roch Formation. Paleocurrent data from Strong's (1977) study suggest that sediments were derived from the northerly Canadian Precambrian Shield. Similarly, no evidence exists to support a southerly source area for the Lévis-Lauzon (Bréakey, 1975), Cap Enragé (Lajoie et al, 1974; Mathey, 1970; Johnson and Walker, in prep.; and, this study), or the Cap des Rosiers (Hendry, 1973, 1976, 1978) conglomerates. This suggests that the obstruction was, most likely, a smaller-scale topographic feature, that did not extend up to sea level, but was able to influence sedimentation patterns throughout Cap Enragé and Cap des Rosiers time.

In summary, the Cambro-Ordovician tectonic setting for the Cap Enragé sediments is inferred to consist of a marginal oceanic basin. This basin was bounded, to the south, by small-scale, uplifted continental block and, to the north, by the Canadian Precambrian Shield. This small-scale uplifted continental block did not extend to sea level, but did force main channels of the Cap Enragé system to swing parallel to the base-of-slope. A similar influence was exerted upon the Cap des Rosiers conglomerate. The continental block did not supply detritus to the depocentre. The northern marginal basin closed by late Ordovician time.



## REFERENCES

- Aalto, K.R., 1972, Flysch pebble conglomerate of the Cap-des-Rosiers Formation (Ordovician), Gaspé Peninsula, Québec: Jour. Sed. Petrol., V. 42, p. 922-926.
- , 1976, Sedimentology of a mélange: Franciscan of Trinidad, California: Jour. Sed. Petrol., V. 46, p. 913-929.
- and Dott, R.H., Jr., 1970, Late Mesozoic conglomeratic flysch in southwestern Oregon, and the problem of transport of coarse gravel in deep water, in Lajoie, J. (Ed.), Flysch sedimentology in North America, Geol. Assoc. Canada, Sp. Paper 7, p. 53-65.
- Allen, J.R.L., 1964, Primary current lineation in the lower Old Red Sandstone (Devonian), Anglo-Welsh Basin: Sedimentology, V.3, p.89-108.
- , 1965, A review of the origin and characteristics of recent alluvial sediments: Sedimentology, V.5, p. 89-191.
- , 1970, The sequence of sedimentary structures in turbidites, with special reference to dunes: Scottish Jour. Geol., V.6, p.146-161.
- American Geological Institute, 1957, Dictionary of geological terms: Doubleday and Co., Inc., Garden City, New York, 545 p.
- Andresen, A. and Bjerrum, L., 1967, Slides in subaqueous slopes in loose sand and silt in Richards, A.A. (Ed.), Marine geotechnique, Univ. Illinois Press, Urbana, p.221-239.
- Bagnold, R.A., 1954, Experiments on gravity-free dispersion of large solid spheres in a Newtonian fluid under shear: Proc. Roy. Soc. London Ser. A, V. 225, p. 49-63.
- , 1973, The nature of saltation and of "bed-load" transport in water: Proc. Roy. Soc. London, Ser. A, V.332, p. 473-504.
- Bennets, K.R. and Pilkey, O.H., 1976, Characteristics of three turbidites, Hispaniola-Caicos Basin: Geol. Soc. Amer. Bull., V. 87, p.1291-1300.
- Bird, J.M. and Dewey, J.F., 1970, Lithosphere plate - continental margin tectonics and the evolution of the Appalachian orogen: Geol. Soc. Amer. Bull., V. 81, p. 1031-1060.
- Bouma, A.H., 1962, Sedimentology of some flysch deposits: a graphic approach to facies interpretation: Elsevier Publ. Co., Amsterdam, 168 p.
- , 1972, Recent and ancient turbidites and contourites: Trans. Gulf Coast Assoc. Geol. Socs., V. 22, p. 205-221.

- , and Hollister, C.D., 1973, Deep ocean basin sedimentation in Middleton, G.V. and Bouma, A.H. (Eds.), Turbidites and deep water sedimentation, Pacific Section Soc. Econ. Paleont. Mineral. Short Course Notes, Anaheim 1973, p. 79-118.
- Breakey, E.C., 1975, Sedimentology of the Lower Paleozoic shelf-slope transition Lévis, Québec: M.Sc. thesis, McGill University, Montréal.
- Bussièrès, L., Mehrtens, C.J., Belt, E.S., and Riva, J., 1977, Late Middle Ordovician shelf, slope and flysch facies between Baie St. Paul and La Malbaie, Québec, in Béland, R. and LaSalle, P. (Eds.), 69 th Ann. Mtg. NEIGC, Québec City, Canada, p. B9-1 to B9-26.
- Cant, D.J., in press, Bedforms and bar types in the South Saskatchewan River: Jour. Sed. Petrol.
- and Walker, R.G., 1976, Development of a braided fluvial facies model for the Devonian Battery Point Sandstone, Quebec: Canadian Jour. Earth Sci., V. 13, p.102-119.
- Cherkis, N.Z., Fleming, H.S. and Feden, R.H., 1973, Morphology and structure of Maury Channel, northeast Atlantic Ocean: Geol. Soc. Amer. Bull., V. 84, p. 1601-1606.
- Chevalier, J., 1976, Diagenèse de Grès Cambro-Ordovicien, St-Fabien, Québec: M.Sc. thesis, Univ. de Montréal, Montréal, 86p.
- Chipping, D.H., 1972, Sedimentary structures and environment of some thick sandstone beds of turbidite type: Jour. Sed. Petrol., V.42, p. 587-595.
- Chough, S.K. and Hesse, R., 1976, Submarine meandering thalweg and turbidity currents flowing for 4000 km in the Northeast Atlantic Mid-Ocean Channel, Labrador Sea: Geology, V. 4, p. 529-533.
- Church, W.R. and Stevens, R.K., 1971, Early Paleozoic ophiolite complexes of the Newfoundland Appalachians as mantle-oceanic crust sequences: Jour. Geophys. Res., V. 76, p. 1460-1466.
- Cleary, W.J. and Conolly, J.R., 1974, Hatteras deep-sea fan: Jour. Sed. Petrol., V. 44, p. 1140-1148.
- Colburn, I.P., 1968, Grain fabrics in turbidite sandstone beds and their relationship to sole mark trends on the same beds: Jour. Sed. Petrol., V. 38, p. 146-158.
- Cook, H.E., McDaniel, P.N., Mountjoy, E.N., and Pray, L.C., 1972, Allocthonous carbonate debris flows at Devonian bank ("reef") margins, Alberta, Canada: Canadian Petrol. Geol. Bull., V.20, p. 439-497.
- Costello, W.R. and Walker, R.G., 1972, Pleistocene sedimentology, Credit River, Southern Ontario: a new component of the braided-river

- model: Jour. Sed. Petrol., V. 42, p. 389-400.
- Crowe, B.M. and Fisher, R.V., 1973, Sedimentary structures in base-surge deposits with special reference to cross-bedding, Ubehebe Craters, Death Valley, California: Geol. Soc. Amer. Bull., V.84, p.663-682.
- Curray, J.R., 1956, The analysis of two-dimensional orientation data: Jour. Geology, V. 64, p. 117-131.
- Dalrymple, R.W., Knight, R.J. and Lambiase, J.J., 1978, Bedforms and their hydraulic stability relationships in a tidal environment, Bay of Fundy, Canada: Nature, V. 275, p. 100-104.
- Dapples, E.C. and Rominger, J.F., 1945, Orientation analysis of fine-grained clastic sediments: Jour. Geology, V. 53, p. 246-261.
- Davies, I.C., 1972, Transport of conglomerate into deep water: a study of the Cambro-Ordovician Cap Enragé conglomerate at St. Simon de Rimouski, Québec: M.Sc. thesis, McMaster Univ., Hamilton, 91 p.
- and Walker, R.G., 1974, Transport and deposition of resedimented conglomerates: the Cap Enragé Formation, Gaspé, Québec: Jour. Sed. Petrol., V. 44, p. 1200-1216.
- Davis, J.C., 1973, Statistics and data analysis in geology: Wiley, New York, 550 p.
- and Cocks, J.M., 1972, Interpretation of complex lithologic successions by substitutability analysis in Merriam, D.F. (Ed.), Mathematical models of sedimentary processes: Plenum Press, New York, p. 27-52.
- DeLong, R.C., 1977, Field observations on the Cape Cormorant Breccia, Cape Cormorant, western Newfoundland: Tech. Memo 77-6, Dec. 1977, McMaster Univ., Hamilton, Dept. Geology, 25 p.
- and Middleton, G.V., 1978, Ordovician carbonate megabreccias at Cape Cormorant, western Newfoundland: submarine debris flow: Geol. Soc. Amer.- Geol. Assoc. Canada Ann. Mtg. Abstracts, Toronto, p.326.
- DeRaaf, J.F.M., Reading, H.G. and Walker, R.G., 1965, Cyclic sedimentation in the lower Westphalian of No. Devon, England: Sedimentology, V. 4, p. 1-52.
- Dewey, J.F. and Bird, J.M., 1970, Mountain belts and the New Global Tectonics: Jour. Geophys. Res., V. 75, p. 2625-2647.
- Dott, R.H., 1963, Dynamics of subaqueous gravity depositional processes: Amer. Assoc. Petrol. Geol. Bull., V. 47, p. 104-128.

- Doveton, J.H. and Skipper, K., 1974, Markov chain and substitutability analysis of a turbidite succession, Cloridorme Formation (Middle Ordovician) Gaspé, Québec: Canadian Jour. Earth Sci., V.11, p.472-488.
- Eder, F.W., Genese Riff-näher detritus-kalke bei Balne im Rheinischen Schiefergebirge (Garbecker Kalk): Verh. Geol. B-A, V.4, p.551-569.
- Engel, W., 1974, Sedimentologische Untersuchungen im Flysch des Beckens von Ajdovscina (Slovenien): Goettinger Arb. Geol. Paleont., V.16, 65 p.
- Enos, P., 1969, Anatomy of a flysch: Jour. Sed. Petrol., V.39, p.680-723.
- Fisher, R.A., 1953, Dispersion on a sphere: Proc. Roy. Soc. London, Ser. A., V.217, p. 295-305.
- Fisher, R.V. and Mattinson, J.M., 1968, Wheeler Gorge turbidite-conglomerate series, California: inverse grading: Jour. Sed. Petrol., V. 38, p. 1013-1023.
- Fleischer, P., 1970, Mineralogy of hemipelagic basin sediments, California continental borderland: a technical report: Rept. No. USC Geol. 70-7, Ocean Science and Technology Division, Office of Naval Research, Washington, D.C., 208 p.
- Gingerich, P.D., 1969, Markov analysis of cyclic alluvial sediments: Jour. Sed. Petrol., V. 39, p. 330-332.
- Gonzalez-Bonorino, G. and Middleton, G.V., 1976, A Devonian submarine fan in western Argentina: Jour. Sed. Petrol., V.46, p. 56-69.
- Gorler, K. and Reutter, K.J., 1968, Entstehung und Merkmale der Olistostrome: Geol. Rund., V. 57, p. 484-514.
- Griggs, G.B. and Kulm, L.D., 1970, Sedimentation in Cascadia deep sea channel: Geol. Soc. Amer. Bull., V.81, p. 1361-1384.
- , Waters, A.C. and Fowler, G.A., 1970, Deep sea gravels from Cascadia Channel: Jour. Geol., V. 78, p. 611-619.
- Guy, H.P., Simons, D.B. and Richardson, E.V., 1966, Summary of alluvial channel data from flume experiments, 1956-61: Prof. Pap. U.S. Geol. Surv., V. 462-I, p. 1-96.
- Hampton, M.A., 1972, The role of subaqueous debris flow in generating turbidity currents: Jour. Sed. Petrol., V.42, p. 775-793.
- Hand, B. M., 1961, Grain orientation in turbidites: The Compass of Sigma Gamma Epsilon, V. 38, p. 133-144.

- and Emery, K.O., 1964, Turbidites and topography of north end of San Diego Trough, California: Jour. Geology, V.72, p. 526-542.
- Haner, B.E., 1971, Morphology and sediments of Redondo submarine fan: Geol. Soc. Amer. Bull., V.82, p. 2413-2432.
- Harbaugh, J.W. and Bonham-Carter, G.F., 1970, Computer simulation in geology: John Wiley & Sons, New York, 575 p.
- Harms, J.C., 1974, Brushy Canyon Formation, Texas: a deep-water density current deposit: Geol. Soc. Amer. Bull., V.85, p. 1763-1784.
- and Fahnestock, R.K., 1965, Stratification, bed forms and flow phenomena (with an example from the Rio Grande) in Middleton, G.V., (Ed.), Primary sedimentary structures and their hydrodynamic interpretation: Soc. Econ. Paleont. Mineral. Spec. Pub. 12, p. 84-115.
- , Southard, J.B., Spearing, D.R. and Walker, R.G., 1975, Depositional environments as interpreted from primary sedimentary structures and stratification sequences: Soc. Econ. Paleont. Mineral. Short Course 2 Notes, 161 p.
- Hattori, I., 1976, Entropy in Markov chains and discrimination of cyclic patterns in lithologic successions: Math. Geol., V.8, p.477-497.
- Heezen, B.C. and Drake, C.L., 1964, Grand Banks slump: Geol. Soc. Amer. Bull., V.48, p. 221-225.
- and Ewing, M., 1952, Turbidity currents and submarine slumps, and the 1929 Grand Banks earthquake: Amer. Jour. Sci., V.250, p.849-873.
- Heim, A., 1932, Bergsturz und Menschenleben: Fritz & Wasmuth Verlag, Zurich, 218 p.
- Helwig, J. and Sarpi, E., 1969, Plutonic pebble conglomerates, New World Island, and history of eugeosynclines in Kay, M. (Ed.), North Atlantic -- geology and continental drift: Amer. Assoc. Petrol. Geol. Mem. 12, p. 443-466.
- Hendry, H.E., 1972, Breccias deposited by mass flow in the Breccia Nappe of the French pre-Alps: Sedimentology, V.18, p.277-292.
- , 1973, Sedimentation of deep-water conglomerates in Lower Ordovician rocks of Quebec -- composite bedding produced by progressive liquefaction of sediment?: Jour. Sed. Petrol., V.43, p. 125-136.
- , 1976, The orientation of discoidal clasts in resedimented conglomerates, Cambro-Ordovician, Gaspé, Eastern Québec: Jour. Sed. Petrol. V.46, p. 48-55.
- , 1978, Cap des Rosiers Formation at Grosses Roches, Québec -- deposits of the mid-fan region on an Ordovician submarine fan: Canadian Jour. Earth Sci., V.15, p. 1472-1488.

- Hesse, R., 1975, Turbiditic and non-turbiditic mudstone of Cretaceous flysch sections of the eastern Alps and other basins: *Sedimentology*, V. 22, p. 387-416.
- Heward, A.P., 1978, Alluvial fan and lacustrine sediments from the Stephanian A and B (La Magdalena, Cínera -- Matallana and Sabero) coal fields, northern Spain: *Sedimentology*, V. 25, p. 451-488.
- Hiscott, R.N., 1977, Sedimentology and regional implications of deep-water sandstones of the Tourelle Formation, Ordovician, Québec: Ph.D. Thesis, McMaster University, 542-p.
- Howell, D.G. and McLean, H., 1976, Middle Miocene Paleogeography, Santa Cruz and Santa Rosa Islands, in Howell, D.G. (Ed.), Aspects of the geologic history of the California continental borderland: *Amer. Assoc. Petrol. Geol. Pacific Section, Misc. Pub. 24*, p. 266-293.
- Hsü, K.J., 1975, Catastrophic debris streams (sturzstroms) generated by rockfalls: *Geol. Soc. Amer. Bull.*, V.86, p. 129-140.
- Hubert, C., 1965, Stratigraphy of the Quebec Complex in the L'Islet - Kamouraska area, Quebec: Ph.D. Thesis, McGill Univ., Montreal, 192p.
- , 1973, Région de Kamouraska: La Pocatière - Saint Jean Port Joli area: *Rap. Geol. 151*, Min. des Richesses Naturelles, Québec.
- Lajoie, J. and Léonard, M.A., 1970, Deep sea sediments in the Lower Paleozoic Quebec Supergroup, in Lajoie, J. (Ed.), Flysch sedimentology in North America, *Geol. Assoc. Canada Sp. Paper 7*, p. 103-125.
- Hubert, J.F., 1966, Sedimentary history of Upper Ordovician geosynclinal rocks, Girvan, Scotland: *Jour. Sed. Petrol.*, V. 36, p. 677-699.
- , Suchecki, R.K., Callahan, R.K.M., 1977, The Cow Head Breccia: sedimentology of the Cambro-Ordovician continental margin, Newfoundland: *Soc. Econ. Paleont. Mineral. Spec. Pub. 25*, p. 125-154.
- Irving, E., 1964, Paleomagnetism and its application to geological and geophysical problems: New York, Wiley Interscience, 399 p.
- Jeffrey, G.B., 1922, The motion of ellipsoidal particles immersed in a viscous fluid: *Proc. Roy. Soc. London, Ser. A*, V.102, p. 161-179.
- Johansson, C.E., 1963, Orientation of pebbles in running water. A laboratory study: *Geog. Annaler*, V.XLV (2-3), p. 85-112.
- , 1965, Structural studies of sedimentary deposits: *Geol. Foren. Stockholm Förh.*, V. 87, p. 3-61.
- , 1976, Structural studies of frictional sediments: *Geog. Annaler*, V. 58, p. 201-301.

- Johnson, A.M., 1970, Physical processes in geology: Freeman, Cooper & Co., San Francisco, 577 p.
- Johnson, B.A., 1974, Deep sea fan-valley conglomerate: Cap Enragé Formation, Gaspé, Québec: M.Sc. Thesis, McMaster Univ., Hamilton, 108 p.
- and Walker, R.G., in prep., Paleocurrents and depositional environments of conglomerates in the Cambro-Ordovician Cap Enragé Formation, Québec Appalachians.
- Jopling, A.V., 1965, Laboratory study of the distribution of grain sizes in cross-bedded deposits, in Middleton, G.V. (Ed.), Primary sedimentary structures and their hydrodynamic interpretation: Soc. Econ. Paleont. Mineral. Spec. Pub. 12, p. 53-65.
- Keith, B.D. and Friedman, G.M., 1977, A slope-fan-basin-plain model, Taconic Sequence, New York and Vermont: Jour. Sed. Petrol., V.47, p. 1220-1241.
- Kelling, G. and Williams, P.F., 1967, Flume studies on the reorientation of pebbles and shells: Jour. Geology, V. 75, p. 243-267.
- Kennedy, M.J., 1973, The relationship between pre-Ordovician polyphase deformation and ophiolite obduction in the Newfoundland Appalachian system: Geol. Soc. Amer. N.E. Section 8th Annual Mtg. Abstracts.
- Khan, M.A., 1962, The anisotropy of magnetic susceptibility of some igneous and metamorphic rocks: Jour. Geophys. Res., V.67, p.2873-2885.
- Komar, P.D., 1970, The competence of turbidity current flow: Geol. Soc. Amer. Bull., V. 81, p. 1555-1562.
- , 1977, Computer simulation of turbidity current flow and the study of deep-sea channel and fan sedimentation, in Goldberg, E.D. (Ed.), The sea: ideas and observations on progress in the study of the seas, John Wiley & Sons, New York, p. 603-621.
- Koster, E.H., 1977, A flume study of fluvial gravel fabric: 1st Int. Sym. Fluvial Sedimentology, Calgary, Canada Abstracts, p. 17.
- Krause, F.F. and Oldershaw, A.E., 1968, Continental slope-rise deposits from Lower Cambrian Sekwi Formation, Mackenzie Mountains, Northwest Territories, Canada: Amer. Assoc. Petrol. Geol.-Soc. Econ. Paleont. Mineral. Annual Mtg., Oklahoma City, Abstracts, p. 83.
- Kruit, C., Brouwer, J., Knox, G., Schollnberger, W. and van Vliet, A., 1975, Une excursion aux cones d'alluvions en eau profonde d'âge tertiaire pres de San Sebastian. Guide Excursion Z-23, IX Int. Sediment. Congress, Nice.

- Ksiazkiewicz, M., 1952, Graded and laminated bedding in the Carpathian flysch: *Ann. Soc. Geol. Pologne*, V.22, p. 399-449.
- Kuenen, Ph. H., 1937, Experiments in connection with Daly's hypothesis on the formation of submarine canyons: *Leid. Geol. Meded.*, V. 7, p. 327-351.
- , 1958, Experiments in geology: *Trans. Geol. Soc. Glasgow*, V.23, p. 1-28.
- , 1964, Deep-sea sands and ancient turbidites, in Bouma, A.H. and Brouwer (Eds.), *Turbidites -- Developments in sedimentology*, 3: Elsevier Publ. Co., Amsterdam, p. 3-33.
- and Carozzi, A., 1953, Turbidity currents and sliding in geosynclinal basins in the Alps: *Jour. Geology*, V. 61, p. 363-373.
- Lajoie, J., in press, Region de Rimouski: *Rapp. Geol., Min. des Richesses Naturelles*, Québec.
- , Héroux, Y. and Mathey, B., 1974, The Precambrian Shield and the Lower Paleozoic shelf: the unstable provenance of the Lower Paleozoic flysch sandstones and conglomerates of the Appalachians between Beaumont and Bic, Québec: *Canadian Jour. Earth Sci.*, V. 11, p. 951-963.
- Léonard, M.A., 1969, Le flysch de St. Fabien: M.Sc. Thesis, Univ. de Montréal, Montréal, 80 p.
- Lindsay, J.F., 1966, Carboniferous subaqueous mass-movement in the Manning-Macleay Basin, Kempsey, New South Wales: *Jour. Sed. Petrol.*, V. 36, p. 719-732.
- , 1968, The development of clast fabric in mudflows: *Jour. Sed. Petrol.*, V. 38, p. 1242-1253.
- Lowe, D.R., 1975, Water escape structures in coarse-grained sediments: *Sedimentology*, V.22, p. 157-204.
- , in prep., Gravity flow classification and nomenclature.
- and LoPiccolo, R.D., 1974, The characteristics and origins of dish and pillar structures: *Jour. Sed. Petrol.*, V.44, p. 484-501.
- Malouta, D.N., 1978, Holocene sedimentation in Santa Monica Basin, California: M.Sc. Thesis, Univ. Southern California, Los Angeles, 146p.
- Marshalko, R., 1964, Sedimentary structures and paleocurrents in marginal lithofacies of the central Carpathian flysch, in Bouma, A.H. and Brouwer, A. (Eds.), *Turbidites*, Elsevier Publ. Co., Amsterdam, p. 106-126.



- Mathey, B., 1970, Etude sédimentologique du flysch de la région de Saint-Simon de Rimouski: M.Sc. Thesis, Univ. de Montréal, Montréal, 133 p.
- McBride, E.F., 1962, Flysch and associated beds of the Martinsburg Formation (Ordovician), central Appalachians: Jour. Sed. Petrol., V. 32, p. 39-91.
- and Kimberly, J.E., 1963, Sedimentology of Smithwick Shale (Pennsylvanian), eastern Llano region, Texas: Amer. Assoc. Petrol. Geol. Bull., V. 10, p. 1840-1854.
- McHargue, T.R., Webb, J.E. and Kessler, L.G., 1978, Ancient submarine canyon and channel morphology, Indus Cone, offshore Pakistan: Amer. Assoc. Petrol. Geol. - Soc. Econ. Paleont. Mineral. Annual Mtg., Oklahoma City, Abstracts, p. 93.
- Miall, A.D., 1973, Markov chain analysis applied to an ancient alluvial plain succession: Sedimentology, V. 20, p. 347-364.
- Middleton, G.V., 1966, Experiments on density and turbidity currents: I. Motion of the head: Canadian Jour. Earth Sci., V.3, p.523-546.
- , 1967, Experiments on density and turbidity currents: III. Deposition of sediment: Canadian Jour. Earth Sci., V. 4, p. 475-504.
- , 1970, Experimental studies related to problems of flysch sedimentation, in Lajoie, J. (Ed.), Flysch sedimentology in North America: Geol. Assoc. Canada Spec. Pub. 7, p. 253-272.
- , 1976, Hydraulic interpretation of sand size distributions: Jour. Geology, V. 84, p. 405-426.
- , 1978, Coarse sediments deposited at base of continental slope by sediment-gravity flows (examples from Northern Appalachians): Amer. Assoc. Petrol. Geol. - Soc. Econ. Paleont. Mineral. Annual Mtg., Oklahoma City, Abstracts, p. 94-95.
- and Hampton, M.A., 1973, Sediment gravity flows: mechanisms of flow and deposition, in Middleton, G.V. and Bouma, A.H. (Eds.), Turbidites and deep-water sedimentation: Pacific Coast Section, Soc. Econ. Paleont. Mineral., Short Course Notes, Anaheim, p. 1-38.
- , 1976, Subaqueous sediment transport and deposition by sediment gravity flows, in Stanley, D.J. and Swift, D.J.P., (Eds.), Marine sediment transport and environmental management: Wiley Interscience, New York, p. 197-218.
- and Southard, J.B., 1977, Mechanics of sediment movement: Eastern section Soc. Econ. Paleont. Mineral. Short Course Notes, Binghamton, p.

- Miyamura, M., 1965, The Paleozoic Formation in the Yokoyama District, Gifu Prefecture, central Japan: Jour. Geol. Soc. Japan, V.71 (1), p. 5-17.
- Moore, D.G., 1961, Submarine slumps: Jour. Sed. Petrol., V. 31, p. 343-357.
- Morgenstern, N.R., 1967, Submarine slumping and the initiation of turbidity currents, in Richards, A.F. (Ed.), Marine Geotechnique, p.189-220.
- Mutti, E., 1969, Sedimentologia delle Arenarie di Messanagros (Oligocene-Aquitano) nell'isola di Rodi: Italiana Mem. Geol. Soc., V. 8, p. 1027-1070.
- and Ghibaudo, G., 1972, Un esempio di torbiditi di conoide sottomarina esterna: le Arenarie di San Salvatore (Formazione di Bobbio, Miocene) nell' Appennino di Piacenza: Mem. Acc. Sci. Torino, Classe Sci. Fis., Nat., Ser. 4, n. 16, 40 p.
- and Ricci Lucchi, F., 1972, Le torbiditi del "Appennino settentrionale:" introduzione all'analisi di facies: Soc. Geol. Italiana Mem., V.11, p. 161-199; translated by Nielson, T.H. and published in English in Int. Geology Rev., V. 20 (2), p. 125-166 under the title: "Turbidites of the Northern Appennines: introduction to facies analysis."
- Nederlof, M.H. and Weber, K.J., 1971, A three dimensional vector method as an aid to continuous-dipmeter interpretation: Geol. Mijnbouw, V. 50, p. 725-732.
- Nelson, C.H., Carlson, P.R., Byrne, J.V. and Alpha, T.R., 1970, Development of the Astoria Canyon-Fan: Physiography and comparison with similar systems: Marine Geology, V. 8, p. 259-291.
- Nielson, T.H. and Simony, T.R., 1973, Deep-sea fan paleocurrent patterns of the Eocene Butano Sandstone, Santa Cruz Mountains, California: U.S. Geol. Survey Jour. Research., V.1, p. 439-452.
- Normark, W.R., 1974, Submarine canyons and fan valleys: factors affecting growth patterns of deep-sea fans, in Dott, R.H., Jr. and Shaver, R.H. (Eds.), Modern and ancient geosynclinal sedimentation: Soc. Econ. Paleont. Mineral. Spec. Pub. 19, p. 56-68.
- , 1978, Fan valleys, channels and depositional lobes on modern submarine fans: characters for recognition of sandy turbidite environments: Amer. Assoc. Petrol. Geol. Bull., V.62, p. 912-931.
- , Piper, D.J.W. and Hess, G.R., in prep., Distributary channels, sand lobes, and mesotopography of Navy submarine fan with applications to ancient fan sediments.

- Onions, D. and Middleton, G.V., 1968, Dimensional grain orientation of Ordovician turbidite greywackes: *Jour. Sed. Petrol.*, V.38, p.164-174.
- Osborne, F.F., 1956, Geology near Québec City: *Nat. Can.*, V.83, p. 157-223.
- Parkash, B., 1970, Downcurrent changes in sedimentary structures in Ordovician turbidite greywackes: *Jour. Sed. Petrol.*, V.40, p. 572-590.
- Parkash, B. and Middleton, G.V., 1970, Downcurrent textural changes in Ordovician turbidite greywackes: *Sedimentology*, V.14, p. 259-293.
- Passaga, R., 1957, Texture as characteristic of clastic deposition: *Amer. Assoc. Petrol. Geol. Bull.*, V. 41, p. 1952-1984.
- , 1964, Grain size representation by CM patterns as a geological tool: *Jour. Sed. Petrol.*, V.34, p. 830-847.
- Piper, D.J.W., 1970, A Silurian deep sea fan deposit in western Ireland and its bearing on the nature of turbidity currents: *Jour. Geology*, V. 78, p. 509-522.
- , Panagos, A.G. and Pe, G.G., 1978, Conglomeratic Miocene flysch, western Greece: *Jour. Sed. Petrol.*, V. 48, p. 117-126.
- Poole, W.H., 1976, Plate tectonic evolution of the Canadian Appalachian region: *Geol. Survey Canada Paper*, 76-1B, p. 113-126.
- Rasetti, F., 1948a, Lower Cambrian trilobites from the conglomerates of Quebec (exclusive of the Ptychopariidea): *Jour. Paleont.*, V.22, p. 1-24.
- , 1948b, Middle Cambrian trilobites from the conglomerates of Quebec (exclusive of the Ptychopariidea): *Jour. Paleont.*, V.22, p.315-339.
- Rees, A.I., 1968, The production of a preferred orientation in a concentrated dispersion of elongated and flattened grains: *Jour. Geology*, V. 76, p. 457-465.
- Ricci Lucchi, F., 1969, Composizione e morfometria di un conglomerato resedimentato nel flysch miocenico romagnolo (Fontanelice, Bologna): *Gior. Geologica*, V. 35, p. 1-47.
- , 1975, Depositional cycles in two turbidite formations of northern Appennines (Italy): *Jour. Sed. Petrol.*, V. 45, p. 3-43.
- Rocheleau, M. and Lajoie, J., 1974, Sedimentary structures in resedimented conglomerate of the Cambrian flysch, L'Islet, Québec Appalachians: *Jour. Sed. Petrol.*, V.44, p. 826-836.
- Ruitenberg, A.A., Fyffe, L.R., McOutcheon, S.R., St. Peter, C.J., Irrinki, R.R. and Venugopal, D.V., 1977, Evolution of pre-Carboniferous tectonostratigraphic zones in the New Brunswick Appalachians: *Geosci-*

- ence Canada, p. 171-181.
- Rukavina, N.A., 1965, Particle orientation in turbidites: theory and experiment: Ph.D. Thesis, Univ. of Rochester, New York.
- Rusnak, G.A., 1957, The orientation of sand grains under condition of "unidirectional" fluid flow. I. Theory and experiment: Jour. Geology, V. 65, p. 384-409.
- Rust, B.R., 1966, Late Cretaceous paleogeography near Wheeler Gorge, Ventura County, California: Amer. Assoc. Petrol. Geol. Bull., V. 50, p. 1389-1398.
- Sadler, P.M., in prep., On the significance of bed-thickness in turbidites.
- Scholl, D.W., Buffington, E.C., Hopkins, D.M. and Alpha, T.R., 1970, The structure and origin of the large submarine canyons of the Bearing Sea: Marine Geology, V. 8, p. 187-210.
- Schwarzacher, W., 1951, Grain orientation in sands and sandstones: Jour. Sed. Petrol., V. 21, p. 162-172.
- Scott, K.M., 1966, Sedimentology and dispersal pattern of a Cretaceous flysch sequence, Patagonian Andes, southern Chile: Amer. Assoc. Petrol. Geol. Bull., V. 52, p. 72-107.
- Sestini, G. and Pranzini, G., 1965, Correlation of sedimentary fabric and sole marks as current indicators in turbidites: Jour. Sed. Petrol., V. 35, p. 100-108.
- Shepard, F.P., 1978, Currents in submarine canyons and other types of slope valleys: Amer. Assoc. Petrol. Geol.- Soc. Econ. Paleont. Mineral., Annual Mtg., Oklahoma City, Abstracts, p. 112.
- and Dill, R.F., 1966, Submarine canyons and other sea valleys: Rand McNally, Chicago, 381 p.
- and Emery, K.O., 1973, Congo submarine canyon and fan valley: Amer. Assoc. Petrol. Geol. Bull., V. 57, p. 1679-1691.
- Sheridan, M.F. and Updike, R.G., 1975, Sugarloaf Mountain tephra -- a Pleistocene rhyolitic deposit of base-surge origin in northern Arizona: Geol. Soc. Amer. Bull., V. 86, p. 571-581.
- Simons, D.B., Richardson, E.V., and Nordin, C.F., 1965, Sedimentary structures generated by flow in alluvial channels, in Middleton, G.V. (Ed.), Primary sedimentary structures and their hydrodynamic interpretations: Soc. Econ. Paleont. Mineral. Spec. Pub. 12, p. 34-52.

- Simpson, F., 1970, Sedimentation of the middle Eocene of the Magura series, Polish Western Carpathians: Roczn. Pol. Tow. Geol., V. 40 (2), p. 209-286.
- Skipper, K. and Middleton, G.V., 1975, The sedimentary structures and depositional mechanics of certain Ordovician turbidites: Cloridorme Formation, Gaspé Peninsula, Québec: Canadian Jour. Earth Sci., V. 12, p. 1934-1952.
- Smoor, P.B., 1960, Dimensional grain orientation studies in turbidite greywackes: M.Sc. Thesis, McMaster Univ., Hamilton, 97 p.
- Southard, J.B., 1971, Representation of bed configurations in depth-velocity-size diagrams: Jour. Sed. Petrol., V.41, p. 903-915.
- Srivistana, P., Stern, C.W. and Mountjoy, E.W., 1972, A Devonian megabreccia at the margin of the Ancient Wall carbonate complex, Alberta: Canadian Petrol. Geol. Bull., V.20, p. 412-438.
- Stanley, D.J., 1963, Vertical petrographic variability in Annot sandstone turbidites: some preliminary observations and generalizations: Jour. Sed. Petrol., V.33, p. 783-788.
- St. Julien, P. and Hubert, C., 1975, Evolution of the Taconian orogen in the Quebec Appalachians: Amer. Jour. Sci., V.275-A, p.337-362.
- Stow, D.A.V., 1977, Late Quaternary stratigraphy and sedimentation on the Nova Scotian outer continental margin: Ph.D. Thesis, Dalhousie Univ., Halifax, 360 p.
- Strong, P.G., 1978, The sedimentology and depositional history of the St. Roch Formation near St. Jean-Port-Joli, Quebec: M.Sc. Thesis, McMaster University, Hamilton, 128 p.
- Taira, A., 1976, Settling velocity distributions, magnetic fabrics and sedimentary structures of the Pliocene Pico Formation, Ventura Basin, California: Implications for the depositional processes of turbidites and associated deposits: Ph.D. Thesis, Univ. Texas at Dallas, Dallas, p. 310-365.
- Taylor, G.I., 1923, The motion of ellipsoidal particles in viscous fluid: Proc. Royal Soc. London, Ser. A, V. 103, p. 58-61.
- Thompson, A.F. and Thomasson, M.R., 1969, Shallow to deep water facies development in the Dimple Limestone (Lower Pennsylvanian), Marathon region, Texas, in Friedman, G.M. (Ed.), Depositional environments in carbonate rocks: Soc. Econ. Paleont. Mineral. Spec. Pub. 14, p. 57-78.
- Unrug, R., 1963, Istebna beds -- a fluxoturbidite formation in the Carpathian flysch: Roczn. Pol. Tow. Geol., V.33, p. 49-92.

- Vallières, A., in prep., Unified nomenclature for stratigraphy of Cambro-Ordovician rocks between Québec and the Metapedia region.
- van Andel, T.H. and Komar, P.D., 1969, Ponded sediments of the mid-Atlantic ridge between 22° and 23° north latitude: Geol. Soc. Amer. Bull., V. 80, p. 1163-1190.
- Van der Kamp, P.C., Harper, J.D., Conniff, J.J. and Morris, D.A., 1974, Facies relations in the Eocene-Oligocene in the Santa Ynez Mountains, California: Jour. Geol. Soc. California, V.130, p.545-565.
- Vistelius, A.B. and Faas, A.V., 1965, Variation in thickness of strata in the south Ural Paleozoic flysch section: Doklady Akad. Nauk. SSR, V. 164, p. 77-79.
- and Feygel'son, T.S., 1965, Theory of formation of sedimentary beds: Doklady Akad. Nauk. SSR, V. 164, p. 158-160.
- Walker, R.G., 1973, Mopping up the turbidite mess, in Ginsburg, R.N. (Ed.), Evolving concepts in sedimentology: Baltimore, Johns Hopkins Press, p. 1-37.
- , 1975a, Generalized facies models for resedimented conglomerates of turbidite association: Geol. Soc. Amer. Bull., V.86, p.737-748.
- , 1975b, Conglomerate: Sedimentary structures and facies models, in Harms, J.C., Southard, J.B., Spearing, D.R. and Walker, R.G., Depositional environments as interpreted from primary sedimentary structures and stratification sequences: Soc. Econ. Paleont. Mineral. Short Course 2, p. 133-161.
- , 1975c, Upper Cretaceous resedimented conglomerates at Wheeler Gorge, California: description and field guide: Jour. Sed. Petrol., V. 45, p. 105-112.
- , 1976, Facies models. 2, turbidites and associated coarse clastic deposits: Geoscience Canada, V. 3, p. 25-36.
- , 1977, Deposition of upper Mesozoic resedimented conglomerates and associated turbidites in southwestern Oregon: Geol. Soc. Amer. Bull., V. 88, p. 273-285.
- , 1978, Deep-water sandstone facies and ancient submarine fans: models for exploration for stratigraphic traps: Amer. Assoc. Petrol. Geol. Bull., V. 62, p. 932-966.
- Williams, G.P., 1967, Flume experiments on the transport of a coarse sand: U.S. Geol. Survey Prof. Pap. 562-B, p. 1-31.
- Winn, R.D., Jr. and Dott, R.H., Jr., 1977, Large-scale traction-produced structures in deep-water fan-channel conglomerates in southern Chile: Geology, V. 5, p. 41-44.

LIST OF SYMBOLS AND ABBREVIATIONS (continued)

| <u>Symbol</u>  | <u>Description</u>                                              | <u>Dimensions</u>               |
|----------------|-----------------------------------------------------------------|---------------------------------|
| $R_e$          | Reynold's number = $(U d_s \rho_f) / \mu$                       | —                               |
| $R_x$          | E-W component of vectorial sum                                  | —                               |
| $R_y$          | N-S component of vectorial sum                                  | —                               |
| $R_z$          | vertical component of vectorial sum                             | —                               |
| $R_{xy}$       | horizontal component of vectorial sum                           | —                               |
| $U$            | velocity of the grain relative to the fluid                     | L/T                             |
| $\bar{U}$      | average velocity of the flow                                    | L/T                             |
| $U_*$          | shear velocity                                                  | L/T                             |
| $U_{*c}$       | critical shear velocity using Shield's criterion                | L/T                             |
| $\bar{V}$      | average velocity of the head of a density current               | L/T                             |
| $\beta$        | Shield's parameter = $\frac{\tau_o}{(\gamma_s - \gamma_f) d_s}$ | —                               |
| $\delta_{xyz}$ | three-dimensional mean dip angle = $\arctan (R_{xy} / R_z)$     | —                               |
| $\rho_f$       | fluid density of sediment-gravity flow                          | M/L <sup>3</sup>                |
| $\rho_s$       | sediment density                                                | M/L <sup>3</sup>                |
| $\Delta \rho$  | density difference between flow density and sea water           | M/L <sup>3</sup>                |
| $\gamma_f$     | specific weight of fluid = $\rho_f g$                           | M/L <sup>2</sup> T <sup>2</sup> |
| $\gamma_s$     | specific weight of sediment = $\rho_s g$                        | M/L <sup>2</sup> T <sup>2</sup> |
| $\mu$          | viscosity of the fluid                                          | M/LT                            |
| $\phi$         | phi units = $-\log_2 (d_s \text{ in mm})$                       | —                               |
| $\omega$       | settling velocity of a grain                                    | L/T                             |

## APPENDIX 1

LIST OF SYMBOLS AND ABBREVIATIONS

| <u>Symbol</u> | <u>Description</u>                                                                                                              | <u>Dimensions</u> |
|---------------|---------------------------------------------------------------------------------------------------------------------------------|-------------------|
| a-axis        | apparent long-axis of clasts or grains                                                                                          | L                 |
| ab plane      | plane defined by the apparent long- (a) and intermediate (b) axes of clasts                                                     | —                 |
| c             | cophenetic correlation coefficient, used in substitutability analyses                                                           | —                 |
| C             | constant number                                                                                                                 | —                 |
| $d_1$         | height of turbidity current head                                                                                                | L                 |
| $d_s$         | grain size of sediment                                                                                                          | L                 |
| f             | friction factor                                                                                                                 | —                 |
| fn            | " function of "                                                                                                                 | —                 |
| Fr            | Froude number = $U / (gL)^{1/2}$                                                                                                | —                 |
| g             | acceleration due to gravity                                                                                                     | $L/T^2$           |
| K             | precision constant of a spherical distribution                                                                                  | —                 |
| $\hat{K}$     | estimate of the precision constant K,<br>= $(N-1) / (N-R_{xyz})$                                                                | —                 |
| L             | characteristic length                                                                                                           | L                 |
| LZ            | magnitude of vector mean in terms of percent = $\frac{\{(\sum n \sin \theta)^2 + (\sum n \cos \theta)^2\}^{1/2}}{\sum n} * 100$ | —                 |
| Mz            | graphic mean of grain size cumulative frequency curve in phi units = $(\phi 16 + \phi 50 + \phi 84) / 3$                        | —                 |
| N             | " number of "                                                                                                                   | —                 |
| N Beds        | number of beds                                                                                                                  | —                 |
| P             | pressure, normal force per unit area of surface                                                                                 | $M/LT^2$          |
| r             | correlation coefficient                                                                                                         | —                 |



LIST OF SYMBOLS AND ABBREVIATIONS (continued)

| <u>Symbol</u>    | <u>Description</u>                                                                                                                                                                   | <u>Dimensions</u> |
|------------------|--------------------------------------------------------------------------------------------------------------------------------------------------------------------------------------|-------------------|
| $\tau$           | shear stress, tangential force per unit area of surface                                                                                                                              | M/LT <sup>2</sup> |
| $\tau_0$         | boundary shear stress                                                                                                                                                                | M/LT <sup>2</sup> |
| $\tau_c$         | critical or threshold boundary shear stress                                                                                                                                          | M/LT <sup>2</sup> |
| $\bar{\theta}$   | vector sum azimuth. In three-dimensions $R_{xyz} = (R_x^2 + R_y^2 + R_z^2)^{1/2}$ ; In two dimensions = $\arctan (\sum n \sin \theta) / (\sum n \cos \theta)$                        | —                 |
| $\hat{\theta}$   | estimate of the semi-angle of confidence cone of the 3-D vector mean at probability level (1-P) = $\arccos \left\{ \frac{N}{R_{xyz}} - (N - R_{xyz}) / (R_{xyz} P^{1/N-1}) \right\}$ | —                 |
| $\hat{\theta}_d$ | estimate of the semi-angle of confidence of the azimuth of the 3-D vector mean = $\arccos \left\{ (\cos^2 \hat{\theta} - \cos^2 \delta_{xyz}) / \sin \delta_{xyz} \right\}$          | —                 |

## APPENDIX 2

METHODS1. Field Methods

Field work consisted of detailed descriptions of outcrop sections. Outcrops were selected for description if there was sufficient vertical exposure, generally greater than 5 m in height. Emphasis was placed upon the sandy and pebbly sandstone outcrops within the Cap Enragé Formation. A few selected, mainly conglomeratic, sections were measured to depict sandstone associations within major conglomeratic units. These selected outcrops were measured at Anse à Pierre Jean 2, Anse à Pierre Jean 3, St. Simon sur Mer and Bic, where there is good paleoflow data for the conglomerates (Davies, 1972; Johnson, 1974).

Preliminary examination of individual sections involved picking out major units. After the general description, the section was measured in detail. Beds were distinguished by erosional or load contact features, or abrupt changes in grain size. Beds which had flat bases were solely defined by abrupt, non-gradational, grain size changes. Sedimentary structures were described. Grain size measurements were made in bed portions where there appeared to be a grain size change, as seen in the field. In pebbly or conglomeratic beds (grain diameter greater than 4 mm), measurements of the apparent long-axis (a-axis) of the 10 largest clasts were made. In beds with grain diameters  $\leq$  4 mm the grain size was made by an estimate of the average size of the grains, as seen in the field with a ruler and hand lens.

For material larger than 4 mm in diameter, the classification of Davies (1972, p. 18) was used to distinguish fine-pebble and coarse conglomerate. For material  $\leq$  4 mm in diameter, the Udden-Wentworth scheme was used for lithologic subdivisions (Blatt et al, 1972). Lithologies are listed in Table 14.

Paleocurrent measurements were obtained from beds that displayed flutes, grooves, longitudinal ridges and cross-stratification. Tractional current features, such as crossbedding, are relatively uncommon within the Esp Enragé sediments, although locally within individual outcrops they may be very abundant.

In the sections that had interbedded sandstones and conglomerates, preferred fabric was measured in some of the conglomerate interbeds. Fabric measurements were only made in those beds which did not appear to be tectonized and in which the preferred fabric was thought to represent the true original sedimentary fabric. Only elongate, flattish pebbles (a-axis: b-axis length ratio  $\geq$  1.5) which had a apparent a-axis  $\geq$  1 cm were measured. All of the conglomerate fabric data was measured directly in the field, not from photographs as was done by Davies and Walker (1974) and by Johnson (1974). Because of the relative absence of suitable clasts, neither a grid pattern nor random transverse lines were used in sampling. Rather, all pebbles that fit the above criterion were measured. The clasts, in addition to fulfilling the elongation and size requirements, had to "weather out" from the rock such that a notebook could be placed, by eye, in a direction parallel to the apparent a-b plane of the pebble. Strike and dip were read off the notebook. Regional strike and dip of the bed, in which the fabric was measured, was taken.

Table 14

LITHOLOGIC SUBDIVISIONS BASED UPON FIELD MEASUREMENTS OF GRAIN SIZE

| <u>Lithology</u>       | <u>Grain Size</u> |
|------------------------|-------------------|
| Coarse Conglomerate    | a-axis > 16mm     |
| Fine Conglomerate      | a-axis > 4-16mm   |
| Pebbly Sandstones      | > 2-4 mm          |
| Very Coarse Sandstones | > 1-2 mm          |
| Coarse Sandstones      | > 0.5-1 mm        |
| Medium Sandstones      | > 0.25 - 0.5 mm   |
| Fine Sandstones        | > 0.125 - 0.25 mm |

Table 15

OPERATOR CHECK ON CONGLOMERATE FABRIC MEASUREMENTS \*

| <u>Plot</u> | <u>Operator</u> | <u>3-D Az</u> | <u>3-D Dip</u> | <u><math>\hat{K}</math></u> | <u><math>\hat{\theta}</math></u> | <u><math>\hat{\theta}_\alpha</math></u> | <u>Facies</u> |
|-------------|-----------------|---------------|----------------|-----------------------------|----------------------------------|-----------------------------------------|---------------|
| 1181C       | Author (1)      | 001.9         | 30.2           | 2.71                        | 80                               | 59.85                                   | 1             |
| 1181B       | Field Ass't     | 017.6         | 12.8           | 2.95                        | 75                               | 77.32                                   | 1             |
| Missing     | Author (2)      | 000.6         | 28.5           | 2.70                        | 80                               | 71.95                                   | 1             |
| 1135        | Author (1)      | 004.0         | 15.1           | 5.03                        | 52                               | 75.00                                   | 2             |
| 1135A       | Author (2)      | 360.0         | 9.3            | 8.83                        | 41                               | 80.72                                   | 2             |
| Missing     | Field Ass't     | 008.3         | 13.8           | 6.04                        | 47                               | 72.60                                   | 2             |

- \* Key: Author (1) and (2), repeated measurements by the author.  
 3-D Az: three dimensional vector mean azimuth  
 $\hat{K}$ : estimate of the precision constant K  
 $\hat{\theta}$ : estimate of the semi-angle of the confidence cone of the 3-dimensional vector mean  
 $\hat{\theta}_\alpha$ : estimate of the semi-angle of the confidence cone of the three-dimensional vector mean azimuth

The position of a bed was randomly selected for fabric analysis. Once the first, randomly-selected clast was measured, all those clasts near the first pebble were measured which fit the criterion for selection. This procedure was repeated until 100 clasts were measured per bed. No grid scheme was used, rather all grains were measured from a randomly-selected point. Consequently, depending upon weathering characteristics, shape and size distributions within individual beds, different sampling areas were covered for different beds. This method was used mainly because of the difficulty in trying to decide on an adequate grid-size to cover beds which may be poorly sorted and have individual clasts ranging in size from 1 cm to  $> 1$  m in length.

During each of the two full field seasons, an independent operator check was made on the conglomeratic fabric measurements. Replicate fabric measurements were made on the same bed by the author and two different field assistants. Duplicate measurements were also made by the author. The first bed was a thin, Facies (2) conglomerate. The second bed was a thick, Facies (1) coarse conglomerate. Results of the fabric measurements are listed in Table 15.

For the Facies (2) bed, replicate measurements by the same operator yield vector means within  $4^{\circ}$  of one another. An independent operator check yielded a vector mean within  $6^{\circ}$  of the average vector mean obtained by the author. For the Facies (1) bed, replicate measurements by the author yield vector means within  $2^{\circ}$  of one another. An independent operator check yielded a vector mean within  $17^{\circ}$  of the vector mean obtained by the author.

These results suggest that the author was consistent in fabric

measurement. The independent operator check for the Facies (2) bed yielded about the same vector mean, suggesting that the method is consistent between workers. The independent operator check for the Facies (1) bed was at a high divergence from the values obtained by the author. This check was done during a different field season than the original measurements by the author, and it is possible that the same interval within the bed was not measured. Although this divergence is high it is not high enough to account for the  $90^{\circ}$ + difference in paleoflows commonly seen between Facies (1) coarse conglomerates and the finer-grained facies at many of the outcrops.

The method used in this study to determine conglomerate fabric differs from the photographic technique used by Davies (1972) and Johnson (1974) in their studies of preferred fabrics within the Facies (1) conglomerates. The photographic technique consisted of measurement of apparent long axes of clasts on oriented photographs taken of bedding surfaces. Vertical cross-sections were studied to confirm that long-axes were oriented parallel to the paleoflow direction, as evidenced from the imbrication direction.

As a check on the correspondence between the photographic method and the method used in this study, strike and dip directions of 100 individual clasts were measured at each of the stations of the Anse à Pierre Jean 1 Niveau 3 outcrop, in which conglomerate fabric was determined photographically by Davies (1972) (see discussion Johnson and Walker, in prep). After the individual clasts were rotated back to the horizontal, using a stereonet, the grand vector mean dip direction yielded a paleoflow direction of  $244^{\circ}$ . The grand vector mean obtained by

Davies and Walker (1974) for this outcrop was 236, indicating a divergence of  $8^{\circ}$  in the grand vector mean calculation using the two methods. This amount of divergence falls within the range obtained by independent operators in the present study for the Facies (2) bed. These results suggest that the grand vector mean calculations for the paleoflow directions are compatible for the two methods.

Differences between the two methods arise in measurements of the standard deviation of individual clasts about the grand vector mean for individual beds. In Davies and Walker's (1974) study, the average standard deviation about the grand vector mean was  $30^{\circ}$  for the coarse conglomerates at Anse à Pierre Jean 1. Johnson (1974) computed an average standard deviation of  $40^{\circ}$  for the coarse conglomerates at other outcrops. By contrast, deviations about the grand vector means for individual coarse conglomerates measured in the present study average  $63^{\circ}$ .

The differences in the estimation of the standard deviation of clast orientations within individual beds is thought to be due to actual "averaging" of long-axis orientations, when one takes a photograph of clasts in bedding planes. The photograph is essentially a projection of the three-dimensional clast orientations onto a two-dimensional surface. Some of the dispersion of the orientation pattern is lost in this projection. It is thought that if one is concerned only with the paleoflow direction (and not a measure of the standard deviation of the orientation pattern) the photographic method is quite adequate. The photographic method is less time-consuming and less tedious to do in the field. In the present study, it usually took 3-3½ hours

to measure the orientations of 100 "ab planes" of individual clasts. The photographic technique is also useful in that the measurements can be done at a later date in the laboratory. However, if one is concerned with the actual deviations of individual clasts about the computed grand vector mean for a bed, one should measure the clasts individually in the field.

Some sandstone beds that lacked paleocurrent indicators were sampled for fabric analyses in the laboratory. Strike and dip directions of individual beds were marked on respective samples before removal from the bed. Only those sandstones that did not appear tectonized were sampled; sandstones were not sampled if they showed cleavage, extensive fracturing and/or veining, minor folding or crenulations, slickensides, or if the sandstones were in a fault zone or located on the nose or hinge zone of a fold. By eliminating these occurrences it was fairly certain that the fabric would not represent obvious tectonic features visible in the field. If a preferred fabric were found in the lab, it would probably represent the original sedimentary fabric.

Some sandstone and pebbly sandstone beds were sampled for grain size analysis in thin section. Strike and dip directions of individual beds were marked on respective samples before removal from the bed. This was done to insure that grain size measurements were done in bedding. All samples were taken near the base of beds. These samples were obtained from beds belonging to a variety of facies, including Facies (2), (3), (4) and (6).



## 2. Laboratory Methods

The pebbly sandstone and sandstone fabric was measured in slab sections cut parallel to the strike-and-dip bedding planes, which were marked on the samples in the field. After slabbing, the cut surfaces were polished and then etched in hydrofluoric acid. Etched surfaces were then stained with methylene blue, which preferentially stained the matrix. This staining procedure made the clasts more apparent. Acetate peels were then made of the stained surfaces. Details of etching and staining procedures are listed below in Table 16.

TABLE 16

ETCHING AND STAINING METHODS  
OF PEBBLY SANDSTONE AND SANDSTONE POLISHED SLAB SECTIONS

Solutions:

Mix equal portions of 18% HF Reagent and distilled water.  
Mix staining solution: 2 g methylene blue/ liter of distilled water.

Method:

In fume hood, put small portion of HF solution in a plastic dish. Cover the top of the dish with the slab to be etched. Let the HF fumes etch the slab for 7 minutes. Rinse the slab in distilled water and dry the slab. Put a small portion of methylene blue solution in a shallow pan. Put the slab in the methylene blue solution, etched side down. Let the slab sit in the stain for 10 - 15 minutes. Rinse the slab initially in tap water, then in distilled water. Dry slab and make acetate peel of the etched and stained surface.

Orientation arrows on the original slab surfaces were transferred to the acetate peels before removal of the peels from the slabs. Enlarged photographs were made from the acetate peels, in which the acetate peels were used as "negatives" of the enlarged prints. This resulted in "reverse prints," where the light quartz and feldspar grains on the peel became dark images on the print. Conversely, the dark stained matrix on the peels became light images on the print. The amount of enlargement depended upon the grain size of the sample. Generally, enlargements were 3-4 x the original peel size. A grid was placed over the enlarged photographs. The orientations of the apparent long-axes of grains were measured on the grid. Only elongate grains (a-axis: b-axis length ratio  $\geq 1.5$ ) which had apparent a-axis  $\geq 1$  mm were measured. Only grains that fell on the grid points were measured.

Grid counting was done on a square grid 2x the largest grains on the enlarged photographs. Large, oversized clasts were not used to determine the grid size. If an oversized grain was encountered on more than one grid point, that grid point was skipped until a new grain was encountered. Grains that were fractured, veined or had vague grain boundaries (possibly due to pressure solution) were not measured. The grid was extended across the enlarged photograph until 100 grains were measured per sample.

For about half of the bedding-plane slab sections in which the preferred fabric was determined, a second imbrication study was done. The grand vector mean of the bedding plane fabric was marked on the original sample for those with unimodal and random bedding fabrics. For samples with bimodal bedding fabrics, the major mode direction was marked.

on the original sample. The second cut was made in a direction parallel to the preferred direction in bedding, but in an orientation perpendicular to the bedding plane. Etching, staining and measurement techniques for the imbrication study were identical to the methods used for the study of bedding fabric.

The methods used in this analysis of sandstone fabric are similar to those used by Hiscott (1977) in his analysis of sandstone fabrics for the Tourelle Formation sediments. The major difference is, in this study, grain orientations were measured on enlarged photographs, rather than on "Shadow-master" projections of the acetate peels (as was done by Hiscott, 1977).

At various times throughout the laboratory phases of the present study, operator checks were made on the sandstone fabric measurements. Duplicate measurements were made on samples that were analyzed during the first month of laboratory work. It took approximately 3-4 months to measure all of the bedding plane (116 samples) and imbrication plane (71 samples) photographs. Operator check measurements were made at approximately equally-spaced intervals during the 3-4 month period. Five samples were reanalyzed to determine the consistency of measurement by the author. One sample was also checked by an independent operator.

Most of the samples used for the operator check showed a fairly well pronounced bimodality. It is impossible to conduct an analysis of variance on bimodal distributions, as the assumption of normality is probably invalid. Operator error is generally insignificant in this sort of study (Onions and Middleton, 1968; Smoor, 1960; Hiscott, 1977). Rose diagrams for the five different samples subject to the operator check

are shown in Fig.1. As illustrated, most of the main peaks are maintained during replicate measurements, although the individual numbers differ. The grid sheets were randomly placed upon the enlarged photographs. Hence, it is not surprising that the distributions do not exactly correspond to one another. The results show that there is a consistency in the delineation of major peak(s) of the distributions.

The conglomerate field fabric data were punched onto computer cards. Structural dip and strike were removed by simple rotation about the strike for each bed. Clast orientations in a horizontal position (with structural tilt removed) were calculated and stereonet plots were made for each conglomerate bed. Three- and two-dimensional summary statistics were computed for each bed. Computing and plotting of stereonets for the conglomerate data was done on the computer and plotter facilities at the Denver Research Center of Marathon Oil Company.

The problem of recognizing modes on rose diagrams is one, which at present, cannot be handled statistically. The following arbitrary criterion was used to distinguish bimodal from unimodal or random patterns. A new mode was recognized if the lower of two adjacent classes was 5+ readings above the higher of two adjacent classes, which comprised the minimum of the distribution (see below). This criterion gave reasonably good agreement with the subjective evaluation of the patterns. For about 3% of the bedding plane rose diagrams the subjective designation disagreed with the criterion; and, for the vertical (imbrication) rose diagrams, about 10% disagreed.

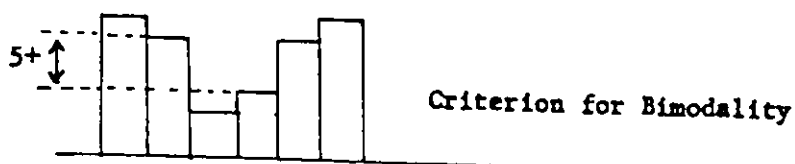
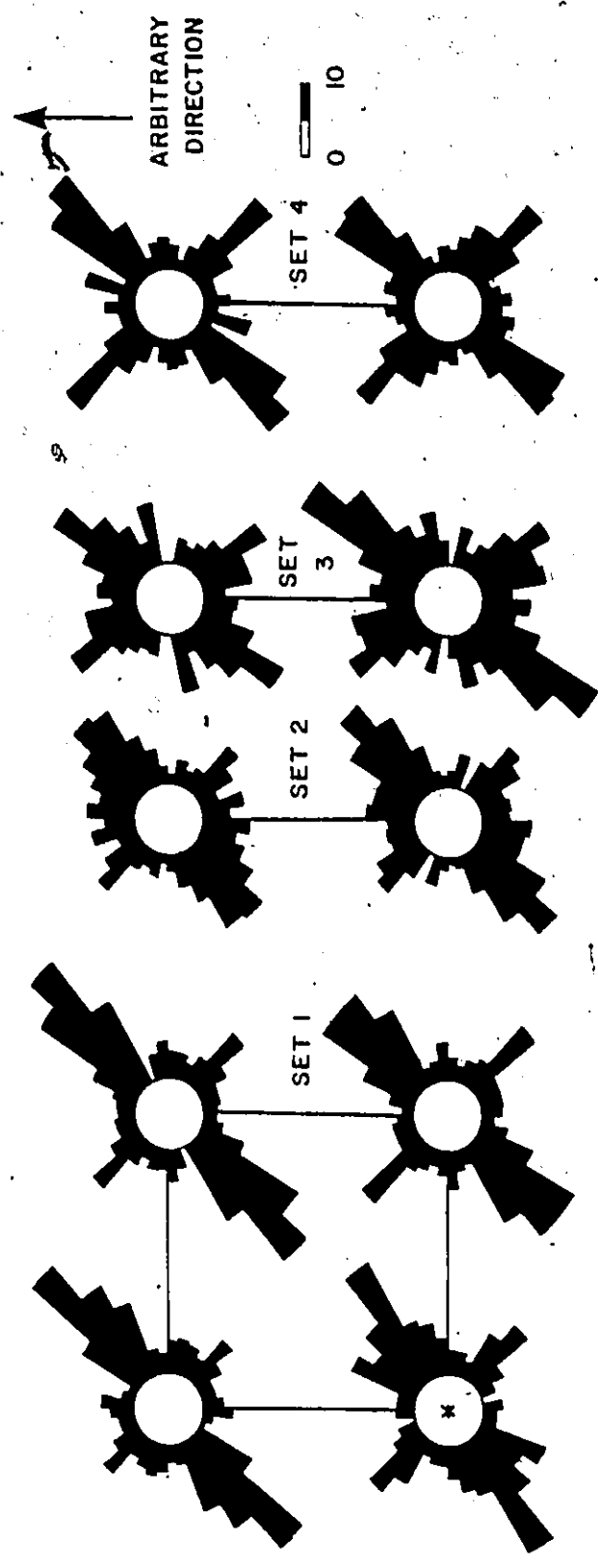


Fig. 77 - Rose diagrams for replicate measurements of sandstone and pebbly sandstone fabrics.

\* - duplicate measurement by D. Hunter, other replicate measurements by the author.

Rose diagrams in sets indicate replicate measurements on the same sample. Measurements in sets 2, 3, and 4 were done on the same photographs. For set 1, two different peels were made of the same slab section. Duplicate measurements of the same photographs are plotted above one another. For each set of data 100 measurements were made.



Grain size measurements were done in thin sections that were made from slabs cut parallel to bedding. The thin sections were projected onto a Shadowmaster screen. A grid overlay was placed over the enlarged projection (magnification = 56.2 x the original). Grains that fell upon the gridpoints were measured. For each grain the apparent a-axis dimension was recorded. The frequencies of a given grain size, as seen in thin section, depend upon the size of the grains. Because of this grain size influence, individual grains were only measured once. If a grain fell on more than one grid point, that grid point was skipped. For each thin section, 300 grains were measured. Recrystallized matrix was classed as being finer than very fine sand (the limit of the size of grains that could be discerned).

For each sample a cumulative frequency percent curve (with probability ordinate) was plotted. Standard statistical methods were used to analyze the grain size distributions (Folk, 1968). The following statistics are important: the graphic mean grain size ( $Mz \phi$ ), the median grain size ( $Md \phi$  or  $\phi_{50}$ ), the inclusive graphic standard deviation ( $\sigma_I$ ), and the inclusive graphic skewness ( $Sk_I$ ). Methods used to calculate these graphic statistics from the cumulative frequency curves are given by Folk (1968). In addition to the statistics, the grain size of the coarsest one-percentile was also noted.

APPENDIX 3

PETROLOGIC ANALYSES OF SANDSTONES AND PEBBLY SANDSTONES

| Bed | Quartz | Feldspar* | Matrix | Muscovite | Biotite | Zircon | Opaque Minerals | Volcanic Rk Frags | Cement + Other |
|-----|--------|-----------|--------|-----------|---------|--------|-----------------|-------------------|----------------|
| 3   | 56%    | 30%       | 9%     | tr        | ---     | tr     | 5%              | ---               | ---            |
| 2A* | 54%    | 35%       | 5%     | --        | 3%      | --     | 3%              | ---               | ---            |
| 2B* | 58%    | 37%       | --     | --        | ---     | tr     | 1%              | 4%                | ---            |
| 46  | 55%    | 39%       | 3%     | --        | ---     | tr     | 2%              | ---               | 1%             |
| 74  | 49%    | 50%       | --     | --        | ---     | --     | 1%              | ---               | ---            |
| 75  | 40%    | 47%       | 11%    | --        | ---     | --     | 2%              | ---               | ---            |
| 100 | 73%    | 20%       | 5%     | --        | ---     | --     | tr              | 1%                | 1%             |
| 123 | 63%    | 21%       | 8%     | tr        | ---     | tr     | 1%              | 3%                | 4%             |
| 179 | 38%    | 20%       | --     | --        | ---     | --     | --              | ---               | 4%             |
| 281 | 61%    | 32%       | 3%     | tr        | tr      | tr     | 3%              | 1%                | ---            |
| 302 | 61%    | 34%       | 3%     | --        | ---     | tr     | 2%              | ---               | ---            |
| 349 | 46%    | 35%       | 13%    | --        | ---     | tr     | 3%              | ---               | 3%             |
| 350 | 51%    | 40%       | 6%     | --        | ---     | 1%     | 2%              | ---               | ---            |
| 357 | 53%    | 33%       | 9%     | tr        | tr      | tr     | 3%              | 2%                | ---            |
| 378 | 68%    | 29%       | 1%     | tr        | ---     | tr     | 1%              | ---               | 1%             |
| 382 | 70%    | 27%       | --     | --        | 1%      | --     | --              | 2%                | tr             |

Notes:

100 grains were measured per thin section.

\*Feldspar: includes plagioclase, orthoclase and perthite grains.

Orthoclase: this is possibly marginally overestimated, as it was sometimes difficult to distinguish untwinned orthoclase from small quartz grains

Cement + Other: includes alteration minerals, mainly hematite and sericite

Grid counting was done on a square grid > 2x the largest grain on the slide, not grain counting. Large grains are "always" quartz and feldspars, less commonly a few large volcanic rock fragments.

tr : < 1%. Bed samples 2A & 2B are from turbidites immediately overlying bed 2.



PETROLOGIC ANALYSES OF SANDSTONES AND PEBBLY SANDSTONES (continued)INDEPENDENT OPERATOR CHECK (Done by Milton Graves, Dalhousie University)

## Bed 100:

| <u>Mineral</u>      | <u>No. Points</u> | <u>Per Cent</u> | <u>of 140 Pts.<br/>Per Cent</u> |
|---------------------|-------------------|-----------------|---------------------------------|
| Quartz              | 105               | 65%             | 75%                             |
| Orthoclase          | 15                | 17%             | 19%                             |
| Microcline          | 12                |                 |                                 |
| Plagioclase         | 8                 | 5%              | 6%                              |
| Alteration Minerals | 22                | 14%             | 100%                            |
| Totals              | 162               | 101%            |                                 |

## Bed 357:

| <u>Mineral</u>      | <u>No. Points</u> | <u>Per Cent</u> | <u>of 139 Pts.<br/>Per Cent</u> |
|---------------------|-------------------|-----------------|---------------------------------|
| Quartz              | 93                | 62%             | 67%                             |
| Orthoclase          | 23                | 16%             | 17%                             |
| Microcline          | 1                 |                 |                                 |
| Plagioclase         | 22                | 14%             | 16%                             |
| Alteration Minerals | 12                | 8%              | 100%                            |
| Totals              | 151               | 100%            |                                 |

Notes:

Alteration Minerals: usually hematite and sericite between grains, several badly weathered opaques included as well.

Orthoclase: this is possibly marginally overestimated as it was sometimes difficult to distinguish from small plagioclase grains.

Plagioclase: various perthitic grains included as well .

Each slide contained several other trace minerals which did not show on the counting. Grid counting was done on a square grid, > 2x the largest grain in the slide, not grain counting. Large grains are "always" quartz and feldspars, usually about the same size.

## APPENDIX 4

DESCRIPTIONS OF SEDIMENTARY FEATURES

In the following section detailed descriptions will be given of the sedimentary features which lay the basis for the definition of lithofacies. The sedimentary features which contribute to the definition of the lithofacies include: sole marks, basal scour margins, irregular upper bed contacts, internal features of beds ( fluid escape features and stratification ) and textural characteristics of beds ( grain size, grading patterns and grain size distributions ). Methods used in the field for section measuring and grain size description are given in Appendix . Detailed logs of the sections measured in the present study are included in Appendix 5.

SOLE MARKS

These features are common on many of the pebbly sandstone and conglomerate beds in the present study. Sole marks originate by three main processes: 1) current activity, 2) gravitational loading processes; or, 3) biologic activity. No sole marks within the Cap Enragé sediments were recognized as being biologic in origin. Within the Cap Enragé deposits the following types of sole marks were observed: scours; flutes; grooves; load casts and detached load coasts; load pebbles, cobbles and boulders; flame structures; and, longitudinal ridges. Flute marks, groove marks and longitudinal ridges are rare in the Cap Enragé sediments but are important in that they are reliable paleocurrent indicators.

Descriptions of these structures are given below, with the exception of scours which are covered under a separate heading.

#### Flute Marks

Flute casts rarely occur in the Cap Enragé sediments. Identification of flute marks is possible only in cases where three-dimensional views of the basal margin of beds are shown. In instances where only a two-dimensional cross-sectional view is seen of a flute mark, it may be identified as an asymmetrical scour or a load cast. In cases where lamination is truncated in the underlying bed the feature would be classed as an asymmetrical scour. Consequently, some flutes may be misidentified as asymmetrical scours or loads.

Flute casts were observed in sandstones, pebbly sandstones and fine conglomerate. Flute casts were most common in Facies (7), (3) and (6) beds. Flutes which could be measured had the following dimensions:

minimum dimensions : length (3 cm), width (1.5 cm), depth (1 cm)  
 maximum dimensions : length (27 cm), width (16 cm), depth (10 cm)  
 average dimensions : length (18 cm), width (11 cm), depth (7 cm)

The largest flute cast was observed at the base of a fine conglomerate bed ( apparent a-axis dimension: 7-8 mm). The smallest casts were filled with medium sandstone (grain diameter: 0.3 mm). Flute marks rarely occur singly, rather they tend to occur in groups. Flute marks are best developed along the basal surface of the Niveau 2 sandstone at the eastern end of the Anse à Pierre Jean 5 outcrop.

#### Groove Marks

These features are raised ridges which may have sharp or rounded edges and are found on the basal surfaces of sandstones.

Groove casts were rarely observed on the base of beds. These features were most common at the base of Facies (7) beds. Grooves which could be measured had the following dimensions:

maximum dimensions: length (80 cm), width (85 cm), depth (26 cm)

minimum dimensions: length (3 cm), width (0.2 cm), depth (0.2 cm)

The largest grooves occurred in conglomerate (a-axis = 200 mm), whilst the smallest grooves occurred at the base of a medium sandstone bed (grain diameter = 0.25 mm). The best example of a grooved surface occurs at the base of Niveau 2 at Greve de la Pointe.

#### Longitudinal Ridges (Fig. 78)

These features are raised ridges which have rounded edges and are found on basal bed surfaces. The lobate ridges are subparallel and occur in sets. Longitudinal ridges were only observed on the basal surfaces of two beds within the measured sections (St. Simon sur Mer, Shrine section, Beds 767, 761). Both of these beds belong to Facies (4). The longitudinal ridges averaged 5 - 8 cm wide and 2 - 2.5 cm in depth. It was impossible to determine the length of individual ridges because basal surfaces were not exposed well-enough. Both beds consisted of fine conglomerate at the base which graded into coarse sandstone. Some of the individual longitudinal ridges had blunt, presumably upcurrent ends as with flute casts, which tapered off in a downcurrent direction.

#### Load Features (Figs. 79 - 83)

These features are very common in the pebbly sandstones and conglomerates. Within the measured sections, 152 beds had loaded bases; 47 beds had loaded and scoured bases. Load structures are produced by the sinking of heavier sediment into less dense, or water saturated,



Fig.78 - Large-scale longitudinal ridges at conglomeratic base of bed.  
Lincation is 169-349 degrees. Rectangles on notebook are 5 cm  
long. Bed 761, St. Simon sur Mer (TwoCottages) Section, p.398

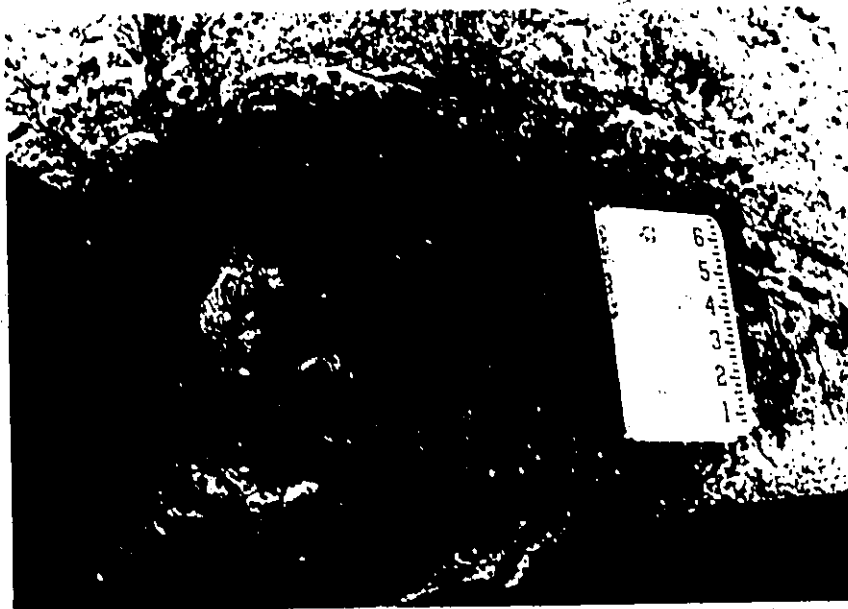


Fig.79 - Sandstone with dish structures which has subsequently been loaded and deformed into a flame structure. Float block, Bic.

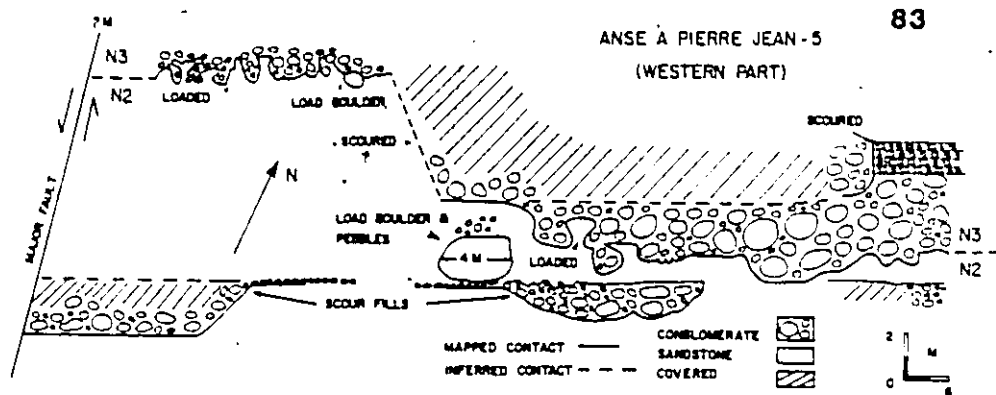
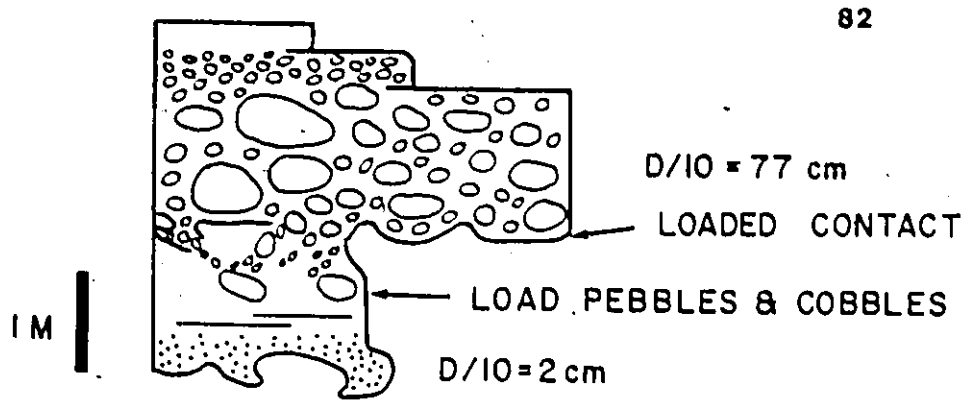
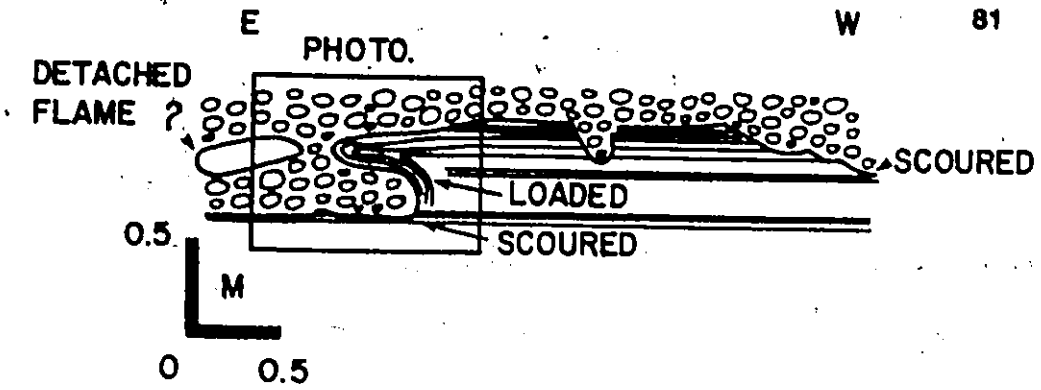


Fig.80 - Load pebbles and boulders (arrows), top of bed 885, St. Simon sur Mer Est. Rectangles on notebooks are 5 cm long. Stratigraphic top of bed is up, p.403

Fig.81 - Detached and undetached flame structures, Top of Bed 295, Grève de la Pointe, p.378

Fig.82 - Sketch of Fig. 80. Load pebbles and boulders in Bed 885, St. Simon sur Mer Est, p.403

Fig.83 - Sketch of load/scour contact between Niveau 2/Niveau 3, Anse à Pierre-Jean 5. Regional paleoflow in Niveau 2 is toward the southeast. Regional paleoflow in Niveau 3 is west-southwest, p.391





sediment. In load casts, the original flat or inclined sedimentary features of underlying sediment are deformed to conform to the shape of the load feature. In cases where the underlying unit is structureless, it is difficult to decide whether a depression is a load cast or a scour. Generally, load casts tend to have steeper margins than scours. In ambiguous cases, no measurement was taken. Load casts had average dimensions of 2.25 m width x 0.6 m height.

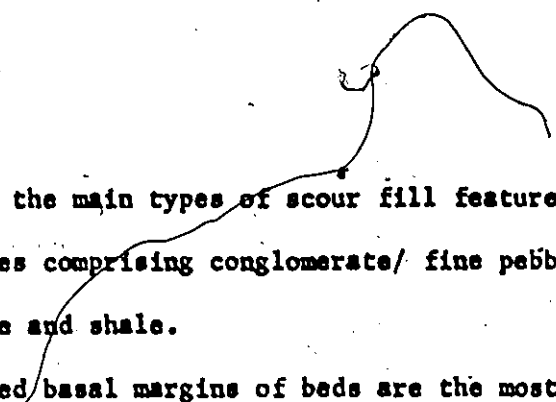
In the Cap Enragé sediments, the load features are best developed when pebbly sandstone to conglomerate is loaded into finer-grained pebbly sandstone to medium sandstone. Loaded or loaded and scoured bases are equally abundant in beds of Facies (1), (2), (3) and (4). Loaded or loaded and scoured bases are rare on beds of Facies (5), (6) and (7). Some outcrops have beds which show a tendency toward loaded or loaded and scoured bases.

Types of load features observed in the measured sections include: load casts (Fig. 79, 83), detached load casts or 'pseudonodules', flame structures and detached flame structures (Figs. 81, 79), and load boulders, cobbles and pebbles (Figs. 80, 82).

Detached load casts are rare within the Cap Enragé sediments. These are most common in the upper part of Niveau 4 at Grève de la Pointe. Load pebbles, cobbles and boulders are equally rare, but are important to recognize, in that they may account for the presence of large out-sized clasts within finer-grained beds.

#### SCOURS AND SCOUR FILL

Emphasis in the present study is placed upon the finer grained units of the Cap Enragé Formation, excluding Facies (1) horizons.



Consequently, the main types of scour fill features will be described for lithologies comprising conglomerate/ fine pebble conglomerate to fine sandstone and shale.

Scoured basal margins of beds are the most common type of sedimentary feature in the Cap Enragé deposits. Within the measured sections, 310 beds had scoured basal margins. As mentioned previously, 47 beds had loaded/scoured bases. Scour fill material ranges from fine sandstone to conglomerate as listed in Table 17. Not all scours were measured. Of the 310 scoured basal margins, 254 scours were measured.

Basal margins may be defined by a single scour ( Figs. 84, 85 ) or they may be delimited by a series of small scours, giving the base a scalloped appearance ( Fig. 85 ). Small scours may occur isolated along the base, or, alternatively, they may be linked together. Some small scours may lie parallel to bedding, whilst others are linked together and are inclined to bedding and actually define the margins of a much larger single scour surface.

Scours may be two-sided (symmetric) or apparently one-sided (asymmetric). This may depend upon the quality of the outcrop and the line of section through the original scour surface. About equal numbers of one- and two-sided scours were recorded ( Figs. 86, 87 ).

Four general types of scours can be distinguished. The first distinction is whether a scour fill is solitary or multiple in origin. The second distinction concerns the geometry of the scour: Is the base defined by a single scour, or does the base consist of a series of linked or unlinked scours? Although four distinctions can be made, only three types of scours were noted: 1) scours with a single scoured

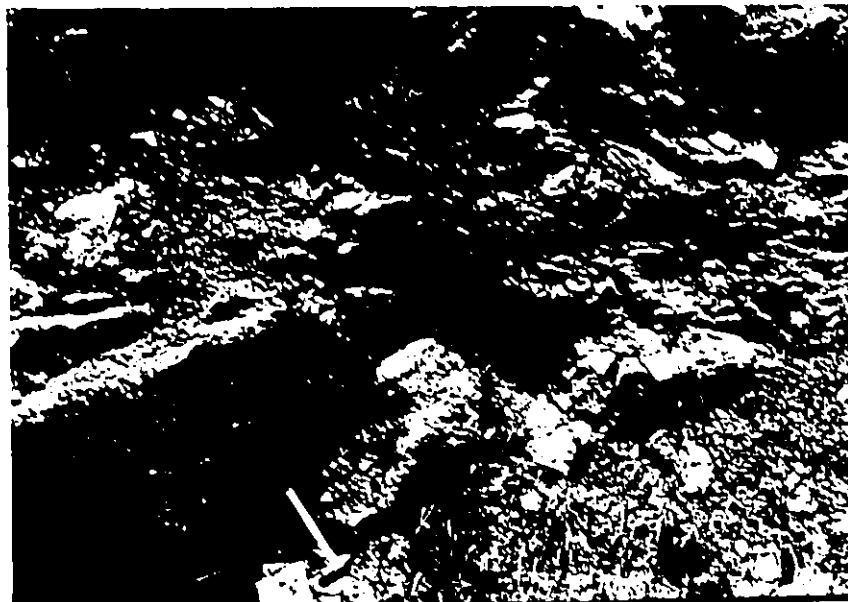


Fig.84 - Solitary scour fill cut into sandstone (near hammer).

Fill consists of conglomerate which is overlain by a slump bed portion (arrow). Bed 383, Rivière Trois Pistoles.

Hammer handle is 35 cm long. Stratigraphic top is to the upper right, p.381

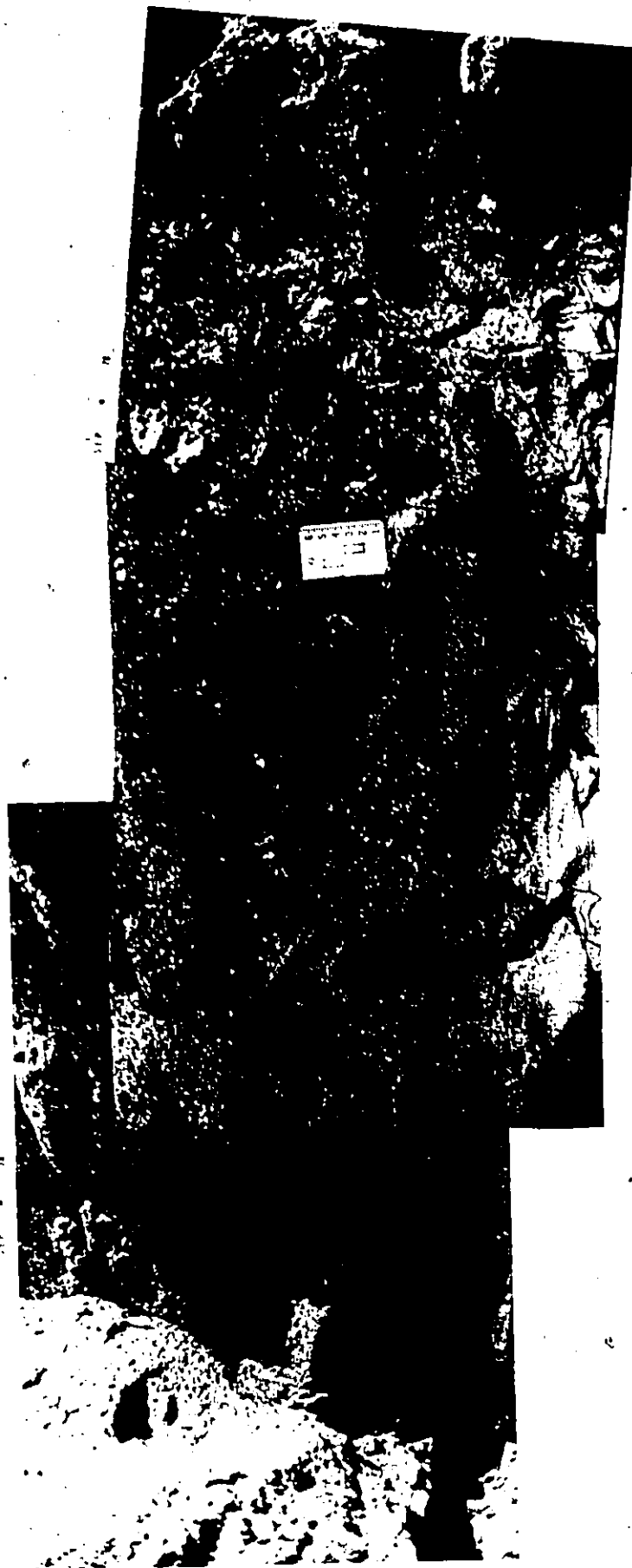


Fig. 85 - Base of Bed defined by many two-sided scours. Base of Bed 1399, Bic. Stratigraphic top is up, p. 422



Fig.86 - Two-sided, symmetrical, solitary scour of conglomerate cut into pebbly sandstone. Base of Bed 495, Anse à Pierre Jean 3. Ms. Hunter is leaning on the scour surface. Stratigraphic top is to the left, p.387



Fig. 87 - Base of bed defined by solitary, asymmetric (one-sided) scour opening up to the left.  
Base of bed 1304, Bfc. Rectangles on book are 5 cm long. Top of bed is up, p. 419

TABLE 17  
RANGE OF GRAIN SIZE IN SCOUR FILLS

| <u>Grain Size Class</u>  | <u>Abbrev.</u> | <u>N Beds</u> | <u>Per Cent (%)</u> |
|--------------------------|----------------|---------------|---------------------|
| Conglomerate             | C              | 79            | 36.5                |
| Fine Conglomerate        | FC             | 62            | 28.7                |
| Coarse Sandstone         | CS             | 28            | 13.0                |
| Medium Sandstone         | MS             | 21            | 9.7                 |
| Pebbly Sandstone         | PS             | 13            | 6.0                 |
| Very Coarse<br>Sandstone | VCS            | 8             | 3.7                 |
| Fine Sandstone           | FS             | 5             | 2.3                 |
| Very Fine<br>Sandstone   | VFS            | --            | ----                |

basal surface which were cut and then filled by many depositional events; 2) scours with a singly scoured basal surface which were cut and then filled by one depositional event; and 3) scours which have many linked or unlinked smaller scours along the base which were cut and filled by one depositional event. All of the scours of multiple fill or multiple cut-and-fill origin have one a singly scoured basal surface and do not display a series of small scours.

Multiple scour fills have complex origins and their fill usually comprises many different facies. For this reason, multiple scour fills will be discussed in Chapter 2, which deals with vertical and lateral facies relationships.

Solitary scours usually do not cut into one another; rather, they define the contacts of superimposed beds. Less commonly solitary scours may dissect one another. Table 18 shows a summary of the dimensions of solitary scours. Subdivisions are according to: 1) grain size of the scour fill, 2) the presence of a singly scoured basal surface; or 3) the presence of many small scours along the base of a single bed. On the average, the smallest scours occur at the bases of the sandstone beds, whilst the largest scours are along the basal margins of conglomerates. This is certainly expected if the cut-and-fill processes are associated with a single transport and depositional event. Conglomeratic flows would, presumably, have greater transport and erosional capabilities than sandy flows (assuming that all sizes were available for transport). In conglomeratic, pebbly sandstone and medium sandstone beds the dimensions of solitary scours are larger than the small scours that occur as sets. In fine conglomerate and fine sandstone beds the dimensions of



TABLE 18

DIMENSIONS OF INDIVIDUAL SCOURS (in metres)

| <u>Fill</u> | <u>No. Scours on<br/>Base of Bed</u> | <u>N</u> | <u>Average<br/>Width</u> | <u>Average<br/>Depth</u> | <u>Range of Dimensions<br/>Width x Depth</u>                                                 |
|-------------|--------------------------------------|----------|--------------------------|--------------------------|----------------------------------------------------------------------------------------------|
| C           | single                               | 19       | 3.74                     | 0.58                     | longest: 16 x 1.2<br>shortest: 0.25 x 0.05<br>deepest: 12 x 2<br>shallowest: 0.25 x 0.05     |
| C           | many                                 | 6        | 1.42                     | 0.37                     | longest: 3.6 x 0.8<br>shortest: 0.3 x 0.07<br>deepest: 3.6 x 0.8<br>shallowest: 0.3 x 0.07   |
| FC          | many                                 | 70       | 1.19                     | 0.17                     | longest: 9.75 x 0.5<br>shortest: 0.3 x 0.17<br>deepest: 3.0 x 0.9<br>shallowest: 1.1 x 0.05  |
| PS          | single                               | 5        | 3.34                     | 0.6                      | longest: 9.7 x 1<br>shortest: 0.96 x 0.48<br>deepest: 9.7 x 1<br>shallowest: 1 x 0.2         |
| VCS &<br>CS | single                               | 4        | 1.49                     | 0.35                     | longest: 1.7 x 0.35<br>shortest: 1.35 x 0.4<br>deepest: 1.5 x 0.4<br>shallowest: 1.4 x 0.25  |
| VCS &<br>CS | many                                 | 11       | 1.6                      | 0.22                     | longest: 3 x 0.6<br>shortest: 0.4 x 0.06<br>deepest: 1.9 x 0.45<br>shallowest: 0.4 x 0.06    |
| MS          | single                               | 5        | 3.66                     | 0.43                     | longest: 10.1 x 0.6<br>shortest: 0.72 x 0.1<br>deepest: 10.1 x 0.6<br>shallowest: 2.5 x 0.25 |
| MS          | many                                 | 3        | 0.95                     | 0.15                     | longest: 1.1 x 0.24<br>shortest: 0.8 x 0.1<br>deepest: 1.1 x 0.24<br>shallowest: 0.95 x 0.1  |
| FS          | single                               | 1        | 0.8                      | 0.08                     |                                                                                              |
| FS          | many                                 | 2        | 1.9                      | 0.23                     |                                                                                              |

single scours are, on the average, smaller than those scours which occur as sets along basal surfaces of beds. In coarse sandstones the scour sizes are the same for beds which have many scours on the base in comparison to those which have a solitary basal scour.

Most of the beds that have basal margins defined by series of scours outcrop in the St. Simon sur Mer Est area. Some beds of Member III at Bic and of Niveau 4 or Niveau 6 at Cap à la Carre Ouest also display this type of scouring, but to a lesser extent than that at St. Simon sur Mer Est. Descriptions of the fill of these scour features will be given in Chapter 2.

Scoured and loaded/scoured bases of beds are common in beds classed as Facies (2), (1) and (5), less common in beds belonging to Facies (6), (3), (2) and rare in beds belonging to Facies (7).

#### IRREGULAR UPPER BED SURFACES

Irregular upper bed or layer contacts occur in cases where clasts at the top of a bed or layer actually protrude above the general level of the top of the bed or level (Fig.89). This feature is not very common in the Cap Enragé sediments. It has been noted at the top of 49 beds within the measured sections.

Irregular upper bed surfaces mainly occur in instances where conglomerate material (a-axis = 225 mm - 820 mm) is overlain abruptly by finer grained conglomerate or pebbly sandstone. The average thickness of beds or layers which display irregular upper contacts is 1.2 m (minimum thickness = 0.2 m; maximum thickness = 3.9 m). Beds are usually clast-supported where coarse clasts touch one another, with very little fine material between the coarser clasts. Most of the beds which show irregu-

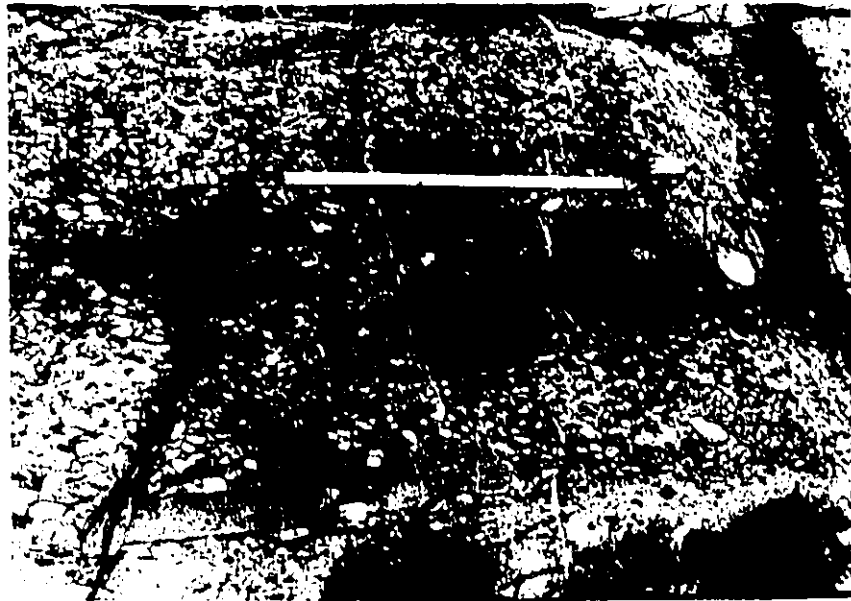


Fig.88 - Pebbles and cobbles protruding above the general bed level.

Note the wedging-out along section of the overlying sandstone.

Top of Bed 803 St. Simon sur Mer (Shrine Section). Tape measure

is extended 50 cm. Stratigraphic top is up, 0.400



Fig.89 - Boulder extending above the general level of the top of a clast-supported, inversely-graded conglomerate. Note the flat top of the overlying sandstone with many small scale irregularities. Boulder is slightly faulted. Top Bed 802, St. Simon sur Mer

lar upper surfaces belong to Facies (1); only two beds were classed as belonging to Facies (3).

Most of the beds with this feature had flat bases (27 beds). The remaining beds had scoured (9 beds), loaded (6 beds) or loaded/scoured bases (6 beds). Of the Facies (1) conglomerates, most showed inverse grading (30 beds), less commonly the conglomerates were ungraded (19 beds). Of the ungraded beds, only eight had a disorganized fabric.

The presence of coarse clasts which are "floating" up above the general top of the bed is an important feature to recognize for subsequent hydraulic interpretation of flow mechanisms. It is also a useful aspect to help separate amalgamated or composite beds in the field.

The best outcrop occurrences of irregular upper bed contacts are seen at the two following sections (Appendix 5): Anse à Pierre Jean 2, Section 1 and at St. Simon sur Mer (Shrine Section). In both cases thin Facies (1) conglomerates are overlain by sandstone or pebbly sandstone units, which wedge out from the base toward the top of the unit, yielding lenses of fine material intercalated among the conglomerate.

#### FLUID ESCAPE FEATURES

Lowe (1975) describes a variety of fluid escape features which characterize coarse (silt size and greater) sediment. In the field, Lowe's (1975) terminology was used, with the exception of the feature that Lowe (1975) calls 'Type D Pillars' or 'stress pillars.' These structures were originally recognized by Laird (1970) who called them 'sheet structures.' This original term was used in the present study.

Of the different types of structures listed by Lowe (1975, pp.

166-189) the following were noted in the Cap Enragé sediments: dish structures, fluid escape pillars ( including Types A, B and C), horizontal fluidization channels, sheet structures, sediment dykes and sills, oversteepened crossbedding, convolute lamination and load structures. Convolute lamination and oversteepened crossbedding arise from both gravitational instabilities and tractional current processes and will be discussed under the heading ' Stratification Types.' Load structures have been discussed in an earlier part of this chapter.

#### Dish Structures (Figs. 90 to 93)

Dish structures consist of concave-up saucer-shaped laminations, when seen in a cross sectional view. The lower contact is generally very sharp and is defined by a dark layer (Fig. 92). Above the lower margin of the structure the sediment becomes lighter colored upsection, to the extent that it is almost white underneath the next row of dish structures ( Fig. 92). Seen in plan view (Fig. 93), dish structures are again defined by dark zones. Upturned edges of dish structures define small circular or oval outlines in plan section . This feature is most common and better defined in coarse and medium sandstones (Figs. 92, 93 ), although it does occur in fine conglomerate and conglomerate beds (Figs. 90, 91). Dish structures tend to be larger and not as well defined in the coarser beds (Fig. 90).

Average widths and depths of dish structures were measured in material of various grain sizes. Thicknesses of dish structure units was also measured, where dish structure units were defined as follows: If dish structures had approximately the same shape and dimensions and occurred within the same part of a bed they were grouped as being in a

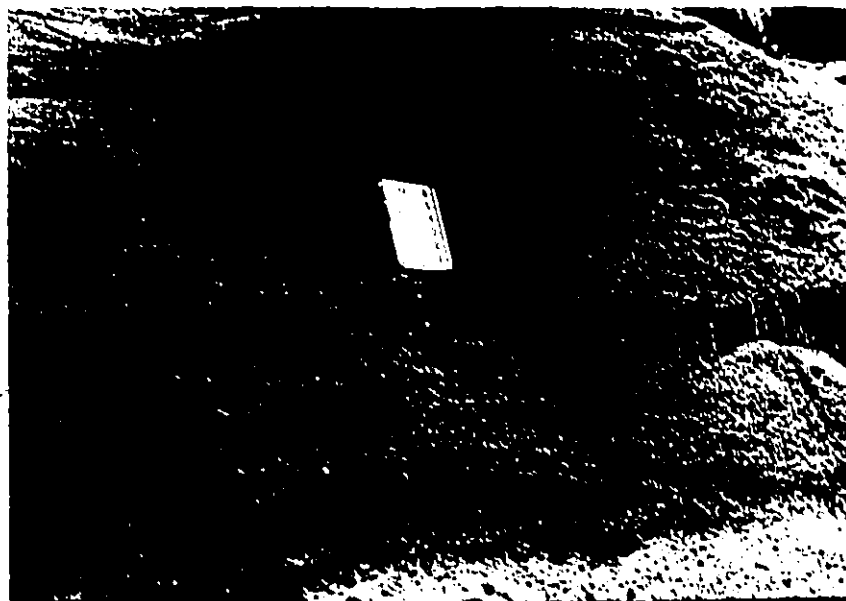


Fig. 90 - Large dish structures in cross-section view. Bed consists of fine-pebble conglomerate. Bed 1298Bic. Top of bed is up, p. 419

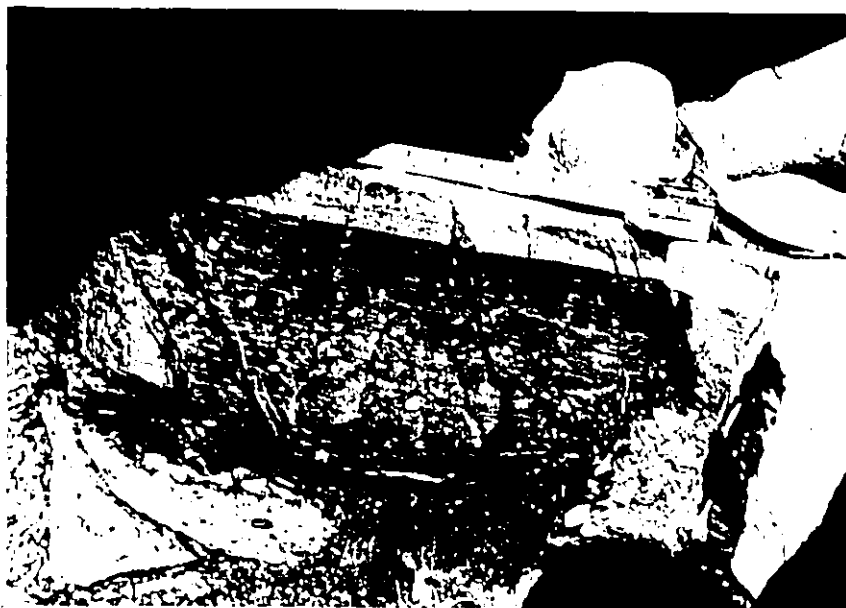


Fig. 91 - Small dish structures in dispersed fine conglomerate-pebbly sandstone. Bed 1345, Bic. Tape is 20 cm long. Top of bed is up, p. 419

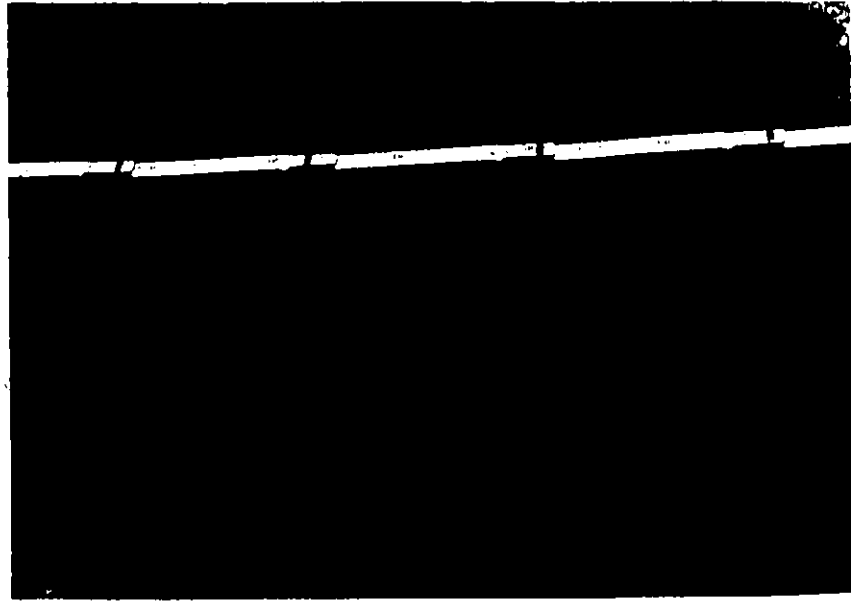


Fig.92 - Small dish-structures in cross-section. Cap à la Carre Ouest,  
between Sections 4 and 5. Scale is in cm. Top of bed is up, p.414



Fig.93 - Small dish structures in top or plan view. Cap à la Carre  
Ouest, between Sections 4 and 5. Scale is in cm, p.414

in a given dish structure unit. If dish shape or size changed significantly, a new dish structure unit would be defined. Average dish width (measured from rim-to-rim) and depth (measured from the top of the up-turned edge down to the lowest part of the lower convex margin) were made for 476 dish structure units. These data are tabulated in Table 19 .

Dish structure dimensions varied as follows:

minimum width x depth : 0.15 cm x 0.1 cm in medium sandstone

maximum width x depth : 60 cm x 3 cm in pebbly sandstone

average width x depth : 8.7 cm x 0.8 cm in conglomerate to fine sandstone

As shown in Table 20 , the average width x depth dimensions decrease with decreasing grain size of the deposit. In conglomerates, the average width x depth was 12.5 cm x 0.9 cm, whilst in fine sandstone the average width x depth was 4.8 cm x 0.5 cm. Average width:depth ratios also decreased from conglomerate to sandstone, indicating that dish structures tend to be flatter in coarser sediments and more curved or more concave in finer sediment. Minimum and maximum dimensions of dishes do not change with decreasing grain size of the deposit.

Dish structures may be well defined (as in Figs. 91 and 92 ) or vague (as in Fig. 90). Ill-defined or vague dish structures seem to occur in all grain sizes of beds, although (on the whole, when one considers all of the liquefied sediments within the Cap Enragé) dish structures seem to be better defined in coarse and medium sandstone ( This is not evident from the data in Table 20 and may reflect sampling error.).

Most dish structures lie parallel to bedding. Of the 476 units that were measured, inclined dish structures were noted in only 28 units.



TABLE 19

DISH STRUCTURE OCCURRENCE IN DIFFERENT SEDIMENT TYPES

| Grain<br>Size<br>Class | N<br>Dish<br>Units | %  | N<br>Vague Dish<br>Units | %   | N<br>Total<br>Units | %   | (in metres)            |                         |
|------------------------|--------------------|----|--------------------------|-----|---------------------|-----|------------------------|-------------------------|
|                        |                    |    |                          |     |                     |     | Unit<br>Thick.<br>Avg. | Unit<br>Thick.<br>Range |
| C                      | 2                  | 1  | ---                      | --- | 2                   | 0.4 | 1.15                   | 0.6-1.7                 |
| FC                     | 51                 | 13 | 8                        | 9   | 59                  | 12  | 0.41                   | 0.02-1.8                |
| PS                     | 43                 | 11 | 18                       | 21  | 61                  | 13  | 0.50                   | 0.08-2.                 |
| VCS                    | 45                 | 12 | 16                       | 19  | 61                  | 13  | 0.40                   | 0.1-1.7                 |
| CS                     | 89                 | 23 | 13                       | 15  | 102                 | 21  | 0.33                   | 0.01-1.2                |
| MS                     | 93                 | 24 | 22                       | 26  | 115                 | 24  | 0.36                   | 0.02-4.                 |
| FS                     | 67                 | 17 | 9                        | 10  | 76                  | 16  | 0.24                   | 0.04-0.8                |
| Total                  | 390                |    | 86                       |     | 476                 |     |                        |                         |

TABLE 20

DIMENSIONS OF DISH STRUCTURES

(width x depth in centimetres)

| Grain<br>Size<br>Class | N<br>Dish<br>Units | Minimum    |     | Maximum   |     | Average    |     |
|------------------------|--------------------|------------|-----|-----------|-----|------------|-----|
|                        |                    | W x D      | W/D | W x D     | W/D | W x D      | W/D |
| C                      | 2                  | 10 x 1.5   | 7   | 15 x 0.3  | 50  | 12.5 x 0.9 | 14  |
| FC                     | 38                 | 1.5 x 0.5  | 3   | 50 x 2    | 25  | 11 x 1.1   | 10  |
| PS                     | 38                 | 1.0 x 0.2  | 5   | 60 x 3    | 20  | 11.3 x 1.1 | 10  |
| VCS                    | 40                 | 1.0 x 0.5  | 2   | 50 x 0.5  | 100 | 8.7 x 0.7  | 12  |
| CS                     | 77                 | 0.3 x 0.1  | 3   | 50 x 1.5  | 33  | 8.0 x 0.8  | 10  |
| MS                     | 99                 | 0.15 x 0.1 | 2   | 50 x 3.8  | 13  | 5.1 x 0.7  | 7   |
| FS                     | 71                 | 1.0 x 0.2  | 5   | 20 x 0.25 | 80  | 4.8 x 0.5  | 10  |

W x D: width x depth dimensions in cm of dish structures

W/D: width:depth ratio of dish structures

Abbreviations for grain size classes are the same as in Table .

Other rare occurrences consisted of smaller dish structures "nested" within larger, and broader dish structures; dish structures which have subsequently been loaded into flame structures; and, dish structures which are in association with fluid escape tubes which pass across the dishes without any disruption of laminae. These specific occurrences, although they do not occur very often, give some hints (for certain beds) of the time of liquefaction that produced the dish structures. Within units, dish structures are usually the only feature observed. Less commonly dish structures occur in the same units as fluid escape pillars, flame and convolute structures.

The average thickness of dish structure units was 0.48 m, with the range from 0.01 m to 4 m. Average unit thicknesses vary with grain size. Maximum average unit thickness (1.15 m) occurs in conglomerate, whilst the fine sandstones had an average unit thickness of 0.24 m. Maximum and minimal unit thicknesses do not vary consistently with sediment size. The thickest dish structure unit was recorded in medium sandstone. Thinnest units were noted in fine conglomerate and coarse sandstone.

Dish structures are well defined in Facies (4) beds and are one of the characteristics of this facies. Vague dish structures occur less commonly in Facies (3) beds and rarely occur in Facies (6) beds. Some of the best places to see beds with dish structures are : Niveau 2 at Anse à Pierre Jean 1; Niveau 4 at Greve de la Pointe and the top of Member I at Bic.

### Fluid Escape Pillar Structures (Figs. 94 - 98)

Pillar structures were named by Wentworth (1966, p. 133) and consist of circular columns or curtain-like sheets of light-colored sandstone. Fluid escape pillar structures were recognized in 130 beds in the present study in material ranging in size from fine sandstone to conglomerate. As with dish structures, not all fluid escape pillars were measured. Similar to the criterion used in dish structures, fluid escape pillar units were defined within beds. Average apparent lengths and widths were measured as seen in cross sectional view for 265 pillar units. Using Lowe's (1975) classification two types of fluid escape pillars were recognized: Type A pillars and Type B pillars.

(1) Type A Pillars (Fig. 20) - occur between the upturned edges of adjacent dish structures. Type A pillars are very common in units in which they occur. These structures tend to have a somewhat regular spacing, that is probably related to the spacing of intervening dish structures. Average length x width measurements were made in 43 Type A pillar units out of a total of 50 units. The results are summarized in Table 21.

Type A pillar structure dimensions varied as follows:

- minimum length x width: 1 cm x 0.1 cm in coarse sandstone
- maximum length x width: 45 cm x 0.5 cm in fine conglomerate
- average length x width: 6 cm x 0.5 cm in fine conglomerate to fine sandstone material

In conglomerates the average length x width was 11.2 cm x 0.7 cm, which decreased to an average length x width of 2.9 cm x 0.3 cm in fine sand-



Fig. 94 - Straight Type B fluid escape pillars in plan view. Bed  
761, St. Simon sur Mer (Two Cottages) Section, p.398

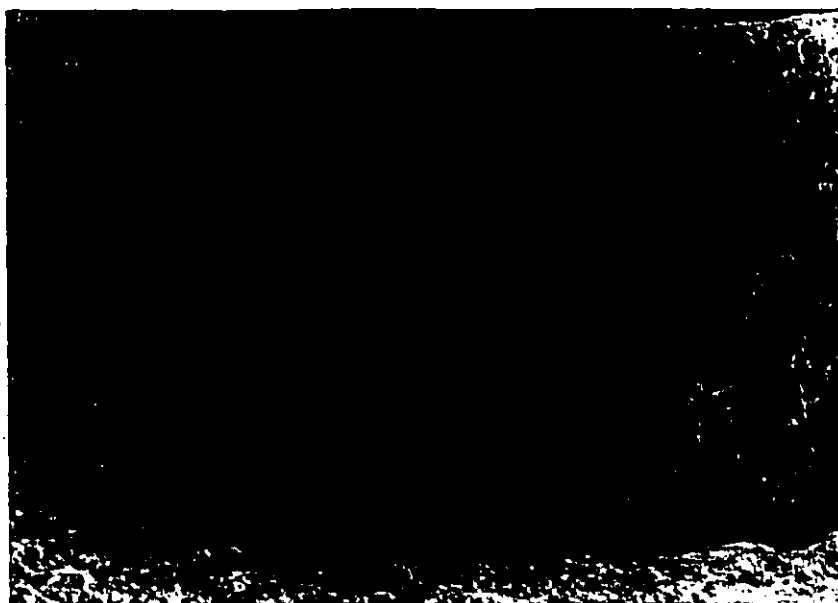


Fig.95 - Branching Type B fluid escape pillars in cross-section. Bed  
1217, Cap à la Carpe Ouest. Rectangles on notebook are 5 cm  
long. Stratigraphic top is up, p.415

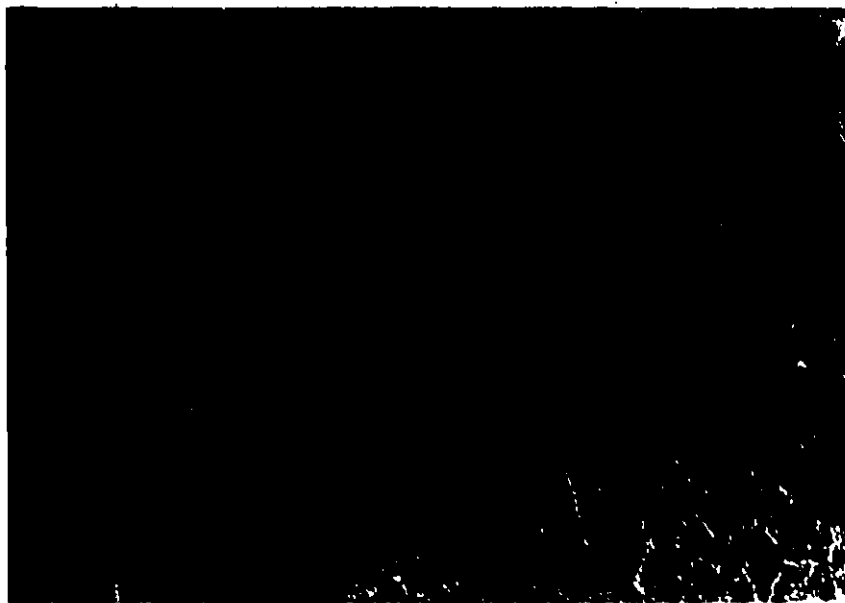


Fig.96 - Branching Type B fluid escape pillars in plan view.  
 Bed 1217, Cap à la Carre Ouest. . Rectangle on book is  
 5 cm long, p.415

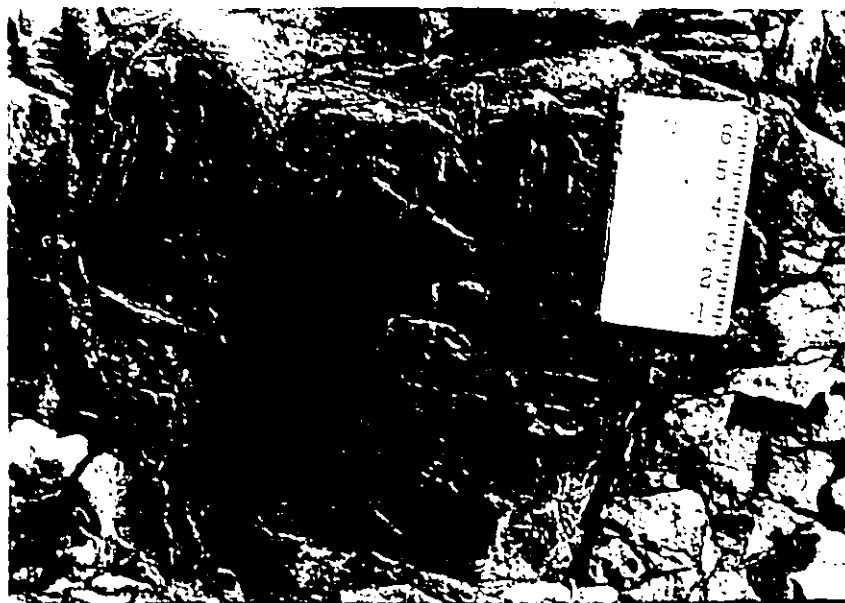


Fig.97 - Irregular Type B fluid escape pillars in cross-section.  
 Bed 1352, Bic. Stratigraphic top is up, p.419

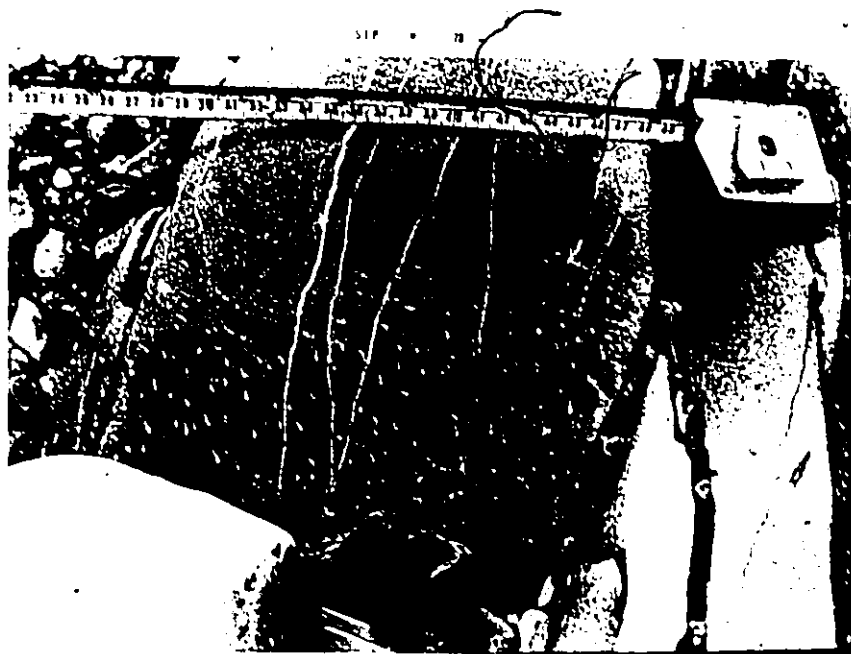


Fig. 98 - Irregularly shaped Type B fluid escape pillars in cross-section. Pillars are bent into a convolute form about half way up the bed. Bed 1256 Cap à la Carre Ouest. Bottom scale is in cm. Stratigraphic top is up, p. 417

TABLE 21

DIMENSIONS OF FLUID ESCAPE PILLARS: TYPE A

| Grain<br>Size<br>Class | N  | Maximum<br>l x w<br>(cm) | Minimum<br>l x w<br>(cm) | Average<br>l x w<br>(cm) | (in metres)            |                         |
|------------------------|----|--------------------------|--------------------------|--------------------------|------------------------|-------------------------|
|                        |    |                          |                          |                          | Unit<br>Thick.<br>Avg. | Unit<br>Thick.<br>Range |
| FC                     | 9  | 45 x 0.5                 | 1 x 0.15                 | 11.2 x 0.7               | 0.28                   | 0.12-0.5                |
| PS                     | 5  | 10 x 0.5                 | 2.5 x 0.4                | 5.5 x 0.4                | 0.21                   | 0.05-0.5                |
| VCS                    | 3  | 7 x 0.4                  | 4 x 0.4                  | 5.5 x 0.4                | 0.4                    | 0.1-0.7                 |
| CS                     | 10 | 12 x 0.3                 | 1 x 0.1                  | 4.9 x 0.7                | 0.41                   | 0.04-0.95               |
| MS                     | 12 | 10 x 0.8                 | 1.5 x 0.2                | 1.5 x 0.5                | 0.63                   | 0.1-4.0                 |
| FS                     | 11 | 6 x 0.4                  | 1.5 x 0.2                | 2.9 x 0.3                | 0.18                   | 0.05-0.8                |

Average dimensions of Type A pillars: 5.78 cm length x 0.5 cm width

Average unit thickness: 0.35 m

l = length of pillar structure; w = width of pillar structure

Abbreviations for the grain size classes are the same as in Table 17.

TABLE 22

DIMENSIONS OF FLUID ESCAPE PILLARS: TYPE B (STRAIGHT)

| Grain<br>Size<br>Class | N  | Maximum<br>l x w<br>(cm) | Minimum<br>l x w<br>(cm) | Average<br>l x w<br>(cm) | (in metres)            |                         |
|------------------------|----|--------------------------|--------------------------|--------------------------|------------------------|-------------------------|
|                        |    |                          |                          |                          | Unit<br>Thick.<br>Avg. | Unit<br>Thick.<br>Range |
| C                      | 2  | 50 x 7                   | 10 x 5                   | 30 x 6                   | 1.9                    | 1.0-2.8                 |
| FC                     | 21 | 23 x 0.7                 | 1 x 0.7                  | 8.5 x 3.6                | 0.45                   | 0.1-1.4                 |
| PS                     | 30 | 20 x 0.7                 | 1 x 0.5                  | 5.5 x 0.6                | 0.64                   | 0.07-2.5                |
| VCS                    | 29 | 45 x 2                   | 1 x 0.1                  | 8.5 x 0.9                | 0.49                   | 0.1-2.0                 |
| CS                     | 35 | 20 x 0.4                 | 1 x 0.5                  | 5.4 x 0.5                | 0.4                    | 0.04-1.2                |
| MS                     | 34 | 15 x 8.5                 | 1 x 0.1                  | 5.1 x 1.0                | 0.63                   | 0.04-3.3                |
| FS                     | 21 | 25 x 0.2                 | 0.5 x 0.05               | 5.6 x 0.7                | 0.30                   | 0.01-1.4                |

Average dimensions of Type B (straight) pillars: 9.8 cm length x 1.9 cm width

Average unit thickness: 0.69 m

Abbreviations for grain size classes are the same as in Table 17.

stone. This decrease in pillar size is probably related to the concomitant decrease in the size of dish structures from conglomeratic to fine sandstone material. Minimum and maximum dimensions of Type A pillars found in a given pillar unit decreased with decreasing grain size.

Type A pillar units vary in thickness from 4 m (in medium sandstone) to 0.04 m (in coarse sandstone). Average pillar unit thickness was 0.35 m. The thickest units occurred in the finer sediment ranges (coarse-, medium and fine sandstone). Average unit thicknesses were the largest in somewhat coarser sediment ranges (very coarse-, coarse- and medium sandstone). Plots of pillar width versus unit thickness and plots of pillar length versus unit thickness showed no trends.

(2) Type B Pillars (Figs. 94-98) - are those pillar structures which do not occur at upturned edges of dish structures, but occur generally isolated from dish structures. Type B pillars may be vertical or less steeply inclined with respect to bedding. These features may coincide or be discordant with other sedimentary features within a bed. In cross sectional view, Type B pillars may be straight (Fig. 21); branching, where they generally fork upsection (Fig. 95); or, very irregular in shape, resembling curtains (as lights in the aurora borealis) (Fig. 97); amorphous "blobs", or small "inverted commas" (Fig. 98).

In plan view, the branching pillars also show a dendritic pattern (Fig. 96). Plan view of straight, Type B pillars shows small circular, washed-out zones. Irregularly shaped Type B pillars have irregularly shaped zones in plan view. Rarely, Type B pillars appear to be bent, sheared or aligned in convolute structures (Fig. 98).



Type B pillars were noted in 215 fluid escape units. Of these units, most of the Type B pillars were straight (172 units), less commonly branched (16 units) and rarely bent, inclined or in convolute structures (27 units).

Straight Type B pillars were found in conglomeratic to fine sandstone beds. Dimensions of these pillars are as follows (Table 22):  
maximum length x width: 50 cm x 7 cm in conglomerate  
minimum length x width: 0.5 cm x 0.05 cm in fine sandstone  
average length x width: 9.8 cm x 1.9 cm in conglomerate to fine sandstone beds. Aside from the Type B pillars in the conglomerate, most of the pillars average 6.5 cm length x 1.2 cm width in all sediment classes from pebbly- to fine sandstone. Maximum and minimum dimensions also remain fairly constant within the sandstones.

Straight Type B pillars occurred in units which averaged 0.69 m in thickness. The thickest units occurred in medium sandstone (3.3 m). Unit thicknesses tend to be greater, on the average, in the coarser sediment ranges (conglomerate, pebbly- and medium sandstone). The thinnest units were found in fine sandstone. As with the Type A pillars, the dimensions of straight Type B pillars do not seem to be related to the unit thickness.

Branching Type B pillars tend to be larger than those of straight Type B pillars (as seen in cross sectional view) (average length x width: 11.5 cm x 0.42 cm). The branching types also occur in smaller units (average thickness of units: 0.43 m) than the straight types. Branching Type B pillars are rarely observed in fine conglomerate.

Type B pillars in convolute structures, bent or inclined pillars

are less common than the branched type. Only six units showed Type B pillars in convolute structures (Fig. 98). The average unit thickness was 0.53 m; average pillar dimensions were 4.4 cm length x 1.6 cm width. Twenty-one units were noted with bent or inclined Type B pillars. Average unit thickness was 0.3 m; average pillar dimensions were 3.6 cm length, x 0.4 cm width.

In most beds with Type B pillars they are the only structure observed. Less commonly, they are associated with other sedimentary structures. The most common association, when it occurs, is with dish structures. These dish structures are not disrupted by the Type B pillars: pillars may be superimposed upon the dish structures, or they may occur in separate zones intercalated with dishy zones or laterally equivalent to dish units.

The best example of straight Type B pillars occurs at the St. Simon sur Mer Est outcrop (Niveau 4) (Fig. 21). Branching Type B pillars are best developed at Cap à la Carre Ouest, at Section 4 and between Section 4 and Section 5 (Fig. 95, 96). Irregularly shaped Type B pillars are most common in the upper part of Member I at Bic. As with the dish structures, fluid escape pillars characterize Facies (4) sediments. They are rarely developed, to a minor extent, in Facies (6) beds.

#### Horizontal Fluidization Channels (Fig. 99)

Horizontal fluidization channels consist of white, structureless sandstone which underlies darker layers (Lowe, 1975; Lowe and LoPiccolo, 1974) (Fig. 99). These channels are commonly superimposed upon one another in the Cap Enragé sediments, with the basal dark lamina and overlying white sandstone forming a couplet. The dark lower margin is commonly



Fig.99 - Horizontal fluid escape channels in cross-section. Bed 562, Anse à Pierre Jean 5. Stratigraphic top is up. Rectangles on notebook are 5 cm long,  $\rho.390$

very sharp, whereas the upper contact with the white sandstone is more gradual. These features are analagous to "flat" dish structures and are thought to form by horizontal flow of pore fluid through the sediment. Horizontal fluidization channels occurred in material from fine sandstone to fine conglomerate. They are most common in fine sandstone ( 12 beds out of 24 beds were composed of fine sandstone and showed fluidization horizontal channels). The dark and light layers had the following thicknesses:

| Thickness | Light Layers | Dark Layers |
|-----------|--------------|-------------|
| maximum   | 5 cm         | 2.5 cm      |
| minimum   | 0.3 cm       | 0.4 cm      |
| average   | 1.2 cm       | 1 cm        |

As seen by eye, dark and light layers do not appear to differ in grain size. Individual layers are traceable from a minimum of 15 - 100 cm along strike, to a maximum of entire outcrop widths. The average thickness of units with horizontal fluidization channels was 0.42 m (range 0.03 - 1.9 m in fine sandstone). These channels are rarely associated with very flat dish structures or sheet structures ( to be described below).

As with most of the other fluid escape features, horizontal fluidization channels are one of the features that characterize Facies (4) beds and do not occur in any of the other Facies. The best outcrop to see this type of structure is in the beds at the base of Anse a Pierre Jean 5 outcrop near the westerly cottage (see outcrop map Appendix 5).

### Sheet Structures (Fig.100)

In cross sectional view, sheet structures appear as tiny, regularly spaced fluid escape pillars. In plan view they are straight to sinuous white structureless bands. In cross sectional view, the pillars vary from less than 0.5 cm to 2 cm in length x 0.15 cm to 0.25 cm in width. Individual sheets are traceable up to 1 m along bedding surfaces (in plan view).

Sheet structures are rare in the Cap Enragé sediments and were noted only within six beds. The bed material comprised all sediment size ranges from conglomerate to fine sandstone. In the fine sandstone beds, they were always associated with beds that also displayed parting lineation. In some cases, it is possible to see the progressive development of sheet structures from what appear to be tiny white "harrow marks" (Fig. 101). In coarser sediments, sheet structure alignment (as seen in plan view) is usually coincident with other paleocurrent indicators. For these reasons, although sheet structures are rare, they are important features to recognize in that they yield valuable paleocurrent data.

### Large Scale Sediment Intrusions: Dykes and Sills (Fig.102,103)

Large scale sediment intrusions in the form of sediment dykes and sills are rare: only two locations showed these features. Conglomeratic injections in the form of dykes and sills occur along the margins of the basal scour fill of Niveau 2 at Grève de la Pointe (Fig.102). Injections are traceable along strike from a few cm to 1.3 m; injection thicknesses vary from a few cm to 90 cm. A sandstone sill with small dykes occurred at St. Simon sur Mer Est in Niveau 4 deposits (Fig.103).

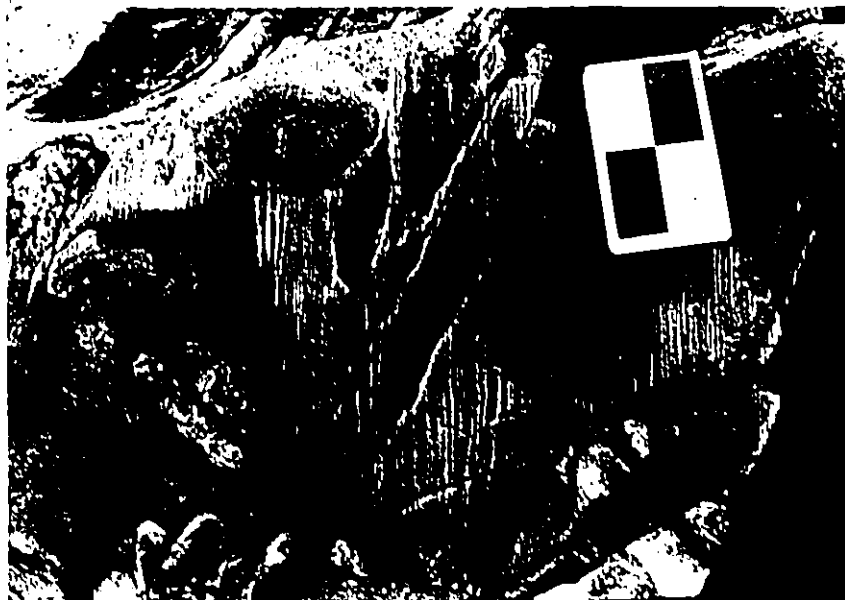


Fig.100 - Sheet structures in top or plan view. Bed 231, Grève de la Pointe. Rectangles on notebook are each 10 cm long, p.377



Fig.101 - "Incipient" sheet structures in plan view, in association with harrow marks. Bed 230, Grève de la Pointe. Lens cap is about 5 cm in diameter, p.377



Fig.102 - Channel margin showing conglomeratic injections into turbidites (lower half of photo beneath notebook). Bed 1, Grève de la Pointe. Stratigraphic top is to the left. Rectangles on notebook are 10 cm long, p.372

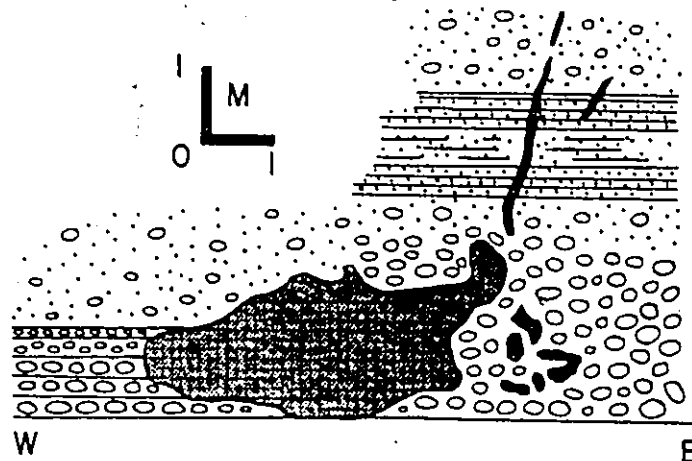


Fig.103 - Sketch of cross-sectional view of sandstone sill and dykes (shaded portion) in beds 907,908 St. Simon sur Mer Est, p.404

## STRATIFICATION TYPES

Many sedimentary deposits display features which are attributable to sorting of different sizes of sediment. These features are called stratification and can be horizontal or inclined. Stratification is a very common feature within the Cap Enrage sediments and was noted in 801 beds of the present study. The following types of stratification and cross-stratification were noted and described: 1) horizontal stratification; 2) low-angle cross-stratification; 3) trough cross-stratification; 4) scour fill stratification; 5) 'coarse clast' stratification; 6) convolute lamination and convolute bedding; and, 7) irregularly inclined stratification.

### Horizontal Stratification (Figs. 104-106)

Horizontal stratification consists of alternating laminae or layers within a bed, where the layering lies parallel to bedding. Units with horizontal stratification vary from less than a centimetre in thickness to greater than 3 m in thickness. Horizontal stratification is found in all grain sizes of sediment from fine sandstone to conglomerate. This is the most common type of stratification observed in beds of the measured sections. Over 80% of the beds that are stratified display horizontal stratification (Table 23), of these about 30% of the beds had vague horizontal stratification.

Vague horizontal stratification is defined by layers which are one or more clasts thick in pebbly sandstones and conglomerates. In finer grained sediments the layers vary from less than a centimetre thick



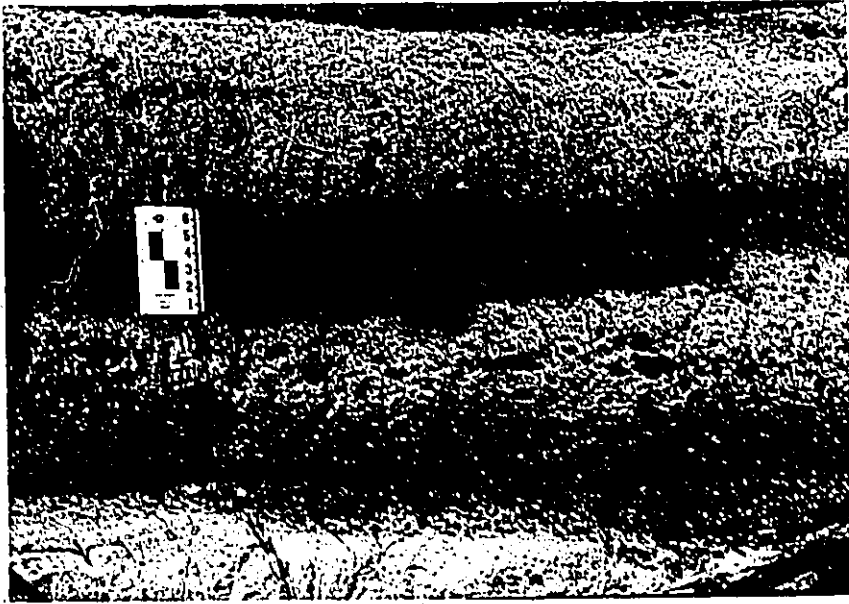


Fig.104 - Cross-section view of parallel stratification in fine conglomerate. Laminae defined by clast-supported and clast dispersed units. Bed 434 Anse à Pierre Jean, p.384

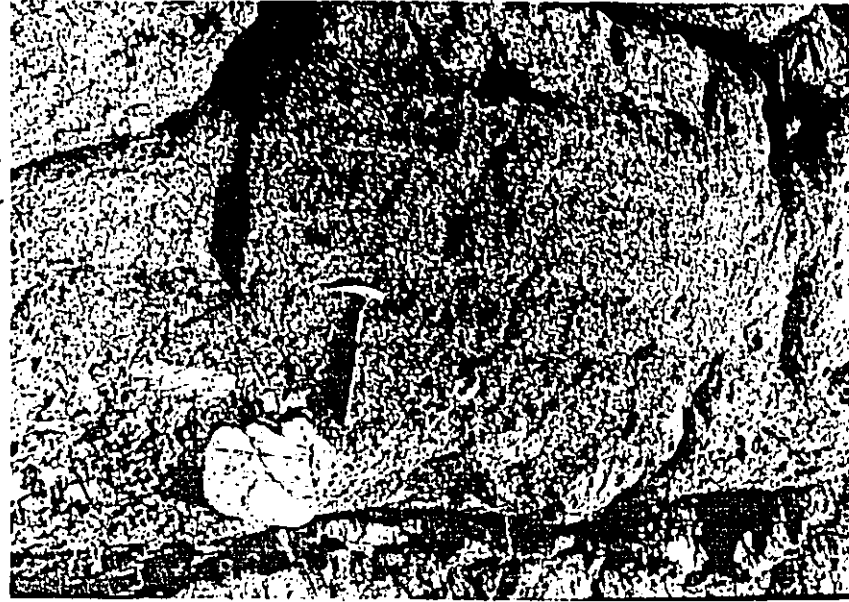


Fig.105 - Parallel stratification in a conglomerate- fine conglomerate bed. Laminae defined by alternating sizes of clasts. Hammer handle is about 30 cm long. Top of bed is up.



Fig.106 - Parallel stratification in medium sandstone (with some small scale ripple cross-lamination). Bed 196, Grève de la Pointe. Rectangles on the notebook are 10 cm long. Stratigraphic top is up, p.376

TABLE 23  
STRATIFICATION TYPES

| <u>Type of Stratification or Crossbedding</u> | <u>N Beds</u> | <u>% *</u> |
|-----------------------------------------------|---------------|------------|
| Well-defined Horizontal Stratification        | 403           | 50         |
| Vague Horizontal Stratification               | 247           | 31         |
| Low-angle, Oblique Crossbedding               | 112           | 14         |
| Vague low-angle, Oblique Crossbedding         | 14            | 2          |
| Irregularly Inclined Cross-stratification     | 125           | 16         |
| Trough Crossbedding                           | 300           | 37         |
| Scour Fill Stratification                     | 84            | 10         |
| Coarse Clast Stratification                   | 10            | 1          |
| Small-scale Convolute Lamination              | 45            | 6          |
| Large-scale Convolute Lamination              | 8             | 1          |

\* Note: percentages are calculated in terms of the number of stratified beds and not the total number of beds measured.

Slight differences in grain size point out the stratification. Individual layers or laminae are traceable along strike for distances between approximately 20-100 cm. Vague horizontal lamination may become better defined towards tops of beds.

Parallel stratification in many of the Facies (1), (2) and (3) pebbly sandstones and conglomerates is marked by an alternation of "clast supported" and "dispersed" (clasts are scattered in a finer bed or layer) clast layers (Fig.104). This type of stratification is best developed toward the base of beds rather than bed tops, although it may also occur in other bed portions. Layers average about 10 cm thick (range: few cm - 50 cm thick). This type of stratification is laterally more continuous than the "vague" parallel stratification and can commonly be traced for entire outcrop widths.

Parallel stratification marked by rows of larger pebbles or cobbles within finer clast-supported conglomerates and pebbly sandstones is rare. This type occurs in only 1% of the beds that are stratified (Table 23). Laminae or layers are one pebble or cobble thick and, in some cases, individual clasts protrude up above the general thickness of the layer. In these cases, the stratification is thought to be due to amalgamation of beds. In most instances, the coarse clast stratification appears to represent segregation of grain sizes within a single bed.

The last type of parallel stratification consists of layers in which there is a clear and distinct alternation of layers of different grain sizes. Layering in fine to medium sandstones is usually in the range of 1mm to several cm thick. In pebbly sandstones and conglomerates this type of stratification is marked by concentrated quartz pebble

trains or layers (Fig.105). In some fine sandstone layers the layer boundaries are parallel sided, whilst in other layers the boundaries are slightly wavy or undulating (Fig.106). Stratification which is defined by alternating sizes of grains is well defined and individual laminae or layers are commonly traceable across entire outcrop widths.

#### Low-angle Cross-stratification

Low-angle cross-stratification consists of alternating layers which are inclined at low angles, usually less than  $10^{\circ}$  but commonly  $4 - 5^{\circ}$ , to regional bedding. In most cases, low-angle cross-stratification occurs as a single set; rarely it occurs as two or three sets. Individual layers average about 0.5 to 1 cm in thickness. Within individual sets, the dips flatten off to near-horizontal at the base of the sets. Sets range in thickness from .1 m to greater than 1 m. This feature was found in 16% of the stratified beds (Table 23), with only 2% of the low-angle cross-stratification being vague.

#### Scour Fill Cross-stratification

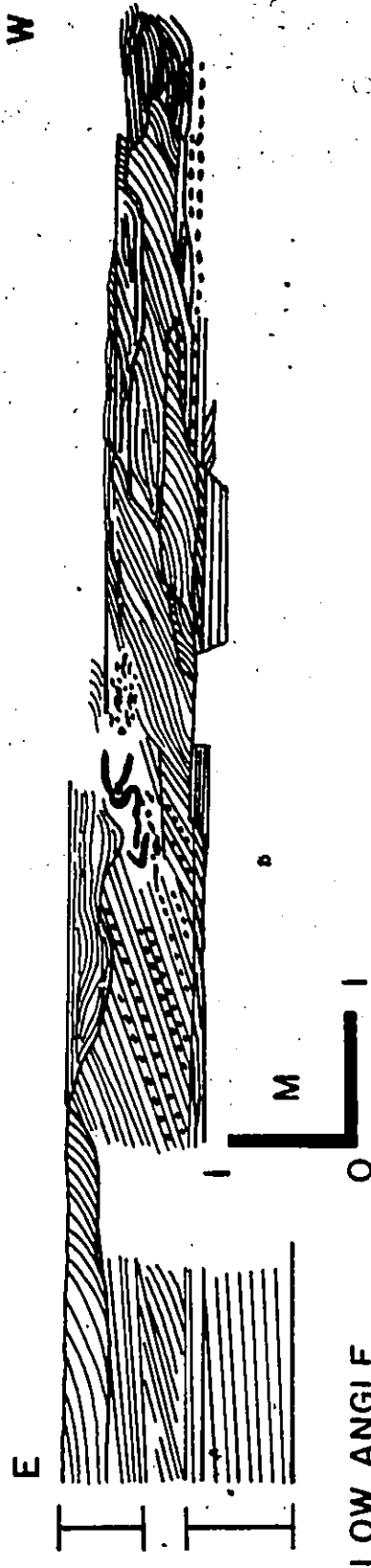
Scour fill cross-stratification consists of stratification which overlies scoured surfaces in which layers or laminae follow the outline of the scour. This type of crossbedding has been noted in material from fine sandstone to coarse conglomerate. The thickness of units with scour fill cross-stratification varies from a few cm to meters, with the upper thickness limit being delimited by the dimensions of the scour being filled. Many of the 'beds' with scour fill crossbedding are thought to be multiple in origin. This is suggested by the occurrence of finer grained laminae which are eroded out by coarser laminae and internal erosion features between laminae or layers.

### Trough Cross-stratification (Figs.107-109)

Trough cross-stratification is characterized by laminae or layers which are inclined at high angles to bedding in cross-sectional view. (Figs.107 - 109). In plan view, trough crossbed sets have horizontal traces which are curved (Fig. 24). Where ever plan views were available, all crossbed sets were identified as trough crossbeds. Individual sets vary in thickness from less than a cm to a maximum of 1 m. Trough crossbedding is commonly observed in stratified beds and occurs within 37% of the stratified beds (Table 23). Trough crossbedding may be classed as small-scale ( sets are a maximum of a few - 10 cm in thickness) or as medium-scale ( sets are 10's of cm to about 1 m in thickness).

(1) Medium-Scale Trough Crossbedding - (Figs.23,107) is thought to form by the migration of dune bedforms . Most of the medium-scale trough crossbedding occurs in fine pebble conglomerate and pebbly sandstone belonging to Facies (2) or (5), with less common occurrences in medium sandstone Facies (5) beds. Trough sets may occur singly or multiply, where up to six sets may be superimposed upon one another (Fig107). Average trough dimensions, as seen in plan view, were: 1.7 m long x 0.97m wide. Maximum trough dimensions in plan view were: 5.9 m long x 2.4 m wide. Average depth of crossbed sets, in cross-sectional view, was about 0.4 m (number of measurements = 141).

The average grain size of the coarse layers was 6 mm (fine conglomerate), whilst the average grain size of fine layers was 0.4 mm (medium sandstone). Layers averaged between 0.5 to 1 cm thick for the coarse grained layers, and 0.2 to 0.4 cm thick for the fine layers. Some



LOW ANGLE  
X.ST.

Fig.107- Multiple sets of ungraded, medium-scale trough crossbedding (Facies 5) in fine conglomerate. Crossbedding becomes low-angle inclined at the east end of the outcrop. Beds 331, 332, Grève de la Pointe. Paleoflow to the east-southeast, p.379

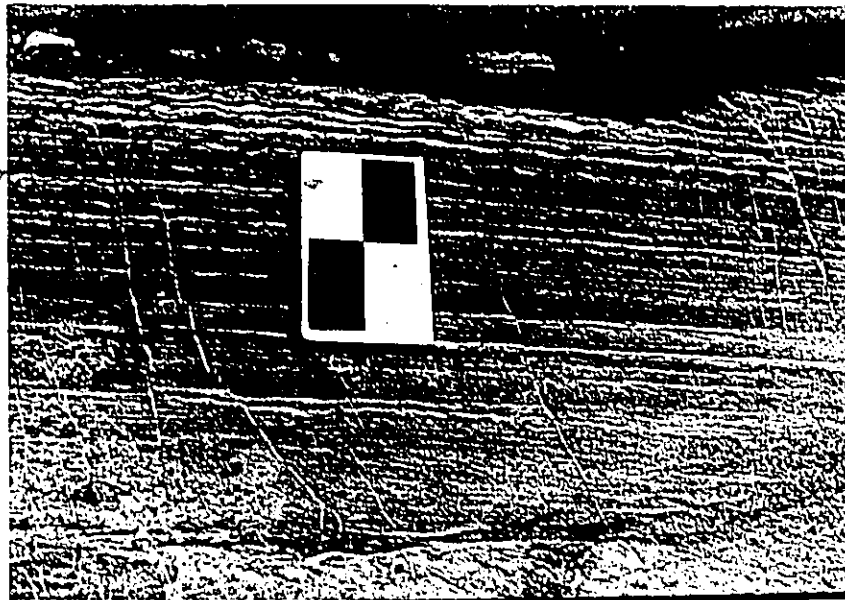
trough sets are scoured and/or loaded into underlying sediment. Where multiple sets occur there is commonly an erosional or reactivation surface between the sets (Figs.23,107).

The best exposure of plan views of medium scale troughs occur at the Cap à la Carré Ouest outcrop (eastern part) (Appendix 5). An excellent vertical exposure of multiple trough crossbed sets occurs at Grève de la Pointe (Fig.107). Load/scour bases of trough crossbeds are most common at the Grève de la Pointe outcrop; at other outcrops the bases are scoured or flat. Medium-scale trough crossbedding is common in graded beds belonging to Facies (2). This feature characterizes coarser Facies (5) beds.

(2) Small-Scale Trough Crossbedding ( Figs.108,109) - is thought to be the product of ripple or small dune migration. Most small-scale trough crossbedding occurs in medium to coarse sandstone, with less common occurrences in fine or very coarse sandstone. Ripple or small dune sets occur multiply within single beds and generally cross-cut one another. Ripple drift cross-lamination is very rare. Less commonly, small troughs occur as single sets. Most sets are less than 1 cm thick in the finer sediment. Units with small cross-stratification average 0.17 m thick (minimum unit thickness = 0.2 m; maximum unit thickness = 1.15 m). Individual laminae average 1-2 mm in thickness. In plan view small troughs are, on the average, 0.12 m long x 0.06 m wide.

Small-scale trough crossbedding may occur as part of graded sequences within classical turbidites (Facies 7), which are most common in the top part of Member III at Bic and in the Niveau 4 deposits at Grève de la Pointe. Small-scale trough crossbedding characterizes fine grained





347

Fig.108 - Small-scale trough cross-stratification (above Notebook).  
 Bed 311, Grève de la Pointe. Paleoflow is to the right.  
 Top of bed is up, p.379



Fig.109 - Small-scale trough crossbedding in cross-sectional view. Cap  
 à la Carre Ouest. Tape is 50 cm long. Between Sections 2  
 and 1. Paleoflow to the left, p.416

Facies (5) beds. These beds are also most common at the top of the Bic section (Member III) and at the top of the Grève de la Pointe section (Niveau 4).

#### Convolute Lamination (Figs. 110, 111)

Convolute laminations are small folds or contortions that affect individual laminations or layers within beds but not the entire bed (Pettijohn *et al.*, 1973). These features are thought to be intraformational folds. In the present study, convolute lamination occurs less commonly than most of the other stratification types. Only 7% of the stratified beds had convolute lamination (Table 23). This feature is most common in medium and fine sandstone classical turbidites (Facies 7). Convolute lamination is less common in fine conglomerate to pebbly sandstone beds and usually occurs at the bases of these coarser beds. These large scale convolutions (amplitudes generally from 0.5 m to several m) are commonly associated with fluid escape features of Facies 4 beds (Fig. 110). The small-scale convolute laminations in classical turbidites vary between a few cm and 0.3 m in thickness and occur in Bouma "c" divisions.

Small-scale convolute laminations are most common in classical turbidites at the top of the Bic section (Member III). Large scale convolute lamination is found in beds of Niveau 2 at Anse à Pierre Jean 5 (middle part) (Appendix 5), beds of Niveau 2 at Anse à Pierre Jean 1 (Appendix 5) and beds of Niveau 4 at Grève de la Pointe (Fig. 111).

#### Irregular Inclined Stratification (Fig. 112)

Irregular inclined stratification is stratification that may undulate up and down as seen in cross-section, but generally follows

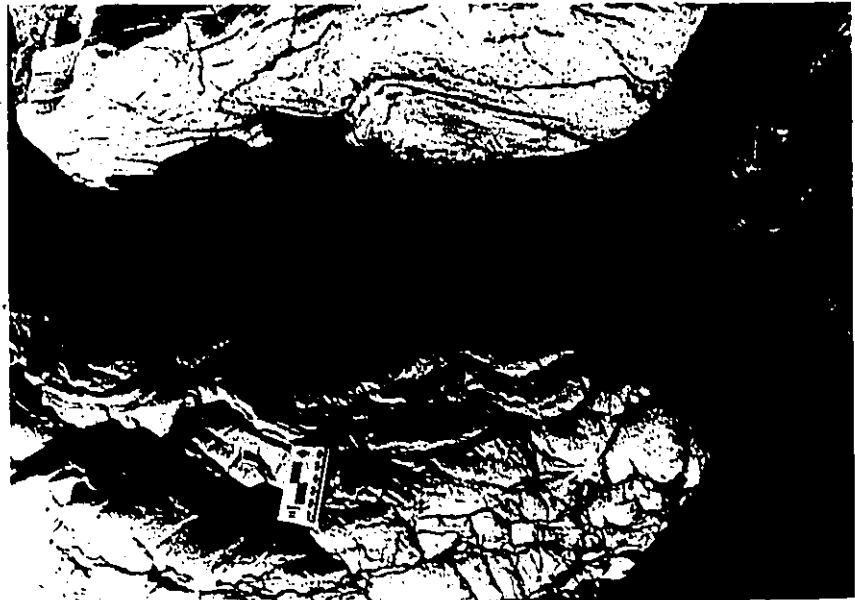


Fig.110 - Large-scale convolute lamination in cross-section. Bed 561, Anse à Pierre Jean 5. Top of bed is in shadow. The rectangles on the notebook are 5 cm long, p.390



Fig.111 - Large-scale convolutions in plan view. Bed 78, Grève de la Pointe. Rectangles on the notebook are 10 cm long, p.373

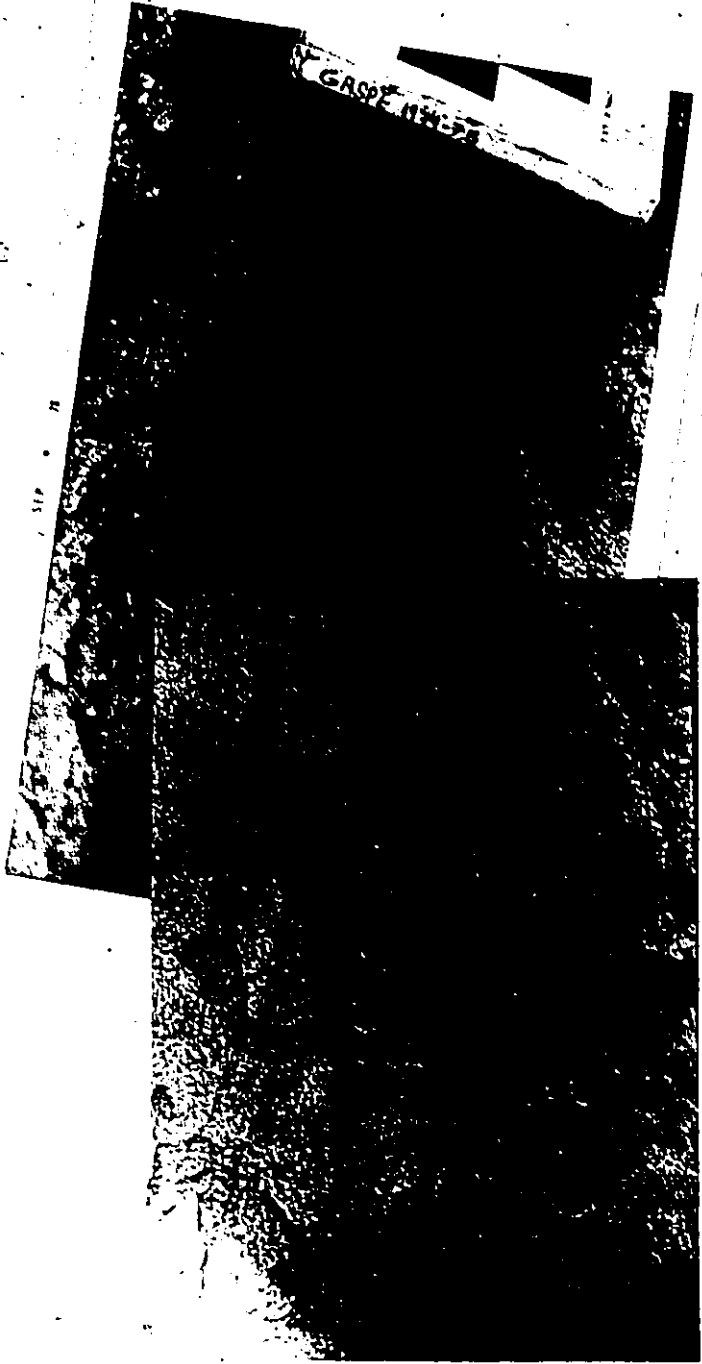


Fig. 112 - Irregular inclined stratification in cross-sectional view (above small scour). Bed 1421

Bic. Rectangles on notebook are 5 cm long. Paleoflow is to the left. Stratigraphic top is up, p. 422

the basal margin of the bed. In cross section it has a sweeping or wavy appearance. No plan views were seen of this feature. Laminations are usually between 0.5 and 1 cm thick and are commonly marked by quartz pebble or granule bands. This feature is most common in deposits that have many scours along the base of a bed, giving the basal margin a scalloped appearance when seen in cross section. Irregular inclined stratified units vary from a few cm to 0.4 m thick. Successive laminae tend to follow the form of the previous laminae. Generally the layering becomes less inclined to nearly horizontal upsection (with respect to bedding).

This type of stratification was observed in 16% of the stratified beds. Most of these beds are classed as belonging to Facies (2) or Facies (3) pebbly sandstones and conglomerates. It is rarely observed in Facies (6) beds. Laminae are generally well defined and traceable for many meters along strike.

#### TEXTURAL FEATURES

Textural features refer to the distribution and orientation of individual grains within beds. In the present study, the sizes of the coarse fraction within beds was measured at various intervals in the field. These data are plotted on the measured sections (Appendix 5) with methods described in Appendix 1.

The distribution of the coarse fraction upsection within individual beds is referred to as "grading." Beds may be classed as inversely graded, normally graded, abrupt normally graded or complexly graded. In addition to describing the grading patterns, one may consider how concentrated the coarse fraction is within a bed. Beds in which the

coarse clasts touch one another are called "clast supported." In beds where coarse clasts do not touch one another are called "dispersed."

The final aspect to consider when looking at the textural features of beds is the orientation of individual grains -- the sedimentary fabric, which is discussed in Chapter 4 of the thesis text.

#### Distribution of the Coarse Fraction Within Beds

The distribution of the coarse fraction within beds (as seen in the field) can be a simple gradation from the base to the top of a bed. This is called simple grading. Alternatively, a bed may show different subunits, which are themselves graded. Such beds would be considered to be multiply or complexly graded. Grading may also occur within small restricted zones of an otherwise homogeneous or slightly graded bed. This type of grading may occur in the basal few to 10's of cm of a bed or at the top few cm of a bed. In cases where the grading occurs suddenly at the base or top of a bed, the bed is said to be "abruptly graded." Various combinations of simple and multiple grading patterns were observed within the Cap Enragé sediments. Eleven different types of grading patterns were noted, of these the eight major patterns will be described in the following section. The occurrence of a dispersed versus clast-supported texture will be discussed in conjunction with the grading patterns. It must be emphasized that the following grading patterns are based upon the distribution of the coarse fraction as observed in the field and do not account for the fine grained or total distribution of sizes within beds. See Figure 113 for examples of grading.

(1) Ungraded Beds - are homogeneous and show no change in the grain size as observed in the field. Ungraded beds are the second most

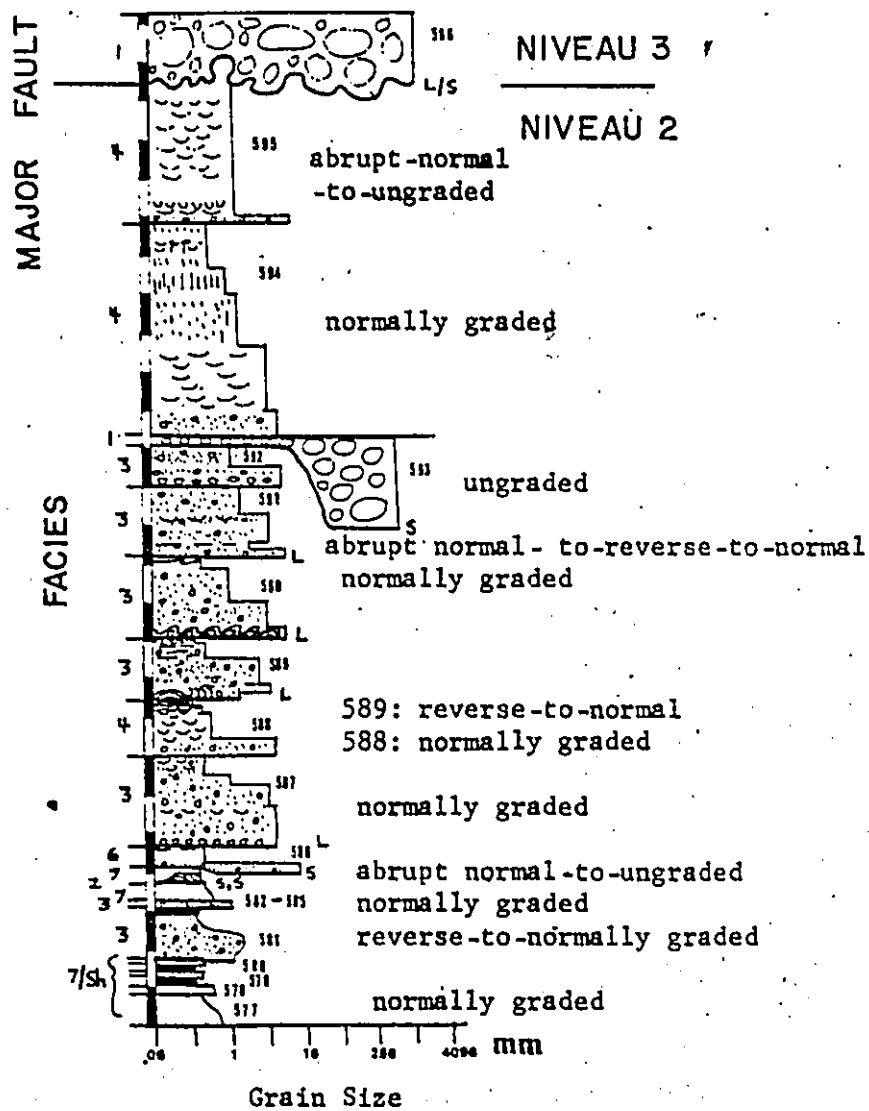



Fig.113 - Example of different grading types. Section 3 Anse à Pierre Jean 5, Niveau 2. Bed numbers indicated to the right of the stratigraphic column. Scale bars are in metres. L- loaded base; S- scoured base; L/S-loaded and scoured base.



common type of "grading" observed in the present study. Grain size of ungraded beds was commonly conglomerate and fine conglomerate as well as fine to coarse sandstone (Table 24). Most of the ungraded beds had flat bases (66%). Less commonly ungraded beds had scoured (26%) bases or rarely had load and load/scour bases. Ungraded beds had an average bed thickness of 0.82 m (Fig.114) (maximum thickness = 12 m, minimum thickness = 0.05 m). Few ungraded beds showed a dispersed texture (63 beds, 16.5%). All of the Facies (5) beds are ungraded. Over a third of the Facies (1) conglomerates are ungraded. All beds of other facies have about  $\frac{1}{2}$  of the beds classed as ungraded.

(2) Inversely Graded Beds or Reverse Graded Beds - rarely occur in beds measured in the present study. Simple reverse graded beds, in which the whole bed is reversely graded, account for only 2% (29 beds) of the measured beds. Reverse graded conglomerate was the most common type of sediment which displayed this grading. Less common sediment types were reverse graded fine conglomerate-to-conglomerate and reverse graded pebbly sandstone-to-fine conglomerate. Transitions between other grain size classes rarely occurred. Most of the simple reverse graded beds had flat bases (50%), with less commonly scoured (27%) or loaded (11.5%) bases. Irregular bases are rarely associated with reverse graded beds. Simple reverse graded beds had an average bed thickness of 1 m (Fig.115) (maximum thickness = 4.1 m, minimum thickness = 0.4 m). Over one-third (35.7%) of the simple reverse graded sediments displayed a dispersed texture in some part of the beds, generally at the base. Most reverse graded beds belong to Facies (1).



TABLE 24  
GRAIN SIZE OF UNGRADED BEDS

| Grain<br>Size<br>Class | N Beds | % *  |
|------------------------|--------|------|
| C                      | 58     | 14.9 |
| FC                     | 83     | 21.2 |
| PS                     | 29     | 7.4  |
| VCS                    | 33     | 8.5  |
| CS                     | 53     | 13.6 |
| MS                     | 65     | 16.7 |
| FS                     | 67     | 17.2 |
| VFS                    | 2      | 0.5  |

\* Note: Percentages calculated in terms of the number of ungraded beds. Abbreviations for grain size classes as in Table .

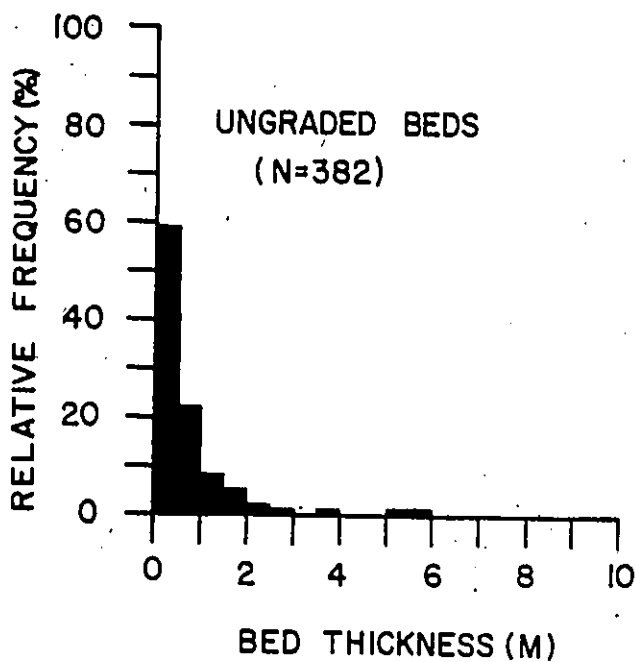


Fig.114- Bed thickness distribution of ungraded beds.

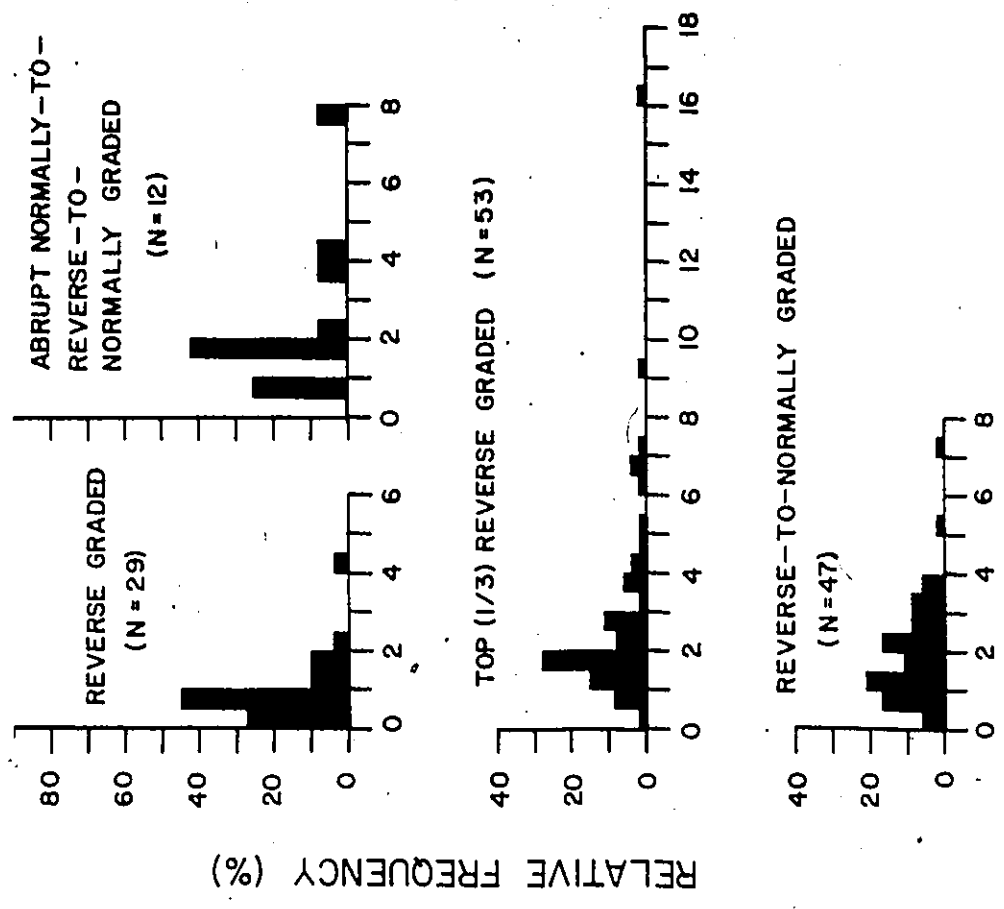


Fig.115 - Bed thickness distribution of beds with grading in some portion of the bed.

(3) Top Reverse Graded Beds - are those beds in which the upper one-third of the bed is reversely graded. This type of grading was noted in 3.9 % (53 beds) of the measured beds. Graded fine conglomerate-to-pebbly sandstone, which became coarser at the top, was the most common type of sediment type. Less common occurrences involved alternations between the following grain size classes: conglomerate-to-fine conglomerate, which became coarser grained upsection; fine conglomerate-to-pebbly sandstone-to-fine conglomerate; conglomerate-to-coarse sandstone-to-very coarse sandstone; and, coarse sandstone-to-medium sandstone-to-coarse sandstone. Transitions amongst other grain size classes are rare, usually with only single occurrences. Most of the top reverse graded beds had flat bases (39.2%), with less commonly scoured (33.3%) or loaded (23.5%) bases. Load/scour and irregular bases are rarely associated with beds of this type of grading. Average bed thickness was 2.91 m (Fig.115) (maximum thickness = 16.1 m, minimum thickness = 0.5 m). Grading patterns in the lower portions are varied: graded-to-top reverse graded is the most common association, with less common occurrences of reverse graded-to-graded-to-top reverse graded. Most of beds with top reverse grading also displayed a dispersed texture within some portion of the bed and are commonly classed as Facies (3).

(4) Normally Graded Beds - are beds in which the grain size gets finer upsection. This is the most common type of grading logged in the present study, with 589 beds (43.4%) being normally graded. Graded fine conglomerate-to-medium sandstone and graded conglomerate-to-fine conglomerate were the most common sediment types. Less common transi-

tions consisted of graded fine conglomerate-to-coarse sandstone; graded fine conglomerate-to-fine sandstone; graded fine conglomerate-to - very coarse sandstone; and, graded medium sandstone-to-fine sandstone,

Transitions amongst other grain size classes are less frequent or rare. Over a third of the normally graded beds showed a dispersed texture within some portion of the beds.

Over half of the normally graded beds had flat bases (56.4%). Less common were beds with scoured (26.7%) or loaded (11.6%) bases. Load/scour and irregular bases rarely occurred. Average bed thickness was 1.41 m (Fig.116) (maximum thickness = 11.5 m, minimum thickness = 0.2 m). Over three-quarters of the Facies (7) beds are normally graded (with respect to the coarse fraction as seen in the field). Over half of the Facies (2), (3) and (4) show normal grading. Normal grading was noted in over a third of the Facies (1) beds and was less common in beds of Facies (6).

(5) Abrupt Normally Graded Beds - are those beds which grade suddenly at the base of the bed, with overlying portions of the bed being ungraded or slightly normally graded. This type of grading is the third most common type of grading noted, with 174 beds (12.9%) being abruptly normally graded. Abruptly graded fine conglomerate-to-medium sandstone was the most common transition. Less common associations consisted of fine conglomerate-to-fine sandstone; conglomerate-to-very coarse sandstone; and, fine conglomerate-to-coarse sandstone. Transitions amongst other grain size classes are less frequent or rare. Most of the abrupt normally graded beds had flat bases (60%), with less commonly scoured (26.5%) or loaded (10%) bases. Load/scour

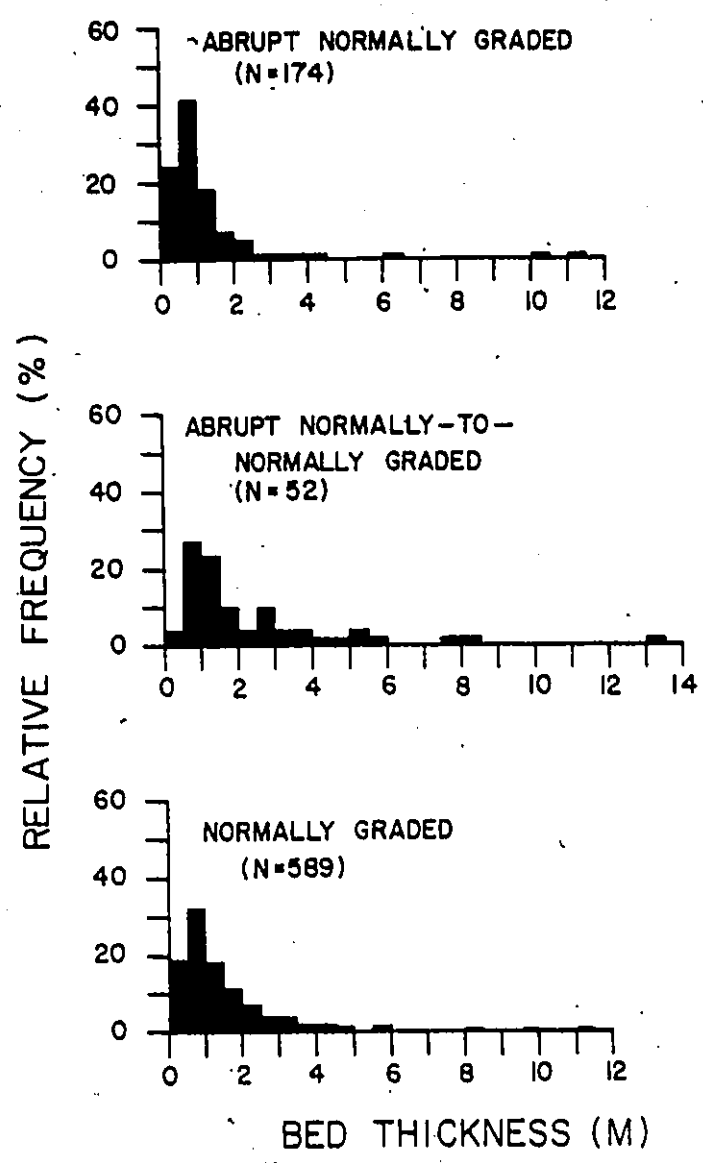


Fig.116 - Bed thickness distributions of beds with normal grading.

and irregular bases are rare. Average bed thickness was 1.11 m (Fig.116) (maximum thickness=11.3 m, minimum thickness = 0.2 m). About 44% of the abrupt normally graded beds showed dispersed texture within some portion of the bed. Most of the abrupt normally graded beds were classed as Facies (6). Less commonly beds were classed as belonging to Facies (2), (3) and (4). Rarely abrupt normally graded Facies (1) and Facies (7) beds were noted.

(6) Abrupt Normally Graded-to-Normally Graded Beds - are those beds which grade suddenly at the base of the bed, with overlying portions of the bed being normally graded. This grading pattern is the fourth most common type of grading type noted, with 52 beds (3.9%) classed in this category. Most of the beds consisted of fine conglomerate, abruptly graded -to- medium sandstone-to-fine sandstone, Less common associations were fine conglomerate, abruptly graded, -to- coarse sandstone-to-fine sandstone and conglomerate, abruptly graded, -to-coarse sandstone-to-medium sandstone, Transitions amongst other grain size classes are very rare.

Most of the beds had flat bases (47%), with less commonly scoured (27.5%) or loaded (17.7%) bases. Load/scour bases are rare. Average bed thickness was 2.38 m (Fig.116) (maximum thickness = 13.2 m, minimum thickness = 0.4 m). Many of the abrupt normally graded-to-graded beds (48%) showed a dispersed texture in some portion of the bed. Most of the beds with this grading pattern were classed as belonging to Facies (6).

(7) Reverse Graded-to-Normally Graded Beds - are reversely graded in the lower third of the bed, with overlying portions of beds being nor-

mally graded. This type of grading is less common than the patterns discussed above, with only 47 beds (3.5%) being reverse graded-to-normally graded. Most of the beds were conglomerate, . Less common associations consisted of reverse graded-to-graded conglomerate-to-fine conglomerate; fine conglomerate-to-conglomerate-to coarse or medium sandstone; and, reverse graded fine conglomerated, graded, -to-medium sandstone. Transitions amongst other grain size classes are very rare.

Over half of these reverse-to-normally graded beds had flat bases (53.2%) with less common occurrences of scoured (27.7%) or loaded (15%) bases. Irregular bases are rare. Average bed thickness of beds with this grading type was 2.03 m (Fig.115) (maximum thickness = 7.5m, minimum thickness = 0.4m). Most of the beds that show this grading pattern are the Facies (1) conglomerates or the Facies (2) fine conglomerates.

(8) Complex Multiply Graded Beds - rarely occur in the Cap Enrage sediments and were only observed in 1% of the beds that were measured. The most common complex grading pattern was abrupt normally graded-to-reverse graded-to-normally graded. Most of these beds involved alternations amongst fine conglomerate, pebbly and medium sandstones. Bases of the beds were usually scoured. Average bed thickness was 1.8 m (maximum thickness = 7.49m, minimum thickness = 0.5 m). Beds with complex grading patterns were slightly more common in Facies (3) and (4) beds.

Chaotic Mixture of Grain Sizes (Fig.117)

Chaotic mixtures of different grain sizes within single beds rarely occur within the Cap Enragé sediments. This type of feature was observed in the following sections (Appendix 2): one bed in Niveau 2 at the Anse à Pierre Jean 5 outcrop; one bed at the contact between Niveau 3 and Niveau 4 at Rivière Trois Pistoles outcrop; and two beds at the Grève de la Pointe outcrop ( Niveau 2 and Niveau 4). All beds with this feature had scoured bases . In two cases (Anse à Pierre Jean 5 and Grève de la Pointe, Niveau 2) beds were part of multiple channel fills. Chaotically mixed units varied in thickness from 0.6 to 1.6 m, with an average thickness of 1.02 m. Upper surfaces of chaotic units were irregular, scoured, loaded or flat. Mixtures ranged in size from conglomerate to coarse sandstone. Shale rafts were also common in chaotically mixed zones, many of which are very contorted. Clasts of a given size may occur singly or as irregular distorted pockets (most likely coarse grained intraclasts or internal load features). Grain sizes varied drastically both in lateral and vertical directions with no apparent ordering or segregation of sizes. In the field, grain fabric appears to be completely disorganized.





Fig.117 - Slump bed which begins just above hammer head. The bed consists of contorted shale clasts and chaotic mixture of pebbles and sandstone. Bed 383, Rivière Trois Pistoles. Hammer handle is 35 cm long. Stratigraphic top is up, p.381

## APPENDIX 5

OUTCROP MAPS AND STRATIGRAPHIC SECTIONS

All of the sections measured in the present study are drawn on the following pages. Most of the sections are preceded by respective outcrop maps. The Grève de la Pointe outcrop map was traced from aerial photographs (scale 1:10,000) of the coastline. All other outcrop maps were drawn in the field as pace-and-compass maps. No outcrop maps were made of the following sections: Rivière Trois Pistoles, Anse à Pierre Jean 1, Niveau 2, Anse aux Saumon Est and Bic.

Topographic maps of the study area are given on the Trois Pistoles 22 C/3 (edition 2) and Rimouski 22 C/7 (edition 2) 1:50,000 scale maps (Canada Map Office, Department of Energy, Mines and Resources, Ottawa). Aerial photographs are as follows (scale 1:10,000): Bic 'type' section - Roll Q76-120, numbers 168,180; Anse à Pierre Jean to Cap à la Carre - Roll Q76-121, numbers 38 through 47; and Grève de la Pointe - Roll Q76-121, numbers 15 through 17 (Ministère des Terres et Forêts, Service de la Cartographie, Photo-cartothèque provinciale, Québec).

Outcrop Map Key

- Shaded map portions indicate outcrops where sections were measured.
  - Striped outcrop patterns indicate covered sections.
  - Solid road lines are major paved roads. Dashed road lines are dirt road, passable by car. Dotted road lines are dirt roads or paths, impassable by car.
- N2, ..., N6: indicate stratigraphic 'niveau' as defined by Mathey (1970) in the St. Simon area. M I, M II, M III: indicate stratigraphic members as defined by Lajoie (in press) in the Bic area.

Numbers and letters in brackets ( ) are survey marks painted on the rocks in the field.

1,2,3, ... : indicate section numbers at specific outcrops. Outcrop area covered under each section is encompassed by heavy, solid lines.

Along generally isolated coastlines, prominent cottages are indicated

as:



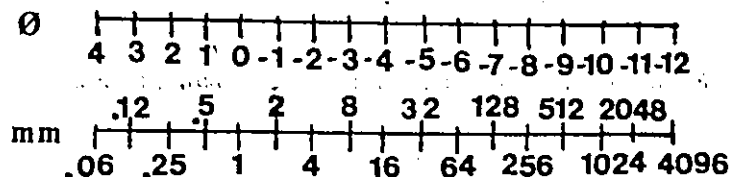
Faults are drawn with apparent direction offset and amount of offset, according to respective map scales.

T: Tectonized section

Dashed lines on the outcrops indicate boundaries between different 'niveau.'

#### Stratigraphic Section Key

Vertical scale is in metres, where 1 bar = 1 m.



Horizontal scale is grain size. Data were plotted as φ units.

The horizontal and vertical scales are the same for all of the sections.

Facies numbers are designated to the left of the metre scale.

Bed numbers are indicated to the right of the sections. Beds are bounded by horizontal lines to the left of the metre scale (between these lines is the facies number). As many beds were measured at more than one location (and bed grain size and facies character may change with location), a new number is usually assigned to each new measurement. Bed numbering is generally from the base to the top of each section. Numbers are the lowest at the Grève de la Pointe section and highest at the Bic section.

Correlative beds or bed portions on single diagrams are joined by solid tie lines. Correlative beds or bed portions on different diagrams are indicated by solid arrows (  $\xrightarrow{212}$   $\xleftarrow{135}$  ).

The north arrow refers only to the orientation arrow, not the outcrop orientation.

Sections which are continued on other diagrams are indicated by arrows

as follows:  $\begin{array}{c} 28 \uparrow \\ \vdots \\ 27 \downarrow \end{array}$  : the next succeeding bed is Bed number 28  
 : the immediately preceding bed is Bed number 27.



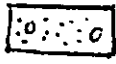

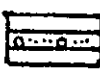

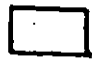

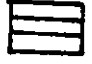


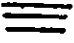


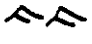
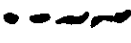


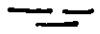


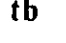

Distances between sections are indicated in metres ( 107M ).

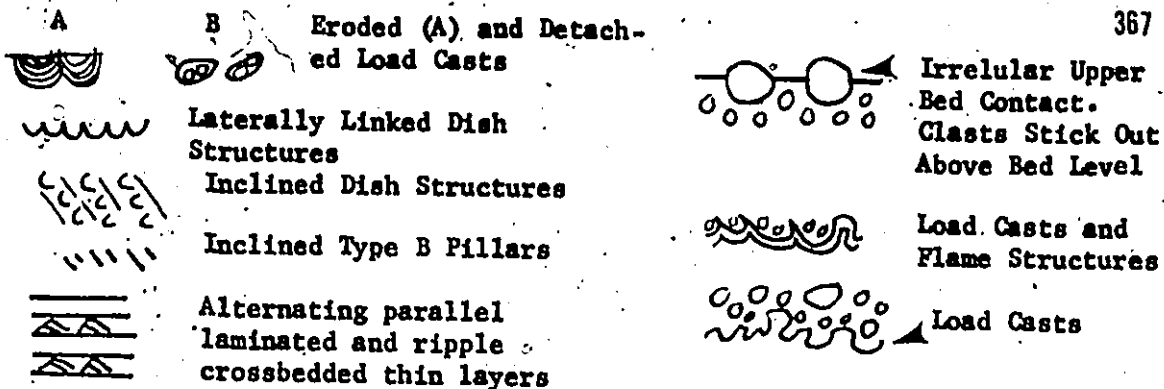
Blank section areas indicate covered intervals.

#### Internal structures of beds:

With the exception of the classical turbidites, all of the internal

structures of the individual beds are drawn on these sections. Key is:

|                                                                                     |                                                                       |                                                                                      |                                                                                                                |
|-------------------------------------------------------------------------------------|-----------------------------------------------------------------------|--------------------------------------------------------------------------------------|----------------------------------------------------------------------------------------------------------------|
|  | Structureless Conglomerate                                            |  | Dish Structures                                                                                                |
|  | Dispersed Texture                                                     |  | Sheet Structures                                                                                               |
|  | Stratification Defined by Alternating concentrated/dispersed layers   |  | Type B Pillars                                                                                                 |
|  | Structureless                                                         |  | Branching Type B Pillars                                                                                       |
|  | Stratification Defined by Alternating layers of Different grain sizes |  | Irregular Type B Pillars                                                                                       |
|  | Low-angle, inclined Crossbedding                                      |  | Horizontal Fluidization Channels                                                                               |
|  | Trough Crossbedding                                                   |  | Dish structures with Type A pillars                                                                            |
|  | Ripple Crossbedding                                                   |  | Shale intraclasts                                                                                              |
|  | Medium-scale trough crossbedding                                      |  | Shale layer                                                                                                    |
|  | Vague stratification                                                  |  | Tectonized                                                                                                     |
|                                                                                     |                                                                       |  | Convolute Lamination                                                                                           |
|                                                                                     |                                                                       |  | tb classical turbidite bed, only indicated on thicker turbidites to avoid confusion with thick, Facies 6 beds. |
|                                                                                     |                                                                       |  | Irregularly inclined Crossbedding                                                                              |



### Bases of Beds:

Notation to the right of the stratigraphic section. Letters indicate different types of basal contacts as follows.

- S - scoured base; L - loaded base; L/S - loaded and scoured base;
- I - irregular base, due to irregular upper bed contact of previous bed. Absence of a letter means that the bed has a flat base.

### Paleocurrent Data:

These data are plotted to the right, generally speaking, of the stratigraphic sections. Position of the paleocurrent determination is indicated by a dashed line. Key to the paleocurrent data is as follows.

- FB Field fabric measurement of conglomerate unit.
- FB Lab fabric measurement of sandstone or pebbly sandstone unit. Grand Vector-Mean is plotted for unimodal bedding plots. Dominant modes are plotted for bimodal bedding plots.
- FB Dotted lines indicate Grand Vector Mean as calculated from random bedding plots. Arrows indicate flow direction as obtained from imbrication plots.
- Line of Motion paleocurrent data.
- Vectorial paleocurrent data.

Letters near the paleocurrent lines and vectors indicate the type of structure from which the paleocurrent information was obtained, i.e. RF

Although the vector mean directions are insignificant in random plots, the computed values were plotted to provide a reference direction for imbrication data.

Source of paleocurrent data:

F - Flute Mark; G - Groove Mark; HR - Harrow Marks; ID - Inclined Dish Structure Units; IT - Inclined Fluid Escape Tubes; LR - Longitudinal Ridges; EL - Parting Lineation; R - Ripple Mark, paleocurrent obtained from dip of stratification as seen in cross-section; RF - Rib-and-Furrow Marks, refers to plan views of both small- and medium-scale trough crossbedding; SA - Scour Axis, taken as the strike of the axis of a scour; SP - Scour Plane, taken as the strike of the side of a scour surface; ST - Sheet Structure; T - Trough Crossbedding, paleocurrent obtained from dip of crossbedding of medium-scale trough crossbeds as seen in cross-section; IMB - trend of apparent field imbrication as seen by eye.

All paleocurrent data was rotated about strike through the angle of dip back to the horizontal (regional strike and dip for each bed was used in this rotation). All of the paleocurrent data are plotted with respect to the north arrows indicated on each section. Any paleocurrent data not found in these sections, but given on the generalized model sections in the text, are from Davies (1972) or Johnson (1974).

Other Notation:

- - - - - A,B,C,D replicate samples for fabric analyses from same bed.
- gs = 107 mm 1037 grain size = 107 mm for Bed 1037
- (235) bed correlation obtained by comparison of sections, not a field correlation
- Sh Shale Unit
- FIG.11 | Line drawing of indicated stratigraphic section given in the thesis text.
- ◆ Grain Size Analysis in thin section; ▲ Petrologic Analysis

TYPES OF CLASSICAL TURBIDITES

Key: 16 (abc) = Bed 16 is an abc turbidite

16 (abc), 22 (abc), 26 (abc), 70 (abc), 80 (b), 111 (ab), 118 (abc),  
 119 (abc),<sup>3</sup> 121 (abc), 135 (b), 146 (abd), 148 (abe), 149 (be), 150 (be),  
 151 (abc), 156 (abc), 157 (bc), 158 (bc), 159 (acd), 166 (bc), 173  
 (abcd), 174 (b), 180 (abc), 181 (b), 184 (abcd), 185 (abcde), 189 (abc),  
 198 (ac), 199 (abc), 200 (abc), 201 (abc), 208 (c), 209 (ac), 211 (bc),  
 214 (abc), 215 (abc), 223 (ab), 229 (abc), 249 (ab), 252 (ab), 254 (abc),  
 260 (ab), 290 (acd), 293 (abc), 297 (abc), 321 (ac), 328 (ac), 333  
 (abcd), 336 (abc), 345 (abe), 346 (abe), 349 (abc), 350 (abc), 354 (abc),  
 357 (abc), 359 (ab), 360 (abc), 364 (ac), 365 (abc), 367 (ac), 373 (ac),  
 376 (ac), 378 (ac), 380 (abc), 399 (ab), 407 (b), 408 (ab), 409 (b),  
 411 (ab), 413 (bce), 414 (be), 508a (bc), 513 (bc), 514 (bc), 535 (abe),  
 537 (bce), 577 (ab), 578 (abe), 579 (abe), 580 (ae), 583 (ab), 585 (ab),  
 742 (abce), 743 (be), 744 (be), 745 (be), 765 (be), 769 (be), 817 (abce),  
 834 (bce), 846 (bc), 861 (ac), 1060 (abc), 1033 (ab), 1072 (acd), 1141  
 (ac), 1219 (ab), 1244 (bc), 1265 (abc), 1266 (ab), 1270 (be), 1271 (be),  
 1272 (b), 1275 (abc), 1286 (ac), 1312 (ac), 1313 (ab), 1314 (ab), 1315  
 (b), 1316 (abc), 1317 (ac), 1318 (ab), 1329 (abcde), 1349 (bce), 1405  
 (abce), 1408 (abc), 1414 (abc), 1428 (ab), 1433 (be), 1444 (ac), 1445  
 (abc), 1445a (bc), 1449 (acd), 1450 (acd), 1454 (abc), 1461 (ac), 1463  
 (abc), 1464 (abc), 1465 (abc), 1467 (ac), 1468 (abc), 1476 (ac), 1476a  
 (bc), 1488 (abc), 1489 (abce)

CHRONOLOGICAL ORDER OF SANDSTONES AND SHALES AT THE TOP OF BIC SECTION

These beds immediately overlie bed 1489, see top of Bic Member III.

Key: Sh -shale bed, 5 - ungraded, crossbedded sandstone, all other beds are classical turbidites, with the type of sequence indicated.

Sh  
 ae  
 cde  
 Sh  
 ce  
 bce  
 Sh  
 5  
 Sh  
 5  
 Sh  
 5  
 Sh  
 5  
 abce

↑  
up

Upper Part

Tectonized (T)

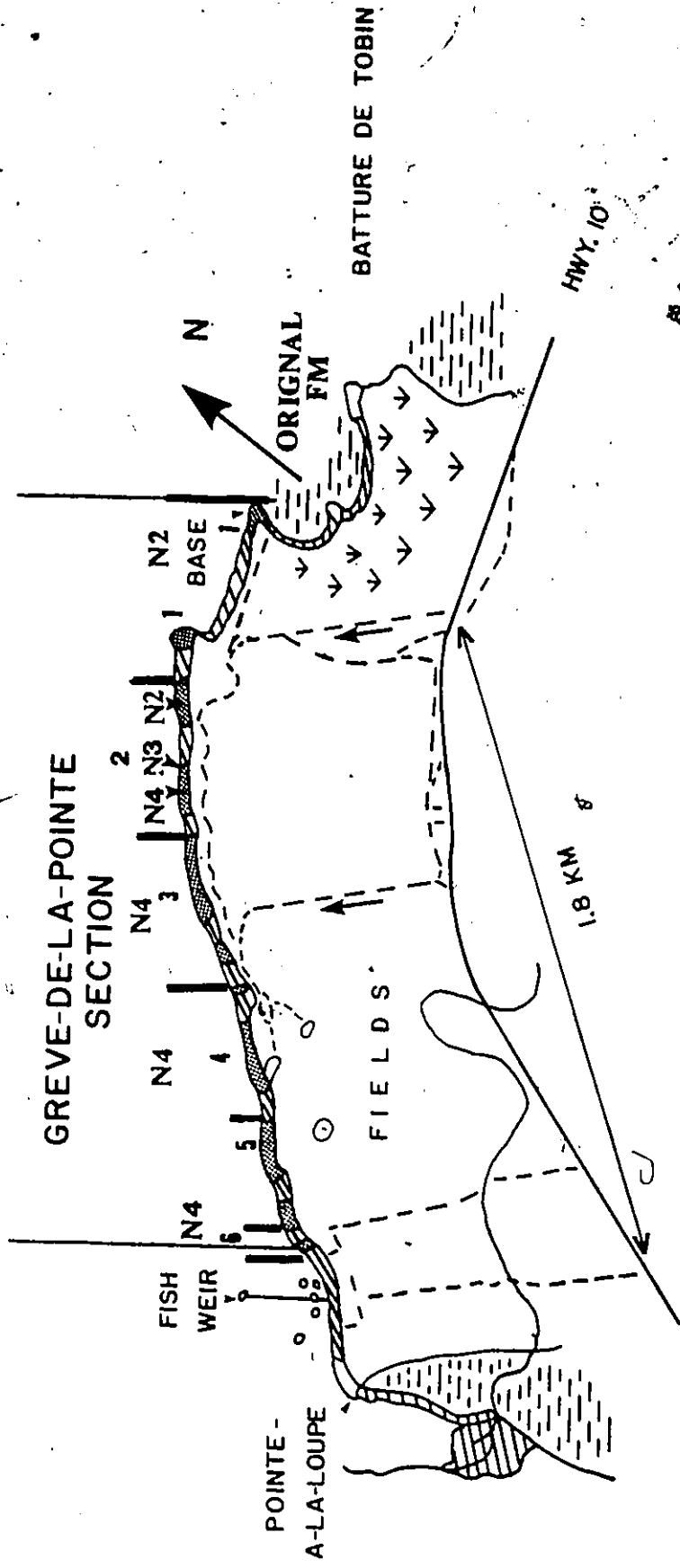
Sh  
 ae  
 Sh  
 ace  
 abe  
 ace  
 Sh  
 ace  
 Sh  
 ae  
 be  
 ac  
 Sh  
 5  
 Sh  
 ace  
 Sh  
 5  
 Sh  
 5  
 Sh  
 5  
 ace  
 acde  
 abc  
 Facies 4, Bed 1494  
 abce  
 Sh  
 5  
 Sh  
 ae  
 Sh  
 5  
 Sh  
 bce  
 ae  
 ae  
 Sh  
 Bed 1489

↑  
up

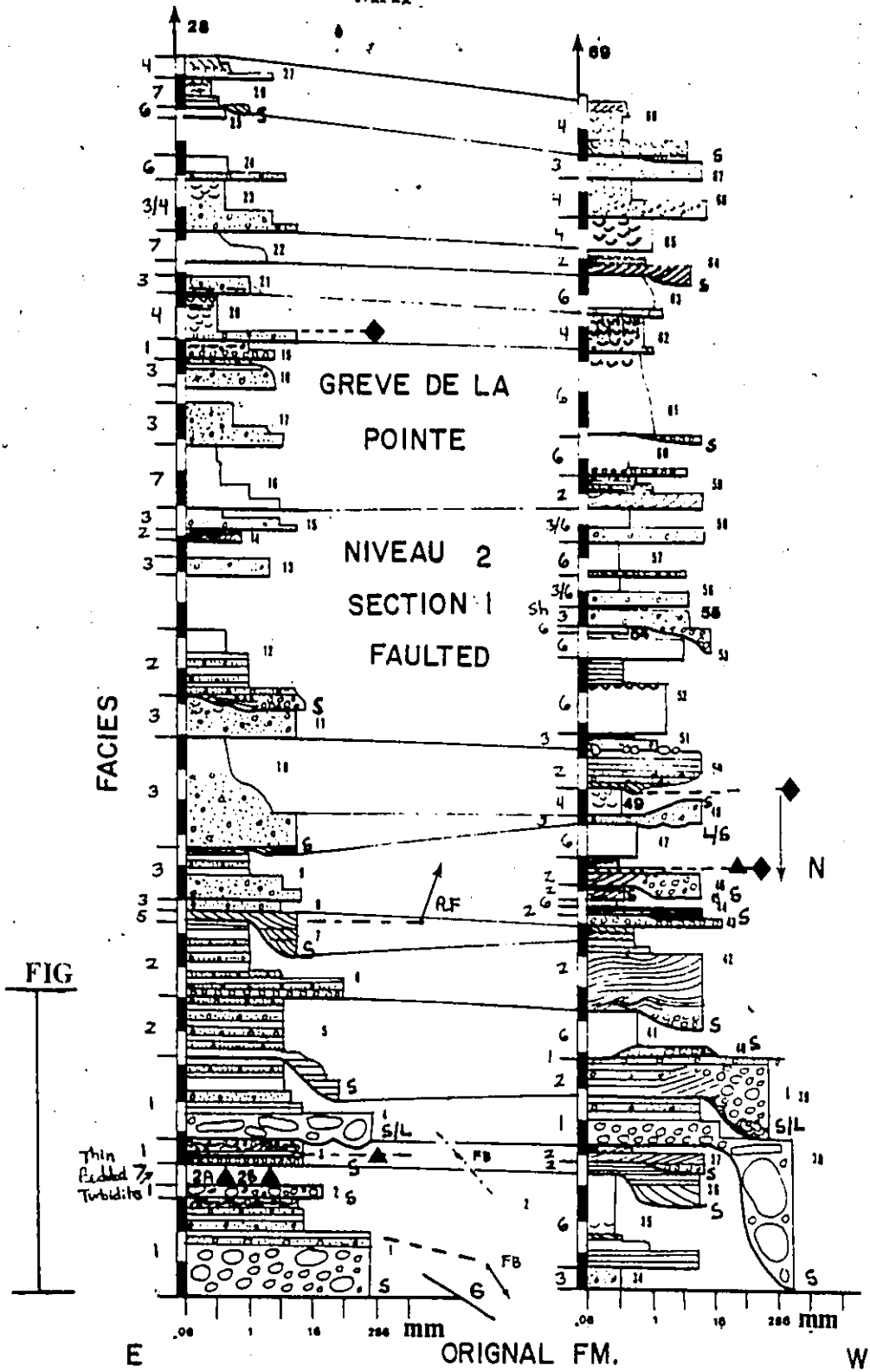
Lower Part

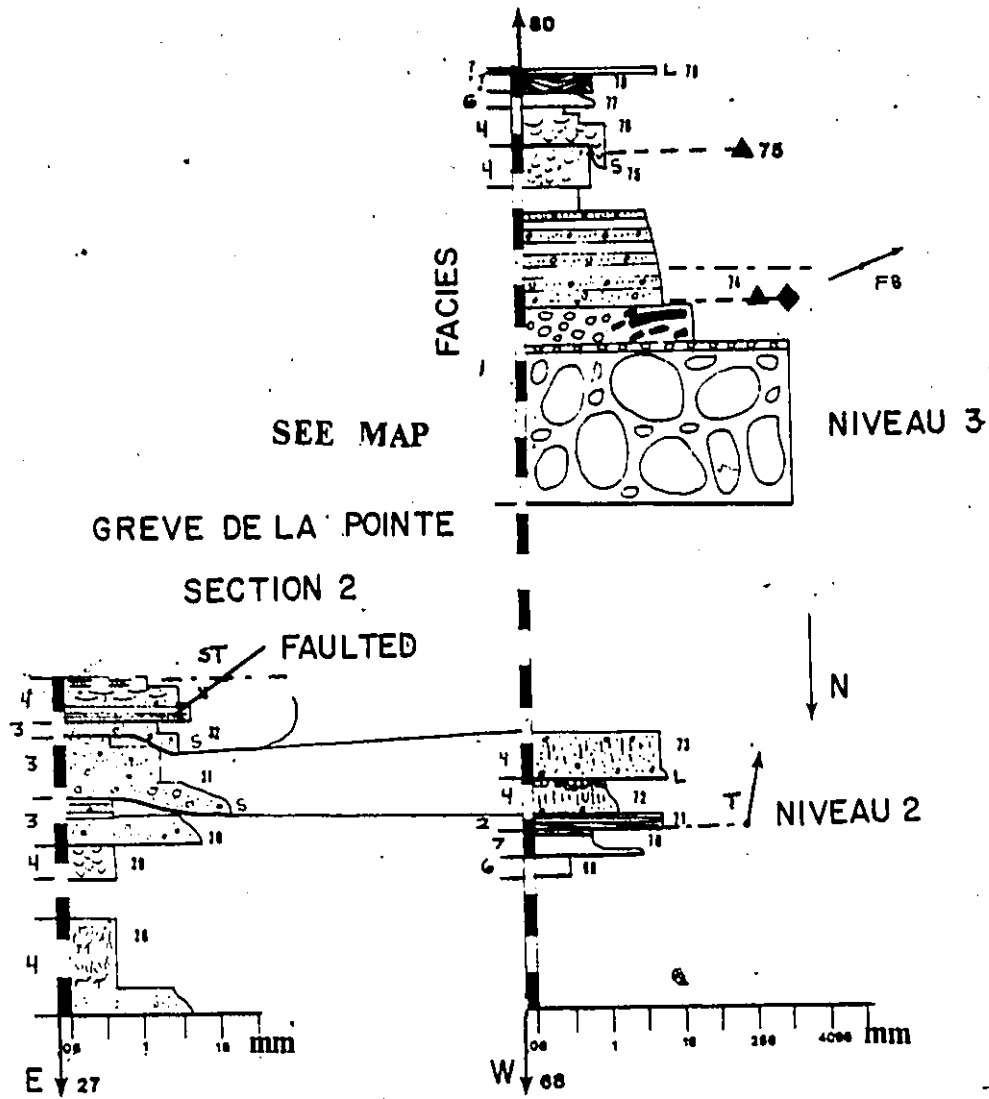
Drafted as one unit

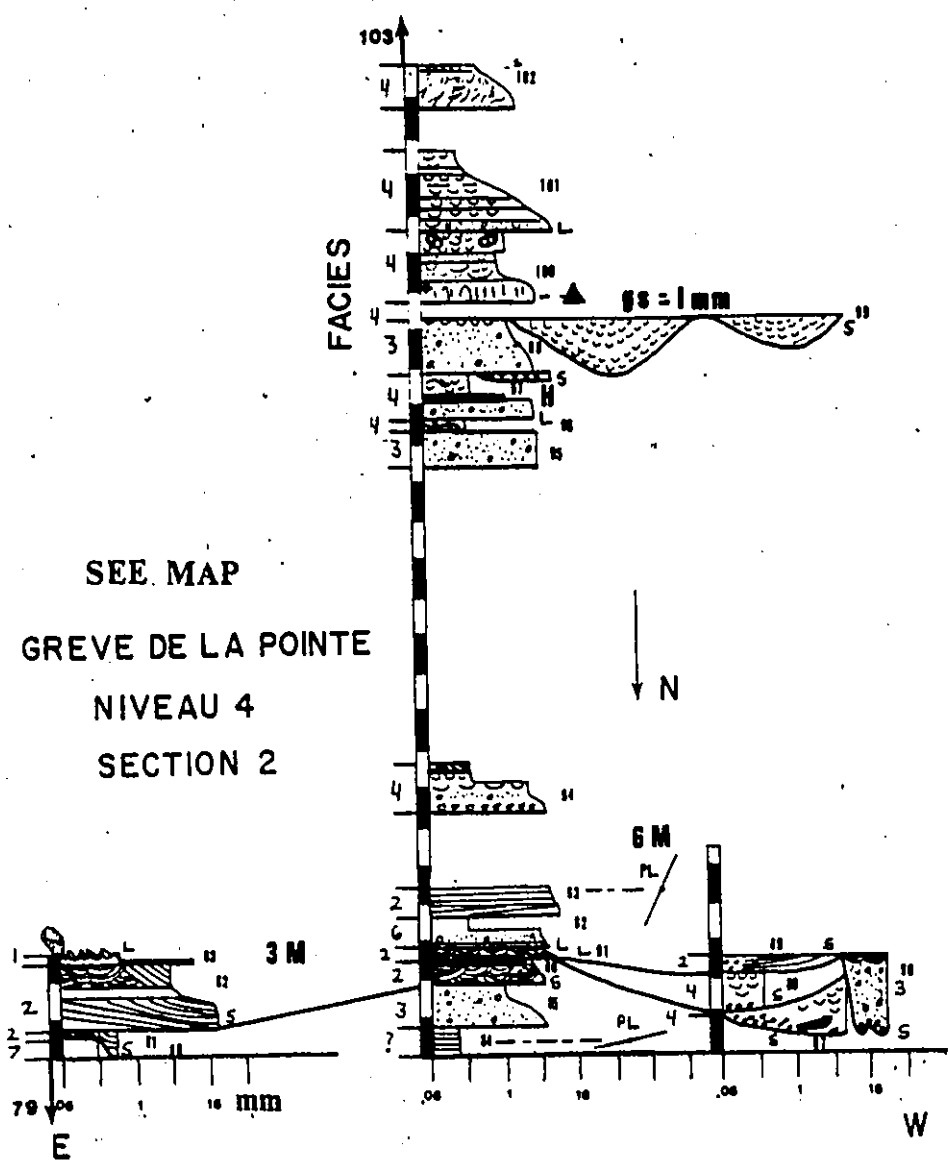


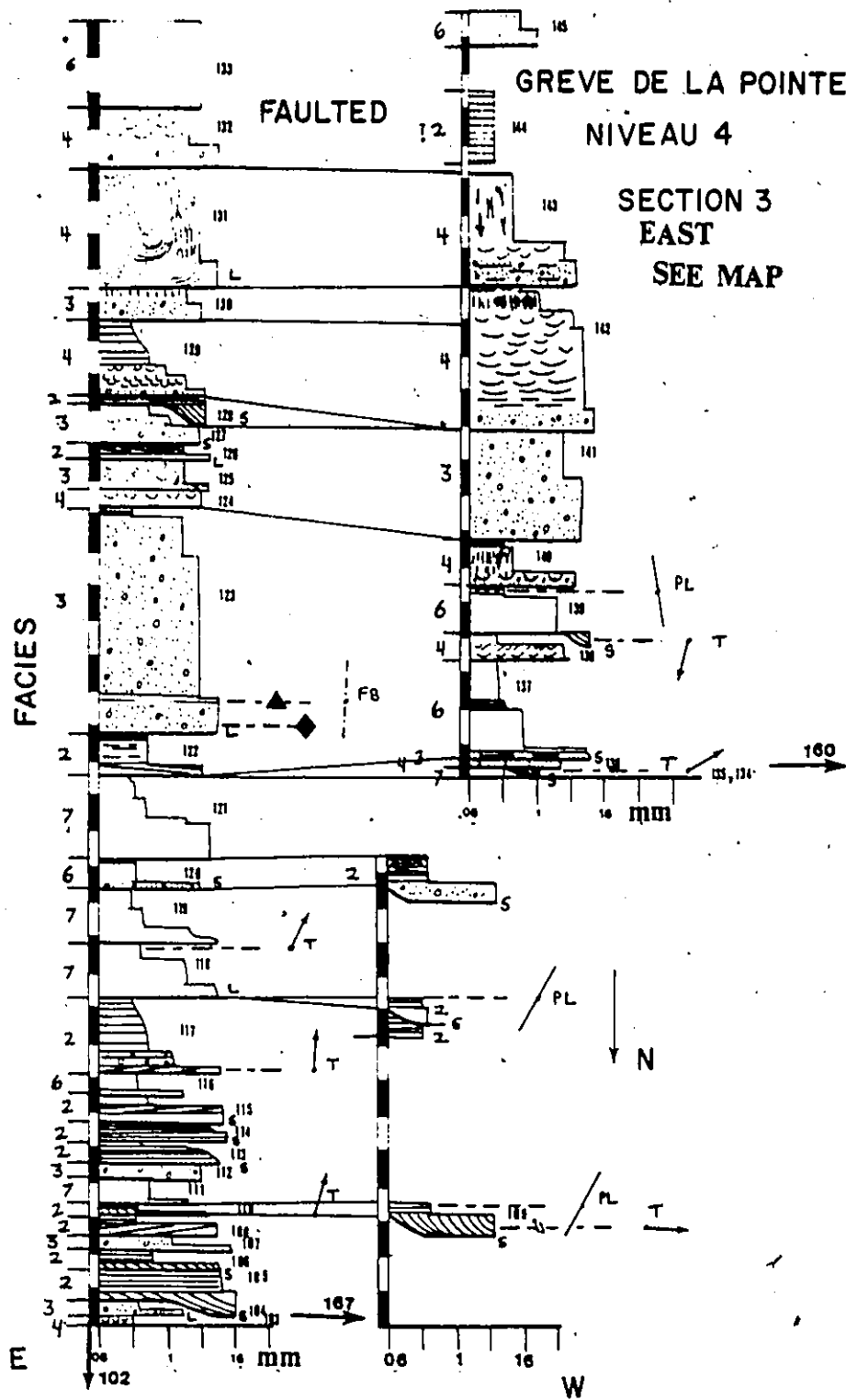


SEE MAP

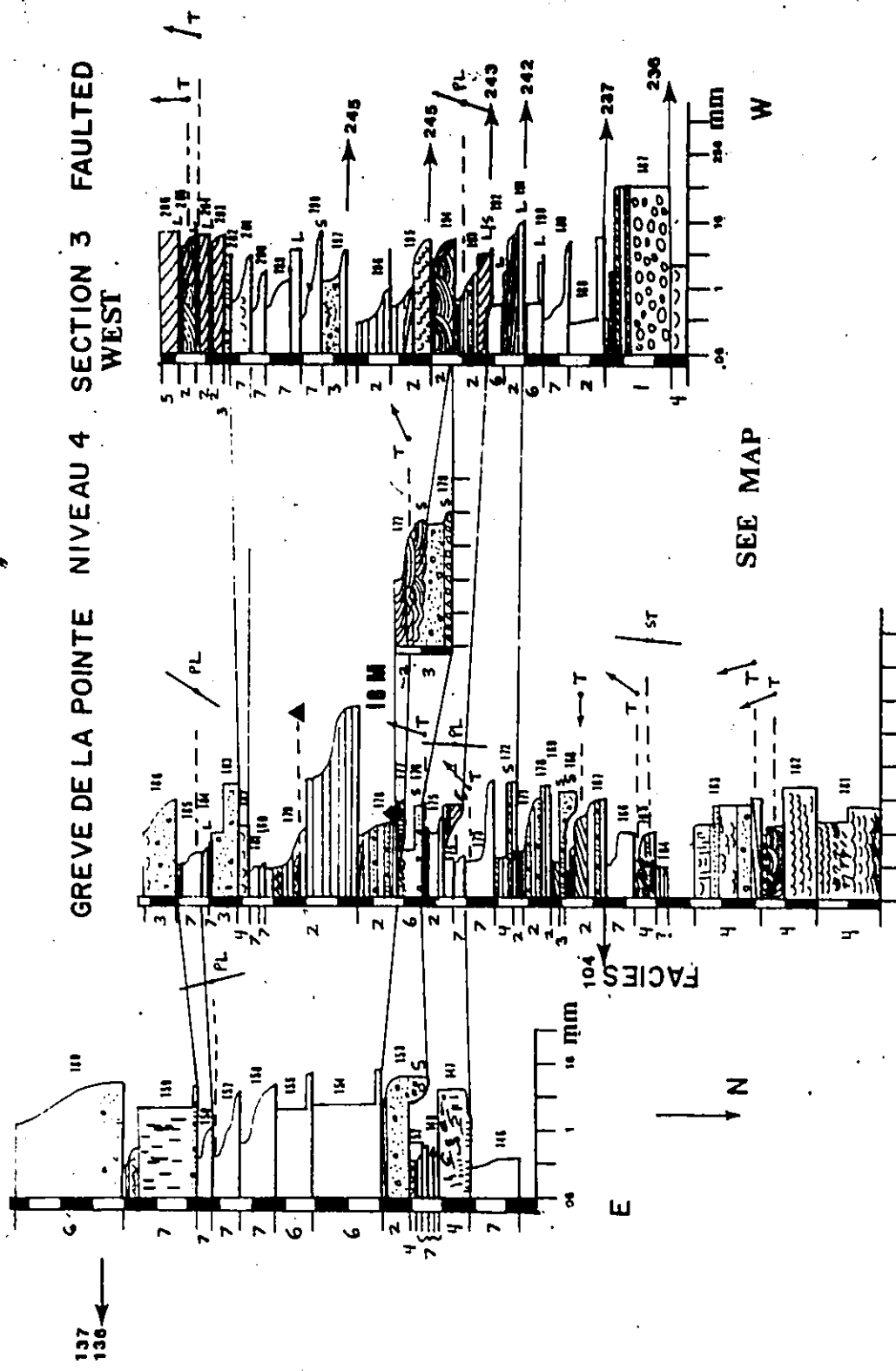


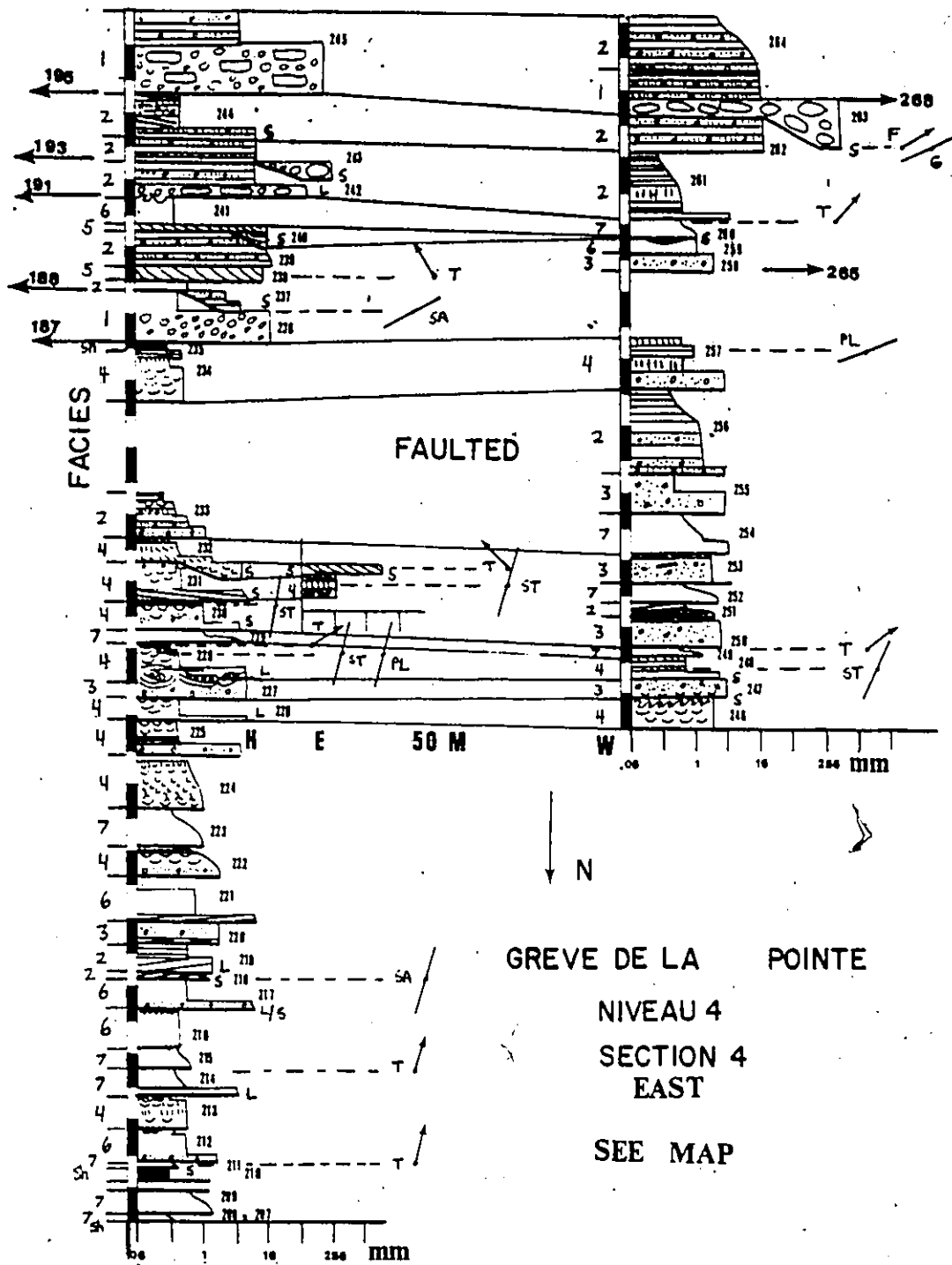






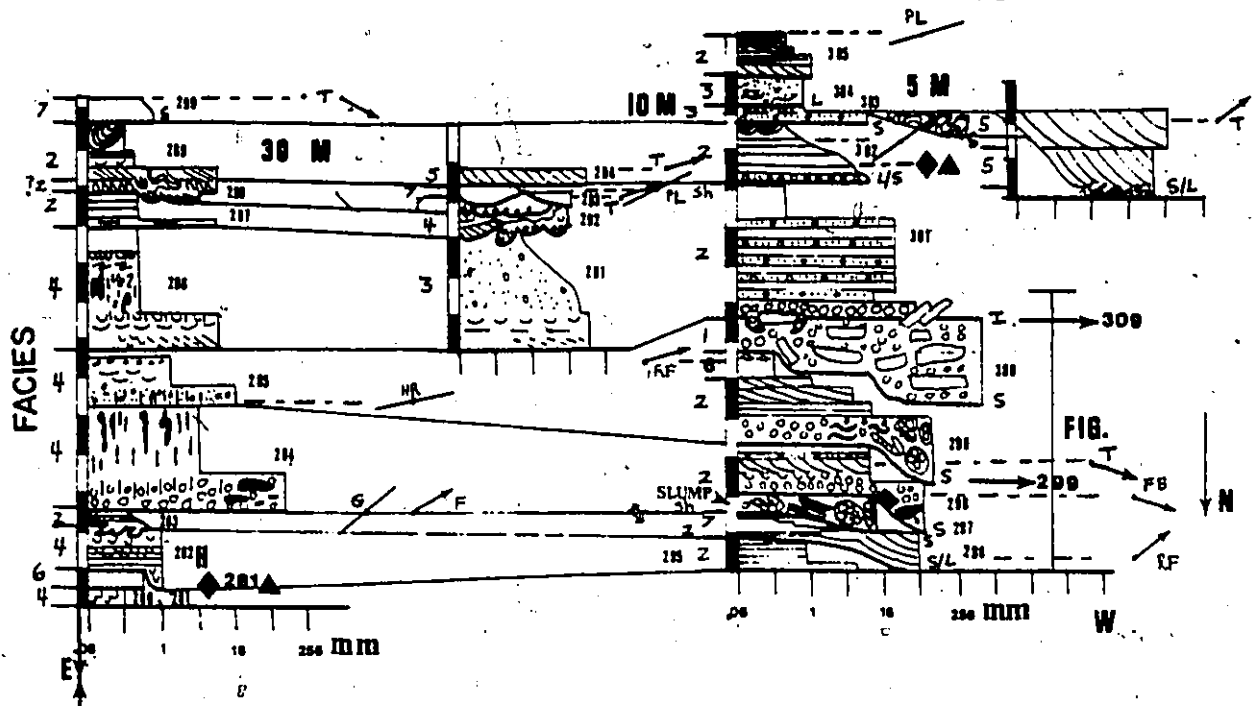
GREVE DE LA POINTE NIVEAU 4 SECTION 3 FAULTED WEST





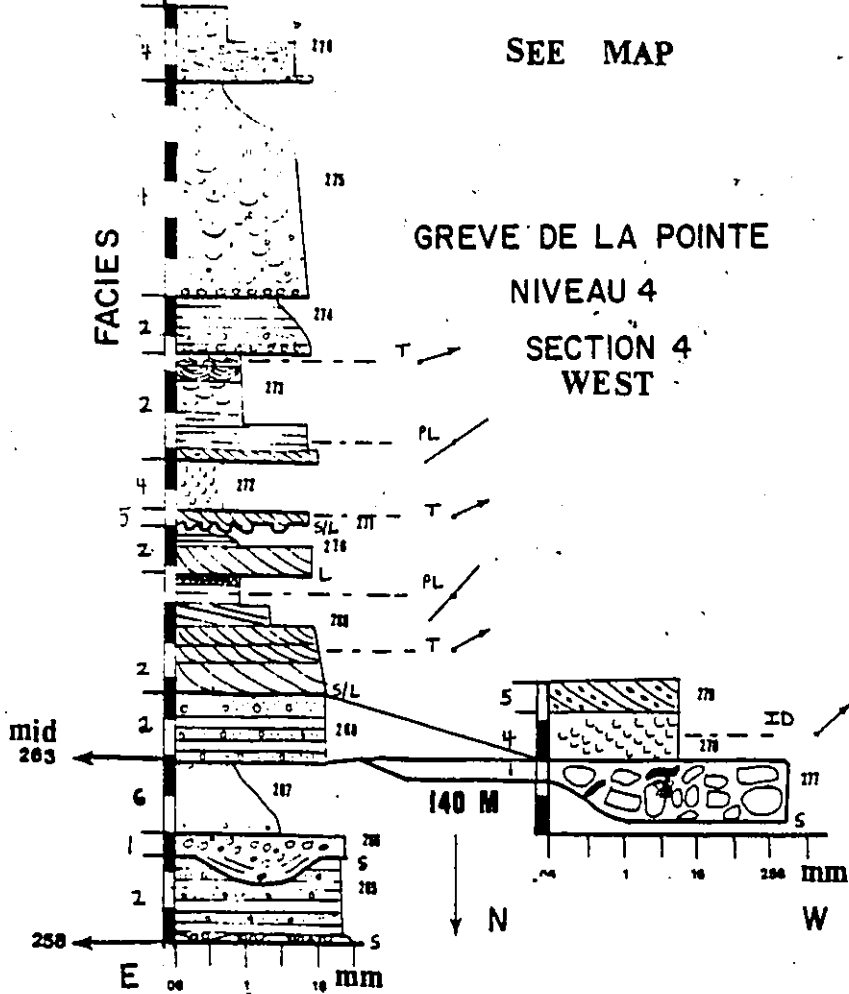
GREVE DE LA POINTE NIVEAU 4 SECTION 5

378



SEE MAP

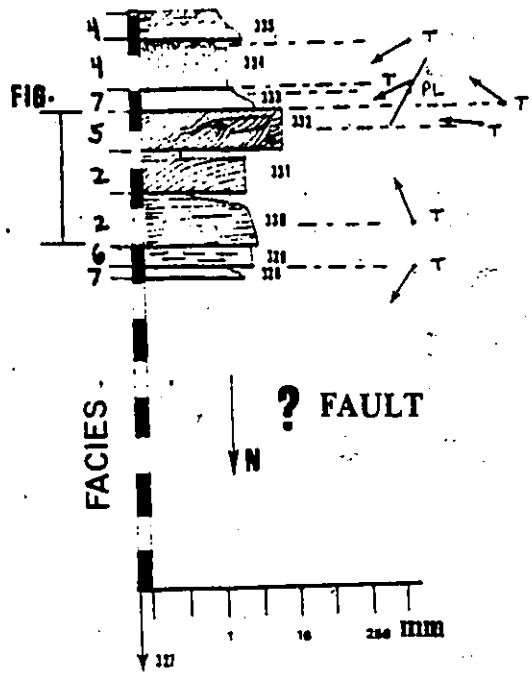
GREVE DE LA POINTE  
NIVEAU 4  
SECTION 4  
WEST



Handwritten mark or signature.

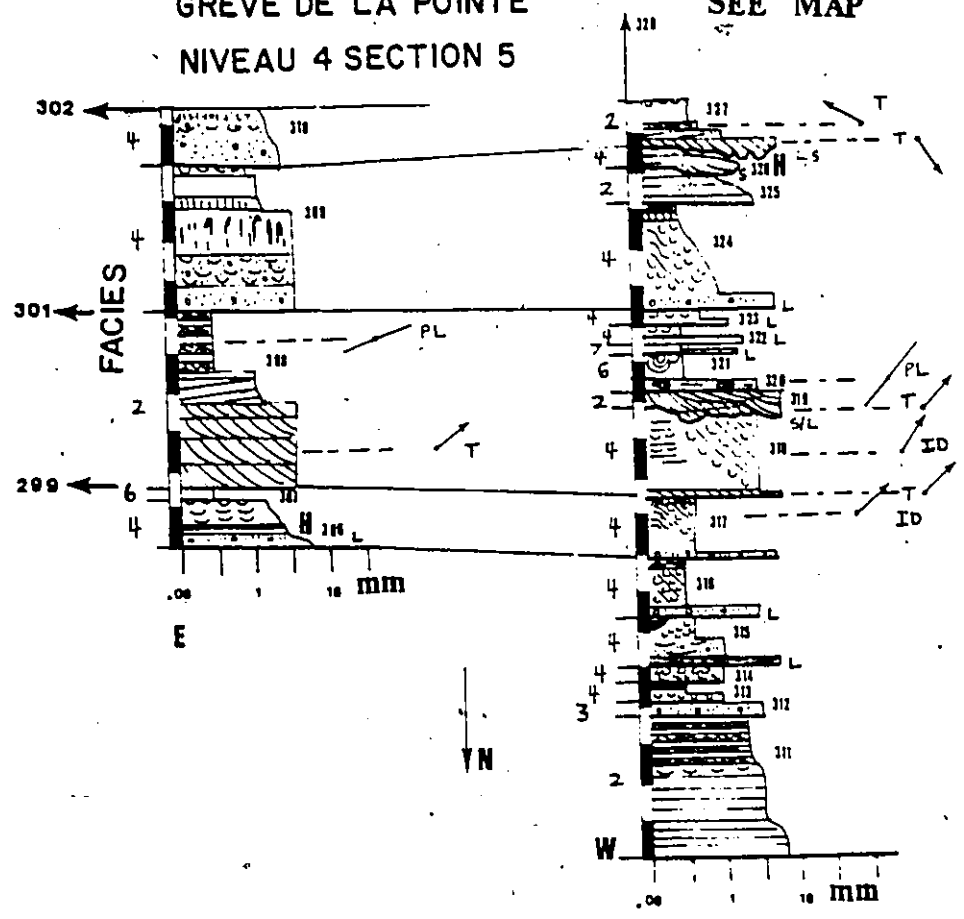


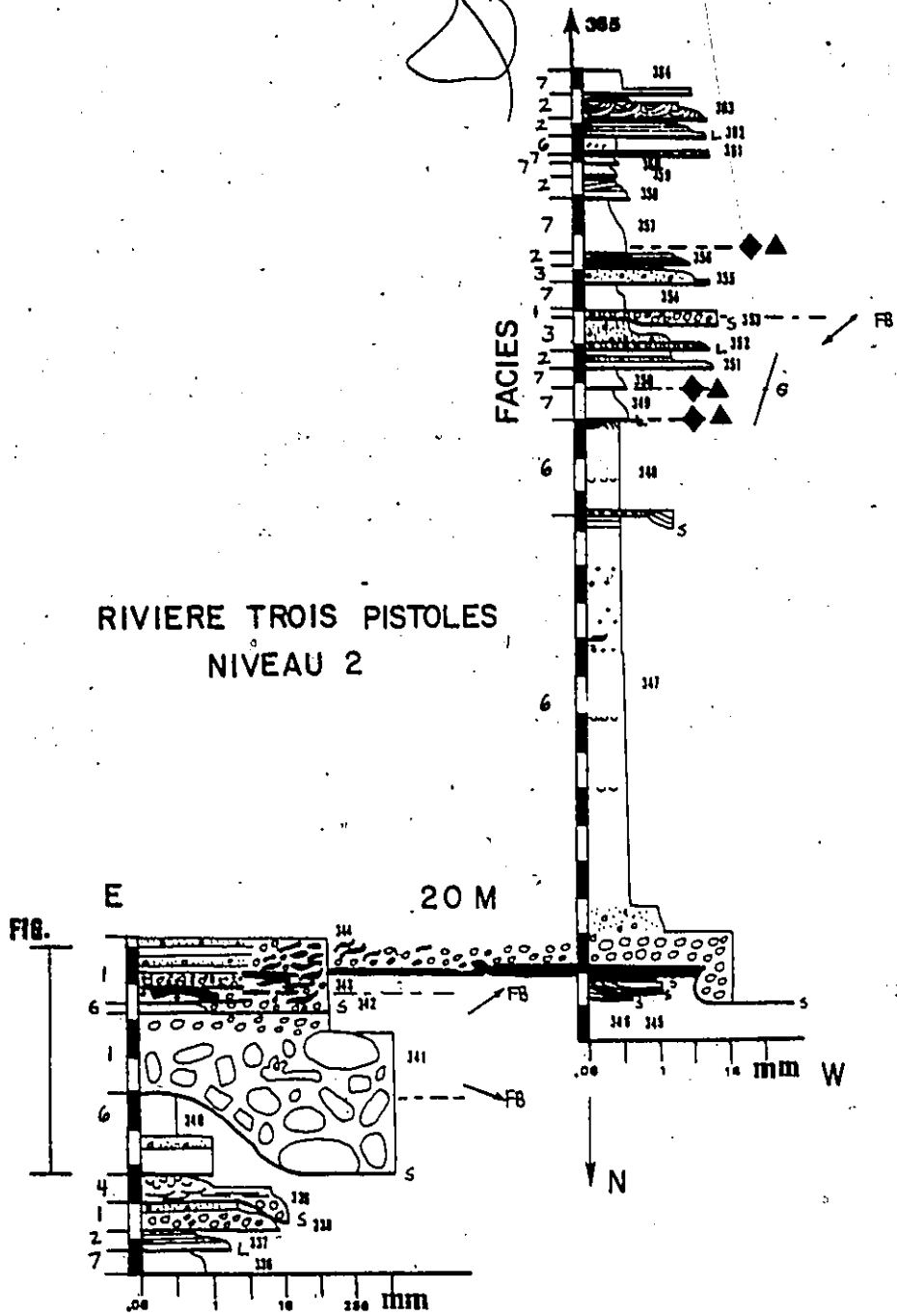
### GREVE DE LA POINTE NIVEAU 4 SECTION 6



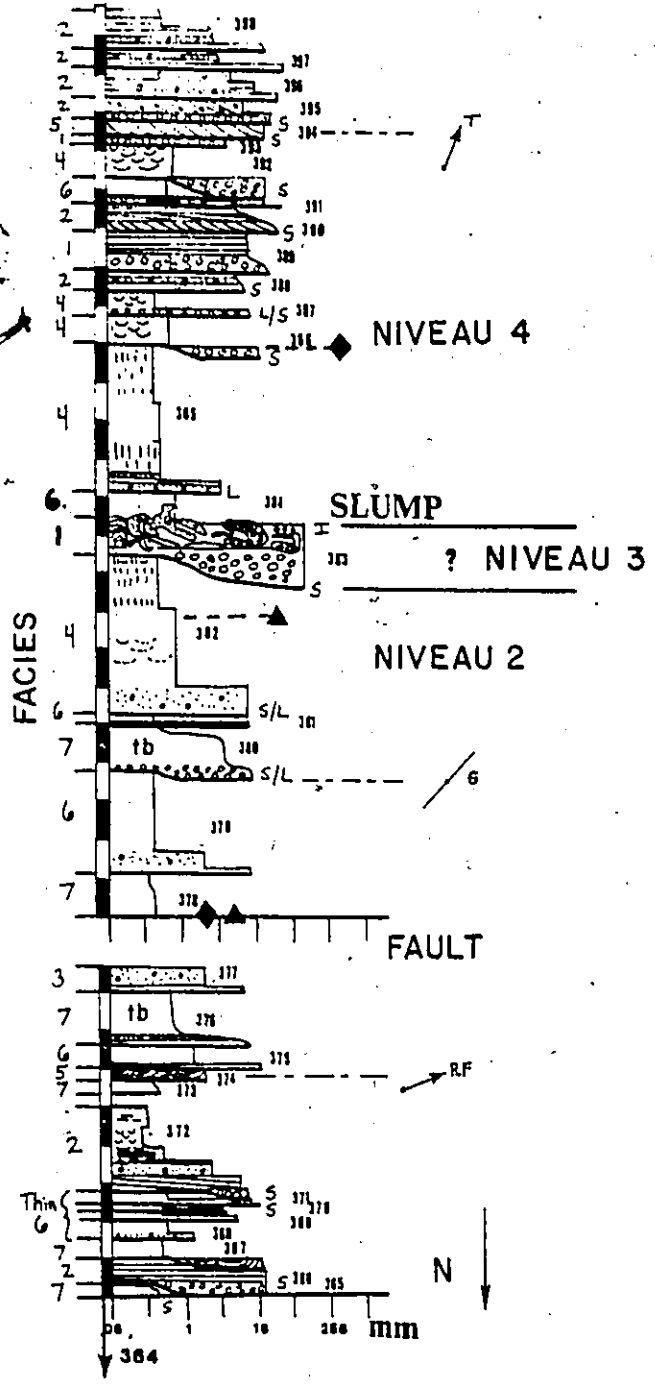
### GREVE DE LA POINTE NIVEAU 4 SECTION 5

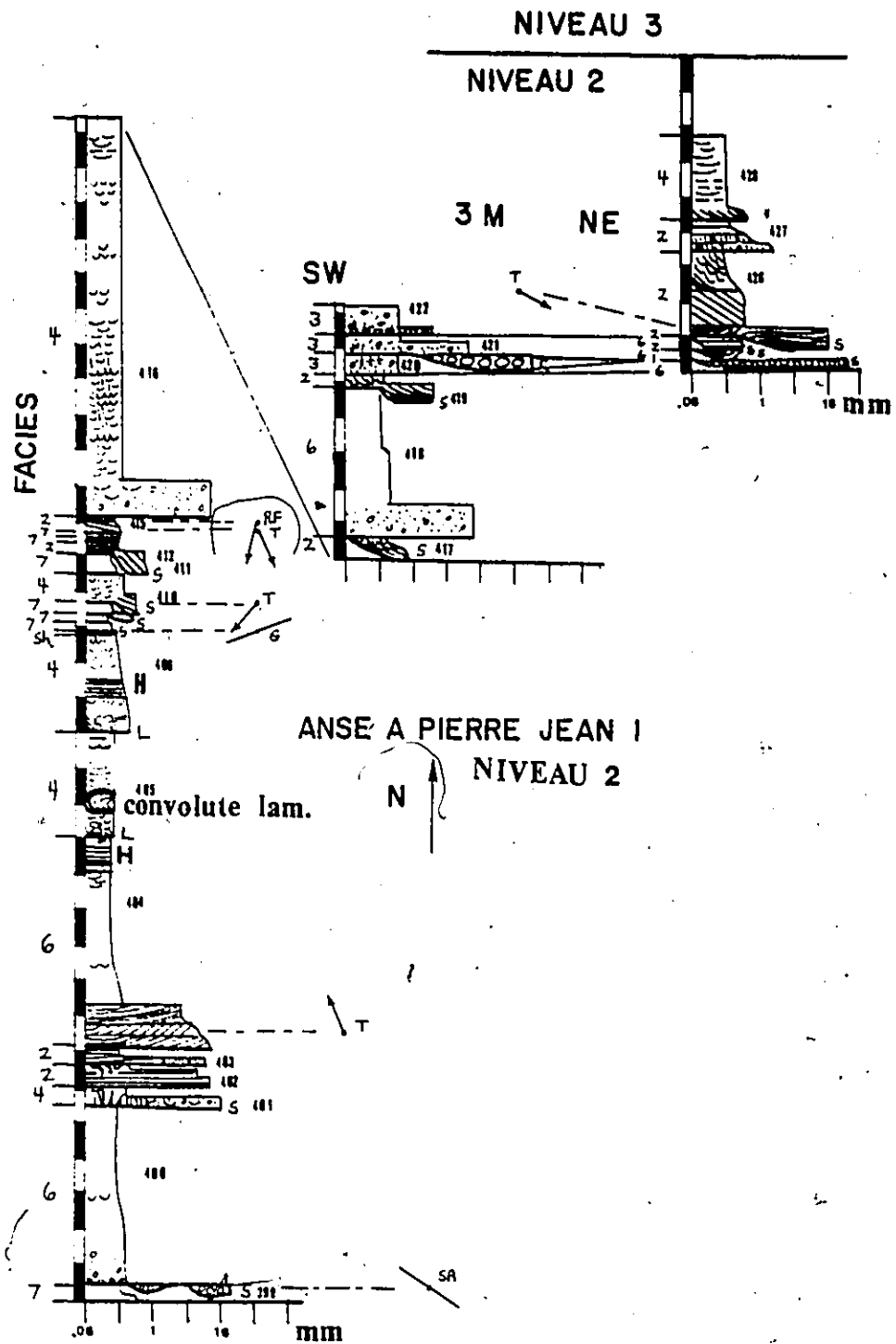
SEE MAP



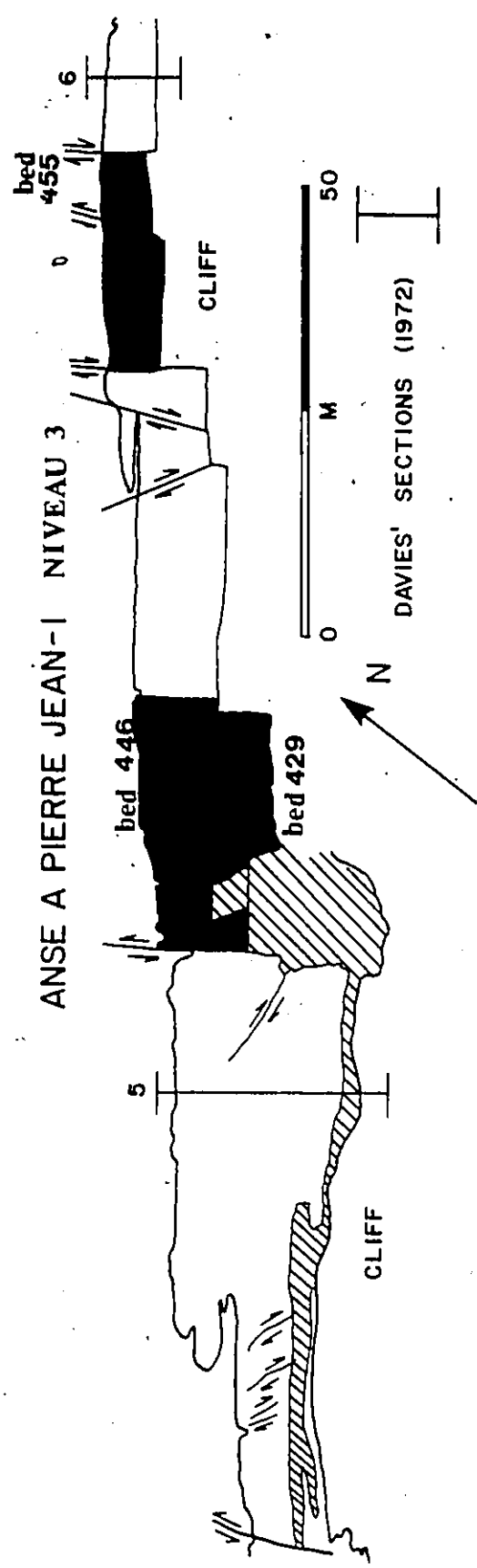


# RIVIERE TROIS PISTOLES



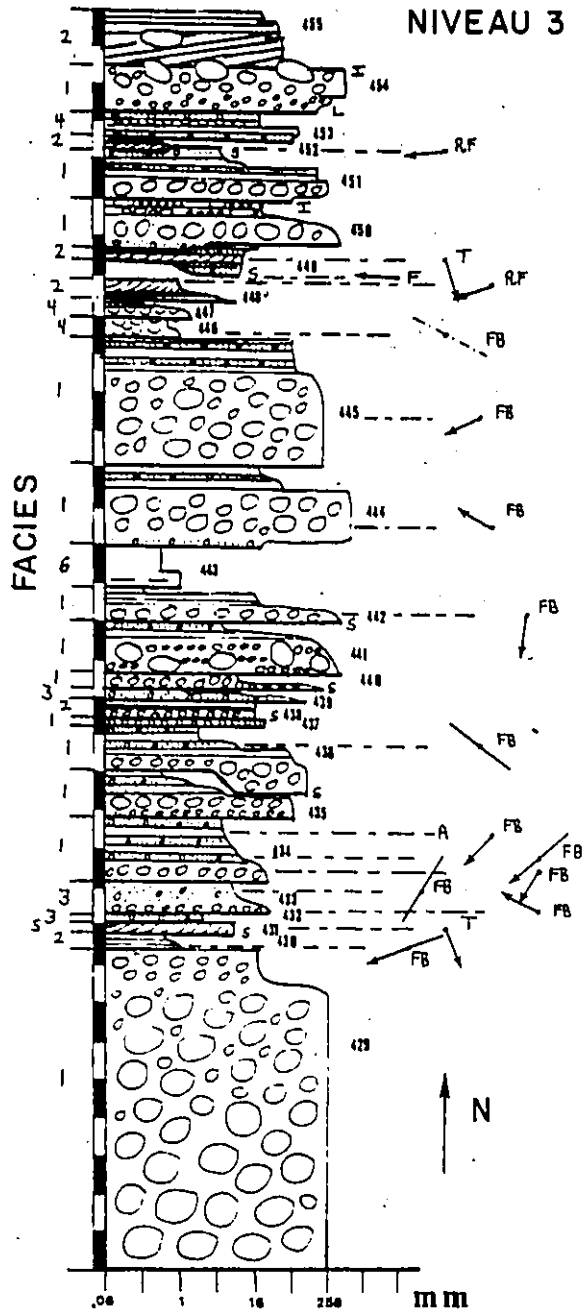


7



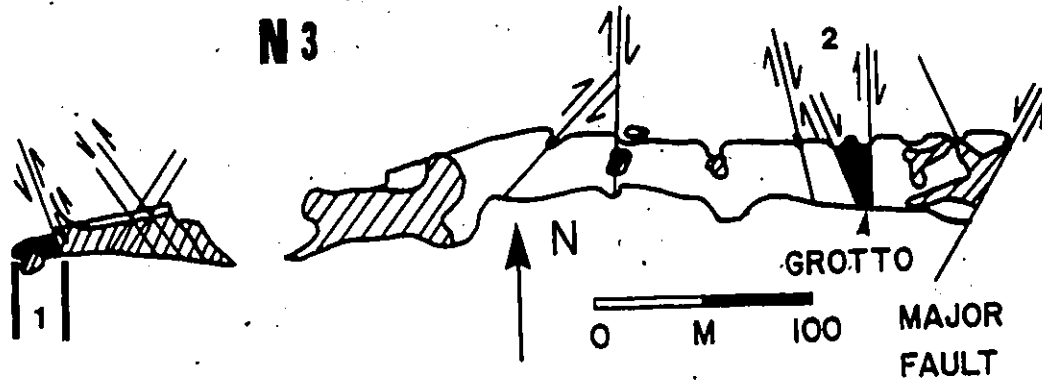
# ANSE A PIERRE JEAN I

## NIVEAU 3

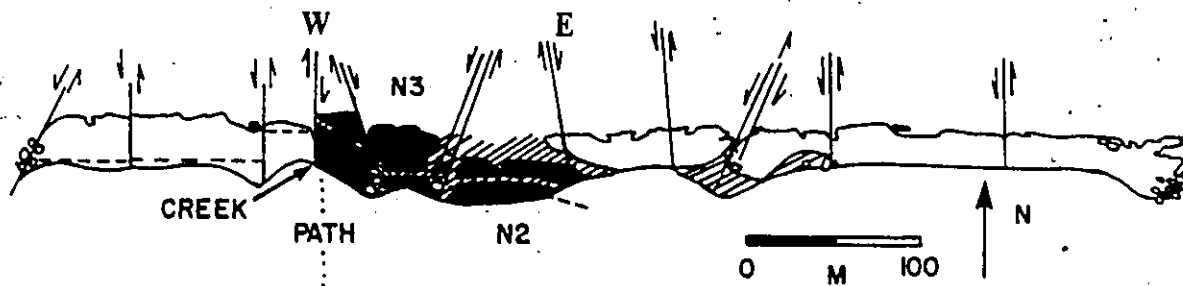


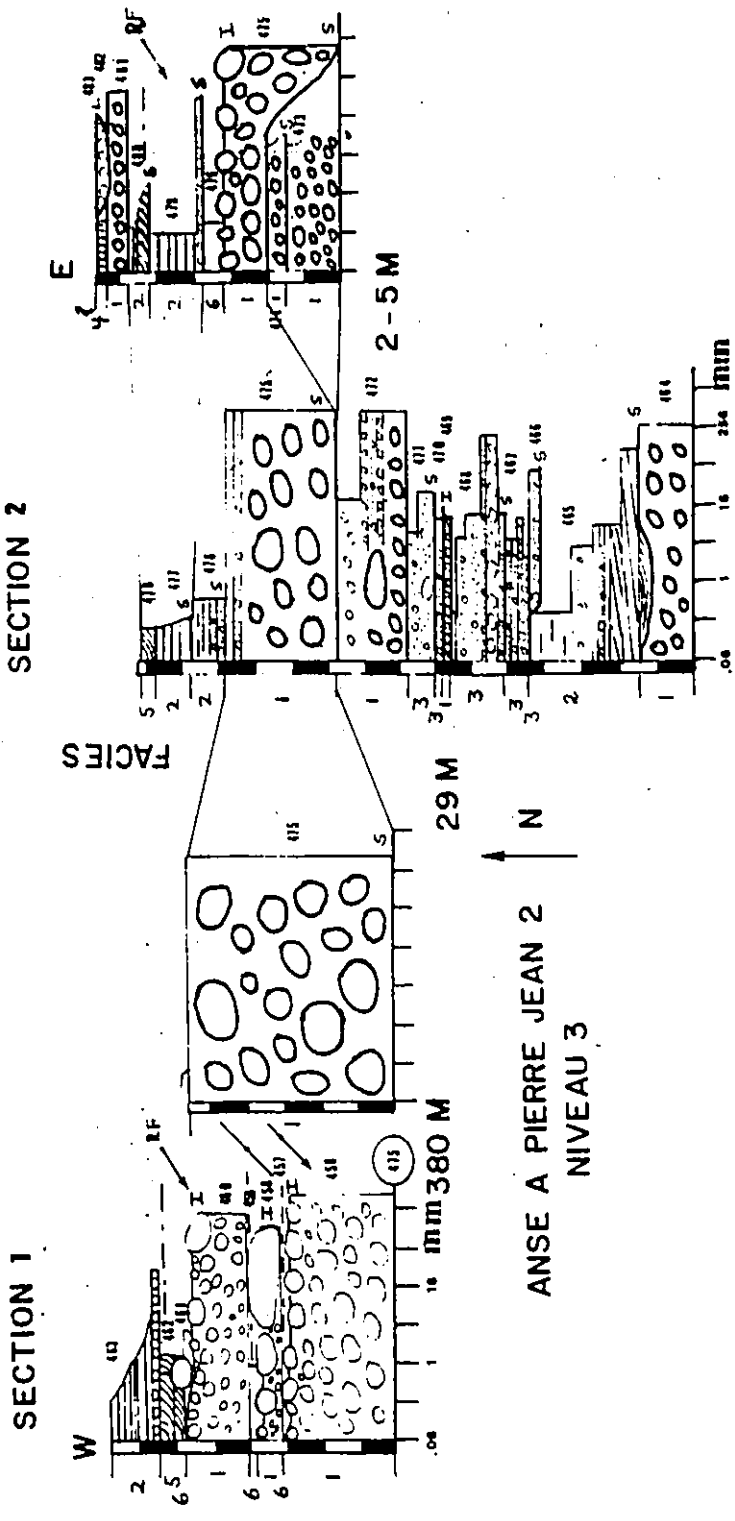
### ANSE A PIERRE JEAN 2

N3

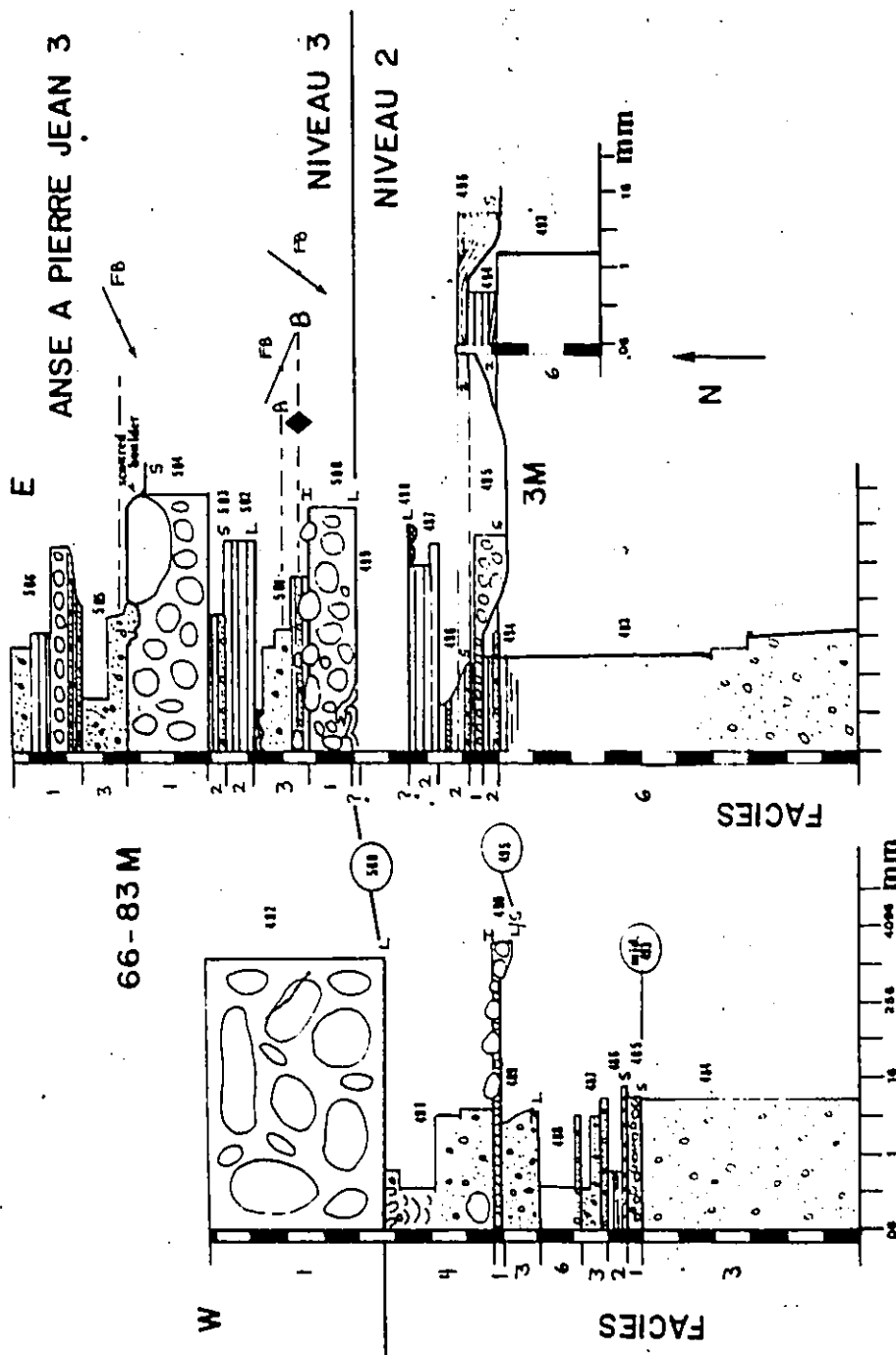


### ANSE A PIERRE JEAN 3









66-83 M

W

FACIES

FACIES

mm

# ANSE A PIERRE JEAN-5

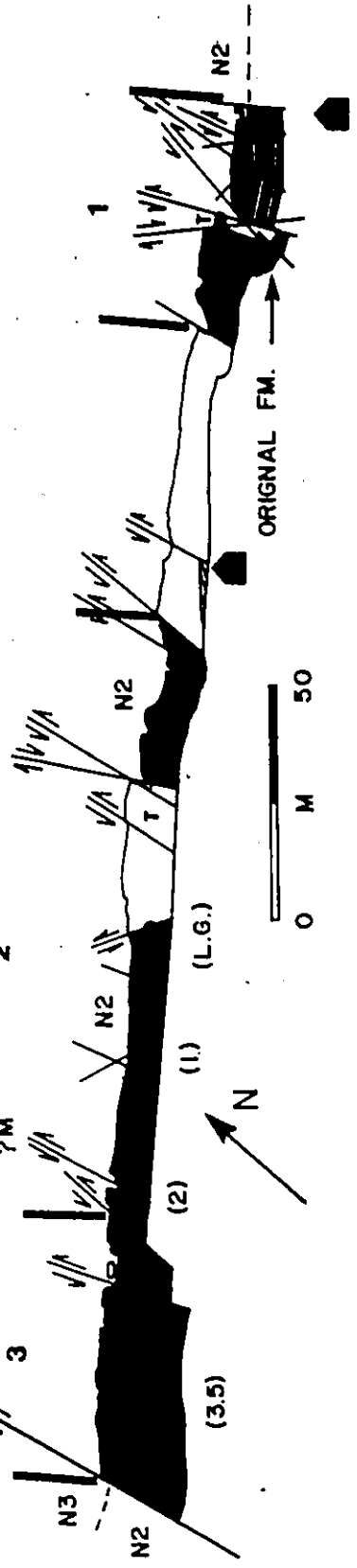
ANSE A  
PIERRE  
JEAN-4  
OUTCROP

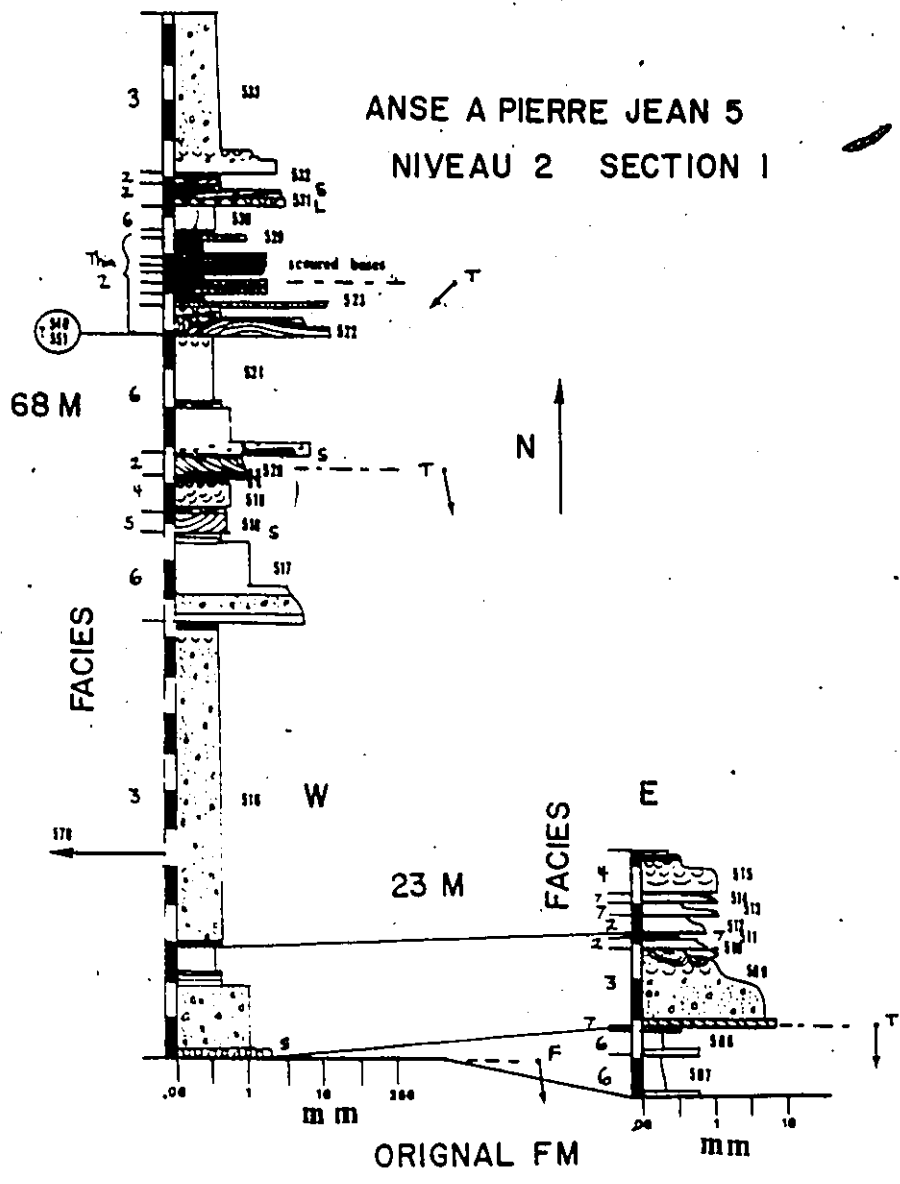
MAJOR  
FAULT  
?M

2

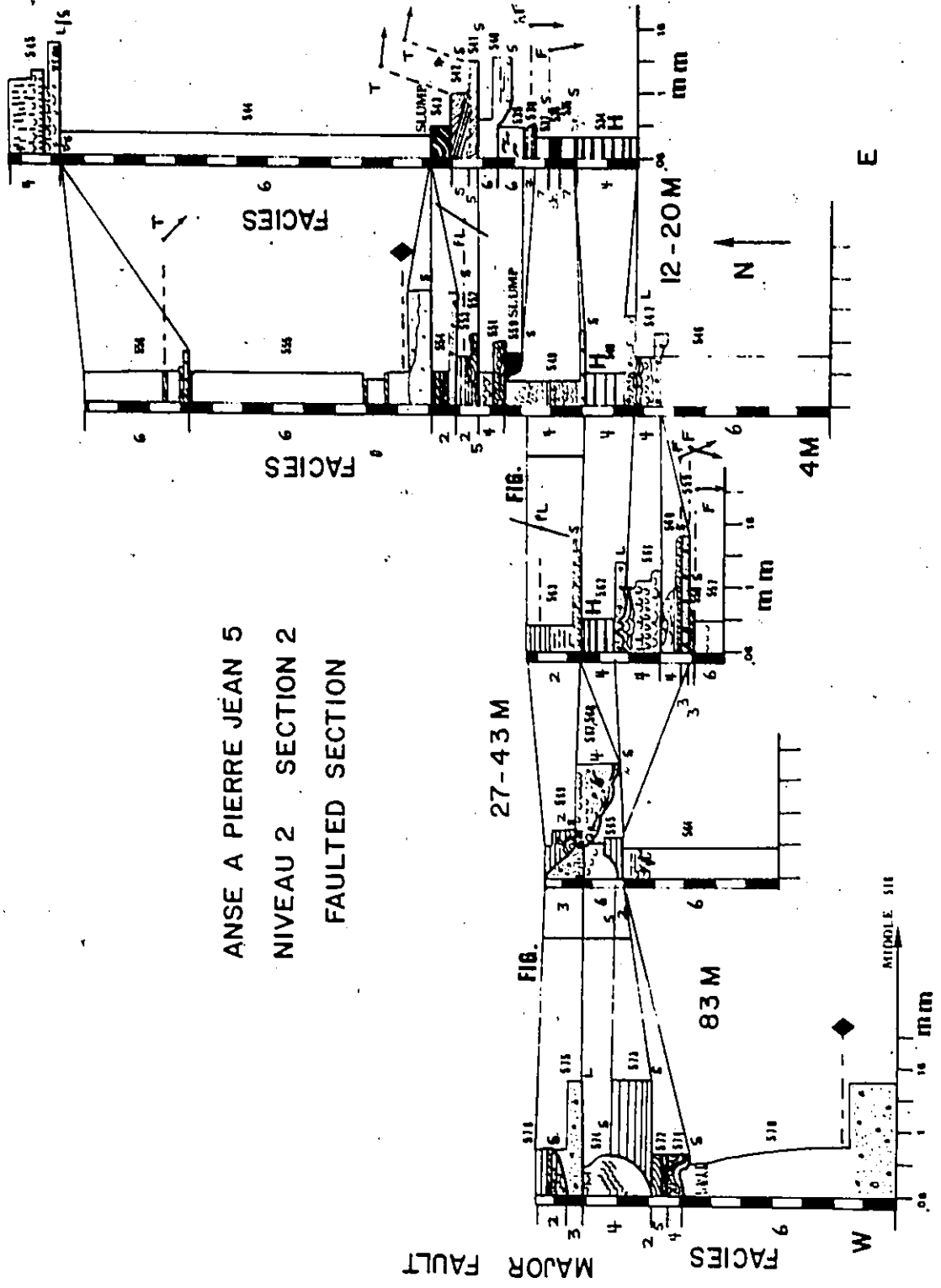
N

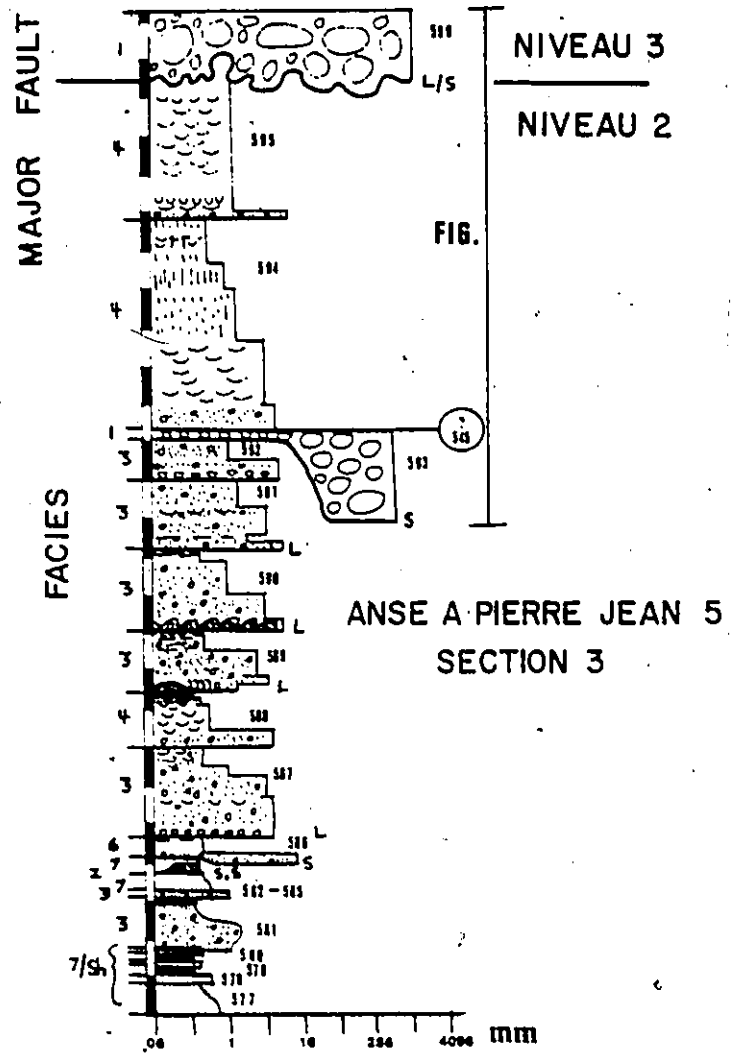
ORIGINAL FM.

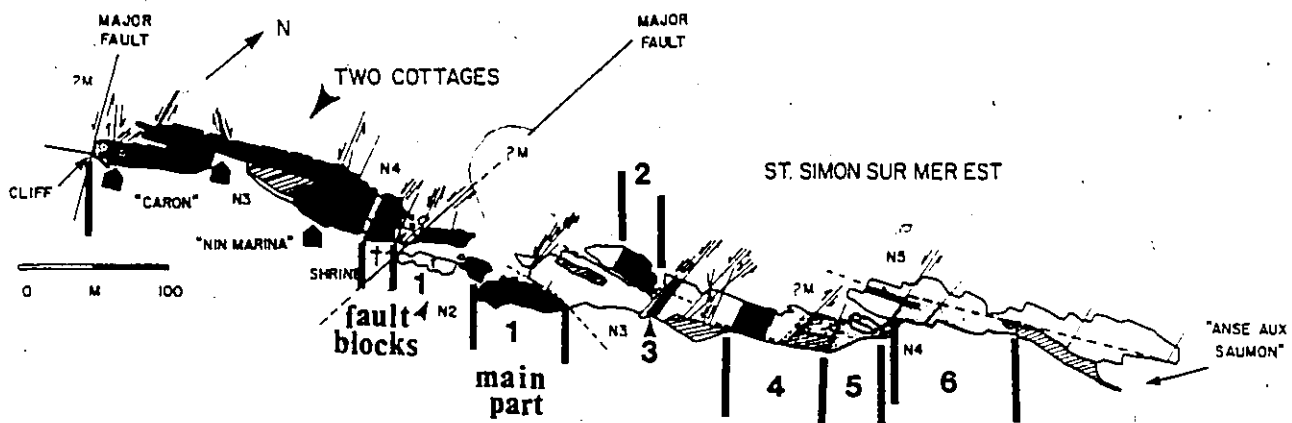
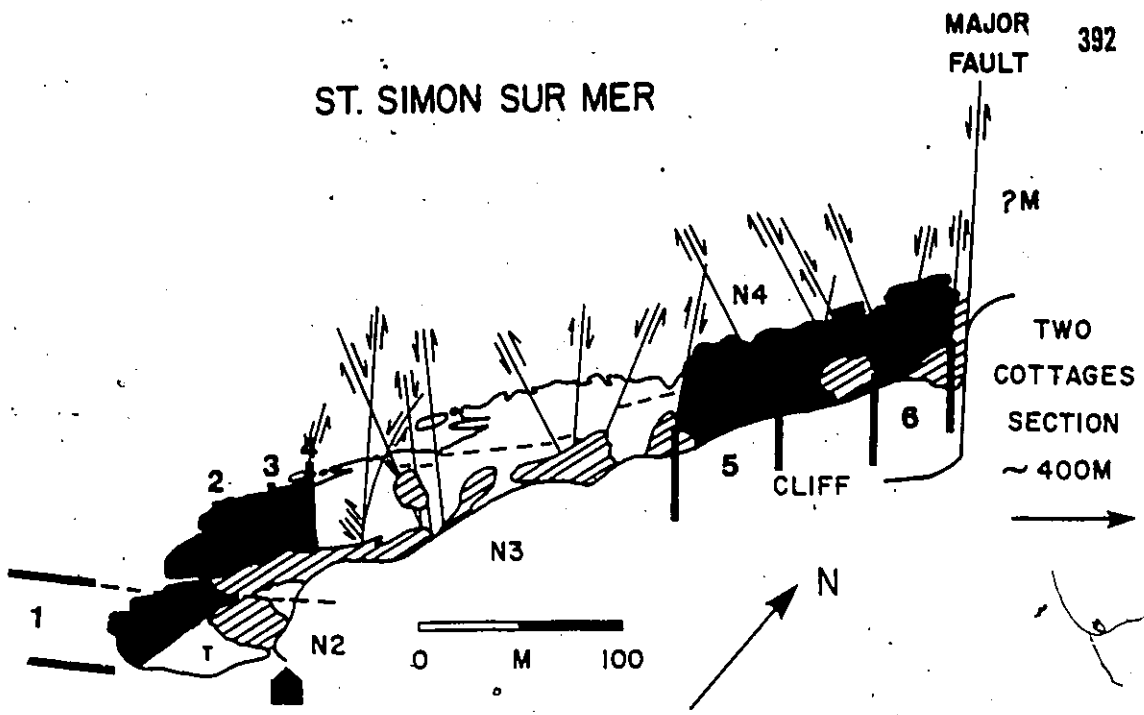


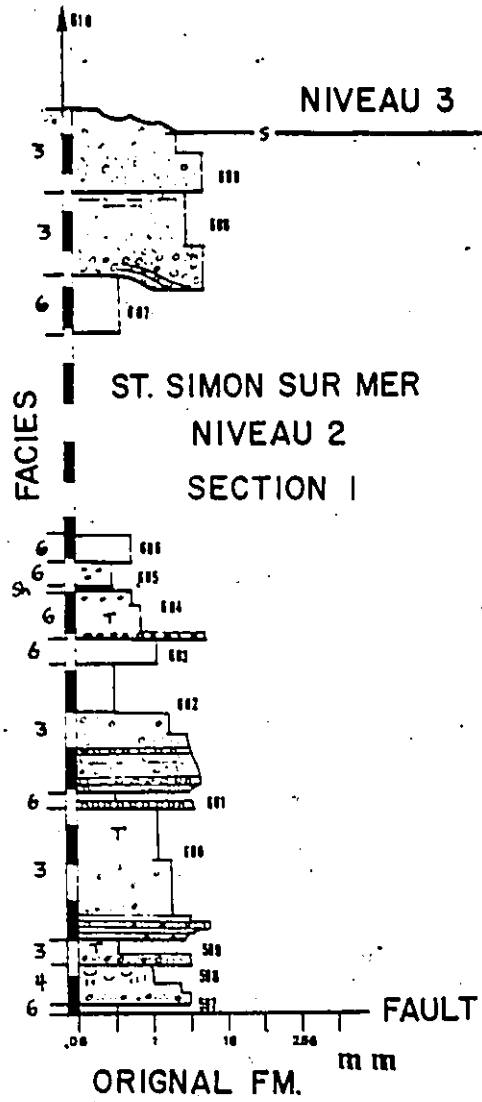


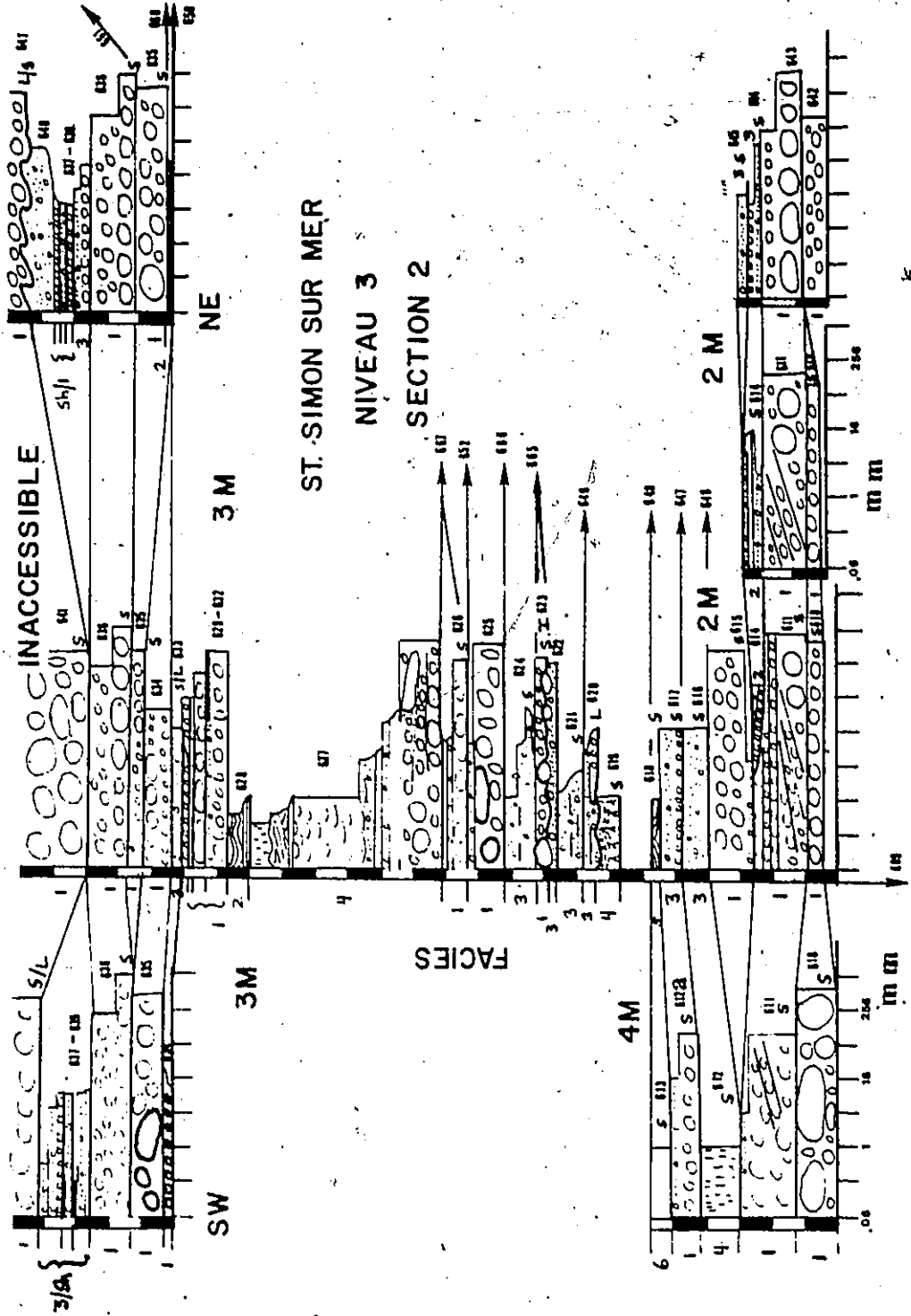
ANSE A PIERRE JEAN 5  
 NIVEAU 2 SECTION 2  
 FAULTED SECTION



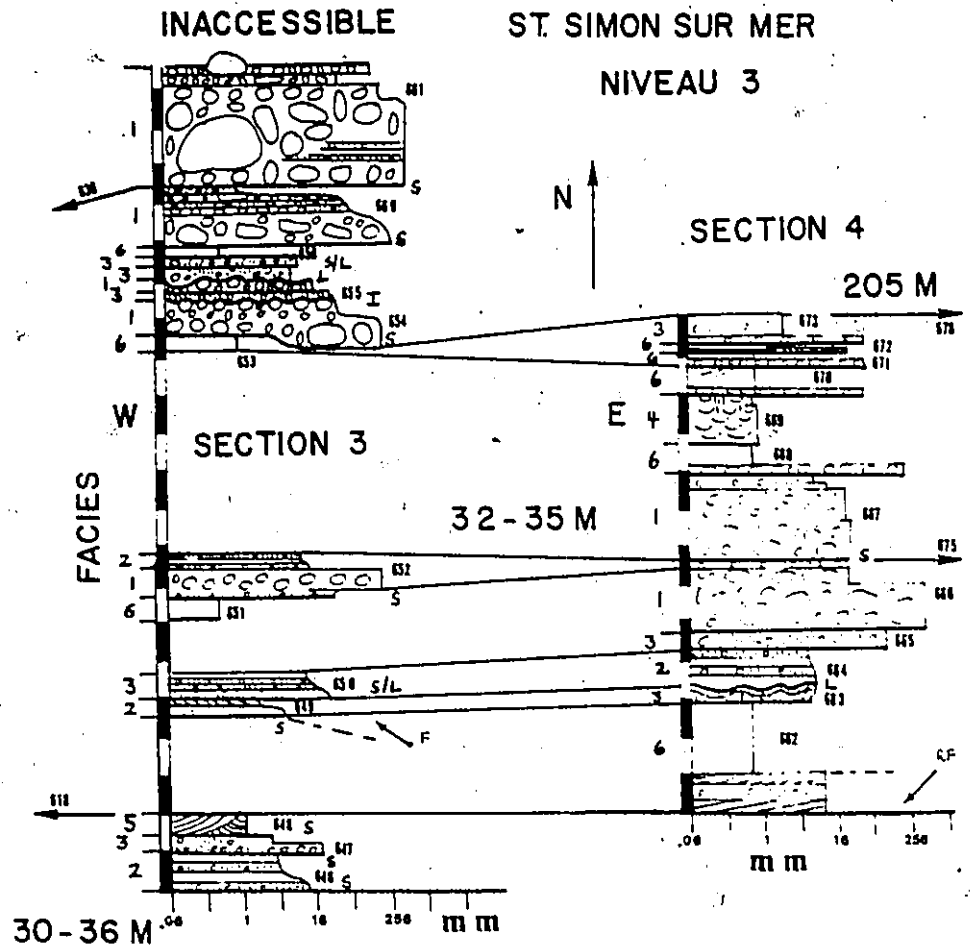




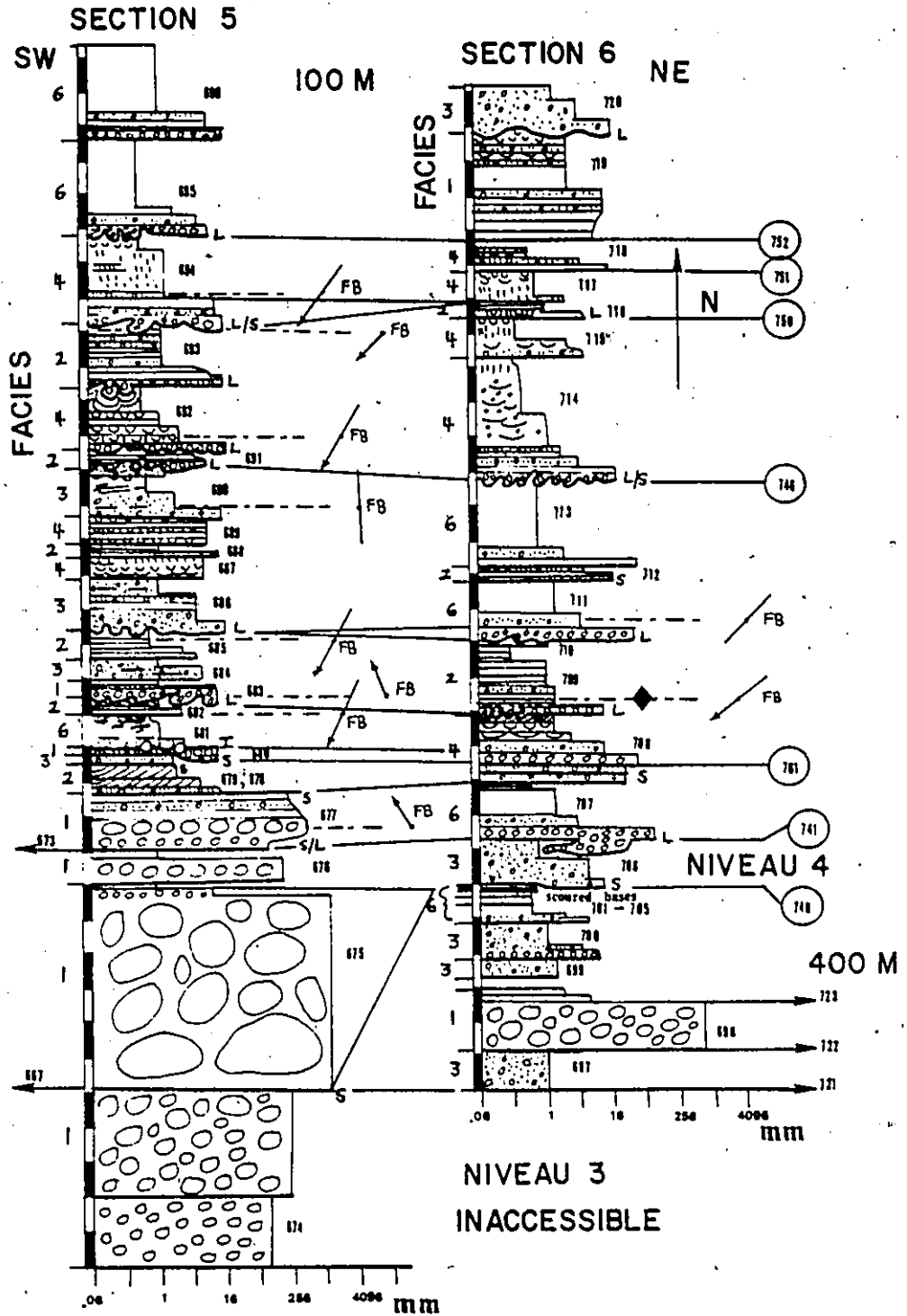


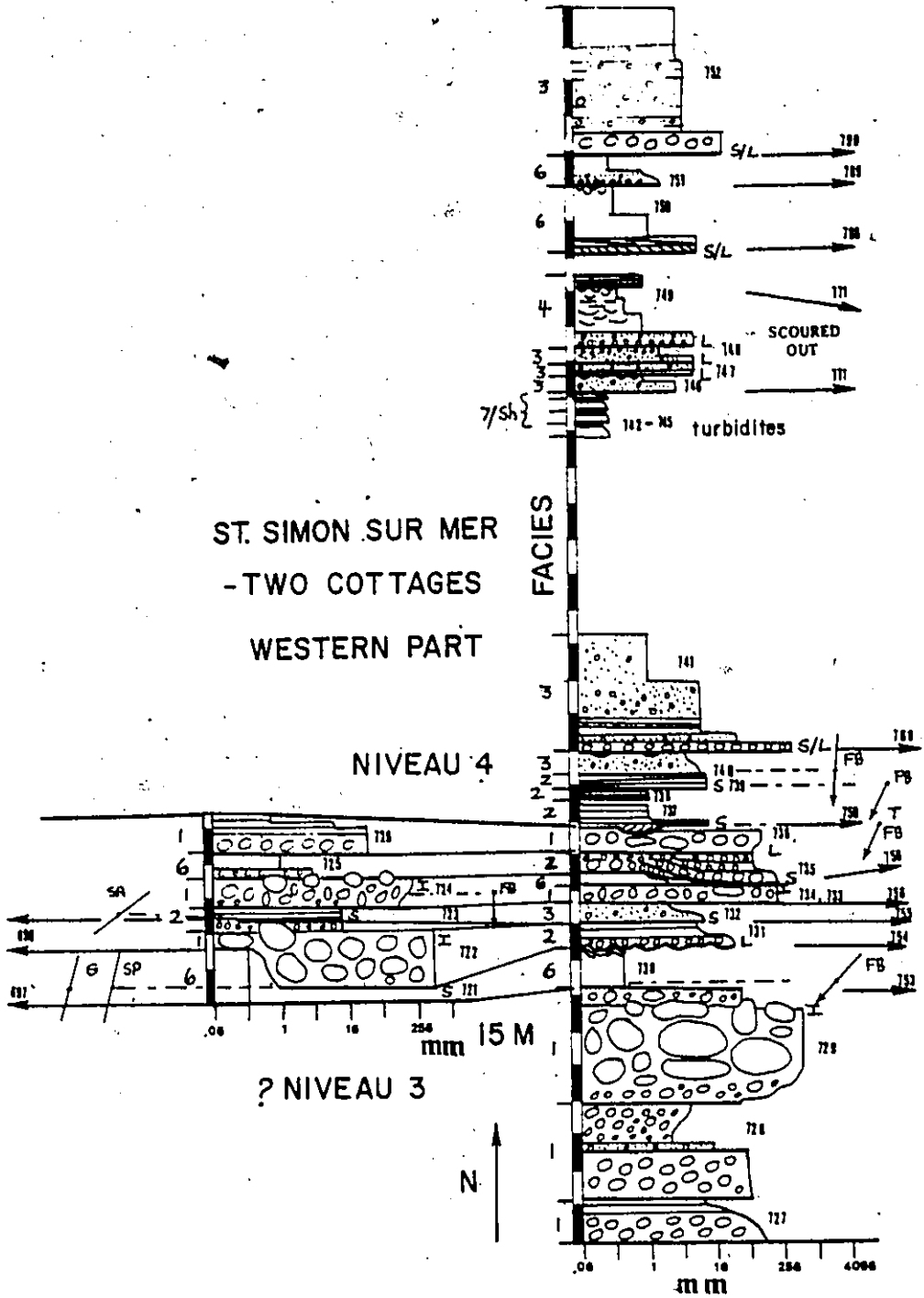




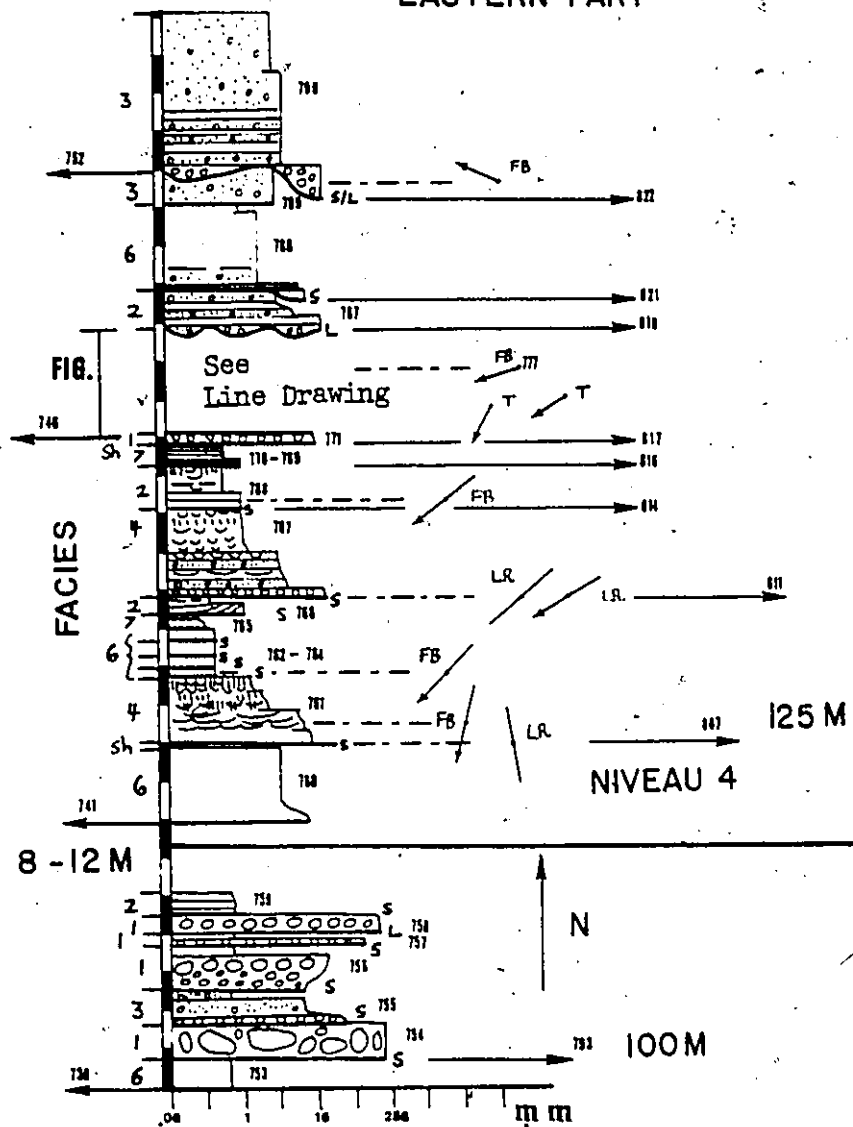


ST. SIMON SUR MER

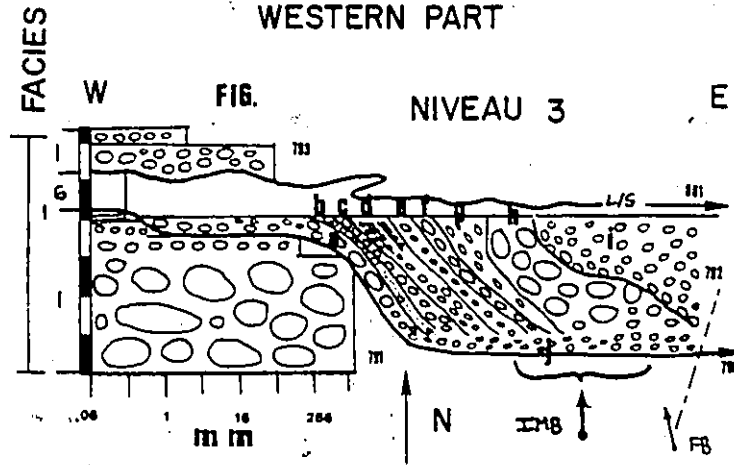




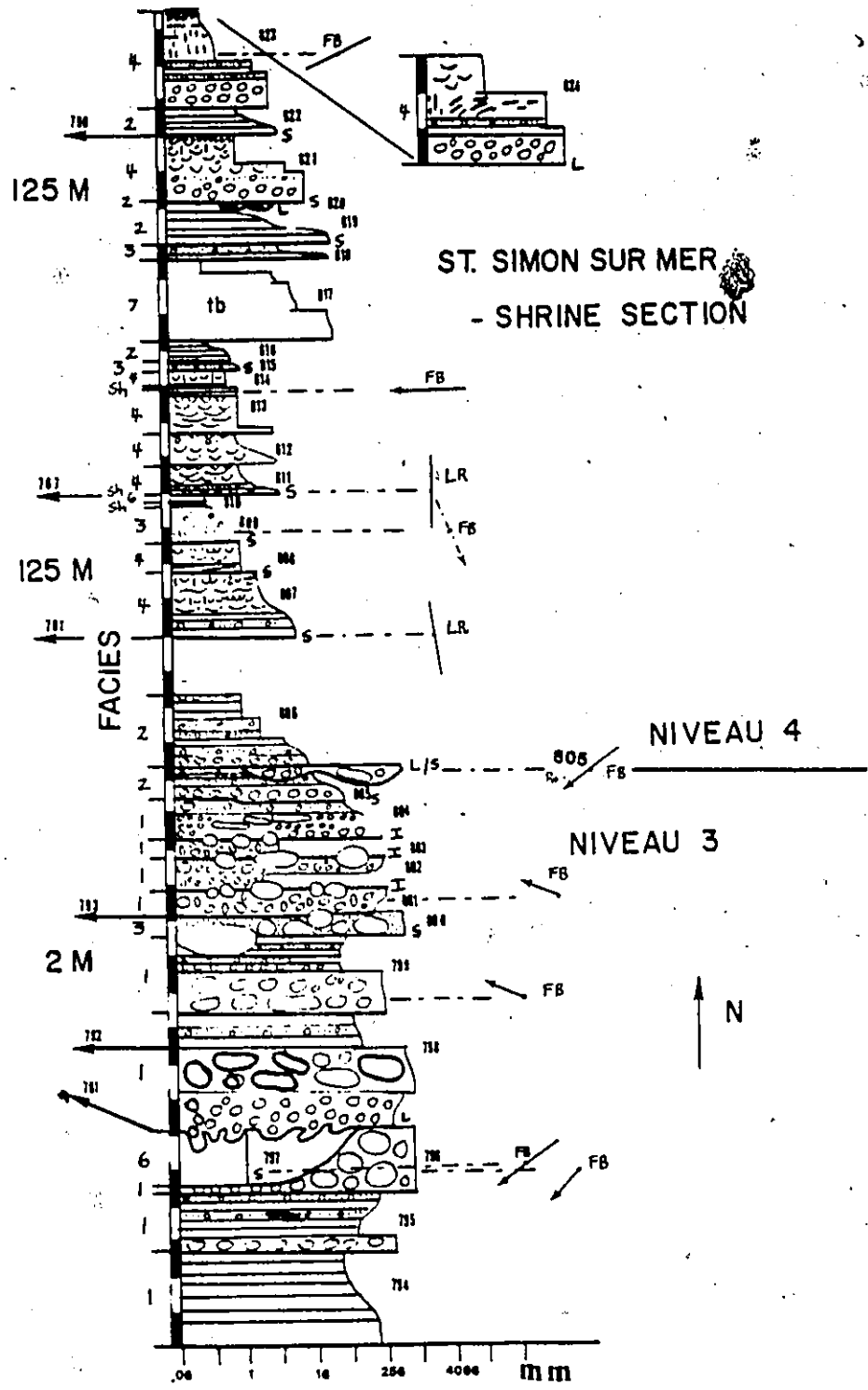
ST. SIMON SUR MER - TWO COTTAGES  
EASTERN PART

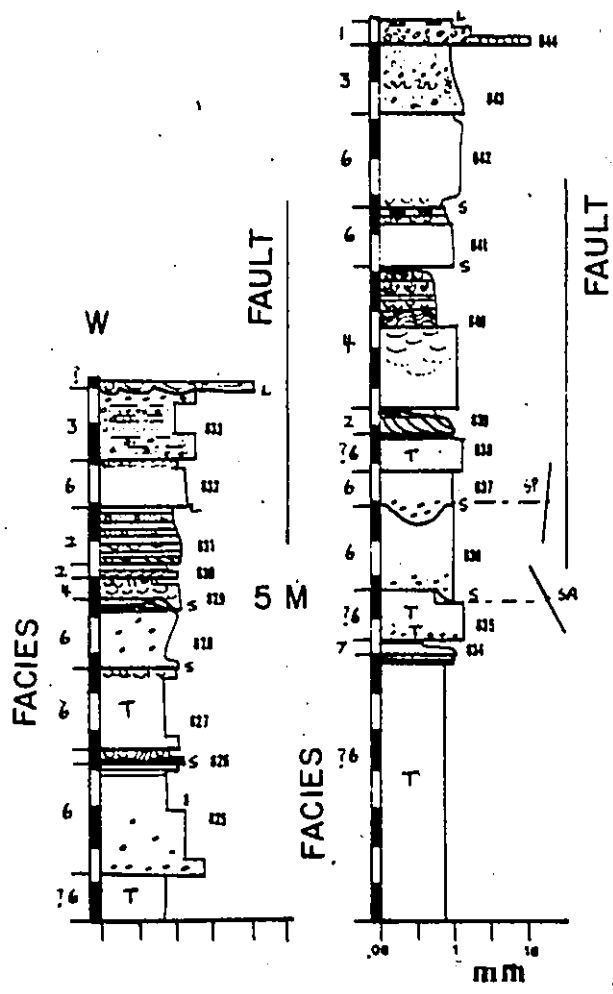


ST. SIMON SUR MER - SHRINE SECTION  
WESTERN PART

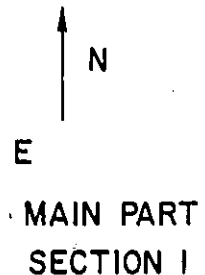


grain size a=190 mm, b=47 mm, c=95 mm, d=44 mm at top,  
d=129 mm at base, e=58 mm, f=172 mm, j  
g=74 mm, h=470 mm, i=56 mm, j=50 mm

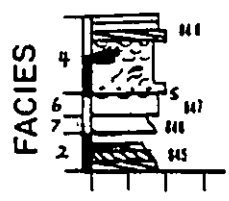




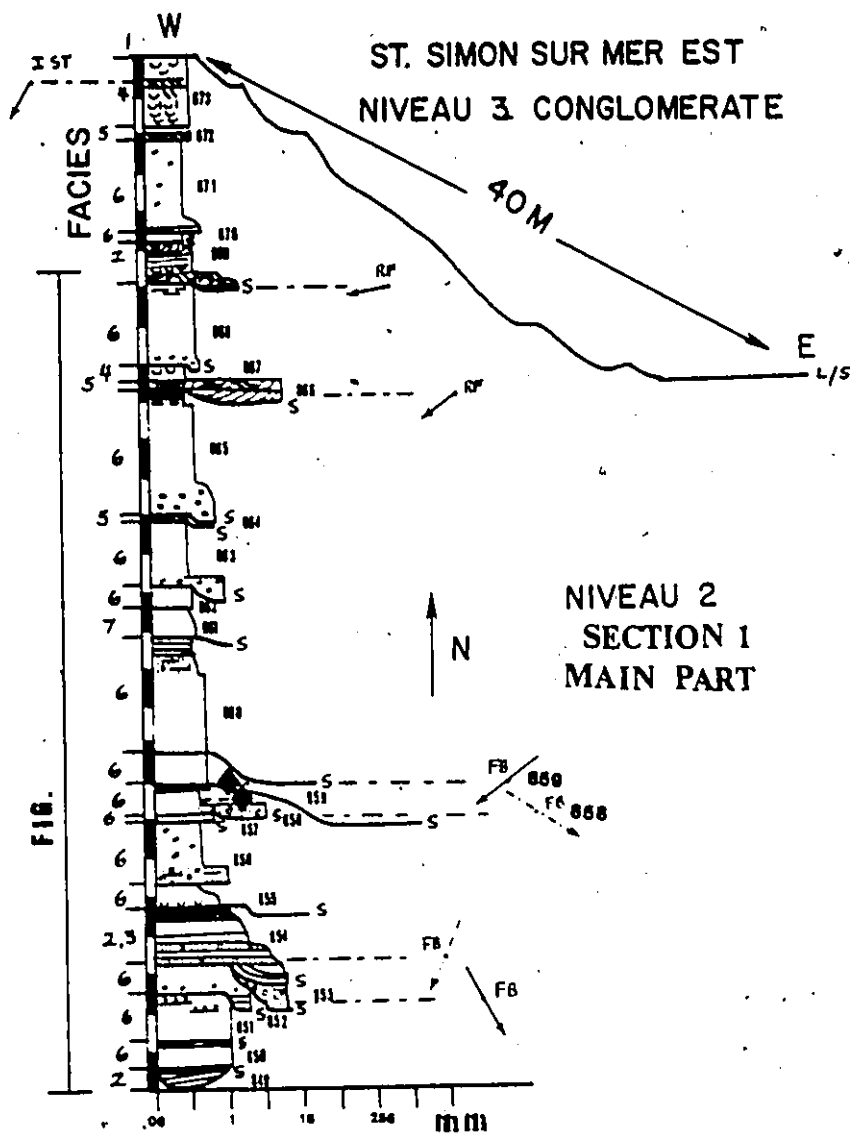
ST. SIMON SUR MER EST  
NIVEAU 2  
SECTION I  
WESTERN FAULT BLOCKS



10M

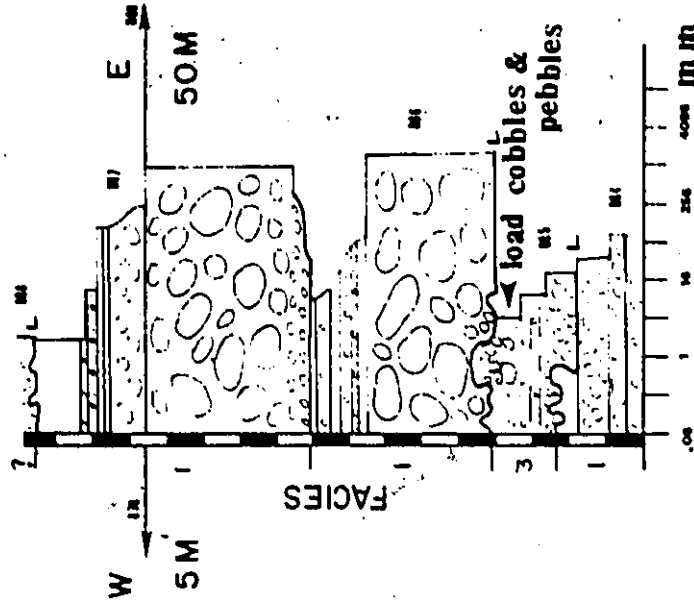


MAIN PART  
SECTION I

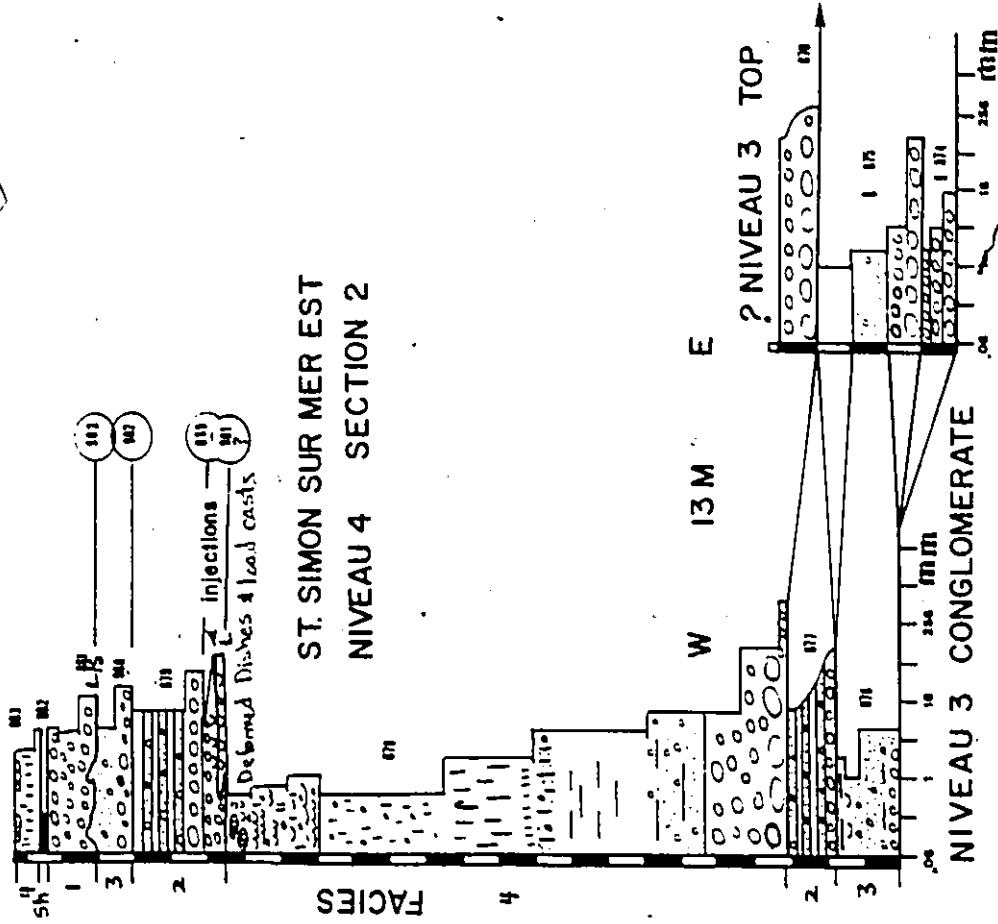


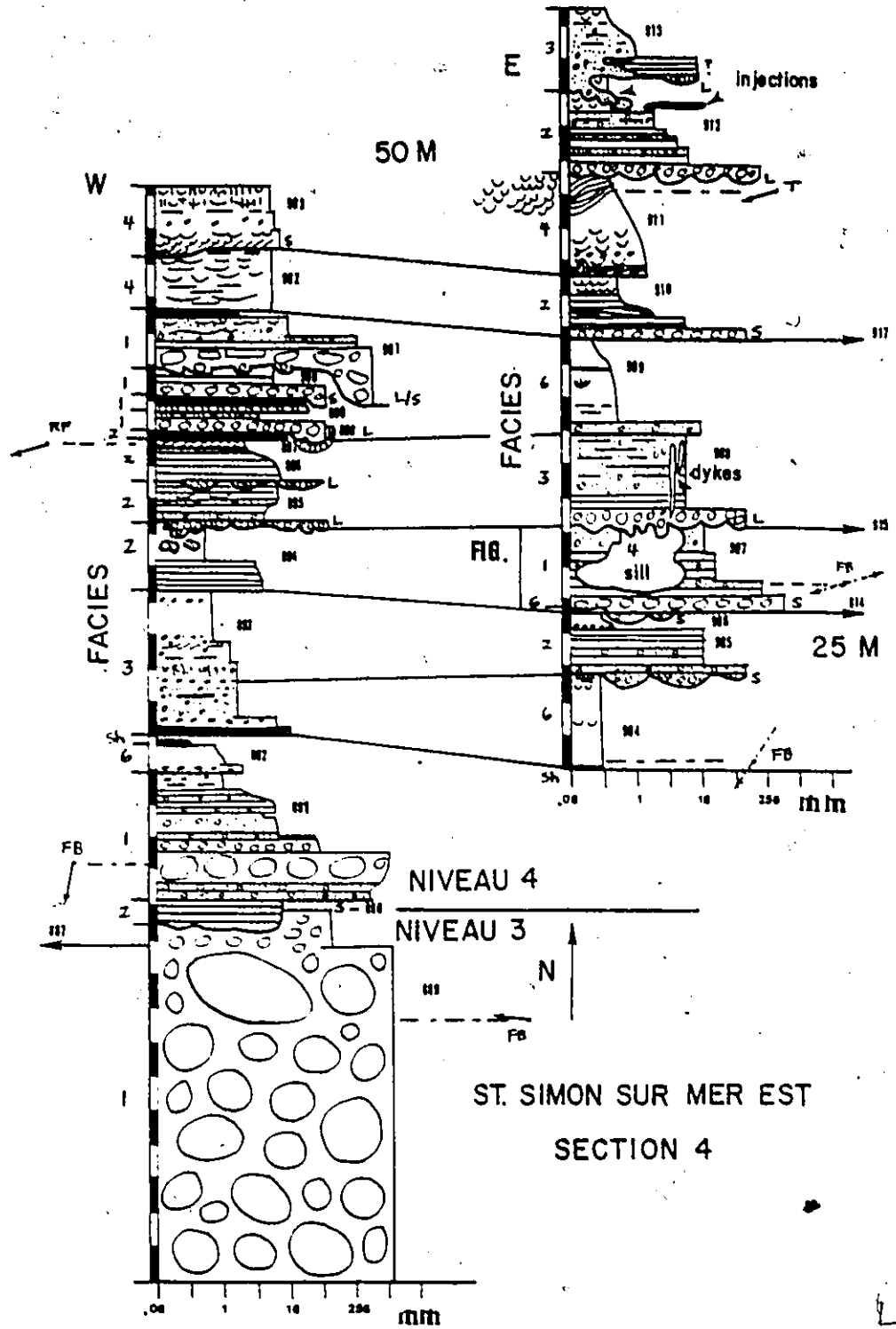


ST. SIMON SUR MER EST  
NIVEAU 3 SECTION 3

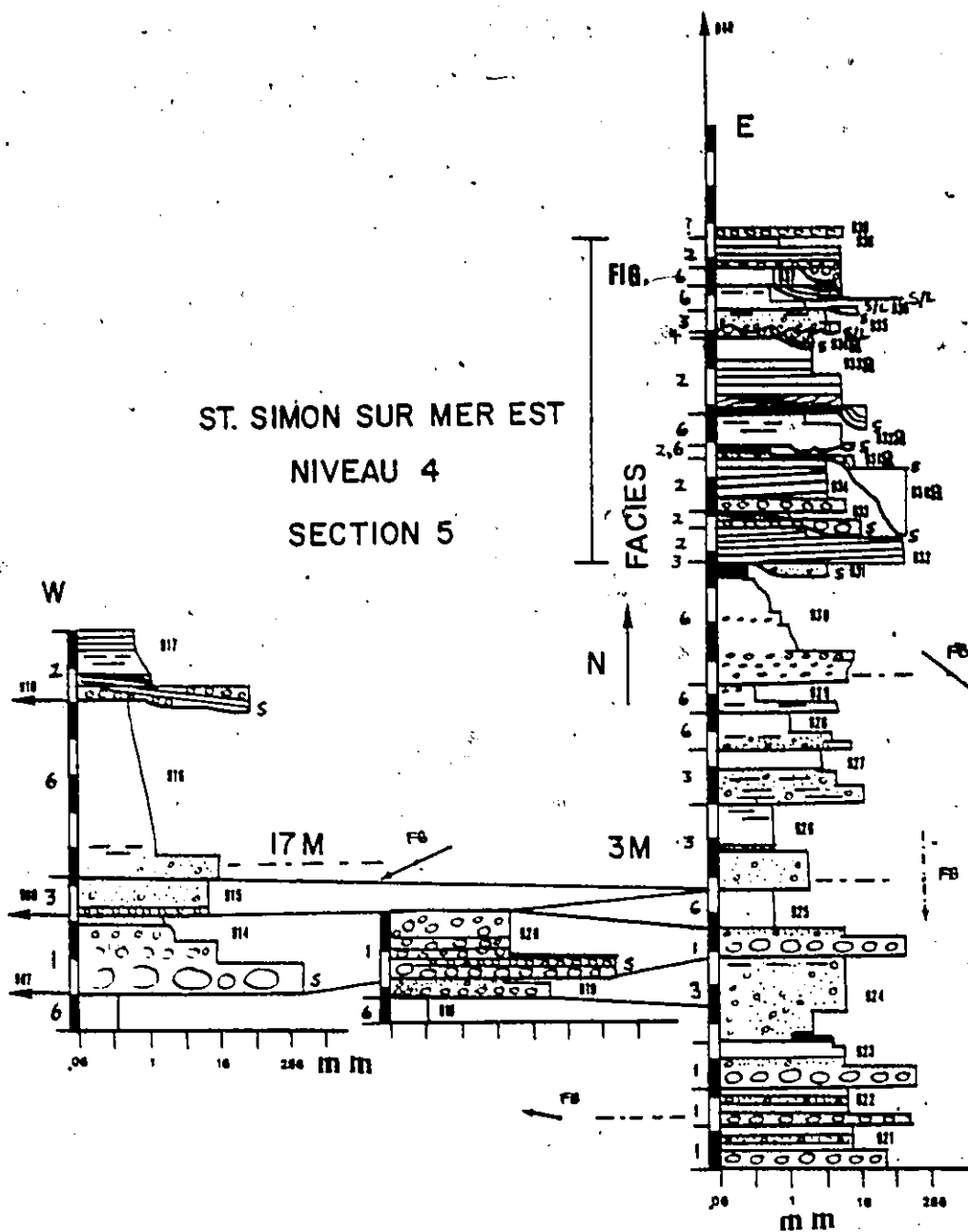


ST. SIMON SUR MER EST  
NIVEAU 4 SECTION 2

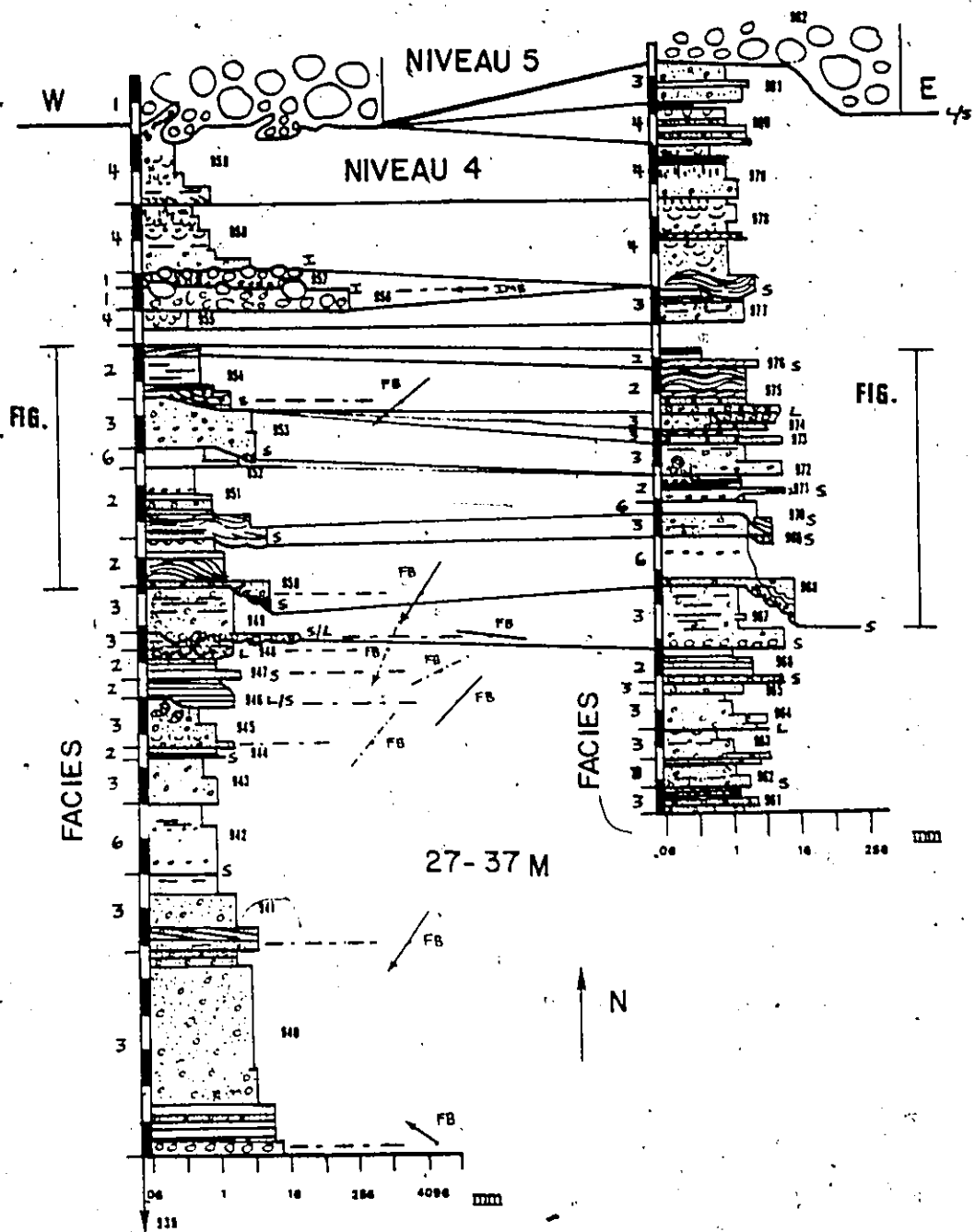


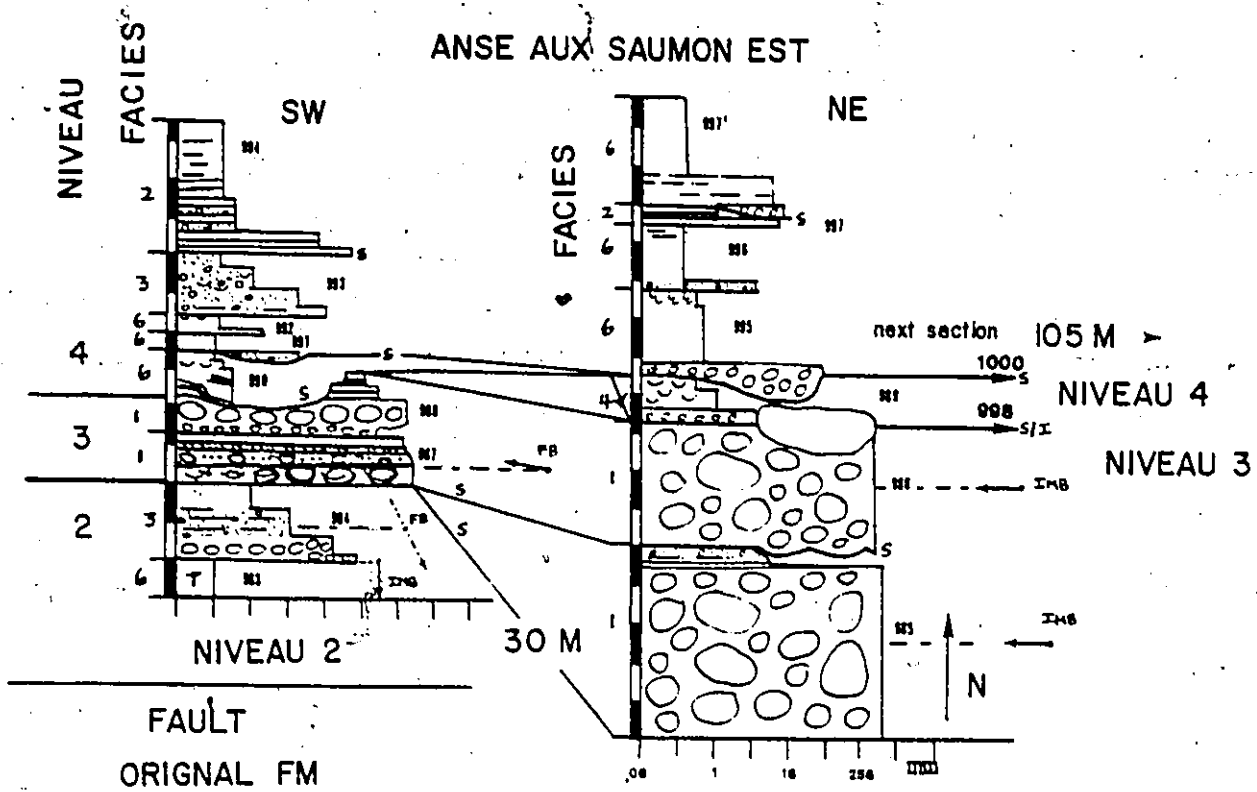


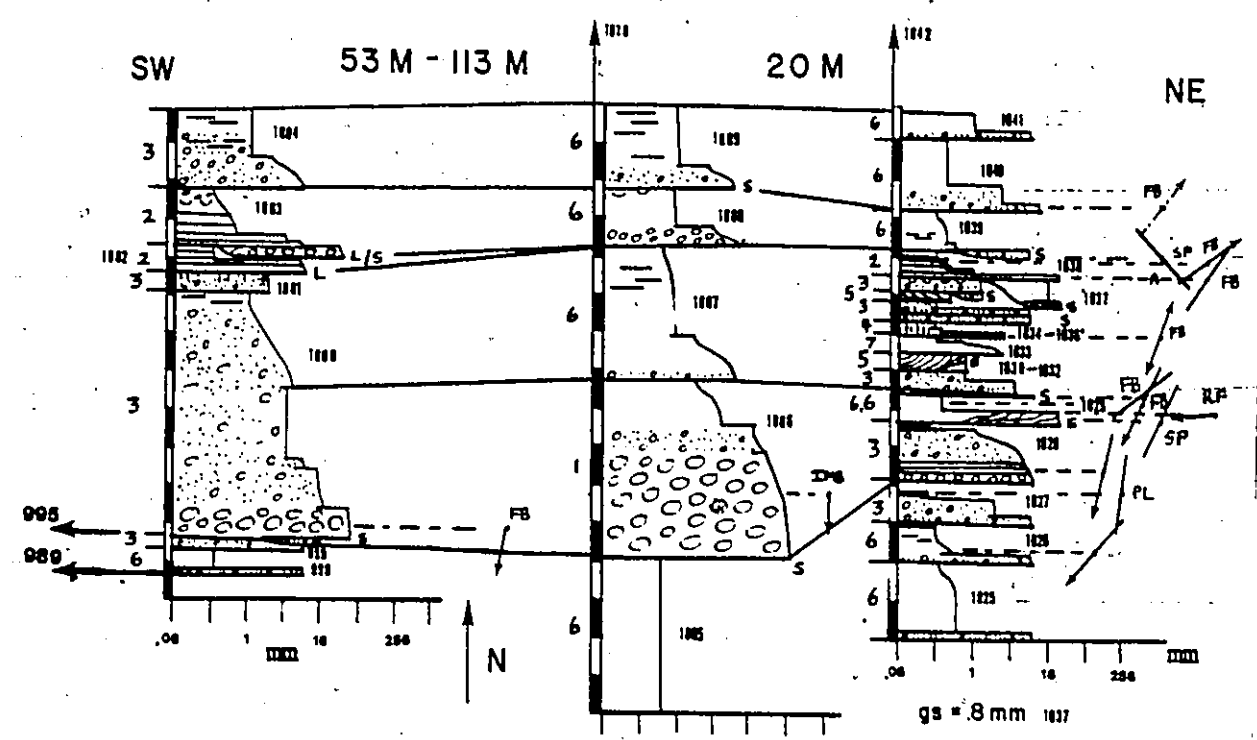
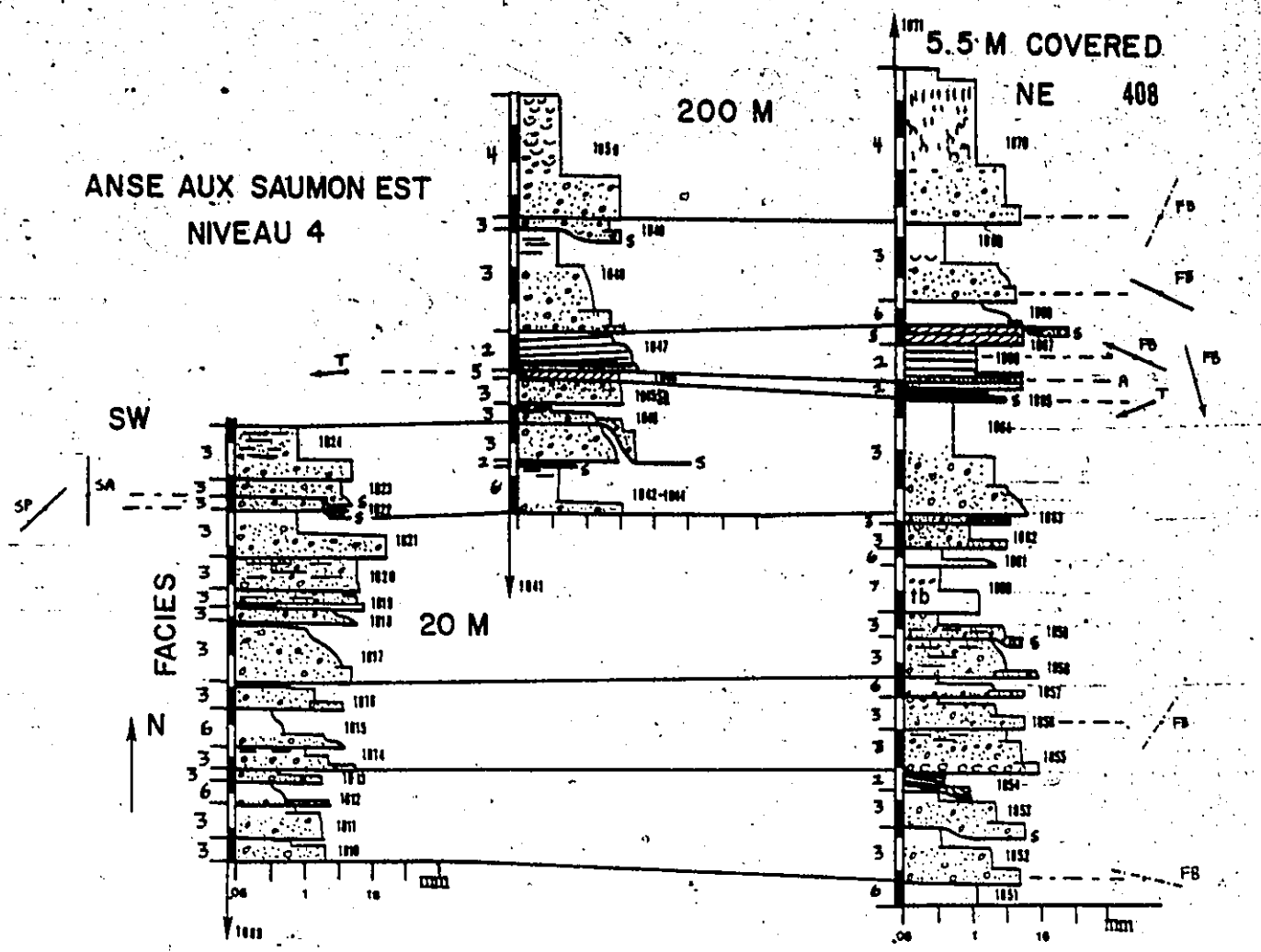
ST. SIMON SUR MER EST  
NIVEAU 4  
SECTION 5



ST. SIMON SUR MER EST SECTION 6

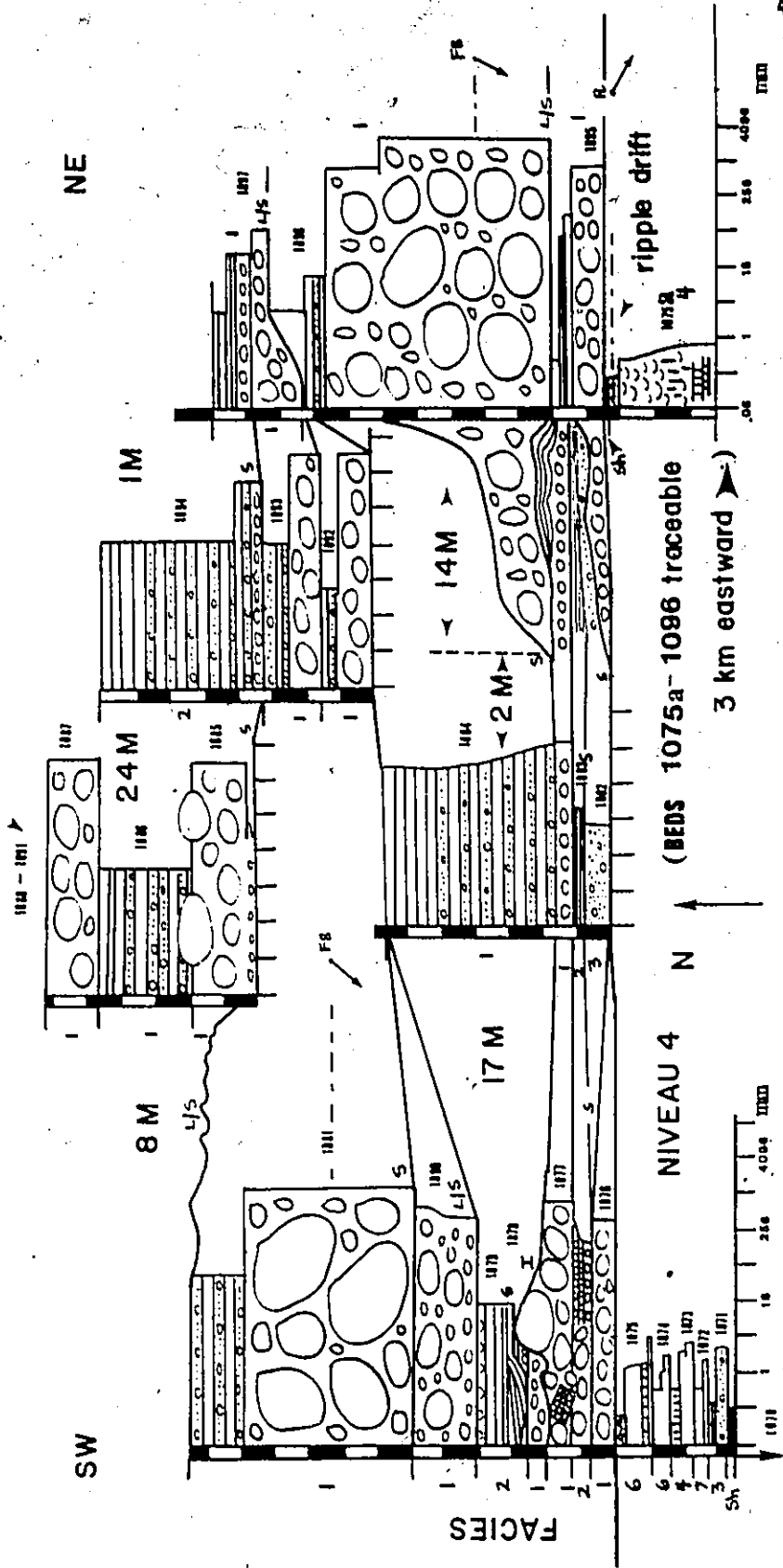






ANSE AUX SAUMON EST NIVEAU 4 / MEMBER II EQUIV.

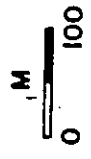
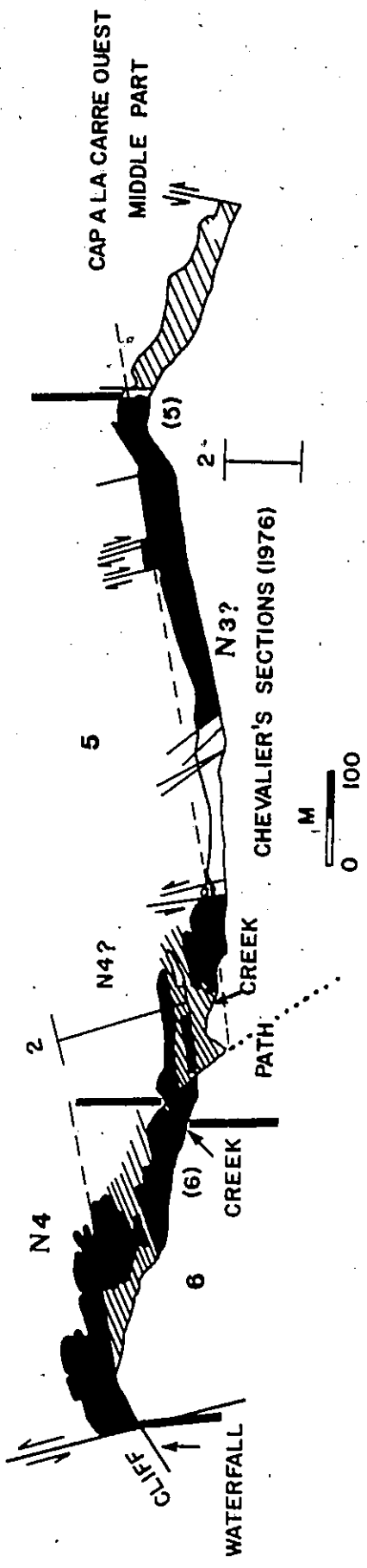
INACCESSIBLE SIMILAR TO 1094



# CAP A LA CARRE OUEST (WESTERN PART)



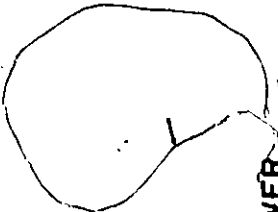
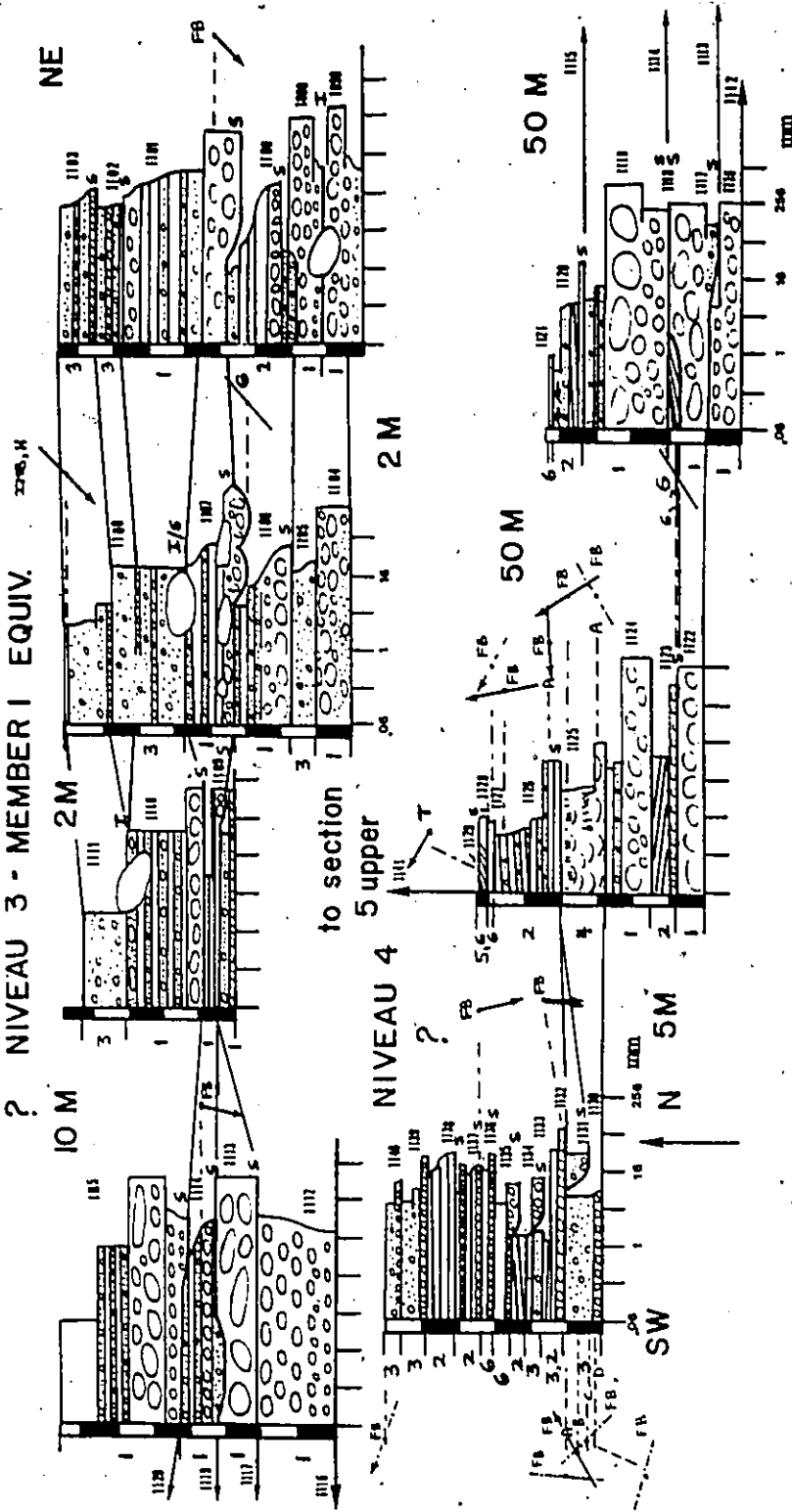
MAJOR FAULT ? M



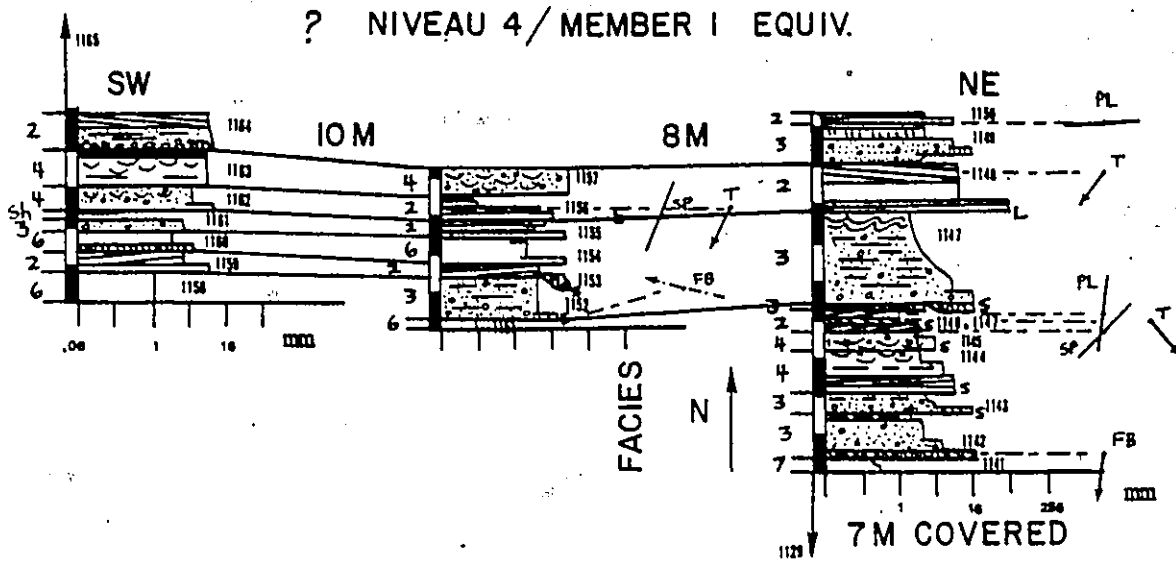


CAP A LA CARRE QUEST SECTION 5 LOWER

? NIVEAU 3 - MEMBER 1 EQUIV.

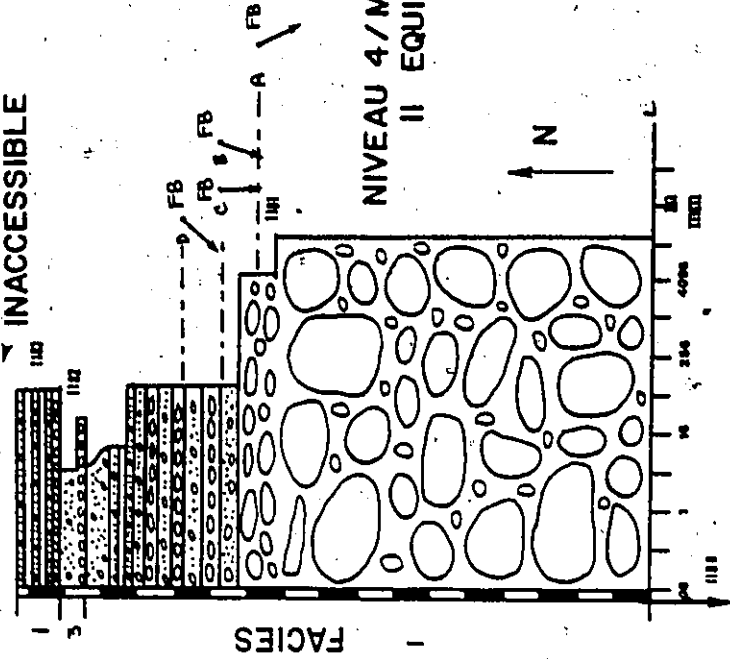


CAP A LA CARRE OUEST SECTION 5 UPPER  
 ? NIVEAU 4 / MEMBER I EQUIV.



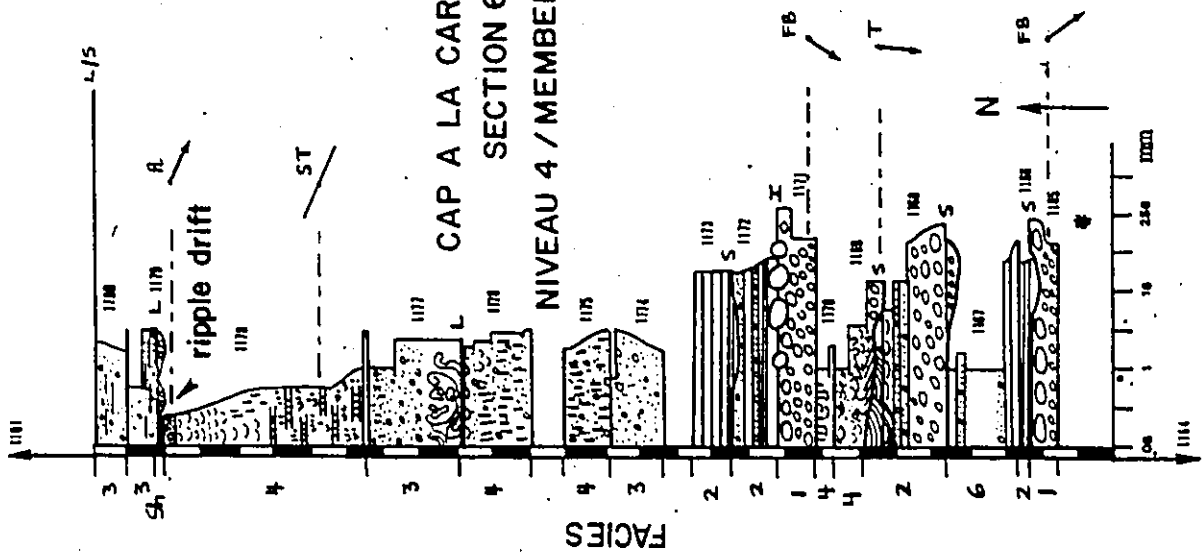
CAP A LA CARRE OUEST  
SECTION 6

INACCESSIBLE



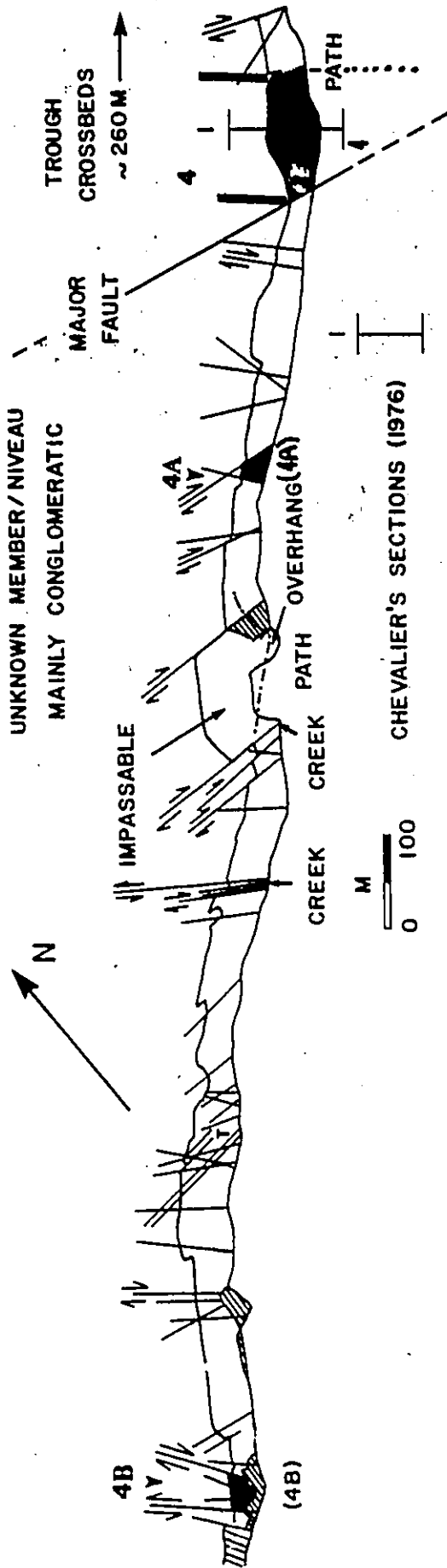
CAP A LA CARRE OUEST  
SECTION 6

NIVEAU 4 / MEMBER I EQUIV.

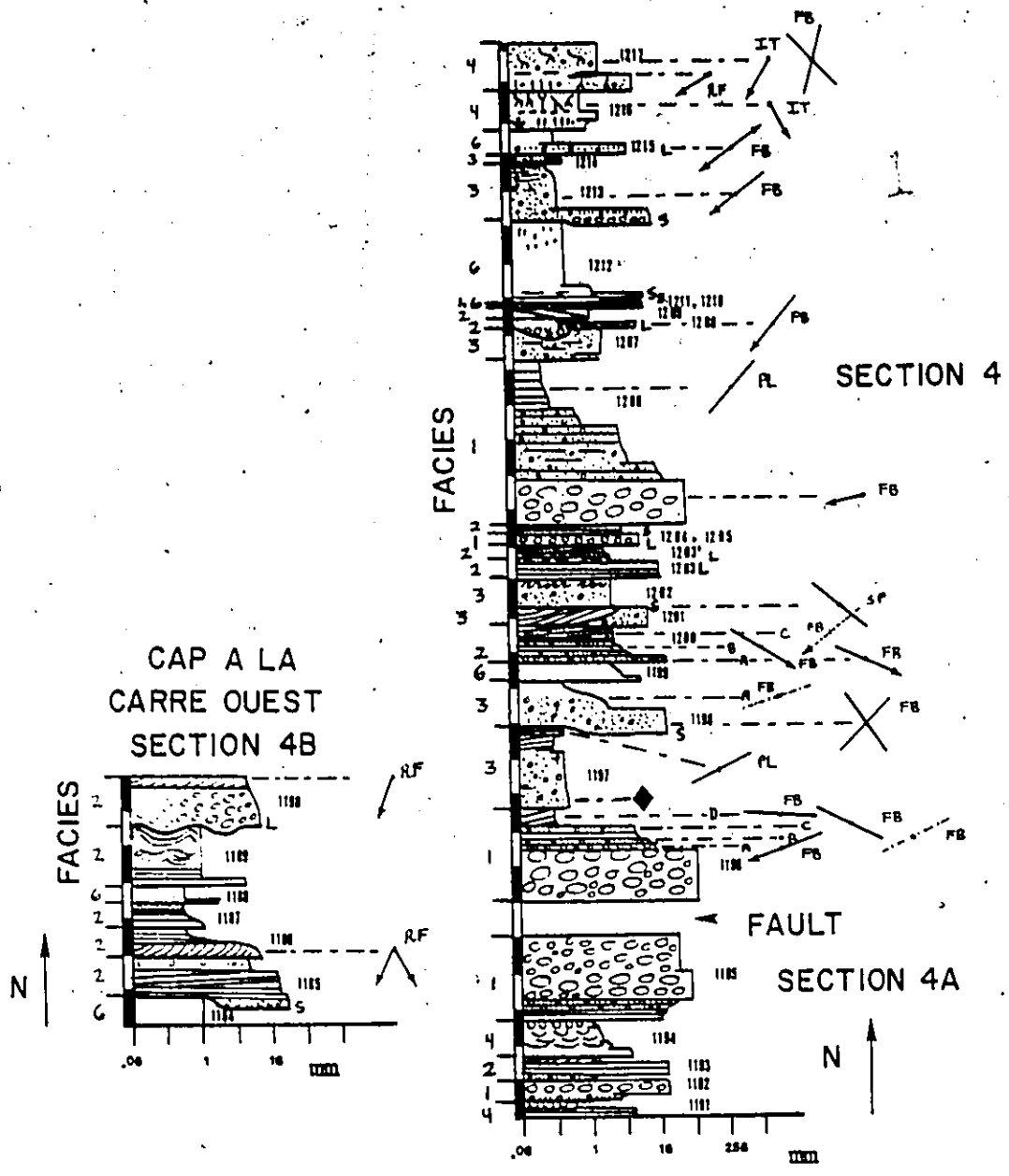


5

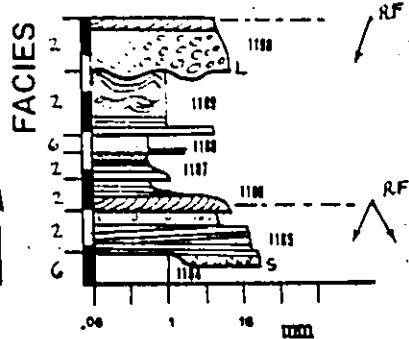
CAP A LA CARRE OUEST (MIDDLE PART)



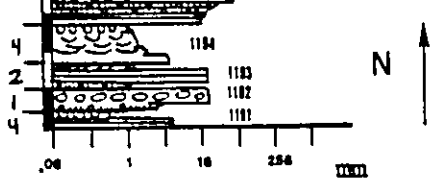
CAP A LA CARRE OUEST

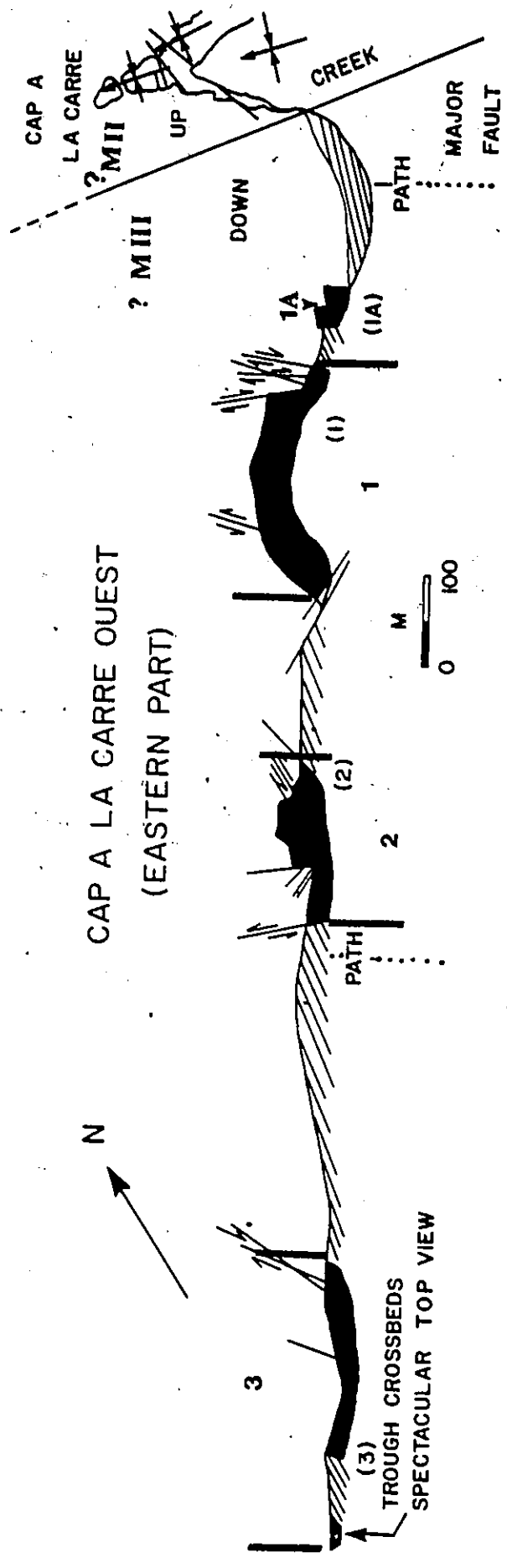


CAP A LA CARRE OUEST  
SECTION 4B



FAULT  
SECTION 4A

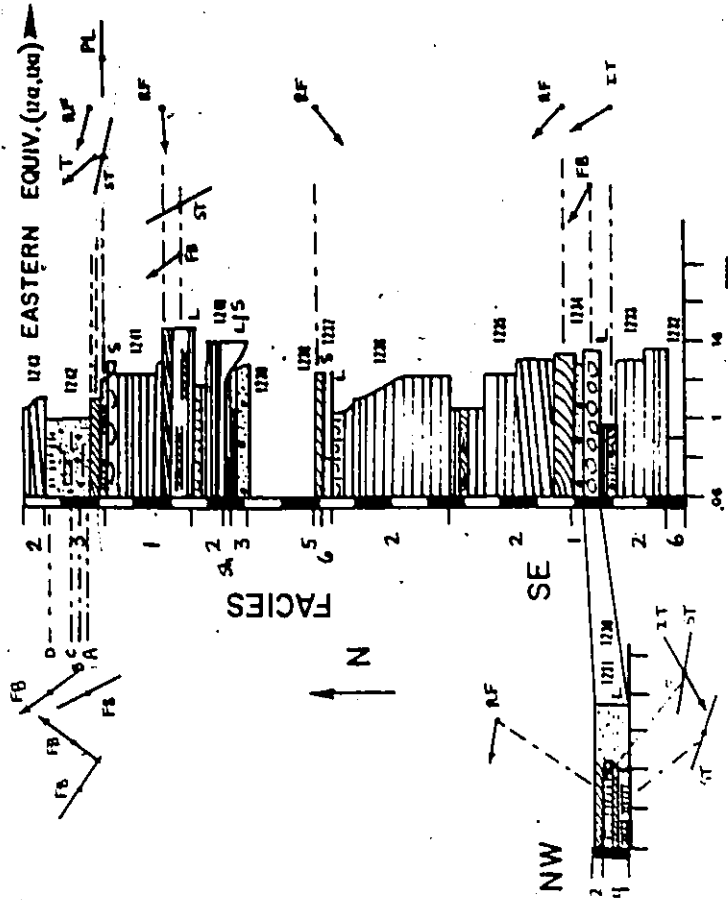




# ? MEMBER III

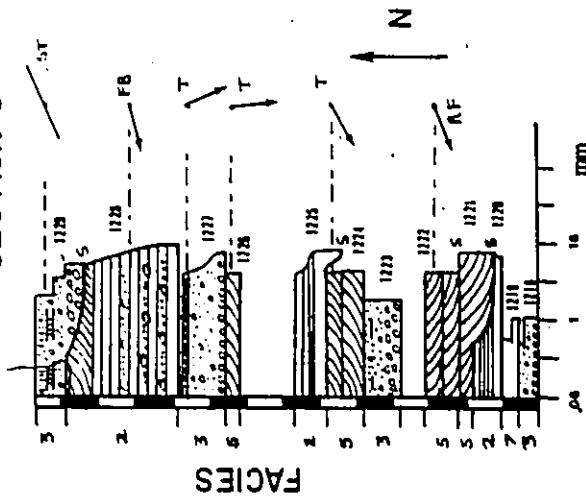
## CAP A LA CARRE OUEST

### SECTION 2

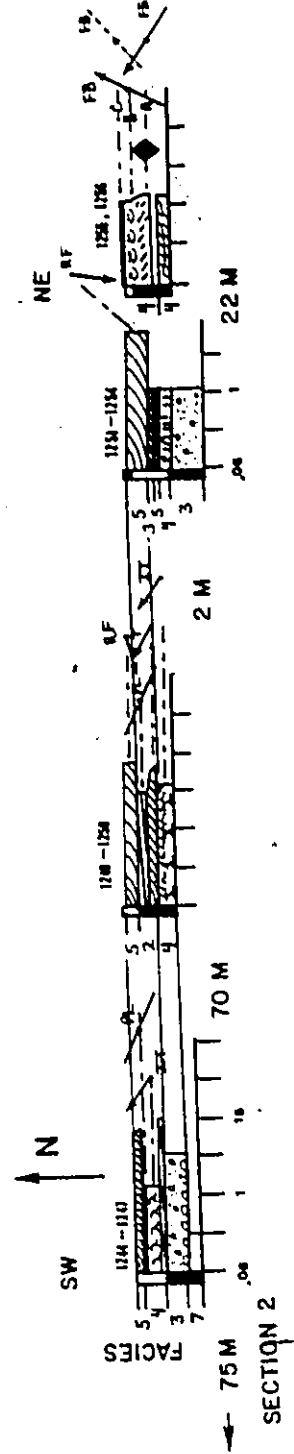


## CAP A LA CARRE OUEST

### SECTION 3



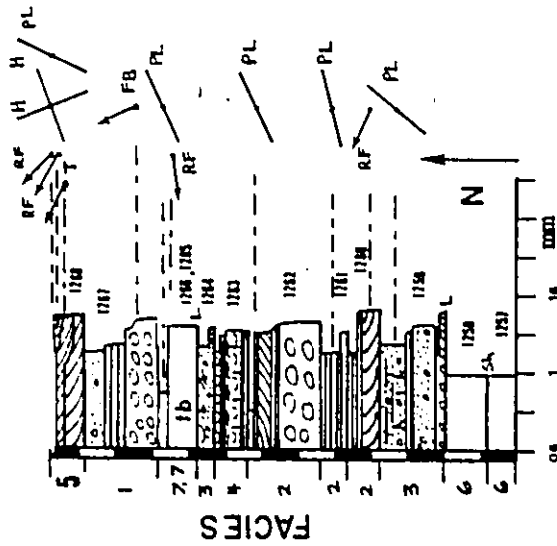
## EASTERN EQUIV. BEDS 1242, 1243



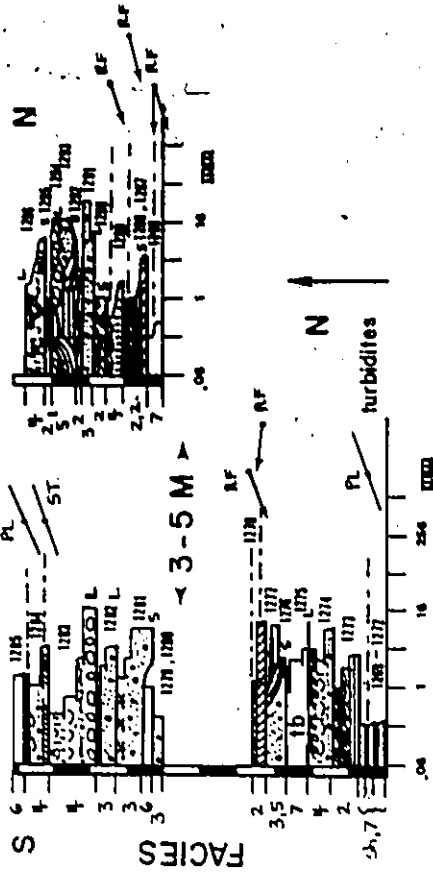
# ? MEMBER III

CAP A LA CARRE OUEST

SECTION I



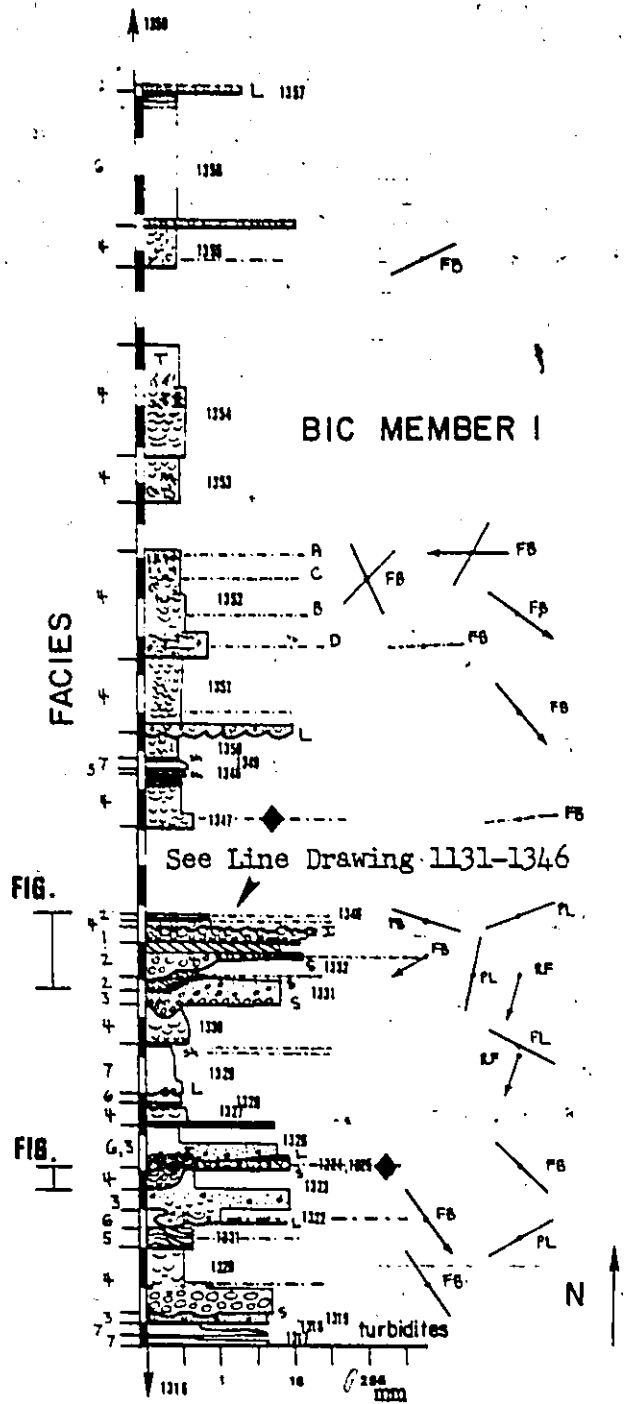
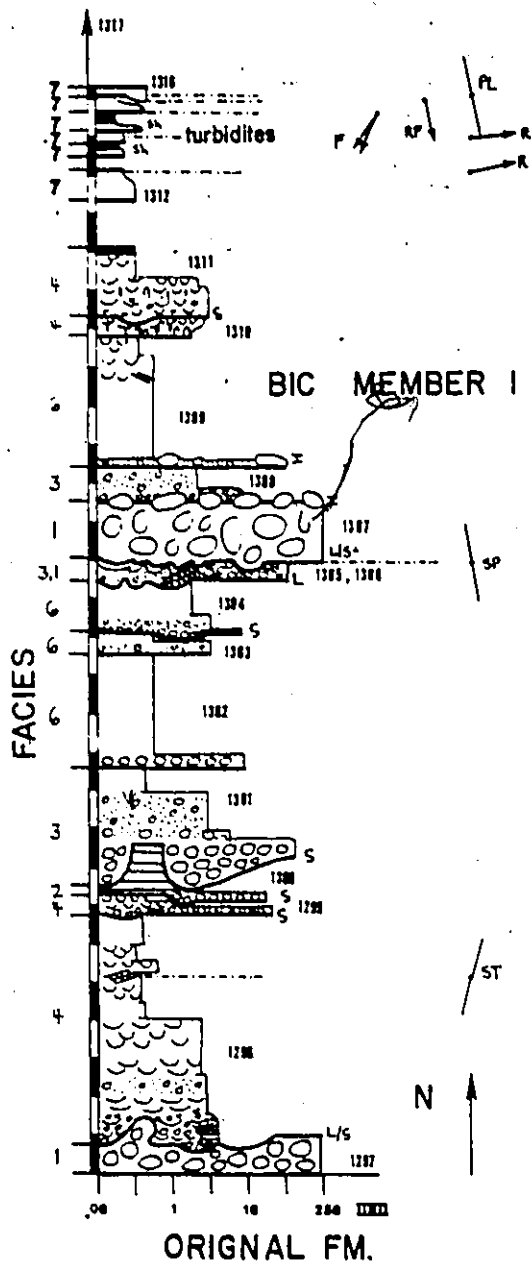
CAP A LA CARRE OUEST SECTION IA

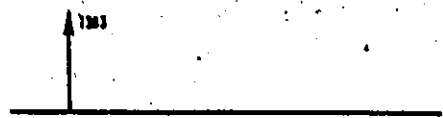


*Handwritten signature or initials.*

*Handwritten mark.*



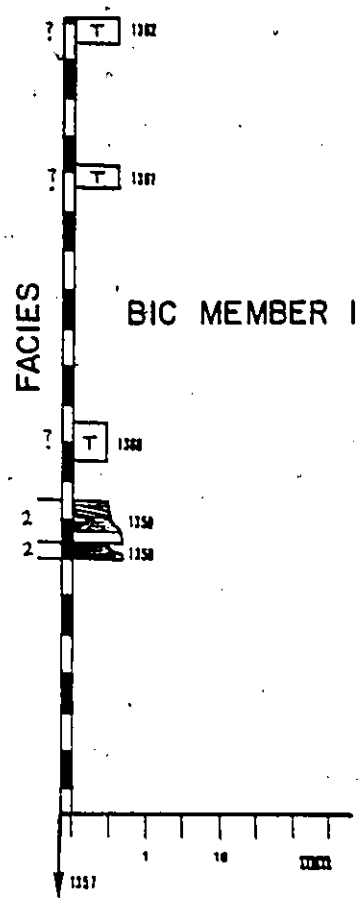


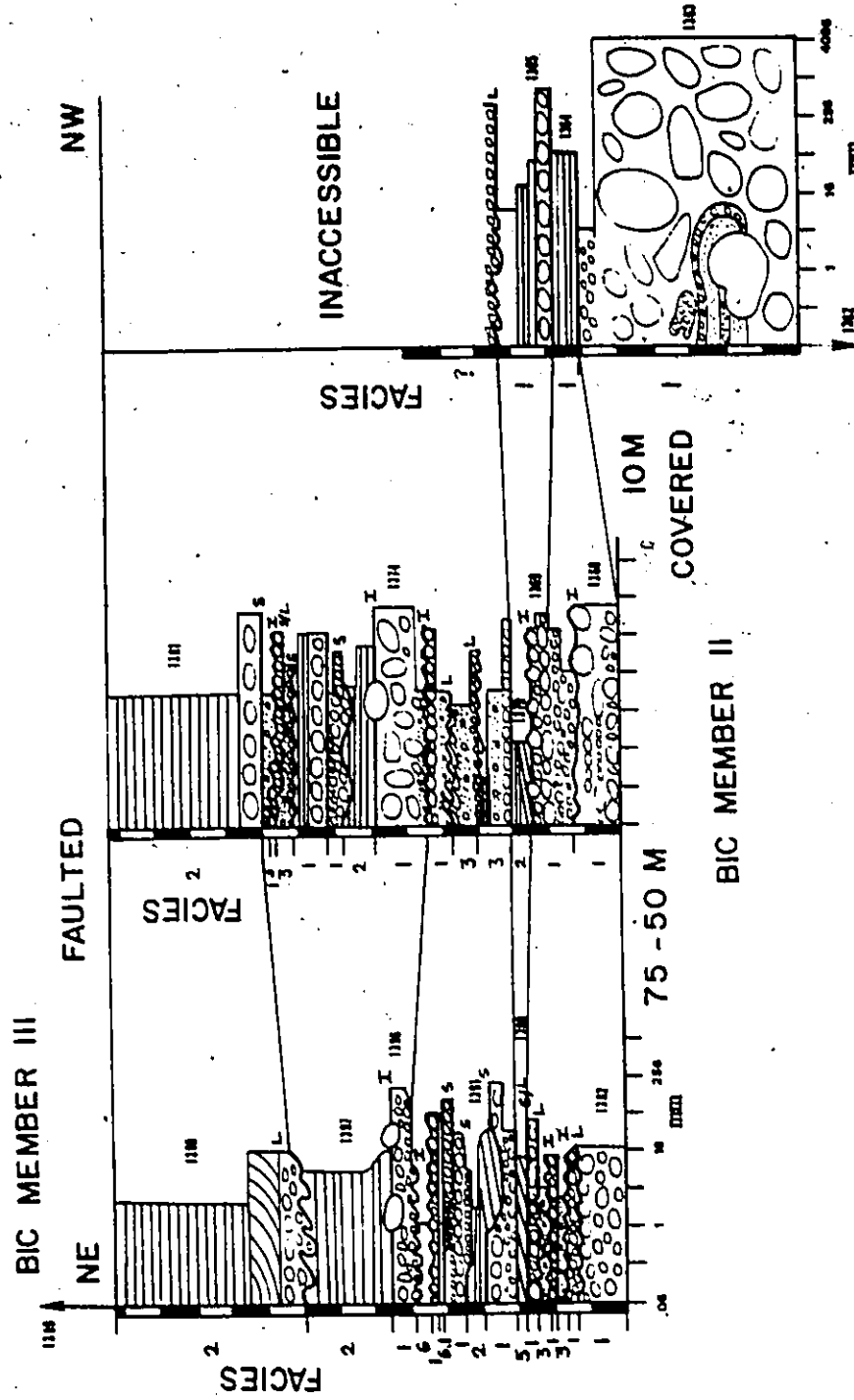


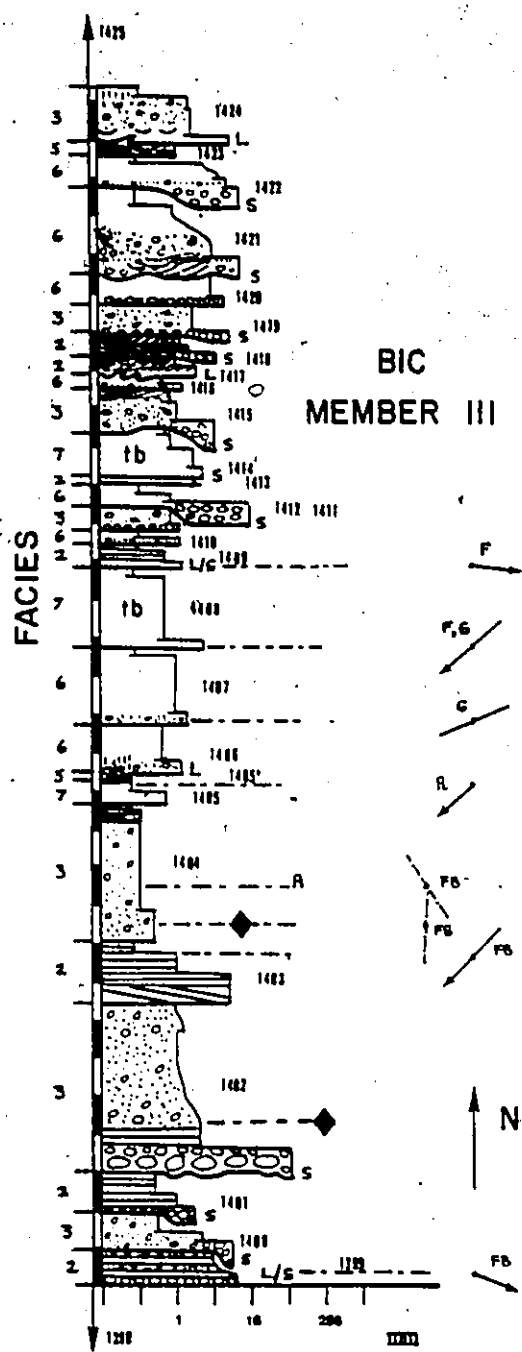
25-30 M CONGLOMERATE &  
SANDSTONE BLOCKS

BIC MEMBER II

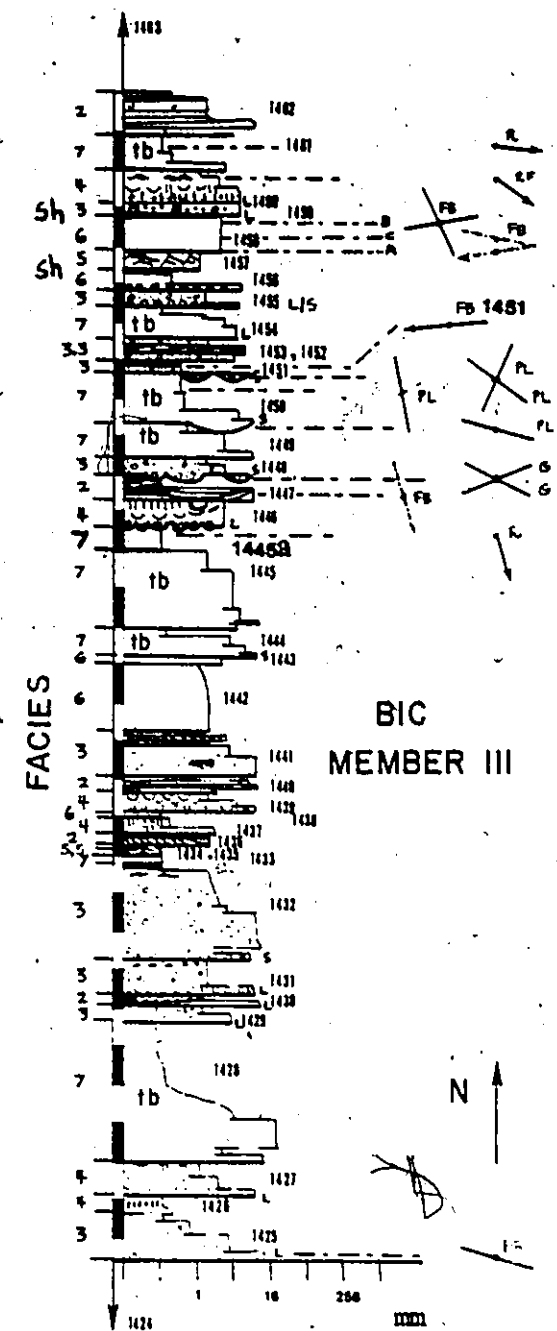
10 M TECTONIZED  
SANDSTONE BLOCKS



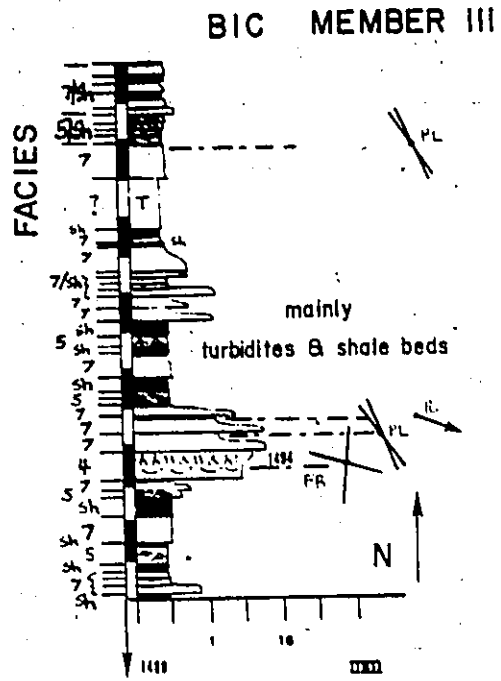
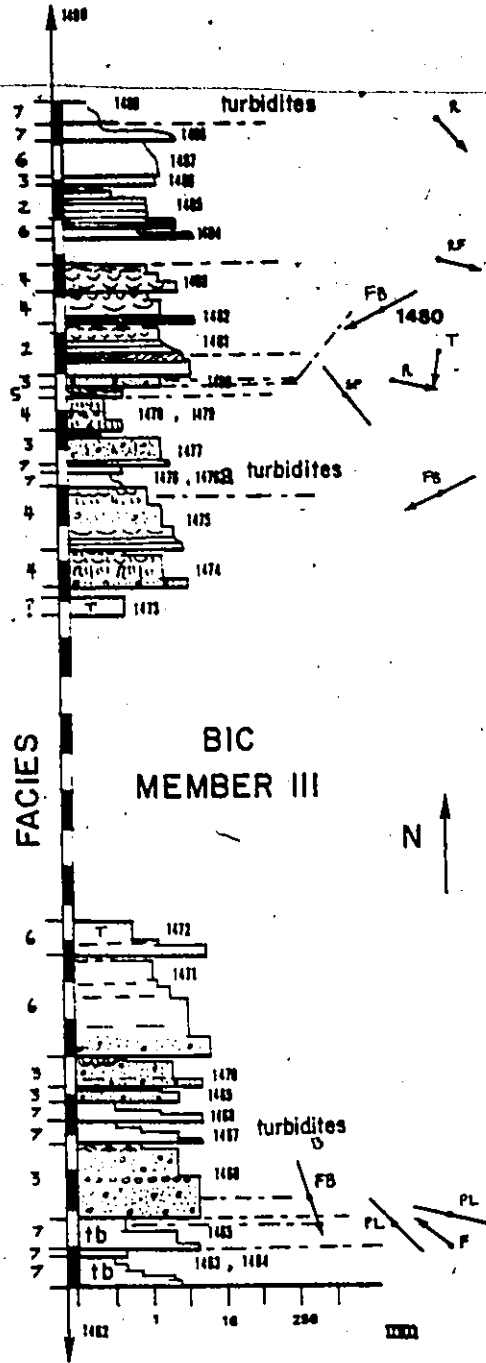




BIC MEMBER III



BIC MEMBER III



## APPENDIX 6

## FABRIC DATA FROM CONGLOMERATES\*

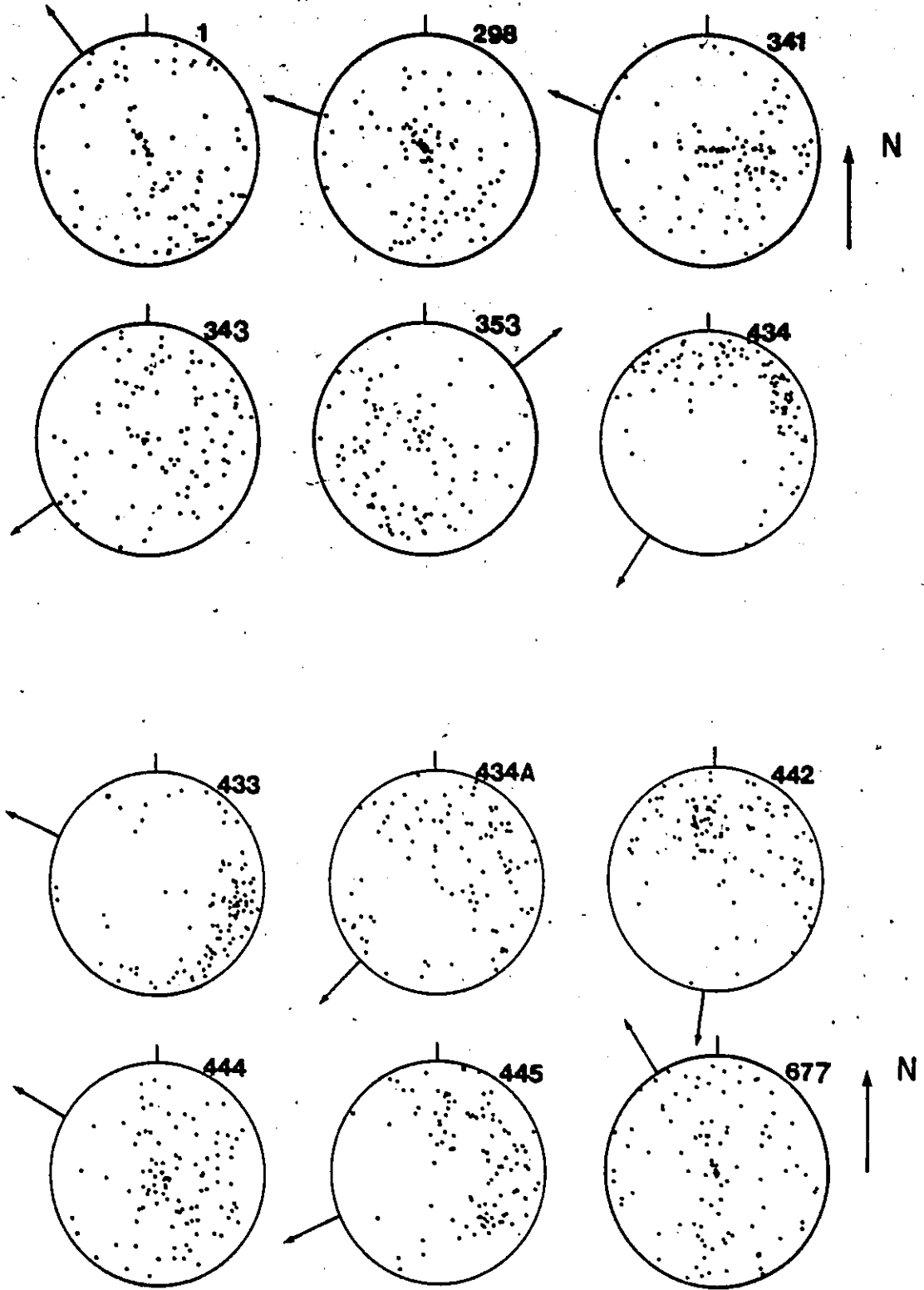
| Bed   | 2-D Az | Avg Dip | 3-D Az | 3-D Dip | $\hat{K}$ | $\hat{\theta}$ | $\hat{\theta}_{\alpha}$ | Paleoflow |
|-------|--------|---------|--------|---------|-----------|----------------|-------------------------|-----------|
| 1     | 139.1  | 35.7    | 144.1  | 5.7     | 3.94      | 61             | 84.53                   | 324.1     |
| 298   | 151.8  | 50.8    | 107.2  | 5.6     | 2.34      | 91             | 84.82                   | 287.2     |
| 341   | 107.6  | 44.9    | 108.5  | 21.5    | 3.29      | 69             | 68.55                   | 288.5     |
| 343   | 062.7  | 39.2    | 057.4  | 6.8     | 3.62      | 65             | 83.35                   | 237.4     |
| 353   | 226.3  | 40.2    | 233.2  | 14.0    | 3.72      | 64             | 76.07                   | 053.2     |
| 434   | 033.5  | 19.8    | 032.7  | 13.4    | 18.95     | 25             | 76.64                   | 212.7     |
| 434A  | 048.4  | 30.7    | 044.8  | 13.4    | 6.06      | 47             | 76.62                   | 224.8     |
| 433   | 116.8  | 22.1    | 114.5  | 14.9    | 15.25     | 28             | 75.09                   | 294.5     |
| 442   | 013.3  | 33.4    | 008.0  | 22.0    | 6.57      | 45             | 68.03                   | 188.0     |
| 444   | 118.8  | 46.5    | 119.1  | 19.5    | 3.01      | 73             | 70.63                   | 299.1     |
| 445   | 069.9  | 34.7    | 067.4  | 19.4    | 6.04      | 47             | 70.59                   | 247.4     |
| 677   | 145.9  | 38.7    | 147.3  | 2.7     | 3.44      | 67             | 87.84                   | 327.3     |
| 683   | 165.3  | 45.0    | 157.8  | 13.5    | 2.95      | 75             | 76.66                   | 337.8     |
| 694   | 038.9  | 41.0    | 046.8  | 4.2     | 3.47      | 67             | 86.11                   | 226.8     |
| 724   | 002.6  | 38.7    | 000.2  | 23.8    | 4.88      | 53             | 66.23                   | 180.2     |
| 739   | 037.9  | 38.9    | 027.0  | 9.0     | 3.38      | 68             | 81.14                   | 207.0     |
| 777   | 056.7  | 36.1    | 071.9  | 12.6    | 4.38      | 57             | 77.52                   | 251.9     |
| 790   | 105.5  | 44.0    | 112.7  | 22.0    | 3.26      | 70             | 68.08                   | 292.7     |
| 792   | 172.2  | 44.6    | 167.9  | 25.7    | 3.72      | 64             | 64.39                   | 347.9     |
| 796   | 040.5  | 45.3    | 044.4  | 17.3    | 3.11      | 72             | 72.77                   | 224.4     |
| 799   | 124.2  | 45.1    | 112.2  | 11.7    | 2.96      | 75             | 78.45                   | 292.2     |
| 801   | 104.4  | 48.6    | 111.5  | 25.2    | 2.95      | 75             | 64.89                   | 291.5     |
| 889   | 096.8  | 43.1    | 093.8  | 15.2    | 3.29      | 69             | 74.90                   | 273.8     |
| 891   | 006.6  | 38.3    | 012.0  | 10.2    | 3.82      | 62             | 79.93                   | 192.0     |
| 922   | 096.8  | 35.8    | 100.7  | 18.5    | 4.82      | 54             | 71.57                   | 280.7     |
| 940   | 070.4  | 41.2    | 123.1  | 9.0     | 3.29      | 69             | 81.21                   | 303.1     |
| 987   | 088.5  | 29.2    | 098.8  | 16.3    | 7.46      | 41             | 73.71                   | 278.8     |
| 1000  | 017.7  | 27.0    | 013.0  | 11.3    | 6.73      | 44             | 78.77                   | 193.0     |
| 1096  | 022.0  | 45.7    | 026.8  | 12.6    | 2.92      | 76             | 77.54                   | 206.8     |
| 1081  | 012.2  | 49.4    | 039.9  | 10.1    | 2.48      | 87             | 80.11                   | 219.9     |
| 1142  | 004.9  | 27.8    | 006.9  | 11.4    | 6.61      | 44             | 78.63                   | 186.9     |
| 1165  | 322.9  | 41.1    | 325.0  | 28.5    | 5.51      | 49             | 61.52                   | 145.0     |
| 1171  | 147.2  | 35.5    | 033.6  | 1.9     | 4.20      | 58             | 88.70                   | 213.6     |
| 1181A | 342.2  | 42.8    | 334.4  | 20.0    | 3.57      | 65             | 70.04                   | 154.4     |
| 1181B | 015.7  | 45.6    | 017.6  | 12.8    | 2.95      | 75             | 77.32                   | 197.6     |
| 1181C | 005.4  | 53.4    | 001.9  | 30.2    | 2.71      | 80             | 59.85                   | 181.9     |
| 1181D | 045.7  | 47.6    | 041.5  | 29.4    | 3.68      | 64             | 60.70                   | 221.5     |
| 1114  | 161.1  | 34.9    | 013.2  | 3.1     | 4.36      | 57             | 87.21                   | 193.2     |
| 1132  | 178.3  | 34.0    | 004.0  | 15.1    | 5.03      | 52             | 75.00                   | 184.0     |
| 1132A | 002.7  | 24.3    | 360.0  | 9.3     | 8.83      | 41             | 80.72                   | 180.0     |
| 1137  | 348.8  | 26.4    | 348.8  | 14.0    | 8.83      | 41             | 76.00                   | 168.8     |
| 1101  | 038.9  | 49.7    | 044.3  | 18.2    | 2.71      | 80             | 71.95                   | 224.3     |
| 1206  | 079.4  | 30.3    | 077.6  | 11.5    | 6.11      | 46             | 78.57                   | 257.6     |

FABRIC DATA FROM CONGLOMERATES (continued)

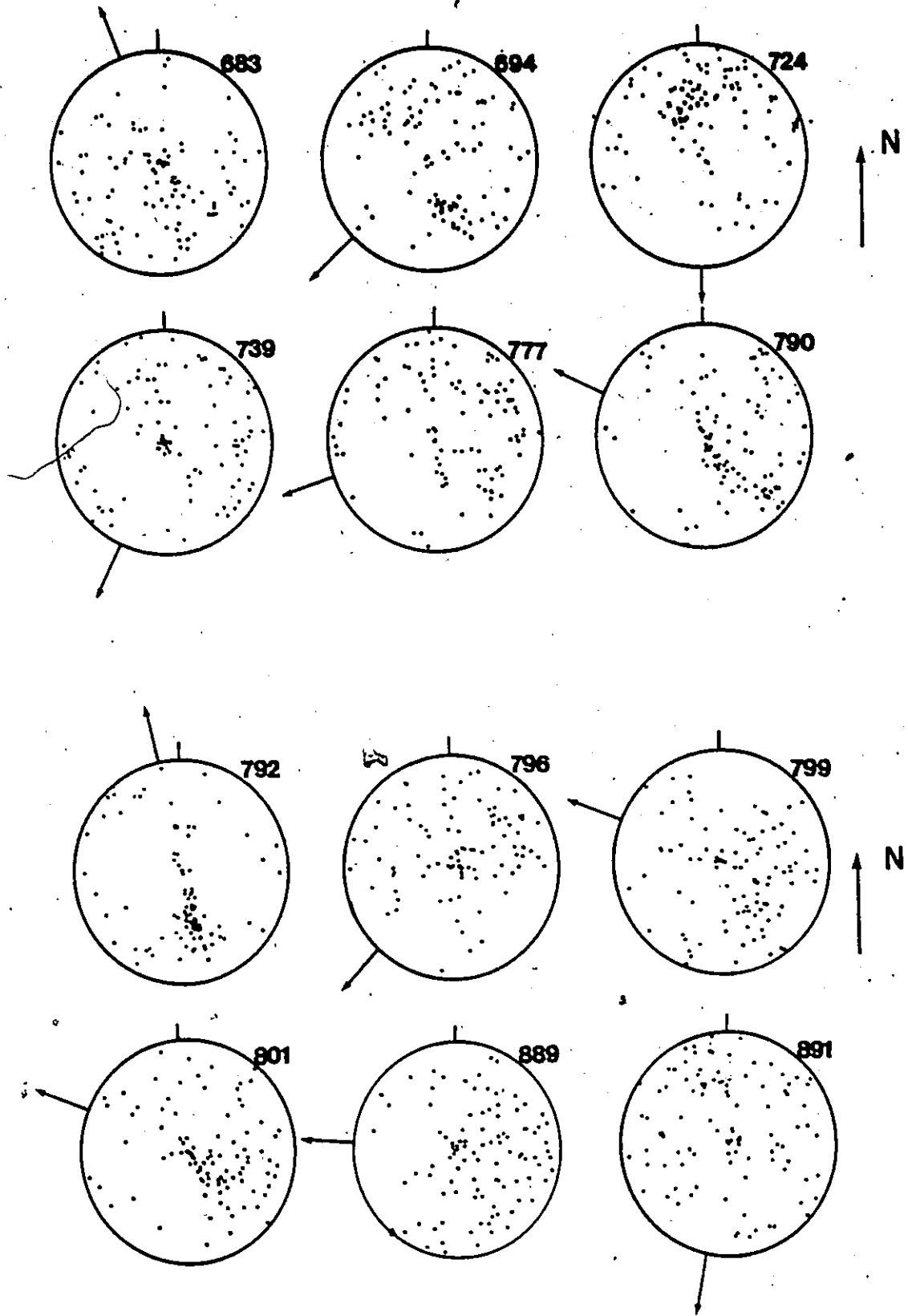
| <u>Bed</u> | <u>2-D Az</u> | <u>Avg Dip</u> | <u>3-D Az</u> | <u>3-D Dip</u> | $\hat{K}$ | $\hat{\theta}$ | $\hat{\theta}_\alpha$ | <u>Paleoflow</u> |
|------------|---------------|----------------|---------------|----------------|-----------|----------------|-----------------------|------------------|
| 1228       | 088.3         | 32.2           | 074.9         | 9.7            | 5.17      | 52             | 80.34                 | 254.9            |
| 1234       | 119.0         | 39.5           | 119.3         | 23.5           | 4.66      | 55             | 66.58                 | 299.3            |
| 1241       | 126.3         | 39.5           | 142.9         | 10.4           | 3.61      | 65             | 79.73                 | 322.9            |
| 1267       | 154.9         | 45.3           | 155.7         | 16.6           | 3.26      | 70             | 73.51                 | 335.7            |
| 1342       | 042.0         | 26.4           | 060.4         | 4.2            | 6.67      | 44             | 85.92                 | 240.4            |
| 1399       | 124.1         | 40.9           | 290.0         | 7.6            | 3.40      | 68             | 82.54                 | 110.0            |

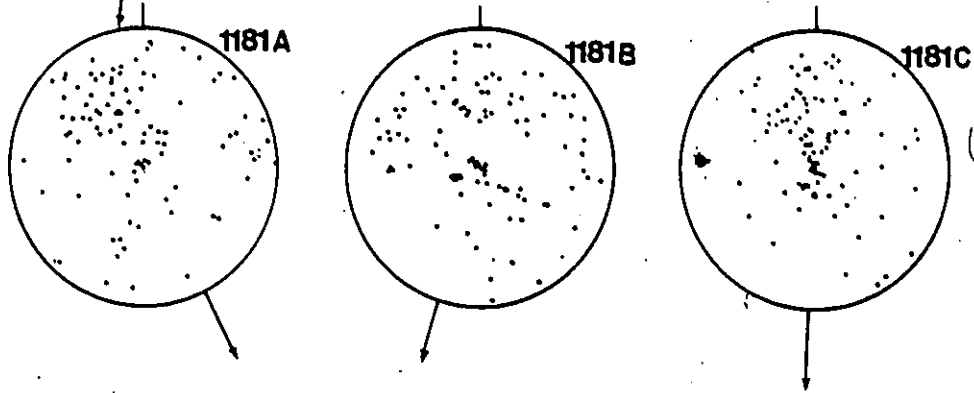
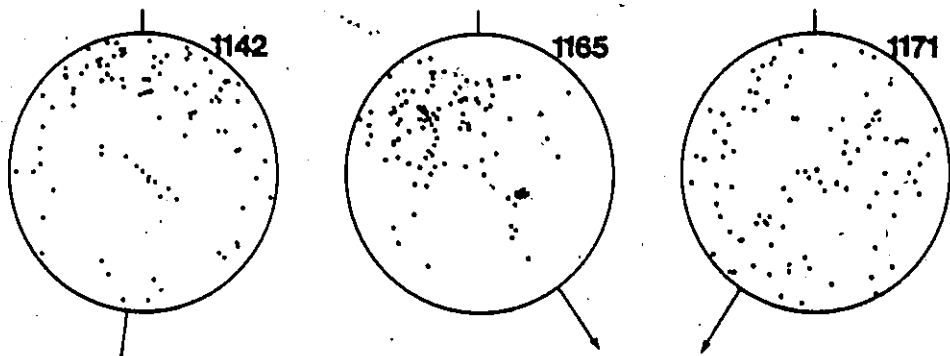
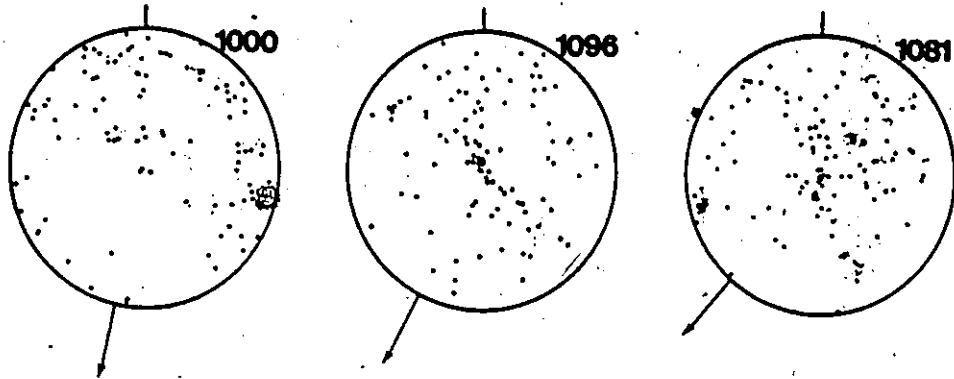
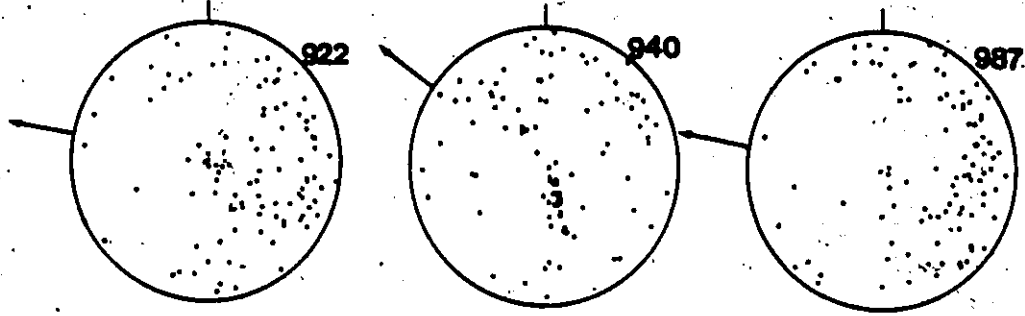
\* Key: 2-D Az - two dimensional vector mean of the projections of the pebble orientations onto a flat surface; Avg Dip - average dip of pebbles, measured as an absolute deviation from the horizontal, regardless of direction of dip; 3-D Az: three dimensional vector mean azimuth; 3-D Dip - three dimensional vector mean dip (takes into account direction of dip);  $\hat{K}$  - precision constant K estimate;  $\hat{\theta}$  - estimate of the semi-angle of the confidence of the three-dimensional vector mean;  $\hat{\theta}_\alpha$  - estimate of the semi-angle of the confidence of the three-dimensional vector mean azimuth ( $\hat{\theta}$  and  $\hat{\theta}_\alpha$  calculated at the 95% confidence level); Paleoflow - direction of the paleoflow direction, Paleoflow = 3-D vector mean azimuth  $\pm 180^\circ$  = current direction. (see Nederlof and Weber, 1971, for discussion of these statistics)

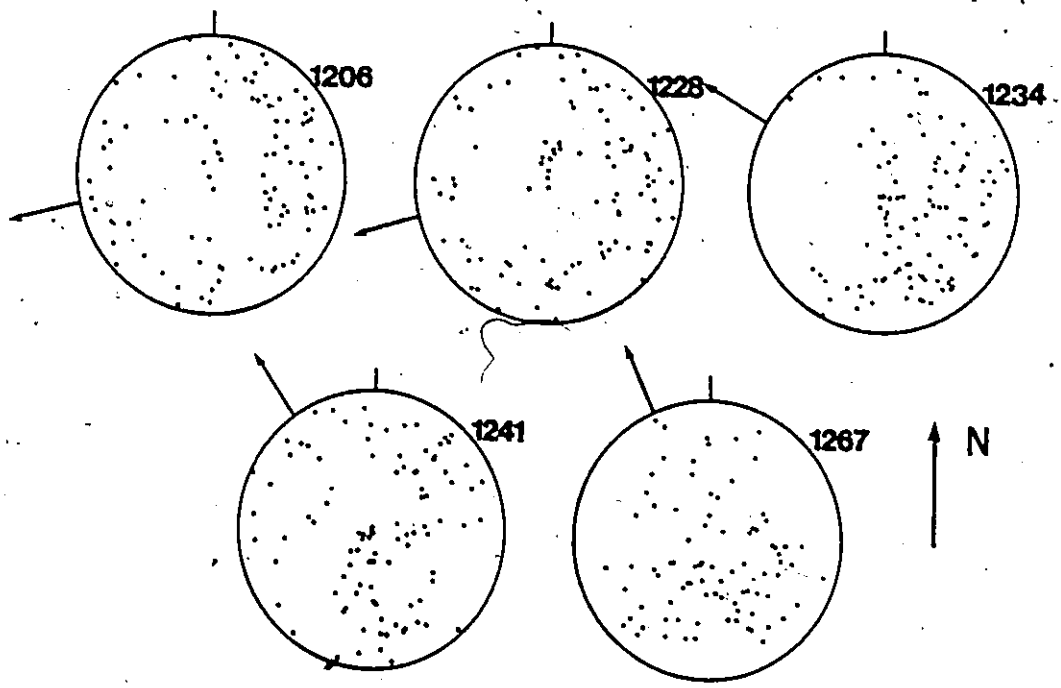
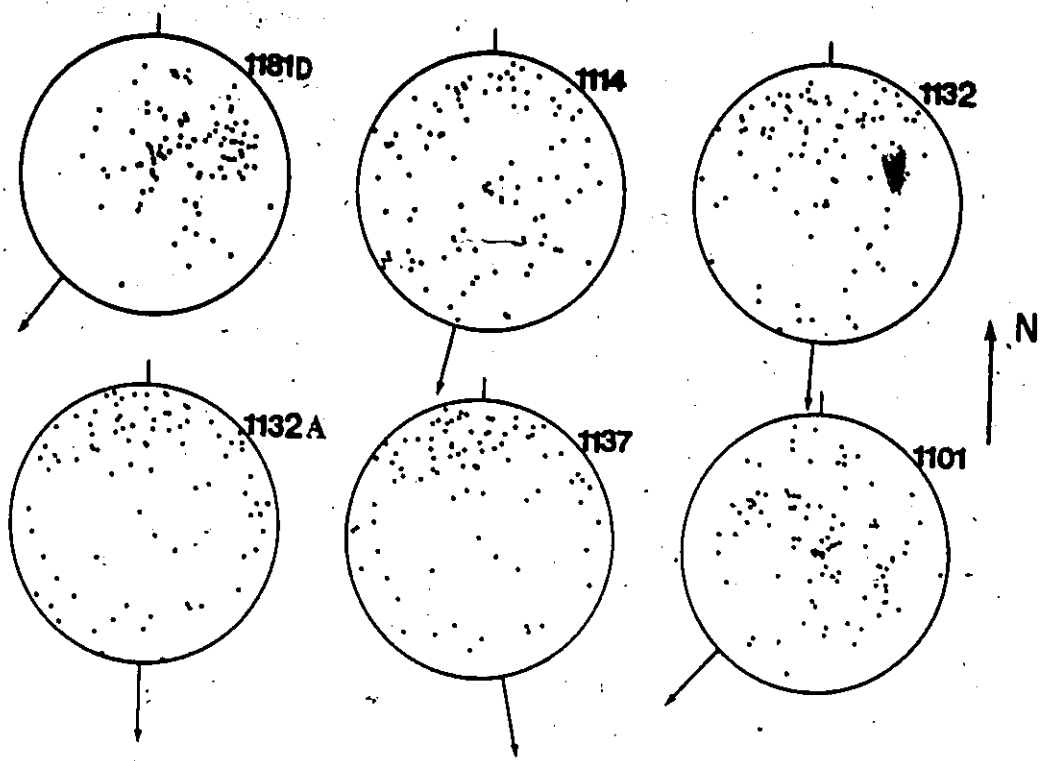
Southern hemisphere stereonet plots of the conglomerate fabric data are given on the following pages. Each point is the direction of the maximum dip of each clast. Arrows show the computed vector-mean flow direction (paleoflow). North arrow indicates north direction. Tick marks on the top of each stereonet are the north direction. Numbers indicate bed numbers. Letters indicate positions within individual beds (see sections).

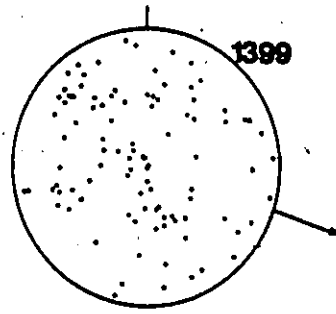
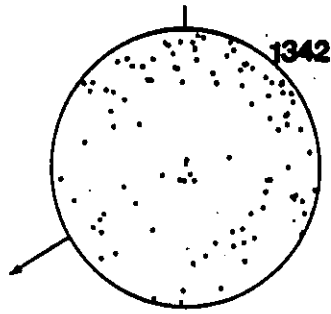












↑ N

## APPENDIX 7

## FABRIC DATA FROM PEBBLY SANDSTONES AND SANDSTONES

## SUMMARY STATISTICS OF FABRIC IN BEDDING \*

| Bed  | $\bar{\theta}$ | $\% ^2$ | $\chi^2 = 2 \text{ df}$<br>Sig. Level | L% | $s^0$ | N   | Orientation<br>Pattern |
|------|----------------|---------|---------------------------------------|----|-------|-----|------------------------|
| 3    | 136            | 1.77    | 1.0 - 0.2                             | 9  | --    | 100 | Random                 |
| 74   | 069            | 7.78    | .025 - .01                            | 20 | 46    | 100 | Unimodal               |
| 123  | 003            | 0.61    | 1.0 - 0.2                             | 5  | --    | 100 | Random                 |
| 430  | 071            | 5.34    | 0.1 - 0.05                            | 16 | 47    | 100 | Unimodal               |
| 432  | 033            | 4.11    | 0.2 - 0.1                             | 14 | 47    | 100 | Unimodal (Poor)        |
| 434  | 051            | 12.07   | <0.005                                | 25 | 44    | 100 | Unimodal (Good)        |
| 436  | ---            | ---     | -----                                 | -- | --    | 100 | Bimodal (125-305)      |
| 446  | 117            | 0.97    | 1.0 - 0.2                             | 7  | --    | 100 | Random                 |
| 457  | ---            | ---     | -----                                 | -- | --    | 100 | Bimodal (045-225)      |
| 459  | ---            | ---     | -----                                 | -- | --    | 101 | Bimodal (035-215)      |
| 501A | 115            | 10.52   | 0.01 - 0.005                          | 23 | 44    | 100 | Unimodal               |
| 501B | ---            | ---     | -----                                 | -- | --    | 101 | Bimodal (035-215)      |
| 505  | ---            | ---     | -----                                 | -- | --    | 100 | Bimodal (065-245)      |
| 682  | 026            | 13.48   | <0.005                                | 26 | 44    | 099 | Unimodal (Good)        |
| 685  | ---            | ---     | -----                                 | -- | --    | 100 | Bimodal (030-210)      |
| 690  | 177            | 12.72   | <0.005                                | 25 | 44    | 100 | Unimodal (Good)        |
| 692  | 031            | 7.98    | 0.025 - 0.1                           | 20 | 46    | 100 | Unimodal               |
| 694  | 038            | 18.11   | <0.005                                | 30 | 43    | 100 | Unimodal (Good)        |
| 709  | 054            | 4.38    | 0.2 - 0.1                             | 15 | 47    | 100 | Unimodal (Poor)        |
| 711  | ---            | ---     | -----                                 | -- | --    | 099 | Bimodal (045-225)      |
| 730  | 044            | 7.36    | 0.05 - 0.025                          | 19 | 45    | 100 | Unimodal               |
| 740  | ---            | ---     | -----                                 | -- | --    | 100 | Bimodal (005-185)      |
| 761  | ---            | ---     | -----                                 | -- | --    | 100 | Bimodal (015-195)      |
| 762  | ---            | ---     | -----                                 | -- | --    | 100 | Bimodal (045-225)      |
| 768  | 053            | 12.94   | <0.005                                | 25 | 44    | 100 | Unimodal (Good)        |
| 797  | ---            | ---     | -----                                 | -- | --    | 100 | Bimodal (055-235)      |
| 805  | ---            | ---     | -----                                 | -- | --    | 100 | Bimodal (055-235)      |
| 809  | 156            | 2.30    | 1.0 - 0.2                             | 11 | --    | 100 | Random                 |
| 813  | 089            | 14.06   | <0.005                                | 27 | 44    | 100 | Unimodal (Good)        |
| 823  | ---            | ---     | -----                                 | -- | --    | 100 | Bimodal (065-245)      |
| 853  | ---            | ---     | -----                                 | -- | --    | 100 | Bimodal (150-330)      |
| 854  | 025            | 1.19    | 1.0 - 0.2                             | 8  | --    | 099 | Random                 |
| 858  | 121            | 0.05    | 1.0 - 0.2                             | 2  | --    | 100 | Random                 |
| 859  | 055            | 3.30    | 0.2 - 0.1                             | 13 | 48    | 100 | Unimodal (Poor)        |
| 904  | 035            | 1.94    | 1.0 - 0.2                             | 10 | --    | 100 | Random                 |
| 907  | 074            | 0.04    | 1.0 - 0.2                             | 1  | --    | 100 | Random                 |
| 916  | 067            | 7.50    | 0.025 - 0.1                           | 19 | 45    | 100 | Unimodal               |
| 926  | 179            | 1.43    | 1.0 - 0.2                             | 8  | --    | 100 | Random                 |
| 930  | ---            | ---     | -----                                 | -- | --    | 101 | Bimodal (125-305)      |
| 941  | ---            | ---     | -----                                 | -- | --    | 100 | Bimodal (035-215)      |
| 945  | 042            | 0.34    | 1.0 - 0.2                             | 4  | --    | 100 | Random                 |
| 946  | 045            | 17.86   | <0.005                                | 30 | 43    | 100 | Unimodal (Good)        |
| 947  | 066            | 0.11    | 1.0 - 0.2                             | 2  | --    | 100 | Random                 |

## SUMMARY STATISTICS OF FABRIC IN BEDDING (continued)

| Bed   | $\bar{\theta}$ | $\chi^2$ | $\chi^2 = 2 \text{ df}$<br>Sig. Level | L% | $s^\circ$ | N   | Orientation<br>Pattern         |
|-------|----------------|----------|---------------------------------------|----|-----------|-----|--------------------------------|
| 948   | 024            | 2.81     | 1.0 - 0.2                             | 12 | --        | 100 | Random                         |
| 949   | 097            | 4.23     | 0.2 - 0.1                             | 15 | 47        | 100 | Unimodal (Poor)                |
| 950   | ---            | ----     | -----                                 | -- | --        | 100 | Bimodal (035-215)              |
| 954   | 052            | 6.40     | 0.05 - 0.025                          | 18 | 46        | 100 | Unimodal                       |
| 984   | 152            | 0.62     | 1.0 - 0.2                             | 6  | --        | 100 | Random                         |
| 1026  | 042            | 18.99    | <0.005                                | 31 | 42        | 100 | Unimodal (Good)                |
| 1028  | 014            | 5.43     | 0.1 - 0.05                            | 17 | 47        | 100 | Unimodal                       |
| 1029  | 027            | 13.04    | <0.005                                | 26 | 44        | 100 | Unimodal (Good)                |
| 1030  | 052            | 3.48     | 0.2 - 0.1                             | 13 | 48        | 100 | Unimodal (Poor)                |
| 1034  | ---            | ----     | -----                                 | -- | --        | 100 | Bimodal (020-200)              |
| 1038  | ---            | ----     | -----                                 | -- | --        | 099 | Bimodal (055-235)              |
| 1038A | ---            | ----     | -----                                 | -- | --        | 097 | Bimodal (035-215)              |
| 1040  | 040            | 1.18     | 1.0 - 0.2                             | 8  | --        | 100 | Random                         |
| 1056  | 034            | 0.28     | 1.0 - 0.2                             | 4  | --        | 100 | Random                         |
| 1066  | 114            | 6.91     | 0.05 - 0.025                          | 19 | 45        | 100 | Unimodal                       |
| 1066A | ---            | ----     | -----                                 | -- | --        | 100 | Bimodal (165-345)              |
| 1069  | ---            | ----     | -----                                 | -- | --        | 100 | Bimodal (115-295)              |
| 1070  | 026            | 2.93     | 1.0 - 0.2                             | 12 | --        | 100 | Random                         |
| 1125  | 149            | 7.40     | 0.025 - 0.01                          | 19 | 45        | 100 | Unimodal                       |
| 1125A | 059            | 2.98     | 1.0 - 0.2                             | 12 | --        | 100 | Random                         |
| 1126  | 171            | 14.09    | <0.005                                | 27 | 44        | 100 | Unimodal (Good)                |
| 1126A | 087            | 8.26     | 0.025 - 0.01                          | 20 | 46        | 100 | Unimodal                       |
| 1127  | 119            | 2.23     | 1.0 - 0.2                             | 11 | --        | 100 | Random                         |
| 1130A | 004            | 0.73     | 1.0 - 0.2                             | 6  | --        | 100 | Random                         |
| 1130B | ---            | ----     | -----                                 | -- | --        | 100 | Bimodal (060-240)              |
| 1130C | 138            | 0.69     | 1.0 - 0.2                             | 6  | --        | 098 | Random                         |
| 1130D | 117            | 1.30     | 1.0 - 0.2                             | 8  | --        | 100 | Random                         |
| 1140  | 110            | 0.47     | 1.0 - 0.2                             | 9  | --        | 100 | Random                         |
| 1152  | 103            | 0.19     | 1.0 - 0.2                             | 3  | --        | 100 | Random                         |
| 1196A | 071            | 4.72     | 0.1 - 0.05                            | 15 | 47        | 100 | Unimodal                       |
| 1196B | 065            | 1.19     | 1.0 - 0.2                             | 8  | --        | 100 | Random                         |
| 1196C | ---            | ----     | -----                                 | -- | --        | 100 | Bimodal (115-295)              |
| 1196D | 093            | 12.53    | <0.005                                | 25 | 44        | 100 | Unimodal (Good)                |
| 1198  | ---            | ----     | -----                                 | -- | --        | 100 | Bimodal (045-225)<br>(145-325) |
| 1198A | 073            | 2.88     | 1.0 - 0.2                             | 12 | --        | 100 | Random                         |
| 1200A | 112            | 11.71    | <0.005                                | 24 | 45        | 101 | Unimodal (Good)                |
| 1200B | ---            | ----     | -----                                 | -- | --        | 100 | Bimodal (120-300)              |
| 1200C | 053            | 2.05     | 1.0 - 0.2                             | 10 | --        | 100 | Random                         |
| 1208  | 040            | 6.61     | 0.05 - 0.025                          | 18 | 46        | 100 | Unimodal                       |
| 1213  | 055            | 3.53     | 0.2 - 0.1                             | 13 | 48        | 100 | Unimodal (Poor)                |
| 1215  | ---            | ----     | -----                                 | -- | --        | 097 | Bimodal (055-235)              |
| 1217  | ---            | ----     | -----                                 | -- | --        | 100 | Bimodal (015-195)<br>(135-315) |
| 1242A | ---            | ----     | -----                                 | -- | --        | 100 | Bimodal (155-335)              |

SUMMARY STATISTICS OF FABRIC IN BEDDING (continued)

| <u>Bed</u> | <u><math>\bar{\theta}</math></u> | <u><math>\chi^2</math></u> | <u><math>\nu = 2</math> df<br/>Sig. Level</u> | <u>L<math>\bar{x}</math></u> | <u>s<math>^\circ</math></u> | <u>N</u> | <u>Orientation<br/>Pattern</u> |
|------------|----------------------------------|----------------------------|-----------------------------------------------|------------------------------|-----------------------------|----------|--------------------------------|
| 1242B      | ---                              | ----                       | -----                                         | --                           | --                          | 099      | Bimodal (125-305)              |
| 1242C      | 035                              | 3.31                       | 0.2 - 0.1                                     | 13                           | 48                          | 100      | Unimodal (Poor)                |
| 1242D      | 145                              | 11.67                      | <0.005                                        | 24                           | 45                          | 099      | Unimodal (Good)                |
| 1256A      | 124                              | 6.57                       | 0.05 - 0.025                                  | 18                           | 46                          | 100      | Unimodal                       |
| 1256B      | ---                              | ----                       | -----                                         | --                           | --                          | 100      | Bimodal (027-207)              |
| 1256C      | 046                              | 0.36                       | 1.0 - 0.2                                     | 4                            | --                          | 097      | Random                         |
| 1320       | ---                              | ----                       | -----                                         | --                           | --                          | 102      | Bimodal (145-325)              |
| 1322       | 144                              | 18.25                      | <0.005                                        | 31                           | 42                          | 096      | Unimodal (Good)                |
| 1324       | 132                              | 10.98                      | <0.005                                        | 24                           | 45                          | 099      | Unimodal (Good)                |
| 1345       | 108                              | 4.44                       | 0.2 - 0.1                                     | 15                           | 47                          | 100      | Unimodal                       |
| 1347       | 084                              | 0.43                       | 1.0 - 0.2                                     | 5                            | --                          | 100      | Random                         |
| 1351       | 139                              | 10.66                      | <0.005                                        | 23                           | 44                          | 100      | Unimodal (Good)                |
| 1352A      | ---                              | ----                       | -----                                         | --                           | --                          | 100      | Bimodal (090-270)<br>(030-210) |
| 1352B      | ---                              | ----                       | -----                                         | --                           | --                          | 099      | Bimodal (125-305)              |
| 1352C      | ---                              | ----                       | -----                                         | --                           | --                          | 100      | Bimodal (045-225)<br>(155-335) |
| 1352D      | 087                              | 2.04                       | 1.0 - 0.2                                     | 10                           | --                          | 099      | Random                         |
| 1355       | ---                              | ----                       | -----                                         | --                           | --                          | 100      | Bimodal (065-245)              |
| 1403       | ---                              | ----                       | -----                                         | --                           | --                          | 100      | Bimodal (045-225)              |
| 1404       | 003                              | 1.77                       | 1.0 - 0.2                                     | 9                            | --                          | 100      | Random                         |
| 1404A      | 145                              | 1.87                       | 1.0 - 0.2                                     | 10                           | --                          | 100      | Random                         |
| 1425       | ---                              | ----                       | -----                                         | --                           | --                          | 100      | Bimodal (115-295)              |
| 1447       | 164                              | 1.40                       | 1.0 - 0.2                                     | 8                            | --                          | 100      | Random                         |
| 1451       | 085                              | 6.70                       | 0.05 - 0.025                                  | 18                           | 46                          | 100      | Unimodal                       |
| 1458A      | 081                              | 0.56                       | 1.0 - 0.2                                     | 6                            | --                          | 100      | Random                         |
| 1458B      | ---                              | ----                       | -----                                         | --                           | --                          | 100      | Bimodal (080-260)<br>(155-235) |
| 1458C      | 101                              | 0.08                       | 1.0 - 0.2                                     | 2                            | --                          | 100      | Random                         |
| 1466       | 162                              | 6.55                       | 0.05 - 0.025                                  | 18                           | 46                          | 099      | Unimodal                       |
| 1475       | ---                              | ----                       | -----                                         | --                           | --                          | 100      | Bimodal (065-245)              |
| 1480       | 064                              | 4.75                       | 0.1 - 0.05                                    | 15                           | 47                          | 100      | Unimodal                       |
| 1494       | ---                              | ----                       | -----                                         | --                           | --                          | 100      | Bimodal (005-185)<br>(105-285) |

\*Key: Bed - bed number;  $\bar{\theta}$  - vector mean;  $\chi^2$  - calculated chi-squared value of the observed distribution; sig. level - significance level of the calculated chi-squared value on a chi-squared distribution with 2 degrees of freedom; L $\bar{x}$  - vector strength of the vector mean; s $^\circ$  - standard deviation of the observed distribution in degrees; N - number of measurements.

Rose diagrams of the individual distributions are plotted on the following pages. Diagrams are plotted in 10 $^\circ$  class intervals. Arrow indicates the north direction. Scale bar is 10 measurements. Numbers in the centres of the diagrams indicate the bed numbers.

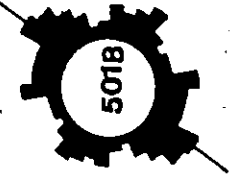
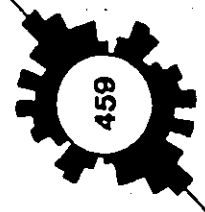
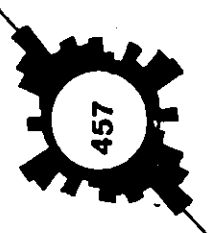
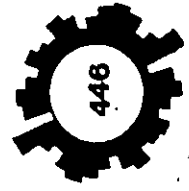
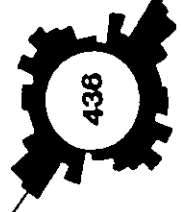
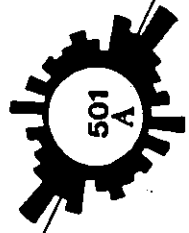
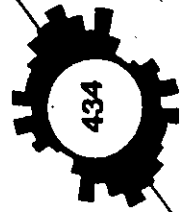
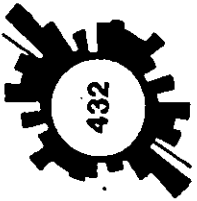
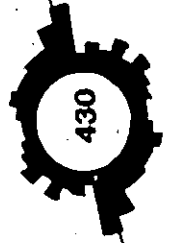
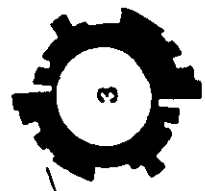
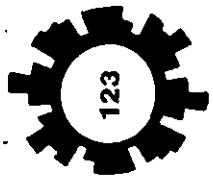
Fig. 118 - Rose diagrams of bedding fabric patterns are plotted on the following pages. About 100 measurements were made on each sample. Data is line-of-motion data. Hence the distributions were drawn as symmetrical patterns. Scale bar indicates 10 measurements. North direction is plotted. Numbers in the centres of the rose diagrams indicate bed numbers from which the samples were taken. Narrow lines indicate vector means in unimodal distributions and directions of dominant modes in bimodal distributions. A, B, C, ... indicate replicate samples upsection within individual beds.



BEDDING FABRIC  
ROSE DIAGRAMS

N

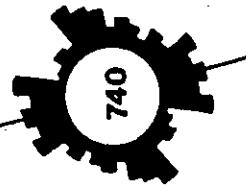
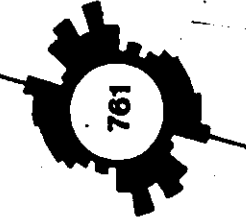
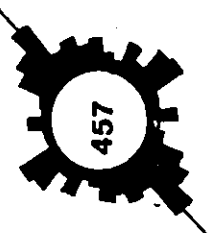
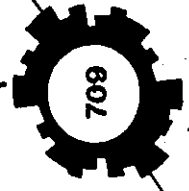
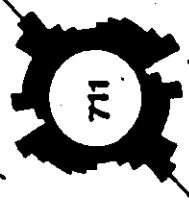
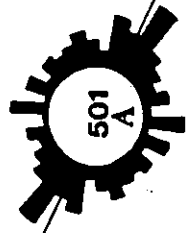
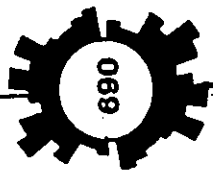
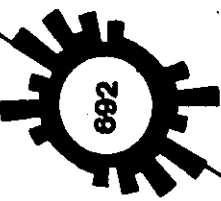
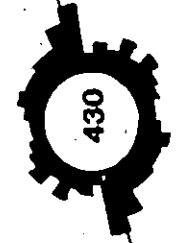
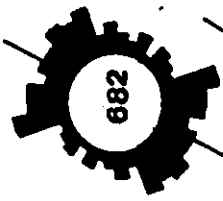
10



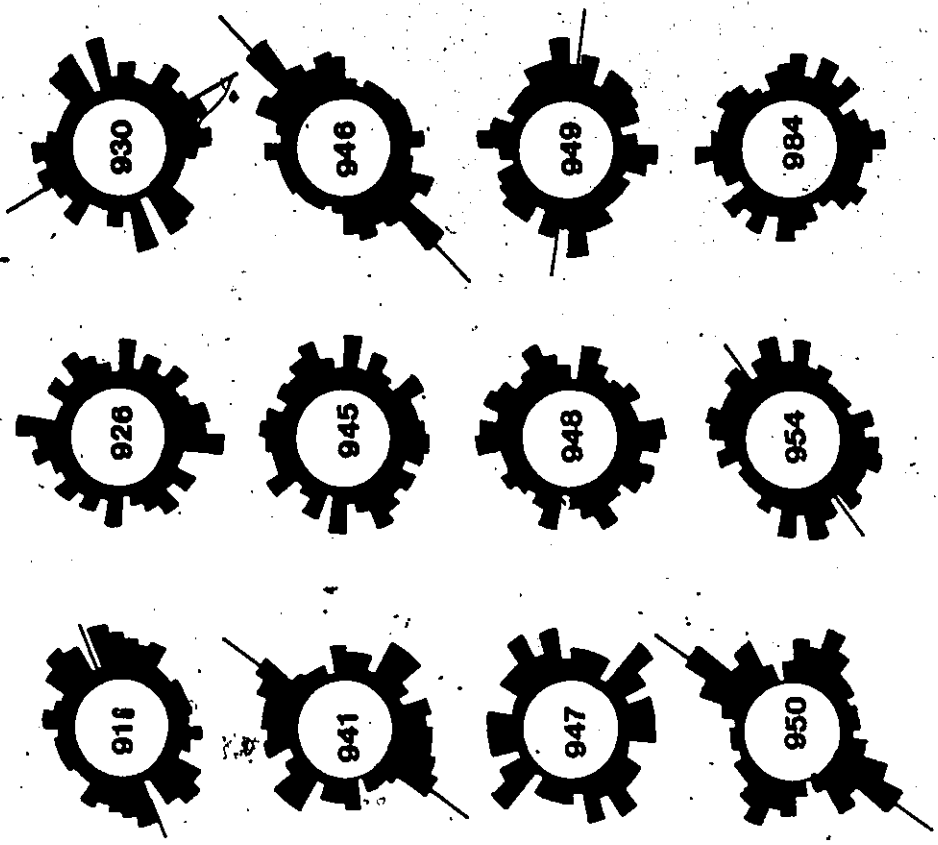
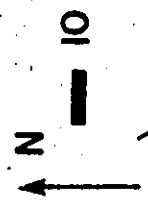
BEDDING FABRIC  
ROSE DIAGRAMS

N

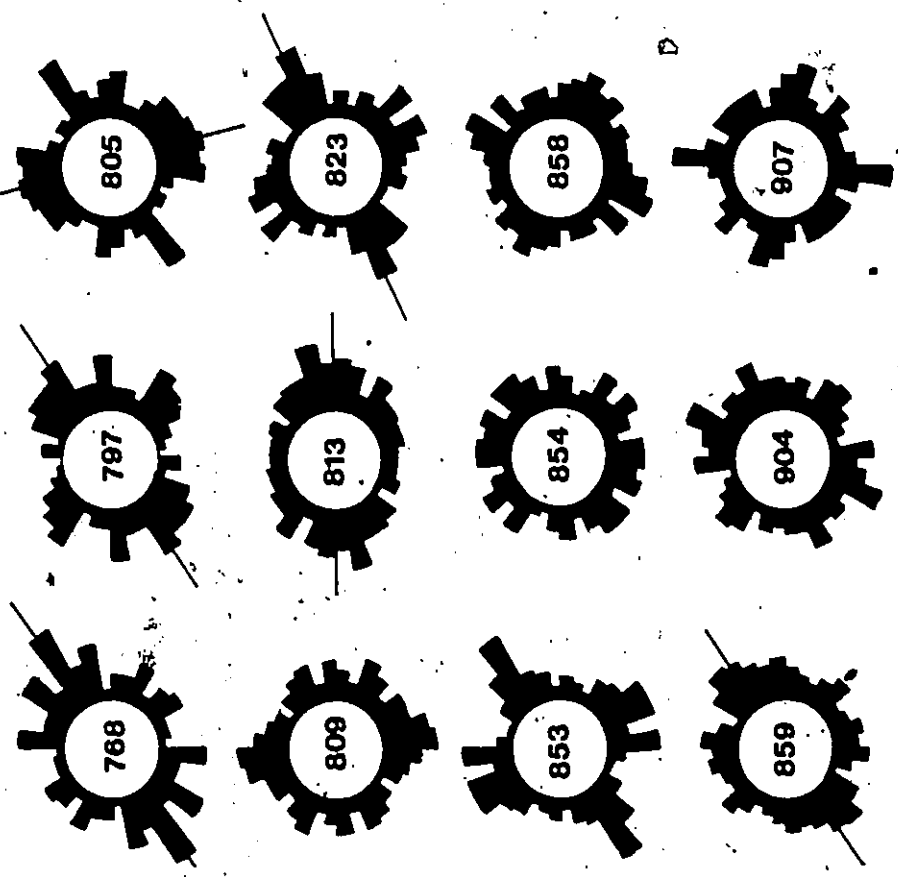
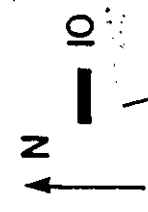
10



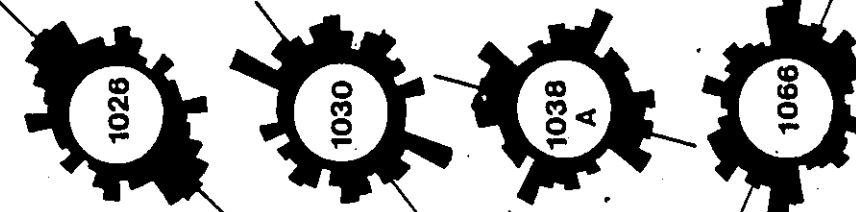
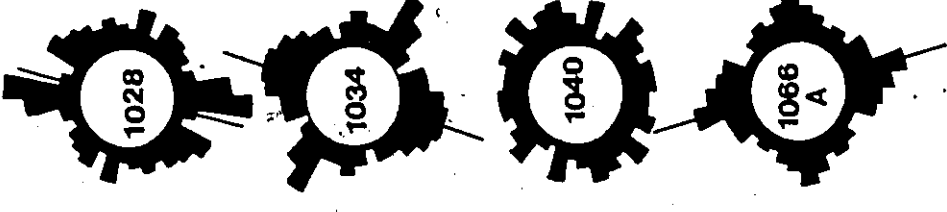
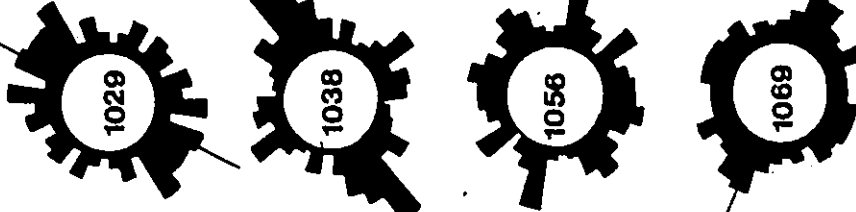
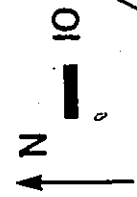
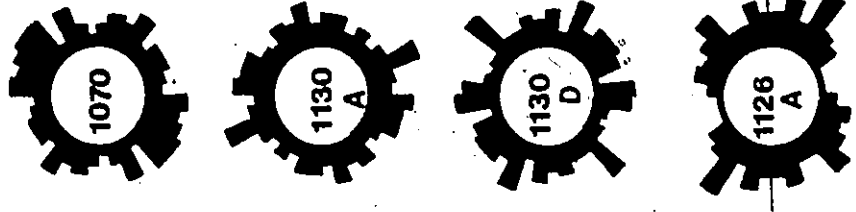
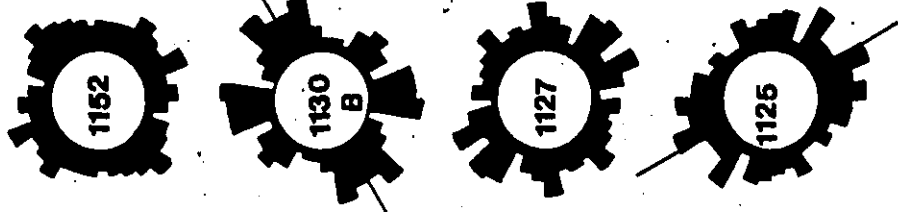
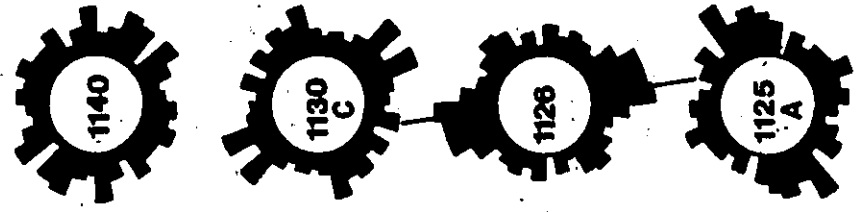
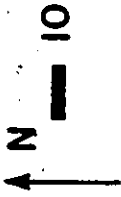
BEDDING FABRIC  
ROSE DIAGRAMS



BEDDING FABRIC  
ROSE DIAGRAMS

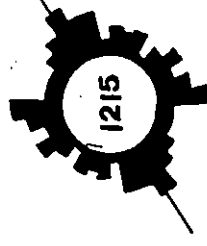
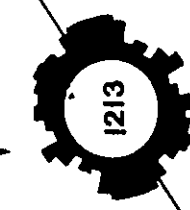
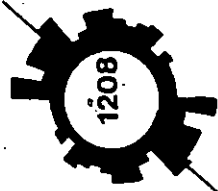
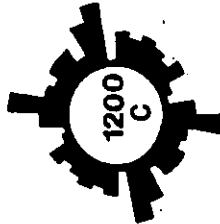
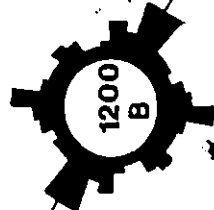
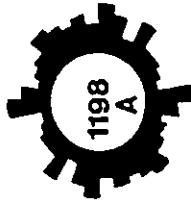
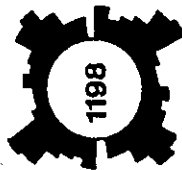
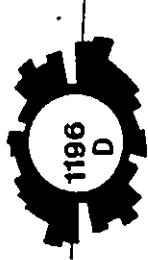
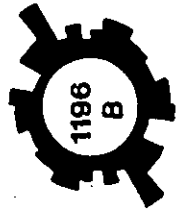
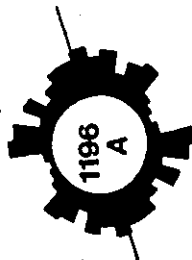
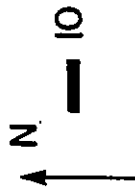


BEDDING FABRIC  
ROSE DIAGRAMS

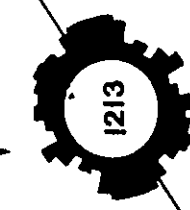
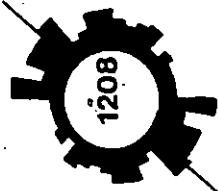
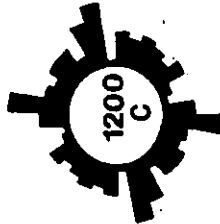
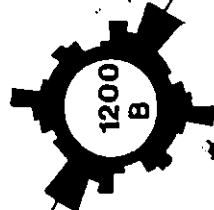
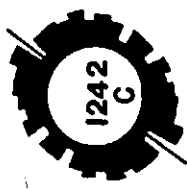
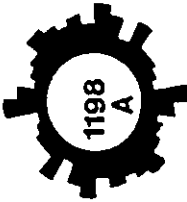
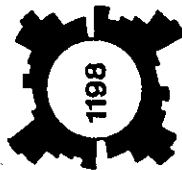
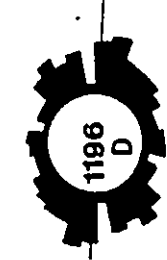
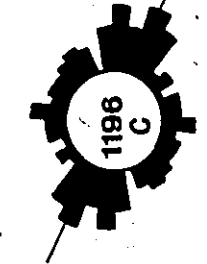
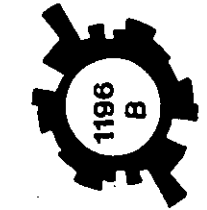
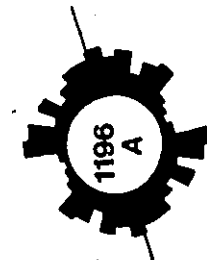
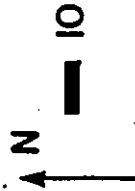


BEDDING FABRIC  
ROSE DIAGRAMS

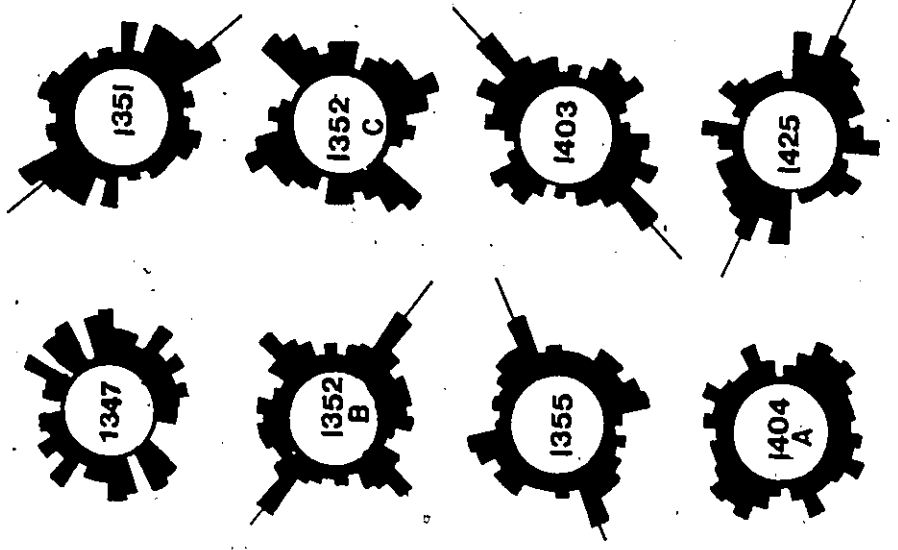
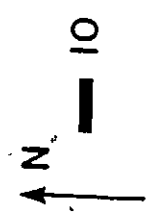
BEDDING FABRIC  
ROSE, DIAGRAMS



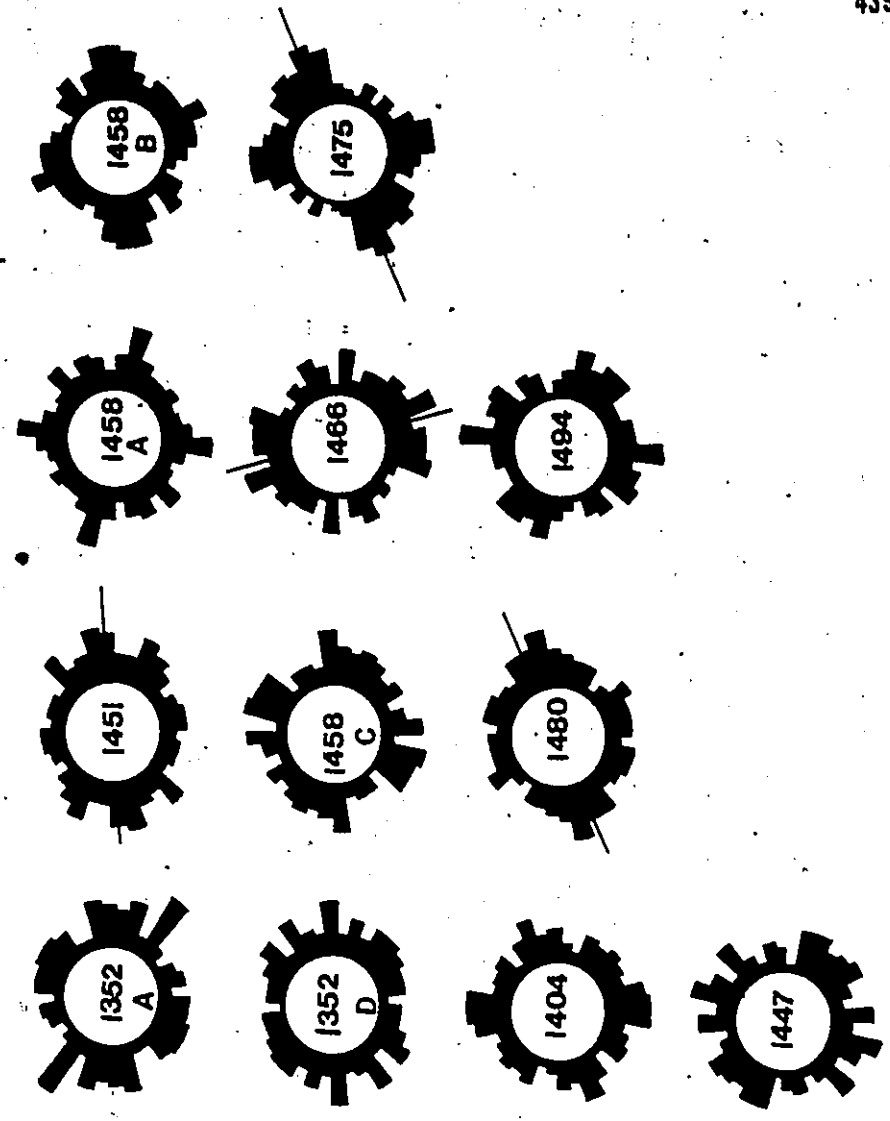
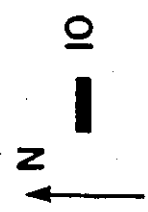
BEDDING FABRIC  
ROSE, DIAGRAMS



BEDDING FABRIC  
ROSE DIAGRAMS



BEDDING FABRIC  
ROSE DIAGRAMS



## SUMMARY STATISTICS OF IMBRICATION PATTERNS \*

| Bed   | $\bar{\theta}$ | °  |    | Modal Dip | L% Bed: |  | Imbrication Pattern |
|-------|----------------|----|----|-----------|---------|--|---------------------|
|       |                | S  | LZ |           | L% Imb  |  |                     |
| 74    | ---            | -- | -- | 35 (45)   | ----    |  | Bimodal             |
| 430   | ----           | -- | -- | 15 (15)   | ----    |  | Bimodal             |
| 434   | ----           | -- | -- | 10 (15)   | ----    |  | Bimodal             |
| 457   | 093            | 53 | 62 | 35 (25)   | ----    |  | Random              |
| 501B  | ----           | -- | -- | 55 (45)   | ----    |  | Bimodal             |
| 505   | ----           | -- | -- | 25 (55)   | ----    |  | Bimodal             |
| 682   | 113            | 62 | 50 | 20        | 0.52    |  | Unimodal (Poor)     |
| 685   | ----           | -- | -- | 35 (35)   | ----    |  | Bimodal             |
| 692   | 113            | 53 | 63 | 35        | 0.32    |  | Unimodal (Poor)     |
| 694   | ----           | -- | -- | 25 (30)   | ----    |  | Bimodal             |
| 709   | 119            | 41 | 78 | 35        | 0.19    |  | Unimodal (Good)     |
| 730   | 073            | 57 | 58 | 35        | 0.33    |  | Unimodal (Poor)     |
| 740   | 064            | 52 | 65 | 35        | ----    |  | Unimodal            |
| 761   | 066            | 52 | 65 | 40        | ----    |  | Unimodal            |
| 762   | ----           | -- | -- | 45 (35)   | ----    |  | Bimodal             |
| 768   | ----           | -- | -- | 30 (35)   | ----    |  | Bimodal             |
| 797   | 081            | 54 | 61 | 45        | ----    |  | Unimodal (Poor)     |
| 805   | 067            | 60 | 54 | 15 (35)   | ----    |  | Unimodal (Poor)     |
| 809   | ----           | -- | -- | 30 (40)   | ----    |  | Bimodal             |
| 813   | ----           | -- | -- | 25 (15)   | ----    |  | Bimodal             |
| 853   | ----           | -- | -- | 25 (35)   | ----    |  | Bimodal             |
| 854   | 077            | 55 | 60 | 35        | 0.13    |  | Unimodal (Poor)     |
| 858   | ----           | -- | -- | 35 (25)   | ----    |  | Bimodal             |
| 859   | ----           | -- | -- | 35 (15)   | ----    |  | Bimodal             |
| 904   | 105            | 52 | 65 | 50        | 0.15    |  | Unimodal            |
| 907   | ----           | -- | -- | 55 (25)   | ----    |  | Bimodal             |
| 916   | 072            | 60 | 51 | 15        | 0.38    |  | Unimodal            |
| 926   | ----           | -- | -- | 25 (10)   | ----    |  | Bimodal             |
| 941   | ----           | -- | -- | 35 (30)   | ----    |  | Bimodal             |
| 948   | ----           | -- | -- | 30 (25)   | ----    |  | Bimodal             |
| 950   | 059            | 60 | 55 | 25        | ----    |  | Unimodal            |
| 954   | ----           | -- | -- | 30 (30)   | ----    |  | Bimodal             |
| 984   | ----           | -- | -- | 35 (30)   | ----    |  | Bimodal             |
| 1026  | ----           | -- | -- | 10 (10)   | ----    |  | Bimodal             |
| 1026R | ----           | -- | -- | 20 (25)   | ----    |  | Bimodal             |
| 1028  | 071            | 53 | 62 | 35        | 0.27    |  | Unimodal (Poor)     |
| 1029  | ----           | -- | -- | 25 (20)   | ----    |  | Bimodal             |
| 1034  | ----           | -- | -- | 40 (25)   | ----    |  | Bimodal             |
| 1038  | ----           | -- | -- | 40 (35)   | ----    |  | Bimodal             |
| 1040  | 109            | 56 | 59 | 45        | 0.13    |  | Unimodal (Poor)     |
| 1066  | 106            | 54 | 61 | 35        | 0.30    |  | Unimodal            |
| 1066A | 075            | 55 | 60 | 35        | ----    |  | Unimodal (Poor)     |
| 1125  | ----           | -- | -- | 50 (35)   | ----    |  | Bimodal             |
| 1126  | ----           | -- | -- | 35 (15)   | ----    |  | Bimodal             |
| 1126A | ----           | -- | -- | 35 (50)   | ----    |  | Bimodal             |
| 1127  | 081            | 53 | 63 | 40        | 0.17    |  | Unimodal (Poor)     |
| 1130B | ----           | -- | -- | 65 (35)   | ----    |  | Bimodal             |

SUMMARY STATISTICS OF IMBRICATION PATTERNS (continued)

| <u>Bed</u> | <u><math>\bar{\theta}</math></u> | <u><math>s^{\circ}</math></u> | <u>L%</u> | <u>Modal Dip</u> | <u>L% Bed:</u><br><u>L% Imb</u> | <u>Imbrication Pattern</u> |
|------------|----------------------------------|-------------------------------|-----------|------------------|---------------------------------|----------------------------|
| 1140       | 108                              | 51                            | 65        | 45               | 0.07                            | Unimodal                   |
| 1152       | ---                              | --                            | --        | 40 (40)          | ----                            | Bimodal                    |
| 1196A      | 088                              | 46                            | 70        | 55               | 0.22                            | Unimodal (Poor)            |
| 1200A      | 069                              | 58                            | 58        | 25               | 0.42                            | Unimodal                   |
| 1200B      | 080                              | 58                            | 55        | 15               | ----                            | Unimodal (Poor)            |
| 1200C      | ---                              | --                            | --        | 35 (25)          | ----                            | Bimodal                    |
| 1208       | ---                              | --                            | --        | 30 (45)          | ----                            | Bimodal                    |
| 1213       | ---                              | --                            | --        | 15 (15)          | ----                            | Bimodal                    |
| 1215       | ---                              | --                            | --        | 30 (15)          | ----                            | Bimodal                    |
| 1242C      | ---                              | --                            | --        | 45 (25)          | ----                            | Bimodal                    |
| 1242D      | 095                              | 55                            | 60        | 15 (50)          | 0.41                            | Unimodal (Poor)            |
| 1256A      | 068                              | 48                            | 70        | 40               | 0.26                            | Unimodal (Good)            |
| 1256C      | 087                              | 55                            | 60        | 35               | 0.07                            | Unimodal (Poor)            |
| 1322       | ---                              | --                            | --        | 35 (55)          | ----                            | Bimodal                    |
| 1351       | ---                              | --                            | --        | 30 (30)          | ----                            | Bimodal                    |
| 1352B      | ---                              | --                            | --        | 35 (25)          | ----                            | Bimodal                    |
| 1352D      | ---                              | --                            | --        | 20 (40)          | ----                            | Bimodal                    |
| 1403       | 080                              | 50                            | 67        | 45               | ----                            | Unimodal                   |
| 1451       | ---                              | --                            | --        | 45 (40)          | ----                            | Bimodal                    |
| 1458A      | 091                              | 49                            | 67        | 55               | 0.08                            | Unimodal (Poor)            |
|            |                                  |                               |           |                  |                                 | ? Random                   |
| 1466       | ---                              | --                            | --        | 45 (25)          | ----                            | Bimodal                    |
| 1475       | 105                              | 57                            | 58        | 30               | ----                            | Unimodal (Poor)            |
| 1480       | ---                              | --                            | --        | 45 (25)          | ----                            | Bimodal                    |

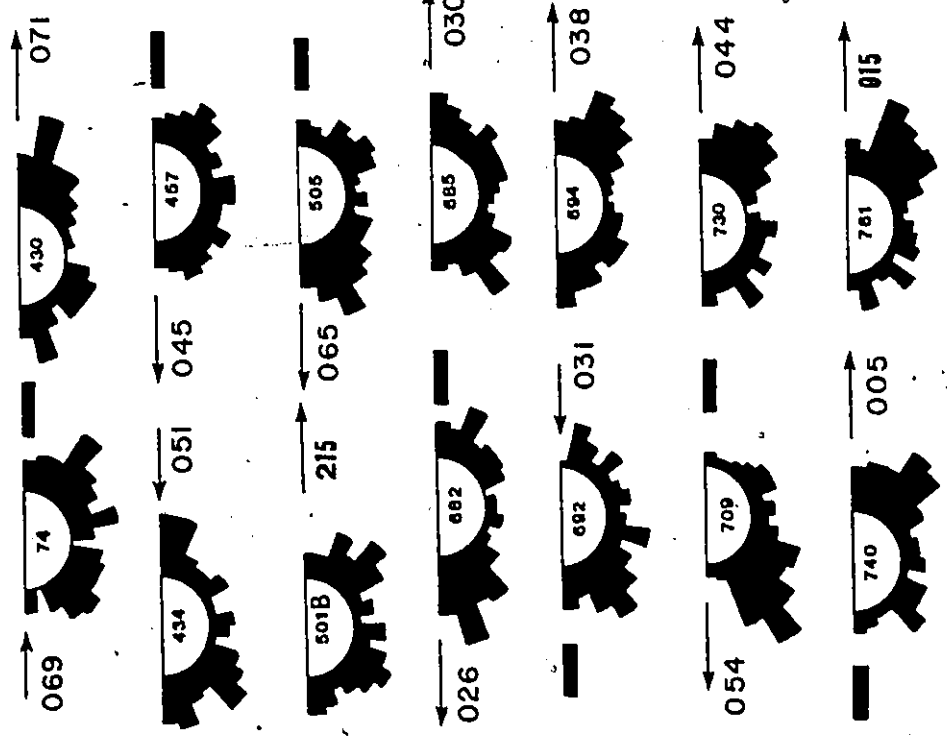
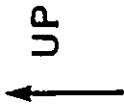
**\*Key:**  $\bar{\theta}$  - vector mean;  $s^{\circ}$  - standard deviation in degrees; L% - vector strength of the vector mean; Modal Dip - degrees from horizontal of major mode (midpoint) determined from rose diagrams. In bimodal imbrication plots, the secondary mode is given in brackets; L% Bed: L% Imb - ratio of the vector strength in bedding versus the strength in the imbrication plane; n = 100 measurements for each sample.

Rose diagrams of the individual samples are given on the following pages. Diagrams are plotted in  $10^{\circ}$  class intervals. Scale bars indicate 10 measurements. The "up" direction is toward the binding of the thesis. Orientation arrows, to the side of the rose diagrams, indicate the direction of the vector mean for random and unimodal plots; and the direction of the major mode for bimodal plots, as observed in bedding plane plots.

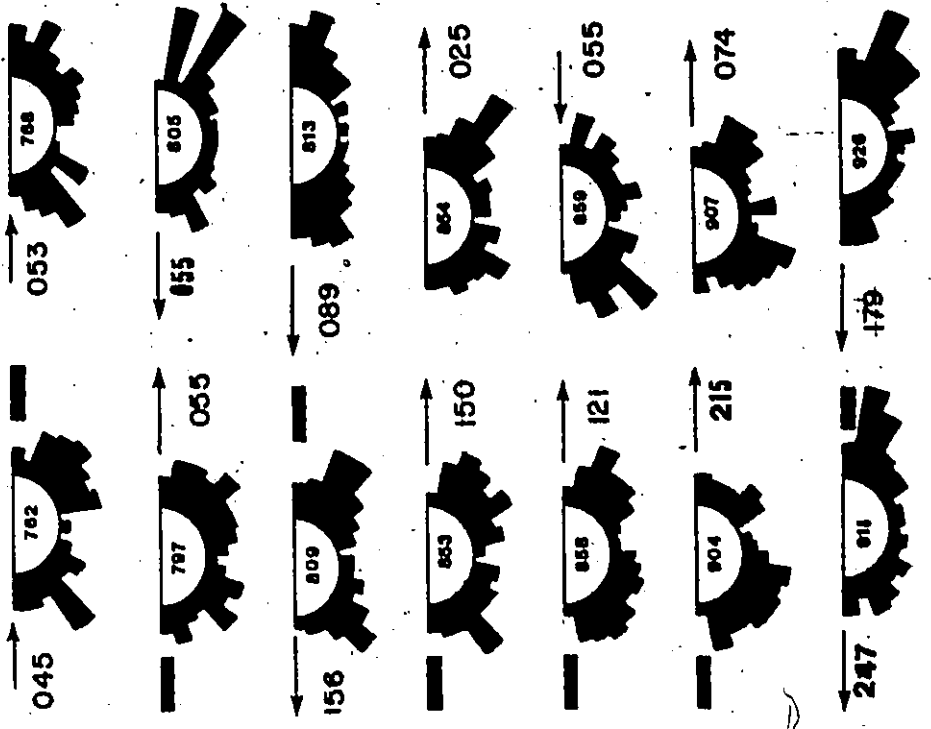
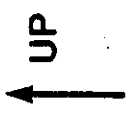
Fig.119 - Rose diagrams of imbrication fabric patterns are shown on the following pages. About 100 measurements were made on each sample. Data is vectorial data, hence the distributions are not necessary symmetrical. Vertically upward direction indicated. Small arrows with numbers to the side of the rose diagrams give the orientations of the imbrication sections. Small numbers in the centres of the rose diagrams indicate bed numbers of the samples. Scale bar indicates 10 measurements. A, B indicate different samples upsection within individual beds. R indicates a repeat measurement by the author of the same sample.



IMBRICATION ROSE DIAGRAMS



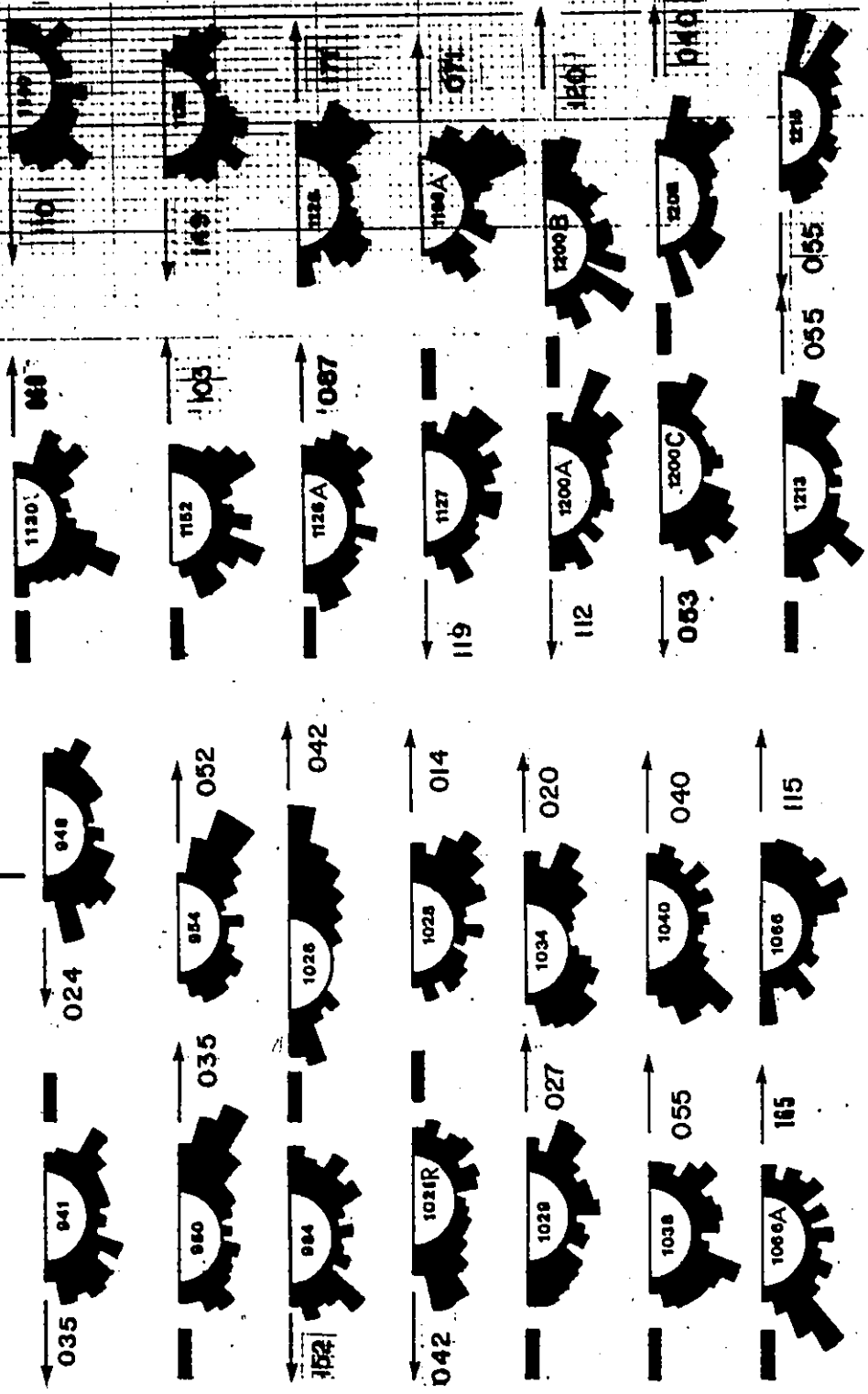
IMBRICATION ROSE DIAGRAMS



**IMBRICATION  
ROSE DIAGRAMS**

UP

**IMBRICATION  
ROSE DIAGRAMS**





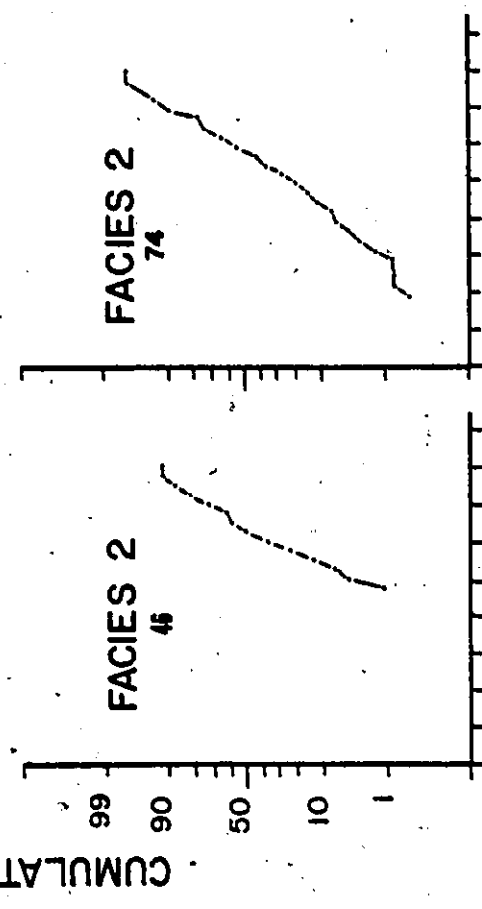
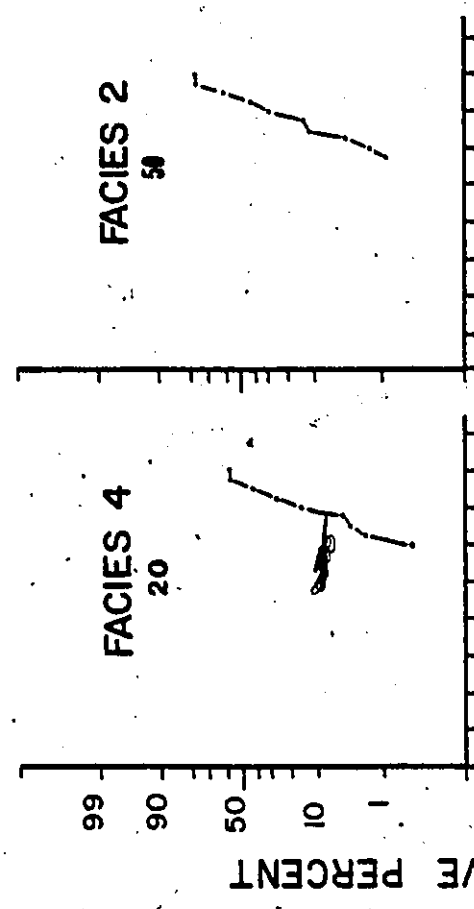
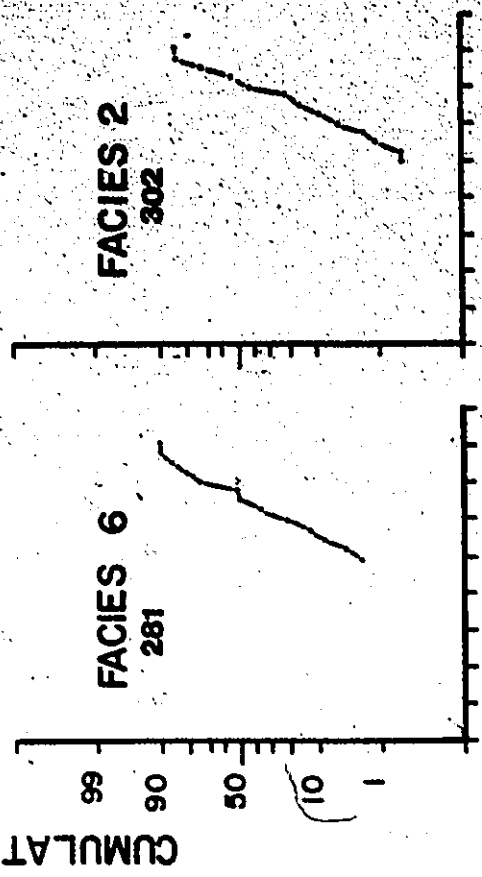
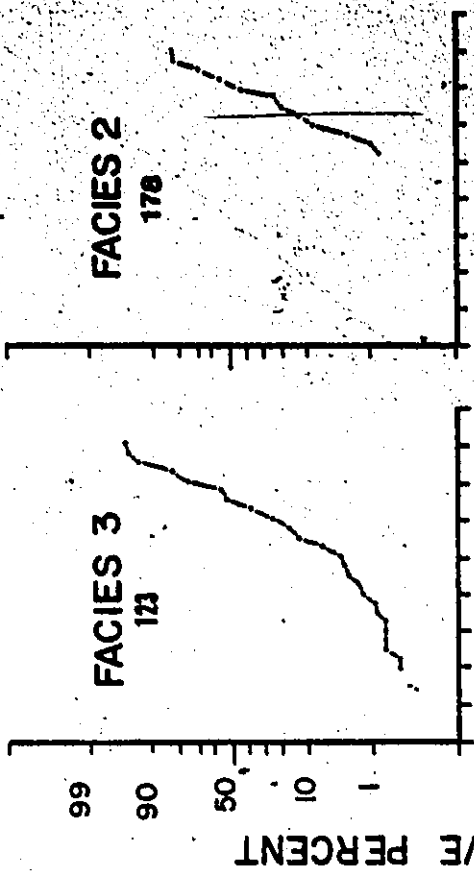
## APPENDIX B

## GRAIN SIZE ANALYSES OF PEBBLY SANDSTONES AND SANDSTONES \*

| Bed No. | Mz $\phi$ | $\sigma_I$ | Sk <sub>I</sub> | Skewness Description | C $\phi$ | M $\phi$ 50 | Sorting Description |
|---------|-----------|------------|-----------------|----------------------|----------|-------------|---------------------|
| 20      | 3.46      | 0.55       | +0.69           | Strong Fine Skew.    | 2.14     | 3.13        | Moderately Well     |
| 50      | 3.44      | 0.63       | +0.02           | Near Symmetrical     | 1.88     | 3.40        | Moderately Well     |
| 46      | 2.43      | 0.91       | +0.20           | Fine Skewed          | 0.75     | 2.32        | Moderate            |
| 74      | 1.91      | 1.05       | -0.08           | Near Symmetrical     | -0.90    | 1.93        | Poor                |
| 123     | 2.45      | 0.80       | +0.01           | Near Symmetrical     | -0.20    | 2.44        | Moderate            |
| 178     | 3.17      | 0.78       | +0.03           | Near Symmetrical     | 1.50     | 3.12        | Moderate            |
| 281     | 2.64      | 0.81       | +0.03           | Near Symmetrical     | 0.94     | 2.65        | Moderate            |
| 302     | 3.26      | 0.69       | +0.06           | Near Symmetrical     | 1.50     | 3.18        | Moderately Well     |
| 349     | 3.22      | 0.78       | +0.12           | Fine Skewed          | 1.68     | 3.12        | Moderate            |
| 350     | 3.16      | 0.71       | +0.19           | Fine Skewed          | 1.38     | 3.04        | Moderate            |
| 357     | 2.31      | 0.90       | +0.09           | Near Symmetrical     | 0.42     | 2.28        | Moderate            |
| 378     | 2.08      | 0.84       | +0.36           | Strong Fine Skew.    | 0.70     | 1.93        | Moderate            |
| 386     | 2.53      | 0.89       | +0.17           | Fine Skewed          | 0.50     | 2.43        | Moderate            |
| 501     | 2.39      | 1.14       | -0.06           | Near Symmetrical     | -0.50    | 2.45        | Poor                |
| 555D    | 2.49      | 0.91       | +0.29           | Fine Skewed          | 0.95     | 2.30        | Moderate            |
| 555F    | 2.37      | 0.89       | +0.13           | Fine Skewed          | 0.25     | 2.33        | Moderate            |
| 570     | 2.83      | 1.08       | -0.03           | Near Symmetrical     | 0.62     | 2.80        | Poor                |
| 709FF   | 2.71      | 1.00       | -0.14           | Coarse Skewed        | 0.14     | 2.80        | Moderate            |
| 709D    | 2.52      | 0.98       | +0.06           | Near Symmetrical     | 0.34     | 2.47        | Moderate            |
| 709F    | 2.89      | 1.03       | .00             | Symmetrical          | -0.35    | 2.83        | Poor                |
| 858     | 2.26      | 0.85       | +0.06           | Near Symmetrical     | 0.66     | 2.30        | Moderate            |
| 859     | 2.34      | 0.96       | +0.18           | Fine Skewed          | -0.25    | 2.23        | Moderate            |
| 1197    | 2.42      | 1.19       | -0.13           | Coarse Skewed        | -1.20    | 2.47        | Poor                |
| 1256    | 2.82      | 1.08       | -0.01           | Near Symmetrical     | 0.04     | 2.77        | Poor                |
| 1324D   | 2.58      | 0.89       | +0.19           | Fine Skewed          | -2.75    | 2.50        | Moderate            |
| 1324F   | 2.40      | 0.77       | +0.24           | Fine Skewed          | 1.00     | 2.32        | Moderate            |
| 1347    | 2.97      | 0.99       | -0.04           | Near Symmetrical     | 0.75     | 2.94        | Moderate            |
| 1402    | 2.85      | 1.12       | -0.15           | Coarse Skewed        | -0.38    | 2.90        | Poor                |
| 1404D   | 1.84      | 1.19       | +0.13           | Fine Skewed          | -0.88    | 1.75        | Poor                |
| 1404F   | 2.53      | 1.38       | +0.01           | Near Symmetrical     | -0.85    | 2.42        | Poor                |

\* Key: Mz  $\phi$  - graphic mean in phi units;  $\sigma_I$  - inclusive graphic standard deviation; SK<sub>I</sub> - inclusive graphic skewness. Formulae for these calculations are given by Folk (1965). C  $\phi$  - coarsest one percentile of the distribution; M  $\phi$  50 - median grain size corresponding to the 50% mark on the distribution. Sorting and skewness descriptions are those used by Folk (1965) for different sorting and skewness values.

Cumulative frequency grain size curves (on probability scale) are given on the following pages. Facies types are indicated. Numbers underneath the facies designation indicate bed numbers; letters indicate replicate measurements from the same thin section. : measurements by the author; D: measurements by Douglas J. Cant.

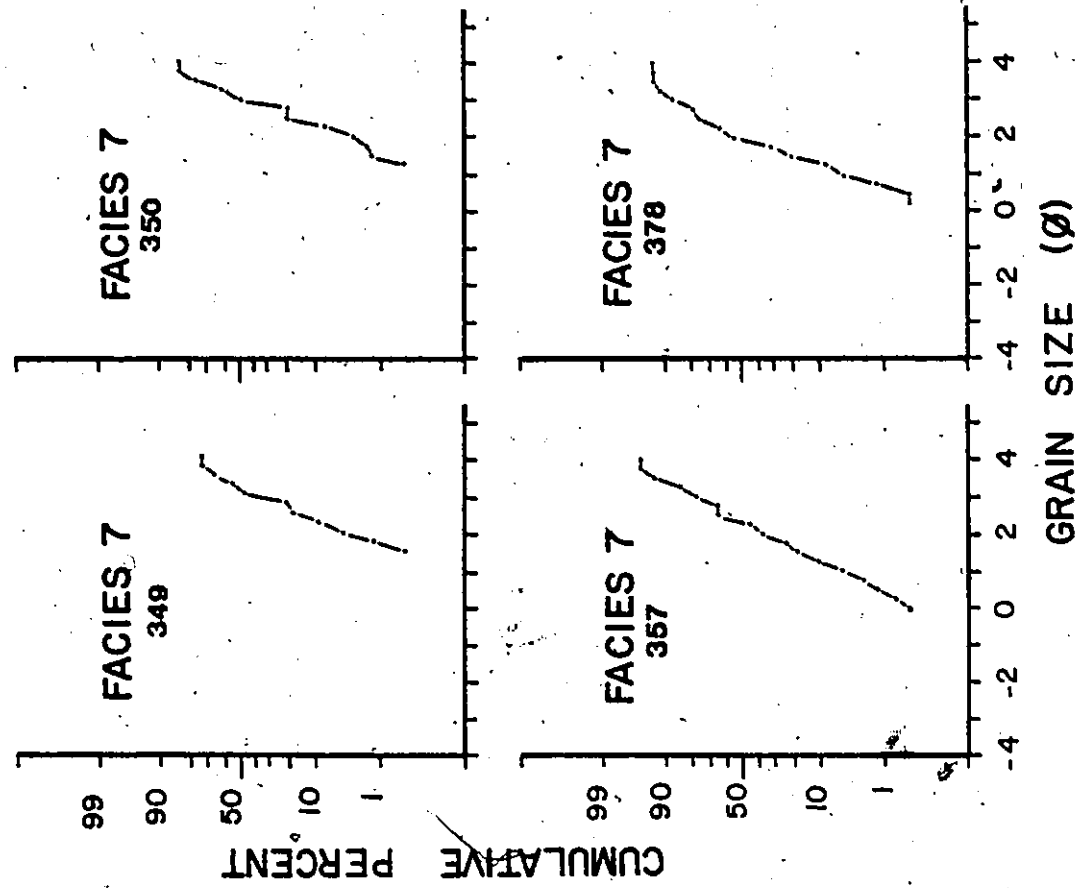
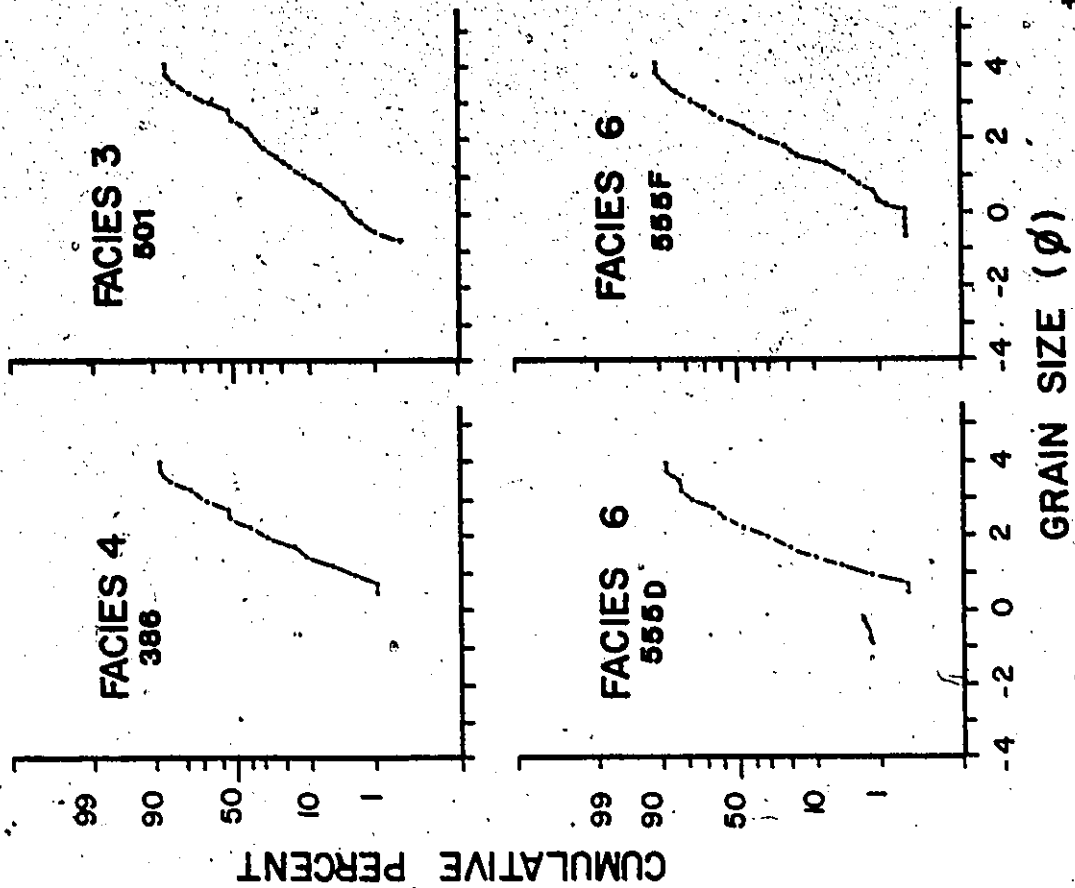


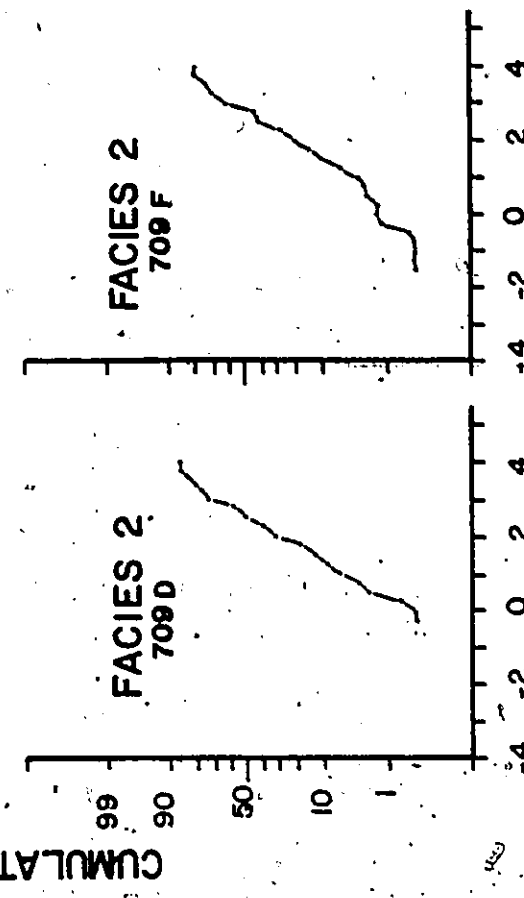
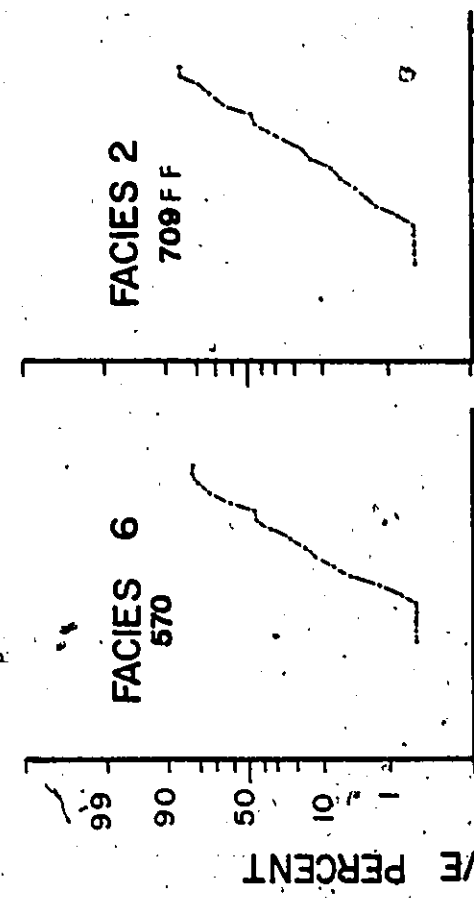
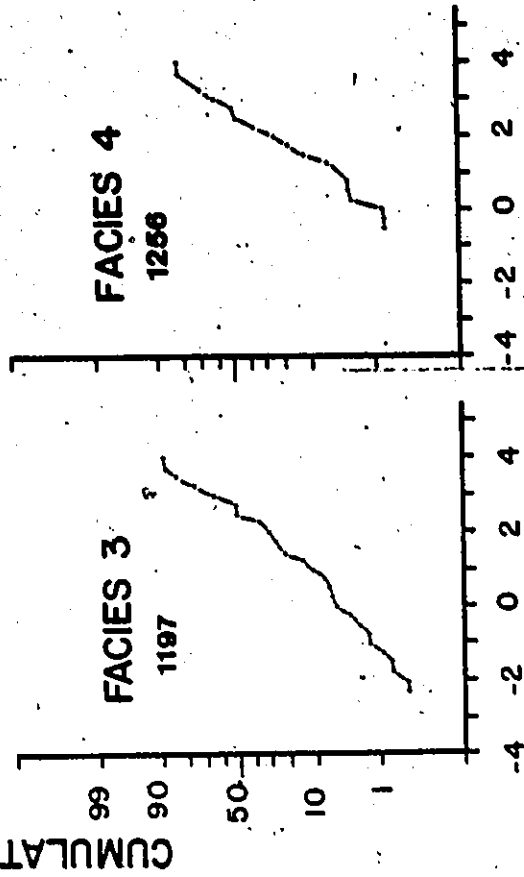
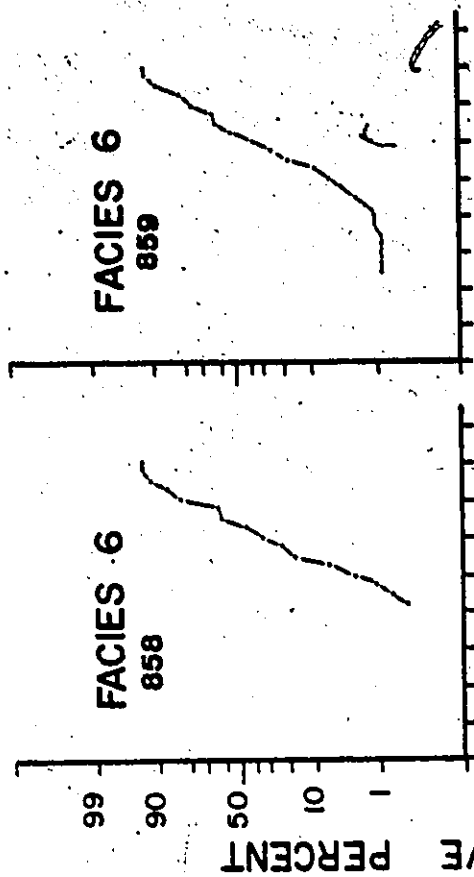
GRAIN SIZE (φ)

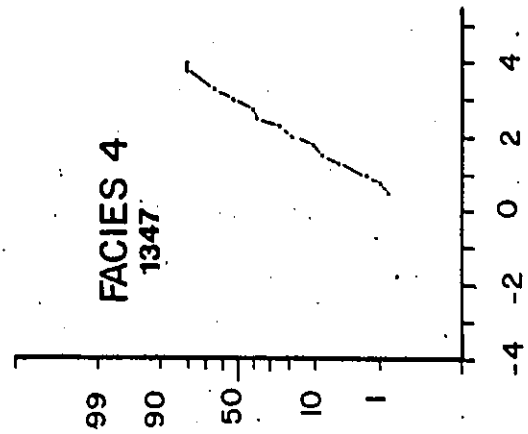
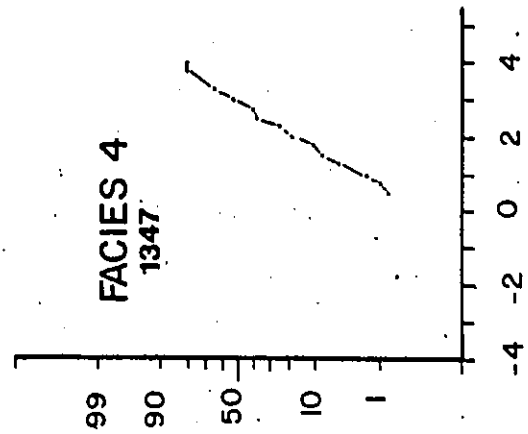
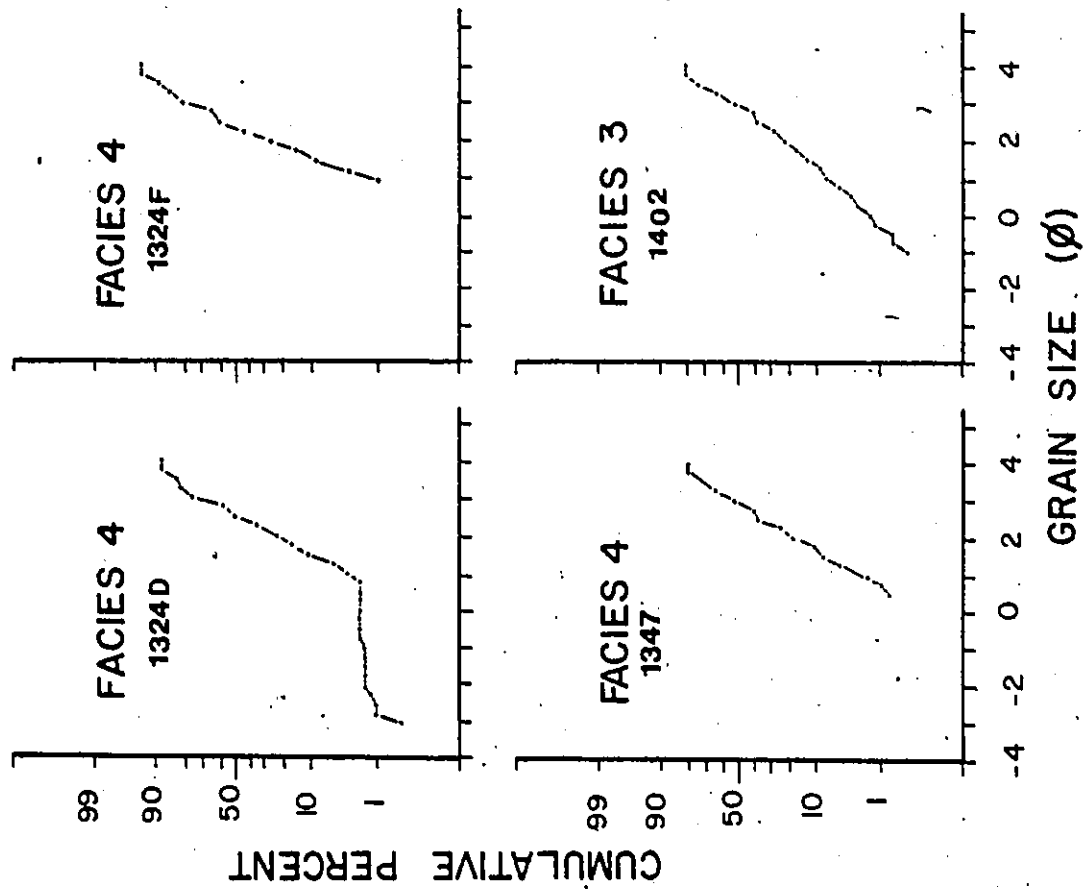
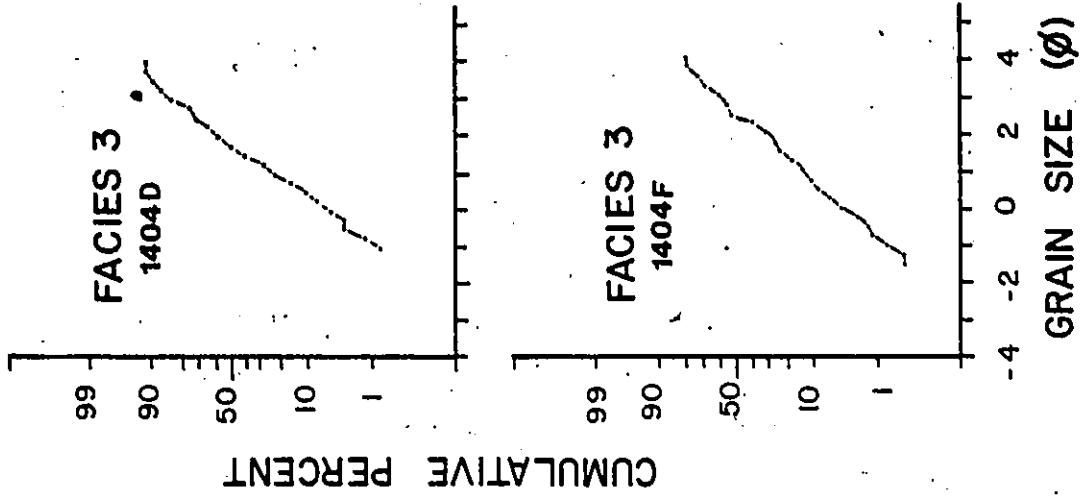
GRAIN SIZE (φ)

CUMULATIVE PERCENT

CUMULATIVE PERCENT









## APPENDIX 9

STATISTICAL ANALYSES OF VERTICAL FACIES SEQUENCES

## Part 1

Preliminary Analysis:Embedded Markov Chain Analysis of  
All the Sections Measured in the Present Study

## Computational Techniques Given by Miall (1973)

Note: In calculation of the random matrix, one must use the sum of the elements in the columns ( $s_j$ ) and not the sum of the elements in the rows ( $s_i$ ) as the numerator (contrary to Gingerich, 1969; in agreement with Miall, 1973). This is mainly due to truncated sequences, as a consequence of faulting or covered intervals. In the present study, there are transitions into a state ( $\rightarrow$  col  $j$ ) which occur more often than transitions from a state (row  $i \rightarrow$ ), due to this truncation. Consequently,  $s_i$  does not necessarily equal  $s_j$ .

For the spider diagram, given in the thesis text, a cutoff value of +0.05 for difference matrix scores was used as the boundary between random and non-random transitions. Also eliminated, were those transitions which only occurred once.

Key: 1, ..., 7: Facies 1 through Facies 7  
Sh: Shale Facies  
SS: Scoured Surfaces

EMBEDDED MARKOV CHAIN ANALYSIS

POOLED DATA FROM ALL OF THE SECTIONS MEASURED IN THE PRESENT STUDY

|     | SS   | 1    | 2    | 3    | 4    | 5    | 6    | 7    | Sh   | Sum |                                                      |
|-----|------|------|------|------|------|------|------|------|------|-----|------------------------------------------------------|
| SS  | --   | 33   | 14   | 5    | 6    | 2    | 7    | 0    | 0    | 67  |                                                      |
| 1   | 26   | --   | 26   | 28   | 16   | 3    | 9    | 3    | 1    | 112 |                                                      |
| 2   | 15   | 18   | --   | 44   | 31   | 8    | 33   | 20   | 1    | 170 | <u>TOTAL<br/>TALLY<br/>MATRIX</u>                    |
| 3   | 6    | 27   | 49   | --   | 26   | 4    | 38   | 15   | 2    | 167 |                                                      |
| 4   | 8    | 9    | 31   | 27   | --   | 6    | 16   | 21   | 0    | 118 |                                                      |
| 5   | 0    | 3    | 9    | 8    | 5    | --   | 5    | 7    | 0    | 37  |                                                      |
| 6   | 8    | 9    | 44   | 31   | 23   | 9    | --   | 14   | 0    | 138 |                                                      |
| 7   | 4    | 2    | 22   | 23   | 15   | 13   | 13   | --   | 0    | 102 |                                                      |
| Sh  | 0    | 1    | 1    | 3    | 0    | 0    | 2    | 0    | --   | 7   |                                                      |
| Sum | 67   | 102  | 196  | 172  | 122  | 45   | 123  | 80   | 4    | 911 |                                                      |
| SS  | ---  | .49  | .21  | .07  | .09  | .03  | .10  | 0    | 0    |     |                                                      |
| 1   | .23  | ---  | .23  | .25  | .14  | .03  | .08  | .03  | .01  |     |                                                      |
| 2   | .09  | .11  | ---  | .26  | .18  | .05  | .19  | .12  | .01  |     | <u>TOTAL<br/>OBSERVED<br/>PROBABILITY<br/>MATRIX</u> |
| 3   | .04  | .16  | .29  | ---  | .16  | .02  | .23  | .09  | .01  |     |                                                      |
| 4   | .07  | .08  | .26  | .23  | ---  | .05  | .14  | .18  | 0    |     |                                                      |
| 5   | 0    | .08  | .24  | .22  | .14  | ---  | .14  | .19  | 0    |     |                                                      |
| 6   | .06  | .07  | .32  | .22  | .17  | .07  | ---  | .10  | 0    |     |                                                      |
| 7   | .04  | .02  | .22  | .23  | .15  | .13  | .13  | ---  | 0    |     |                                                      |
| Sh  | 0    | .14  | .14  | .43  | 0    | 0    | .29  | 0    | ---  |     |                                                      |
| SS  | ---  | .12  | .23  | .20  | .14  | .05  | .15  | .09  | 0    |     |                                                      |
| 1   | .08  | ---  | .24  | .21  | .15  | .05  | .15  | .10  | 0    |     |                                                      |
| 2   | .09  | .14  | ---  | .24  | .17  | .06  | .17  | .11  | .01  |     | <u>TOTAL<br/>RANDOM<br/>MATRIX</u>                   |
| 3   | .09  | .14  | .27  | ---  | .17  | .05  | .17  | .11  | .01  |     |                                                      |
| 4   | .08  | .13  | .25  | .22  | ---  | .06  | .16  | .10  | .01  |     |                                                      |
| 5   | .08  | .12  | .23  | .20  | .14  | ---  | .14  | .09  | 0    |     |                                                      |
| 6   | .09  | .13  | .25  | .22  | .15  | .05  | ---  | .10  | .01  |     |                                                      |
| 7   | .09  | .12  | .24  | .21  | .15  | .05  | .15  | ---  | 0    |     |                                                      |
| Sh  | .07  | .11  | .22  | .19  | .13  | .05  | .14  | .09  | ---  |     |                                                      |
| SS  | ---  | +.37 | -.02 | -.13 | -.05 | -.02 | -.05 | -.09 | 0    |     |                                                      |
| 1   | +.15 | ---- | -.01 | +.04 | -.01 | -.02 | -.07 | -.07 | -.01 |     |                                                      |
| 2   | 0    | -.03 | ---- | +.02 | +.01 | -.01 | +.02 | +.01 | 0    |     | <u>TOTAL<br/>DIFFERENCE<br/>MATRIX</u>               |
| 3   | -.05 | +.02 | +.02 | ---- | -.01 | -.03 | +.06 | -.02 | 0    |     |                                                      |
| 4   | -.01 | -.05 | +.01 | +.01 | ---- | -.01 | -.02 | +.08 | -.01 |     |                                                      |
| 5   | -.08 | -.04 | +.01 | +.02 | 0    | ---- | 0    | +.10 | 0    |     |                                                      |
| 6   | -.03 | -.06 | +.07 | 0    | +.02 | +.02 | ---- | 0    | 0    |     |                                                      |
| 7   | -.05 | -.10 | -.02 | +.02 | 0    | +.08 | -.02 | ---- | 0    |     |                                                      |
| Sh  | -.07 | +.03 | -.08 | +.24 | -.13 | -.05 | +.15 | -.09 | ---- |     |                                                      |

## Part 2

Detailed Analyses:Tests for Differences in Facies Occurrences  
in Major Sedimentation Horizons

Computational Techniques Are Given in Most Basic Statistics Books.

Note: As discussed in the text, major sedimentation horizons are:

1. Sandstone Horizons (Member I and Niveau 2: Anse à Pierre Jean - St. Simon area and Bic)
2. Conglomerate Horizons (Member II, Niveau 3 and Niveau 5: Anse à Pierre Jean - Cap à la Carre region and Bic)
3. Bic Member III Section
4. Pebbly Sandstone Horizons ( Niveau 4 and Niveau 6: St. Simon - Cap à la Carre Ouest area)
5. Rivière Trois Pistoles Section
6. Grève de la Pointe Section

### Chi-squared Test Results

The number of facies per major sedimentation horizon, estimated bivariate probabilities and differences between observed and expected frequencies are given on the next page. Results of this Chi-squared test are as follows:

$$\chi^2_{\text{calc}} = 476.53$$

df = number of cells - 1 - no. estimated parameters  
 =  $(r - 1)(c - 1)$ , where  $r$  = no. of rows and  $c$  = no. of columns.  
 = 40

$$\chi^2_{40} = 55.8$$

The prob value of the calculated  $\chi^2$  value is much less than 0.001 on a  $\chi^2$  distribution with 40 df. This suggests that the null hypothesis of identical bivariate probabilities ( $H_0 = \hat{\pi}_{ij} = \hat{\pi}_i \hat{\pi}_j$ ) is false.

NUMBER OF FACIES OCCURRENCES / MAJOR SEDIMENTATION HORIZONS ( $O_{ij}$ 's)

| Facies<br>Horizon   | SS   | 1    | 2    | 3    | 4    | 5    | 6    | 7    | Sh   | Sum  | % ( $\hat{\pi}_i$ ) |
|---------------------|------|------|------|------|------|------|------|------|------|------|---------------------|
| 1                   | 11   | 7    | 47   | 30   | 47   | 12   | 63   | 33   | 1    | 251  | .167                |
| 2                   | 16   | 76   | 29   | 34   | 8    | 5    | 11   | 0    | 3    | 182  | .121                |
| 3                   | 0    | 0    | 15   | 22   | 11   | 14   | 17   | 42   | 6    | 127  | .084                |
| 4                   | 19   | 76   | 114  | 138  | 54   | 11   | 85   | 17   | 3    | 517  | .344                |
| 5                   | 3    | 7    | 17   | 3    | 6    | 2    | 13   | 16   | 0    | 67   | .045                |
| 6                   | 23   | 15   | 85   | 50   | 77   | 14   | 42   | 53   | 2    | 361  | .240                |
| Sum                 | 72   | 181  | 307  | 277  | 203  | 58   | 231  | 161  | 15   | 1505 |                     |
| % ( $\hat{\pi}_j$ ) | .048 | .120 | .204 | .184 | .135 | .039 | .153 | .107 | .010 |      | 1.000               |

ESTIMATED BIVARIATE PROBABILITIES (ASSUMING INDEPENDENCE) ( $\hat{\pi}_{ij} = \hat{\pi}_i \hat{\pi}_j$ )

| Facies<br>Horizon | SS   | 1    | 2    | 3    | 4    | 5    | 6    | 7    | Sh   | $\hat{\pi}_i$ |
|-------------------|------|------|------|------|------|------|------|------|------|---------------|
| 1                 | .008 | .020 | .034 | .031 | .023 | .007 | .026 | .018 | .002 | .167          |
| 2                 | .006 | .015 | .025 | .022 | .016 | .005 | .019 | .013 | .001 | .121          |
| 3                 | .004 | .010 | .017 | .015 | .011 | .003 | .013 | .009 | .001 | .084          |
| 4                 | .017 | .041 | .070 | .063 | .046 | .013 | .053 | .037 | .003 | .344          |
| 5                 | .002 | .005 | .009 | .008 | .006 | .002 | .007 | .005 | .001 | .045          |
| 6                 | .012 | .029 | .049 | .044 | .032 | .009 | .037 | .026 | .002 | .240          |
| $\hat{\pi}_j$     | .048 | .120 | .204 | .184 | .135 | .039 | .153 | .107 | .010 |               |

DIFFERENCE BETWEEN OBSERVED AND EXPECTED FREQUENCIES ( $O_{ij} - E_{ij}$ )

$$(E_{ij} = n \hat{\pi}_{ij} = (1505) \hat{\pi}_{ij})$$

| Facies<br>Horizon | SS    | 1      | 2      | 3      | 4      | 5     | 6      | 7      | Sh    |
|-------------------|-------|--------|--------|--------|--------|-------|--------|--------|-------|
| 1                 | -1.04 | -23.10 | -4.17  | -16.66 | 12.39  | 1.47  | 23.87  | 5.91   | -2.01 |
| 2                 | 6.97  | 53.43  | -8.63  | 0.89   | 16.08  | -2.53 | -17.60 | -19.57 | 1.50  |
| 3                 | 6.02  | -15.05 | -10.59 | -0.58  | -5.56  | 9.49  | -2.57  | 28.46  | 4.50  |
| 4                 | -6.59 | 14.29  | 8.65   | 43.19  | -15.23 | -8.57 | 5.24   | -38.69 | -1.52 |
| 5                 | -0.01 | -0.53  | 3.46   | -9.04  | -3.03  | -1.01 | 2.47   | 8.48   | -1.51 |
| 6                 | 4.94  | -28.65 | 11.26  | -16.22 | 28.84  | 0.46  | -13.69 | 13.87  | -1.01 |

SUMMARY OF ONE-WAY ANOVA OF % FACIES OCCURRENCES  
IN DIFFERENT SEDIMENTATION HORIZONS

df = 5/10

$F_{0.05} = 3.33$  (critical F-value)

| Facies | Decision                    | Results of One-Way ANOVA of % Facies Occurrences                                                                                                                             |
|--------|-----------------------------|------------------------------------------------------------------------------------------------------------------------------------------------------------------------------|
| 1      | Reject<br>$H_0$             | F-ratio = 70.2. The computed F-ratio exceeds $F_{.05}$ ; therefore, reject the null hypothesis that the horizons are similar at the 5% significance level                    |
| 2      | Accept<br>$H_0$             | F-ratio = 0.55. The critical $F_{.05}$ value exceeds the computed F-ratio; therefore, accept the null hypothesis that the horizons are similar at the 5% significance level. |
| 3      | Accept<br>$H_0$             | F-ratio = 1.95. The critical $F_{.05}$ value exceeds the computed F-ratio; therefore, accept the null hypothesis that the horizons are similar at the 5% sig. level.         |
| 4      | Accept<br>$H_0$             | F-ratio = 0.96. The critical $F_{.05}$ value exceeds the computed F-ratio; therefore, accept the null hypothesis that the horizons are similar at the 5% sig. level.         |
| 5      | Marginal<br>Accept<br>$H_0$ | F-ratio = 2.16. The critical $F_{.05}$ value exceeds the computed F-ratio; therefore, accept the null hypothesis that the horizons are similar at the 5% sig. level.         |
| 6      | Accept<br>$H_0$             | F-ratio = 1.72. The critical $F_{.05}$ value exceeds the computed F-ratio; therefore, accept the null hypothesis that the horizons are similar at the 5% sig. level.         |
| 7      | Marginal<br>Reject<br>$H_0$ | F-ratio = 6.92. The computed F-ratio exceeds the critical $F_{.05}$ value; therefore, reject the null hypothesis that the horizons are similar at the 5% sig. level.         |
| SS     | Marginal<br>Accept<br>$H_0$ | F-ratio = 2.72. The critical $F_{.05}$ value exceeds the computed F-ratio; therefore, accept the null hypothesis that the horizons are similar at the 5% sig. level.         |

## ONE-WAY ANOVA OF % FACIES OCCURRENCES IN DIFFERENT SEDIMENTATION HORIZONS

## FACIES 1

| Maj. Sed. Horizon    | 1             | 2              | 3   | 4              | 5   | 6   |        |
|----------------------|---------------|----------------|-----|----------------|-----|-----|--------|
| Individual           | 3             | 42             | 0   | 24             |     | 4   |        |
| Per Cent             | 1             | 33             |     | 17             |     |     |        |
| at Different         | 0             | 55             |     | 5              |     |     |        |
| Sections             | 2             | 48             |     | 12             |     |     |        |
|                      | 8             |                |     |                |     |     | Totals |
| $n_i$                | 5             | 4              | 1   | 4              | 1   | 1   | 16     |
| $\sum x_{ij}$        | 14            | 178            | 0   | 58             | 10  | 4   | 264    |
| $\sum x_{ij}^2$      | 78            | 8182           | 0   | 1034           | 100 | 16  | 9410   |
| $\bar{x}_i$          | 2.8           | 44.5           | 0   | 14.5           | 10  | 4   |        |
| $s_i^2$              | 9.70          | 87             | --- | 64.33          | --- | --- |        |
| $s_i$                | 3.11          | 9.33           | --- | 8.02           | --- | --- |        |
| $\bar{x}_i \pm 2s_i$ | (-3.43, 9.03) | (25.85, 63.15) | --- | (-1.54, 30.54) | --- | --- |        |

| Source of Variation | Sum of Squares | df | Mean Square | F-ratio  | P Prob Value | Decision     |
|---------------------|----------------|----|-------------|----------|--------------|--------------|
| Grand Mean          | 4356           | 1  | 4356        | 982.8/14 | $p \ll .001$ | Reject $H_0$ |
| Between Horiz       | 4914           | 5  | 982.8       | = 70.2   |              |              |
| Residual            | 140            | 10 | 14          |          |              |              |
| Total               | 9410           | 16 |             |          |              |              |

ONE-WAY ANOVA OF % FACIES OCCURRENCES IN DIFFERENT SEDIMENTATION HORIZONS

FACIES 2

| Maj. Sed. Horizon    | 1              | 2             | 3   | 4             | 5   | 6   |        |
|----------------------|----------------|---------------|-----|---------------|-----|-----|--------|
| Individual           | 29             | 21            | 12  | 20            | 25  | 24  |        |
| Per Cent at          | 24             | 10            |     | 22            |     |     |        |
| Different            | 0              | 10            |     | 12            |     |     |        |
| Sections             | 15             | 19            |     | 29            |     |     | Totals |
|                      | 12             |               |     |               |     |     |        |
| $n_i$                | 5              | 4             | 1   | 4             | 1   | 1   | 16     |
| $\sum x_{ij}$        | 80             | 60            | 12  | 83            | 25  | 24  | 284    |
| $\sum x_{ij}^2$      | 1786           | 1002          | 144 | 1869          | 625 | 576 | 6002   |
| $\bar{x}_i$          | 16             | 15            | 12  | 20.75         | 25  | 24  |        |
| $s_i^2$              | 126.5          | 34            | --- | 48.92         | --- | --- |        |
| $s_i$                | 11.25          | 5.83          | --- | 6.99          | --- | --- |        |
| $\bar{x}_i \pm 2s_i$ | (-6.49, 38.49) | (3.34, 26.66) | --- | (6.76, 34.74) | --- | --- |        |

| Source of Variation | Sum of Squares | df | Mean Square | F-ratio     | p Prob Value | Decision     |
|---------------------|----------------|----|-------------|-------------|--------------|--------------|
| Grand Mean          | 5041           | 1  | 5041        | 41.25/75.48 | p > .25      | Accept $H_0$ |
| Between Horiz       | 206.25         | 5  | 41.25       | = 0.55      |              |              |
| Residual            | 754.75         | 10 |             |             |              |              |
| Total               | 6002           | 16 |             |             |              |              |



## ONE-WAY ANOVA OF % FACIES OCCURRENCES IN DIFFERENT SEDIMENTATION HORIZONS

## FACIES 3

| Maj. Sed. Horizon    | 1              | 2             | 3   | 4       | 5   | 6   |        |
|----------------------|----------------|---------------|-----|---------|-----|-----|--------|
| Individual           | 16             | 14            | 17  | 17      | 4   | 14  |        |
| Per Cent at          | 11             | 25            |     | 29      |     |     |        |
| Different            | 27             | 10            |     | 41      |     |     |        |
| Sections             | 7              | 23            |     | 25      |     |     | Totals |
|                      | 12             |               |     |         |     |     |        |
| $n_i$                | 5              | 4             | 1   | 4       | 1   | 1   | 16     |
| $\sum x_{ij}$        | 73             | 72            | 17  | 112     | 4   | 14  | 292    |
| $\sum x_{ij}^2$      | 1299           | 1450          | 289 | 3436    | 16  | 196 | 6686   |
| $\bar{x}_i$          | 14.6           | 18            | 17  | 28      | 4   | 14  |        |
| $s_i^2$              | 58.3           | 51.33         | --- | 100     | --- | --- |        |
| $s_i$                | 7.64           | 7.16          | --- | 10      | --- | --- |        |
| $\bar{x}_i \pm 2s_i$ | (-0.67, 29.87) | (3.67, 32.22) | --- | (8, 48) | --- | --- |        |

| Source of Variation | Sum of Squares | df | Mean Square | F-ratio      | p Prob Value | Decision     |
|---------------------|----------------|----|-------------|--------------|--------------|--------------|
| Grand Mean          | 5329           | 1  | 5329        | 133.96/68.72 | .25 > p > .1 | Accept $H_0$ |
| Between Horiz       | 669.8          | 5  | 133.96      | = 1.95       |              |              |
| Residual            | 687.2          | 10 | 68.72       |              |              |              |
| Total               | 6686           | 16 |             |              |              |              |

## ONE-WAY ANOVA OF % FACIES OCCURRENCES IN DIFFERENT SEDIMENTATION HORIZONS

| Maj. Sed. Horizon    | FACIES 4        |              |     |               |     |     | Totals |
|----------------------|-----------------|--------------|-----|---------------|-----|-----|--------|
|                      | 1               | 2            | 3   | 4             | 5   | 6   |        |
| Individual           | 16              | 6            | 9   | 14            | 9   | 21  |        |
| Per Cent at          | 20              | 7            |     | 10            |     |     |        |
| Different            | 13              | 0            |     | 4             |     |     |        |
| Sections             | 9               | 0            |     | 12            |     |     |        |
|                      | 31              |              |     |               |     |     |        |
| $n_i$                | 5               | 4            | 1   | 4             | 1   | 1   | 16     |
| $\sum x_{ij}$        | 89              | 13           | 9   | 40            | 9   | 21  | 181    |
| $\sum x_{ij}^2$      | 2692            | 85           | 81  | 456           | 81  | 441 | 3836   |
| $\bar{x}_i$          | 17.8            | 3.25         | 9   | 10            | 9   | 21  |        |
| $s_i^2$              | 276.95          | 14.25        | --- | 18.67         | --- | --- |        |
| $s_i$                | 16.64           | 3.77         | --- | 4.32          | --- | --- |        |
| $\bar{x}_i \pm 2s_i$ | (-15.48, 51.08) | (-4.3, 10.8) | --- | (1.36, 18.64) | --- | --- |        |

| Source of Variation | Sum of Squares | df | Mean Square | F-ratio       | p Prob Value | Decision     |
|---------------------|----------------|----|-------------|---------------|--------------|--------------|
| Grand Mean          | 2047.56        | 1  | 2047.56     | 116.38/120.66 | p > .25      | Accept $H_0$ |
| Between Horiz       | 581.89         | 5  | 116.38      | = 0.96        |              |              |
| Residual            | 1206.55        | 10 | 120.66      |               |              |              |
| Total               | 3836           | 16 |             |               |              |              |

## ONE-WAY ANOVA OF % FACIES OCCURRENCES IN DIFFERENT SEDIMENTATION HORIZONS

## FACIES 5

| Maj. Sed. Horizon    | 1              | 2             | 3   | 4             | 5   | 6   |        |
|----------------------|----------------|---------------|-----|---------------|-----|-----|--------|
| Individual           | 0              | 4             | 11  | 0             | 3   | 4   |        |
| Per Cent at          | 5              | 2             |     | 1             |     |     |        |
| Different            | 0              | 0             |     | 1             |     |     |        |
| Sections             | 7              | 3             |     | 5             |     |     |        |
|                      | 6              |               |     |               |     |     | Totals |
| $n_1$                | 5              | 4             | 1   | 4             | 1   | 1   | 16     |
| $\sum x_{ij}$        | 18             | 9             | 11  | 7             | 3   | 4   | 52     |
| $\sum x_{ij}^2$      | 110            | 29            | 121 | 27            | 9   | 16  | 312    |
| $\bar{x}_1$          | 3.6            | 2.25          | 11  | 1.75          | 3   | 4   |        |
| $s_1^2$              | 11.3           | 2.92          | --- | 4.92          | --- | --- |        |
| $s_1$                | 3.36           | 1.71          | --- | 2.22          | --- | --- |        |
| $\bar{x}_1 \pm 2s_1$ | (-3.12, 10.32) | (-1.17, 5.67) | --- | (-2.68, 6.18) | --- | --- |        |

| Source of Variation | Sum of Squares | df | Mean Square | F-ratio    | P Prob Value  | Decision                  |
|---------------------|----------------|----|-------------|------------|---------------|---------------------------|
| Grand Mean          | 169            | 1  | 169         | 14.86/6.87 | .10 > p > .05 | Some evidence $H_0$ false |
| Between Horiz       | 74.3           | 5  | 14.86       | = 2.16     |               |                           |
| Residual            | 68.7           | 10 | 6.87        |            |               |                           |
| Total               | 312            | 16 |             |            |               |                           |

## ONE-WAY ANOVA OF % FACIES OCCURRENCES IN DIFFERENT SEDIMENTATION HORIZONS

## FACIES 6

| Maj. Sed. Horizon    | 1              | 2            | 3   | 4             | 5   | 6   |        |
|----------------------|----------------|--------------|-----|---------------|-----|-----|--------|
| Individual           | 18             | 3            | 13  | 17            | 19  | 12  |        |
| Per Cent at          | 16             | 12           |     | 17            |     |     |        |
| Different            | 47             | 0            |     | 27            |     |     |        |
| Sections             | 49             | 6            |     | 10            |     |     |        |
|                      | 13             |              |     |               |     |     | Totals |
| $n_i$                | 5              | 4            | 1   | 4             | 1   | 1   | 16     |
| $\sum x_{ij}$        | 143            | 21           | 13  | 71            | 19  | 12  | 279    |
| $\sum x_{ij}^2$      | 5359           | 169          | 169 | 1407          | 361 | 144 | 7609   |
| $\bar{x}_i$          | 28.6           | 5.25         | 13  | 17.75         | 19  | 12  |        |
| $s_i^2$              | 317.3          | 19.58        | --- | 48.92         | --- | --- |        |
| $s_i$                | 17.81          | 4.43         | --- | 6.99          | --- | --- |        |
| $\bar{x}_i \pm 2s_i$ | (-7.03, 64.23) | (-3.6, 14.1) | --- | (3.76, 31.74) | --- | --- |        |

| Source of Variation | Sum of Squares | df | Mean Square | F-ratio       | P Prob Value | Decision              |
|---------------------|----------------|----|-------------|---------------|--------------|-----------------------|
| Grand Mean          | 4865.06        | 1  | 4865.06     | 253.85/147.47 | .25 > p > .1 | Accept H <sub>0</sub> |
| Between Horiz       | 1269.24        | 5  | 253.85      | = 1.72        |              |                       |
| Residual            | 1474.7         | 10 | 147.47      |               |              |                       |
| Total               | 7609           | 16 |             |               |              |                       |

## ONE-WAY ANOVA OF % FACIES OCCURRENCES IN DIFFERENT SEDIMENTATION HORIZONS

## FACIES 7

| Maj. Sed. Horizon    | 1                 | 2 | 3    | 4                | 5   | 6   |        |
|----------------------|-------------------|---|------|------------------|-----|-----|--------|
| Individual           | 18                | 0 | 33   | 4                | 24  | 15  |        |
| Per Cent at          | 15                | 0 |      | 0                |     |     |        |
| Different            | 0                 | 0 |      | 3                |     |     |        |
| Sections             | 5                 | 0 |      | 5                |     |     |        |
|                      | 17                |   |      |                  |     |     | Totals |
| $n_i$                | 5                 | 4 | 1    | 4                | 1   | 1   | 16     |
| $\sum x_{ij}$        | 50                | 0 | 33   | 12               | 24  | 15  | 134    |
| $\sum x_{ij}^2$      | 863               | 0 | 1089 | 50               | 576 | 225 | 2803   |
| $\bar{x}_i$          | 10                | 0 | 33   | 3                | 24  | 15  |        |
| $s_i^2$              | 90.75             | 0 | ---  | 4.67             | --- | --- |        |
| $s_i$                | 9.53              | 0 | ---  | 2.16             | --- | --- |        |
| $\bar{x}_i \pm 2s_i$ | (-9.05,<br>29.05) | 0 | ---  | (-1.32,<br>7.32) | --- | --- |        |

| Source of Variation | Sum of Squares | df | Mean Square | F-ratio     | P Prob Value   | Decision                  |
|---------------------|----------------|----|-------------|-------------|----------------|---------------------------|
| Grand Mean          | 1122.25        | 1  | 1122.25     | 260.75/37.7 | .01 > p > .001 | Some evidence $H_0$ false |
| Between Horiz       | 1303.75        | 5  | 260.75      | = 6.92      |                |                           |
| Residual            | 377            | 10 | 37.7        |             |                |                           |
| Total               | 2803           | 16 |             |             |                |                           |

## ONE-WAY ANOVA OF 7 FACIES OCCURRENCES IN DIFFERENT SEDIMENTATION HORIZONS

## SCoured SURFACES

| Maj. Sed. Horizon     | 1            | 2               | 3   | 4            | 5   | 6   |        |
|-----------------------|--------------|-----------------|-----|--------------|-----|-----|--------|
| Individual            | 0            | 10              | 0   | 4            | 4   | 6   |        |
| Per Cent              | 5            | 7               |     | 5            |     |     |        |
| at Different Sections | 13           | 25              |     | 5            |     |     |        |
|                       | 5            | 0               |     | 2            |     |     |        |
|                       | 2            |                 |     |              |     |     | Totals |
| $n_i$                 | 5            | 4               | 1   | 4            | 1   | 1   | 16     |
| $\sum x_{ij}$         | 25           | 42              | 0   | 16           | 4   | 6   | 93     |
| $\sum x_{ij}^2$       | 223          | 774             | 0   | 70           | 16  | 36  | 1119   |
| $\bar{x}_i$           | 5.0          | 10.5            | 0   | 4.0          | 4   | 6   |        |
| $s_i^2$               | 24.5         | 111.0           | --- | 2.0          | --- | --- |        |
| $s_i$                 | 4.95         | 10.54           | --- | 1.41         | --- | --- |        |
| $\bar{x}_i \pm 2s_i$  | (-4.9, 14.9) | (-10.58, 31.58) | --- | (1.18, 6.82) | --- | --- |        |

| Source of Variation | Sum of Squares | df | Mean Square | F-ratio    | P Prob value  | Decision      |
|---------------------|----------------|----|-------------|------------|---------------|---------------|
| Grand Mean          | 540.56         | 1  | 540.56      |            |               |               |
| Between Horiz       | 333.44         | 5  | 66.69       | 66.69/24.5 | .10 > p > .05 | Some evidence |
| Residual            | 245            | 10 | 24.5        | = 2.72     |               | $H_0$ false   |
| Total               | 1119           | 16 |             |            |               |               |

## Part 3

Detailed Analyses:Sequences of Beds:  
Non-embedded Markov Chain Analysis

## Computational Techniques Given by Davis (1973)

Note: The transitions of scoured surfaces - to - scoured surfaces (SS  $\rightarrow$  SS) and of shale facies - to - shale facies (Sh  $\rightarrow$  Sh) are not discernable in the field. All other transitions are possible. Random probabilities from scoured surfaces and shale facies must take into account the impossibility of these two types of transitions. Hence, for rows from scoured surfaces, the random probabilities are calculated as:  $r_{SS j} = \frac{\text{no. transitions in column } j}{\text{total no. observations} - \text{no. scoured surfaces}}$

Similarly, the rows from shale facies have the random probabilities calculated as:  $r_{Sh j} = \frac{\text{no. transitions in column } j}{\text{total no. observations} - \text{no. of shale beds}}$

Key: 1, ..., 7: Facies 1 through 7  
SS: Scoured Surfaces  
Sh: Shale Facies

For the spider diagram of the facies relationships, a cutoff value of +0.05 was arbitrary selected as being the boundary between random and non-random transitions (from difference matrix scores). Also eliminated, were those transitions which only occurred once.

Fig.120- Facies relations in different major sedimentation horizons.

Non-embedded Markov chain analysis.

Dotted arrows = difference matrix scores are .05-.10

Dashed arrows = difference matrix scores are .11-.30

Solid arrows = difference matrix scores are  $>$  .30.

1, 2, 3, ...7 = Facies 1 through 7

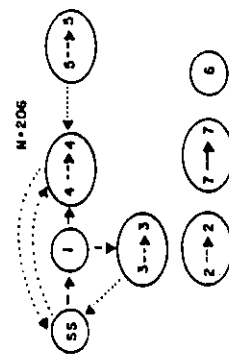
Sh = Shale Facies

SS = Scoured surfaces

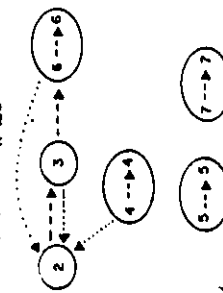
S1 - S11 sections on location map Fig. in text.



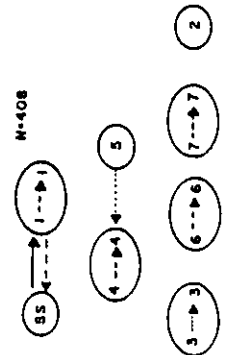
SANDSTONE HORIZONS S9 TO S7, S5 & S1



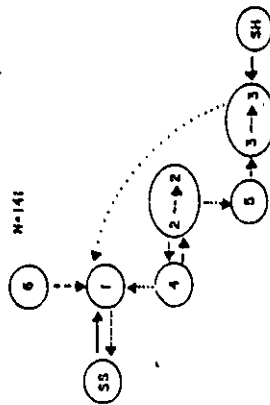
BIC (S1) III N-120



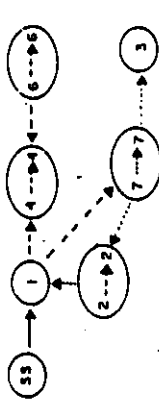
PEBBLY SANDSTONE HORIZONS S9 TO S3



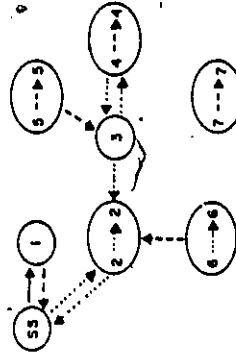
CONGLOMERATE HORIZONS S9 TO S3, S1



RIVIERE TROIS PISTOLES SECTION S10 N-64



GREVE DE LA POINTE SECTION S11 N-327



## NON-EMBEDDED MARKOV CHAIN ANALYSIS

## 1. SANDSTONE HORIZONS

|     | SS   | 1    | 2    | 3    | 4    | 5    | 6    | 7    | Sh  | Sum |                                                        |
|-----|------|------|------|------|------|------|------|------|-----|-----|--------------------------------------------------------|
| SS  | --   | 2    | 2    | 2    | 3    | 0    | 2    | 0    | 0   | 11  |                                                        |
| 1   | 0    | 0    | 0    | 2    | 3    | 0    | 0    | 0    | 0   | 5   |                                                        |
| 2   | 2    | 1    | 14   | 4    | 3    | 0    | 9    | 5    | 1   | 39  |                                                        |
| 3   | 3    | 1    | 3    | 4    | 4    | 0    | 6    | 1    | 0   | 26  | <u>TALLY</u><br><u>MATRIX</u>                          |
| 4   | 5    | 0    | 7    | 4    | 12   | 3    | 4    | 3    | 0   | 38  |                                                        |
| 5   | 0    | 0    | 2    | 0    | 3    | 3    | 1    | 1    | 0   | 10  |                                                        |
| 6   | 3    | 1    | 8    | 4    | 8    | 5    | 17   | 2    | 0   | 48  |                                                        |
| 7   | 0    | 0    | 5    | 2    | 5    | 0    | 3    | 13   | 0   | 28  |                                                        |
| Sh  | 0    | 0    | 0    | 0    | 0    | 0    | 1    | 0    | --  | 1   |                                                        |
| Sum | 13   | 5    | 41   | 26   | 41   | 11   | 43   | 25   | 1   | 206 |                                                        |
| SS  | --   | .18  | .18  | .18  | .27  | 0    | .18  | 0    | 0   |     |                                                        |
| 1   | 0    | 0    | 0    | .40  | .60  | 0    | 0    | 0    | 0   |     |                                                        |
| 2   | .05  | .03  | .36  | .10  | .08  | 0    | .23  | .13  | .03 |     | <u>OBSERVED</u><br><u>PROBABILITY</u><br><u>MATRIX</u> |
| 3   | .12  | .04  | .12  | .31  | .15  | 0    | .23  | .04  | 0   |     |                                                        |
| 4   | .13  | 0    | .18  | .11  | .32  | .08  | .11  | .08  | 0   |     |                                                        |
| 5   | 0    | 0    | .20  | 0    | .30  | .30  | .10  | .10  | 0   |     |                                                        |
| 6   | .06  | .02  | .17  | .08  | .17  | .10  | .35  | .04  | 0   |     |                                                        |
| 7   | 0    | 0    | .18  | .07  | .18  | 0    | .11  | .46  | 0   |     |                                                        |
| Sh  | 0    | 0    | 0    | 0    | 0    | 0    | 1.0  | 0    | --  |     |                                                        |
| SS  | --   | .03  | .21  | .13  | .21  | .06  | .22  | .13  |     |     |                                                        |
| 1   | .06  | .02  | .20  | .13  | .20  | .05  | .21  | .12  |     |     |                                                        |
| 2   | .06  | .02  | .20  | .13  | .20  | .05  | .21  | .12  |     |     | <u>RANDOM</u><br><u>MATRIX</u>                         |
| 3   | .06  | .02  | .20  | .13  | .20  | .05  | .21  | .12  |     |     |                                                        |
| 4   | .06  | .02  | .20  | .13  | .20  | .05  | .21  | .12  |     |     |                                                        |
| 5   | .06  | .02  | .20  | .13  | .20  | .05  | .21  | .12  |     |     |                                                        |
| 6   | .06  | .02  | .20  | .13  | .20  | .05  | .21  | .12  |     |     |                                                        |
| 7   | .06  | .02  | .20  | .13  | .20  | .05  | .21  | .12  |     |     |                                                        |
| SS  | --   | +.15 | -.03 | +.05 | +.06 | -.06 | -.04 | -.13 |     |     |                                                        |
| 1   | -.06 | -.02 | -.20 | +.27 | +.40 | -.05 | -.21 | -.12 |     |     |                                                        |
| 2   | -.01 | +.01 | +.16 | -.03 | -.12 | -.05 | +.02 | +.01 |     |     | <u>DIFFERENCE</u><br><u>MATRIX</u>                     |
| 3   | +.06 | +.02 | -.08 | +.18 | -.05 | -.05 | +.02 | -.08 |     |     |                                                        |
| 4   | +.07 | -.02 | -.02 | -.02 | +.12 | +.03 | -.10 | -.04 |     |     |                                                        |
| 5   | -.06 | -.02 | 0    | -.13 | +.10 | +.25 | -.11 | -.02 |     |     |                                                        |
| 6   | 0    | 0    | -.03 | -.05 | -.03 | +.05 | +.14 | -.08 |     |     |                                                        |
| 7   | -.06 | -.02 | -.02 | -.06 | -.02 | -.05 | -.10 | +.34 |     |     |                                                        |

## NON-EMBEDDED MARKOV CHAIN ANALYSIS

## 2. CONGLOMERATE HORIZONS

|     | SS   | 1    | 2    | 3    | 4    | 5    | 6    | Sh   | Sum |                                                        |
|-----|------|------|------|------|------|------|------|------|-----|--------------------------------------------------------|
| SS  | --   | 10   | 1    | 0    | 0    | 1    | 0    | 0    | 12  |                                                        |
| 1   | 10   | 22   | 11   | 9    | 3    | 2    | 4    | 1    | 62  |                                                        |
| 2   | 0    | 5    | 7    | 4    | 2    | 2    | 0    | 0    | 20  | <u>TALLY</u><br><u>MATRIX</u>                          |
| 3   | 1    | 13   | 2    | 7    | 0    | 1    | 1    | 2    | 27  |                                                        |
| 4   | 0    | 3    | 2    | 1    | 0    | 0    | 0    | 0    | 6   |                                                        |
| 5   | 0    | 2    | 1    | 2    | 1    | 0    | 0    | 0    | 6   |                                                        |
| 6   | 0    | 3    | 1    | 1    | 0    | 0    | 0    | 0    | 5   |                                                        |
| Sh  | 0    | 1    | 0    | 2    | 0    | 0    | 0    | --   | 3   |                                                        |
| Sum | 11   | 59   | 25   | 26   | 6    | 6    | 5    | 3    | 141 |                                                        |
| SS  | --   | .83  | .08  | 0    | 0    | .08  | 0    | 0    |     | <u>OBSERVED</u><br><u>PROBABILITY</u><br><u>MATRIX</u> |
| 1   | .16  | .35  | .18  | .15  | .05  | .03  | .06  | .02  |     |                                                        |
| 2   | 0    | .25  | .35  | .20  | .10  | .10  | 0    | 0    |     |                                                        |
| 3   | .04  | .48  | .07  | .26  | 0    | .04  | .04  | .07  |     |                                                        |
| 4   | 0    | .50  | .33  | .17  | 0    | 0    | 0    | 0    |     |                                                        |
| 5   | 0    | .33  | .17  | .33  | .17  | 0    | 0    | 0    |     |                                                        |
| 6   | 0    | .60  | .20  | .20  | 0    | 0    | 0    | 0    |     |                                                        |
| Sh  | 0    | .33  | 0    | .66  | 0    | 0    | 0    | --   |     |                                                        |
| SS  | --   | .45  | .19  | .20  | .05  | .05  | .04  | .02  |     | <u>RANDOM</u><br><u>MATRIX</u>                         |
| 1   | .08  | .42  | .18  | .18  | .04  | .04  | .04  | .02  |     |                                                        |
| 2   | .08  | .42  | .18  | .18  | .04  | .04  | .04  | .02  |     |                                                        |
| 3   | .08  | .42  | .18  | .18  | .04  | .04  | .04  | .02  |     |                                                        |
| 4   | .08  | .42  | .18  | .18  | .04  | .04  | .04  | .02  |     |                                                        |
| 5   | .08  | .42  | .18  | .18  | .04  | .04  | .04  | .02  |     |                                                        |
| 6   | .08  | .42  | .18  | .18  | .04  | .04  | .04  | .02  |     |                                                        |
| Sh  | .08  | .43  | .18  | .19  | .04  | .04  | .04  | --   |     |                                                        |
| SS  | --   | +.38 | -.11 | -.20 | -.05 | +.03 | -.04 | -.02 |     | <u>DIFFERENCE</u><br><u>MATRIX</u>                     |
| 1   | +.08 | -.07 | 0    | -.03 | +.01 | -.01 | +.02 | 0    |     |                                                        |
| 2   | -.08 | -.17 | +.17 | +.02 | +.06 | +.06 | -.04 | -.02 |     |                                                        |
| 3   | -.04 | +.06 | -.11 | +.08 | -.04 | 0    | 0    | +.05 |     |                                                        |
| 4   | -.08 | +.08 | +.15 | -.01 | -.04 | -.04 | -.04 | -.02 |     |                                                        |
| 5   | -.08 | -.09 | -.01 | +.15 | +.13 | -.04 | -.04 | -.02 |     |                                                        |
| 6   | -.08 | +.18 | +.02 | +.02 | -.04 | -.04 | -.04 | -.02 |     |                                                        |
| Sh  | -.08 | -.10 | -.18 | +.47 | -.04 | -.04 | -.04 | --   |     |                                                        |

## NON-EMBEDDED MARKOV CHAIN ANALYSIS

## 3. BIC MEMBER III

|     | 2    | 3    | 4    | 5    | 6    | 7    | Sum |                    |
|-----|------|------|------|------|------|------|-----|--------------------|
| 2   | 2    | 6    | 2    | 0    | 2    | 3    | 15  |                    |
| 3   | 4    | 5    | 3    | 0    | 6    | 4    | 22  |                    |
| 4   | 2    | 0    | 3    | 1    | 1    | 4    | 11  | <u>TALLY</u>       |
| 5   | 1    | 2    | 0    | 7    | 2    | 5    | 17  | <u>MATRIX</u>      |
| 6   | 3    | 2    | 1    | 2    | 5    | 3    | 16  |                    |
| 7   | 2    | 7    | 2    | 7    | 0    | 21   | 39  |                    |
| Sum | 14   | 22   | 11   | 17   | 16   | 40   | 120 |                    |
| 2   | .13  | .40  | .13  | 0    | .13  | .20  |     |                    |
| 3   | .18  | .23  | .14  | 0    | .27  | .18  |     | <u>OBSERVED</u>    |
| 4   | .18  | 0    | .27  | .09  | .09  | .36  |     | <u>PROBABILITY</u> |
| 5   | .06  | .12  | 0    | .41  | .12  | .29  |     | <u>MATRIX</u>      |
| 6   | .19  | .13  | .06  | .13  | .31  | .19  |     |                    |
| 7   | .05  | .18  | .05  | .18  | 0    | .54  |     |                    |
| 2   | .12  | .18  | .09  | .14  | .13  | .33  |     |                    |
| 3   | .12  | .18  | .09  | .14  | .13  | .33  |     |                    |
| 4   | .12  | .18  | .09  | .14  | .13  | .33  |     | <u>RANDOM</u>      |
| 5   | .12  | .18  | .09  | .14  | .13  | .33  |     | <u>MATRIX</u>      |
| 6   | .12  | .18  | .09  | .14  | .13  | .33  |     |                    |
| 7   | .12  | .18  | .09  | .14  | .13  | .33  |     |                    |
| 2   | +.01 | +.22 | +.04 | -.14 | 0    | -.13 |     |                    |
| 3   | +.06 | +.05 | +.05 | -.14 | +.14 | -.15 |     |                    |
| 4   | +.06 | -.18 | +.18 | -.05 | -.04 | +.03 |     | <u>DIFFERENCE</u>  |
| 5   | -.06 | -.06 | -.09 | +.27 | -.01 | -.04 |     | <u>MATRIX</u>      |
| 6   | +.07 | -.05 | -.03 | -.01 | +.18 | -.14 |     |                    |
| 7   | -.07 | 0    | -.04 | +.04 | -.13 | +.21 |     |                    |

## NON-EMBEDDED MARKOV CHAIN ANALYSIS

## 4. PEBBLY SANDSTONE HORIZONS

|     | SS   | 1    | 2    | 3    | 4    | 5    | 6    | 7    | Sum |                                                        |
|-----|------|------|------|------|------|------|------|------|-----|--------------------------------------------------------|
| SS  | --   | 11   | 4    | 2    | 1    | 0    | 3    | 0    | 21  |                                                        |
| 1   | 12   | 17   | 11   | 16   | 5    | 0    | 3    | 0    | 64  |                                                        |
| 2   | 3    | 7    | 23   | 21   | 13   | 2    | 12   | 2    | 83  |                                                        |
| 3   | 2    | 12   | 24   | 38   | 8    | 2    | 18   | 4    | 109 | <u>TALLY</u><br><u>MATRIX</u>                          |
| 4   | 1    | 5    | 9    | 6    | 11   | 1    | 5    | 1    | 39  |                                                        |
| 5   | 0    | 1    | 2    | 1    | 1    | 0    | 1    | 0    | 6   |                                                        |
| 6   | 2    | 5    | 16   | 21   | 4    | 2    | 21   | 0    | 71  |                                                        |
| 7   | 0    | 1    | 3    | 3    | 1    | 0    | 2    | 2    | 12  |                                                        |
| Sh  | 0    | 0    | 1    | 1    | 0    | 0    | 1    | 0    | 3   |                                                        |
| Sum | 20   | 59   | 93   | 109  | 44   | 7    | 66   | 9    | 408 |                                                        |
| SS  | ---  | .52  | .19  | .10  | .05  | 0    | .14  | 0    |     | <u>OBSERVED</u><br><u>PROBABILITY</u><br><u>MATRIX</u> |
| 1   | .19  | .27  | .17  | .25  | .08  | 0    | .05  | 0    |     |                                                        |
| 2   | .04  | .08  | .28  | .25  | .16  | .02  | .14  | .02  |     |                                                        |
| 3   | .02  | .11  | .22  | .35  | .07  | .02  | .17  | .04  |     |                                                        |
| 4   | .03  | .13  | .23  | .15  | .28  | .03  | .13  | .03  |     |                                                        |
| 5   | 0    | .17  | .33  | .17  | .17  | 0    | .17  | 0    |     |                                                        |
| 6   | .03  | .07  | .23  | .30  | .06  | .03  | .30  | 0    |     |                                                        |
| 7   | 0    | .08  | .25  | .25  | .08  | 0    | .17  | .17  |     |                                                        |
| Sh  | 0    | 0    | .33  | .33  | 0    | 0    | .33  | 0    |     |                                                        |
| SS  | ---  | .15  | .24  | .28  | .11  | .02  | .17  | .02  |     | <u>RANDOM</u><br><u>MATRIX</u>                         |
| 1   | .05  | .14  | .23  | .27  | .11  | .02  | .16  | .02  |     |                                                        |
| 2   | .05  | .14  | .23  | .27  | .11  | .02  | .16  | .02  |     |                                                        |
| 3   | .05  | .14  | .23  | .27  | .11  | .02  | .16  | .02  |     |                                                        |
| 4   | .05  | .14  | .23  | .27  | .11  | .02  | .16  | .02  |     |                                                        |
| 5   | .05  | .14  | .23  | .27  | .11  | .02  | .16  | .02  |     |                                                        |
| 6   | .05  | .14  | .23  | .27  | .11  | .02  | .16  | .02  |     |                                                        |
| 7   | .05  | .14  | .23  | .27  | .11  | .02  | .16  | .02  |     |                                                        |
| Sh  | .05  | .14  | .23  | .27  | .11  | .02  | .16  | .02  |     |                                                        |
| SS  | ---  | +.37 | -.05 | -.18 | -.06 | -.02 | -.03 | -.02 |     | <u>DIFFERENCE</u><br><u>MATRIX</u>                     |
| 1   | +.14 | +.13 | -.06 | -.02 | -.03 | -.02 | -.11 | -.02 |     |                                                        |
| 2   | -.01 | -.06 | +.05 | -.02 | +.05 | 0    | -.02 | 0    |     |                                                        |
| 3   | -.03 | -.03 | -.01 | +.08 | -.04 | 0    | +.01 | +.02 |     |                                                        |
| 4   | -.02 | -.01 | 0    | -.12 | +.17 | +.01 | -.03 | +.01 |     |                                                        |
| 5   | -.05 | +.03 | +.10 | -.10 | +.06 | -.02 | +.01 | -.02 |     |                                                        |
| 6   | -.02 | -.07 | 0    | +.03 | -.05 | +.01 | +.14 | -.02 |     |                                                        |
| 7   | -.05 | -.06 | +.02 | -.02 | -.03 | -.02 | +.01 | +.15 |     |                                                        |
| Sh  | -.05 | -.14 | +.10 | +.06 | -.11 | -.02 | +.17 | -.02 |     |                                                        |

## NON-EMBEDDED MARKOV CHAIN ANALYSIS

## 5. RIVIERE TROIS PISTOLES SECTION

|     | SS   | 1    | 2    | 3    | 4    | 5    | 6    | 7    | Sum |                    |
|-----|------|------|------|------|------|------|------|------|-----|--------------------|
| SS  | --   | 2    | 0    | 0    | 0    | 0    | 1    | 0    | 3   |                    |
| 1   | 0    | 0    | 1    | 0    | 2    | 1    | 0    | 2    | 6   |                    |
| 2   | 1    | 3    | 5    | 1    | 0    | 0    | 2    | 2    | 14  |                    |
| 3   | 0    | 0    | 1    | 0    | 0    | 0    | 0    | 1    | 2   | <u>TALLY</u>       |
| 4   | 1    | 1    | 1    | 0    | 2    | 0    | 1    | 1    | 7   | <u>MATRIX</u>      |
| 5   | 0    | 0    | 1    | 0    | 0    | 0    | 1    | 0    | 2   |                    |
| 6   | 1    | 0    | 1    | 0    | 3    | 0    | 5    | 3    | 13  |                    |
| 7   | 0    | 1    | 5    | 2    | 0    | 1    | 3    | 5    | 17  |                    |
| Sum | 3    | 7    | 15   | 3    | 7    | 2    | 13   | 14   | 64  |                    |
| SS  | ---  | .67  | 0    | 0    | 0    | 0    | .33  | 0    |     |                    |
| 1   | 0    | 0    | .17  | 0    | .33  | .17  | 0    | .33  |     |                    |
| 2   | .07  | .21  | .36  | .07  | 0    | 0    | .14  | .14  |     |                    |
| 3   | 0    | 0    | .50  | 0    | 0    | 0    | 0    | .50  |     | <u>OBSERVED</u>    |
| 4   | .14  | .14  | .14  | 0    | .29  | 0    | .14  | .14  |     | <u>PROBABILITY</u> |
| 5   | 0    | 0    | .50  | 0    | 0    | 0    | .50  | 0    |     | <u>MATRIX</u>      |
| 6   | .08  | 0    | .08  | 0    | .23  | 0    | .38  | .23  |     |                    |
| 7   | 0    | .06  | .29  | .12  | 0    | .06  | .18  | .29  |     |                    |
| SS  | ---  | .11  | .25  | .05  | .11  | .03  | .21  | .23  |     |                    |
| 1   | .05  | .11  | .23  | .05  | .11  | .03  | .20  | .22  |     |                    |
| 2   | .05  | .11  | .23  | .05  | .11  | .03  | .20  | .22  |     |                    |
| 3   | .05  | .11  | .23  | .05  | .11  | .03  | .20  | .22  |     | <u>RANDOM</u>      |
| 4   | .05  | .11  | .23  | .05  | .11  | .03  | .20  | .22  |     | <u>MATRIX</u>      |
| 5   | .05  | .11  | .23  | .05  | .11  | .03  | .20  | .22  |     |                    |
| 6   | .05  | .11  | .23  | .05  | .11  | .03  | .20  | .22  |     |                    |
| 7   | .05  | .11  | .23  | .05  | .11  | .03  | .20  | .22  |     |                    |
| SS  | ---  | +.56 | -.25 | -.05 | -.11 | -.03 | +.12 | -.23 |     |                    |
| 1   | -.05 | -.11 | -.06 | -.05 | +.22 | +.14 | -.20 | +.11 |     |                    |
| 2   | +.02 | +.10 | +.13 | +.02 | -.11 | -.03 | -.06 | -.08 |     |                    |
| 3   | -.05 | -.11 | +.27 | -.05 | -.11 | -.03 | -.20 | +.28 |     | <u>DIFFERENCE</u>  |
| 4   | +.09 | +.03 | -.09 | -.05 | +.18 | -.03 | -.06 | -.08 |     | <u>MATRIX</u>      |
| 5   | -.05 | -.11 | +.27 | -.05 | -.11 | -.03 | +.30 | -.22 |     |                    |
| 6   | +.03 | -.11 | -.15 | -.05 | +.12 | -.03 | +.18 | +.01 |     |                    |
| 7   | -.05 | -.05 | +.06 | +.07 | -.11 | +.03 | -.02 | +.07 |     |                    |

## NON-EMBEDDED MARKOV CHAIN ANALYSIS

## 6. GREVE DE LA POINTE SECTION

|    | SS   | 1    | 2    | 3    | 4    | 5    | 6    | 7    | Sum |                                                        |  |
|----|------|------|------|------|------|------|------|------|-----|--------------------------------------------------------|--|
| SS | ---  | 8    | 7    | 1    | 2    | 1    | 1    | 0    | 20  |                                                        |  |
| 1  | 4    | 1    | 3    | 1    | 3    | 0    | 2    | 1    | 15  |                                                        |  |
| 2  | 9    | 2    | 28   | 8    | 11   | 4    | 8    | 8    | 78  | <u>TALLY</u><br><u>MATRIX</u>                          |  |
| 3  | 0    | 1    | 15   | 5    | 11   | 1    | 7    | 5    | 45  |                                                        |  |
| 4  | 1    | 0    | 10   | 16   | 21   | 1    | 5    | 12   | 66  |                                                        |  |
| 5  | 0    | 0    | 2    | 3    | 0    | 2    | 0    | 1    | 8   |                                                        |  |
| 6  | 2    | 0    | 15   | 3    | 7    | 0    | 7    | 6    | 40  |                                                        |  |
| 7  | 4    | 0    | 7    | 9    | 7    | 2    | 8    | 17   | 54  |                                                        |  |
| SS | ---  | .40  | .35  | .05  | .10  | .05  | .05  | 0    |     |                                                        |  |
| 1  | .27  | .07  | .20  | .07  | .20  | 0    | .13  | .07  |     |                                                        |  |
| 2  | .12  | .03  | .36  | .10  | .14  | .05  | .10  | .10  |     |                                                        |  |
| 3  | 0    | .02  | .33  | .11  | .24  | .02  | .16  | .11  |     | <u>OBSERVED</u><br><u>PROBABILITY</u><br><u>MATRIX</u> |  |
| 4  | .02  | 0    | .15  | .24  | .32  | .02  | .08  | .18  |     |                                                        |  |
| 5  | 0    | 0    | .25  | .38  | 0    | .25  | 0    | .13  |     |                                                        |  |
| 6  | .05  | 0    | .38  | .08  | .18  | 0    | .18  | .15  |     |                                                        |  |
| 7  | .07  | 0    | .13  | .17  | .13  | .04  | .15  | .31  |     |                                                        |  |
| SS | ---  | .04  | .28  | .15  | .20  | .04  | .12  | .17  |     |                                                        |  |
| 1  | .06  | .04  | .27  | .14  | .19  | .03  | .12  | .16  |     |                                                        |  |
| 2  | .06  | .04  | .27  | .14  | .19  | .03  | .12  | .16  |     |                                                        |  |
| 3  | .06  | .04  | .27  | .14  | .19  | .03  | .12  | .16  |     | <u>RANDOM</u><br><u>MATRIX</u>                         |  |
| 4  | .06  | .04  | .27  | .14  | .19  | .03  | .12  | .16  |     |                                                        |  |
| 5  | .06  | .04  | .27  | .14  | .19  | .03  | .12  | .16  |     |                                                        |  |
| 6  | .06  | .04  | .27  | .14  | .19  | .03  | .12  | .16  |     |                                                        |  |
| 7  | .06  | .04  | .27  | .14  | .19  | .03  | .12  | .16  |     |                                                        |  |
| SS | ---  | +.36 | +.07 | -.10 | -.10 | +.01 | -.07 | -.17 |     |                                                        |  |
| 1  | +.21 | +.03 | -.07 | -.07 | +.01 | -.03 | +.01 | -.09 |     |                                                        |  |
| 2  | +.06 | -.01 | +.09 | -.04 | -.05 | +.02 | -.02 | -.06 |     |                                                        |  |
| 3  | -.06 | -.02 | +.06 | -.03 | +.05 | -.01 | +.04 | -.05 |     | <u>DIFERENCE</u><br><u>MATRIX</u>                      |  |
| 4  | -.04 | -.04 | -.12 | +.10 | +.13 | -.01 | -.04 | +.02 |     |                                                        |  |
| 5  | -.06 | -.04 | -.02 | +.24 | -.19 | +.22 | -.12 | -.03 |     |                                                        |  |
| 6  | -.01 | -.04 | +.11 | -.06 | -.01 | -.03 | +.06 | -.01 |     |                                                        |  |
| 7  | +.01 | -.04 | -.14 | +.03 | -.06 | +.01 | +.03 | +.15 |     |                                                        |  |

## FACIES STABILITIES FOR DIFFERENT SEDIMENTATION HORIZONS

| Horizon | Facies | $\bar{x}$ | $s^2$ | s   | $\bar{x} \pm 2s$ |
|---------|--------|-----------|-------|-----|------------------|
| 1       | 1-7    | .30       | .02   | .15 | (.01, .59)       |
| 2       | 1-7    | .14       | .03   | .18 | (-.23, .51)      |
| 3       | 1-7    | .27       | .03   | .18 | (-.08, .62)      |
| 4       | 1-7    | .24       | .01   | .12 | (0, .48)         |
| 5       | 1-7    | .19       | .04   | .19 | (-.18, .56)      |
| 6       | 1-7    | .23       | .01   | .12 | (-.01, .47)      |

## STABILITIES OF DIFFERENT FACIES

| Horizon | Facies | $\bar{x}$ | $s^2$ | s   | $\bar{x} \pm 2s$ |
|---------|--------|-----------|-------|-----|------------------|
| 1-6     | 1      | .12       | .02   | .15 | (-.18, .42)      |
| 1-6     | 2      | .31       | .01   | .09 | (.13, .49)       |
| 1-6     | 3      | .21       | .02   | .13 | (-.05, .47)      |
| 1-6     | 4      | .25       | .02   | .13 | (-.01, .51)      |
| 1-6     | 5      | .16       | .04   | .19 | (-.22, .54)      |
| 1-6     | 6      | .25       | .02   | .14 | (-.04, .54)      |
| 1-6     | 7      | .30       | .04   | .20 | (-.10, .70)      |

In the following two-factor ANOVA, one assumes that the distribution is normal and the variances are equal (homoscedasticity).

The confidence bands of the mean facies stability ( $\bar{x} \pm 2s$ ) listed above suggest that there is little variability in the facies stability values. Similarly, the variances are all about the same. This suggests that the assumption of homoscedasticity is probably valid.

There is not enough data to test the assumption of normality.



## TWO-FACTOR ANOVA: FACIES STABILITY

| Facies<br>Horizon | 1   | 2   | 3   | 4   | 5   | 6   | 7   | Horizon<br>Mean |
|-------------------|-----|-----|-----|-----|-----|-----|-----|-----------------|
| 1                 | 0   | .36 | .31 | .32 | .30 | .35 | .46 | .30             |
| 2                 | .35 | .35 | .26 | 0   | 0   | 0   | 0   | .14             |
| 3                 | 0   | .13 | .23 | .27 | .41 | .31 | .54 | .27             |
| 4                 | .27 | .28 | .35 | .28 | 0   | .30 | .17 | .24             |
| 5                 | 0   | .36 | 0   | .29 | 0   | .38 | .29 | .19             |
| 6                 | .07 | .36 | .11 | .32 | .25 | .18 | .31 | .23             |
| Facies<br>Mean    | .12 | .31 | .21 | .25 | .16 | .25 | .30 | .23             |

| Source of<br>Variation | Sum of<br>Squares | df | Mean<br>Square | F-ratio |
|------------------------|-------------------|----|----------------|---------|
| Between<br>Horizons    | .0978             | 5  | .0196          | .8978   |
| Between<br>Facies      | .2065             | 6  | .0344          | 1.5758  |
| Unexplained            | .6549             | 30 | .0218          |         |
| Total                  | .9592             | 41 |                |         |

## Results:

- 1) Test for differences between horizons: F-ratio = 0.90 (df = 5/30);  
 $F_{.05}$  critical = 2.53. The computed F-ratio does not exceed the  $F_{.05}$  value. The null hypothesis (facies stability is similar in different horizons) is accepted at the 5% significance level. The Prob Value (p) > 0.25, which suggests that there is no evidence from this sample that the null hypothesis is false.
- 2) Test for differences between facies: F-ratio = 1.58 (df = 6/30);  
 $F_{.05}$  = 2.42. The computed F-ratio does not exceed  $F_{.05}$  value. Hence, the null hypothesis (facies stability is similar in different facies) is acceptable at the 5% significance level. The prob value (p):  $0.25 > p > 0.10$ , which suggests that there is no evidence from this sample that the null hypothesis is false.

## Part 4

Detailed Analyses:

Sequences of Facies and Clustering of Facies  
Embedded Markov Chain and Substitutability Analyses

Computational Techniques for Embedded Markov Chain Analysis (Miall, 1973)

Computational Techniques for Substitutability and Cluster Analysis  
(Davis, 1973)

Chi-squared Test for Markov Property (Gingerich, 1969)

Techniques and conventions used are the same as in the preliminary  
analysis, Part 1, Appendix 9.

Fig.121 - Facies relations in major sedimentation units: embedded

Markov chain analysis.

Dotted arrows = difference matrix scores = .05-.10

Dashed arrows = difference matrix scores = .11-.30

Solid arrows = difference matrix scores  $>$ .30.

1, 2, ... 7 = Facies 1 through 7.

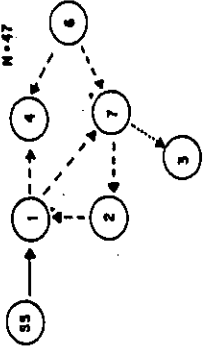
Sh = Shale Facies

SS = Scoured surfaces

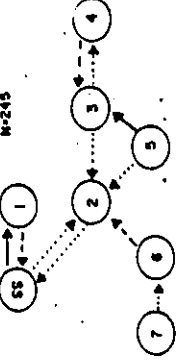
S1 - S11 are sections on location map Fig.10 in text.



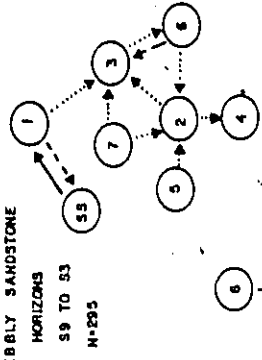
RIVIERE TROIS PISTOLES SECTION S10  
M-47



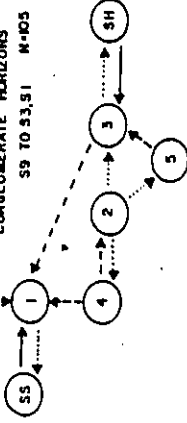
GREVE DE LA POINTE SECTION S11  
M-245



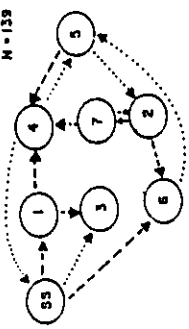
PEBBLY SANDSTONE  
HORIZONS  
S9 TO S3  
M-295



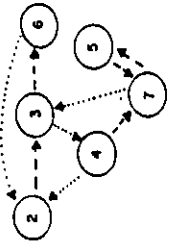
CONGLOMERATE HORIZONS  
S9 TO S3, S1  
M-405



SANDSTONE HORIZONS S9 TO S7, S5 & S1  
M-139



BIC (S1) III M-77



TEST FOR MARKOV PROPERTY OF WHOLE OBSERVED TRANSITION MATRIX: EMBEDDED MARKOV CHAINS

| Maj. Sed. Horizon | Calculated $\chi^2$ | d.f. | $\chi^2$ | P Value        | Decision     | no. obs. | Off-diag. 0 entries |
|-------------------|---------------------|------|----------|----------------|--------------|----------|---------------------|
| 1                 | 56.7                | 63   | 82.5     | .7 > p > .6    | Accept $H_0$ | 139      | 21%                 |
| 2                 | 40.25               | 48   | 65.2     | .8 > p > .7    | Accept $H_0$ | 105      | 23%                 |
| 3                 | 27.8                | 24   | 36.4     | .3 > p > .2    | Accept $H_0$ | 77       | 6%                  |
| 4                 | 75.17               | 55   | 73.3     | .05 > p > .025 | Reject $H_0$ | 295      | 5%                  |
| 5                 | 37.14               | 48   | 65.2     | .9 > p > .8    | Accept $H_0$ | 47       | 57%                 |
| 6                 | 113.90              | 48   | 65.2     | p < .0005      | Reject $H_0$ | 245      | 4%                  |

$H_0$ : No difference between the independent trials (random) probability matrix and the observed transition probability matrix

$H_1$ : There is a significant difference between the independent trials (random) probability matrix and the observed transition probability matrix

.95  $\chi^2$ : limiting value at the 95% confidence level

$\nu$  d.f.: number of possible entries in the tally matrix - the rank of the matrix

$$\chi^2 = \sum_{i=1}^n \sum_{j=1}^n \left\{ \frac{(f_{ij} - s_i r_{ij})^2}{s_i r_{ij}} \right\}$$

## MAJOR GROUPS OF FACIES FOR DIFFERENT SEDIMENTATION HORIZONS

### Results of Cluster Analysis

#### 1. Sandstone Horizons

Underlying substitutability dendrogram: (Sh,7) (4,3) (5,SS)  
 Overlying substitutability dendrogram: (7,6,Sh) (5,2,SS)  
 Mutual substitutability dendrogram: (Sh,7) (4,3) (2,SS)

#### 2. Conglomerate Horizons

Underlying substitutability dendrogram: (2,5,Sh) (6,4,3,SS)  
 Overlying substitutability dendrogram: (2,6,SS) (4,3,5)  
 Mutual substitutability dendrogram: (2,6,SS) (3,4)

#### 3. Bic Member III Section

Underlying substitutability dendrogram: (3,4) (2,6,7)  
 Overlying substitutability dendrogram: (2,7) (6,4) (3,5)  
 Mutual substitutability dendrogram: (2,7) (4,6)

#### 4. Pebbly Sandstone Horizons

Underlying substitutability dendrogram: (2,6) (5,7) (3,4)  
 Overlying substitutability dendrogram: (4,5,6,7)  
 Mutual substitutability dendrogram: (4,5,6,7)

#### 5. Rivière Trois Pistoles Section

Underlying substitutability dendrogram: (2,6) (4,5,7)  
 Overlying substitutability dendrogram: (2,3,6) (4,7)  
 Mutual substitutability dendrogram: (4,7) (1,6)

#### 6. Grève de la Pointe Section

Underlying substitutability dendrogram: (4,6,SS) (3,7)  
 Overlying substitutability dendrogram: (3,7) (4,6) (5,SS)  
 Mutual substitutability dendrogram: (4,5,6) (3,7)

Note: The major groups of facies were selected as being the three highest clusters on the dendrogram. If clusters are completely nested about one central facies, then the three highest clusters (with the highest probabilities) were selected. All clusters with a mutual substitutability greater than 0.8 were counted as being major groups of facies for further Markov analysis. If the mutual substitutabilities were less than 0.5, then the clusters were not used in the Markov analysis and were not considered to be facies groups.

Fig.122- Dendrograms constructed by weight pair-group method using arithmetic averages of correlation coefficients).

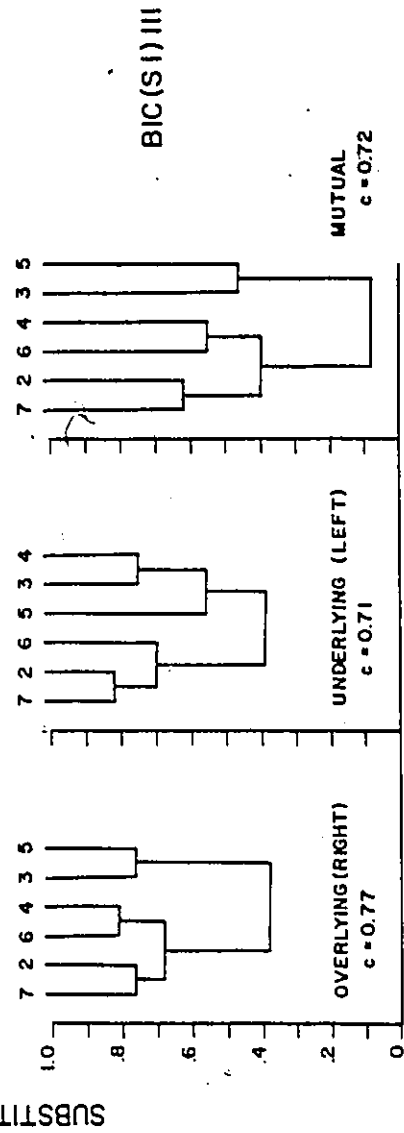
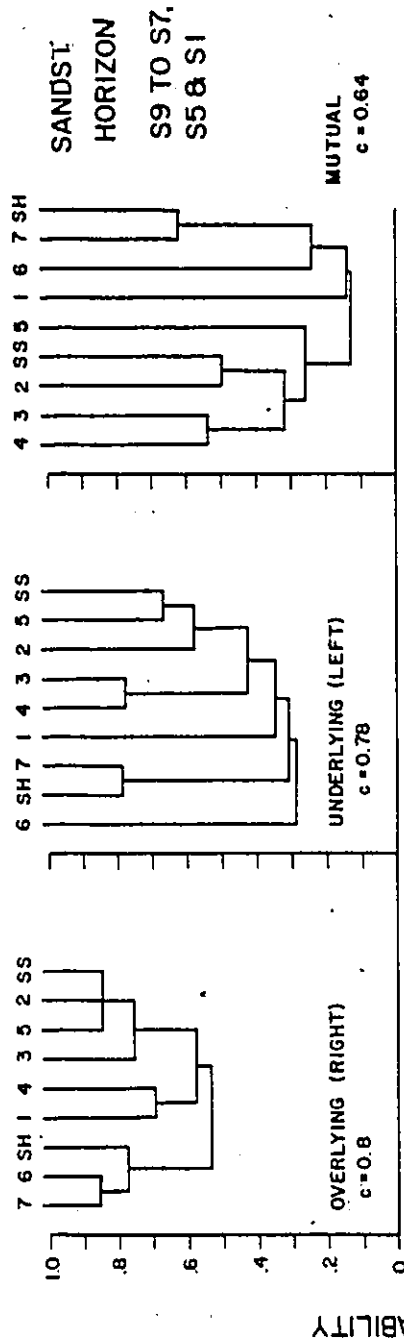
C : Cophenetic correlation coefficients.

S1 - S11: Sections on location map Fig.10 in text.

1, 2, ...7 = Facies 1 through 7

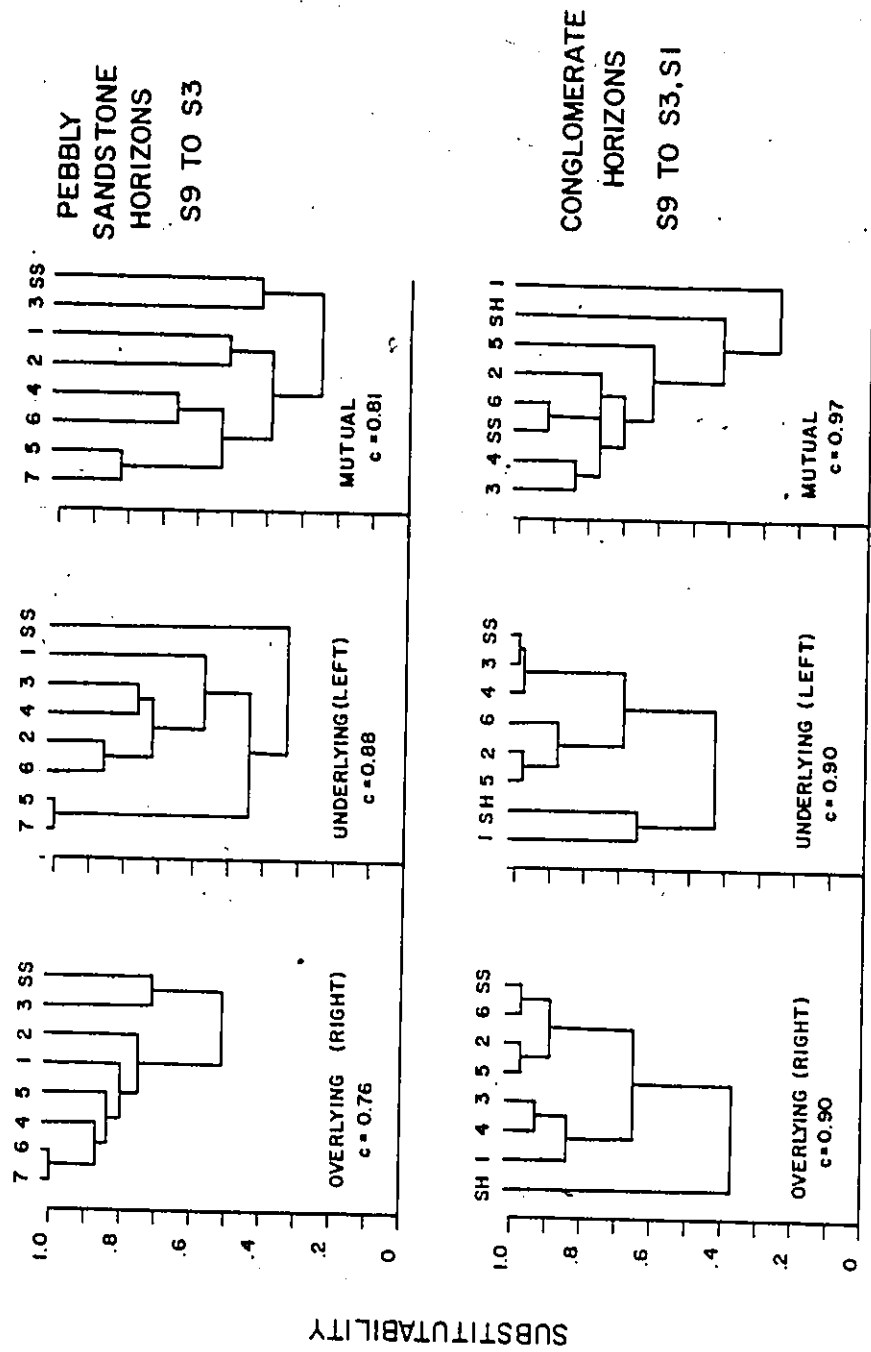
Sh = Shale Facies

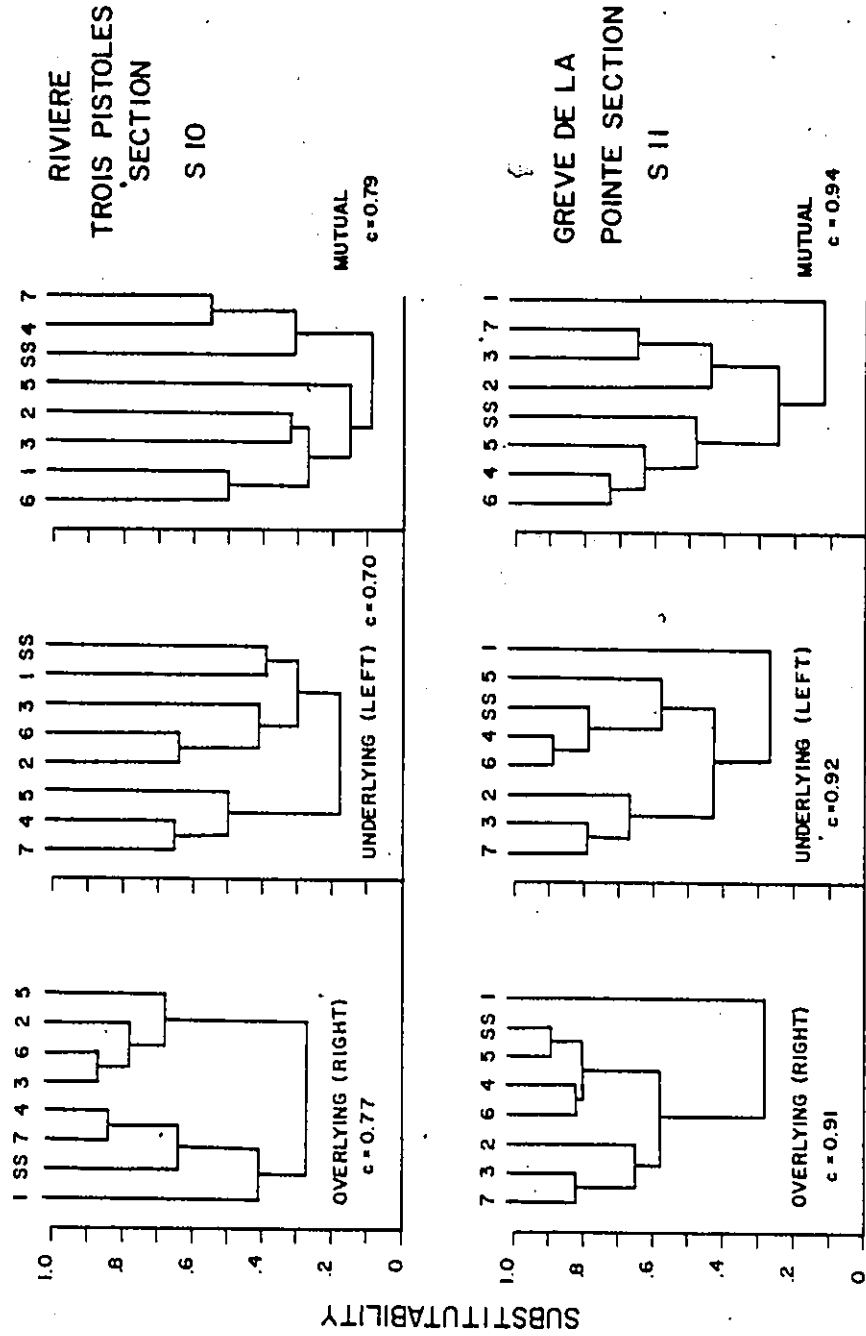
SS = Scoured surfaces.



FACIES







1. SANDSTONE HORIZONS

|     | SS   | 1    | 2    | 3    | 4    | 5    | 6    | 7    | Sh   | Sum                                                                       |                                |
|-----|------|------|------|------|------|------|------|------|------|---------------------------------------------------------------------------|--------------------------------|
| SS  | --   | 2    | 2    | 2    | 3    | 0    | 2    | 0    | 0    | 11                                                                        | <u>TALLY</u><br><u>MATRIX</u>  |
| 1   | 0    | --   | 0    | 2    | 3    | 0    | 0    | 0    | 0    | 5                                                                         |                                |
| 2   | 2    | 1    | --   | 4    | 3    | 0    | 9    | 5    | 1    | 25                                                                        |                                |
| 3   | 3    | 1    | 3    | --   | 4    | 0    | 6    | 1    | 0    | 18                                                                        |                                |
| 4   | 5    | 0    | 7    | 4    | --   | 3    | 4    | 3    | 0    | 26                                                                        |                                |
| 5   | 0    | 0    | 2    | 0    | 3    | --   | 1    | 1    | 0    | 7                                                                         |                                |
| 6   | 3    | 1    | 8    | 4    | 8    | 5    | --   | 2    | 0    | 31                                                                        |                                |
| 7   | 0    | 0    | 5    | 2    | 5    | 0    | 3    | --   | 0    | 15                                                                        |                                |
| Sh  | 0    | 0    | 0    | 0    | 0    | 0    | 1    | 0    | --   | 1                                                                         |                                |
| Sum | 13   | 5    | 27   | 18   | 29   | 8    | 26   | 12   | 1    | 139                                                                       |                                |
| SS  | ---  | .18  | .18  | .18  | .27  | 0    | .18  | 0    | 0    | <u>UPWARD</u><br><u>TRANSITION</u><br><u>PROBABILITY</u><br><u>MATRIX</u> |                                |
| 1   | 0    | ---  | 0    | .40  | .60  | 0    | 0    | 0    | 0    |                                                                           |                                |
| 2   | .08  | .04  | ---  | .16  | .12  | 0    | .36  | .20  | .04  |                                                                           |                                |
| 3   | .17  | .06  | .17  | ---  | .22  | 0    | .33  | .06  | 0    |                                                                           |                                |
| 4   | .19  | 0    | .27  | .15  | ---  | .12  | .15  | .12  | 0    |                                                                           |                                |
| 5   | 0    | 0    | .29  | 0    | .43  | ---  | .14  | .14  | 0    |                                                                           |                                |
| 6   | .10  | .03  | .26  | .13  | .26  | .16  | ---  | .06  | 0    |                                                                           |                                |
| 7   | 0    | 0    | .33  | .13  | .33  | 0    | .20  | ---  | 0    |                                                                           |                                |
| Sh  | 0    | 0    | 0    | 0    | 0    | 0    | 1.0  | 0    | ---  |                                                                           |                                |
| SS  | ---  | .04  | .21  | .14  | .23  | .06  | .20  | .09  | .01  |                                                                           | <u>RANDOM</u><br><u>MATRIX</u> |
| 1   | .10  | ---  | .20  | .13  | .22  | .06  | .19  | .09  | .01  |                                                                           |                                |
| 2   | .11  | .04  | ---  | .16  | .25  | .07  | .23  | .11  | .01  |                                                                           |                                |
| 3   | .11  | .04  | .22  | ---  | .24  | .07  | .21  | .10  | .01  |                                                                           |                                |
| 4   | .12  | .04  | .24  | .16  | ---  | .07  | .23  | .11  | .01  |                                                                           |                                |
| 5   | .10  | .04  | .20  | .14  | .22  | ---  | .20  | .09  | .01  |                                                                           |                                |
| 6   | .12  | .05  | .25  | .17  | .27  | .07  | ---  | .11  | .01  |                                                                           |                                |
| 7   | .10  | .04  | .22  | .15  | .23  | .06  | .21  | ---  | .01  |                                                                           |                                |
| Sh  | .09  | .04  | .20  | .13  | .21  | .06  | .19  | .09  | ---  |                                                                           |                                |
| SS  | ---- | +.14 | -.03 | +.04 | +.04 | -.06 | -.02 | -.09 | -.01 | <u>DIFFERENCE</u><br><u>MATRIX</u>                                        |                                |
| 1   | -.10 | ---- | -.20 | +.27 | +.38 | -.06 | -.19 | -.09 | -.01 |                                                                           |                                |
| 2   | -.03 | 0    | ---- | 0    | -.13 | -.07 | +.13 | +.09 | +.03 |                                                                           |                                |
| 3   | +.06 | +.02 | -.05 | ---- | -.02 | -.07 | +.12 | -.04 | -.01 |                                                                           |                                |
| 4   | +.07 | -.04 | +.03 | -.01 | ---- | +.05 | -.08 | +.01 | -.01 |                                                                           |                                |
| 5   | -.10 | -.04 | +.09 | -.14 | +.21 | ---- | -.06 | +.05 | -.01 |                                                                           |                                |
| 6   | -.02 | -.02 | +.01 | -.04 | -.01 | +.09 | ---- | -.05 | -.01 |                                                                           |                                |
| 7   | -.10 | -.04 | +.11 | -.02 | +.10 | -.06 | -.01 | ---- | -.01 |                                                                           |                                |
| Sh  | -.09 | -.04 | -.20 | -.13 | -.21 | -.06 | +.81 | -.09 | ---- |                                                                           |                                |

1. SANDSTONE HORIZONS

|    | SS  | 1   | 2   | 3   | 4   | 5   | 6   | 7   | Sh  |                                                              |
|----|-----|-----|-----|-----|-----|-----|-----|-----|-----|--------------------------------------------------------------|
| SS | 1.0 | .33 | .59 | .31 | .29 | .67 | .34 | .71 | .22 | <u>UNDERLYING<br/>(LEFT)<br/>SUBSTITUTABILITY<br/>MATRIX</u> |
| 1  | .33 | 1.0 | .40 | .38 | .38 | .13 | .26 | .35 | .22 |                                                              |
| 2  | .59 | .40 | 1.0 | .42 | .68 | .56 | .33 | .57 | 0   |                                                              |
| 3  | .31 | .38 | .42 | 1.0 | .78 | .38 | .23 | .40 | .42 |                                                              |
| 4  | .29 | .38 | .68 | .78 | 1.0 | .22 | .27 | .42 | .12 |                                                              |
| 5  | .67 | .13 | .56 | .38 | .22 | 1.0 | .09 | .35 | 0   |                                                              |
| 6  | .34 | .26 | .33 | .23 | .27 | .09 | 1.0 | .40 | .19 |                                                              |
| 7  | .71 | .35 | .57 | .40 | .42 | .35 | .40 | 1.0 | .79 |                                                              |
| Sh | .22 | .22 | 0   | .42 | .12 | 0   | .19 | .79 | 1.0 |                                                              |
| SS | --- | .40 | .07 | .11 | .10 | 0   | .08 | 0   | 0   | <u>DOWNWARD<br/>TRANSITION<br/>PROBABILITY<br/>MATRIX</u>    |
| 1  | 0   | --- | 0   | .11 | .10 | 0   | 0   | 0   | 0   |                                                              |
| 2  | .15 | .20 | --- | .22 | .10 | 0   | .35 | .42 | 1.0 |                                                              |
| 3  | .23 | .20 | .11 | --- | .14 | 0   | .23 | .08 | 0   |                                                              |
| 4  | .38 | 0   | .26 | .22 | --- | .38 | .15 | .25 | 0   |                                                              |
| 5  | 0   | 0   | .07 | 0   | .10 | --- | .04 | .08 | 0   |                                                              |
| 6  | .23 | .20 | .30 | .22 | .28 | .63 | --- | .17 | 0   |                                                              |
| 7  | 0   | 0   | .19 | .11 | .17 | 0   | .12 | --- | 0   |                                                              |
| Sh | 0   | 0   | 0   | 0   | 0   | 0   | .04 | 0   | --- |                                                              |
| SS | 1.0 | .48 | .84 | .74 | .52 | .75 | .68 | .80 | .29 | <u>OVERLYING<br/>(RIGHT)<br/>SUBSTITUTABILITY<br/>MATRIX</u> |
| 1  | .48 | 1.0 | .44 | .53 | .69 | .33 | .62 | .46 | .38 |                                                              |
| 2  | .84 | .44 | 1.0 | .80 | .78 | .84 | .47 | .55 | 0   |                                                              |
| 3  | .74 | .53 | .80 | 1.0 | .69 | .71 | .67 | .83 | .52 |                                                              |
| 4  | .52 | .69 | .78 | .69 | 1.0 | .59 | .53 | .50 | .24 |                                                              |
| 5  | .75 | .33 | .84 | .71 | .59 | 1.0 | .18 | .53 | 0   |                                                              |
| 6  | .68 | .62 | .47 | .67 | .53 | .18 | 1.0 | .85 | .76 |                                                              |
| 7  | .80 | .46 | .55 | .83 | .50 | .53 | .85 | 1.0 | .78 |                                                              |
| Sh | .29 | .38 | 0   | .52 | .24 | 0   | .76 | .78 | 1.0 |                                                              |
| SS | 1.0 | .16 | .50 | .23 | .15 | .50 | .23 | .57 | .06 | <u>MUTUAL<br/>SUBSTITUTABILITY<br/>MATRIX</u>                |
| 1  | .16 | 1.0 | .18 | .20 | .26 | .04 | .16 | .16 | .08 |                                                              |
| 2  | .50 | .18 | 1.0 | .34 | .53 | .47 | .16 | .31 | 0   |                                                              |
| 3  | .23 | .20 | .34 | 1.0 | .54 | .27 | .15 | .33 | .22 |                                                              |
| 4  | .15 | .26 | .53 | .54 | 1.0 | .13 | .14 | .21 | .03 |                                                              |
| 5  | .50 | .04 | .47 | .27 | .13 | 1.0 | .02 | .19 | 0   |                                                              |
| 6  | .23 | .16 | .16 | .15 | .14 | .02 | 1.0 | .34 | .14 |                                                              |
| 7  | .57 | .16 | .31 | .33 | .21 | .19 | .34 | 1.0 | .62 |                                                              |
| Sh | .06 | .08 | 0   | .22 | .03 | 0   | .14 | .62 | 1.0 |                                                              |

1. SANDSTONE HORIZONS

Cophenetic Correlations Based Upon Dendrograms

|    | SS  | 1   | 2   | 3   | 4   | 5   | 6   | 7   | Sh  |                                                                                                    |
|----|-----|-----|-----|-----|-----|-----|-----|-----|-----|----------------------------------------------------------------------------------------------------|
| SS | 1.0 | .57 | .84 | .75 | .57 | .84 | .53 | .53 | .53 | <u>OVERLYING</u><br><u>(RIGHT)</u><br><u>SUBSTITUTABILITY</u><br><u>DENDROGRAM</u><br><br>c = 0.80 |
| 1  | .57 | 1.0 | .57 | .57 | .69 | .57 | .53 | .53 | .53 |                                                                                                    |
| 2  | .84 | .57 | 1.0 | .75 | .57 | .84 | .53 | .53 | .53 |                                                                                                    |
| 3  | .75 | .57 | .75 | 1.0 | .57 | .75 | .53 | .53 | .53 |                                                                                                    |
| 4  | .57 | .69 | .57 | .57 | 1.0 | .57 | .53 | .53 | .53 |                                                                                                    |
| 5  | .84 | .57 | .84 | .75 | .57 | 1.0 | .53 | .53 | .53 |                                                                                                    |
| 6  | .53 | .53 | .53 | .53 | .53 | .53 | 1.0 | .85 | .77 |                                                                                                    |
| 7  | .53 | .53 | .53 | .53 | .53 | .53 | .85 | 1.0 | .77 |                                                                                                    |
| Sh | .53 | .53 | .53 | .53 | .53 | .53 | .77 | .77 | 1.0 |                                                                                                    |
| SS | 1.0 | .35 | .58 | .43 | .43 | .67 | .29 | .31 | .31 |                                                                                                    |
| 1  | .35 | 1.0 | .35 | .35 | .35 | .35 | .29 | .31 | .31 |                                                                                                    |
| 2  | .58 | .35 | 1.0 | .43 | .43 | .58 | .29 | .31 | .31 |                                                                                                    |
| 3  | .43 | .35 | .43 | 1.0 | .78 | .43 | .29 | .31 | .31 |                                                                                                    |
| 4  | .43 | .35 | .43 | .78 | 1.0 | .43 | .29 | .31 | .31 |                                                                                                    |
| 5  | .67 | .35 | .58 | .43 | .43 | 1.0 | .29 | .31 | .31 |                                                                                                    |
| 6  | .29 | .29 | .29 | .29 | .29 | .29 | 1.0 | .29 | .29 |                                                                                                    |
| 7  | .31 | .31 | .31 | .31 | .31 | .31 | .29 | 1.0 | .79 |                                                                                                    |
| Sh | .31 | .31 | .31 | .31 | .31 | .31 | .29 | .79 | 1.0 |                                                                                                    |
| SS | 1.0 | .13 | .50 | .32 | .32 | .26 | .13 | .13 | .13 | <u>MUTUAL</u><br><u>SUBSTITUTABILITY</u><br><u>DENDROGRAM</u><br><br>c = 0.64                      |
| 1  | .13 | 1.0 | .13 | .13 | .13 | .13 | .14 | .14 | .14 |                                                                                                    |
| 2  | .50 | .13 | 1.0 | .32 | .32 | .26 | .13 | .13 | .13 |                                                                                                    |
| 3  | .32 | .13 | .32 | 1.0 | .54 | .26 | .13 | .13 | .13 |                                                                                                    |
| 4  | .32 | .13 | .32 | .54 | 1.0 | .26 | .13 | .13 | .13 |                                                                                                    |
| 5  | .26 | .13 | .26 | .26 | .26 | 1.0 | .13 | .13 | .13 |                                                                                                    |
| 6  | .13 | .14 | .13 | .13 | .13 | .13 | 1.0 | .24 | .24 |                                                                                                    |
| 7  | .13 | .14 | .13 | .13 | .13 | .13 | .24 | 1.0 | .62 |                                                                                                    |
| Sh | .13 | .14 | .13 | .13 | .13 | .13 | .24 | .62 | 1.0 |                                                                                                    |

## EMBEDDED MARKOV CHAIN AND SUBSTITUTABILITY ANALYSES

## 2. CONGLOMERATE HORIZONS

|     | SS   | 1    | 2    | 3    | 4    | 5    | 6    | Sh   | Sum |                                                                           |
|-----|------|------|------|------|------|------|------|------|-----|---------------------------------------------------------------------------|
| SS  | --   | 10   | 1    | 0    | 0    | 1    | 0    | 0    | 12  |                                                                           |
| 1   | 10   | --   | 11   | 9    | 3    | 2    | 4    | 1    | 40  |                                                                           |
| 2   | 0    | 5    | --   | 4    | 2    | 2    | 0    | 0    | 13  | <u>TALLY</u><br><u>MATRIX</u>                                             |
| 3   | 1    | 13   | 2    | --   | 0    | 1    | 1    | 2    | 20  |                                                                           |
| 4   | 0    | 3    | 2    | 1    | --   | 0    | 0    | 0    | 6   |                                                                           |
| 5   | 0    | 2    | 1    | 2    | 1    | --   | 0    | 0    | 6   |                                                                           |
| 6   | 0    | 3    | 1    | 1    | 0    | 0    | --   | 0    | 5   |                                                                           |
| Sh  | 0    | 1    | 0    | 2    | 0    | 0    | 0    | --   | 3   |                                                                           |
| Sum | 11   | 37   | 18   | 19   | 6    | 6    | 5    | 3    | 105 |                                                                           |
| SS  | ---  | .83  | .08  | 0    | 0    | .08  | 0    | 0    |     | <u>UPWARD</u><br><u>TRANSITION</u><br><u>PROBABILITY</u><br><u>MATRIX</u> |
| 1   | .25  | ---  | .28  | .23  | .08  | .05  | .10  | .03  |     |                                                                           |
| 2   | 0    | .38  | ---  | .31  | .15  | .15  | 0    | 0    |     |                                                                           |
| 3   | .05  | .65  | .10  | ---  | 0    | .05  | .05  | .10  |     |                                                                           |
| 4   | 0    | .50  | .33  | .17  | ---  | 0    | 0    | 0    |     |                                                                           |
| 5   | 0    | .33  | .17  | .33  | .17  | ---  | 0    | 0    |     |                                                                           |
| 6   | 0    | .60  | .20  | .20  | 0    | 0    | ---  | 0    |     |                                                                           |
| Sh  | 0    | .33  | 0    | .66  | 0    | 0    | 0    | ---  |     |                                                                           |
| SS  | ---  | .40  | .19  | .20  | .06  | .06  | .05  | .03  |     | <u>RANDOM</u><br><u>MATRIX</u>                                            |
| 1   | .17  | ---  | .28  | .29  | .09  | .09  | .08  | .05  |     |                                                                           |
| 2   | .12  | .40  | ---  | .21  | .07  | .07  | .05  | .03  |     |                                                                           |
| 3   | .13  | .44  | .21  | ---  | .07  | .07  | .06  | .04  |     |                                                                           |
| 4   | .11  | .37  | .18  | .19  | ---  | .06  | .05  | .03  |     |                                                                           |
| 5   | .11  | .37  | .18  | .19  | .06  | ---  | .05  | .03  |     |                                                                           |
| 6   | .11  | .37  | .18  | .19  | .06  | .06  | ---  | .03  |     |                                                                           |
| Sh  | .11  | .36  | .18  | .19  | .06  | .06  | .05  | ---  |     |                                                                           |
| SS  | ---- | +.43 | -.11 | -.20 | -.06 | +.02 | -.05 | -.03 |     | <u>DIFFERENCE</u><br><u>MATRIX</u>                                        |
| 1   | +.08 | ---- | 0    | -.06 | -.01 | -.04 | +.02 | -.02 |     |                                                                           |
| 2   | -.12 | -.02 | ---- | +.10 | +.08 | +.08 | -.05 | -.03 |     |                                                                           |
| 3   | -.08 | +.21 | -.11 | ---- | -.07 | -.02 | -.01 | +.06 |     |                                                                           |
| 4   | -.11 | +.13 | +.15 | -.02 | ---- | -.06 | -.05 | -.03 |     |                                                                           |
| 5   | -.11 | -.04 | -.01 | +.14 | +.11 | ---- | -.05 | -.03 |     |                                                                           |
| 6   | -.11 | +.23 | +.02 | +.01 | -.06 | -.06 | ---- | -.03 |     |                                                                           |
| Sh  | -.11 | -.03 | -.18 | +.47 | -.06 | -.06 | -.05 | ---- |     |                                                                           |

## EMBEDDED MARKOV CHAIN AND SUBSTITUTABILITY ANALYSES

## 2. CONGLOMERATE HORIZONS

|    | SS   | 1    | 2   | 3   | 4   | 5   | 6   | Sh  |                                                              |
|----|------|------|-----|-----|-----|-----|-----|-----|--------------------------------------------------------------|
| SS | 1.0  | .05  | .74 | .97 | .86 | .63 | .93 | .43 | <u>UNDERLYING<br/>(LEFT)<br/>SUBSTITUTABILITY<br/>MATRIX</u> |
| 1  | .05  | 1.0  | .37 | .20 | .45 | .58 | .36 | .44 |                                                              |
| 2  | .74  | .37  | 1.0 | .73 | .73 | .93 | .83 | .84 |                                                              |
| 3  | .97  | .20  | .73 | 1.0 | .86 | .65 | .92 | .42 |                                                              |
| 4  | .86  | .45  | .73 | .86 | 1.0 | .88 | .97 | .60 |                                                              |
| 5  | .63  | .58  | .93 | .65 | .88 | 1.0 | .86 | .84 |                                                              |
| 6  | .93  | .36  | .83 | .92 | .97 | .86 | 1.0 | .67 |                                                              |
| Sh | .43  | .44  | .84 | .42 | .60 | .84 | .67 | 1.0 |                                                              |
| SS | ---  | .27  | .06 | 0   | 0   | .17 | 0   | 0   | <u>DOWNWARD<br/>TRANSITION<br/>PROBABILITY<br/>MATRIX</u>    |
| 1  | .91  | ---  | .61 | .47 | .50 | .33 | .80 | .33 |                                                              |
| 2  | 0    | .14  | --- | .21 | .33 | .33 | 0   | 0   |                                                              |
| 3  | .09  | .35  | .11 | --- | 0   | .17 | .20 | .66 |                                                              |
| 4  | 0    | .08  | .11 | .05 | --- | 0   | 0   | 0   |                                                              |
| 5  | 0    | .05  | .06 | .11 | .17 | --- | 0   | 0   |                                                              |
| 6  | 0    | .08  | .06 | .05 | 0   | 0   | --- | 0   |                                                              |
| Sh | 0    | .03  | 0   | .11 | 0   | 0   | 0   | --- |                                                              |
| SS | 1.0  | .07  | .98 | .87 | .80 | .81 | .99 | .53 | <u>OVERLYING<br/>(RIGHT)<br/>SUBSTITUTABILITY<br/>MATRIX</u> |
| 1  | .07  | 1.0  | .26 | .19 | .20 | .67 | .18 | .65 |                                                              |
| 2  | .98  | .26  | 1.0 | .91 | .81 | .73 | .98 | .58 |                                                              |
| 3  | .87  | .19  | .91 | 1.0 | .98 | .85 | .86 | .40 |                                                              |
| 4  | .80  | .20  | .81 | .98 | 1.0 | .90 | .78 | .37 |                                                              |
| 5  | .81  | .67  | .73 | .85 | .90 | 1.0 | .70 | .59 |                                                              |
| 6  | .99  | .18  | .98 | .86 | .78 | .70 | 1.0 | .64 |                                                              |
| Sh | .53  | .65  | .58 | .40 | .37 | .59 | .64 | 1.0 |                                                              |
| SS | 1.0  | .004 | .73 | .84 | .69 | .51 | .92 | .23 | <u>MUTUAL<br/>SUBSTITUTABILITY<br/>MATRIX</u>                |
| 1  | .004 | 1.0  | .10 | .04 | .09 | .39 | .06 | .29 |                                                              |
| 2  | .73  | .10  | 1.0 | .66 | .59 | .68 | .81 | .49 |                                                              |
| 3  | .84  | .04  | .66 | 1.0 | .84 | .55 | .79 | .17 |                                                              |
| 4  | .69  | .09  | .59 | .84 | 1.0 | .79 | .76 | .22 |                                                              |
| 5  | .51  | .39  | .68 | .55 | .79 | 1.0 | .60 | .50 |                                                              |
| 6  | .92  | .06  | .81 | .79 | .76 | .60 | 1.0 | .43 |                                                              |
| Sh | .23  | .29  | .49 | .17 | .22 | .50 | .43 | 1.0 |                                                              |

## EMBEDDED MARKOV CHAIN AND SUBSTITUTABILITY ANALYSES

## 2. CONGLOMERATE HORIZONS

## Cophenetic Correlations Based Upon Dendrograms

|    | SS  | 1   | 2   | 3   | 4   | 5   | 6   | Sh  |                                                                  |
|----|-----|-----|-----|-----|-----|-----|-----|-----|------------------------------------------------------------------|
| SS | 1.0 | .43 | .98 | .69 | .69 | .69 | .99 | .43 | <u>OVERLYING<br/>(RIGHT)<br/>SUBSTITUTABILITY<br/>DENDROGRAM</u> |
| 1  | .43 | 1.0 | .43 | .43 | .43 | .43 | .43 | .65 |                                                                  |
| 2  | .98 | .43 | 1.0 | .69 | .69 | .69 | .98 | .43 |                                                                  |
| 3  | .69 | .43 | .69 | 1.0 | .98 | .88 | .69 | .43 |                                                                  |
| 4  | .69 | .43 | .69 | .98 | 1.0 | .88 | .69 | .43 |                                                                  |
| 5  | .69 | .43 | .69 | .88 | .88 | 1.0 | .69 | .43 |                                                                  |
| 6  | .99 | .43 | .98 | .69 | .69 | .69 | 1.0 | .43 |                                                                  |
| Sh | .43 | .65 | .43 | .43 | .43 | .43 | .43 | 1.0 |                                                                  |
| SS | 1.0 | .37 | .65 | .97 | .89 | .65 | .89 | .65 | <u>UNDERLYING<br/>(LEFT)<br/>SUBSTITUTABILITY<br/>DENDROGRAM</u> |
| 1  | .37 | 1.0 | .37 | .37 | .37 | .37 | .37 | .37 |                                                                  |
| 2  | .65 | .37 | 1.0 | .65 | .65 | .93 | .65 | .84 |                                                                  |
| 3  | .97 | .37 | .65 | 1.0 | .89 | .65 | .89 | .65 |                                                                  |
| 4  | .89 | .37 | .65 | .89 | 1.0 | .65 | .97 | .65 |                                                                  |
| 5  | .65 | .37 | .93 | .65 | .65 | 1.0 | .65 | .84 |                                                                  |
| 6  | .89 | .37 | .65 | .89 | .97 | .65 | 1.0 | .65 |                                                                  |
| Sh | .65 | .37 | .84 | .65 | .65 | .84 | .65 | 1.0 |                                                                  |
| SS | 1.0 | .26 | .77 | .77 | .77 | .62 | .92 | .42 | <u>MUTUAL<br/>SUBSTITUTABILITY<br/>DENDROGRAM</u>                |
| 1  | .26 | 1.0 | .26 | .26 | .26 | .26 | .26 | .26 |                                                                  |
| 2  | .77 | .26 | 1.0 | .70 | .70 | .62 | .77 | .42 |                                                                  |
| 3  | .77 | .26 | .70 | 1.0 | .84 | .62 | .77 | .42 |                                                                  |
| 4  | .77 | .26 | .70 | .84 | 1.0 | .62 | .77 | .42 |                                                                  |
| 5  | .62 | .26 | .62 | .62 | .62 | 1.0 | .62 | .42 |                                                                  |
| 6  | .92 | .26 | .77 | .77 | .77 | .62 | 1.0 | .42 |                                                                  |
| Sh | .42 | .26 | .42 | .42 | .42 | .42 | .42 | 1.0 |                                                                  |



## - EMBEDDED MARKOV CHAIN AND SUBSTITUTABILITY ANALYSES

## 3. BIC MEMBER III

|     | 2    | 3    | 4    | 5    | 6    | 7    | Sum                      |               |
|-----|------|------|------|------|------|------|--------------------------|---------------|
| 2   | --   | 6    | 2    | 0    | 2    | 3    | 13                       |               |
| 3   | 4    | --   | 3    | 0    | 6    | 4    | 17                       |               |
| 4   | 2    | 0    | --   | 1    | 1    | 4    | 8                        | <u>TALLY</u>  |
| 5   | 1    | 2    | 0    | --   | 2    | 5    | 10                       | <u>MATRIX</u> |
| 6   | 3    | 2    | 1    | 2    | --   | 3    | 11                       |               |
| 7   | 2    | 7    | 2    | 7    | 0    | --   | 18                       |               |
| Sum | 12   | 17   | 8    | 10   | 11   | 19   | 77                       |               |
| 2   | ---  | .46  | .15  | 0    | .15  | .23  |                          |               |
| 3   | .24  | ---  | .18  | 0    | .35  | .24  |                          |               |
| 4   | .25  | 0    | ---  | .13  | .13  | .50  | <u>UPWARD TRANSITION</u> |               |
| 5   | .10  | .20  | 0    | ---  | .20  | .50  | <u>PROBABILITY</u>       |               |
| 6   | .27  | .18  | .09  | .18  | ---  | .27  | <u>MATRIX</u>            |               |
| 7   | .11  | .39  | .11  | .39  | 0    | ---  |                          |               |
| 2   | ---  | .27  | .13  | .16  | .17  | .30  |                          |               |
| 3   | .20  | ---  | .13  | .17  | .18  | .32  |                          |               |
| 4   | .17  | .25  | ---  | .14  | .16  | .28  | <u>RANDOM MATRIX</u>     |               |
| 5   | .18  | .25  | .12  | ---  | .16  | .28  |                          |               |
| 6   | .18  | .26  | .12  | .15  | ---  | .29  |                          |               |
| 7   | .20  | .29  | .14  | .17  | .19  | ---  |                          |               |
| 2   | ---- | +.19 | +.02 | -.16 | -.02 | -.07 |                          |               |
| 3   | +.04 | ---- | +.05 | -.17 | +.17 | -.08 | <u>DIFFERENCE</u>        |               |
| 4   | +.08 | -.25 | ---- | -.01 | -.03 | +.22 | <u>MATRIX</u>            |               |
| 5   | -.08 | -.05 | -.12 | ---- | +.04 | +.22 |                          |               |
| 6   | +.09 | -.08 | -.03 | +.03 | ---- | -.02 |                          |               |
| 7   | -.09 | +.10 | -.03 | +.22 | -.19 | ---- |                          |               |

## EMBEDDED MARKOV CHAIN AND SUBSTITUTABILITY ANALYSES

## 3. BIC MEMBER III

|   | 2              | 3              | 4              | 5              | 6              | 7              |                                                                      |
|---|----------------|----------------|----------------|----------------|----------------|----------------|----------------------------------------------------------------------|
| 2 | <del>1.0</del> | .37            | .58            | .59            | .63            | .82            | <u>UNDERLYING (LEFT)</u><br><u>SUBSTITUTABILITY</u><br><u>MATRIX</u> |
| 3 | .37            | <del>1.0</del> | .75            | .61            | .38            | .48            |                                                                      |
| 4 | .58            | .75            | <del>1.0</del> | .51            | .68            | .37            |                                                                      |
| 5 | .59            | .61            | .51            | <del>1.0</del> | .10            | .33            |                                                                      |
| 6 | .63            | .38            | .68            | .10            | <del>1.0</del> | .76            |                                                                      |
| 7 | .82            | .48            | .37            | .33            | .76            | <del>1.0</del> |                                                                      |
| 2 | ---            | .35            | .25            | 0              | .18            | .16            |                                                                      |
| 3 | .33            | ---            | .38            | 0              | .55            | .21            |                                                                      |
| 4 | .17            | 0              | ---            | .10            | .09            | .21            |                                                                      |
| 5 | .08            | .12            | 0              | ---            | .18            | .26            |                                                                      |
| 6 | .25            | .12            | .13            | .20            | ---            | .16            |                                                                      |
| 7 | .17            | .41            | .25            | .70            | 0              | ---            |                                                                      |
| 2 | <del>1.0</del> | .40            | .77            | .53            | .70            | .76            | <u>OVERLYING (RIGHT)</u><br><u>SUBSTITUTABILITY</u><br><u>MATRIX</u> |
| 3 | .40            | <del>1.0</del> | .71            | .76            | .24            | .43            |                                                                      |
| 4 | .77            | .71            | <del>1.0</del> | .54            | .81            | .58            |                                                                      |
| 5 | .53            | .76            | .54            | <del>1.0</del> | .02            | .15            |                                                                      |
| 6 | .70            | .24            | .81            | .02            | <del>1.0</del> | .65            |                                                                      |
| 7 | .76            | .43            | .58            | .15            | .65            | <del>1.0</del> |                                                                      |
| 2 | <del>1.0</del> | .15            | .45            | .31            | .44            | .62            |                                                                      |
| 3 | .15            | <del>1.0</del> | .53            | .46            | .09            | .21            |                                                                      |
| 4 | .45            | .53            | <del>1.0</del> | .28            | .55            | .21            |                                                                      |
| 5 | .31            | .46            | .28            | <del>1.0</del> | .002           | .05            |                                                                      |
| 6 | .44            | .09            | .55            | .002           | <del>1.0</del> | .49            |                                                                      |
| 7 | .62            | .21            | .21            | .05            | .49            | <del>1.0</del> |                                                                      |

## EMBEDDED MARKOV CHAIN AND SUBSTITUTABILITY ANALYSES

## 3. BIC MEMBER III

## Cophenetic Correlations Based Upon Dendrograms

|   | 2   | 3   | 4   | 5   | 6   | 7   |                          |
|---|-----|-----|-----|-----|-----|-----|--------------------------|
| 2 | 1.0 | .38 | .68 | .38 | .68 | .76 |                          |
| 3 | .38 | 1.0 | .38 | .76 | .38 | .38 | <u>OVERLYING (RIGHT)</u> |
| 4 | .68 | .38 | 1.0 | .38 | .81 | .68 | <u>SUBSTITUTABILITY</u>  |
| 5 | .38 | .76 | .38 | 1.0 | .38 | .38 | <u>DENDROGRAM</u>        |
| 6 | .68 | .38 | .81 | .38 | 1.0 | .68 |                          |
| 7 | .76 | .38 | .68 | .38 | .68 | 1.0 | c = 0.77                 |
| 2 | 1.0 | .39 | .39 | .39 | .70 | .82 |                          |
| 3 | .39 | 1.0 | .75 | .56 | .39 | .39 | <u>UNDERLYING (LEFT)</u> |
| 4 | .39 | .75 | 1.0 | .56 | .39 | .39 | <u>SUBSTITUTABILITY</u>  |
| 5 | .39 | .56 | .56 | 1.0 | .39 | .39 | <u>DENDROGRAM</u>        |
| 6 | .70 | .39 | .39 | .39 | 1.0 | .70 |                          |
| 7 | .82 | .39 | .39 | .39 | .70 | 1.0 | c = 0.71                 |
| 2 | 1.0 | .08 | .40 | .08 | .40 | .62 |                          |
| 3 | .08 | 1.0 | .08 | .46 | .08 | .08 | <u>MUTUAL</u>            |
| 4 | .40 | .08 | 1.0 | .08 | .55 | .40 | <u>SUBSTITUTABILITY</u>  |
| 5 | .08 | .46 | .08 | 1.0 | .08 | .08 | <u>DENDROGRAM</u>        |
| 6 | .40 | .08 | .55 | .08 | 1.0 | .40 |                          |
| 7 | .62 | .08 | .40 | .08 | .40 | 1.0 | c = 0.72                 |

## EMBEDDED MARKOV CHAIN AND SUBSTITUTABILITY ANALYSES

## 4. PEBBLY SANDSTONE HORIZONS

|     | SS   | 1    | 2    | 3    | 4    | 5    | 6    | 7    | Sum |                                                                           |
|-----|------|------|------|------|------|------|------|------|-----|---------------------------------------------------------------------------|
| SS  | --   | 11   | 4    | 2    | 1    | 0    | 3    | 0    | 21  | <u>TALLY</u><br><u>MATRIX</u>                                             |
| 1   | 12   | --   | 11   | 16   | 5    | 0    | 3    | 0    | 47  |                                                                           |
| 2   | 3    | 7    | --   | 21   | 13   | 2    | 12   | 2    | 60  |                                                                           |
| 3   | 2    | 12   | 24   | --   | 8    | 2    | 18   | 4    | 70  |                                                                           |
| 4   | 1    | 5    | 9    | 6    | --   | 1    | 5    | 1    | 28  |                                                                           |
| 5   | 0    | 1    | 2    | 1    | 1    | --   | 1    | 0    | 6   |                                                                           |
| 6   | 2    | 5    | 16   | 21   | 4    | 2    | --   | 0    | 50  |                                                                           |
| 7   | 0    | 1    | 3    | 3    | 1    | 0    | 2    | --   | 10  |                                                                           |
| Sh  | 0    | 0    | 1    | 1    | 0    | 0    | 1    | 0    | 3   |                                                                           |
| Sum | 20   | 42   | 70   | 71   | 33   | 7    | 45   | 7    | 295 |                                                                           |
| SS  | ---  | .52  | .19  | .10  | .05  | 0    | .14  | 0    |     | <u>UPWARD</u><br><u>TRANSITION</u><br><u>PROBABILITY</u><br><u>MATRIX</u> |
| 1   | .26  | ---  | .23  | .34  | .11  | 0    | .06  | 0    |     |                                                                           |
| 2   | .05  | .12  | ---  | .35  | .22  | .03  | .20  | .03  |     |                                                                           |
| 3   | .03  | .17  | .34  | ---  | .11  | .03  | .25  | .06  |     |                                                                           |
| 4   | .04  | .18  | .32  | .21  | ---  | .04  | .18  | .04  |     |                                                                           |
| 5   | 0    | .17  | .33  | .17  | .17  | ---  | .17  | 0    |     |                                                                           |
| 6   | .04  | .10  | .32  | .42  | .08  | .04  | ---  | 0    |     |                                                                           |
| 7   | 0    | .10  | .30  | .30  | .10  | 0    | .20  | ---  |     |                                                                           |
| Sh  | 0    | 0    | .33  | .33  | 0    | 0    | .33  | 0    |     |                                                                           |
| SS  | ---  | .15  | .25  | .26  | .12  | .03  | .16  | .03  |     | <u>RANDOM</u><br><u>MATRIX</u>                                            |
| 1   | .08  | ---  | .28  | .29  | .13  | .03  | .18  | .04  |     |                                                                           |
| 2   | .08  | .18  | ---  | .30  | .14  | .03  | .19  | .04  |     |                                                                           |
| 3   | .09  | .19  | .31  | ---  | .15  | .03  | .20  | .04  |     |                                                                           |
| 4   | .07  | .16  | .26  | .26  | ---  | .03  | .17  | .03  |     |                                                                           |
| 5   | .07  | .14  | .24  | .24  | .11  | ---  | .16  | .03  |     |                                                                           |
| 6   | .08  | .17  | .28  | .29  | .13  | .03  | ---  | .04  |     |                                                                           |
| 7   | .07  | .15  | .24  | .25  | .12  | .02  | .16  | ---  |     |                                                                           |
| Sh  | .07  | .14  | .24  | .24  | .11  | .02  | .15  | .03  |     |                                                                           |
| SS  | ---- | +.37 | -.06 | -.16 | -.07 | -.03 | -.02 | -.03 |     | <u>DIFFERENCE</u><br><u>MATRIX</u>                                        |
| 1   | +.18 | ---- | -.05 | +.05 | -.02 | -.03 | -.12 | -.04 |     |                                                                           |
| 2   | -.03 | -.06 | ---- | +.05 | +.08 | 0    | +.01 | -.01 |     |                                                                           |
| 3   | -.06 | -.02 | +.03 | ---- | -.04 | 0    | +.05 | +.02 |     |                                                                           |
| 4   | -.03 | +.02 | +.06 | -.05 | ---- | +.01 | +.01 | +.01 |     |                                                                           |
| 5   | -.07 | +.03 | +.09 | -.07 | +.06 | ---- | +.01 | -.03 |     |                                                                           |
| 6   | -.04 | -.07 | +.04 | +.13 | -.05 | +.01 | ---- | -.04 |     |                                                                           |
| 7   | -.07 | +.05 | +.06 | +.05 | +.02 | -.02 | +.04 | ---- |     |                                                                           |
| Sh  | -.07 | -.14 | +.09 | +.09 | -.11 | -.02 | +.18 | -.03 |     |                                                                           |

EMBEDDED MARKOV CHAIN AND SUBSTITUTABILITY ANALYSES

4. PEBBLY SANDSTONE HORIZONS

|    | SS  | 1   | 2   | 3   | 4   | 5   | 6   | 7   |                                                              |
|----|-----|-----|-----|-----|-----|-----|-----|-----|--------------------------------------------------------------|
| SS | 1.0 | .17 | .38 | .59 | .51 | .35 | .31 | .35 | <u>UNDERLYING<br/>(LEFT)<br/>SUBSTITUTABILITY<br/>MATRIX</u> |
| 1  | .17 | 1.0 | .64 | .44 | .60 | .48 | .59 | .32 |                                                              |
| 2  | .38 | .64 | 1.0 | .79 | .68 | .35 | .86 | .35 |                                                              |
| 3  | .59 | .44 | .79 | 1.0 | .76 | .48 | .71 | .24 |                                                              |
| 4  | .51 | .60 | .68 | .76 | 1.0 | .58 | .70 | .58 |                                                              |
| 5  | .35 | .48 | .35 | .48 | .58 | 1.0 | .52 | 1.0 |                                                              |
| 6  | .31 | .59 | .86 | .71 | .70 | .52 | 1.0 | .70 |                                                              |
| 7  | .35 | .32 | .35 | .24 | .58 | 1.0 | .70 | 1.0 |                                                              |
| SS | --- | .26 | .06 | .03 | .03 | 0   | .07 | 0   | <u>DOWNWARD<br/>TRANSITION<br/>PROBABILITY<br/>MATRIX</u>    |
| 1  | .60 | --- | .16 | .23 | .15 | 0   | .07 | 0   |                                                              |
| 2  | .15 | .17 | --- | .30 | .39 | .29 | .27 | .29 |                                                              |
| 3  | .10 | .29 | .34 | --- | .24 | .29 | .40 | .57 |                                                              |
| 4  | .05 | .12 | .13 | .08 | --- | .14 | .11 | .14 |                                                              |
| 5  | 0   | .02 | .03 | .01 | .03 | --- | .02 | 0   |                                                              |
| 6  | .10 | .12 | .23 | .30 | .12 | .29 | --- | 0   |                                                              |
| 7  | 0   | .02 | .04 | .04 | .03 | 0   | .04 | --- |                                                              |
| SS | 1.0 | .28 | .53 | .71 | .58 | .34 | .41 | .27 | <u>OVERLYING<br/>(RIGHT)<br/>SUBSTITUTABILITY<br/>MATRIX</u> |
| 1  | .28 | 1.0 | .79 | .50 | .73 | .79 | .89 | .83 |                                                              |
| 2  | .53 | .79 | 1.0 | .55 | .55 | .78 | .71 | .68 |                                                              |
| 3  | .71 | .50 | .55 | 1.0 | .79 | .76 | .49 | .31 |                                                              |
| 4  | .58 | .73 | .55 | .79 | 1.0 | .84 | .94 | .79 |                                                              |
| 5  | .34 | .79 | .78 | .76 | .84 | 1.0 | .86 | .82 |                                                              |
| 6  | .41 | .89 | .71 | .49 | .94 | .86 | 1.0 | 1.0 |                                                              |
| 7  | .27 | .83 | .68 | .31 | .79 | .82 | 1.0 | 1.0 |                                                              |
| SS | 1.0 | .05 | .20 | .42 | .30 | .12 | .13 | .09 | <u>MUTUAL<br/>SUBSTITUTABILITY<br/>MATRIX</u>                |
| 1  | .05 | 1.0 | .51 | .22 | .44 | .38 | .53 | .27 |                                                              |
| 2  | .20 | .51 | 1.0 | .43 | .37 | .27 | .61 | .24 |                                                              |
| 3  | .42 | .22 | .43 | 1.0 | .60 | .36 | .35 | .07 |                                                              |
| 4  | .30 | .44 | .37 | .60 | 1.0 | .49 | .66 | .46 |                                                              |
| 5  | .12 | .38 | .27 | .36 | .49 | 1.0 | .45 | .82 |                                                              |
| 6  | .13 | .53 | .61 | .35 | .66 | .45 | 1.0 | .70 |                                                              |
| 7  | .09 | .27 | .24 | .07 | .46 | .82 | .70 | 1.0 |                                                              |

## EMBEDDED MARKOV CHAIN AND SUBSTITUTABILITY ANALYSES

## 4. PEBBLY SANDSTONE HORIZONS

## Cophenetic Correlations Based Upon Dendrograms

|    | SS  | 1   | 2   | 3   | 4   | 5   | 6   | 7   |                         |
|----|-----|-----|-----|-----|-----|-----|-----|-----|-------------------------|
| SS | 1.0 | .51 | .51 | .71 | .51 | .51 | .51 | .51 |                         |
| 1  | .51 | 1.0 | .75 | .51 | .80 | .80 | .80 | .80 |                         |
| 2  | .51 | .75 | 1.0 | .51 | .75 | .75 | .75 | .75 |                         |
| 3  | .71 | .51 | .51 | 1.0 | .51 | .51 | .51 | .51 | <u>OVERLYING</u>        |
| 4  | .51 | .80 | .75 | .51 | 1.0 | .84 | .87 | .87 | <u>(RIGHT)</u>          |
| 5  | .51 | .80 | .75 | .51 | .84 | 1.0 | .84 | .84 | <u>SUBSTITUTABILITY</u> |
| 6  | .51 | .80 | .75 | .51 | .87 | .84 | 1.0 | 1.0 | <u>DENDROGRAM</u>       |
| 7  | .51 | .80 | .75 | .51 | .87 | .84 | 1.0 | 1.0 | c = 0.76                |
| SS | 1.0 | .33 | .33 | .33 | .33 | .33 | .33 | .33 |                         |
| 1  | .33 | 1.0 | .57 | .57 | .57 | .44 | .57 | .44 |                         |
| 2  | .33 | .57 | 1.0 | .72 | .72 | .44 | .86 | .44 |                         |
| 3  | .33 | .57 | .72 | 1.0 | .76 | .44 | .72 | .44 | <u>UNDERLYING</u>       |
| 4  | .33 | .57 | .72 | .76 | 1.0 | .44 | .72 | .44 | <u>(LEFT)</u>           |
| 5  | .33 | .44 | .44 | .44 | .44 | 1.0 | .44 | 1.0 | <u>SUBSTITUTABILITY</u> |
| 6  | .33 | .57 | .86 | .72 | .72 | .44 | 1.0 | .44 | <u>DENDROGRAM</u>       |
| 7  | .33 | .44 | .44 | .44 | .44 | 1.0 | .44 | 1.0 | c = 0.88                |
| SS | 1.0 | .25 | .25 | .42 | .25 | .25 | .25 | .25 |                         |
| 1  | .25 | 1.0 | .51 | .25 | .39 | .39 | .39 | .39 |                         |
| 2  | .25 | .51 | 1.0 | .25 | .39 | .39 | .39 | .39 |                         |
| 3  | .42 | .25 | .25 | 1.0 | .25 | .25 | .25 | .25 | <u>MUTUAL</u>           |
| 4  | .25 | .39 | .39 | .25 | 1.0 | .53 | .66 | .53 | <u>SUBSTITUTABILITY</u> |
| 5  | .25 | .39 | .39 | .25 | .53 | 1.0 | .53 | .82 | <u>DENDROGRAM</u>       |
| 6  | .25 | .39 | .39 | .25 | .66 | .53 | 1.0 | .53 |                         |
| 7  | .25 | .39 | .39 | .25 | .53 | .82 | .53 | 1.0 | c = 0.81                |

## EMBEDDED MARKOV CHAIN AND SUBSTITUTABILITY ANALYSES

## 5. RIVIERE TROIS PISTOLES SECTION

|     | SS   | 1    | 2    | 3    | 4    | 5    | 6    | 7    | Sum |                                                                           |
|-----|------|------|------|------|------|------|------|------|-----|---------------------------------------------------------------------------|
| SS  | --   | 2    | 0    | 0    | 0    | 0    | 1    | 0    | 3   |                                                                           |
| 1   | 0    | --   | 1    | 0    | 2    | 1    | 0    | 2    | 6   |                                                                           |
| 2   | 1    | 3    | --   | 1    | 0    | 0    | 2    | 2    | 9   | <u>TALLY</u><br><u>MATRIX</u>                                             |
| 3   | 0    | 0    | 1    | --   | 0    | 0    | 0    | 1    | 2   |                                                                           |
| 4   | 1    | 1    | 1    | 0    | --   | 0    | 1    | 1    | 5   |                                                                           |
| 5   | 0    | 0    | 1    | 0    | 0    | --   | 1    | 0    | 2   |                                                                           |
| 6   | 1    | 0    | 1    | 0    | 3    | 0    | --   | 3    | 8   |                                                                           |
| 7   | 0    | 1    | 5    | 2    | 0    | 1    | 3    | --   | 12  |                                                                           |
| Sum | 3    | 7    | 10   | 3    | 5    | 2    | 8    | 9    | 47  |                                                                           |
| SS  | ---  | .67  | 0    | 0    | 0    | 0    | .33  | 0    |     |                                                                           |
| 1   | 0    | ---  | .17  | 0    | .33  | .17  | 0    | .33  |     |                                                                           |
| 2   | .11  | .33  | ---  | .11  | 0    | 0    | .22  | .22  |     | <u>UPWARD</u><br><u>TRANSITION</u><br><u>PROBABILITY</u><br><u>MATRIX</u> |
| 3   | 0    | 0    | .50  | ---  | 0    | 0    | 0    | .50  |     |                                                                           |
| 4   | .20  | .20  | .20  | 0    | ---  | 0    | .20  | .20  |     |                                                                           |
| 5   | 0    | 0    | .50  | 0    | 0    | ---  | .50  | 0    |     |                                                                           |
| 6   | .13  | 0    | .13  | 0    | .38  | 0    | ---  | .38  |     |                                                                           |
| 7   | 0    | .08  | .42  | .17  | 0    | .08  | .25  | ---  |     |                                                                           |
| SS  | ---  | .16  | .23  | .07  | .11  | .05  | .18  | .20  |     |                                                                           |
| 1   | .07  | ---  | .24  | .07  | .12  | .05  | .20  | .22  |     |                                                                           |
| 2   | .08  | .18  | ---  | .08  | .13  | .05  | .21  | .24  |     | <u>RANDOM</u><br><u>MATRIX</u>                                            |
| 3   | .07  | .16  | .22  | ---  | .11  | .04  | .18  | .20  |     |                                                                           |
| 4   | .07  | .17  | .24  | .07  | ---  | .05  | .19  | .21  |     |                                                                           |
| 5   | .07  | .16  | .22  | .07  | .11  | ---  | .18  | .20  |     |                                                                           |
| 6   | .08  | .18  | .26  | .08  | .13  | .05  | ---  | .23  |     |                                                                           |
| 7   | .09  | .20  | .29  | .09  | .14  | .06  | .23  | ---  |     |                                                                           |
| SS  | ---- | +.51 | -.23 | -.07 | -.11 | -.05 | +.15 | -.20 |     |                                                                           |
| 1   | -.07 | ---- | -.07 | -.07 | +.21 | +.12 | -.20 | +.11 |     |                                                                           |
| 2   | +.03 | +.15 | ---- | +.03 | -.13 | -.05 | +.01 | -.02 |     | <u>DIFFERENCE</u><br><u>MATRIX</u>                                        |
| 3   | -.07 | -.16 | +.28 | ---- | -.11 | -.04 | -.18 | +.30 |     |                                                                           |
| 4   | +.13 | +.03 | +.04 | -.07 | ---- | -.05 | +.01 | -.01 |     |                                                                           |
| 5   | -.07 | -.16 | +.28 | -.07 | -.11 | ---- | +.32 | -.20 |     |                                                                           |
| 6   | +.05 | -.18 | +.13 | -.08 | +.25 | -.05 | ---- | +.15 |     |                                                                           |
| 7   | -.09 | +.12 | +.13 | +.08 | -.14 | +.02 | +.02 | ---- |     |                                                                           |

## EMBEDDED MARKOV CHAIN AND SUBSTITUTABILITY ANALYSES

## 5. RIVIERE TROIS PISTOLES SECTION

|    | SS  | 1   | 2   | 3   | 4   | 5   | 6   | 7   |                                                              |
|----|-----|-----|-----|-----|-----|-----|-----|-----|--------------------------------------------------------------|
| SS | 1.0 | .39 | .26 | .19 | .38 | 0   | .32 | .54 | <u>UNDERLYING<br/>(LEFT)<br/>SUBSTITUTABILITY<br/>MATRIX</u> |
| 1  | .39 | 1.0 | .10 | .32 | 0   | .06 | .63 | .18 |                                                              |
| 2  | .26 | .10 | 1.0 | .40 | .25 | .34 | .64 | .59 |                                                              |
| 3  | .19 | .32 | .40 | 1.0 | 0   | .25 | .42 | .13 |                                                              |
| 4  | .38 | 0   | .25 | 0   | 1.0 | .60 | 0   | .65 |                                                              |
| 5  | 0   | .06 | .34 | .25 | .60 | 1.0 | .14 | .39 |                                                              |
| 6  | .32 | .63 | .64 | .42 | 0   | .14 | 1.0 | .16 |                                                              |
| 7  | .54 | .18 | .59 | .13 | .65 | .39 | .16 | 1.0 |                                                              |
| SS | --- | .29 | 0   | 0   | 0   | 0   | .13 | 0   | <u>DOWNWARD<br/>TRANSITION<br/>PROBABILITY<br/>MATRIX</u>    |
| 1  | 0   | --- | .10 | 0   | .40 | .50 | 0   | .22 |                                                              |
| 2  | .33 | .43 | --- | .33 | 0   | 0   | .25 | .22 |                                                              |
| 3  | 0   | 0   | .10 | --- | 0   | 0   | 0   | .11 |                                                              |
| 4  | .33 | .14 | .10 | 0   | --- | 0   | .13 | .11 |                                                              |
| 5  | 0   | 0   | .10 | 0   | 0   | --- | .13 | 0   |                                                              |
| 6  | .33 | 0   | .10 | 0   | .60 | 0   | --- | .33 |                                                              |
| 7  | 0   | .14 | .50 | .66 | 0   | .50 | .38 | --- |                                                              |
| SS | 1.0 | .60 | .19 | .26 | .48 | 0   | .41 | .80 | <u>OVERLYING<br/>(RIGHT)<br/>SUBSTITUTABILITY<br/>MATRIX</u> |
| 1  | .60 | 1.0 | .27 | .57 | 0   | .18 | .79 | .42 |                                                              |
| 2  | .19 | .27 | 1.0 | .81 | .25 | .77 | .75 | .27 |                                                              |
| 3  | .26 | .57 | .81 | 1.0 | 0   | .63 | .87 | .20 |                                                              |
| 4  | .48 | 0   | .25 | 0   | 1.0 | .39 | 0   | .84 |                                                              |
| 5  | 0   | .18 | .77 | .63 | .39 | 1.0 | .53 | .32 |                                                              |
| 6  | .41 | .79 | .75 | .87 | 0   | .53 | 1.0 | .29 |                                                              |
| 7  | .80 | .42 | .27 | .20 | .84 | .32 | .29 | 1.0 |                                                              |
| SS | 1.0 | .23 | .05 | .05 | .18 | 0   | .13 | .43 | <u>MUTUAL<br/>SUBSTITUTABILITY<br/>MATRIX</u>                |
| 1  | .23 | 1.0 | .03 | .18 | 0   | .01 | .50 | .08 |                                                              |
| 2  | .05 | .03 | 1.0 | .32 | .06 | .26 | .48 | .16 |                                                              |
| 3  | .05 | .18 | .32 | 1.0 | 0   | .16 | .37 | .03 |                                                              |
| 4  | .18 | 0   | .06 | 0   | 1.0 | .23 | 0   | .55 |                                                              |
| 5  | 0   | .01 | .26 | .16 | .23 | 1.0 | .07 | .12 |                                                              |
| 6  | .13 | .50 | .48 | .37 | 0   | .07 | 1.0 | .05 |                                                              |
| 7  | .43 | .08 | .16 | .03 | .55 | .12 | .05 | 1.0 |                                                              |





## EMBEDDED MARKOV CHAIN AND SUBSTITUTABILITY ANALYSES

## 6. GREVE DE LA POINTE SECTION

|     | SS   | 1    | 2    | 3    | 4    | 5    | 6    | 7    | Sum |                                                                           |
|-----|------|------|------|------|------|------|------|------|-----|---------------------------------------------------------------------------|
| SS  | --   | 8    | 7    | 1    | 2    | 1    | 1    | 0    | 20  |                                                                           |
| 1   | 4    | --   | 3    | 1    | 3    | 0    | 2    | 1    | 14  |                                                                           |
| 2   | 9    | 2    | --   | 8    | 11   | 4    | 8    | 8    | 50  | <u>TALLY</u><br><u>MATRIX</u>                                             |
| 3   | 0    | 1    | 15   | --   | 11   | 1    | 7    | 5    | 40  |                                                                           |
| 4   | 1    | 0    | 10   | 16   | --   | 1    | 5    | 12   | 45  |                                                                           |
| 5   | 0    | 0    | 2    | 3    | 0    | --   | 0    | 1    | 6   |                                                                           |
| 6   | 2    | 0    | 15   | 3    | 7    | 0    | --   | 6    | 33  |                                                                           |
| 7   | 4    | 0    | 7    | 9    | 7    | 2    | 8    | --   | 37  |                                                                           |
| Sum | 20   | 11   | 59   | 41   | 41   | 9    | 31   | 33   | 245 |                                                                           |
| SS  | ---  | .40  | .35  | .05  | .10  | .05  | .05  | 0    |     | <u>UPWARD</u><br><u>TRANSITION</u><br><u>PROBABILITY</u><br><u>MATRIX</u> |
| 1   | .29  | ---  | .21  | .07  | .21  | 0    | .14  | .07  |     |                                                                           |
| 2   | .18  | .04  | ---  | .16  | .22  | .08  | .16  | .16  |     |                                                                           |
| 3   | 0    | .03  | .38  | ---  | .28  | .03  | .18  | .13  |     |                                                                           |
| 4   | .02  | 0    | .22  | .36  | ---  | .02  | .11  | .27  |     |                                                                           |
| 5   | 0    | 0    | .33  | .50  | 0    | ---  | 0    | .17  |     |                                                                           |
| 6   | .06  | 0    | .45  | .09  | .21  | 0    | ---  | .18  |     |                                                                           |
| 7   | .11  | 0    | .19  | .24  | .19  | .05  | .22  | ---  |     |                                                                           |
| SS  | ---  | .05  | .26  | .18  | .18  | .04  | .14  | .15  |     | <u>RANDOM</u><br><u>MATRIX</u>                                            |
| 1   | .09  | ---  | .26  | .18  | .18  | .04  | .13  | .14  |     |                                                                           |
| 2   | .10  | .06  | ---  | .21  | .21  | .05  | .16  | .17  |     |                                                                           |
| 3   | .10  | .05  | .29  | ---  | .20  | .04  | .15  | .16  |     |                                                                           |
| 4   | .10  | .06  | .30  | .21  | ---  | .05  | .16  | .17  |     |                                                                           |
| 5   | .08  | .05  | .25  | .17  | .17  | ---  | .13  | .14  |     |                                                                           |
| 6   | .09  | .05  | .28  | .19  | .19  | .04  | ---  | .16  |     |                                                                           |
| 7   | .10  | .05  | .28  | .20  | .20  | .04  | .15  | ---  |     |                                                                           |
| SS  | ---- | +.35 | +.09 | -.08 | -.08 | +.01 | -.09 | -.15 |     | <u>DIFFERENCE</u><br><u>MATRIX</u>                                        |
| 1   | +.20 | ---- | -.05 | -.11 | +.03 | -.04 | +.01 | -.07 |     |                                                                           |
| 2   | +.08 | -.02 | ---- | -.05 | +.01 | +.03 | 0    | -.01 |     |                                                                           |
| 3   | -.10 | -.02 | +.09 | ---- | +.08 | -.01 | +.03 | -.03 |     |                                                                           |
| 4   | -.08 | -.06 | -.08 | +.15 | ---- | -.03 | -.05 | +.10 |     |                                                                           |
| 5   | -.08 | -.05 | +.08 | +.33 | -.17 | ---- | -.13 | +.03 |     |                                                                           |
| 6   | -.03 | -.05 | +.17 | -.10 | +.02 | -.04 | ---- | +.02 |     |                                                                           |
| 7   | +.01 | -.05 | -.09 | +.04 | -.01 | +.01 | +.07 | ---- |     |                                                                           |

## EMBEDDED MARKOV CHAIN AND SUBSTITUTABILITY ANALYSES

## 6. GREVE DE LA POINTE SECTION

|    | SS  | 1   | 2   | 3   | 4   | 5   | 6   | 7   |                                                              |
|----|-----|-----|-----|-----|-----|-----|-----|-----|--------------------------------------------------------------|
| SS | 1.0 | .08 | .40 | .43 | .77 | .43 | .81 | .48 | <u>UNDERLYING<br/>(LEFT)<br/>SUBSTITUTABILITY<br/>MATRIX</u> |
| 1  | .08 | 1.0 | .45 | .11 | .29 | .35 | .27 | .06 |                                                              |
| 2  | .40 | .45 | 1.0 | .63 | .75 | .34 | .57 | .71 |                                                              |
| 3  | .43 | .11 | .63 | 1.0 | .36 | .40 | .53 | .79 |                                                              |
| 4  | .77 | .29 | .75 | .36 | 1.0 | .69 | .89 | .58 |                                                              |
| 5  | .43 | .35 | .34 | .40 | .69 | 1.0 | .76 | .32 |                                                              |
| 6  | .81 | .27 | .57 | .53 | .89 | .76 | 1.0 | .55 |                                                              |
| 7  | .48 | .06 | .71 | .79 | .58 | .32 | .55 | 1.0 |                                                              |
| SS | --- | .73 | .12 | .02 | .05 | .11 | .03 | 0   | <u>DOWNWARD<br/>TRANSITION<br/>PROBABILITY<br/>MATRIX</u>    |
| 1  | .20 | --- | .05 | .02 | .07 | 0   | .06 | .03 |                                                              |
| 2  | .45 | .18 | --- | .20 | .27 | .44 | .26 | .24 |                                                              |
| 3  | 0   | .09 | .25 | --- | .27 | .11 | .23 | .15 |                                                              |
| 4  | .05 | 0   | .17 | .39 | --- | .11 | .16 | .36 |                                                              |
| 5  | 0   | 0   | .03 | .07 | 0   | --- | 0   | .03 |                                                              |
| 6  | .10 | 0   | .25 | .07 | .17 | 0   | --- | .18 |                                                              |
| 7  | .20 | 0   | .12 | .22 | .17 | .22 | .26 | --- |                                                              |
| SS | 1.0 | .20 | .31 | .63 | .73 | .89 | .74 | .61 | <u>OVERLYING<br/>(RIGHT)<br/>SUBSTITUTABILITY<br/>MATRIX</u> |
| 1  | .20 | 1.0 | .34 | .13 | .32 | .43 | .25 | .14 |                                                              |
| 2  | .31 | .34 | 1.0 | .57 | .72 | .41 | .64 | .72 |                                                              |
| 3  | .63 | .13 | .57 | 1.0 | .44 | .69 | .71 | .82 |                                                              |
| 4  | .73 | .32 | .72 | .44 | 1.0 | .84 | .82 | .58 |                                                              |
| 5  | .89 | .43 | .41 | .69 | .84 | 1.0 | .88 | .67 |                                                              |
| 6  | .74 | .25 | .64 | .71 | .82 | .88 | 1.0 | .64 |                                                              |
| 7  | .61 | .14 | .72 | .82 | .58 | .67 | .64 | 1.0 |                                                              |
| SS | 1.0 | .20 | .12 | .27 | .56 | .38 | .60 | .29 | <u>MUTUAL<br/>SUBSTITUTABILITY<br/>MATRIX</u>                |
| 1  | .20 | 1.0 | .15 | .01 | .09 | .15 | .07 | .01 |                                                              |
| 2  | .12 | .15 | 1.0 | .36 | .54 | .14 | .36 | .51 |                                                              |
| 3  | .27 | .01 | .36 | 1.0 | .16 | .28 | .38 | .65 |                                                              |
| 4  | .56 | .09 | .54 | .16 | 1.0 | .58 | .73 | .34 |                                                              |
| 5  | .38 | .15 | .14 | .28 | .58 | 1.0 | .67 | .21 |                                                              |
| 6  | .60 | .07 | .36 | .38 | .73 | .67 | 1.0 | .35 |                                                              |
| 7  | .29 | .01 | .51 | .65 | .34 | .21 | .35 | 1.0 |                                                              |

## EMBEDDED MARKOV CHAIN AND SUBSTITUTABILITY ANALYSES

## 6. GREVE DE LA POINTE SECTION

## Cophenetic Correlations Based upon Dendrograms

|    | SS  | 1   | 2   | 3   | 4   | 5   | 6   | 7   |                                                                                                    |
|----|-----|-----|-----|-----|-----|-----|-----|-----|----------------------------------------------------------------------------------------------------|
| SS | 1.0 | .28 | .58 | .58 | .80 | .89 | .80 | .58 | <u>OVERLYING</u><br><u>(RIGHT)</u><br><u>SUBSTITUTABILITY</u><br><u>DENDROGRAM</u><br><br>c = 0.91 |
| 1  | .28 | 1.0 | .28 | .28 | .28 | .28 | .28 | .28 |                                                                                                    |
| 2  | .58 | .28 | 1.0 | .65 | .58 | .58 | .58 | .65 |                                                                                                    |
| 3  | .58 | .28 | .65 | 1.0 | .58 | .58 | .58 | .82 |                                                                                                    |
| 4  | .80 | .28 | .58 | .58 | 1.0 | .80 | .82 | .58 |                                                                                                    |
| 5  | .89 | .28 | .58 | .58 | .80 | 1.0 | .80 | .58 |                                                                                                    |
| 6  | .80 | .28 | .58 | .58 | .82 | .80 | 1.0 | .58 |                                                                                                    |
| 7  | .58 | .28 | .65 | .82 | .58 | .58 | .58 | 1.0 |                                                                                                    |
| SS | 1.0 | .27 | .43 | .43 | .79 | .58 | .79 | .43 | <u>UNDERLYING</u><br><u>(LEFT)</u><br><u>SUBSTITUTABILITY</u><br><u>DENDROGRAM</u><br><br>c = 0.92 |
| 1  | .27 | 1.0 | .27 | .27 | .27 | .27 | .27 | .27 |                                                                                                    |
| 2  | .43 | .27 | 1.0 | .67 | .43 | .43 | .43 | .67 |                                                                                                    |
| 3  | .43 | .27 | .67 | 1.0 | .43 | .43 | .43 | .79 |                                                                                                    |
| 4  | .79 | .27 | .43 | .43 | 1.0 | .58 | .89 | .43 |                                                                                                    |
| 5  | .58 | .27 | .43 | .43 | .58 | 1.0 | .58 | .43 |                                                                                                    |
| 6  | .79 | .27 | .43 | .43 | .89 | .58 | 1.0 | .43 |                                                                                                    |
| 7  | .43 | .27 | .67 | .79 | .43 | .43 | .43 | 1.0 |                                                                                                    |
| SS | 1.0 | .12 | .25 | .25 | .48 | .48 | .48 | .25 | <u>MUTUAL</u><br><u>SUBSTITUTABILITY</u><br><u>DENDROGRAM</u><br><br>c = 0.94                      |
| 1  | .12 | 1.0 | .12 | .12 | .12 | .12 | .12 | .12 |                                                                                                    |
| 2  | .25 | .12 | 1.0 | .44 | .25 | .25 | .25 | .44 |                                                                                                    |
| 3  | .25 | .12 | .44 | 1.0 | .25 | .25 | .25 | .65 |                                                                                                    |
| 4  | .48 | .12 | .25 | .25 | 1.0 | .63 | .73 | .25 |                                                                                                    |
| 5  | .48 | .12 | .25 | .25 | .63 | 1.0 | .63 | .25 |                                                                                                    |
| 6  | .48 | .12 | .25 | .25 | .73 | .63 | 1.0 | .25 |                                                                                                    |
| 7  | .25 | .12 | .44 | .65 | .25 | .25 | .25 | 1.0 |                                                                                                    |

## Part 5

Detailed Analyses:

## Sequences of Facies Groups

Embedded and Non-embedded Markov Chain Analyses: Facies Groups

Computational Techniques for Embedded Markov Chain Analysis (Miall, 1973)

Computational Techniques for Non-embedded Markov Chain Analysis

(Davis, 1973)

Techniques and conventions used are the same as the analyses in Parts 1 and 3, Appendix 9.

Note: As for the other Markov chain analyses, those transitions with a difference matrix score less than +.05 were eliminated from the spider diagrams, as were those transitions which only occurred once. The exception to this convention, were those individual transitions at the Riviere Trois Pistoles Section that had a difference matrix score greater to or equal to +.05. This was done because of the small number of transitions observed at this section.



EMBEDDED MARKOV CHAIN ANALYSIS: FACIES GROUPS

2. CONGLOMERATE HORIZONS

|          | 1    | 5    | Sh   | (6,2,SS) | (3,4) | Sum |                                                        |
|----------|------|------|------|----------|-------|-----|--------------------------------------------------------|
| 1        | --   | 1    | 1    | 25       | 12    | 39  | <u>TALLY</u><br><u>MATRIX</u>                          |
| 5        | 1    | --   | 0    | 1        | 2     | 4   |                                                        |
| Sh       | 1    | 0    | --   | 0        | 3     | 4   |                                                        |
| (6,2,SS) | 18   | 3    | 0    | --       | 7     | 28  |                                                        |
| (3,4)    | 16   | 1    | 2    | 7        | --    | 26  |                                                        |
| Sum      | 36   | 5    | 3    | 33       | 24    | 101 |                                                        |
| 1        | ---  | .03  | .03  | .64      | .31   |     | <u>OBSERVED</u><br><u>PROBABILITY</u><br><u>MATRIX</u> |
| 5        | .25  | ---  | 0    | .25      | .50   |     |                                                        |
| Sh       | .25  | 0    | ---  | 0        | .75   |     |                                                        |
| (6,2,SS) | .64  | .11  | 0    | ---      | .25   |     |                                                        |
| (3,4)    | .62  | .04  | .08  | .27      | ---   |     |                                                        |
| 1        | ---  | .06  | .06  | .45      | .58   |     | <u>RANDOM</u><br><u>MATRIX</u>                         |
| 5        | .40  | ---  | .04  | .29      | .27   |     |                                                        |
| Sh       | .40  | .04  | ---  | .29      | .27   |     |                                                        |
| (6,2,SS) | .53  | .05  | .05  | ---      | .36   |     |                                                        |
| (3,4)    | .52  | .05  | .05  | .37      | ---   |     |                                                        |
| 1        | ---  | -.03 | -.03 | +.19     | -.27  |     | <u>DIFFERENCE</u><br><u>MATRIX</u>                     |
| 5        | -.15 | ---  | -.04 | -.04     | +.23  |     |                                                        |
| Sh       | -.15 | -.04 | ---  | -.29     | +.48  |     |                                                        |
| (6,2,SS) | +.11 | +.06 | -.05 | ---      | -.09  |     |                                                        |
| (3,4)    | +.10 | -.01 | +.03 | -.10     | ---   |     |                                                        |

## EMBEDDED MARKOV CHAIN ANALYSIS: FACIES GROUPS

## 3. BIC MEMBER III SECTION

|       | (7,2) | (6,4) | 3    | 5    | Sum |                                                        |
|-------|-------|-------|------|------|-----|--------------------------------------------------------|
| (7,2) | ---   | 7     | 12   | 7    | 26  |                                                        |
| (6,4) | 12    | ---   | 2    | 3    | 17  | <u>TALLY</u><br><u>MATRIX</u>                          |
| 3     | 8     | 8     | ---  | 0    | 16  |                                                        |
| 5     | 6     | 2     | 2    | ---  | 10  |                                                        |
| Sum   | 26    | 17    | 16   | 10   | 69  |                                                        |
| (7,2) | ---   | .27   | .46  | .27  |     | <u>OBSERVED</u><br><u>PROBABILITY</u><br><u>MATRIX</u> |
| (6,4) | .71   | ---   | .12  | .18  |     |                                                        |
| 3     | .50   | .50   | ---  | 0    |     |                                                        |
| 5     | .60   | .20   | .20  | ---  |     |                                                        |
| (7,2) | ---   | .40   | .37  | .23  |     | <u>RANDOM</u><br><u>MATRIX</u>                         |
| (6,4) | .50   | ---   | .31  | .19  |     |                                                        |
| 3     | .49   | .32   | ---  | .19  |     |                                                        |
| 5     | .44   | .29   | .27  | ---  |     |                                                        |
| (7,2) | ----  | -.13  | +.09 | +.04 |     | <u>DIFFERENCE</u><br><u>MATRIX</u>                     |
| (6,4) | +.21  | ----  | -.19 | -.01 |     |                                                        |
| 3     | +.01  | +.18  | ---- | -.19 |     |                                                        |
| 5     | +.16  | -.09  | -.07 | ---- |     |                                                        |



## EMBEDDED MARKOV CHAIN ANALYSIS: FACIES GROUPS

## 4. PEBBLY SANDSTONE HORIZONS

|           | 1    | 2    | 3    | SS   | (4,5<br>6,7) | Sh   | Sum |                    |
|-----------|------|------|------|------|--------------|------|-----|--------------------|
| 1         | ---  | 11   | 16   | 11   | 8            | 0    | 46  |                    |
| 2         | 7    | ---  | 20   | 3    | 29           | 0    | 59  |                    |
| 3         | 12   | 24   | ---  | 2    | 31           | 1    | 69  |                    |
| SS        | 10   | 4    | 2    | ---  | 4            | 0    | 20  | <u>TALLY</u>       |
| (7,5,6,4) | 12   | 30   | 31   | 3    | ---          | 0    | 76  | <u>MATRIX</u>      |
| Sh        | 0    | 1    | 0    | 0    | 1            | ---  | 2   |                    |
| Sum       | 41   | 70   | 69   | 19   | 73           | 1    | 272 |                    |
| 1         | ---  | .24  | .35  | .24  | .17          | 0    |     |                    |
| 2         | .12  | ---  | .34  | .05  | .49          | 0    |     | <u>OBSERVED</u>    |
| 3         | .17  | .35  | ---  | .03  | .45          | .01  |     | <u>PROBABILITY</u> |
| SS        | .50  | .20  | .10  | ---  | .20          | 0    |     | <u>MATRIX</u>      |
| (7,5,6,4) | .16  | .39  | .41  | .04  | ---          | 0    |     |                    |
| Sh        | 0    | .50  | 0    | 0    | .50          | ---  |     |                    |
| 1         | ---  | .26  | .31  | .09  | .34          | .01  |     |                    |
| 2         | .22  | ---  | .32  | .09  | .36          | .01  |     | <u>RANDOM</u>      |
| 3         | .23  | .29  | ---  | .10  | .37          | .01  |     | <u>MATRIX</u>      |
| SS        | .18  | .23  | .27  | ---  | .30          | .01  |     |                    |
| (4,5,6,7) | .23  | .30  | .35  | .10  | ---          | .01  |     |                    |
| Sh        | .17  | .22  | .26  | .07  | .28          | ---  |     |                    |
| 1         | ---- | -.02 | +.04 | +.13 | -.17         | -.01 |     |                    |
| 2         | -.10 | ---- | +.02 | -.04 | +.13         | -.01 |     | <u>DIFFERENCE</u>  |
| 3         | -.06 | +.06 | ---- | -.07 | +.08         | 0    |     | <u>MATRIX</u>      |
| SS        | +.32 | -.03 | -.17 | ---- | -.10         | -.01 |     |                    |
| (4,5,6,7) | -.07 | +.09 | +.06 | -.06 | ----         | -.01 |     |                    |
| Sh        | -.17 | +.28 | -.26 | -.07 | +.22         | ---- |     |                    |

## EMBEDDED MARKOV CHAIN ANALYSIS: FACIES GROUPS

## 5. RIVIERE TROIS PISTOLES

|       | (7,4) | (6,1) | SS   | 2    | 3    | 5    | Sum |                                                        |
|-------|-------|-------|------|------|------|------|-----|--------------------------------------------------------|
| (7,4) | ---   | 6     | 1    | 6    | 2    | 1    | 16  |                                                        |
| (6,1) | 10    | --    | 1    | 2    | 0    | 1    | 14  |                                                        |
| SS    | 0     | 3     | --   | 0    | 0    | 0    | 3   | <u>TALLY</u><br><u>MATRIX</u>                          |
| 2     | 2     | 5     | 1    | --   | 1    | 0    | 9   |                                                        |
| 3     | 1     | 0     | 0    | 1    | --   | 0    | 2   |                                                        |
| 5     | 0     | 1     | 0    | 1    | 0    | --   | 2   |                                                        |
| Sum   | 13    | 15    | 3    | 10   | 3    | 2    | 46  |                                                        |
| (7,4) | ---   | .38   | .06  | .38  | .13  | .06  |     | <u>OBSERVED</u><br><u>PROBABILITY</u><br><u>MATRIX</u> |
| (6,1) | .71   | ---   | .07  | .14  | 0    | .07  |     |                                                        |
| SS    | 0     | 1.0   | ---  | 0    | 0    | 0    |     |                                                        |
| 2     | .22   | .56   | .11  | ---  | .11  | 0    |     |                                                        |
| 3     | .50   | 0     | 0    | .50  | ---  | 0    |     |                                                        |
| 5     | 0     | .50   | 0    | .50  | 0    | ---  |     |                                                        |
| (7,4) | ---   | .47   | .10  | .30  | .07  | .07  |     | <u>RANDOM</u><br><u>MATRIX</u>                         |
| (6,1) | .47   | ---   | .10  | .30  | .07  | .07  |     |                                                        |
| SS    | .34   | .34   | ---  | .22  | .05  | .05  |     |                                                        |
| 2     | .40   | .40   | .09  | ---  | .06  | .06  |     |                                                        |
| 3     | .33   | .33   | .07  | .21  | ---  | .05  |     |                                                        |
| 5     | .33   | .33   | .07  | .21  | .05  | ---  |     |                                                        |
| (7,4) | ---   | -.04  | -.03 | +.13 | +.07 | 0    |     | <u>DIFFERENCE</u><br><u>MATRIX</u>                     |
| (6,1) | +.24  | ----  | -.03 | -.16 | -.07 | 0    |     |                                                        |
| SS    | -.34  | +.66  | ---- | -.22 | -.05 | -.05 |     |                                                        |
| 2     | -.18  | +.14  | +.02 | ---- | +.05 | -.06 |     |                                                        |
| 3     | +.17  | -.33  | -.07 | +.29 | ---- | -.05 |     |                                                        |
| 5     | -.33  | +.17  | -.07 | +.29 | -.05 | ---- |     |                                                        |

EMBEDDED MARKOV CHAIN ANALYSIS: FACIES GROUPS

6. GREVE DE LA POINTE SECTION

|         | SS   | 1    | 2    | (4,5,6) | (3,7) | Sh   | Sum |                    |
|---------|------|------|------|---------|-------|------|-----|--------------------|
| SS      | --   | 9    | 5    | 4       | 1     | 0    | 19  |                    |
| 1       | 4    | --   | 4    | 5       | 2     | 0    | 15  |                    |
| 2       | 9    | 1    | --   | 22      | 15    | 0    | 47  |                    |
| (4,5,6) | 3    | 0    | 25   | --      | 36    | 0    | 64  | <u>TALLY</u>       |
| (3,7)   | 4    | 1    | 20   | 35      | --    | 0    | 60  | <u>MATRIX</u>      |
| Sh      | 0    | 0    | 0    | 0       | 1     | --   | 1   |                    |
| Sum     | 20   | 11   | 54   | 66      | 55    | 0    | 206 |                    |
| SS      | ---  | .47  | .26  | .21     | .05   |      |     |                    |
| 1       | .27  | ---  | .27  | .33     | .13   |      |     | <u>OBSERVED</u>    |
| 2       | .19  | .02  | ---  | .47     | .32   |      |     | <u>PROBABILITY</u> |
| (4,5,6) | .05  | 0    | .39  | ---     | .56   |      |     | <u>MATRIX</u>      |
| (3,7)   | .07  | .02  | .33  | .58     | ---   |      |     |                    |
| Sh      | 0    | 0    | 0    | 0       | 1.0   |      |     |                    |
| SS      | ---  | .08  | .25  | .34     | .32   | .01  |     |                    |
| 1       | .10  | ---  | .25  | .34     | .31   | .01  |     | <u>RANDOM</u>      |
| 2       | .12  | .09  | ---  | .40     | .38   | .01  |     | <u>MATRIX</u>      |
| (4,5,6) | .13  | .11  | .33  | ---     | .42   | .01  |     |                    |
| (3,7)   | .13  | .10  | .32  | .44     | ---   | .01  |     |                    |
| Sh      | .09  | .07  | .23  | .31     | .29   | ---  |     |                    |
| SS      | ---- | +.39 | +.11 | -.13    | -.27  | -.01 |     |                    |
| 1       | +.17 | ---- | +.02 | -.01    | -.18  | -.01 |     | <u>DIFFERENCE</u>  |
| 2       | +.07 | -.07 | ---- | +.07    | -.06  | -.01 |     | <u>MATRIX</u>      |
| (4,5,6) | -.08 | -.11 | +.06 | ----    | +.14  | -.01 |     |                    |
| (3,7)   | -.06 | -.08 | +.01 | +.14    | ----  | -.01 |     |                    |
| Sh      | -.09 | -.07 | -.23 | -.31    | +.71  | ---- |     |                    |

## NON-EMBEDDED MARKOV CHAIN ANALYSIS: FACIES GROUPS

## 1. SANDSTONE HORIZONS

|        | (Sh,7) | (4,3) | (2,SS) | 1    | 5    | 6    | Sum |                                                        |
|--------|--------|-------|--------|------|------|------|-----|--------------------------------------------------------|
| (Sh,7) | 14     | 7     | 5      | 0    | 0    | 4    | 30  | <u>TALLY</u><br><u>MATRIX</u>                          |
| (4,3)  | 4      | 28    | 17     | 1    | 3    | 9    | 62  |                                                        |
| (2,SS) | 7      | 12    | 16     | 3    | 0    | 11   | 49  |                                                        |
| 1      | 0      | 5     | 0      | 0    | 0    | 0    | 5   |                                                        |
| 5      | 1      | 3     | 2      | 0    | 3    | 1    | 10  |                                                        |
| 6      | 2      | 12    | 12     | 1    | 5    | 18   | 50  |                                                        |
| Sum    | 28     | 67    | 52     | 5    | 11   | 43   | 206 |                                                        |
| (Sh,7) | .47    | .23   | .17    | 0    | 0    | .13  |     | <u>OBSERVED</u><br><u>PROBABILITY</u><br><u>MATRIX</u> |
| (4,3)  | .06    | .45   | .27    | .02  | .05  | .15  |     |                                                        |
| (2,SS) | .14    | .24   | .33    | .06  | 0    | .22  |     |                                                        |
| 1      | 0      | 1.0   | 0      | 0    | 0    | 0    |     |                                                        |
| 5      | .10    | .30   | .20    | 0    | .30  | .10  |     |                                                        |
| 6      | .04    | .24   | .24    | .02  | .10  | .36  |     |                                                        |
| (Sh,7) | .14    | .33   | .25    | .02  | .05  | .21  |     |                                                        |
| (4,3)  | .14    | .33   | .25    | .02  | .05  | .21  |     |                                                        |
| (2,SS) | .14    | .33   | .25    | .02  | .05  | .21  |     |                                                        |
| 1      | .14    | .33   | .25    | .02  | .05  | .21  |     |                                                        |
| 5      | .14    | .33   | .25    | .02  | .05  | .21  |     |                                                        |
| 6      | .14    | .33   | .25    | .02  | .05  | .21  |     |                                                        |
| (Sh,7) | +.33   | -.10  | -.08   | -.02 | -.05 | -.08 |     | <u>DIFFERENCE</u><br><u>MATRIX</u>                     |
| (4,3)  | -.08   | +.12  | +.02   | 0    | 0    | -.06 |     |                                                        |
| (2,SS) | 0      | -.09  | +.08   | +.04 | -.05 | -.01 |     |                                                        |
| 1      | -.14   | +.67  | -.25   | -.02 | -.05 | -.21 |     |                                                        |
| 5      | -.04   | -.03  | -.05   | -.02 | +.25 | -.11 |     |                                                        |
| 6      | -.10   | -.09  | -.01   | 0    | +.05 | +.15 |     |                                                        |

## NON-EMBEDDED MARKOV CHAIN ANALYSIS: FACIES GROUPS

## 2. CONGLOMERATE HORIZONS

|          | 1    | 5    | Sh   | (6,2,SS) | (3,4) | Sum |                    |
|----------|------|------|------|----------|-------|-----|--------------------|
| 1        | 21   | 1    | 1    | 25       | 12    | 60  |                    |
| 5        | 1    | 0    | 0    | 1        | 2     | 4   |                    |
| Sh       | 1    | 0    | ---  | 0        | 3     | 4   |                    |
| (6,2,SS) | 18   | 3    | 0    | 10       | 7     | 38  | <u>TALLY</u>       |
| (3,4)    | 16   | 1    | 2    | 7        | 8     | 34  | <u>MATRIX</u>      |
| Sum      | 57   | 5    | 3    | 43       | 32    | 140 |                    |
| 1        | .35  | .02  | .02  | .42      | .20   |     | <u>OBSERVED</u>    |
| 5        | .25  | 0    | 0    | .25      | .50   |     | <u>PROBABILITY</u> |
| Sh       | .25  | 0    | ---  | 0        | .75   |     | <u>MATRIX</u>      |
| (6,2,SS) | .47  | .08  | 0    | .26      | .18   |     |                    |
| (3,4)    | .47  | .03  | .06  | .21      | .24   |     |                    |
| 1        | .41  | .04  | .02  | .31      | .23   |     |                    |
| 5        | .41  | .04  | .02  | .31      | .23   |     |                    |
| Sh       | .42  | .04  | ---  | .32      | .24   |     | <u>RANDOM</u>      |
| (6,2,SS) | .41  | .04  | .02  | .31      | .23   |     | <u>MATRIX</u>      |
| (3,4)    | .41  | .04  | .02  | .31      | .23   |     |                    |
| 1        | -.06 | -.02 | 0    | +.11     | -.03  |     |                    |
| 5        | -.16 | -.04 | -.02 | -.06     | +.27  |     | <u>DIFFERENCE</u>  |
| Sh       | -.17 | -.04 | ---- | -.32     | +.51  |     | <u>MATRIX</u>      |
| (6,2,SS) | +.06 | +.04 | -.02 | -.05     | -.05  |     |                    |
| (3,4)    | +.06 | -.01 | +.04 | -.10     | +.01  |     |                    |

## NON-EMBEDDED MARKOV CHAIN ANALYSIS: FACIES GROUPS

## 3. BIC MEMBER III SECTION

|       | (7,2) | (6,4) | 3    | 5    | Sum |                                                        |
|-------|-------|-------|------|------|-----|--------------------------------------------------------|
| (7,2) | 27    | 7     | 12   | 7    | 53  |                                                        |
| (6,4) | 12    | 10    | 2    | 3    | 27  | <u>TALLY</u><br><u>MATRIX</u>                          |
| 3     | 8     | 8     | 5    | 0    | 21  |                                                        |
| 5     | 6     | 2     | 2    | 7    | 17  |                                                        |
| Sum   | 53    | 27    | 21   | 17   | 118 |                                                        |
| (7,2) | .51   | .13   | .23  | .13  |     | <u>OBSERVED</u><br><u>PROBABILITY</u><br><u>MATRIX</u> |
| (6,4) | .44   | .37   | .07  | .11  |     |                                                        |
| 3     | .38   | .38   | .24  | 0    |     |                                                        |
| 5     | .35   | .12   | .12  | .41  |     |                                                        |
| (7,2) | .44   | .23   | .18  | .14  |     | <u>RANDOM</u><br><u>MATRIX</u>                         |
| (6,4) | .45   | .22   | .18  | .14  |     |                                                        |
| 3     | .45   | .23   | .17  | .14  |     |                                                        |
| 5     | .45   | .23   | .18  | .14  |     |                                                        |
| (7,2) | +.07  | -.10  | +.05 | -.01 |     | <u>DIFFERENCE</u><br><u>MATRIX</u>                     |
| (6,4) | -.01  | +.15  | -.11 | -.03 |     |                                                        |
| 3     | -.07  | +.15  | +.07 | -.14 |     |                                                        |
| 5     | -.10  | -.11  | -.06 | +.27 |     |                                                        |



## NON-EMBEDDED MARKOV CHAIN ANALYSIS: FACIES GROUPS

## 5. RIVIERE TROIS PISTOLES SECTION

|       | (7,4) | (6,1) | SS   | 2    | 3    | 5    | Sum |                                                        |
|-------|-------|-------|------|------|------|------|-----|--------------------------------------------------------|
| (7,4) | 7     | 6     | 1    | 6    | 2    | 1    | 23  |                                                        |
| (6,1) | 10    | 5     | 1    | 2    | 0    | 1    | 19  |                                                        |
| SS    | 0     | 3     | --   | 0    | 0    | 0    | 3   | <u>TALLY</u><br><u>MATRIX</u>                          |
| 2     | 2     | 5     | 1    | 5    | 1    | 0    | 14  |                                                        |
| 3     | 1     | 0     | 0    | 1    | 0    | 0    | 2   |                                                        |
| 5     | 0     | 1     | 0    | 1    | 0    | 0    | 2   |                                                        |
| Sum   | 20    | 20    | 3    | 15   | 3    | 2    | 63  |                                                        |
| (7,4) | .30   | .26   | .04  | .26  | .09  | .04  |     | <u>OBSERVED</u><br><u>PROBABILITY</u><br><u>MATRIX</u> |
| (6,1) | .53   | .26   | .05  | .11  | 0    | .05  |     |                                                        |
| SS    | 0     | 1.0   | ---  | 0    | 0    | 0    |     |                                                        |
| 2     | .14   | .36   | .07  | .36  | .07  | 0    |     |                                                        |
| 3     | .50   | 0     | 0    | .50  | 0    | 0    |     |                                                        |
| 5     | 0     | .50   | 0    | .50  | 0    | 0    |     |                                                        |
| (7,4) | .32   | .32   | .05  | .24  | .05  | .03  |     | <u>RANDOM</u><br><u>MATRIX</u>                         |
| (6,1) | .32   | .32   | .05  | .24  | .05  | .03  |     |                                                        |
| SS    | .33   | .33   | ---  | .25  | .05  | .03  |     |                                                        |
| 2     | .32   | .32   | .05  | .24  | .05  | .03  |     |                                                        |
| 3     | .32   | .32   | .05  | .24  | .05  | .03  |     |                                                        |
| 5     | .32   | .32   | .05  | .24  | .05  | .03  |     |                                                        |
| (7,4) | -.02  | -.06  | -.01 | +.02 | +.04 | +.01 |     | <u>DIFFERENCE</u><br><u>MATRIX</u>                     |
| (6,1) | +.21  | -.06  | 0    | -.13 | -.05 | +.02 |     |                                                        |
| SS    | -.33  | +.67  | ---- | -.25 | -.05 | -.03 |     |                                                        |
| 2     | -.18  | +.04  | +.02 | +.12 | +.02 | -.03 |     |                                                        |
| 3     | +.18  | -.32  | -.05 | +.26 | -.05 | -.03 |     |                                                        |
| 5     | -.32  | +.18  | -.05 | +.26 | -.05 | -.03 |     |                                                        |



## NON-EMBEDDED MARKOV CHAIN ANALYSIS: FACIES GROUPS

## 6. GREVE DE LA POINTE SECTION

|         | SS   | 1    | 2    | (4,5,6) | (3,7) | Sh  | Sum |                                                        |
|---------|------|------|------|---------|-------|-----|-----|--------------------------------------------------------|
| SS      | --   | 9    | 5    | 4       | 1     | 0   | 19  | <u>TALLY</u><br><u>MATRIX</u>                          |
| 1       | 4    | 1    | 4    | 5       | 2     | 0   | 16  |                                                        |
| 2       | 9    | 1    | 28   | 22      | 15    | 0   | 75  |                                                        |
| (4,5,6) | 3    | 0    | 25   | 37      | 36    | 0   | 101 |                                                        |
| (3,7)   | 4    | 1    | 20   | 35      | 35    | 0   | 95  |                                                        |
| Sh      | 0    | 0    | 0    | 0       | 1     | --  | 1   |                                                        |
| Sum     | 20   | 12   | 82   | 103     | 90    | 0   | 307 |                                                        |
| SS      | ---  | .47  | .26  | .21     | .05   |     |     | <u>OBSERVED</u><br><u>PROBABILITY</u><br><u>MATRIX</u> |
| 1       | .25  | .06  | .25  | .31     | .13   |     |     |                                                        |
| 2       | .12  | .01  | .37  | .29     | .20   |     |     |                                                        |
| (4,5,6) | .03  | 0    | .25  | .37     | .36   |     |     |                                                        |
| (3,7)   | .04  | .01  | .21  | .37     | .37   |     |     |                                                        |
| Sh      | 0    | 0    | 0    | 0       | 1.0   |     |     |                                                        |
| SS      | ---  | .04  | .28  | .36     | .31   | 0   |     | <u>RANDOM</u><br><u>MATRIX</u>                         |
| 1       | .07  | .04  | .27  | .34     | .29   | 0   |     |                                                        |
| 2       | .07  | .04  | .27  | .34     | .29   | 0   |     |                                                        |
| (4,5,6) | .07  | .04  | .27  | .34     | .29   | 0   |     |                                                        |
| (3,7)   | .07  | .04  | .27  | .34     | .29   | 0   |     |                                                        |
| Sh      | .07  | .04  | .27  | .34     | .29   | --- |     |                                                        |
| SS      | ---- | +.43 | -.02 | -.15    | -.26  | 0   |     | <u>DIFFERENCE</u><br><u>MATRIX</u>                     |
| 1       | +.18 | +.02 | -.02 | -.03    | -.16  | 0   |     |                                                        |
| 2       | +.05 | -.03 | +.10 | -.05    | -.09  | 0   |     |                                                        |
| (4,5,6) | -.04 | -.04 | -.02 | +.03    | +.07  | 0   |     |                                                        |
| (3,7)   | -.03 | -.03 | -.06 | +.03    | +.08  | 0   |     |                                                        |
| Sh      | -.07 | -.04 | -.27 | -.34    | +.71  | --- |     |                                                        |